

Waste Isolation Pilot Plant

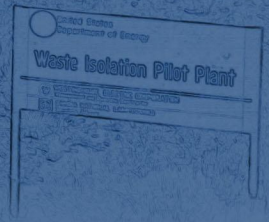


HalfPACT

Safety Analysis Report



Revision 5
February 2009



This page intentionally left blank to facilitate duplex printing.

TABLE OF CONTENTS

1.0 GENERAL INFORMATION.....	1.1-1
1.1 Introduction	1.1-1
1.2 Package Description.....	1.2-1
1.2.1 Packaging	1.2-1
1.2.1.1 Packaging Description.....	1.2-1
1.2.1.2 Gross Weight.....	1.2-5
1.2.1.3 Neutron Moderation and Absorption	1.2-5
1.2.1.4 Receptacles, Valves, Testing, and Sampling Ports	1.2-5
1.2.1.5 Heat Dissipation	1.2-6
1.2.1.6 Coolants.....	1.2-6
1.2.1.7 Protrusions.....	1.2-6
1.2.1.8 Lifting and Tie-down Devices.....	1.2-6
1.2.1.9 Pressure Relief System.....	1.2-7
1.2.1.10 Shielding.....	1.2-7
1.2.2 Operational Features.....	1.2-7
1.2.3 Contents of Packaging.....	1.2-8
1.3 Appendices	1.3-1
1.3.1 Packaging General Arrangement Drawings	1.3.1-1
1.3.2 Glossary of Terms and Acronyms.....	1.3.2-1
2.0 STRUCTURAL EVALUATION	2.1-1
2.1 Structural Design.....	2.1-1
2.1.1 Discussion	2.1-1
2.1.1.1 Containment Vessel Structures	2.1-2
2.1.1.2 Non-Containment Vessel Structures	2.1-3
2.1.2 Design Criteria	2.1-3
2.1.2.1 Analytic Design Criteria (Allowable Stresses)	2.1-3
2.1.2.2 Miscellaneous Structural Failure Modes.....	2.1-4
2.2 Weights and Centers of Gravity	2.2-1
2.2.1 Effect of a Radial Payload Imbalance	2.2-1
2.2.2 Effect of an Axial Payload Imbalance.....	2.2-3
2.3 Mechanical Properties of Materials.....	2.3-1
2.3.1 Mechanical Properties Applied to Analytic Evaluations	2.3-1
2.3.2 Mechanical Properties Applied to Certification Testing.....	2.3-2
2.4 General Standards for All Packages.....	2.4-1
2.4.1 Minimum Package Size.....	2.4-1
2.4.2 Tamper-indicating Feature	2.4-1

2.4.3	Positive Closure.....	2.4-1
2.4.4	Chemical and Galvanic Reactions.....	2.4-1
2.4.4.1	Packaging Materials of Construction	2.4-2
2.4.4.2	Payload Interaction with Packaging Materials of Construction..	2.4-3
2.4.5	Valves	2.4-3
2.4.6	Package Design	2.4-3
2.4.7	External Temperatures	2.4-3
2.4.8	Venting	2.4-4
2.5	Lifting and Tie-down Standards for All Packages	2.5-1
2.5.1	Lifting Devices	2.5-1
2.5.2	Tie-down Devices.....	2.5-2
2.5.2.1	Tie-down Forces.....	2.5-2
2.5.2.2	Tie-down Stress Due to a Vertical Tensile Load	2.5-3
2.5.2.3	Tie-down Stress Due to a Vertical Compressive Load	2.5-7
2.5.2.4	Tie-down Stresses Due to a Horizontal Compressive Load.....	2.5-9
2.5.2.5	Response of the Package if Treated as a Fixed Cantilever Beam	2.5-11
2.5.2.6	Summary.....	2.5-11
2.6	Normal Conditions of Transport	2.6-1
2.6.1	Heat	2.6-2
2.6.1.1	Summary of Pressures and Temperatures	2.6-2
2.6.1.2	Differential Thermal Expansion.....	2.6-3
2.6.1.3	Stress Calculations	2.6-3
2.6.1.4	Comparison with Allowable Stresses.....	2.6-4
2.6.1.5	Range of Primary Plus Secondary Stress Intensities.....	2.6-5
2.6.2	Cold	2.6-6
2.6.2.1	Stress Calculations	2.6-6
2.6.2.2	Comparison with Allowable Stresses.....	2.6-7
2.6.3	Reduced External Pressure	2.6-7
2.6.4	Increased External Pressure	2.6-7
2.6.4.1	Stress Calculations	2.6-8
2.6.4.2	Comparison with Allowable Stresses.....	2.6-8
2.6.4.3	Buckling Assessment of the Torispherical Heads.....	2.6-9
2.6.4.4	Buckling Assessment of the Cylindrical Shells	2.6-10
2.6.5	Vibration.....	2.6-10
2.6.5.1	Vibratory Loads Determination.....	2.6-10
2.6.5.2	Calculation of Alternating Stresses	2.6-11
2.6.5.3	Stress Limits and Results	2.6-12
2.6.6	Water Spray	2.6-13
2.6.7	Free Drop.....	2.6-13
2.6.8	Corner Drop.....	2.6-13
2.6.9	Compression.....	2.6-13

2.6.10	Penetration.....	2.6-13
2.7	Hypothetical Accident Conditions	2.7-1
2.7.1	Free Drop.....	2.7-2
2.7.1.1	Technical Basis for the Free Drop Tests	2.7-2
2.7.1.2	Test Sequence for the Selected Tests	2.7-3
2.7.1.3	Summary of Results from the Free Drop Tests	2.7-3
2.7.2	Crush	2.7-3
2.7.3	Puncture	2.7-4
2.7.3.1	Technical Basis for the Puncture Drop Tests	2.7-4
2.7.3.2	Test Sequence for the Selected Tests	2.7-5
2.7.3.3	Summary of Results from the Puncture Drop Tests.....	2.7-5
2.7.4	Thermal	2.7-6
2.7.4.1	Summary of Pressures and Temperatures	2.7-6
2.7.4.2	Differential Thermal Expansion.....	2.7-8
2.7.4.3	Stress Calculations	2.7-8
2.7.4.4	Comparison with Allowable Stresses.....	2.7-8
2.7.5	Immersion – Fissile Material.....	2.7-8
2.7.6	Immersion – All Packages.....	2.7-8
2.7.6.1	Buckling Assessment of the Torispherical Heads.....	2.7-9
2.7.6.2	Buckling Assessment of the Cylindrical Shells	2.7-10
2.7.7	Deep Water Immersion Test.....	2.7-10
2.7.8	Summary of Damage.....	2.7-10
2.8	Special Form.....	2.8-1
2.9	Fuel Rods.....	2.9-1
2.10	Appendices	2.10-1
2.10.1	Finite Element Analysis (FEA) Models	2.10.1-1
2.10.1.1	Outer Containment Assembly (OCA) Structural Analysis	2.10.1-1
2.10.1.2	Inner Containment Assembly (ICV) Structural Analysis.....	2.10.1-5
2.10.2	Elastomer O-ring Seal Performance Tests	2.10.2-1
2.10.2.1	Introduction	2.10.2-1
2.10.2.2	Test Specimens and Equipment	2.10.2-1
2.10.2.3	Test Conditions.....	2.10.2-2
2.10.2.4	Test Procedure.....	2.10.2-3
2.10.2.5	Example O-ring Seal Compression Calculation.....	2.10.2-3
2.10.2.6	Test Results	2.10.2-4
2.10.2.7	Designating an Alternative Seal Material	2.10.2-5
2.10.3	Certification Tests	2.10.3-1
2.10.3.1	Introduction	2.10.3-1
2.10.3.2	Summary.....	2.10.3-1
2.10.3.3	Test Facilities	2.10.3-3
2.10.3.4	Test Unit Description	2.10.3-3
2.10.3.5	Technical Basis for Tests	2.10.3-8

2.10.3.6	Test Sequence for Selected Free Drop, Puncture Drop, and Fire Tests	2.10.3-18
2.10.3.7	Test Results	2.10.3-25
3.0	THERMAL EVALUATION	3.1-1
3.1	Discussion	3.1-1
3.1.1	Packaging	3.1-1
3.1.2	Payload Configuration.....	3.1-2
3.1.3	Boundary Conditions.....	3.1-3
3.1.4	Analysis Summary	3.1-4
3.2	Summary of Thermal Properties of Materials.....	3.2-1
3.3	Technical Specifications of Components	3.3-1
3.4	Thermal Evaluation for Normal Conditions of Transport.....	3.4-1
3.4.1	Thermal Model	3.4-1
3.4.1.1	Analytical Model.....	3.4-1
3.4.1.2	Test Model.....	3.4-3
3.4.2	Maximum Temperatures	3.4-3
3.4.3	Minimum Temperatures	3.4-3
3.4.4	Maximum Internal Pressure	3.4-3
3.4.4.1	Design Pressure	3.4-3
3.4.4.2	Maximum Pressure for Normal Conditions of Transport	3.4-3
3.4.4.3	Maximum Normal Operating Pressure.....	3.4-10
3.4.5	Maximum Thermal Stresses	3.4-10
3.4.6	Evaluation of Package Performance for Normal Conditions of Transport	3.4-11
3.5	Thermal Evaluation for Hypothetical Accident Conditions.....	3.5-1
3.5.1	Thermal Model	3.5-1
3.5.1.1	Analytical Model.....	3.5-1
3.5.1.2	Test Model.....	3.5-1
3.5.2	Package Conditions and Environment	3.5-1
3.5.3	Package Temperatures.....	3.5-2
3.5.4	Maximum Internal Pressure	3.5-3
3.5.5	Maximum Thermal Stresses	3.5-4
3.5.6	Evaluation of Package Performance for the Hypothetical Accident Thermal Conditions.....	3.5-4
3.6	Appendices	3.6-1
3.6.1	Computer Analysis Results	3.6.1-1
3.6.1.1	Seven 55-Gallon Drum Payload with 100 °F Ambient and Full Solar Loading, Uniformly Distributed Decay Heat Load (Case 1).....	3.6.1-1

3.6.1.2	Seven 55-Gallon Drum Payload with 100 °F Ambient and Full Solar Loading, All Decay Heat Load in Center Drum Only (Case 2).....	3.6.1-2
3.6.1.3	Seven 55-Gallon Drum Payload with 100 °F Ambient and No Solar Loading, Uniformly Distributed Decay Heat Load (Case 1).....	3.6.1-3
3.6.1.4	Seven 55-Gallon Drum Payload with 100 °F Ambient and No Solar Loading, All Decay Heat Load in Center Drum Only (Case 2).....	3.6.1-4
3.6.2	Thermal Model Details.....	3.6.2-1
3.6.2.1	Convection Coefficient Calculation.....	3.6.2-1
3.6.2.2	Aluminum Honeycomb Conductivity Calculation.....	3.6.2-1
3.6.2.3	Polyethylene Plastic Wrap Transmittance Calculation.....	3.6.2-3
4.0	CONTAINMENT.....	4.1-1
4.1	Containment Boundary.....	4.1-1
4.1.1	Containment Vessel.....	4.1-1
4.1.1.1	Outer Containment Assembly (Primary Level of Containment).....	4.1-1
4.1.1.2	Inner Containment Vessel (Secondary Level of Containment).....	4.1-1
4.1.2	Containment Penetrations.....	4.1-1
4.1.3	Seals and Welds.....	4.1-2
4.1.3.1	Seals.....	4.1-2
4.1.3.2	Welds.....	4.1-2
4.1.4	Closure.....	4.1-3
4.1.4.1	Outer Containment Assembly (OCA) Closure.....	4.1-3
4.1.4.2	Inner Containment Vessel (ICV) Closure.....	4.1-3
4.2	Containment Requirements for Normal Conditions of Transport.....	4.2-1
4.2.1	Containment of Radioactive Material.....	4.2-1
4.2.2	Pressurization of Containment Vessel.....	4.2-1
4.2.3	Containment Criterion.....	4.2-1
4.3	Containment Requirements for Hypothetical Accident Conditions.....	4.3-1
4.3.1	Fission Gas Products.....	4.3-1
4.3.2	Containment of Radioactive Material.....	4.3-1
4.3.3	Containment Criterion.....	4.3-1
4.4	Special Requirements.....	4.4-1
4.4.1	Plutonium Shipments.....	4.4-1
4.4.2	Interchangeability.....	4.4-1
5.0	SHIELDING EVALUATION.....	5-1

6.0	CRITICALITY EVALUATION	6.1-1
6.1	Discussion and Results	6.1-2
6.2	Package Contents	6.2-1
6.2.1	Applicability of Case A Limit	6.2-2
6.2.2	Applicability of Case B Limit	6.2-3
6.2.3	Applicability of Case C Limit	6.2-3
6.2.4	Applicability of Case D Limit	6.2-4
6.2.5	Applicability of Case E Limit	6.2-5
6.2.6	Applicability of Case F Limit	6.2-5
6.2.7	Applicability of Case G Limit	6.2-5
6.2.8	Applicability of Case H Limit	6.2-5
6.3	Model Specification	6.3-1
6.3.1	Contents Model	6.3-1
6.3.1.1	Case A Contents Model	6.3-1
6.3.1.2	Case B Contents Model	6.3-2
6.3.1.3	Case C Contents Model	6.3-2
6.3.1.4	Case D Contents Model	6.3-2
6.3.2	Packaging Model	6.3-3
6.3.3	Single-Unit Models	6.3-5
6.3.4	Array Models	6.3-5
6.3.5	Package Regional Densities	6.3-6
6.4	Criticality Calculations	6.4-1
6.4.1	Calculational or Experimental Method	6.4-1
6.4.2	Fuel Loading or Other Contents Loading Optimization	6.4-1
6.4.3	Criticality Results	6.4-2
6.4.3.1	Criticality Results for a Single HalfPACT Package	6.4-3
6.4.3.2	Criticality Results for Infinite Arrays of HalfPACT Packages	6.4-4
6.4.3.3	Special Reflectors in CH-TRU Waste	6.4-7
6.4.3.4	Machine Compacted CH-TRU Waste	6.4-8
6.4.3.5	Applicable Criticality Limits for CH-TRU Waste	6.4-9
6.5	Critical Benchmark Experiments	6.5-1
6.5.1	Benchmark Experiments and Applicability	6.5-1
6.5.2	Details of Benchmark Calculations	6.5-2
6.5.3	Results of Benchmark Calculations	6.5-2
7.0	OPERATING PROCEDURES	7.1-1
7.1	Procedures for Loading the Package	7.1-1
7.1.1	Removal of the HalfPACT Package from the Transport Trailer/Railcar	7.1-1
7.1.2	Outer Containment Assembly (OCA) Lid Removal	7.1-1

7.1.3	Inner Containment Vessel (ICV) Lid Removal.....	7.1-2
7.1.4	Loading the Payload into the HalfPACT Package	7.1-2
7.1.5	Inner Containment Vessel (ICV) Lid Installation	7.1-3
7.1.6	Outer Containment Assembly (OCA) Lid Installation.....	7.1-4
7.1.7	Final Package Preparations for Transport (Loaded)	7.1-6
7.2	Procedures for Unloading the Package	7.2-1
7.2.1	Removal of the HalfPACT Package from the Transport Trailer/Railcar ...	7.2-1
7.2.2	Outer Containment Assembly (OCA) Lid Removal	7.2-1
7.2.3	Inner Containment Vessel (ICV) Lid Removal.....	7.2-2
7.2.4	Unloading the Payload from the HalfPACT Package	7.2-2
7.2.5	Inner Containment Vessel (ICV) Lid Installation	7.2-2
7.2.6	Outer Containment Assembly (OCA) Lid Installation.....	7.2-3
7.2.7	Final Package Preparations for Transport (Unloaded).....	7.2-4
7.3	Preparation of an Empty Package for Transport	7.3-1
7.4	Preshipment Leakage Rate Test	7.4-1
7.4.1	Gas Pressure Rise Leakage Rate Test Acceptance Criteria	7.4-1
7.4.2	Determining the Test Volume and Test Time	7.4-1
7.4.3	Performing the Gas Pressure Rise Leakage Rate Test	7.4-2
7.4.4	Optional Preshipment Leakage Rate Test	7.4-2
8.0	ACCEPTANCE TESTS AND MAINTENANCE PROGRAM.....	8.1-1
8.1	Acceptance Tests.....	8.1-1
8.1.1	Visual Inspection.....	8.1-1
8.1.2	Structural and Pressure Tests	8.1-1
8.1.2.1	Lifting Device Load Testing	8.1-1
8.1.2.2	Containment Vessel Pressure Testing	8.1-1
8.1.3	Fabrication Leakage Rate Tests	8.1-2
8.1.3.1	Fabrication Leakage Rate Test Acceptance Criteria	8.1-2
8.1.3.2	Helium Leakage Rate Testing the ICV Structure Integrity	8.1-2
8.1.3.3	Helium Leakage Rate Testing the ICV Main O-ring Seal	8.1-3
8.1.3.4	Helium Leakage Rate Testing the ICV Outer Vent Port Plug O-ring Seal	8.1-4
8.1.3.5	Helium Leakage Rate Testing the OCV Structure Integrity	8.1-4
8.1.3.6	Helium Leakage Rate Testing the OCV Main O-ring Seal Integrity	8.1-5
8.1.3.7	Helium Leakage Rate Testing the OCV Vent Port Plug O-ring Seal Integrity	8.1-5
8.1.4	Component Tests.....	8.1-6
8.1.4.1	Polyurethane Foam.....	8.1-6
8.1.5	Tests for Shielding Integrity.....	8.1-18

8.1.6	Thermal Acceptance Test	8.1-18
8.2	Maintenance Program	8.2-1
8.2.1	Structural and Pressure Tests	8.2-1
8.2.1.1	Containment Vessel Pressure Testing	8.2-1
8.2.1.2	ICV Interior Surfaces Inspection	8.2-1
8.2.2	Maintenance/Periodic Leakage Rate Tests	8.2-1
8.2.2.1	Maintenance/Periodic Leakage Rate Test Acceptance Criteria ..	8.2-2
8.2.2.2	Helium Leakage Rate Testing the ICV Main O-ring Seal	8.2-2
8.2.2.3	Helium Leakage Rate Testing the ICV Outer Vent Port Plug O-ring Seal	8.2-3
8.2.3	Subsystems Maintenance	8.2-3
8.2.3.1	Fasteners	8.2-3
8.2.3.2	Locking Rings	8.2-3
8.2.3.3	Seal Areas and Grooves	8.2-4
8.2.4	Valves, Rupture Discs, and Gaskets on the Containment Vessel	8.2-7
8.2.4.1	Valves	8.2-7
8.2.4.2	Rupture Discs	8.2-7
8.2.4.3	Gaskets	8.2-7
8.2.5	Shielding	8.2-7
8.2.6	Thermal	8.2-7
9.0	QUALITY ASSURANCE	9.1-1
9.1	Introduction	9.1-1
9.2	Quality Assurance Requirements	9.2-1
9.2.1	U.S. Nuclear Regulatory Commission	9.2-1
9.2.2	U.S. Department of Energy	9.2-1
9.2.3	Transportation to or from WIPP	9.2-1
9.3	Quality Assurance Program	9.3-1
9.3.1	NRC Regulatory Guide 7.10	9.3-1
9.3.2	Design	9.3-1
9.3.3	Fabrication, Assembly, and Testing	9.3-1
9.3.4	Procurement	9.3-1
9.3.5	Use	9.3-1
9.3.5.1	DOE Shipments: To/From WIPP	9.3-1
9.3.5.2	Other DOE Shipments: Non-WIPP	9.3-2
9.3.5.3	Non-DOE Users of HalfPACT	9.3-2
9.3.6	Maintenance and Repair	9.3-2

LIST OF TABLES

Table 2.1-1 – Containment Structure Allowable Stress Limits	2.1-7
Table 2.1-2 – Non-Containment Structure Allowable Stress Limits.....	2.1-7
Table 2.2-1 – HalfPACT Weight and Center of Gravity	2.2-5
Table 2.3-1 – Mechanical Properties of Type 304 Stainless Steel Components (for Analysis)	2.3-5
Table 2.3-2 – Mechanical Properties of Polyurethane Foam (for Analysis).....	2.3-7
Table 2.3-3 – Mechanical Properties of Metallic Materials (for Testing).....	2.3-7
Table 2.6-1 – Summary of Stress Results for OCA Load Case 1	2.6-14
Table 2.6-2 – Summary of Stress Results for OCA Load Case 2	2.6-15
Table 2.6-3 – Summary of Stress Results for OCA Load Case 3	2.6-16
Table 2.6-4 – Summary of Stress Results for OCA Load Case 4	2.6-17
Table 2.6-5 – Summary of Stress Results for ICV Load Case 1	2.6-18
Table 2.6-6 – Summary of Stress Results for ICV Load Case 2	2.6-19
Table 2.6-7 – Buckling Geometry Parameters per Code Case N-284-1	2.6-20
Table 2.6-8 – Stress Results for 14.7 psig External Pressure	2.6-20
Table 2.6-9 – Buckling Summary for 14.7 psig External Pressure	2.6-21
Table 2.6-10 – Tie-down Lug Weld Shear Stresses	2.6-22
Table 2.6-11 – OCA Outer Shell Compressive Membrane Stresses	2.6-22
Table 2.6-12 – OCA Tie-down Weldment Compressive Membrane Stresses	2.6-22
Table 2.6-13 – Maximum Unit Alternating Stress Intensities	2.6-22
Table 2.7-1 – Summary of HalfPACT Engineering Test Unit (ETU) Tests and Results.....	2.7-11
Table 2.7-2 – Summary of Selected Certification Test Unit (CTU) Tests	2.7-12
Table 2.7-3 – Buckling Geometry Parameters per Code Case N-284-1	2.7-13
Table 2.7-4 – Stress Results for 21 psig External Pressure	2.7-13
Table 2.7-5 – Buckling Summary for 21 psig External Pressure	2.7-14
Table 2.10.1-1 – ANSYS [®] Input Listing for OCA Load Case 1	2.10.1-7
Table 2.10.1-2 – ANSYS [®] Input Listing for OCA Load Case 2	2.10.1-12
Table 2.10.1-3 – ANSYS [®] Input Listing for OCA Load Case 3	2.10.1-17
Table 2.10.1-4 – ANSYS [®] Input Listing for OCA Load Case 4	2.10.1-22
Table 2.10.1-5 – ANSYS [®] Input Listing for ICV Load Case 1	2.10.1-27
Table 2.10.1-6 – ANSYS [®] Input Listing for ICV Load Case 2.....	2.10.1-30

Table 2.10.2-1 – O-ring Seal Performance Test Results	2.10.2-9
Table 2.10.3-1 – TRUPACT-II / HalfPACT Comparison Using NUREG/CR-3966.....	2.10.3-41
Table 2.10.3-2 – Summary of HalfPACT ETU Test Results in Sequential Order [®]	2.10.3-42
Table 2.10.3-3 – Summary of HalfPACT CTU Test Results in Sequential Order [®]	2.10.3-43
Table 2.10.3-4 – Summary of HalfPACT CTU Temperature Indicating Label Readings	2.10.3-44
Table 3.1-1 – NCT Steady-State Temperatures with 30 Watts Decay Heat Load and Insolation; Seven, 55-Gallon Drums.....	3.1-5
Table 3.2-1 – Thermal Properties of Homogenous Materials	3.2-2
Table 3.2-2 – Thermal Properties of Non-Homogenous Materials	3.2-3
Table 3.2-3 – Thermal Properties of Air.....	3.2-4
Table 3.2-4 – Thermal Radiative Properties	3.2-5
Table 3.4-1 – NCT Steady-State Temperatures with 30 Watts Decay Heat Load and Insolation; Seven 55-Gallon Drums.....	3.4-12
Table 3.4-2 – Summary of Temperatures for Determining MNOP for the ICV.....	3.4-13
Table 3.4-3 – HalfPACT Pressure Increase with a 7-Drum Payload, 60-Day Duration*	3.4-15
Table 3.4-4 – HalfPACT Pressure Increase with a 1 SWB Payload, 60-Day Duration*	3.4-15
Table 3.4-5 – HalfPACT Pressure Increase with 4 Drums Overpacked in 1 SWB, 60-Day Duration*	3.4-15
Table 3.4-6 – HalfPACT Pressure Increase with 4 85-Gallon Drums or 4 55-Gallon Drums Overpacked in 4 85-Gallon Drums, 60-Day Duration*	3.4-16
Table 3.4-7 – HalfPACT Pressure Increase with 3 100-Gallon Drums, 60-Day Duration*	3.4-16
Table 3.4-8 – HalfPACT Pressure Increase with 3 Shielded Containers, 60-Day Duration*	3.4-16
Table 3.5-1 – NCT Steady-State Temperatures with 30 Watts Decay Heat Load and Zero Insolation; Seven 55-Gallon Drums	3.5-5
Table 3.5-2 – HAC Thermal Event Temperature Readings	3.5-6
Table 3.6.2-1– Effective Thermal Conductivity of Aluminum Honeycomb.....	3.6.2-2
Table 6.1-1 – Fissile Material Limit per Payload Container	6.1-4
Table 6.1-2 – Fissile Material Limit per HalfPACT Package	6.1-4
Table 6.1-3 – Summary of Criticality Analysis Results	6.1-5
Table 6.2-1 – Special Reflector Material Parameters that Achieve the Reactivity of a 25%/75% Polyethylene/Water Mixture Reflector	6.2-6
Table 6.3-1 – Description of Contents Displacement in Array Models	6.3-6
Table 6.3-2 – Fissile Contents Model Properties for Various H/Pu Ratios.....	6.3-7

Table 6.3-3 – Composition of Modeled Steels	6.3-8
Table 6.3-4 – Composition of the Polyethylene/Water/Beryllium Reflector	6.3-8
Table 6.4-1 – Single-Unit, NCT, Case A, 325 FGE; k_s vs. H/Pu Ratio with Different Moderator and Reflector Compositions.....	6.4-10
Table 6.4-2 – Single Unit, NCT, Case A, 325 FGE; Variation of Reflector Volume Fraction (VF) at Near-Optimal H/Pu Ratio	6.4-11
Table 6.4-3 – Single-Unit, HAC, Case A, 325 FGE; k_s vs. H/Pu at Maximum Reflection Conditions	6.4-11
Table 6.4-4 – Infinite Array Variation 0, HAC, Case A, 325 FGE; k_s vs. H/Pu at Extremes of Reflection Conditions.....	6.4-12
Table 6.4-5 – Infinite Array Variation 0, HAC, Case A, 325 FGE; Variation of Reflector Volume Fraction at Near-Optimal H/Pu Ratios.....	6.4-13
Table 6.4-6 – Infinite Array Variation 1, HAC, Case A, 325 FGE; Variation of H/Pu Ratio at Extremes of Reflection Conditions	6.4-14
Table 6.4-7 – Infinite Array Variation 0, HAC, Case A; Variation of H/Pu Ratio for Various Gram Quantities of Pu-240 at Maximum Reflection Conditions.....	6.4-15
Table 6.4-8 – Infinite Array Variation 0, HAC, Case A, 5 g Pu-240, 340 FGE; k_s vs. H/Pu for Various Combinations of U-235 and Pu-239 under Maximum Reflection Conditions	6.4-16
Table 6.4-9 – Infinite Array Variation 0, HAC, Case B, 100 FGE; k_s vs. H/Pu at Maximum Reflection Conditions.....	6.4-17
Table 6.4-10 – Infinite Array Variation 0, HAC, Case B, 100 FGE; k_s vs. H/Pu for Various Moderator Volume Fractions of Beryllium under Maximum Reflection Conditions	6.4-18
Table 6.4-11 – Infinite Array Variation 0, HAC, Case B, 100 FGE; Variation of Reflector Volume Fraction at Near-Optimal H/Pu Ratio	6.4-19
Table 6.4-12 – Infinite Array Variation 1, HAC, Case B, 100 FGE; Variation of H/Pu Ratio at Reflector Volume Fraction to Maximize Interaction while Maintaining Beryllium Reflection.....	6.4-19
Table 6.4-13 – Infinite Array Variation 0, HAC, Case C, 250 FGE; k_s vs. H/Pu at Maximum Reflection Conditions.....	6.4-20
Table 6.4-14 – Infinite Array Variation 0, HAC, Case C, 250 FGE; Variation of Reflector Volume Fraction at Near-Optimal H/Pu Ratio	6.4-20
Table 6.4-15 – Infinite Array Variation 1, HAC, Case C, 250 FGE; Variation of H/Pu Ratio at Reflector Volume Fraction to Maximize Interaction while Maintaining Reflection	6.4-21
Table 6.4-16 – Infinite Array Variation 0, HAC, Case D, 325 FGE; k_s vs. H/Pu at Maximum Reflection Conditions	6.4-22

Table 6.4-17 – Infinite Array Variation 0, HAC, Case D, 325 FGE; Variation of Reflector Volume Fraction at Near-Optimal H/Pu Ratio	6.4-23
Table 6.4-18 – Infinite Array Variation 1, HAC, Case D, 325 FGE; Variation of H/Pu Ratio at Reflector Volume Fraction to Maximize Interaction while Maintaining Reflection ...	6.4-23
Table 6.5-1 – Benchmark Experiment Description with Experimental Uncertainties	6.5-4
Table 6.5-2 – Benchmark Case Parameters and Computed Results	6.5-5
Table 6.5-3 – Calculation of USL	6.5-13
Table 8.1-1 – Acceptable Compressive Stress Ranges for Foam (psi)	8.1-18
Table 8.2-1 – Calculation of Minimum O-ring Compression	8.2-4

LIST OF FIGURES

Figure 1.1-1 – HalfPACT Package Assembly	1.1-3
Figure 1.1-2 – HalfPACT Packaging Closure/Seal Region Details	1.1-4
Figure 1.2-1 – OCV Closure Design (ICV closure is Similar)	1.2-9
Figure 2.2-1 – HalfPACT Package Components	2.2-6
Figure 2.2-2 – Radial Shift of CG for Seven 55-Gallon Drum Payload	2.2-7
Figure 2.2-3 – Radial Shift of CG for SWB Payload	2.2-8
Figure 2.2-4 – Radial Shift of CG for Four 85-Gallon Drum Payload	2.2-9
Figure 2.2-5 – Radial Shift of CG for Three 100-Gallon Drum Payload	2.2-10
Figure 2.2-6 – Radial Shift of CG for Three Shielded Container Payload	2.2-11
Figure 2.5-1 – Tie-down Device Layout	2.5-12
Figure 2.5-2 – Tie-down Device Detail	2.5-13
Figure 2.5-3 – Tie-down Plan View and Reaction Force Diagram	2.5-14
Figure 2.5-4 – Tie-down Tensile/Shear Failure Modes	2.5-15
Figure 2.5-5 – Tie-down Lug Dimensions and Load Diagram	2.5-16
Figure 2.5-6 – Horizontal Doubler and Tripler Plate Details	2.5-17
Figure 2.6-1 – OCA Load Case 1, Overall Model	2.6-23
Figure 2.6-2 – OCA Load Case 1, Seal Region Detail	2.6-24
Figure 2.6-3 – OCA Load Case 2, Overall Model	2.6-25
Figure 2.6-4 – OCA Load Case 2, Seal Region Detail	2.6-26
Figure 2.6-5 – OCA Load Case 3, Overall Model	2.6-27
Figure 2.6-6 – OCA Load Case 3, Seal Region Detail	2.6-28
Figure 2.6-7 – OCA Load Case 4, Overall Model	2.6-29

Figure 2.6-8 – OCA Load Case 4, Seal Region Detail	2.6-30
Figure 2.6-9 – ICV Load Case 1, Overall Model	2.6-31
Figure 2.6-10 – ICV Load Case 1, Seal Region Detail.....	2.6-32
Figure 2.6-11 – ICV Load Case 2, Overall Model	2.6-33
Figure 2.6-12 – ICV Load Case 2, Seal Region Detail.....	2.6-34
Figure 2.10.1-1 – OCA FEA Model Element Plot.....	2.10.1-33
Figure 2.10.1-2 – ICV FEA Model Element Plot	2.10.1-34
Figure 2.10.2-1 – Test Fixture for O-ring Seal Performance Testing.....	2.10.2-11
Figure 2.10.3-1 – Drop Pad at the Coyote Canyon Aerial Cable Facility	2.10.3-45
Figure 2.10.3-2 – Design Comparison between a TRUPACT-II Packaging and a HalfPACT Packaging.....	2.10.3-47
Figure 2.10.3-3 – Design Comparison between 55-Gallon Drum Payload Assemblies..	2.10.3-48
Figure 2.10.3-4 – Making the HalfPACT ETU OCA from TRUPACT-II Unit 104	2.10.3-49
Figure 2.10.3-5 – Making the HalfPACT ETU OCA from TRUPACT-II Unit 104	2.10.3-50
Figure 2.10.3-6 – Making the HalfPACT CTU OCA from TRUPACT-II Unit 107	2.10.3-51
Figure 2.10.3-7 – Making the HalfPACT CTU ICV from TRUPACT-II Unit 107	2.10.3-52
Figure 2.10.3-8 – Dimensional Comparison of TRUPACT-II and HalfPACT for NUREG/CR-3966 (Lower Figures are Simplifying Representations Used in <i>CASKDROP</i>).....	2.10.3-53
Figure 2.10.3-9 – Schematic of HalfPACT ETU Test Orientations	2.10.3-54
Figure 2.10.3-10 – Schematic of HalfPACT CTU Test Orientations.....	2.10.3-55
Figure 2.10.3-11 – Schematic of HalfPACT CTU Temperature Indicating Label Location	2.10.3-57
Figure 2.10.3-12 – ETU Free Drop Test 1; Top-End Damage; ~16" Wide Flat	2.10.3-59
Figure 2.10.3-13 – ETU Free Drop Test 1; Bottom-End Damage; ~18" Wide Flat.....	2.10.3-59
Figure 2.10.3-14 – ETU Free Drop Test 2; Top-End Damage; ~36" Wide Flat	2.10.3-60
Figure 2.10.3-15 – ETU Free Drop Test 2; Bottom-End Damage; ~33" Wide Flat.....	2.10.3-60
Figure 2.10.3-16 – ETU Free Drop Test 3; View Just Prior to NCT Free Drop Test	2.10.3-61
Figure 2.10.3-17 – ETU Free Drop Test 3; Top-End Damage; ~18" Wide Flat	2.10.3-61
Figure 2.10.3-18 – ETU Free Drop Test 4; Top-End Damage; ~34" Wide Flat	2.10.3-62
Figure 2.10.3-19 – ETU Free Drop Test 4; Bottom-End Damage; ~34" Wide Flat.....	2.10.3-62
Figure 2.10.3-20 – ETU Free Drop Test 5; Bottom Corner Damage; ~26" Wide Flat ...	2.10.3-63
Figure 2.10.3-21 – ETU Free Drop Test 5; Bottom Corner Damage; ~5½" Deep Flat...	2.10.3-63

Figure 2.10.3-22 – ETU Free Drop Test 6; Bottom Corner Damage; ~40" Wide Flat ...	2.10.3-64
Figure 2.10.3-23 – ETU Free Drop Test 6; Bottom Corner Damage; ~12" Deep Flat....	2.10.3-64
Figure 2.10.3-24 – ETU Puncture Drop Test 7; ~10½" High × ~11½" Wide Hole	2.10.3-65
Figure 2.10.3-25 – ETU Puncture Drop Test 7; Radial Penetration ~8" Deep.....	2.10.3-65
Figure 2.10.3-26 – ETU Puncture Drop Test 8; View of Damage; ~2½" Deep Dent	2.10.3-66
Figure 2.10.3-27 – ETU Puncture Drop Test 8; Close-up View of Damage; ~2½" Deep Dent	2.10.3-66
Figure 2.10.3-28 – ETU Puncture Drop Test 9; View of Impact on Puncture Bar	2.10.3-67
Figure 2.10.3-29 – ETU Puncture Drop Test 9; Bottom Corner Damage; ~3" Deep Dent	2.10.3-67
Figure 2.10.3-30 – ETU Puncture Drop Test 10; 3/8–to-1/4 Transition; ~27" Long Tear	2.10.3-68
Figure 2.10.3-31 – ETU Puncture Drop Test 10; 3/8–to-1/4 Transition; ~5½" Deep Dent	2.10.3-68
Figure 2.10.3-32 – ETU Fire Test 11; Side 1 View Showing Tests 1, 2, 7, & 10 Damage	2.10.3-69
Figure 2.10.3-33 – ETU Fire Test 11; Side 2 View Showing Tests 3, 4, 5, 6, 8, & 9 Damage	2.10.3-69
Figure 2.10.3-34 – ETU Fire Test 11; Overall View ~5 Minutes after Start of Fire.....	2.10.3-70
Figure 2.10.3-35 – ETU Fire Test 11; View ~12 Minutes after Start of Fire.....	2.10.3-71
Figure 2.10.3-36 – ETU Fire Test 11; View ~25 Minutes after Start of Fire.....	2.10.3-71
Figure 2.10.3-37 – ETU Fire Test 11; View ~32 Minutes after Start of Fire.....	2.10.3-72
Figure 2.10.3-38 – ETU Fire Test 11; View ~17 Minutes after End of Fire.....	2.10.3-72
Figure 2.10.3-39 – ETU Fire Test 11; View ~37 Minutes after End of Fire.....	2.10.3-73
Figure 2.10.3-40 – ETU; View Before Disassembly	2.10.3-73
Figure 2.10.3-41 – ETU; Removal of the OCA Lid Outer Shell (Note Crumbling Foam Char)	2.10.3-74
Figure 2.10.3-42 – ETU; Residual Foam in OCA Lid Side; Aligned with Test 1, 2, & 7 Damage.....	2.10.3-74
Figure 2.10.3-43 – ETU; Residual Foam in OCA Lid Side; Remote From Test Damage	2.10.3-75
Figure 2.10.3-44 – ETU; Residual Foam in OCA Lid Top (~11").....	2.10.3-75
Figure 2.10.3-45 – ETU; View of OCV Seal Test Port Plug (As Removed; Not Cleaned).....	2.10.3-76
Figure 2.10.3-46 – ETU; View of OCV Vent Port Cover (As Removed; Not Cleaned).	2.10.3-76

Figure 2.10.3-47 – ETU; View of OCV Vent Port Plug (As Removed; Not Cleaned)...	2.10.3-77
Figure 2.10.3-48 – ETU; View of 55-Gallon Payload Drums Following ICV Lid Removal.....	2.10.3-77
Figure 2.10.3-49 – ETU; View of ICV Body Cavity Following Payload Drum Removal.....	2.10.3-78
Figure 2.10.3-50 – ETU; View of Debris Inside ICV Body Cavity After Payload Drum Removal.....	2.10.3-78
Figure 2.10.3-51 – CTU; 5 Inch Thick Payload Spacer (Wood Simulation) in Bottom of ICV	2.10.3-79
Figure 2.10.3-52 – CTU; Aligning 55-Gallon Drum Payload Assembly for Installation into ICV.....	2.10.3-79
Figure 2.10.3-53 – CTU; Final ICV Lid Alignment During ICV Lid Installation	2.10.3-80
Figure 2.10.3-54 – CTU; Final OCA Lid Alignment During OCA Lid Installation.....	2.10.3-80
Figure 2.10.3-55 – CTU; Certification Test Unit (TRUPACT-II Unit 107) After Final Assembly.....	2.10.3-81
Figure 2.10.3-56 – CTU Free Drop Test 1; Lid-End Damage; ~13" Wide Flat.....	2.10.3-82
Figure 2.10.3-57 – CTU Free Drop Test 1; Bottom-End Damage; ~13" Wide Flat.....	2.10.3-83
Figure 2.10.3-58 – CTU Free Drop Test 2; Lid-End Damage; ~37" Wide Flat.....	2.10.3-84
Figure 2.10.3-59 – CTU Free Drop Test 2; Bottom-End Damage; ~37" Wide Flat.....	2.10.3-85
Figure 2.10.3-60 – CTU Free Drop Test 3; Lid-End Damage; ~41½" Wide Flat.....	2.10.3-86
Figure 2.10.3-61 – CTU Free Drop Test 3; Bottom-End Damage	2.10.3-87
Figure 2.10.3-62 – CTU Puncture Drop Test 4; Mounting the Puncture Bar.....	2.10.3-88
Figure 2.10.3-63 – CTU Puncture Drop Test 4; Close-up View of Damage.....	2.10.3-89
Figure 2.10.3-64 – CTU Puncture Drop Test 4; Close-up Profile View of Damage; ~3¾" Deep.....	2.10.3-90
Figure 2.10.3-65 – CTU Puncture Drop Test 5; Close-up View of Damage.....	2.10.3-91
Figure 2.10.3-66 – CTU Puncture Drop Test 5; Profile Views of Damage; ~4" Deep ...	2.10.3-92
Figure 2.10.3-67 – CTU Puncture Drop Test 6; Overall View of Damage.....	2.10.3-93
Figure 2.10.3-68 – CTU Puncture Drop Test 6; Close-up Views of Damage; ~3½" Deep	2.10.3-94
Figure 2.10.3-69 – CTU Fire Test 7; Side 1 View Before Fire Showing Tests 1, 2, & 4 Damage.....	2.10.3-95
Figure 2.10.3-70 – CTU Fire Test 7; Side 2 View Before Fire Showing Test 5 Damage	2.10.3-96
Figure 2.10.3-71 – CTU Fire Test 7; Overall View ~5 Minutes after Start	2.10.3-97

Figure 2.10.3-72 – CTU Fire Test 7; View ~10 Minutes after Start	2.10.3-98
Figure 2.10.3-73 – CTU Fire Test 7; View ~15 Minutes after Start (Showing Wind Effects)	2.10.3-99
Figure 2.10.3-74 – CTU Fire Test 7; View ~28 Minutes after Start (Note Flares at Vents)	2.10.3-100
Figure 2.10.3-75 – CTU Fire Test 7; Side 1 View ~33 Minutes after Start (End of Fire).....	2.10.3-101
Figure 2.10.3-76 – CTU Fire Test 7; Side 2 View ~33 Minutes after Start (End of Fire).....	2.10.3-102
Figure 2.10.3-77 – CTU Fire Test 7; Side 1/2 Views ~10 Minutes after End of Fire ...	2.10.3-103
Figure 2.10.3-78 – CTU; View Before Disassembly (OCV Seal Test Port in Foreground)	2.10.3-104
Figure 2.10.3-79 – CTU; Removal of the OCA Lid Outer Shell (Note Crumbling Foam Char)	2.10.3-105
Figure 2.10.3-80 – CTU; Residual Foam in OCA Lid Side; Aligned with Test 1, 2, & 4 Damage.....	2.10.3-106
Figure 2.10.3-81 – CTU; Residual Foam in OCA Lid Knuckle; Aligned with Test 1, 2, & 4 Damage.....	2.10.3-106
Figure 2.10.3-82 – CTU; Residual Foam in OCA Lid Top (~11")	2.10.3-107
Figure 2.10.3-83 – CTU; Residual Foam in OCA Lid Side; Remote from Test Damage	2.10.3-107
Figure 2.10.3-84 – CTU; Close-up of OCV Seal Test Port Plug (As Removed/Not Cleaned).....	2.10.3-108
Figure 2.10.3-85 – CTU; OCV Vent Port Region After Removing Excess Foam Char.....	2.10.3-108
Figure 2.10.3-86 – CTU; Close-up of OCV Vent Port Cover (As Removed/Not Cleaned).....	2.10.3-109
Figure 2.10.3-87 – CTU; Close-up of OCV Vent Port Plug (As Removed/Not Cleaned).....	2.10.3-109
Figure 2.10.3-88 – CTU; Close-up of Damage to ICV Locking Ring	2.10.3-110
Figure 2.10.3-89 – CTU; End View of OCV Cavity Showing Deformed Lower Seal Flange.....	2.10.3-110
Figure 2.10.3-90 – CTU; Residual Foam in OCA Lid Side; Aligned with Test 1, 2, & 4 Damage.....	2.10.3-111
Figure 2.10.3-91 – CTU; Residual Foam in OCA Body Side; Remote from Test Damage	2.10.3-111
Figure 2.10.3-92 – CTU; Helium Leakage Rate Testing the ICV Lid Structure.....	2.10.3-112

Figure 2.10.3-93 – CTU; Helium Leakage Rate Testing the OCV Body Structure	2.10.3-112
Figure 2.10.3-94 – CTU; Close-up View of Cracked OCV Vent Port Coupling Inner Weld	2.10.3-113
Figure 2.10.3-95 – CTU; Close-up View of Cracked OCV Vent Port Coupling Inner Weld	2.10.3-113
Figure 3.4-1 – HalfPACT Packaging Thermal Model Node Layout.....	3.4-17
Figure 3.4-2 – Seven 55-Gallon Drum Payload Thermal Node Layout.....	3.4-18
Figure 3.5-1 – HAC Thermal Event Temperature Indicating Label Locations	3.5-6
Figure 6.3-1 – Case A Contents Model	6.3-9
Figure 6.3-2 – Case B Contents Model.....	6.3-10
Figure 6.3-3 – Case C Contents Model.....	6.3-11
Figure 6.3-4 – Case D Contents Model	6.3-12
Figure 6.3-5 – NCT, Single-Unit Model; R-Z Slice	6.3-13
Figure 6.3-6 – HAC, Single-Unit Model; R-Z Slice.....	6.3-14
Figure 6.3-7 – Array Model Variation 0 (Reflective Boundary Conditions Imposed).....	6.3-15
Figure 6.3-8 – Array Model Variation 1; X-Y Slice Through Top Axial Layer	6.3-16
Figure 7.4-1 – Pressure Rise Leakage Rate Test Schematic.....	7.4-2
Figure 8.2-1 – Method of Measuring Upper Seal Flange Groove Widths	8.2-8
Figure 8.2-2 – Method of Measuring Lower Seal Flange Groove Widths	8.2-9
Figure 8.2-3 – Method of Measuring Upper Seal Flange Tab Widths	8.2-10
Figure 8.2-4 – Method of Measuring Lower Seal Flange Tab Widths.....	8.2-11

This page intentionally left blank.

1.0 GENERAL INFORMATION

This chapter of the Safety Analysis Report (SAR) presents a general introduction and description of the HalfPACT contact-handled transuranic waste (CH-TRU) package. The major components comprising the HalfPACT package are presented as [Figure 1.1-1](#) and [Figure 1.1-2](#). [Figure 1.1-1](#) presents an exploded view of all major HalfPACT packaging components. [Figure 1.1-2](#) presents a detailed view of the closure and seal region. Detailed drawings presenting the HalfPACT packaging design are presented in [Appendix 1.3.1, *Packaging General Arrangement Drawings*](#). All details relating to payloads and payload preparation for shipment in a HalfPACT package are presented in the [Contact-Handled Transuranic Waste Authorized Methods for Payload Control \(CH-TRAMPAC\)](#)¹. Descriptions of the standard, S100, S200, and S300 pipe overpack payload configurations are provided in [Appendices 4.1, 4.2, 4.3, and 4.4](#), respectively, of the [CH-TRU Payload Appendices](#)². A description of the shielded container payload configuration is provided in [Appendix 4.5](#) of the [CH-TRU Payload Appendices](#). Terminology and acronyms used throughout this document are presented as [Appendix 1.3.2, *Glossary of Terms and Acronyms*](#).

1.1 Introduction

The model HalfPACT package has been developed for the United States Department of Energy (DOE) as a safe means for transportation of CH-TRU materials and other authorized payloads. The packaging design is based very closely on the currently licensed TRUPACT-II package. The primary difference between the two packages is the body length. The TRUPACT-II packaging body length is shortened by 30 inches to create the HalfPACT packaging. Other minor differences are present, as described in subsequent sections.

The HalfPACT package is designed for truck transport. As many as three, loaded HalfPACT packages can be transported on a single semi-trailer. The rugged, lightweight design of the HalfPACT package allows the efficient transport of heavier-than-average payloads, thereby reducing the total number of radioactive shipments. The HalfPACT is also suitable for rail transport. As many as seven loaded HalfPACT packages can be transported per railcar.

The goals of maintaining public safety while achieving a lightweight design are satisfied by use of a deformable sealing region that can absorb both normal conditions of transport (NCT) and hypothetical accident condition (HAC) deformations without loss of leaktight capability³. This same design was extensively tested on the TRUPACT-II package, and the HalfPACT packaging program utilized the knowledge of the TRUPACT-II packaging program as background information. Nevertheless, both a full scale HalfPACT engineering test unit (ETU), and a certification test unit (CTU) were subjected to a series of free drops and puncture drops, and a fully engulfing pool fire test. These tests conclusively demonstrated containment integrity of the HalfPACT package.

¹ U.S. Department of Energy (DOE), [Contact-Handled Transuranic Waste Authorized Methods for Payload Control \(CH-TRAMPAC\)](#), U.S. Department of Energy, Carlsbad Field Office, Carlsbad, New Mexico.

² U.S. Department of Energy (DOE), [CH-TRU Payload Appendices](#), U.S. Department of Energy, Carlsbad Field Office, Carlsbad, New Mexico.

³ Leaktight is defined as 1×10^{-7} standard cubic centimeters per second (scc/s), or less, air leakage per the definition in ANSI N14.5-1997, [American National Standard for Radioactive Materials - Leakage Tests on Packages for Shipment](#), American National Standards Institute, (ANSI), Inc.

The payload within each HalfPACT package will be within 55-gallon drums, 85-gallon drums, 100-gallon drums, standard waste boxes (SWBs), or shielded containers (SCs). Hereafter, the term “85-gallon drum” is used to refer to 75- to 88-gallon drums that may, with the appropriate dimensions, overpack a single 55-gallon drum. Pipe overpacks utilize 55-gallon drums as overpacks. A single HalfPACT package can transport seven 55-gallon drums (with or without pipe components), one SWB, four 85-gallon drums (with or without 55-gallon drums), three 100-gallon drums, or three SCs. Specifications for payload containers are provided in [Section 2.0, *Container and Physical Properties Requirements*](#), of [CH-TRAMPAC](#).

The HalfPACT packaging provides two leakage rate testable levels of containment for the payload during both normal conditions of transport (NCT) and hypothetical accident conditions (HAC).

Based on the shielding and criticality assessments provided in [Chapter 5.0, *Shielding Evaluation*](#), and [Chapter 6.0, *Criticality Evaluation*](#), the Criticality Safety Index (CSI) for the HalfPACT package is zero (0.0), and the shielding Transport Index (TI) is determined at the time of shipment.

Authorization is sought for shipment of the HalfPACT package by truck or railcar as a Type B(U)F-96 package per the definition delineated in 10 CFR §71.4⁴.

⁴ Title 10, Code of Federal Regulations, Part 71 (10 CFR 71), *Packaging and Transportation of Radioactive Material*, 01-01-07 Edition.

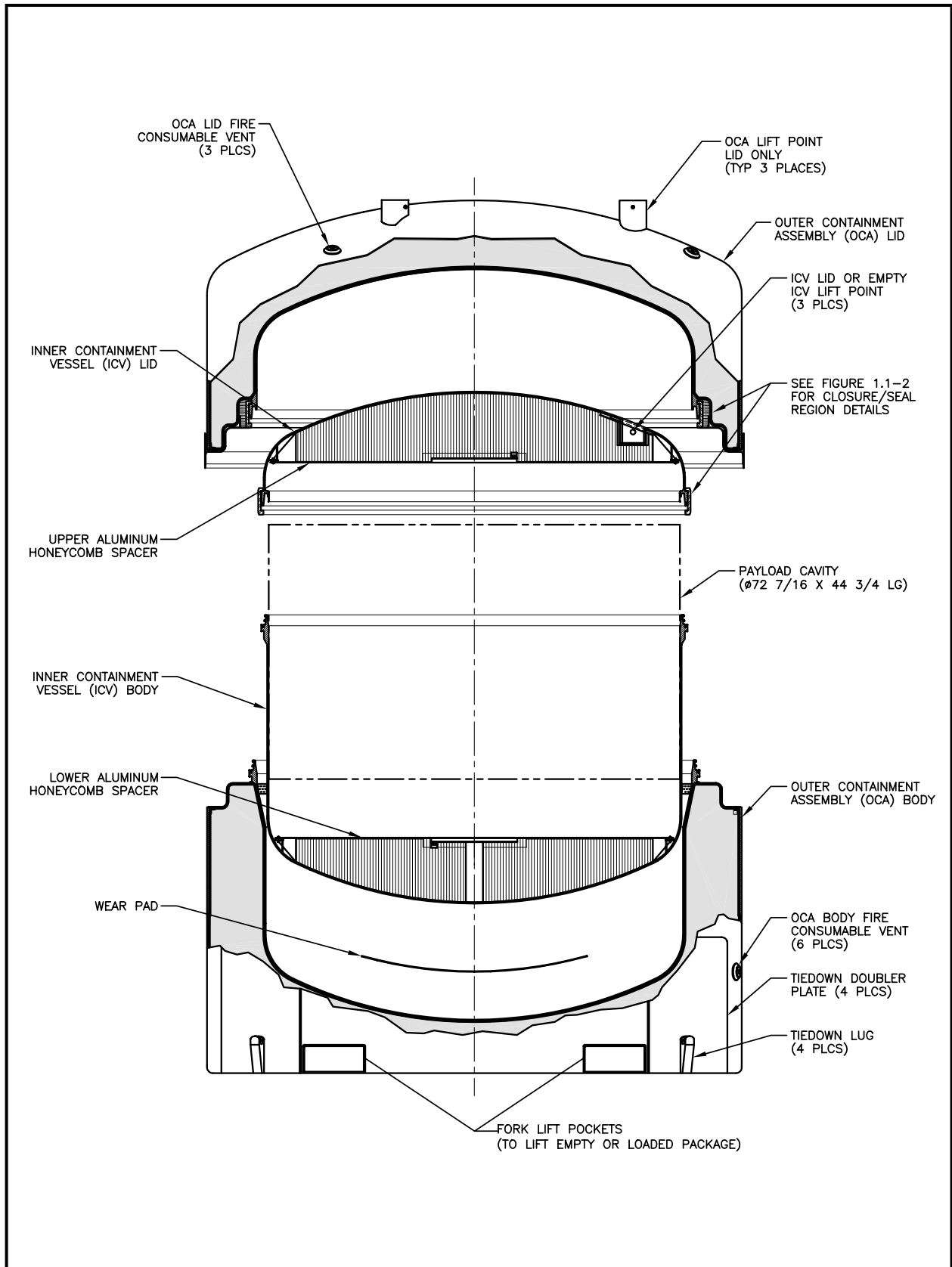


Figure 1.1-1 – HalfPACT Package Assembly

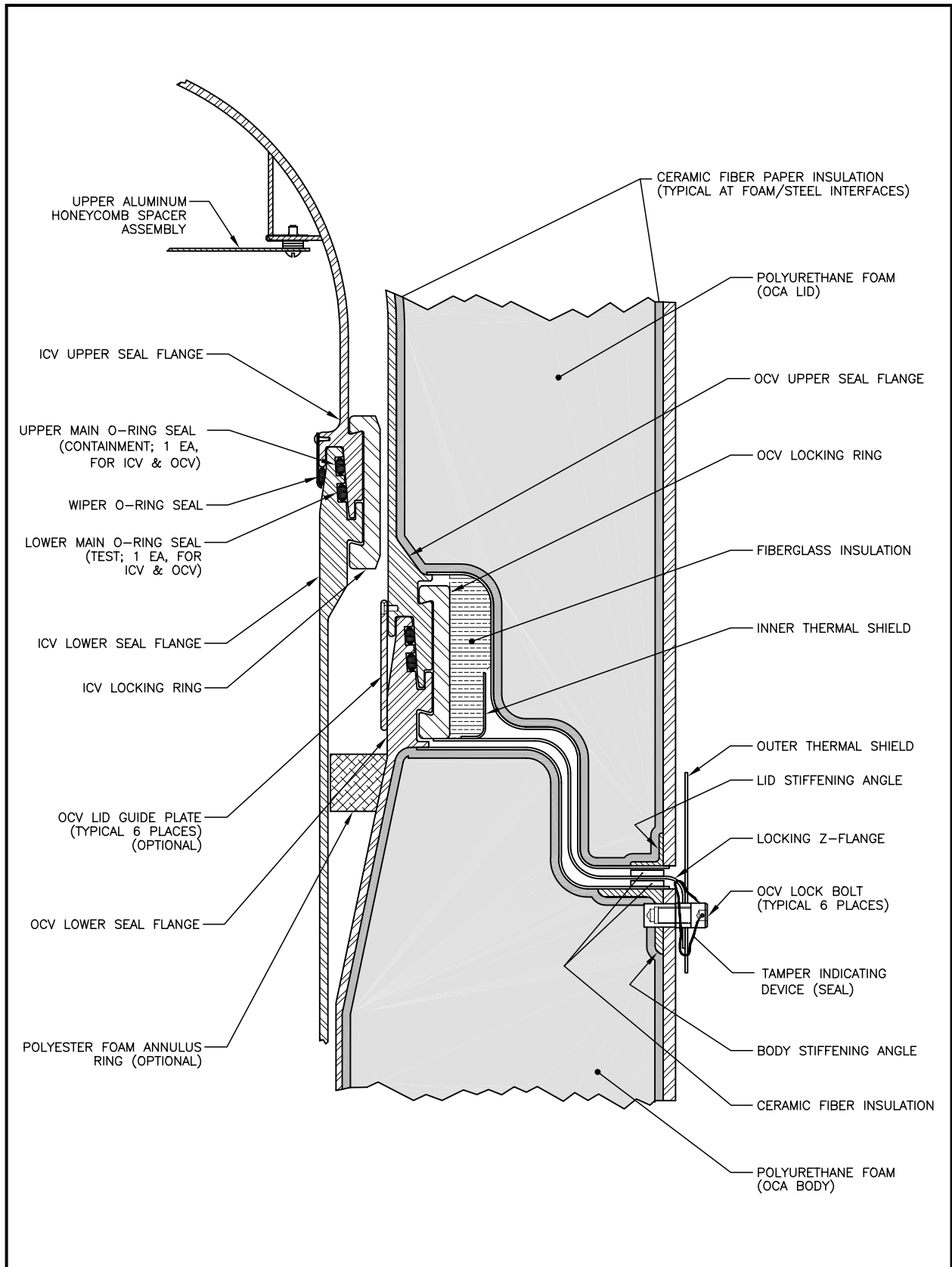


Figure 1.1-2 – HalfPACT Packaging Closure/Seal Region Details

1.2 Package Description

This section presents a basic description of the HalfPACT package. General arrangement drawings of the HalfPACT packaging are presented in [Appendix 1.3.1, *Packaging General Arrangement Drawings*](#). Drawings illustrating payload assembly details are presented in the [CH-TRAMPAC¹](#).

1.2.1 Packaging

1.2.1.1 Packaging Description

The HalfPACT packaging is comprised of an outer containment assembly (OCA) that provides the primary containment boundary, and an inner containment vessel (ICV) that provides the secondary containment boundary. Two aluminum honeycomb spacer assemblies are used within the ICV, one inside each ICV torispherical head. A silicone wear pad is utilized at the interface between the bottom exterior of the ICV and the bottom interior of the OCA. An optional polyester foam annulus ring may be used in the annulus between the ICV and OCV, just below the OCV lower seal flange to prevent debris from becoming entrapped between the vessels.

Inside the ICV, the payload will be within 55-gallon drums, 85-gallon drums, 100-gallon drums, standard waste boxes (SWBs), or shielded containers (SCs). The OCA, ICV, and the aluminum honeycomb spacer assemblies are fully described in the following subsections. The design details and overall arrangement of the HalfPACT packaging are presented in the [Appendix 1.3.1, *Packaging General Arrangement Drawings*](#). Drawings illustrating payload assembly details are presented in the [CH-TRAMPAC](#).

1.2.1.1.1 Outer Containment Assembly (OCA)

The outer containment assembly (OCA) consists of an OCA lid and OCA body, each primarily comprised of an inner stainless steel shell structure, a relatively thick layer of rigid polyurethane foam, and an external stainless steel shell structure. The inner OCA shell structure comprises the outer containment vessel (OCV).

Not considering the seal flange region, the OCA lid has a nominal external diameter of $94\frac{3}{8}$ inches and a nominal internal diameter of $76\frac{13}{16}$ inches. Likewise, not considering the seal flange region, the OCA body has a nominal external diameter of $94\frac{3}{8}$ inches and a nominal internal diameter of $73\frac{5}{8}$ inches, tapering outward to a nominal inside diameter of $76\frac{7}{8}$ inches at the OCV lower seal flange. The nominal external diameter of the OCV seal region is 95 inches, and the nominal internal diameter of the OCV seal region is $76\frac{7}{16}$ inches. With the OCA lid installed onto the OCA body, the OCA has a nominal external length of $91\frac{1}{2}$ inches, and a nominal internal height is 70 inches at the OCV cavity centerline.

The containment boundary provided by the OCA consists of the inner stainless steel vessel formed by a mating lid and body, plus the uppermost of two main O-ring seals enclosed between an upper and lower seal flange. The upper main O-ring seal (containment seal) is butyl rubber

¹ U.S. Department of Energy (DOE), [Contact-Handled Transuranic Waste Authorized Methods for Payload Control \(CH-TRAMPAC\)](#), U.S. Department of Energy, Carlsbad Field Office, Carlsbad, New Mexico.

with a nominal 0.400 inch diameter cross-section. The lower main O-ring seal (test seal) may be neoprene or ethylene propylene with a nominal 0.375 inch diameter cross-section. The purpose of the lower main O-ring seal is for establishing a vacuum on the exterior side of the upper main O-ring seal for helium and pressure rise leakage rate testing.

A vent port feature in the OCV body's lower seal flange is the only other containment boundary penetration. A vent port coupling, a seal welded threaded fitting, and an OCV vent port plug with an O-ring seal defines the containment boundary at the OCV vent port penetration. Access to the OCV vent port is gained through an external penetration in the OCA outer shell once an outer 1½ NPT plug and a foam or ceramic fiber material plug is removed. The connecting tube is fabricated of non-thermally conductive fiberglass.

Leakage rate testing of the OCV's upper main O-ring seal (containment seal) is performed through an OCV seal test port that is located in the OCA lid. Similar in design to the OCV vent port, access to the OCV seal test port is gained through an external penetration in the OCA outer shell once an outer 1½ NPT plug and a foam or ceramic fiber material plug is removed. The connecting tube is fabricated of thin-walled stainless steel.

The cylindrical portion of the OCV body is 3/16 inch nominal thickness, Type 304, stainless steel. All other shells comprising the OCV are 1/4 inch nominal thickness, Type 304, stainless steel, including the lower and upper torispherical heads. The OCA outer shell varies between 1/4 and 3/8 inch nominal thickness, Type 304, stainless steel. The 3/8 inch nominal thickness material is used adjacent to the closure interface to ensure protection from HAC puncture bar penetration near the sealing regions. All other shells comprising the OCA exterior are 1/4 inch nominal thickness, Type 304, stainless steel, including the lower flat head and upper torispherical head. As illustrated in [Figure 1.1-2](#), the inner and outer shell structures for both the OCA lid and OCA body are connected together via 14 gauge (0.075 inch thick), Type 304, stainless steel Z-flanges. Secure attachment of the 14 gauge Z-flanges to the 3/8 inch thick OCA outer shell is assured by the use of rolled angle reinforcements (2 × 2 × 1/4 inch for the OCA body junction, and 1 × 1 × 1/8 inch for the OCA lid junction). A locking Z-flange between the upper and lower (i.e., OCA lid and OCA body) Z-flanges allows rotation of the OCV locking ring from the HalfPACT package exterior. The Z-flanges serve the purpose of precluding direct flame impingement on the OCV seal flanges during the hypothetical accident condition (HAC) thermal event (fire). To further preclude flame and hot gas entry into the Z-flange channel, inner and outer thermal shields are included as part of the locking Z-flange assembly.

The OCA lid is secured to the OCA body via the OCV locking ring located at the outer diameter of the OCV upper and lower seal flanges. Closure design and operation is illustrated in [Figure 1.2-1](#). The lower end of the OCV locking ring has 18 tabs that mate with a corresponding set of 18 tabs on the OCV lower seal flange. To install the OCA lid, the OCV locking ring is rotated to the "unlocked" position, using alignment marks on the OCA exterior for reference. The unlocked position aligns the tabs on the OCV locking ring with the cutouts between the tabs on the OCV lower seal flange. Next, install the OCA lid onto the OCA body, optionally evacuating the OCV cavity through the OCV vent port sufficiently to allow free movement of the OCV locking ring. Positive closure is attained by rotating the OCV locking ring to the "locked" position, again using the alignment marks on the OCA exterior for reference. In order to allow rotation of the OCV locking ring from the HalfPACT packaging exterior, a locking Z-flange extends radially outward to the OCA exterior. Six, 1/2 inch diameter, stainless steel socket head

cap screws secure the locking Z-flange in the locked position. A single, localized cutout in the OCV locking ring is provided for access to the OCV seal test port feature.

Within the annular void between the OCV and the OCA outer shell structure is a relatively thick layer of thermally insulating and energy absorbing, rigid, polyurethane foam. Surrounding the periphery of the polyurethane foam cavity is a layer of 1/4 inch nominal thickness, ceramic fiber paper capable of resisting temperatures in excess of 2,000 °F. The combination of OCA exterior shell, fire resistant polyurethane foam, and insulating ceramic fiber paper is sufficient to protect the containment boundary from the consequences of all regulatory defined tests.

Two fork lift pockets are incorporated into the base of the OCA body. These pockets provide the handling interface for lifting a HalfPACT package. Three sets of lifting straps are included in the OCA lid assembly for lifting of the OCA lid only, and are so appropriately identified. Four tie-down lugs with reinforcing doubler plates are also provided at the base of the OCA body.

Rubber materials used in the OCA include butyl, and ethylene propylene or neoprene, as applicable, for the main O-ring seals, silicone for the wear pad, and polyester foam for the optional annulus foam ring. Plastic is used for the polyurethane foam cavity, fire-consumable vent plugs. The OCA lid lift pockets, vent port access tube, and a portion of the seal test port access tube are made from fiberglass. Brass is used for the OCV vent and seal test port plugs. High alloy stainless steel is used for the OCV locking ring joint pins. Insulating materials such as ceramic fiber paper along the periphery of the polyurethane foam cavity, and fiberglass-type insulation for the inner thermal shield are also used. Finally, a variety of stainless steel fasteners, greases and lubricants, and adhesives are also utilized, as specified in [Appendix 1.3.1, *Packaging General Arrangement Drawings*](#).

1.2.1.1.2 Inner Containment Vessel (ICV) Assembly

The inner containment vessel (ICV) assembly consists of an ICV lid and ICV body, each primarily comprised of a stainless steel shell structure. Not considering the seal flange region, the ICV lid has a nominal external diameter of 74³/₈ inches and a nominal internal diameter of 73⁷/₈ inches. Likewise, not considering the seal flange region, the ICV body has a nominal external diameter of 73¹/₈ inches and a nominal internal diameter of 72⁵/₈ inches. The nominal external diameter of the ICV seal region is 76⁵/₁₆ inches, and the nominal internal diameter of the ICV seal region is 72⁷/₁₆ inches. With the ICV lid installed onto the ICV body, the ICV has a nominal external length of 69 inches, and a nominal internal height is 68¹/₂ inches at the ICV cavity centerline.

The containment boundary provided by the ICV consists of a stainless steel vessel formed by a mating lid and body, plus the uppermost of two main O-ring seals enclosed between an upper and lower seal flange. The upper main O-ring seal (containment) is butyl rubber with a nominal 0.400 inch diameter cross-section. The lower main O-ring seal (test) may be neoprene or ethylene propylene with a nominal 0.375 inch diameter cross-section. The purpose of the lower main O-ring seal is for establishing a vacuum on the exterior side of the upper main O-ring seal for helium and pressure rise leakage rate testing. To protect the main O-ring seals from debris that may be associated with some payloads, a wiper O-ring seal is used between the ICV upper and lower seal flanges. In addition to the wiper O-ring seal, a silicone debris shield, located at the top of the ICV lower seal flange, provides a secondary debris barrier to the upper main O-ring seal. To ensure that helium tracer gas reaches the region directly above the upper main

O-ring seal (containment) during helium leakage rate testing, a helium fill port is integral to the ICV vent port configuration (see [Appendix 1.3.1, Packaging General Arrangement Drawings](#)). In addition, to allow for pressure equalization across the silicone debris shield during ICV lid installation and removal, three, 1/8 inch nominal diameter holes are located in the top of the ICV lower seal flange.

A vent port feature in the ICV body's lower seal flange is the only other containment boundary penetration. A vent port insert and an outer ICV vent port plug with an O-ring seal define the containment boundary at the ICV vent port penetration.

Leakage rate testing of the ICV's upper main O-ring seal (containment seal) is performed through an ICV seal test port that is located in the ICV lid.

All shells comprising the ICV are 1/4 inch nominal thickness, Type 304, stainless steel, including the lower and upper torispherical heads.

Similar to the OCV, the ICV lid is secured to the ICV body via the ICV locking ring located at the outer diameter of the ICV upper and lower seal flanges. Closure design and operation is almost identical to the OCV, as illustrated in [Figure 1.2-1](#). The lower end of the ICV locking ring has 18 tabs that mate with a corresponding set of 18 tabs on the ICV lower seal flange. To install the ICV lid, the ICV locking ring is rotated to the "unlocked" position, using alignment marks for reference. The unlocked position will align the tabs on the ICV locking ring with the cutouts between the tabs on the ICV lower seal flange. Next, the ICV lid is installed onto the ICV body, optionally evacuating the ICV cavity through the ICV vent port sufficiently to allow free movement of the ICV locking ring. Positive closure is attained by rotating the ICV locking ring to the "locked" position, using the alignment marks for reference. Three, 1/2 inch diameter, stainless steel socket head cap screws secure the ICV locking ring in the locked position.

Three lift sockets, each containing a lift pin, are integrated into the ICV lid for lifting the ICV lid or an empty ICV assembly. Any lifting of the loaded ICV is performed using the OCA forklift pockets with the ICV located within the OCA.

Rubber materials used in the ICV include butyl, ethylene propylene, neoprene, buna-N, fluoro-silicone or fluoro-carbon, as applicable, for the main and wiper O-ring seals, and silicone for the debris shield. Brass is used for the ICV vent and seal test port plugs. High alloy stainless steel is used for the ICV locking ring joint pins. Finally, a variety of stainless steel fasteners, and greases and lubricants are also utilized, as specified in [Appendix 1.3.1, Packaging General Arrangement Drawings](#).

1.2.1.1.3 Aluminum Honeycomb Spacer Assemblies

Aluminum honeycomb spacer assemblies are designed to fit within the torispherical heads at each end of the ICV cavity. Each aluminum honeycomb spacer assembly includes an optional, 18 inch nominal diameter by 1½ inch nominal depth pocket that may be used in the future to accommodate a catalyst assembly. The lower spacer assembly also includes a 3 inch nominal diameter hole at the center that serves as an inspection port to check for water accumulation in the ICV lower head. With the spacer assemblies in place, the nominal ICV cavity height becomes 44¾ inches.

1.2.1.2 Gross Weight

The gross shipping weight of a HalfPACT package is 18,100 pounds maximum. A summary of overall component weights is delineated in [Table 2.2-1](#) of [Section 2.2, *Weights and Centers of Gravity*](#).

1.2.1.3 Neutron Moderation and Absorption

The HalfPACT package does not require specific design features to provide neutron moderation and absorption for criticality control. Fissile materials in the payload are limited to amounts that ensure safely subcritical packages for both NCT and HAC. The fissile material limits for a single HalfPACT Package are based on optimally moderated and reflected fissile material. The structural materials in the HalfPACT packaging are sufficient to maintain reactivity between the fissile material in an infinite array of damaged HalfPACT packages at an acceptable level. Further discussion of neutron moderation and absorption is provided in [Chapter 6.0, *Criticality Evaluation*](#).

1.2.1.4 Receptacles, Valves, Testing, and Sampling Ports

There are no receptacles or valves used on the HalfPACT packaging, however, the OCV and ICV each have a seal test port and a vent port (see [Appendix 1.3.1, *Packaging General Arrangement Drawings*](#)). For each containment vessel, a seal test port provides access to the region between the upper and lower (containment and test) main O-ring seals between the upper and lower (lid and body) seal flanges. The seal test ports are used to leakage rate test the seals to verify proper assembly of the HalfPACT package prior to shipment.

The vent port is used during loading and unloading to facilitate lid installation and removal, and to allow blowdown of internal vacuum or pressure prior to opening a loaded package. As an option, a low vacuum may be applied to the vent port to fully seat the lid and assure free rotation of the locking ring.

Two separate penetrations through the polyurethane foam within the OCA are provided to access the seal test port and vent port plugs. The access ports are capped at the OCA exterior surface with 1½ inch pipe plugs (NPT) within 3 inch diameter couplings. Reinforcing doubler plates are also included on the inner surface of the OCA exterior shell, adjacent to the couplings. In addition, removable foam or ceramic fiber plugs fill the region within the access hole tubes to provide a level of thermal protection from the HAC thermal event. The vent port access tube is comprised of a non-metallic fiberglass, and a fiberglass link is included with the stainless steel, seal test port access tube as a lining to reduce radial thermal conductivity. When the OCA lid is removed, the ICV vent and seal test port plugs are readily accessible.

The OCV seal test port and both the ICV seal test and vent port plugs are accessed through localized cutouts in the corresponding vessel locking rings. An elongated cutout in the ICV locking ring is utilized at the ICV vent port location to allow locking ring rotation while an optional vacuum pump is installed. Smaller cutouts are provided in the ICV and OCV locking rings at the seal test port locations since these ports are only used with the locking rings in the locked position. The OCV vent port feature is located in the OCA body, therefore a cutout in the OCV locking ring is not necessary.

Detailed drawings of the test and vent port features and the associated local cutouts in the locking rings are provided in [Appendix 1.3.1, *Packaging General Arrangement Drawings*](#).

1.2.1.5 Heat Dissipation

The HalfPACT package design capacity is 30 thermal watts maximum. The HalfPACT package dissipates this relatively low internal heat load entirely by passive heat transfer for both NCT and HAC. No special devices or features are needed or utilized to enhance the dissipation of heat. Features are included in the design to enhance thermal performance in the HAC thermal event. These include the use of a high temperature insulating material (ceramic fiber paper) at polyurethane foam-to-steel interfaces and the presence of an inner and outer thermal shield at the OCA lid-to-body interface. A more detailed discussion of the package thermal characteristics is provided in [Chapter 3.0, *Thermal Evaluation*](#).

1.2.1.6 Coolants

Due to the passive design of the HalfPACT package with regard to heat transfer, there are no coolants utilized within the HalfPACT package.

1.2.1.7 Protrusions

The only significant protrusions on the HalfPACT package exterior are those associated with the lifting and tie-down features on the OCA exterior. The only significant external protrusions from the OCA lid are lift straps and corresponding guide pockets that extend from three equally spaced locations at the lid top. These lift features protrude above the OCA upper torispherical head, but are radially located such that they remain below torispherical head's crown and do not affect overall package height. The guide pockets are made of a fiberglass material that is designed to break away for lid-end impacts. The only significant external protrusions from the OCA body are the tie-down features at the bottom end of the package. Four tie-down lugs, with associated doubler plates, are used at locations corresponding with the main beams of the trailer. These tie-down protrusions extend a maximum of 2 $\frac{1}{8}$ inch radially from the OCA body exterior shell.

The only significant protrusion on the ICV exterior is the ICV locking ring. The ICV locking ring extends radially outward approximately one inch from the outside surface of the upper ICV torispherical head. With its 3 $\frac{7}{8}$ inch axial length directly backed and supported by the OCV (the nominal radial gap is 1/4 inch), this external protrusion is of little consequence for the package. The only significant protrusions on the ICV interior are the three lift pockets that penetrate the upper ICV torispherical head. These lift pockets are equally spaced on a 56 inch diameter, extending into the ICV cavity a maximum of 4 $\frac{1}{2}$ inches from the inner surface of the upper ICV torispherical head. The ICV lift pockets are of little consequence as they are protected by the surrounding aluminum honeycomb spacer assembly. There are no significant internal or external protrusions associated with the ICV body.

1.2.1.8 Lifting and Tie-down Devices

Three sets of lift pins, lift straps and associated doubler plates used in the OCA lid are designed to handle the OCA lid only (including overcoming any resistance to lid removal associated with the presence of the main O-ring seals). The OCA lid lifting devices are not designed to lift a loaded package or empty OCA. Under excessive load, failure occurs in the region of the OCA

lift pin locations (at the pin-to-strap welds), away from the OCA torispherical head. A loaded HalfPACT package or any portion thereof can be lifted via the pair of fork lift pockets that are located at the base of the OCA body. These pockets are sized to accommodate forks up to 10 inches wide and up to 4 inches thick. An overhead crane can also be used to lift the loaded package, utilizing lifting straps, through the fork lift pockets.

Lifting of the ICV is via the three lift pockets inset into the upper ICV torispherical head. These lift pockets, with their associated lift pins and adjacent doubler plates, are sized to lift an empty ICV or handle the ICV lid (including overcoming any resistance to lid removal associated with the presence of the main O-ring seals). A loaded ICV must be fully supported with the OCA body and lifted via the OCA fork lift pockets. Under excessive load, the ICV lift pins are designed to fail in shear prior to compromising the ICV containment boundary.

Both the OCA and ICV lifting points are appropriately labeled to limit their use to the intended manner.

Four tie-down lugs, with associated doubler plates, are used at locations corresponding with the main beams of the trailer. At each tie-down location, one doubler is used on the outside surface of the OCA side wall and one on the inside surface of the OCA lower flanged head. At each tie-down lug location, an internal gusset plate is also used between the inside of the OCA exterior shell and the doubler in the lower head to stiffen the tie-down regions. The doubler plates are sized to adequately distribute the regulatory-defined tie-down loads (10 gs longitudinal, 5 gs lateral, and 2 gs vertical, applied simultaneously) outwardly into the 1/4 inch thick OCA exterior shell. Each tie-down lug is welded directly to the adjacent side doubler plate. In an excessive load condition, these tie-down lug welds are sized to shear from the corresponding doubler plate.

A detailed discussion of lifting and tie-down designs, with corresponding structural analyses, is provided in [Section 2.5, *Lifting and Tie-down Standards for All Packages*](#).

1.2.1.9 Pressure Relief System

There are no pressure relief systems included in the HalfPACT package design to relieve pressure from within the ICV or OCV. Fire-consumable vents in the form of plastic pipe plugs are employed on the exterior surface of the OCA. These vents are included to release any gases generated by charring polyurethane foam in the HAC thermal event (fire). During the HAC fire, the plastic pipe plugs melt allowing the release of gasses generated by the foam as it flashes to a char. Three vents are used on the OCA lid and six on the OCA body, located at the center of foam mass in each component. For optimum performance, the vents are located uniformly around the circumference of the OCA lid and body.

1.2.1.10 Shielding

Due to the nature of the contact-handled transuranic (CH-TRU) payload, no biological shielding is necessary or provided by the HalfPACT packaging.

1.2.2 Operational Features

The HalfPACT package is not considered to be operationally complex. All operational features are readily apparent from an inspection of the drawings provided in [Appendix 1.3.1, *Packaging General Arrangement Drawings*](#), and the previous discussions presented in [Section 1.2.1](#),

Packaging. Operational procedures and instructions for loading, unloading, and preparing an empty HalfPACT package for transport are provided in [Chapter 7.0, *Operating Procedures*](#).

1.2.3 Contents of Packaging

The HalfPACT packaging is designed to transport contact-handled transuranic (CH-TRU) and other authorized payloads such as tritium-contaminated materials that do not exceed 10^5 A₂ quantities.

The *Contact-Handled Transuranic Waste Authorized Methods for Payload Control (CH-TRAMPAC)*¹ is the governing document for shipments of solid or solidified CH-TRU and tritium-contaminated wastes in the HalfPACT package. All users of the HalfPACT package shall comply with all payload requirements outlined in the *CH-TRAMPAC*, using one or more of the methods described in that document.

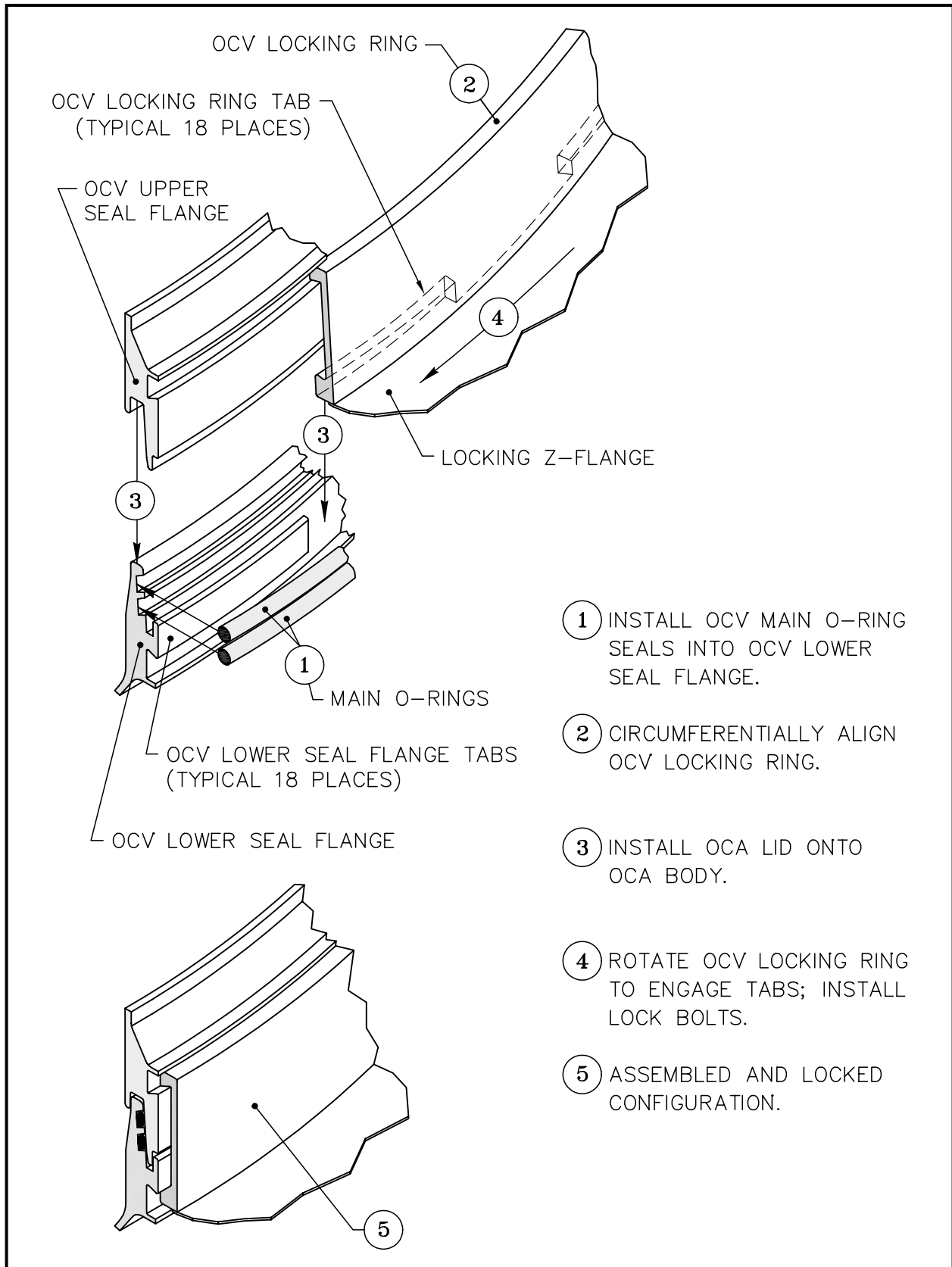


Figure 1.2-1 – OCV Closure Design (ICV closure is Similar)

This page intentionally left blank.

1.3 Appendices

1.3.1 *Packaging General Arrangement Drawings*

1.3.2 *Glossary of Terms and Acronyms*

This page intentionally left blank.

1.3.1 Packaging General Arrangement Drawings

This section presents the HalfPACT packaging general arrangement drawing¹, consisting of 12 sheets entitled, *HalfPACT Packaging SAR Drawing, Drawing Number 707-SAR*. In addition, the standard pipe overpack general arrangement drawing, consisting of 3 sheets entitled, *Standard Pipe Overpack, Drawing Number 163-001*, is presented in this section. The S100 pipe overpack, the S200 pipe overpack, and the S300 pipe overpack are depicted in *Drawing Numbers 163-002, 163-003, and 163-004*, respectively. The 55-gallon, 85-gallon, and 100-gallon compacted puck drum spacers are depicted in *Drawing Number 163-006*. The shielded containers and associated dunnage assemblies are depicted in *Drawing Number 163-008*.

Within the packaging general arrangement drawing, dimensions important to the packaging's safety are dimensioned and toleranced (e.g., structural shell thicknesses, polyurethane foam thicknesses, and the sealing regions on the seal flanges). All other dimensions are provided as a reference dimension, and are toleranced in accordance with the general tolerance block.

¹ The HalfPACT packaging, pipe overpack, compacted puck drum spacer, and shielded container general arrangement drawings utilize the uniform standard practices of ASME Y14.5M, *Dimensioning and Tolerancing*, American National Standards Institute, Inc. (ANSI).

This page intentionally left blank.

8

7

6

5

4

3

707-SAR

1

8

1

D

D

C

C

B

B

A

A

Figure Withheld Under 10 CFR 2.390

Prepared for
U.S. Department of Energy

by PACKAGING TECHNOLOGY, INC.

HalfPACT PACKAGING
SAR DRAWING



SCALE: N/A	WT. N/A
REV: 8	SHEET 1 OF 12
DWG NO. 707-SAR	
CADFILE: 707S_018.DWG	

8

7

6

5

4

3

2

1

8

7

6

5

4

3

707-SAR

2

8

1

D

D

C

C

B

B

A

A

Figure Withheld Under 10 CFR 2.390

Prepared for
U.S. Department of Energy
by PACKAGING TECHNOLOGY, INC.

HalfPACT PACKAGING
SAR DRAWING



SCALE: 1/10	WT. N/A
REV: 8	SHEET 2 OF 12
DWG NO. 707-SAR	
CADFILE: 707S_028.DWG	

8

7

6

5

4

3

2

1

8

7

6

5

4

3

707-SAR

3

8

1

D

D

C

C

B

B

A

A

Figure Withheld Under 10 CFR 2.390

Prepared for
U.S. Department of Energy
by PACKAGING TECHNOLOGY, INC.

HalfPACT PACKAGING
SAR DRAWING



SCALE: 1/10	WT. N/A
REV: 8	SHEET 3 OF 12
DWG NO. 707-SAR	
CADFILE: 707S_038.DWG	

8

7

6

5

4

3

2

1

8

7

6

5

4

3

707-SAR

4

8

1

D

D

C

C

B

B

A

A

Figure Withheld Under 10 CFR 2.390

Prepared for
U.S. Department of Energy
by PACKAGING TECHNOLOGY, INC.

HalfPACT PACKAGING
SAR DRAWING



SCALE: 1/4	WT. N/A
REV: 8	SHEET 4 OF 12
DWG NO. 707-SAR	
CADFILE: 707S_048.DWG	

8

7

6

5

4

3

2

1

8

7

6

5

4

3

707-SAR

5

8

1

D

D

C

C


B

B

A

A

Figure Withheld Under 10 CFR 2.390

Prepared for		
U.S. Department of Energy		
<small>by PACKAGING TECHNOLOGY, INC.</small>		
HalfPACT PACKAGING SAR DRAWING		
	SCALE: 1/2	WT. N/A
	REV: 8	SHEET 5 OF 12
	DWG NO. 707-SAR	
DWG SIZE D	CADFILE: 707S_058.DWG	

8

7

6

5

4

3

2

1

8

7

6

5

4

3

707-SAR

6

8

1

D

D

C

C


B

B

A

A

Figure Withheld Under 10 CFR 2.390

Prepared for		U.S. Department of Energy	
		by PACKAGING TECHNOLOGY, INC.	
HalfPACT PACKAGING SAR DRAWING			
	SCALE: FULL	WT. N/A	
	REV: 8	SHEET 6 OF 12	
DWG SIZE: D	DWG NO. 707-SAR		
CADFILE: 707S_068.DWG			

8

7

6

5

4

3

2

1

8

7

6

5

4

3

707-SAR

7

8

1

D

D

C

C


B

B

A

A

Figure Withheld Under 10 CFR 2.390

Prepared for		
U.S. Department of Energy		
<small>by PACKAGING TECHNOLOGY, INC.</small>		
HalfPACT PACKAGING SAR DRAWING		
	SCALE: 1/2	WT. N/A
	REV: 8	SHEET 7 OF 12
	DWG NO.	707-SAR
	CADFILE: 707S_078.DWG	

8

7

6

5

4

3

2

1

8

7

6

5

4

3

2

707-SAR

8

8

1

D

D

C

C


B

B

A

A

Figure Withheld Under 10 CFR 2.390

Prepared for		
U.S. Department of Energy		
<small>by PACKAGING TECHNOLOGY, INC.</small>		
HalfPACT PACKAGING SAR DRAWING		
	SCALE: 1/4	WT. N/A
	REV: 8	SHEET 8 OF 12
	DWG NO.	707-SAR
	CADFILE: 707S_088.DWG	

8

7

6

5

4

3

2

1

1

8

7

6

5

4

3

707-SAR

9

8

1

D

D

C

C


B

B

A

A

Figure Withheld Under 10 CFR 2.390

Prepared for		
U.S. Department of Energy		
<small>by PACKAGING TECHNOLOGY, INC.</small>		
HalfPACT PACKAGING SAR DRAWING		
	SCALE: 1/8	WT. N/A
	REV: 8	SHEET 9 OF 12
DWG NO.	707-SAR	
DWG SIZE	CADFILE: 707S_098.DWG	

8

7

6

5

4

3

2

1

8

7

6

5

4

3

707-SAR

10

8

1

D

D

C

C

B

B

A

A

Figure Withheld Under 10 CFR 2.390

Prepared for
U.S. Department of Energy
by PACKAGING TECHNOLOGY, INC.

HalfPACT PACKAGING
SAR DRAWING



SCALE: 1/8	WT. N/A
REV: 8	SHEET 10 OF 12
DWG NO. D	707-SAR
CADFILE: 707S_108.DWG	

8

7

6

5

4

3

2

1

8

7

6

5

4

3

707-SAR

11

8

1

D

D

C

C

B

B

A

A

Figure Withheld Under 10 CFR 2.390

Prepared for
U.S. Department of Energy
by PACKAGING TECHNOLOGY, INC.

HalfPACT PACKAGING
SAR DRAWING



SCALE: 2/1	WT. N/A
REV: 8	SHEET 11 OF 12
DWG NO. 707-SAR	
CADFILE: 707S_118.DWG	

8

7

6

5

4

3

2

1

8

7

6

5

4

3

707-SAR

12

8

1

D

D

C

C

B

B

A

A

Figure Withheld Under 10 CFR 2.390

Prepared for
U.S. Department of Energy

by PACKAGING TECHNOLOGY, INC.

HalfPACT PACKAGING
SAR DRAWING



SCALE: FULL	WT. N/A
REV: 8	SHEET 12 OF 12
DWG NO. 707-SAR	
CADFILE: 707S_128.DWG	

8

7

6

5

4

3

2

1

8

7

6

5

4

3

163-001

1

6

1

D

D

C

C

B

B

A

A

Figure Withheld Under 10 CFR 2.390

Prepared for
U.S. Department of Energy
by PACRAGING TECHNOLOGY, INC.

STANDARD PIPE OVERPACK
SAR DRAWING



SCALE: 1/2	WT. N/A
REV: 6	SHEET 1 OF 3
DWG NO. 163-001	
CADFILE: 163_0116.DWG	

8

7

6

5

4

3

2

1

8

7

6

5

4

3

163-001

2

6

1

D

D

C

C

B

B

A

A

Figure Withheld Under 10 CFR 2.390

Prepared for
U.S. Department of Energy
by PACRAGING TECHNOLOGY, INC.

STANDARD PIPE OVERPACK
SAR DRAWING



SCALE: 1/4	WT. N/A
REV: 6	SHEET 2 OF 3
DWG NO. 163-001	
CADFILE: 163_0126.DWG	

8

7

6

5

4

3

2

1

8

7

6

5

4

3

163-001

3

6

1

D

D

C

C

B

B

A

A

Figure Withheld Under 10 CFR 2.390

Prepared for
U.S. Department of Energy

by PACRAGING TECHNOLOGY, INC.

STANDARD PIPE OVERPACK
SAR DRAWING



SCALE: 1/4	WT. N/A
REV: 6	SHEET 3 OF 3
DWG NO. 163-001	
CADFILE: 163_0136.DWG	

8

7

6

5

4

3

2

1

8

7

6

5

4

3

163-002

1

4

1

D

D

C

C

B

B

A

A

Figure Withheld Under 10 CFR 2.390

Prepared for
U.S. Department of Energy
by PACKAGING TECHNOLOGY, INC.

S100 PIPE OVERPACK
SAR DRAWING



SCALE: 1/2	WT. N/A
REV: 4	SHEET 1 OF 2
DWG NO. 163-002	
CADFILE: 163_0214.DWG	

8

7

6

5

4

3

2

1

8

7

6

5

4

3

163-002

2

4

1

D

D

C

C

B

B

A

A

Figure Withheld Under 10 CFR 2.390

Prepared for
U.S. Department of Energy
by PACKAGING TECHNOLOGY, INC.

S100 PIPE OVERPACK
SAR DRAWING



SCALE: 3/8	WT. N/A
REV: 4	SHEET 2 OF 2
DWG NO. D	163-002
CADFILE: 163_0224.DWG	

8

7

6

5

4

3

2

1

8

7

6

5

4

3

163-003

1

3

1

D

D

C

C

B

B

A

A

Figure Withheld Under 10 CFR 2.390

Prepared for
U.S. Department of Energy

by PACKAGING TECHNOLOGY, INC.

S200 PIPE OVERPACK
SAR DRAWING



SCALE: 1/2	WT. N/A
REV: 3	SHEET 1 OF 2
DWG NO. 163-003	
CADFILE: 163_0313.DWG	

8

7

6

5

4

3

2

1

8

7

6

5

4

3

163-003

2

3

1

D

D

C

C

B

B

A

A

Figure Withheld Under 10 CFR 2.390

Prepared for
U.S. Department of Energy

by PACKAGING TECHNOLOGY, INC.

S200 PIPE OVERPACK
SAR DRAWING



SCALE: 1/2	WT. N/A
REV: 3	SHEET 2 OF 2
DWG NO. D	163-003
CADFILE: 163_0323.DWG	

8

7

6

5

4

3

2

1

8

7

6

5

4

3

163-004

1

1

1

D

D

C

C

B

B

A

A

Figure Withheld Under 10 CFR 2.390

Prepared for
U.S. Department of Energy
by PACKAGING TECHNOLOGY, INC.

S300 PIPE OVERPACK
SAR DRAWING



SCALE: 1/2	WT. N/A
REV: 1	SHEET 1 OF 1
DWG SIZE: D	DWG NO. 163-004
CADFILE: 163_0411.DWG	

8

7

6

5

4

3

2

1

8

7

6

5

4

3

163-006

1

0

1

D

D

C

C


B

B

A

A

Figure Withheld Under 10 CFR 2.390

Prepared for		
U.S. Department of Energy		
by PACKAGING TECHNOLOGY, INC.		
COMPACTED PUCK DRUM SPACERS 55-, 85-, & 100-GALLON SAR DRAWING		
	SCALE: 1/4	WT. N/A
	REV: 0	SHEET 1 OF 1
	DWG NO. 163-006	
DWG SIZE D	CADFILE: 163_0610.DWG	

8

7

6

5

4

3

2

1

8

7

6

5

4

3

163-008

1

1

1

D

D

C

C

B

B

A

A

Figure Withheld Under 10 CFR 2.390

Prepared for
U.S. Department of Energy
by PACKAGING TECHNOLOGY, INC.

SHIELDED CONTAINER
SAR DRAWING



SCALE: 1/8	WT. N/A
REV: 1	SHEET 1 OF 6
DWG NO. 163-008	
CADFILE: 163_0811.DWG	

8

7

6

5

4

3

2

1

8

7

6

5

4

3

163-008

2

1

1

D

D

C

C

B

B

A

A

Figure Withheld Under 10 CFR 2.390

Prepared for
U.S. Department of Energy
by PACKAGING TECHNOLOGY, INC.

SHIELDED CONTAINER
SAR DRAWING



SCALE: 1/4	WT. N/A
REV: 1	SHEET 2 OF 6
DWG NO. 163-008	
CADFILE: 163_0821.DWG	

8

7

6

5

4

3

2

1

8

7

6

5

4

3

163-008

3

1

1

D

D

C

C


B

B

A

A

Figure Withheld Under 10 CFR 2.390

Prepared for		
U.S. Department of Energy		
<small>by PACKAGING TECHNOLOGY, INC.</small>		
SHIELDED CONTAINER SAR DRAWING		
	SCALE: 1/4	WT. N/A
	REV: 1	SHEET 3 OF 6
	DWG NO. 163-008	
	CADFILE: 163_0831.DWG	

8

7

6

5

4

3

2

1

8

7

6

5

4

3

163-008

4

1

1

D

D

C

C

B

B

A

A

Figure Withheld Under 10 CFR 2.390

Prepared for
U.S. Department of Energy

by PACKAGING TECHNOLOGY, INC.

SHIELDED CONTAINER
SAR DRAWING



SCALE: 1/4	WT. N/A
REV: 1	SHEET 4 OF 6
DWG NO. D	163-008
CADFILE: 163_0841.DWG	

8

7

6

5

4

3

2

1

8

7

6

5

4

3

163-008

5

1

1

D

D

C

C

B

B

A

A

Figure Withheld Under 10 CFR 2.390

Prepared for
U.S. Department of Energy

by PACKAGING TECHNOLOGY, INC.

SHIELDED CONTAINER
SAR DRAWING



SCALE: 1/8	WT. N/A
REV: 1	SHEET 5 OF 6
DWG NO. 163-008	
CADFILE: 163_0851.DWG	

8

7

6

5

4

3

2

1

8

7

6

5

4

3

163-008

6

1

1

D

D

C

C

B

B

A

A

Figure Withheld Under 10 CFR 2.390

Prepared for
U.S. Department of Energy

by PACKAGING TECHNOLOGY, INC.

SHIELDED CONTAINER
SAR DRAWING



SCALE: 1/8	WT. N/A
REV: 1	SHEET 6 OF 6
DWG NO. 163-008	
DWG SIZE D	CADFILE: 163_0861.DWG

8

7

6

5

4

3

2

1

This page intentionally left blank to facilitate duplex printing.

1.3.2 Glossary of Terms and Acronyms

55-Gallon Drum – A payload container yielding 55 gallons.

85-Gallon Drum – A payload container with a range of dimensions yielding 75 to 88 gallons.

85-Gallon Drum Overpacks – A payload container consisting of a 55-gallon drum overpacked within an 85-gallon drum of the appropriate dimensions.

100-Gallon Drum – A payload container yielding 100 gallons.

Aluminum Honeycomb Spacer Assembly – An assembly that is located within each end of the ICV. The aluminum honeycomb spacer assembly supplements the ICV void volume to accommodate gas generated by the payload material, and acts as an energy-absorbing barrier between the payload and the ICV torispherical heads for axial loads.

ASME – American Society of Mechanical Engineers.

ASME B&PVC – ASME Boiler and Pressure Vessel Code.

CTU – Certification Test Unit

CH-TRAMPAC – Contact-Handled Transuranic Waste Authorized Methods for Payload Control.

CH-TRU Waste – Contact-Handled Transuranic Waste.

HalfPACT Package – The package consisting of a HalfPACT packaging and the Payload.

HalfPACT Packaging – The packaging consisting of an outer containment assembly (OCA), an inner containment vessel (ICV), and two aluminum honeycomb spacer assemblies.

ETU – Engineering Test Unit.

ICV – Inner Containment Vessel.

ICV Body – The assembly consisting of the ICV lower seal flange, the cylindrical vessel, and the ICV lower torispherical head.

ICV Inner Vent Port Plug – The brass plug and accompanying O-ring seal that provides the pressure boundary in the ICV vent port penetration.

ICV Lid – The assembly consisting of the ICV upper seal flange, the ICV locking ring, a short section of cylindrical vessel, and the ICV upper torispherical head.

ICV Lock Bolts – The three, 1/2 inch, socket head cap screws used to secure the ICV locking ring in the locked position.

ICV Locking Ring – The component that connects and locks the ICV upper seal flange to the ICV lower seal flange; included as an ICV lid component.

ICV Lower Seal Flange – The ICV body's sealing interface containing two O-ring grooves, the ICV vent port access, and the ICV test port.

ICV Main O-ring Seal – The upper elastomeric O-ring seal in the ICV lower seal flange; forms the containment boundary.

ICV Outer Vent Port Plug – The brass plug and accompanying O-ring seal that provides the containment boundary in the ICV vent port penetration.

ICV Seal Test Port – The radial penetration between the ICV main O-ring seal and ICV main test O-ring seal to allow leakage rate testing of the ICV main O-ring seal.

ICV Seal Test Port Plug – The brass plug and accompanying O-ring seal for the ICV seal test port.

ICV Seal Test Port Insert – A welded-in, replaceable component within the ICV lower seal flange that interfaces with the ICV seal test port plug.

ICV Main Test O-ring Seal – The lower elastomeric O-ring seal in the ICV lower seal flange; forms the test boundary for leakage rate testing.

ICV Upper Seal Flange – The ICV lid's sealing interface containing a mating sealing surface for the ICV lower seal flange and location for a wiper O-ring seal.

ICV Vent Port – The radial penetration into the ICV cavity that is located in the ICV lower seal flange.

ICV Vent Port Cover – The outer brass cover that directly protects the ICV vent port plugs.

Inner Containment Vessel – The assembly (comprised of an ICV lid and ICV body) providing a secondary level of containment for the payload. Within each end of the inner containment vessel (ICV) is an aluminum honeycomb spacer assembly.

Locking Z-Flange – The z-shaped shell situated between the upper and lower Z-flanges that connects to the OCV locking ring; allows external operation of the OCV locking ring.

Lower Z-Flange – The z-shaped shell in the OCA body, connecting the OCA outer shell to the OCV lower seal flange.

OCA – Outer Containment Assembly.

OCA Body – The assembly consisting of the OCV lower seal flange, the OCV cylindrical and conical shells, the OCV lower torispherical head, the lower Z-flange, the OCA cylindrical shell, the OCA lower flat head, corner reinforcing angles, tie-down structures, ceramic fiber paper, and polyurethane foam.

OCA Inner Thermal Shield – The L-shaped, 16 gauge (0.060 inch thick), inner shield that holds fiberglass insulating material against the OCV locking ring thereby preventing hot gasses and flames from directly impinging on the OCV sealing region in the event of a HAC fire.

OCA Lid – The assembly consisting of the OCV upper seal flange, the OCV locking ring, a short section of cylindrical vessel, the OCV upper torispherical head, the upper and locking Z-flanges, the inner and outer thermal shields, a short section of cylindrical shell, the OCA upper torispherical head, corner reinforcing angles, ceramic fiber paper, and polyurethane foam.

OCA Lock Bolts – The six 1/2 inch, socket head cap screws used to secure the OCV locking ring in the locked position.

OCA Lower Head – The lower ASME flat head comprising the OCA outer shell.

OCA Outer Thermal Shield – The 14 gauge (0.075 inch thick) × 6¹/₈ inch wide outer shield surrounding the OCA lid-to-body joint that prevents hot gasses and flames from entering the joint in the event of a HAC fire.

OCA Upper Head – The upper ASME torispherical head comprising the OCA outer shell.

OCV – Outer Containment Vessel.

OCV Locking Ring – The component that connects and locks the OCV upper seal flange to the OCV lower seal flange; included as an OCA lid component.

OCV Lower Seal Flange – The OCA body's sealing interface containing two O-ring grooves.

OCV Main O-ring Seal – The upper O-ring seal in the OCV lower seal flange; forms the containment boundary.

OCV Seal Test Port – The radial penetration between the OCV main O-ring seal and OCV main test O-ring seal to allow leakage rate testing of the OCV main O-ring seal.

OCV Seal Test Port Access Plug – The 1½ inch NPT plug located at the outside end of the OCV seal test port access tube (i.e., at the outside surface of the OCA lid outer shell).

OCV Seal Test Port Insert – A welded-in, replaceable component within the OCV lower seal flange that interfaces with the OCV seal test port plug.

OCV Seal Test Port Plug – The brass plug and accompanying O-ring seal for the OCV seal test port.

OCV Seal Test Port Thermal Plug – The foam or ceramic fiber plug located within the OCV seal test port access tube that thermally protects the OCV seal test port region.

OCV Main Test O-ring Seal – The lower O-ring seal in the OCV lower seal flange; forms the test boundary for leakage rate testing.

OCV Upper Seal Flange – The OCA lid's sealing interface containing a mating sealing surface for the OCV lower seal flange.

OCV Vent Port – The radial penetration into the OCV cavity that is located in the OCV conical shell.

OCV Vent Port Access Plug – The 1½ NPT plug located at the outside end of the OCV vent port access tube (i.e., at the outside surface of the OCA body outer shell).

OCV Vent Port Access Tube – The fiberglass tube allowing external access to the OCV vent port.

OCV Vent Port Cover – The outer brass cover that directly protects the OCV vent port plug.

OCV Vent Port Plug – The brass plug and accompanying O-ring seal that provides the containment boundary in the OCV vent port penetration.

OCV Vent Port Thermal Plug – The foam or ceramic fiber plug located within the OCV vent port access tube that thermally protects the OCV vent port region.

Outer Containment Assembly – The assembly (comprised of an OCA lid and OCA body) providing a primary level of containment for the payload. The Outer Containment Assembly

(OCA) completely surrounds the Inner Containment Vessel and consists of an exterior stainless steel shell, a relatively thick layer of polyurethane foam and an inner stainless steel boundary that forms the Outer Containment Vessel (OCV).

Outer Containment Vessel – The innermost boundary of the Outer Containment Assembly.

Packaging – The assembly of components necessary to ensure compliance with packaging requirements as defined in 10 CFR §71.4. Within this SAR, the packaging is denoted as the HalfPACT packaging.

Package – The packaging with its radioactive contents, or payload, as presented for transportation as defined in 10 CFR §71.4. Within this SAR, the package is denoted as the HalfPACT contact-handled transuranic waste package, or equivalently, the HalfPACT package.

Payload – Contact-handled transuranic (CH-TRU) waste or other authorized contents such as tritium-contaminated materials contained within approved payload containers. In this SAR, the payload includes a payload pallet for handling when drums are used. Any additional dunnage used that is external to the payload containers is also considered to be part of the payload. Payload requirements are defined by the [CH-TRAMPAC](#).

Payload Container – Payload containers may be 55-gallon drums, pipe overpacks, 85-gallon drums (including overpacks), 100-gallon drums, standard waste boxes (SWB), or shielded containers (SC).

Payload Pallet – A lightweight pallet used for handling drum-type payload containers.

Payload Spacer – A component of the same basic design as the payload pallet; used to control (reduce) vertical clearance within the ICV with 55-gallon drum, short 85-gallon drum, 100-gallon drum, and SWB payload containers.

Pipe Component – A stainless steel container used for packaging specific waste forms within a 55-gallon drum. The pipe component is exclusively used as part of the pipe overpack.

Pipe Overpack – A payload container consisting of a pipe component positioned by dunnage within a 55-gallon drum with a rigid, polyethylene liner and lid. Seven pipe overpack assemblies will fit within the HalfPACT packaging.

RTV – Room Temperature Vulcanizing.

SAR – Safety Analysis Report (this document).

Shielded Container – A specialized payload container for use within the HalfPACT packaging that provides gamma shielding. Three shielded containers are surrounded by radial and axial dunnage assemblies and loaded using a triangular payload pallet within the HalfPACT packaging.

Standard Waste Box – A specialized payload container for use within the HalfPACT packaging. One standard waste box can fit within the HalfPACT packaging.

SWB – Standard Waste Box.

Upper Z-Flange – The z-shaped shell in the OCA lid, connecting the OCA outer shell to the OCV upper seal flange.

2.0 STRUCTURAL EVALUATION

This section presents evaluations demonstrating that the HalfPACT package meets all applicable structural criteria. The HalfPACT packaging, consisting of an outer containment assembly (OCA), with an integral outer containment vessel (OCV), and an inner containment vessel (ICV), with aluminum honeycomb spacer assemblies, is evaluated and shown to provide adequate protection for the payload. Normal conditions of transport (NCT) and hypothetical accident condition (HAC) evaluations, using analytic and empirical techniques, are performed to address 10 CFR 71¹ performance requirements. Analytic demonstration techniques comply with the methodology presented in NRC Regulatory Guides 7.6² and 7.8³.

The HalfPACT package possesses strong similarities with the licensed TRUPACT-II package (NRC Certificate of Compliance No. 9218). All features of the HalfPACT package are essentially identical to those of the TRUPACT-II package. The only major exception is the removal of 30 inches of cylindrical sidewall length from the OCA and ICV bodies.

Numerous component and scale tests were successfully performed on the TRUPACT-II package during its development phase. Subsequent TRUPACT-II certification testing involved three, full scale certification test units (CTUs). The TRUPACT-II CTUs were subjected to a series of free drop and puncture drop tests, and two of the three TRUPACT-II CTUs were subjected to fire testing. Despite the great degree of similarity between the HalfPACT and TRUPACT-II packages, a full scale HalfPACT engineering test unit (ETU) and CTU were also subjected to a series of free drop, puncture drop, and fire tests. Both the HalfPACT ETU and CTU remained leaktight⁴ throughout certification testing. Details of the certification test program are provided in [Appendix 2.10.3, Certification Tests](#).

2.1 Structural Design

2.1.1 Discussion

A comprehensive discussion on the HalfPACT package design and configuration is provided in [Section 1.2, Package Description](#). Specific discussions relating to the aspects important to demonstrating the structural configuration and performance to design criteria for the HalfPACT package are provided in the following sections. Standard fabrication methods are utilized to fabricate the HalfPACT packaging.

¹ Title 10, Code of Federal Regulations, Part 71 (10 CFR 71), *Packaging and Transportation of Radioactive Material*, 01-01-07 Edition.

² U. S. Nuclear Regulatory Commission, Regulatory Guide 7.6, *Design Criteria for the Structural Analysis of Shipping Cask Containment Vessels*, Revision 1, March 1978.

³ U. S. Nuclear Regulatory Commission, Regulatory Guide 7.8, *Load Combinations for the Structural Analysis of Shipping Casks for Radioactive Material*, Revision 1, March 1989.

⁴ Leaktight is defined as leakage of 1×10^{-7} standard cubic centimeters per second (scc/s), air, or less per ANSI N14.5-1997, *American National Standard for Radioactive Materials – Leakage Tests on Packages for Shipment*, American National Standards Institute, Inc. (ANSI).

2.1.1.1 Containment Vessel Structures

All containment vessel cylindrical and conical shell structures are fabricated in accordance with the tolerance requirements of the ASME Boiler and Pressure Vessel Code, Section III⁵, Division 1, Subsection NE, Article NE-4220, as delineated on the drawings in [Appendix 1.3.1, Packaging General Arrangement Drawings](#). All containment vessel shell-to-shell joints and transitions in thickness, such as from the 1/4 inch thick OCV lower head to the 3/16 inch thick OCV shell, are fabricated in accordance with the ASME Boiler and Pressure Vessel Code, Section III, Division 1, Subsection NB, Article NB-4230, as delineated on the drawings in [Appendix 1.3.1, Packaging General Arrangement Drawings](#).

All containment vessel heads are flanged torispherical heads, fabricated in accordance with the ASME Boiler and Pressure Vessel Code, Section VIII, Division 1⁶, as delineated on the drawings in [Appendix 1.3.1, Packaging General Arrangement Drawings](#).

All seal flange material is ultrasonically or radiographically test inspected in accordance with the ASME Boiler and Pressure Vessel Code, Section III, Division 1, Subsection NB, Article NB-2500 and Section V⁷, Article 5 (ultrasonic) or Article 2 (radiograph), as delineated on the drawings in [Appendix 1.3.1, Packaging General Arrangement Drawings](#).

Circumferential and longitudinal welds for the containment vessel shells, seal flanges, and locking ring are full penetration welds, subjected to visual and liquid penetrant examinations, and radiographically test inspected, as delineated on the drawings in [Appendix 1.3.1, Packaging General Arrangement Drawings](#). Visual weld examinations are performed in accordance with AWS D1.1⁸. Liquid penetrant examinations are performed on the final pass in accordance with the ASME Boiler and Pressure Vessel Code, Section III, Division 1, Subsection NB, Article NB-5000 and Section V, Article 6. Radiograph test inspections are performed in accordance with the ASME Boiler and Pressure Vessel Code, Section III, Division 1, Subsection NB, Article NB-2500 and Section V, Article 2.

For both the OCV and ICV vent port penetrations, and the ICV lifting sockets, liquid penetrant examinations are performed on the final pass for single pass welds and on the root and final passes for multipass welds in accordance with the ASME Boiler and Pressure Vessel Code, Section III, Division 1, Subsection NB, Article NB-5000 and Section V, Article 6, as delineated on the drawings in [Appendix 1.3.1, Packaging General Arrangement Drawings](#).

The maximum weld reinforcement for containment vessel welds shall be 3/32 inch in accordance with the ASME Boiler and Pressure Vessel Code, Section III, Division 1, Subsection NB, Article NB-4426, Paragraph NB-4426.1, as delineated on the drawings in [Appendix 1.3.1, Packaging General Arrangement Drawings](#).

⁵ American Society of Mechanical Engineers (ASME) Boiler and Pressure Vessel Code, Section III, *Rules for Construction of Nuclear Power Plant Components*, 1995 Edition, 1997 Addenda.

⁶ American Society of Mechanical Engineers (ASME) Boiler and Pressure Vessel Code, Section VIII, Division 1, *Rules for Construction of Pressure Vessels*, 1995 Edition, 1997 Addenda.

⁷ American Society of Mechanical Engineers (ASME) Boiler and Pressure Vessel Code, Section V, *Nondestructive Examination*, 1995 Edition, 1997 Addenda.

⁸ ANSI/AWS D1.1, *Structural Welding Code--Steel*, American Welding Society (AWS).

2.1.1.2 Non-Containment Vessel Structures

All non-containment vessel shell-to-shell joints and transitions in thickness, such as from the 3/8-to-1/4 inch thick OCA outer shell transition, are fabricated in accordance with the ASME Boiler and Pressure Vessel Code, Section III, Division 1, Subsection NF, Article NF-4230, as delineated on the drawings in [Appendix 1.3.1, *Packaging General Arrangement Drawings*](#).

The OCA outer shell has a top, flanged torispherical head and bottom, flanged flat head that are fabricated in accordance with the ASME Boiler and Pressure Vessel Code, Section VIII, Division 1, as delineated on the drawings in [Appendix 1.3.1, *Packaging General Arrangement Drawings*](#).

Circumferential and longitudinal welds for the non-containment vessel shells are full penetration welds, subjected to visual and liquid penetrant examinations, as delineated on the drawings in [Appendix 1.3.1, *Packaging General Arrangement Drawings*](#). Visual weld examinations are performed in accordance with AWS D1.1. Liquid penetrant examinations are performed on the final pass in accordance with the ASME Boiler and Pressure Vessel Code, Section III, Division 1, Subsection NF, Article NF-5000.

The maximum weld reinforcement for non-containment vessel welds shall be 3/32 inch in accordance with the ASME Boiler and Pressure Vessel Code, Section III, Division 1, Subsection NF, Article NF-4400, as delineated on the drawings in [Appendix 1.3.1, *Packaging General Arrangement Drawings*](#).

2.1.2 Design Criteria

Proof of performance for the HalfPACT package is achieved by a combination of analytic and empirical evaluations. The acceptance criteria for analytic assessments are in accordance with Regulatory Guide 7.6 and Section III of the ASME Boiler and Pressure Vessel Code. The acceptance criterion for empirical assessments is a demonstration that both containment boundaries remain leaktight throughout NCT and HAC certification testing. Additionally, package deformations obtained from certification testing must be such that deformed geometry assumptions used in subsequent thermal, shielding, and criticality evaluations are validated.

The remainder of this section presents the detailed acceptance criteria used for all analytic structural assessments of the HalfPACT package.

2.1.2.1 Analytic Design Criteria (Allowable Stresses)

This section defines the stress allowables for primary membrane, primary bending, secondary, shear, peak, and buckling stresses for containment and non-containment structures. These stress allowables are used for all analytic assessments of HalfPACT package structural performance. Regulatory Guide 7.6 is used in conjunction with Regulatory Guide 7.8 to evaluate the package integrity. Material yield strengths used in the analytic acceptance criteria, S_y , ultimate strengths, S_u , and design stress intensity values, S_m , are presented in [Table 2.3-1 of Section 2.3, *Mechanical Properties of Materials*](#).

2.1.2.1.1 Containment Structures

A summary of allowable stresses used for containment structures is presented in [Table 2.1-1](#). These data are consistent with Regulatory Guide 7.6, and the ASME Boiler and Pressure Vessel Code, Section III, Subsection NB-3000 and Appendix F.

2.1.2.1.2 Non-Containment Structures

A summary of allowable stresses used for non-containment structures is presented in [Table 2.1-2](#).

For evaluation of lifting devices, the allowable stresses are limited to one-third of the material yield strength, consistent with the requirements of 10 CFR §71.45(a). For evaluation of tie-down devices, the allowable stresses are limited to the material yield strength, consistent with the requirements of 10 CFR §71.45(b).

For evaluations involving polyurethane foam, primary, load controlled compressive stresses are limited to two-thirds of the parallel-to-rise or perpendicular-to-rise compressive strength (as applicable) at 10% strain. Use of a two-thirds factor on compressive strength ensures elastic behavior of the polyurethane foam.

2.1.2.2 Miscellaneous Structural Failure Modes

2.1.2.2.1 Brittle Fracture

By avoiding the use of ferritic steels in the HalfPACT packaging, brittle fracture concerns are precluded. Specifically, most primary structural components are fabricated of Type 304 austenitic stainless steel. Since this material does not undergo a ductile-to-brittle transition in the temperature range of interest (down to -40 °F), it is safe from brittle fracture.

The lock bolts used to secure the ICV and OCV locking rings in the locked position are stainless steel, socket head cap screws ensuring that brittle fracture is not of concern. Other fasteners used in the HalfPACT packaging assembly, such as the 36, 1/4 inch screws attaching the locking Z-flange to the OCV locking ring, provide redundancy and are made from stainless steel, again eliminating brittle fracture concerns.

2.1.2.2.2 Fatigue Assessment

2.1.2.2.2.1 Normal Operating Cycles

Normal operating cycles do not present a fatigue concern for the various HalfPACT packaging components. Most HalfPACT packaging components exhibit little-to-no stress concentrations, and by satisfying the allowable limit for range of primary-plus-secondary stress intensity for NCT ($3.0S_m$), the allowable fatigue stress limit for the expected number of operating cycles is satisfied. For HalfPACT packaging components that do exhibit stress concentrations, stresses are low enough that allowable fatigue stress limits are again satisfied.

The maximum number of operating cycles reasonably expected for the HalfPACT package is 3,640, and is based on two round trips per week for 35 years. Conservatively, 5,000 cycles (or in excess of 1 cycle every 3 days) is used in the following calculations. A cycle is defined as the process of the internal pressure within the OCV and ICV increasing gradually from zero psig at the time of loading, to 50 psig (the maximum normal operating pressure, MNOP, per [Section 3.4.4, Maximum Internal Pressure](#)) during transport and then returning to 0 psig when the containment vessel is vented prior to unloading the payload. This scenario is conservative because most shipments will never generate pressure to the magnitude of the MNOP, and the system could never achieve MNOP in less than the assumed transportation cycle of three days.

From Figure I-9.2.1 and Table I-9.1 of the ASME Boiler and Pressure Vessel Code⁹, the fatigue allowable alternating stress intensity amplitude, S_a , for 5,000 cycles is 76,000 psi. This value, when multiplied by the ratio of elastic hot NCT modulus at 160 °F (the package wall temperature from [Section 2.6.1, Heat](#)) to a modulus at 70 °F, $27.8(10)^6/28.3(10)^6$, results in a fatigue allowable alternating stress intensity amplitude at 160 °F of 74,657 psi. The non-fatigue allowable stress intensity range, from the ASME Boiler and Pressure Vessel Code, Section III, Division 1, Subsection NB-3222.2, is 60,000 psi ($3.0S_m$, where S_m is 20,000 psi from [Table 2.3-1](#) in [Section 2.3, Mechanical Properties of Materials](#), at 160 °F). The alternating stress intensity is one-half of this range, or 30,000 psi. Thus, in the absence of stress concentrations, the fatigue allowable alternating stress intensity will not govern the HalfPACT packaging design.

Regions of stress concentrations for the package occur in the ICV and OCV seal flanges and locking rings. The maximum range of primary-plus-secondary stress intensity occurs between the case of maximum internal pressure under NCT hot conditions (see [Section 2.6.1.3, Stress Calculations](#)) and the vacuum case. For the seal flanges or locking rings the maximum primary-plus-secondary stress intensity is 27,922 psi from [Table 2.6-5](#) (ICV Load Case 1). The stress range is therefore 27,922 psi.

In accordance with Paragraph C.3 of Regulatory Guide 7.6, a stress concentration factor of four will conservatively be applied to the value of maximum stress intensity from above. The resultant range of peak stress intensity, correcting the modulus of elasticity for temperature, becomes:

$$S_{\text{range}} = (27,922)(4) \left(\frac{28.3(10)^6}{27.8(10)^6} \right) = 113,697 \text{ psi}$$

where the modulus of elasticity at 70 °F is $28.3(10)^6$ psi, and the modulus of elasticity at 160 °F is $27.8(10)^6$ psi, both from [Table 2.3-1](#) in [Section 2.3, Mechanical Properties of Materials](#). The alternating stress intensity is one-half of this range, or:

$$S_{\text{alt}} = \left(\frac{1}{2} \right) 113,697 = 56,849 \text{ psi}$$

From Figure I-9.2.1 and Table I-9.1 of the ASME Boiler and Pressure Vessel Code, the allowable number of cycles for an alternating stress intensity amplitude of 56,849 psi is 16,627, or 233% more than the 5,000 cycles conservatively considered herein.

2.1.2.2.2 Normal Vibration Over the Road

Fatigue associated with normal vibration over the road is addressed in [Section 2.6.5, Vibration](#).

2.1.2.2.3 Extreme Total Stress Intensity Range

Per paragraph C.7 of Regulatory Guide 7.6:

The extreme total stress intensity range (including stress concentrations) between the initial state, the fabrication state, the normal operating conditions, and the accident conditions should be less

⁹ American Society of Mechanical Engineers (ASME) Boiler and Pressure Vessel Code, Section III, *Rules for Construction of Nuclear Power Plant Components*, Appendix I, *Design Stress Intensity Values, Allowable Stresses, Material Properties, and Design Fatigue Curves*, 1995 Edition, 1997 Addenda.

than twice the adjusted value (adjusted to account for modulus of elasticity at the highest temperature) of S_a at 10 cycles given by the appropriate design fatigue curves.

Since the response of the HalfPACT package to accident conditions is typically evaluated empirically rather than analytically, the extreme total stress intensity range has not been quantified. However, the full scale certification test unit (see [Appendix 2.10.3, Certification Tests](#)) was tested at relatively low ambient temperatures during free drop and puncture testing, as well as exposure to a fully engulfing pool fire event. The CTU was also fabricated in accordance with the drawings in [Appendix 1.3.1, Packaging General Arrangement Drawings](#), thus incurring prototypic fabrication induced stresses, increased internal pressure equal to 150% of MNOP during fabrication pressure testing, and reduced internal pressure (i.e., a full vacuum during leak testing) conditions as part of initial acceptance. Exposure to these extreme conditions while demonstrating two levels of leaktight containment resulting from certification testing satisfy the intent of the previously defined extreme total stress intensity range requirement.

2.1.2.2.3 Buckling Assessment

Buckling, per Regulatory Guide 7.6, is an unacceptable failure mode for the containment vessels. The intent of this provision is to preclude large deformations that would compromise the validity of linear analysis assumptions and quasi-linear stress allowables, as given in Paragraph C.6 of Regulatory Guide 7.6.

Buckling prevention criteria are applicable to both the OCV and ICV containment boundaries within the HalfPACT packaging. Both containment vessel shells incorporate cylindrical mid-sections with torispherical heads at each end. The different geometric regions are considered separately to demonstrate that buckling will not occur for the two containment shells. The methodology of ASME Boiler and Pressure Vessel Code Case N-284-1¹⁰ is applied for the cylindrical regions of the containment vessels (buckling analysis details are provided in [Section 2.7.6, Immersion – All Packages](#)). The methodology of the ASME Boiler and Pressure Vessel Code, Section III, Subsection NE, is applied for the torispherical heads.

Consistent with Regulatory Guide 7.6 philosophy, factors of safety corresponding to ASME Boiler and Pressure Vessel Code, Level A and Level D service conditions are employed for NCT and HAC loadings, respectively, with factors of safety of 2.00 and 1.34, respectively.

It is also noted that 30 foot drop tests performed on full scale models with the package in various orientations produced no evidence of buckling of any of the containment boundary shells (see [Appendix 2.10.3, Certification Tests](#)). Certification testing does not provide a specific determination of the margin of safety against buckling, but is considered as evidence that buckling will not occur.

¹⁰ American Society of Mechanical Engineers (ASME) Boiler and Pressure Vessel Code, Section III, *Rules for Construction of Nuclear Power Plant Components*, Division 1, Class MC, Code Case N-284-1, *Metal Containment Shell Buckling Design Methods*, 1995 Edition, 1997 Addenda.

Table 2.1-1 – Containment Structure Allowable Stress Limits

Stress Category	NCT	HAC
General Primary Membrane Stress Intensity	S_m	Lesser of: $2.4S_m$ $0.7S_u$
Local Primary Membrane Stress Intensity	$1.5S_m$	Lesser of: $3.6S_m$ S_u
Primary Membrane + Bending Stress Intensity	$1.5S_m$	Lesser of: $3.6S_m$ S_u
Range of Primary + Secondary Stress Intensity	$3.0S_m$	Not Applicable
Pure Shear Stress	$0.6S_m$	$0.42S_u$
Peak	Per Section 2.1.2.2.2 , <i>Fatigue Assessment</i>	
Buckling	Per Section 2.1.2.2.3 , <i>Buckling Assessment</i>	

Table 2.1-2 – Non-Containment Structure Allowable Stress Limits

Stress Category	NCT	HAC
General Primary Membrane Stress Intensity	Greater of: S_m S_y	$0.7S_u$
Local Primary Membrane Stress Intensity	Greater of: $1.5S_m$ S_y	S_u
Primary Membrane + Bending Stress Intensity	Greater of: $1.5S_m$ S_y	S_u
Range of Primary + Secondary Stress Intensity	Greater of: $3.0S_m$ S_y	Not Applicable
Pure Shear Stress	Greater of: $0.6S_m$ $0.6S_y$	$0.42S_u$
Peak	Per Section 2.1.2.2.2 , <i>Fatigue Assessment</i>	
Buckling	Per Section 2.1.2.2.3 , <i>Buckling Assessment</i>	

This page intentionally left blank.

2.2 Weights and Centers of Gravity

The maximum gross weight of the HalfPACT package, including a maximum payload weight of 7,600 pounds, is 18,100 pounds. The vertical center of gravity (CG) is situated 43.8 inches above the bottom surface of the package. These values are used in the lifting and tie-down calculations presented in [Section 2.5, *Lifting and Tie-down Standards for All Packages*](#). These results are based on an assumption of a payload configuration consisting of seven, 1,000 pound, 55-gallon drums having their individual CGs located at the drum mid-height. All other payload configurations result in a lower, package gross weight and CG than the 55-gallon drum payload configuration. With reference to [Figure 2.2-1](#), a detailed breakdown of the HalfPACT package component weights and CG is summarized in [Table 2.2-1](#). The five inch thick payload spacer is used with the 55-gallon drum, short 85-gallon drum, 100-gallon drum, and standard waste box (SWB) payload configurations. The shielded container payload configuration utilizes a triangular payload pallet, an upper and lower axial dunnage assembly, and a radial dunnage assembly in lieu of the payload pallet and payload spacer utilized for drums and the SWB.

2.2.1 Effect of a Radial Payload Imbalance

A radial offset of the CG could occur if the payload drums do not all have the same weight, or if the SWB is not uniformly loaded. The maximum offset of the radial CG is calculated in the following paragraphs.

Seven 55-Gallon Drum Payload Configuration:

Since the maximum weight of any one drum is 1,000 pounds, and since the arrangement of seven drums is symmetric, the maximum payload weight can be associated only with a payload CG located on the package centerline. Deviation from the package centerline can only occur with a less-than-maximum total payload weight. The worst case CG offset occurs for an arrangement of four minimum weight (empty) 55-gallon drums, each having a weight of 60 pounds, together with three maximum weight (fully loaded) 55-gallon drums, each having a weight of 1,000 pounds, located in adjacent outside positions, as illustrated in [Figure 2.2-2](#). A 55-gallon drum has a nominal outer diameter of 24 inches. For this case, the worst case radial location of the payload CG is:

$$\bar{r} = \frac{(24.00)(1,000) + (2)(12.00)(1,000) + (0)(60) - 2(12.00)(60) - (24.00)(60)}{3(1,000) + 4(60)} = 13.93 \text{ inches}$$

The pipe overpack payload configurations, since they are enclosed and centered by dunnage within a 55-gallon drum, are enveloped by the foregoing considerations. For an empty package weight of 10,500 pounds, a payload pallet weight of 350 pounds, and a payload spacer weight of 250 pounds, (see [Table 2.2-1](#)), the worst case radial offset of the CG of the entire HalfPACT package is:

$$\bar{R} = \frac{(13.93)[3(1,000) + 4(60)]}{10,500 + 350 + 250 + 3(1,000) + 4(60)} = 3.15 \text{ inches}$$

This radial offset equates to only 3.3% of the HalfPACT package's outer diameter of 94³/₈ inches. The effect of this relatively small radial offset may be neglected.

Standard Waste Box Payload Configuration:

The maximum weight of a loaded SWB is 4,000 pounds; the weight of an empty SWB is 640 pounds. The maximum contents therefore amount to $4,000 - 640 = 3,360$ pounds. The CG of the contents is conservatively assumed to be located at a distance of 17.75 inches from the geometric center (i.e., one-quarter the SWB length), as shown in [Figure 2.2-3](#). For this case, the worst case radial location of the payload CG is:

$$\bar{r} = \frac{(17.75)(3,360)}{4,000} = 14.9 \text{ inches}$$

For an empty package weight of 10,500 pounds and a payload spacer weight of 250 pounds, (see [Table 2.2-1](#)), the maximum radial offset of the CG of the entire HalfPACT is:

$$\bar{R} = \frac{(14.9)(4,000)}{10,500 + 250 + 4,000} = 4.04 \text{ inches}$$

This radial offset equates to only 4.3% of the HalfPACT package's outer diameter of $94\frac{3}{8}$ inches. As before, the effect of this relatively small radial offset may be neglected.

Four 85-Gallon Drum Payload Configuration:

The term "85-gallon drum" refers to drums of 75 to 88 gallons, as discussed in [Section 1.1, Introduction](#). As for the 55-gallon drum payload configuration, the maximum weight of a loaded 85-gallon drum is 1,000 pounds. The worst case CG offset occurs for an arrangement of two minimum weight (empty), tall 85-gallon drums, each having a weight of approximately 81 pounds, together with two maximum weight (fully loaded), tall 85-gallon drums, each having a weight of 1,000 pounds, located adjacent, as illustrated in [Figure 2.2-4](#). A tall 85-gallon drum has a nominal outer diameter of $28\frac{3}{8}$ inches. For this case, the worst case radial location of the payload CG is:

$$\bar{r} = \frac{2(14.31)(1,000) - 2(14.31)(81)}{2(1,000) + 2(81)} = 12.2 \text{ inches}$$

For an empty package weight of 10,500 pounds, a payload pallet weight of 350 pounds, and a payload spacer weight of 250 pounds, (see [Table 2.2-1](#)), the maximum radial offset of the CG of the entire HalfPACT is:

$$\bar{R} = \frac{(12.2)[2(1,000) + 2(81)]}{10,500 + 350 + 2(1,000) + 2(81)} = 2.03 \text{ inches}$$

This radial offset equates to only 2.1% of the HalfPACT package's outer diameter of $94\frac{3}{8}$ inches. As before, the effect of this relatively small radial offset may be neglected.

Three 100-Gallon Drum Payload Configuration:

As for the 55-gallon drum payload configuration, the maximum weight of a loaded 100-gallon drum is 1,000 pounds. The worst case CG offset occurs for an arrangement of two minimum weight (empty), 100-gallon drums, each having a weight of 95 pounds, together with one maximum weight (fully loaded), 100-gallon drum of 1,000 pounds, as illustrated in [Figure 2.2-5](#).

A 100-gallon drum has a nominal outer diameter of 32 inches. For this case, the worst case radial location of the payload CG is:

$$\bar{r} = \frac{(18.48)(1,000) - 2(9.24)(95)}{1,000 + 2(95)} = 14.1 \text{ inches}$$

For an empty package weight of 10,500 pounds, a payload pallet weight of 350 pounds, and a payload spacer weight of 250 pounds, (see [Table 2.2-1](#)), the maximum radial offset of the CG of the entire HalfPACT is:

$$\bar{R} = \frac{(14.1)[1,000 + 2(95)]}{10,500 + 350 + 250 + 1,000 + 2(95)} = 1.37 \text{ inches}$$

This radial offset equates to only 1.5% of the HalfPACT package's outer diameter of 94³/₈ inches. As before, the effect of this relatively small radial offset may be neglected.

Three Shielded Container Payload Configuration:

The maximum weight of a loaded shielded container is 2,260 pounds; the weight of an empty shielded container is 1,726 pounds. The worst case CG offset occurs for an arrangement of two minimum weight (empty), shielded containers, each having a weight of 1,726 pounds, together with one maximum weight (fully loaded), shielded container of 2,260 pounds, as illustrated in [Figure 2.2-6](#). A shielded container has a nominal outer diameter of 23 inches. For this case, the worst case radial location of the payload CG is:

$$\bar{r} = \frac{(13.28)(2,260) - 2(6.64)(1,726)}{2,260 + 2(1,726)} = 1.24 \text{ inches}$$

For an empty package weight of 10,500 pounds, a triangular payload pallet weight of 112 pounds, an upper and lower axial dunnage weight of 132 pounds each, and a radial dunnage weight of 444 pounds, (see [Table 2.2-1](#)), the maximum radial offset of the CG of the entire HalfPACT is:

$$\bar{R} = \frac{(1.24)[2,260 + 2(1,726)]}{10,500 + 112 + 2(132) + 444 + 2,260 + 2(1,726)} = 0.42 \text{ inches}$$

This radial offset equates to only 0.4% of the HalfPACT package's outer diameter of 94³/₈ inches. As before, the effect of this relatively small radial offset may be neglected.

2.2.2 Effect of an Axial Payload Imbalance

The maximum height of the package CG is associated with a uniformly loaded payload, where the CG of the payload containers is located at their mid-height. Due to a payload of non-uniform density or possible settling of the payload contents, the CG height of the payload containers may decrease somewhat. The seven 55-gallon drum payload configuration, since it is the heaviest payload, will result in greatest potential shift in axial CG. The greatest shift in location of the CG of an individual drum is bounded by one-quarter of the drum height, i.e., a shift from the drum mid-height to the quarter height. Thus, for a total 55-gallon drum height of 35 inches, the

axial shift is $35/4 = 8.75$ inches downward. Since the empty weight of a 55-gallon drum is 60 pounds, the maximum weight of contents of one drum is $1,000 - 60 = 940$ pounds. The greatest downward shift in CG location of the HalfPACT packaging, assuming the CG location of all seven drums is at one quarter of the drum height instead of at mid-height, therefore is:

$$\Delta \bar{h} = \frac{7(8.75)(940)}{18,100} = 3.2 \text{ inches}$$

The axial offset amounts to only 3.5% of the total HalfPACT package height of $91\frac{1}{2}$ inches. The effect of this relatively small axial offset may be neglected. As an example, in the case of a hypothetical accident condition (HAC) puncture event where the puncture bar axis passes through the CG of the HalfPACT package, the variation in CG location of 3.2 inches slightly exceeds half the puncture bar diameter resulting in a variation of the puncture bar orientation of less than 4 degrees. In addition, vertical reduction of the CG would have no effect on lifting forces, and would serve to reduce tie-down forces. Therefore, the lifting and tie-down calculations, and the HAC free drop and puncture tests, are performed using a value that bounds the maximum CG height presented in [Table 2.2-1](#), and the downward axial offset is conservatively neglected.

Table 2.2-1 – HalfPACT Weight and Center of Gravity

Item	Weight, pounds		Height to CG, inches ^①	
	Component	Assembly	Component	Assembly
Outer Containment Assembly (OCA)		8,250		41.2
Lid	3,600		67.1	
Body	4,650		21.2	
Inner Containment Vessel (ICV)		2,250		47.3
Lid	825		66.5	
Body	1,225		34.9	
Aluminum Honeycomb Spacers	200		43.5	
Total Empty Package		10,500		42.5
Payload and Payload Components		7,600		45.5
Payload (Seven 55-Gallon Drums)	7,000		46.6	
Payload Pallet	350		40.2	
Payload Spacer	250		23.6	
Total Loaded Package (Maximum)		18,100		43.8
Payload and Payload Components		7,600		44.2
Payload (Three Shielded Containers)	6,780		44.5	
Triangular Payload Pallet	112		25.1	
Axial Dunnage Assemblies	264		43.0	
Radial Dunnage Assembly	444		44.5	
Total Load Package (Maximum)		18,100		43.2

Note:

① The reference datum is the bottom of the HalfPACT package.

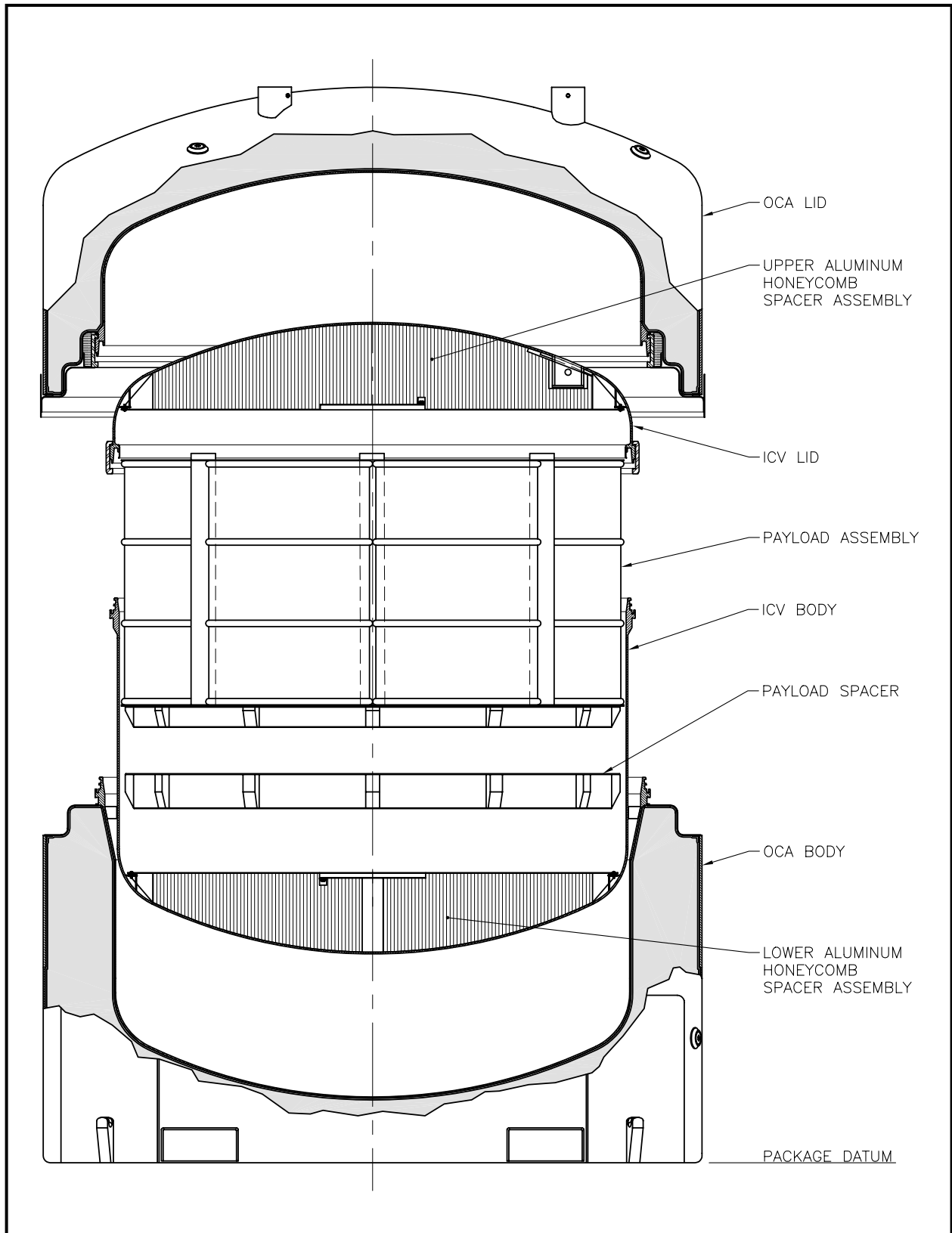


Figure 2.2-1 – HalfPACT Package Components

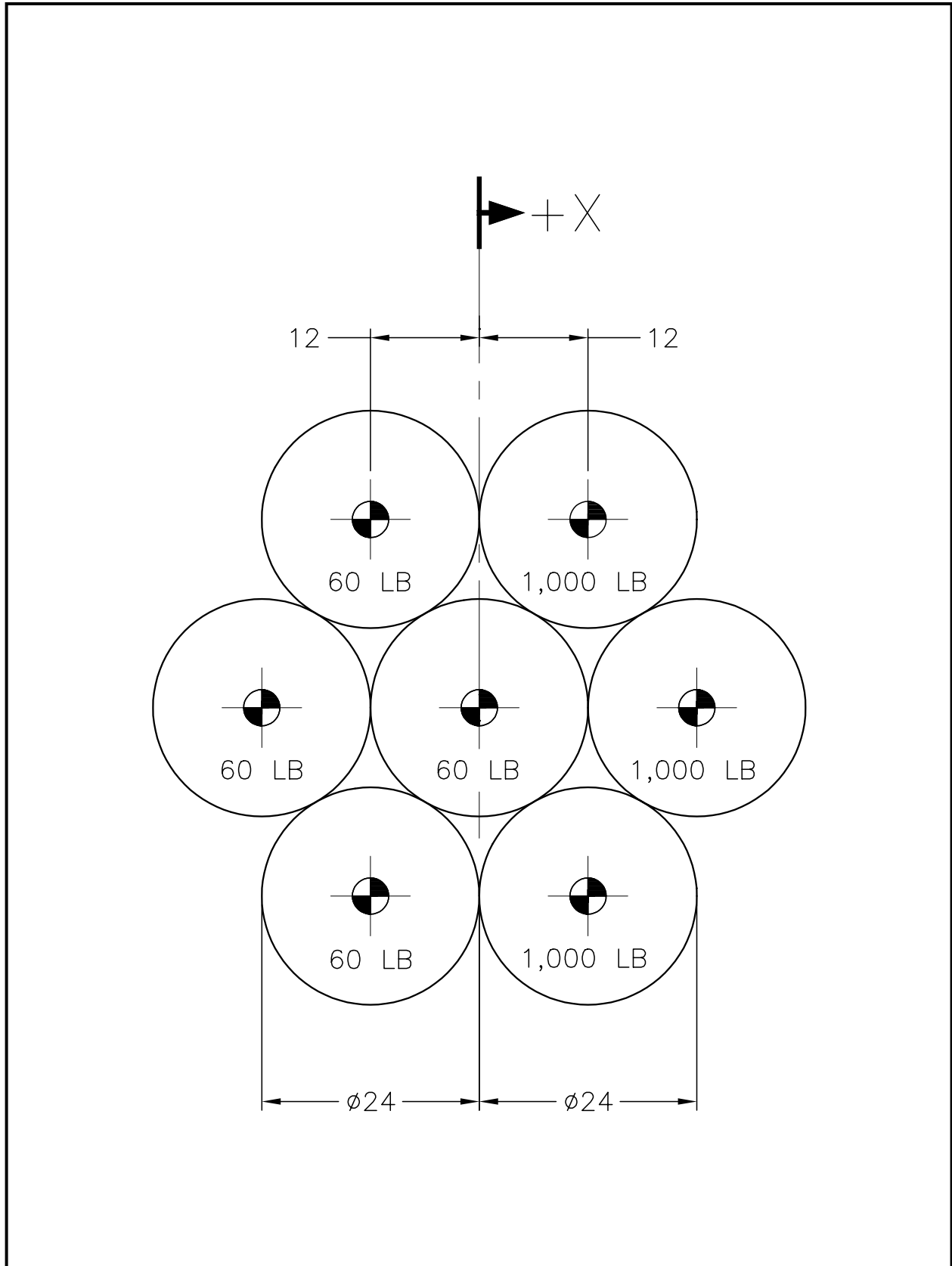


Figure 2.2-2 – Radial Shift of CG for Seven 55-Gallon Drum Payload

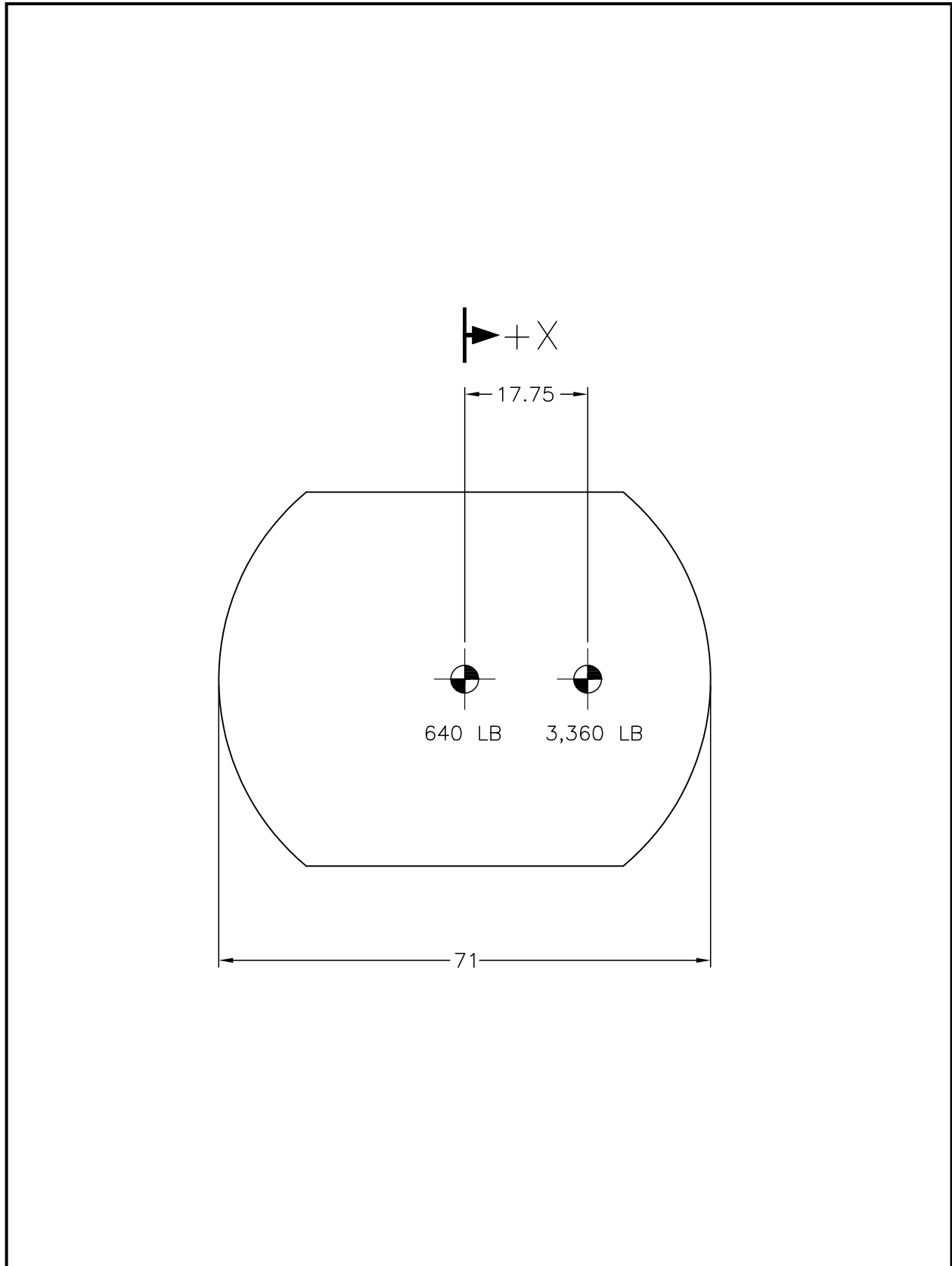


Figure 2.2-3 – Radial Shift of CG for SWB Payload

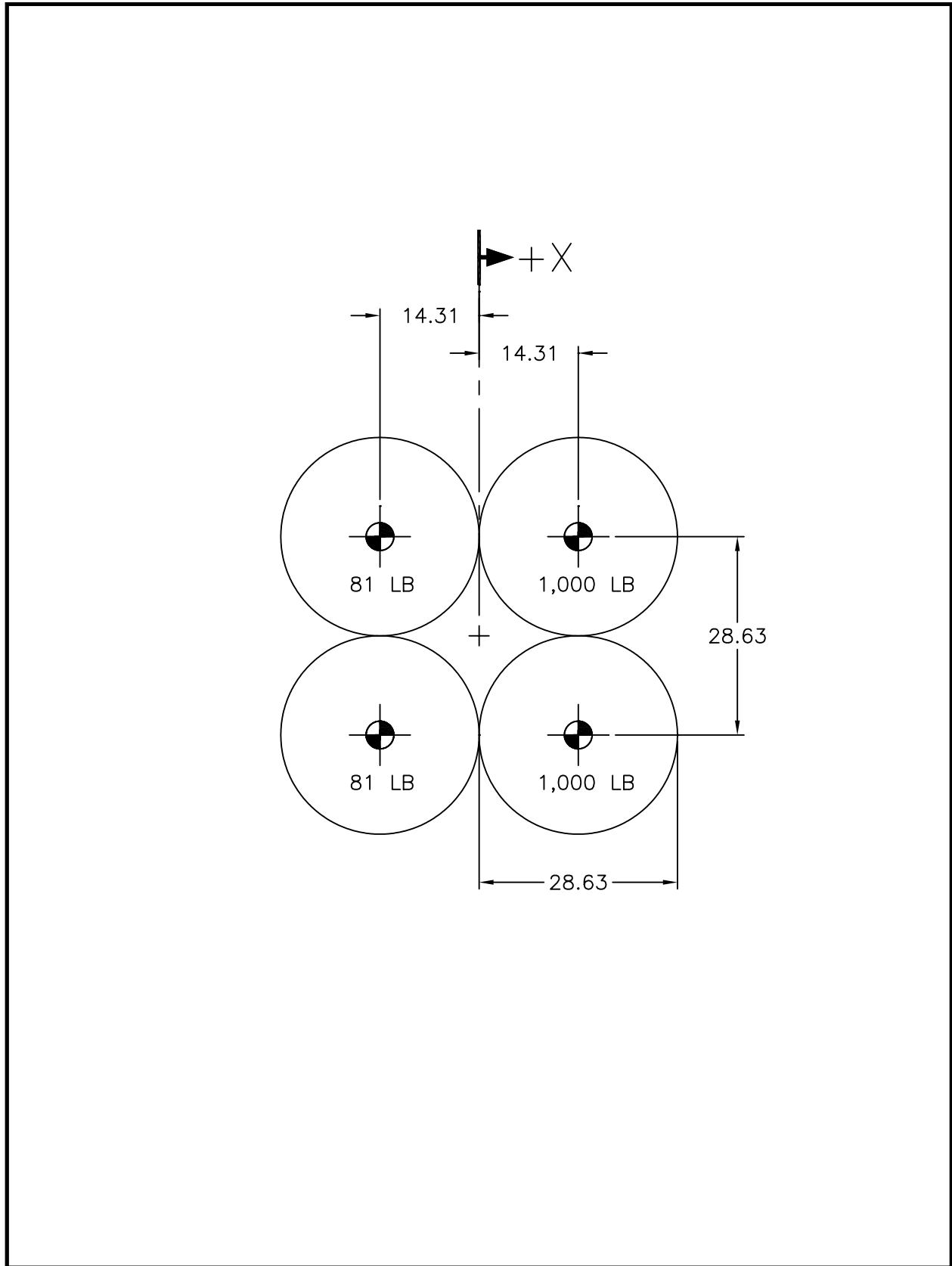


Figure 2.2-4 – Radial Shift of CG for Four 85-Gallon Drum Payload

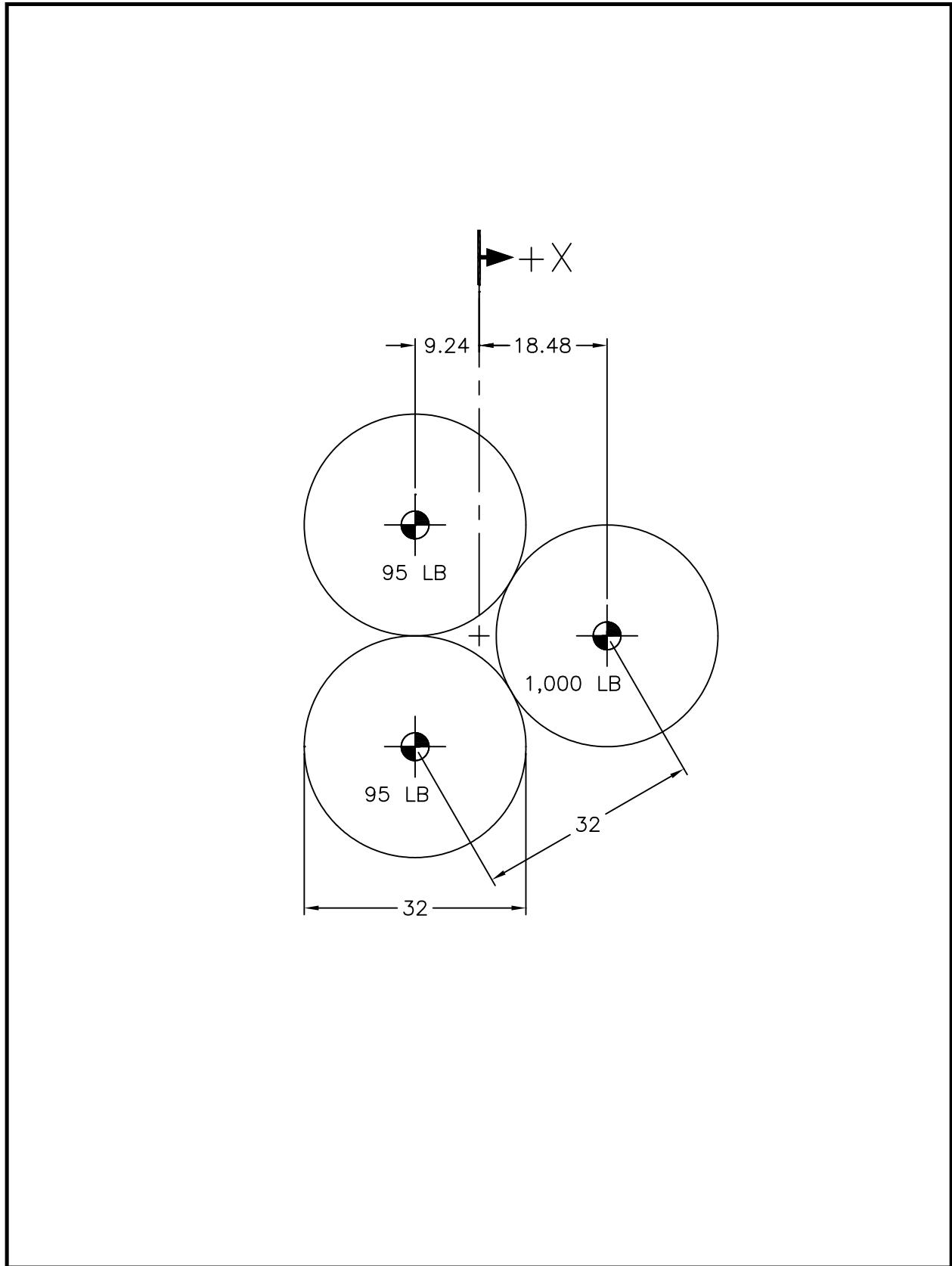


Figure 2.2-5 – Radial Shift of CG for Three 100-Gallon Drum Payload

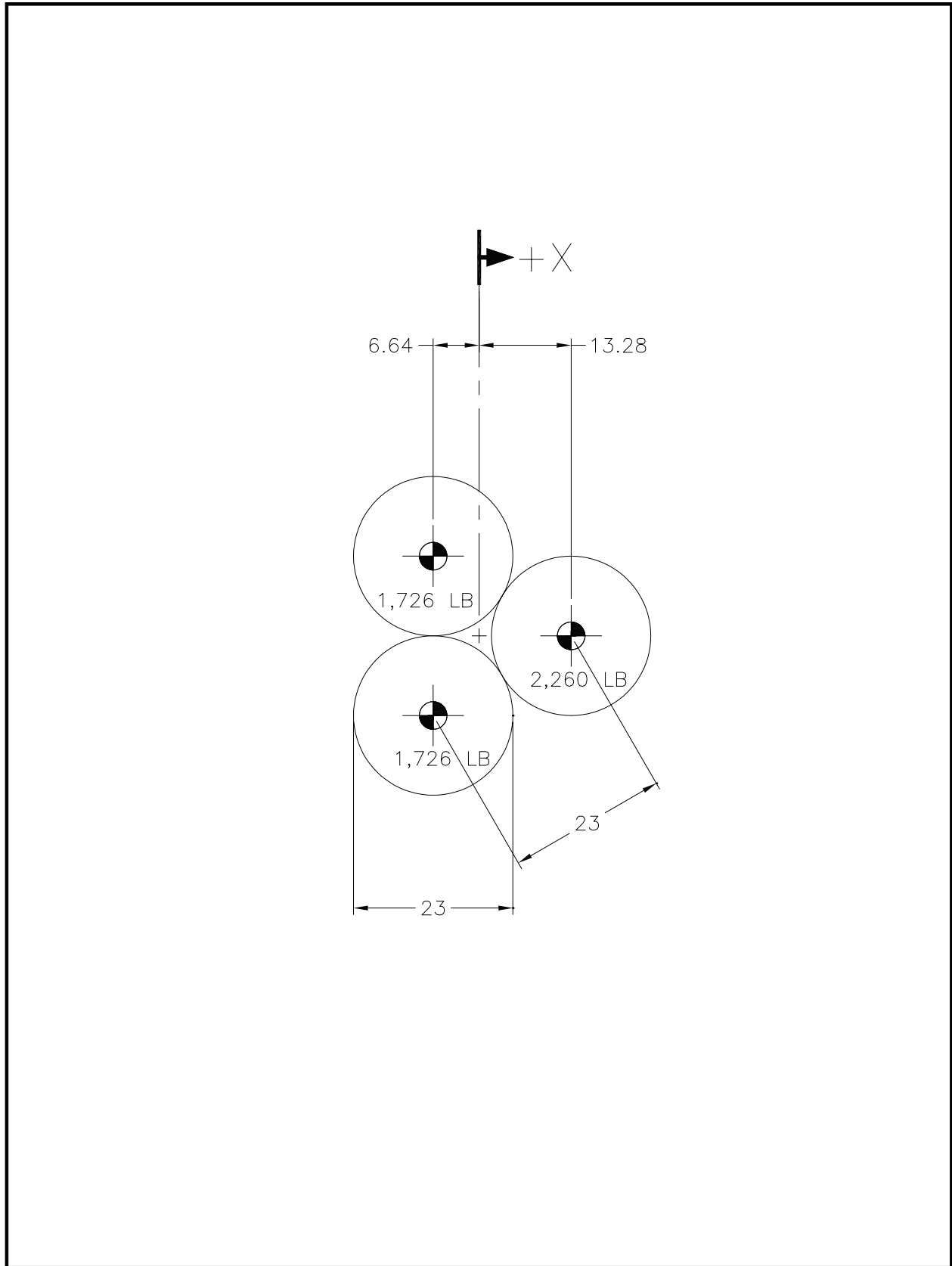


Figure 2.2-6 – Radial Shift of CG for Three Shielded Container Payload

This page intentionally left blank.

2.3 Mechanical Properties of Materials

The major structural components, i.e., the outer containment assembly (OCA) outer shells, outer containment vessel (OCV), and inner containment vessel (ICV), of the HalfPACT packaging are fabricated of Type 304, austenitic stainless steel and 8¼ lb/ft³ (nominal density) polyurethane foam. Other materials performing a structural function are ASTM B16 brass (for the ICV and OCV vent port and seal test port plugs and covers), aluminum honeycomb (for the ICV aluminum honeycomb spacer assemblies), 300 series stainless steel (for the ICV and OCV locking ring lock bolts, and for attaching the locking Z-flange to the OCV locking ring), and ASTM A564, Type 630, stainless steel (joint pins for the OCV and ICV locking rings). Several varieties of non-structural materials are also utilized. Representative non-structural materials include butyl rubber and other elastomeric O-ring seals, a silicone wear pad, aluminum guide tubes for the OCA lid lift operation, ceramic fiber paper, fiberglass insulation, and plastic fire consumable foam cavity vent plugs. The drawings presented in [Appendix 1.3.1, *Packaging General Arrangement Drawings*](#), delineate the specific material(s) used for each HalfPACT packaging component.

The remainder of this section presents and discusses pertinent mechanical properties for the materials that perform a structural function. [Section 2.3.1, *Mechanical Properties Applied to Analytic Evaluations*](#), presents all properties used in analytic structural evaluations of the HalfPACT package. Most normal conditions of transport (NCT) tests are demonstrated analytically. [Section 2.3.2, *Mechanical Properties Applied to Certification Testing*](#), presents the mechanical properties associated with components whose performance is demonstrated via certification testing. With the exception of immersion, all hypothetical accident condition (HAC) tests are demonstrated via certification testing.

2.3.1 Mechanical Properties Applied to Analytic Evaluations

Analytic evaluations are performed for the basic OCA, OCV, and ICV shells, seal flanges, and locking rings, comprised of Type 304 stainless steel. [Table 2.3-1](#) presents the mechanical properties for the Type 304 stainless steel used in the HalfPACT packaging. Each of the mechanical properties of Type 304 stainless steel is taken from Section II, Parts A and D, of the ASME Boiler and Pressure Vessel Code.¹

All analyses of the basic OCA, OCV, and ICV shells, seal flanges and locking rings utilize the properties presented for ASTM A240, Type 304, stainless steel. With the exception of elongation, which is not specifically used in the linear elastic analytic assessments, all materials presented in [Table 2.3-1](#) exhibit equivalent or better properties than the ASTM A240 material. Minimum elongation values are important regarding testing and are therefore discussed in [Section 2.3.2, *Mechanical Properties Applied to Certification Testing*](#). The density of stainless steel is taken as 0.29 lb/in³, and Poisson's Ratio is 0.3.

Unlike the other ASTM materials specified in [Table 2.3-1](#), ASTM A276 material does not have an identical ASME material specification. However, structural use of ASTM A276 is as an

¹ American Society of Mechanical Engineers (ASME) Boiler and Pressure Vessel Code, Section II, *Materials, Part A – Ferrous Material Specifications*, and *Materials, Part D – Properties*, 1995 Edition, 1997 Addenda.

option for the OCA rolled angles used at the lid-to-body interface and the OCA lid lifting straps. As these components are not part of the containment boundary, the use of ASTM A276, whose chemical and mechanical properties are identical to ASTM A479, is justified. Thus, material properties of ASTM A276 versus temperature are taken to be the same as for ASTM A479.

The analytic assessments of the polyurethane foam used in the HalfPACT packaging are limited to the NCT internal pressure, differential thermal expansion, and lifting load cases. The data summarized in [Table 2.3-2](#) are established according to the procedures outlined in [Section 8.1.4.1, *Polyurethane Foam*](#). Detailed stress-strain relationships for the polyurethane foam are not required for analysis since analytic assessments for the NCT or HAC free drop or puncture events are not performed. However, as discussed in [Section 2.3.2, *Mechanical Properties Applied to Certification Testing*](#), since HalfPACT package performance is demonstrated by certification testing, and performance is a function of foam properties, compressive stress-strain characteristics and installation techniques are carefully controlled.

Material properties are linearly interpolated between, or, if necessary, extrapolated beyond the temperature values shown. For example, when a temperature outside a tabulated range is of interest (e.g., low temperature properties to -40 °F), data are extrapolated. When a particular analysis requires data extrapolation, it is identified within the applicable section of this chapter.

2.3.2 Mechanical Properties Applied to Certification Testing

The primary means of demonstrating the structural performance capabilities of the HalfPACT packaging under imposed NCT and HAC free drops, puncture, and thermal (fire) events is via certification testing. The overall response of the HalfPACT packaging to these events is dependent on the characteristics of several structural components. The characteristics of the polyurethane foam used in the OCA are of primary importance regarding HalfPACT package performance. For this reason, the method of installation of the foam material into the OCA, and the foam's compressive stress-strain characteristics are carefully controlled and monitored. [Section 8.1.4.1, *Polyurethane Foam*](#), presents the details associated with foam installation and performance testing. Importantly, all HalfPACT packages will respond similarly to free drop, puncture, and thermal events. Thermal performance of the foam is discussed in [Section 3.2, *Summary of Thermal Properties of Materials*](#).

At the time of polyurethane foam installation, test samples are retained from each foam pour, as discussed in [Section 8.1.4.1, *Polyurethane Foam*](#). Using these samples, each foam pour is tested for compressive strength at strains of 10%, 40%, and 70%, both parallel and perpendicular to the direction of foam rise. To be acceptable, the average compressive strength of all tested samples from a single foamed component (i.e., the OCA lid or OCA body) for a particular rise direction is to fall within $\pm 15\%$ of the corresponding nominal compressive stress. Additionally, the stress value of any single test specimen from a single pour is to fall within $\pm 20\%$ of the corresponding nominal compressive stress.

In addition to controls on foam compressive stress, OCA foam thicknesses are controlled by the tolerances shown on the drawings provided in [Appendix 1.3.1, *Packaging General Arrangement Drawings*](#). The foam thickness tolerance at the OCA top and sides is set at approximately $\pm 5\%$ of the nominal thickness. In regions where foam strains are very small (e.g., bottom end), a slightly greater thickness tolerance (approximately $\pm 8\%$) is allowed. The thickness tolerance is set at approximately one-third the magnitude of the compressive stress tolerance to minimize the effect

on package performance in the unlikely event that both tolerances are simultaneously at their extreme values in a given HalfPACT packaging assembly. Importantly, in the unlikely event that compressive stress and thickness tolerances are simultaneously at their worst case extremes, the net effect of combining the two tolerances is nearly identical to the compressive stress tolerance acting alone. This is directly attributable to the fact that a long portion of the compressive stress-strain curve for foam (at strains of ~50% or less) exhibits a relatively shallow slope (i.e., “plateau”). Consequently, although small changes in foam thickness directly affect foam strains, small changes in strain while on the plateau portion of the stress-strain curve do not significantly affect stress. As demonstrated by testing (documented in [Appendix 2.10.3, Certification Tests](#)), the HalfPACT packaging deformations due to 30 foot free drops were relatively small, demonstrating that resultant foam strains remained within the “plateau” portion of the compressive stress-strain curve.

In addition to the polyurethane foam, the performance of other primary HalfPACT packaging structural components is addressed by certification testing rather than by analysis. These components include the ASTM B16, Alloy 360, half-hard temper, brass vent port plugs, the ICV upper and lower aluminum honeycomb spacer assemblies, the 300 series stainless steel socket head cap screws used to secure the locking rings in the locked position, the ASTM A564, Type 630, Condition 1150, stainless steel pins used in the locking ring joints, and the 1/4 inch, 300 series stainless steel pan head screws used to attach the locking Z-flange to the OCV locking ring. As indicated above, and on the drawings provided in [Appendix 1.3.1, Packaging General Arrangement Drawings](#), each of these components has a specific material callout thereby providing a specific control on its mechanical properties. The structurally significant mechanical properties for these materials are presented in [Table 2.3-3](#).

With the exception of the aluminum honeycomb spacer assemblies, the 1/4 inch stainless steel pan head screws, and the OCV lock bolts, all of the above components remained intact during certification testing, and showed essentially no evidence of distress. By design, the aluminum honeycomb spacer assemblies were partially crushed as a result of the certification test program, but still provided adequate protection for the ICV torispherical heads from the simulated payload of seven, rigid, concrete-filled, 55-gallon drums.

The optional use of Type 304 stainless steel forgings or castings instead of ASTM A240 plate material for the OCV and ICV seal flanges and locking rings is stated on the drawings provided in [Appendix 1.3.1, Packaging General Arrangement Drawings](#). As shown in [Table 2.3-1](#), the ASTM A182 forging option and ASTM A351 casting option provide equivalent or improved strength, but a somewhat reduced elongation than does the ASTM A240. The reduced elongation values (30% for ASTM A182 and 35% for ASTM A351 versus 40% for ASTM A240 material) are acceptable based on the results of the certification testing program. Relatively little permanent deformation was observed for the OCV or ICV seal flanges and locking rings as a result of certification testing, indicating that strains were well below the 30% minimum elongation provided by any of the specified materials. Any of the three material options are therefore acceptable for fabricating HalfPACT packagings.

This page intentionally left blank.

Table 2.3-1 – Mechanical Properties of Type 304 Stainless Steel Components (for Analysis)

Material Specification	① Minimum Elongation (%)	Temperature (°F)	② Yield Strength, S_y ($\times 10^3$ psi)	③ Ultimate Strength, S_u ($\times 10^3$ psi)	④ Allowable Strength, S_m ($\times 10^3$ psi)	⑤ Elastic Modulus, E ($\times 10^6$ psi)	⑥ Thermal Expansion Coefficient, α ($\times 10^{-6}$ in/in/°F)
ASTM A213	35	≤ -20	30.0	75.0	20.0	28.8 ^⑦	8.21 ^⑦
ASTM A240	40	70	30.0	75.0	20.0	28.3	-----
ASTM A312	30	100	30.0	75.0	20.0	-----	8.55
ASTM A376	25	200	25.0	71.0	20.0	27.6	8.79
ASTM A479	30	300	22.5	66.0	20.0	27.0	9.00
Type 304		400	20.7	64.4	18.7	26.5	9.19
ASTM A182 Type F304 (<5 inch thick)	30	-20	30.0	75.0	20.0	28.8 ^⑦	8.21 ^⑦
		70	30.0	75.0	20.0	28.3	-----
		100	30.0	75.0	20.0	-----	8.55
		200	25.0	71.0	20.0	27.6	8.79
		300	22.5	66.0	20.0	27.0	9.00
400	20.7	64.4	18.7	26.5	9.19		
ASTM A351 Grade CF8A	35	-20	35.0	77.0	23.3	28.8 ^⑦	8.21 ^⑦
		70	35.0	77.0	23.3	28.3	-----
		100	35.0	77.0	23.3	-----	8.55
		200	29.1	72.8	23.3	27.6	8.79
		300	26.3	67.8	22.6	27.0	9.00
400	24.2	66.1	21.8	26.5	9.19		

Notes: ① ASME Code, Section II, Part A.

② ASME Code, Section II, Part D, Table Y-1.

③ ASME Code, Section II, Part D, Table U.

⑦ Interpolated/extrapolated

④ ASME Code, Section II, Part D, Table 2A.

⑤ ASME Code, Section II, Part D, Table TM-1, Material Group G.

⑥ ASME Code, Section II, Part D, Table TE-1, 18Cr-8Ni, Coefficient B.

This page intentionally left blank.

Table 2.3-2 – Mechanical Properties of Polyurethane Foam (for Analysis)

Property	Direction	Nominal Room Temperature Value
Compressive Strength, S	Axial (Parallel-to-Rise)	235 psi
	Radial (Perpendicular-to-Rise)	195 psi
Compressive Modulus, E	Axial (Parallel-to-Rise)	6,810 psi
	Radial (Perpendicular-to-Rise)	4,773 psi
Thermal Expansion Coefficient, α	-----	3.5×10^{-5} in/in/°F
Poisson's Ratio, ν	-----	0.33
Density, ρ	-----	8.25 lb/ft ³

Table 2.3-3 – Mechanical Properties of Metallic Materials (for Testing)

Material	Minimum Mechanical Properties (unless otherwise specified)	Notes
ASTM B16, Alloy 360 Brass, Half-Hard Temper	$\sigma_y = 25,000$ psi $\sigma_u = 55,000$ psi	-----
Hexcel ACG-3/8-.003-3.6P Aluminum Honeycomb	$\sigma_{bc} = 340$ psi $\pm 15\%$ (Bare Compressive Strength) $\sigma_c = 120$ psi $\pm 15\%$ (Crush Strength)	①
300 Series Stainless Steel Socket Head Cap Screws	$\sigma_y = 40,000$ psi $\sigma_u = 80,000$ psi	②
ASTM A564, Type 630, Condition 1150, Stainless Steel	$\sigma_y = 105,000$ psi $\sigma_u = 135,000$ psi	③
1/4 inch, 300 Series Stainless Steel Pan Head Screws	$\sigma_y = 30,000$ psi $\sigma_u = 75,000$ psi	④

Notes:

- ① *Mechanical Properties of Hexcel Honeycomb Materials*, TSB-120 (Technical Service Bulletin 120), Hexcel, 1992. The term “Bare Compressive Strength” is defined as the maximum strength that is exhibited by the honeycomb material at the onset of crushing. The term “Crush Strength” is defined as the average compressive strength that is sustained as the honeycomb material undergoes crushing.
- ② UNBRAKO Socket Screw Products Catalog, Copyright 1988, SPS Technologies.
- ③ ASME Code, Section II, Part D, Table 2A, 1995 Edition, 1997 Addenda.
- ④ Industrial Fasteners Institute, *Fastener Standard*, Fifth Edition.

This page intentionally left blank.

2.4 General Standards for All Packages

This section defines the general standards for all packages. The HalfPACT package, with an outer containment vessel (OCV) that is integral to an outer containment assembly (OCA) for primary containment, and an inner containment vessel (ICV) for secondary containment, meets all requirements delineated for this section.

2.4.1 Minimum Package Size

The minimum transverse dimension (i.e., the diameter) of the HalfPACT package is 94 $\frac{3}{8}$ inches, and the minimum longitudinal dimension (i.e., the height) is 91 $\frac{1}{2}$ inches. Thus, the requirement of 10 CFR §71.43(a)¹ is satisfied.

2.4.2 Tamper-indicating Feature

Tamper-indicating seals are installed at one OCA lock bolt location and at the OCV vent port access plug, as delineated on the drawings in [Appendix 1.3.1, *Packaging General Arrangement Drawings*](#). A lock wire device is used between two tie-points. For the OCV lock bolt, the tie-points are the bolt head and the locking Z-flange. The two tie-points for the OCV vent port access plug are the plug itself and a bolt tapped and welded to the OCA body outer shell. Failure of either tamper-indicating device provides evidence of possible unauthorized access. Thus, the requirement of 10 CFR §71.43(b) is satisfied.

2.4.3 Positive Closure

The HalfPACT package cannot be opened unintentionally. Both the OCA and ICV lids are attached to their respective bodies with locking rings. The OCV locking ring is secured with six, 1/2-13UNC, OCA lock bolts through the attached locking Z-flange. Similarly, the ICV locking ring is secured in the locked position with three, 1/2-13UNC, ICV lock bolts. For either lid, the presence of a single, lock bolt will prevent lid removal.

The OCV vent port has three levels of protection against inadvertent opening: 1) the OCV vent port access plug, 2) the OCV vent port cover, and 3) the OCV vent port plug. Each of these components are secured via threaded fittings. The ICV vent port has two levels of protection against inadvertent opening: 1) the ICV vent port cover, and 2) the ICV vent port plug. Thus, the requirements of 10 CFR §71.43(c) are satisfied.

2.4.4 Chemical and Galvanic Reactions

The major materials of construction of the HalfPACT packaging (i.e., austenitic stainless steel, aluminum, brass, polyurethane foam, ceramic fiber paper, fiberglass insulation, butyl rubber O-ring seals and other elastomeric materials) will not have significant chemical, galvanic or other reactions in air, inert gas or water environments, thereby satisfying the requirements of 10 CFR §71.43(d). These materials have been previously used, without incident, in radioactive material (RAM) packages for transport of similar payload materials. Specifically, these

¹ Title 10, Code of Federal Regulations, Part 71 (10 CFR 71), *Packaging and Transportation of Radioactive Material*, 01-01-07 Edition.

materials of construction have been used in the TRUPACT-II package² for many years without incident, utilizing the same materials of construction and carrying identical payloads as will be carried in the HalfPACT package. A successful RAM packaging history combined with successful use of these fabrication materials in similar industrial environments ensures that the integrity of the HalfPACT package will not be compromised by any chemical, galvanic or other reactions. The materials of construction and the payload are further evaluated below for potential reactions.

2.4.4.1 Packaging Materials of Construction

The HalfPACT packaging is primarily constructed of Type 304 stainless steel. This material is highly corrosion resistant to most environments. The metallic structure of the HalfPACT packaging is composed entirely of this material and compatible 300 series weld material. The weld material and processes have been selected in accordance with the ASME Boiler and Pressure Vessel Code³ to provide as good or better material properties, including corrosion resistance, as the base material. Since both the base and weld materials are 300 series materials, they have nearly identical electrochemical potential thereby minimizing any galvanic corrosion that could occur.

The stainless steel within the OCA foam cavity is lined with a ceramic fiber paper, composed of alumina silica. This material is nonreactive with either the polyurethane foam or the stainless steel, both dry or in water. The ceramic fiber paper and the silicone adhesive are very low in free chlorides to minimize the potential for stress corrosion of the OCA structure.

The polyurethane foam that is used in the OCA is essentially identical to previously licensed transportation packagings, such as the TRUPACT-II (Docket 71-9218), NuPac 125B (Docket 71-9200), and NuPac PAS-1 (Docket 71-9184). All of these packagings have had a long and successful record of performance demonstrating that the polyurethane foam does not cause any adverse conditions with the packaging. The polyurethane foam in the OCA is a rigid, closed-cell (non-water absorbent) foam that is very low in free halogens and chlorides, as discussed in [Section 8.1.4.1, Polyurethane Foam](#). The polyurethane foam material cavity is sealed with plastic pipe plugs to preclude the entrance of moisture.

Aluminum honeycomb is used in the HalfPACT packaging for the two, ICV aluminum honeycomb spacer assemblies in the upper and lower ICV torispherical heads. Aluminum honeycomb material is used for dunnage only, and is not used as any part of the HalfPACT packaging's containment boundaries. The aluminum honeycomb is maintained at relatively low temperatures ensuring that no adverse reaction could occur at aluminum/steel interfaces that would compromise the packaging's containment integrity. Of final note, aluminum material is slightly anodic which serves to protect the stainless steel of the ICV.

The various brass fittings and plugs used in the HalfPACT packaging are very corrosion resistant. Like aluminum, brass material is slightly anodic to the stainless steel. Any damage that could occur to the brass is easily detectable since the fittings are all handled each time the HalfPACT package is loaded and unloaded.

² U.S. Department of Energy (DOE), *Safety Analysis Report for the TRUPACT-II Shipping Package*, USNRC Certificate of Compliance 71-9218, U.S. Department of Energy, Carlsbad Field Office, Carlsbad, New Mexico.

³ American Society of Mechanical Engineers (ASME) Boiler and Pressure Vessel Code, Section III, *Rules for Construction of Nuclear Power Plant Components*, 1995 Edition, 1997 Addenda.

The various elastomers (e.g., butyl rubber, polyester, silicone, etc.) that are used in the O-rings, annulus foam ring, debris shield, wear pad, etc., contain no corrosives that would react adversely affect the HalfPACT packaging. These materials are organic in nature and noncorrosive to the stainless steel containment boundaries of the HalfPACT packaging.

2.4.4.2 Payload Interaction with Packaging Materials of Construction

The materials of construction of the HalfPACT packaging are checked for compatibility with the various payload chemistries when the payloads are evaluated for chemical compatibility. All payload materials are in approved payload containers delineated in the [CH-TRAMPAC](#)⁴.

The payload is typically further confined within multiple layers of plastic for radiological health purposes. This configuration ensures that the payload material has an insignificant level of contact with the HalfPACT packaging materials of construction. However, the evaluation of compatibility is based on complete interaction of payload materials with the packaging.

The design of the HalfPACT package is for transport of CH-TRU materials and other authorized payloads that are limited in form to solid or solidified material. Corrosive materials, pressurized containers, explosives, non-radioactive pyrophorics, and liquid volumes greater than 1% are prohibited. These restrictions ensure that the waste in the payload is in a non-reactive form for safe transport in the HalfPACT package. For a comprehensive discussion defining acceptable payload properties, see the [CH-TRAMPAC](#).

2.4.5 Valves

Neither the OCV nor the ICV have valves. However, beside their respective lids, the OCV and the ICV each have a vent port penetration into their containment cavities. These vent port penetrations are sealed using threaded vent port plugs comprised of brass material. Since the ICV is entirely contained within the OCV during transport, a tamper indicating device is not necessary. Access to the OCV vent port penetration is prevented by a lockwire that secures the OCV vent port access plug, as discussed in [Section 2.4.2, Tamper-indicating Feature](#). Thus, the requirements of 10 CFR §71.43(e) are satisfied.

2.4.6 Package Design

As shown in [Chapter 2.0, Structural Evaluation](#), [Chapter 3.0, Thermal Evaluation](#), [Chapter 5.0, Shielding Evaluation](#), and [Chapter 6.0, Criticality Evaluation](#), the structural, thermal, shielding, and criticality requirements, respectively, of 10 CFR §71.43(f) are satisfied for the HalfPACT package.

2.4.7 External Temperatures

As shown in [Table 3.5-1](#) from [Section 3.5.3, Package Temperatures](#), the maximum accessible surface temperature with maximum internal decay heat load and no insolation is 102 °F. Since the maximum external temperature does not exceed 122 °F, the requirements of 10 CFR §71.43(g) are satisfied.

⁴ U.S. Department of Energy (DOE), [Contact-Handled Transuranic Waste Authorized Methods for Payload Control \(CH-TRAMPAC\)](#), U.S. Department of Energy, Carlsbad Field Office, Carlsbad, New Mexico.

2.4.8 Venting

The HalfPACT package does not include any features intended to allow continuous venting during transport. Thus, the requirements of 10 CFR §71.43(h) are satisfied.

2.5 Lifting and Tie-down Standards for All Packages

For analysis of the lifting and tie-down components of the HalfPACT packaging, material properties from [Section 2.3, *Mechanical Properties of Materials*](#), are taken at a bounding temperature of 160 °F per [Section 2.6.1.1, *Summary of Pressures and Temperatures*](#). The primary structural materials are Type 304 stainless steel, and polyurethane foam that is used in the outer containment assembly (OCA).

A loaded HalfPACT package is only lifted by fork lift pockets, located at the bottom of the OCA body. For this case, HalfPACT package lifting loads act parallel to the direction of foam rise. The nominal compressive strength of the polyurethane foam, as delineated in [Table 2.3-2 of Section 2.3.1, *Mechanical Properties Applied to Analytic Evaluations*](#), is reduced by 15% to account for manufacturing tolerance; polyurethane foam manufacturing tolerances are discussed in [Section 8.1.4.1.2.3.2, *Parallel-to-Rise Compressive Stress*](#). The nominal compressive strength of the polyurethane foam is further reduced by 25% to account for elevated temperature effects, as discussed in [Section 2.6.1.1, *Summary of Pressures and Temperatures*](#).

Properties of Type 304 stainless steel and polyurethane foam, parallel to the direction of foam rise accounting for manufacturing tolerances and elevated temperature, are summarized below.

Material Property	Value	Reference
Type 304 Stainless Steel at 160 °F		
Elastic Modulus, E	27.8×10^6 psi	Table 2.3-1
Yield Strength, σ_y	27,000 psi	
Shear Stress, equal to $(0.6)\sigma_y$	16,200 psi	
Polyurethane Foam (parallel-to-rise) at 160 °F		
Minimum compressive strength, σ_c	150 psi	Table 2.3-2
Bearing stress, assumed equal to $(2/3)\sigma_c$	100 psi	

2.5.1 Lifting Devices

This section demonstrates that the fork lift pockets, the only attachments designed to lift the HalfPACT package, are designed with a minimum safety factor of three against yielding, per the requirements of 10 CFR §71.45(a). The lifting devices in the OCA lid are restricted to only lifting the OCA lid, and the lifting devices in the ICV lid are restricted to only lifting an ICV lid or empty ICV. Although these lifting devices are designed with a minimum safety factor of three against yielding, detailed analyses are not specifically included herein since these lifting devices are not intended for lifting a HalfPACT package.

When lifting the entire package, the applied lift force without yielding is simply three times the total package weight of 18,100 pounds, as given in [Section 2.2, *Weights and Centers of Gravity*](#).

$$F_L = (3)(18,100) = 54,300 \text{ pounds}$$

The entire package is lifted via two fork lift pockets located at the bottom of the OCA. Loads are considered to be concentrated at the fork lift pocket interfaces and act parallel to the direction of foam rise. For the purposes of this analysis, the minimum assumed fork width is 8 inches, and the minimum assumed engagement length is 60 inches. The total bearing area for two forks is:

$$A = (2)(8)(60) = 960 \text{ in}^2$$

Assuming the entire lifted load is carried directly into the polyurethane foam, thereby ignoring any beneficial load carrying associated with the presence of the relatively stiff stainless steel fork lift pocket and OCA outer shell, the compressive stress is:

$$\sigma_c = \frac{F_1}{A} = \frac{54,300}{960} = 57 \text{ psi}$$

The allowable compressive stress for the polyurethane foam is 100 psi. Therefore, the margin of safety is:

$$MS = \frac{100}{57} - 1 = +0.75$$

2.5.2 Tie-down Devices

The HalfPACT package is secured to its dedicated semi-trailer at four points, two on each trailer main beam. For railcar shipments, the HalfPACT package is secured to an adapter that mimics the trailer's four attachment points. Subsequent use of the term "trailer" or "trailer main beam(s)" encompass the railcar adapter and railcar frame. The attachment is made using trailer tie-down devices that pass over the tie-down lugs located at the bottom of the OCA body. The semi-trailer is also fitted with kick plates at the four tie-down points to provide horizontal restraint (blocking). The tie-down scheme utilized for the HalfPACT package is illustrated in [Figure 2.5-1](#) and [Figure 2.5-2](#).

Inertial loads of 10g longitudinally, 5g laterally, and 2g vertically, per 10 CFR §71.45(b)(1), are applied through the HalfPACT package center of gravity, conservatively assumed to be 45 inches above the package's base. The horizontal loads of 10g longitudinally and 5g laterally are reacted in compression against the kick plates. The resultant overturning moment is reacted in compression on a trailer main beam and in tension by the four tie-down lugs. The vertical load applied to the center of gravity (2g) is evenly reacted at the four tie-down points, and is assumed to act in the direction (up or down) that maximizes the total tie-down load (i.e., down for the compressive reaction point and up for the tensile reaction points).

2.5.2.1 Tie-down Forces

Tensile tie-down points are on a 48.4 inch radius circle (to the center of the tie-down lugs, in line with the tie-down fixture). The compressive reaction point is at the trailer main beam, occurring at the edge of the tie-down lug's doubler plate, a radius of 47.56 inches. A plan view of the tie-down geometry is depicted in [Figure 2.5-3](#), including a corresponding free-body force diagram. If the HalfPACT package is treated as a rigid body, the reaction forces may be determined from the following set of equations:

$$F_1L_1 + F_2L_2 + F_3L_3 + F_4L_4 = HF_g$$

$$\frac{F_1}{L_1} = \frac{F_2}{L_2} = \frac{F_3}{L_3} = \frac{F_4}{L_4} = k$$

$$F_1 + F_2 + F_3 + F_4 = F_c$$

where, the height of the package center of gravity above its base, $H = 45$ inches, the horizontal inertia force, $F_g = 18,100 \times (10^2 + 5^2)^{1/2} = 202,364$ pounds, and the tie-down lug reaction lengths, $L_1 = 47.56 - 47.52 = 0.04$ inches, $L_2 = 47.56 - 21.16 = 26.40$ inches, $L_3 = 47.56 + 21.16 = 68.72$ inches, and $L_4 = 47.56 + 47.52 = 95.08$ inches. Solving for k :

$$k = \frac{HF_g}{L_1^2 + L_2^2 + L_3^2 + L_4^2} = \frac{(45)(202,364)}{(0.04)^2 + (26.40)^2 + (68.72)^2 + (95.08)^2} = 630 \text{ lb/in}$$

Therefore, $F_1 = k \times L_1 = 25$ pounds, $F_2 = k \times L_2 = 16,632$ pounds, $F_3 = k \times L_3 = 43,294$ pounds, $F_4 = k \times L_4 = 59,900$ pounds, and $F_c = 119,851$ pounds. The maximum vertical tensile force on any single tie-down lug, including the contribution of the vertical load of $2g$, is then found as:

$$F_{t \max} = 59,900 + \frac{(2g)(18,100)}{4 \text{ lugs}} = 68,950 \text{ pounds}$$

Similarly, the maximum compressive force is found as:

$$F_{c \max} = 119,851 + \frac{(2g)(18,100)}{4 \text{ lugs}} = 128,901 \text{ pounds}$$

Since the line of action of the combined $10g$ longitudinal and the $5g$ lateral accelerations pass almost exactly over the centerline of the kickplate (27.6° for the kickplate centerline versus 26.6° for the line of action of the force), the total horizontal reaction force is conservatively assumed to be reacted against a single kickplate. This force is given by:

$$F_h = F_g = 202,364 \text{ pounds}$$

2.5.2.2 Tie-down Stress Due to a Vertical Tensile Load

Several failure modes are considered for the vertical tensile force on the tie-down lug. Shear failure of the tie-down lug itself is not an issue because the shear area of the lug is much greater than the lug attachment welds. The remaining failure modes, as illustrated in [Figure 2.5-4](#), are:

- (a) Shear and bending failure of the tie-down lug welds (shear + bending loads),
- (b) Tearout of the tie-down lug doubler plate at the lug weld outline,
- (c) Shear failure of the welds attaching the lug doubler plate to the OCA outer shell, and
- (d) Tearout of the OCA outer shell at the doubler outline.

2.5.2.2.1 Failure of the Tie-down Lug Welds Due to Shear and Bending Loads

[Figure 2.5-5](#) presents dimensional details of the tie-down, including an appropriate free-body diagram. The length of the tie-down lug weld along the two sides is 5.49 inches. The arc length

of the weld across the top of the lug is 3.38 inches. The groove weld at the bottom is 2.38 inches long. On three sides, the weld is a 3/8 inch fillet over a 3/8 inch groove. The minimum throat length for this weld is $0.375/(\sin 45^\circ) = 0.53$ inches. For the 3/8 inch groove weld at the bottom, the minimum throat length is 0.375 inches. Thus, the total shear area for the weld is:

$$A_s = [(2)(5.49) + 3.38](0.53) + (2.38)(0.375) = 8.50 \text{ in}^2$$

The maximum shearing force, V , is the maximum tensile force, $F_{\text{tmax}} = 68,950$ pounds from [Section 2.5.2.1, Tie-down Forces](#), resulting in a corresponding shear stress of:

$$\tau_v = \frac{V}{A_s} = \frac{68,950}{8.50} = 8,112 \text{ psi}$$

The maximum weld shear stress due to bending is found using the standard beam bending formula, but by treating the weld as a line¹, or:

$$\tau_B = \frac{Mc}{I}$$

where, M is the moment on weld group, c is the maximum weld distance from the weld group centroid, and I is the moment of inertia of weld group. The weld group centroid, relative to the bottom edge of the tie-down lug, is:

$$\bar{y} = \frac{(0.53)(3.38)(6.00) + 2(0.53)(5.49)(5.49/2)}{(0.53)(3.38) + 2(0.53)(5.49) + (0.375)(2.38)} = 3.143 \text{ inches}$$

where the centroid of the arc formed by the weld at the top of the tie-down lug is located 6.00 inches above the base of the lug. For the sides, the contribution to the moment of inertia is:

$$I_s = 2 \left[\frac{tL^3}{12} + Ad^2 \right] = 2 \left[\frac{(0.53)(5.49)^3}{12} + (0.53)(5.49) \left(3.143 - \frac{5.49}{2} \right)^2 \right] = 15.54 \text{ in}^4$$

For the top (arc-shaped) weld, conservatively ignoring the moment of inertia about its own centroid, the contribution to the moment of inertia is:

$$I_t = Ad^2 = (0.53)(3.38)(6.00 - 3.143)^2 = 14.62 \text{ in}^4$$

For the bottom weld, the contribution to the moment of inertia is:

$$I_b = Ad^2 = (0.375)(2.38)(3.143)^2 = 8.82 \text{ in}^4$$

Summing the contributions from each part of the weld group, the total moment of inertia of the weld group, treated as a line, is:

$$I = I_s + I_t + I_b = 15.54 + 14.62 + 8.82 = 38.98 \text{ in}^4$$

¹ Shigley, *Mechanical Engineering Design*, Third Edition, McGraw-Hill, Inc., 1977, Section 7-4, *Bending in Welded Joints*.

The distance from the centroid of the weld group to the extreme fiber is $c = 3.143$ inches. The line of action for the vertical force is 0.7 inches from the side of the tie-down doubler plate, as illustrated in [Figure 2.5-5](#). Therefore, the shear stress on the weld group due to bending is:

$$\tau_B = \frac{Mc}{I} = \frac{(68,950)(0.7)(3.143)}{38.98} = 3,892 \text{ psi}$$

The maximum shear stress in the tie-down lug weld due to the shear and bending loads is:

$$\tau = \sqrt{\tau_V^2 + \tau_B^2} = \sqrt{(8,112)^2 + (3,892)^2} = 8,997 \text{ psi}$$

The allowable shear stress for the tie-down lug welds is 16,200 psi. Therefore, the margin of safety is:

$$MS = \frac{16,200}{8,997} - 1 = +0.80$$

2.5.2.2.2 Tearout of the Tie-down Doubler Plate at the Tie-Down Lug Weld Outline

Assume that a rectangular region equal to $2.88 + 2 \times 0.375 = 3.63$ inches wide by $(6.25 + 0.375) = 6.63$ inches high, tears out from the 3/8 inch thick doubler plate. Under the direct shear load of 68,520 pounds, the top edge will be in direct tension while the sides and bottom will be in direct shear. Conservatively assuming the top and sides are all in direct shear, the shear area in the 3/8 inch thick, tie-down doubler plate is:

$$A_p = [3.63 + 2(6.63)](0.375) = 6.33 \text{ in}^2$$

The shear area of the 1.0 inch groove weld attaching the bottom of the doubler plate to the OCA body flat head is:

$$A_w = (3.63)(1.0) = 3.63 \text{ in}^2$$

Thus, the total shear area is:

$$A_s = A_p + A_w = 6.33 + 3.63 = 9.96 \text{ in}^2$$

The maximum shearing force, V , is the maximum tensile force, $F_{\text{tmax}} = 68,950$ pounds from [Section 2.5.2.1, Tie-down Forces](#), resulting in a corresponding shear stress of:

$$\tau_V = \frac{V}{A_s} = \frac{68,950}{9.96} = 6,923 \text{ psi}$$

The maximum weld shear stress due to bending is found using the standard beam bending formula, but by treating the weld as a line, or:

$$\tau_B = \frac{Mc}{I}$$

where, M is the moment on weld group, c is the maximum weld distance from the weld group centroid, and I is the moment of inertia of weld group. The weld group centroid, relative to the bottom edge of the tie-down lug, is:

$$\bar{y} = \frac{(0.375)(3.63)(6.63) + 2(0.375)(6.63)(6.63/2) + (1.0)(3.63)(1.0/2)}{(0.375)(3.63) + 2(0.375)(6.63) + (1.0)(3.63)} = 2.742 \text{ inches}$$

For the sides of the rectangular region, the contribution to the moment of inertia is:

$$I_s = 2 \left[\frac{tL^3}{12} + Ad^2 \right] = 2 \left[\frac{(0.375)(6.63)^3}{12} + (0.375)(6.63) \left(2.742 - \frac{6.63}{2} \right)^2 \right] = 19.85 \text{ in}^4$$

For the top of the rectangular region, the contribution to the moment of inertia is:

$$I_t = \frac{Lt^3}{12} + Ad^2 = \frac{(3.63)(0.375)^3}{12} + (0.375)(3.63)(6.63 - 2.742)^2 = 20.59 \text{ in}^4$$

For the bottom groove weld, the contribution to the moment of inertia is:

$$I_b = \frac{Lt^3}{12} + Ad^2 = \frac{(3.63)(1.0)^3}{12} + (1.0)(3.63) \left(2.742 - \frac{1.0}{2} \right)^2 = 18.55 \text{ in}^4$$

Summing the contributions from each part of the rectangular region, the total moment of inertia of the weld group, treated as a line, is:

$$I = I_s + I_t + I_b = 19.85 + 20.59 + 18.55 = 58.99 \text{ in}^4$$

The distance from the centroid of the rectangular region to the extreme fiber is $c = 6.63 - 2.742 = 3.888$ inches. The line of action for the vertical force is $0.7 + 0.375/2 = 0.89$ inches from the center of the tie-down doubler plate. Therefore, the shear stress due to bending is:

$$\tau_b = \frac{Mc}{I} = \frac{(68,950)(0.89)(3.888)}{58.99} = 4,103 \text{ psi}$$

The maximum shear stress in the tie-down doubler plate due to the shear and bending loads is:

$$\tau = \sqrt{\tau_v^2 + \tau_b^2} = \sqrt{(6,923)^2 + (4,103)^2} = 8,048 \text{ psi}$$

The allowable shear stress for the tie-down doubler plate is 16,200 psi. Therefore, the margin of safety is:

$$MS = \frac{16,200}{8,048} - 1 = +1.01$$

2.5.2.2.3 Shear Failure of the Tie-down Lug Doubler Plate to OCA Outer Shell Welds

The tie-down lug doubler plate is 24 inches square, and welded to the OCA outer shell on its top and sides with 1/4 inch fillet welds. Although the bottom weld is a groove weld, conservatively

assume it acts as a 1/4 inch fillet weld, resulting in a total weld length of 96 inches. In addition, 30, 1½ inch diameter, 1/4 inch fillet welds supplement the peripheral fillet welds, providing an additional $30 \times \pi(1.5) = 141$ inches of weld. Thus, the total weld length is 237 inches, resulting in a weld shear area of:

$$A_s = (0.25)(\sin 45^\circ)(237) = 41.9 \text{ in}^2$$

The weld shear area is much greater than determined in both previous cases (i.e., $A_s = 8.50 \text{ in}^2$ for [Section 2.5.2.2.1, Failure of the Tie-down Lug Welds Due to Shear and Bending Loads](#), and $A_s = 9.96 \text{ in}^2$ for [Section 2.5.2.2.2, Tearout of the Tie-down Doubler Plate at the Tie-Down Lug Weld Outline](#)). Thus, the weld shear stress for the same vertical load will be correspondingly less. Similarly, a much larger moment of inertia will be determined for a nearly identical bending moment, thereby resulting in a substantially reduced bending stress. In conclusion, by inspection the resulting margin of safety will correspondingly be much greater and does not need to be explicitly determined.

2.5.2.2.4 Tearout of the OCA Outer Shell at the Tie-Down Lug Doubler Plate Outline

A potential failure mode for the tie-down hardware is tearout of the 1/4 inch thick OCA outer shell just outboard of the 24.0 inch square doubler plate. The downward acting force puts the OCA shell adjacent to the top edge of the doubler plate in direct tension. The OCA outer shell immediately adjacent to the sides and bottom edge of the doubler plate is in direct shear.

Assume that the 24 × 24 inch tie-down lug doubler plate tears out from 1/4 inch thick OCA outer shell. Under the direct shear load of 68,520 pounds, the top edge will be in direct tension while the sides and bottom will be in direct shear. Conservatively assuming that all sides are all in direct shear, the shear area in the 1/4 inch thick OCA outer shell is:

$$A_s = 4(24)(0.25) = 24.0 \text{ in}^2$$

Once again, the shell shear area is much greater than determined in both previous cases (i.e., $A_s = 8.50 \text{ in}^2$ for [Section 2.5.2.2.1, Failure of the Tie-down Lug Welds Due to Shear and Bending Loads](#), and $A_s = 9.96 \text{ in}^2$ for [Section 2.5.2.2.2, Tearout of the Tie-down Doubler Plate at the Tie-Down Lug Weld Outline](#)). Thus, the weld shear stress for the same vertical load will be correspondingly less. As before, a much larger moment of inertia will be determined for a nearly identical bending moment, thereby resulting in a substantially reduced bending stress. In conclusion, by inspection the resulting margin of safety will correspondingly be much greater and does not need to be explicitly determined.

2.5.2.3 Tie-down Stress Due to a Vertical Compressive Load

The stresses in the HalfPACT package due to a vertical compressive load may be analyzed by two bounding cases. First, the combination of overturning and vertical, 2g inertial compressive loads carried through the OCA outer shell and tie-down lug doubler plate, and second, the 2g inertial compressive load carried entirely by the polyurethane foam.

2.5.2.3.1 Bearing Stress in the OCA Outer Shell and Tie-down Lug Doubler Plate

The vertical compressive tie-down load is carried in bearing against the semi-trailer main beams. Conservatively assume that this load is carried only by the cylindrical portion of the OCA outer shell and doubler that is directly over the trailer main beams and tie-down support structure. With reference to [Figure 2.5-3](#), the arc length, s , of the OCA that spans the trailer main beams is:

$$s = R \left(\frac{\pi}{180} \right) (\phi_1 - \phi_2) = (47.56) \left(\frac{\pi}{180} \right) \left[\sin^{-1} \left(\frac{32}{47.56} \right) - \sin^{-1} \left(\frac{18}{47.56} \right) \right] = 16.64 \text{ inches}$$

For an OCA outer shell thickness of 1/4 inch, and a tie-down lug doubler plate thickness of 3/8 inch, the area is:

$$A = (16.64)(0.25 + 0.375) = 10.40 \text{ in}^2$$

Thus, from [Section 2.5.2.1](#), *Tie-down Forces*, the maximum compressive force is $F_{\text{cmax}} = 128,901$ pounds, and the corresponding compressive stress is:

$$\sigma_c = \frac{F_{\text{cmax}}}{A} = \frac{128,901}{10.40} = 12,394 \text{ psi}$$

The allowable stress for the OCA outer shell and tie-down lug doubler plate is 27,000 psi. Therefore, the margin of safety is:

$$MS = \frac{27,000}{12,394} - 1 = +1.18$$

2.5.2.3.2 Compressive Stress in the Polyurethane Foam

The HalfPACT package is supported on the two main trailer beams during transport. With reference to [Figure 2.5-3](#), the length, L , under the OCA that spans the trailer main beams is:

$$L = 2\sqrt{(47.56)^2 - (22)^2} = 84.3 \text{ inches}$$

For two, 8 inch wide, trailer main beams, the total compressive area is:

$$A = 2(8)(84.3) = 1,349 \text{ in}^2$$

Conservatively ignoring the load carrying capacity of the OCA outer shell and fork lift pockets, the compressive stress in the polyurethane foam due to a 2g vertical (downward) inertial force is:

$$\sigma_c = \frac{2(18,100)}{A} = \frac{36,200}{1,349} = 27 \text{ psi}$$

The allowable stress for the polyurethane foam is 100 psi. Therefore, the margin of safety is:

$$MS = \frac{100}{27} - 1 = +2.70$$

2.5.2.4 Tie-down Stresses Due to a Horizontal Compressive Load

The horizontal load, $F_h = 202,364$ pounds, determined in [Section 2.5.2.1, Tie-down Forces](#), is reacted by a single tie-down weldment. The following sections consider the bearing stress in the tie-down weldment, and the shear stresses in the welds holding the horizontal tripler plate to the doubler plate, and the doubler plate to the lower OCA flat head. Based on their relative thicknesses, assume that one-quarter the horizontal load is carried through the 1/4 inch thick OCA flat head, one-quarter is carried through the 1/4 inch thick doubler plate, and one-half is carried through the 1/2 inch thick tripler plate.

2.5.2.4.1 Bearing Stress in the Tie-down Weldment

The horizontal load, $F_h = 202,364$ pounds, is carried from the 8.0 inch wide, trailer kickplate through the horizontal doubler and tripler plates welded inside the lower OCA flat head, as illustrated in [Figure 2.5-3](#). For a kickplate length, $L = 8$ inches, a bottom shell thickness, $t_s = 1/4$ inch, a doubler plate thickness, $t_d = 1/4$ inch, and a tripler plate thickness, $t_t = 1/2$ inch, the area available to carry the horizontal compressive load at the kickplate interface is:

$$A = L(t_s + t_d + t_t) = (8.0)(0.25 + 0.25 + 0.5) = 8.0 \text{ in}^2$$

The corresponding compressive (bearing) stress is:

$$\sigma_c = \frac{F_h}{A} = \frac{202,364}{8.0} = 25,296 \text{ psi}$$

The allowable bearing stress for the OCA outer shell, including the horizontal doubler and tripler plates, is 27,000 psi. Therefore, the margin of safety is:

$$MS = \frac{27,000}{25,296} - 1 = +0.07$$

2.5.2.4.2 Shear Stress in the Tripler Plate Welds

Based on the assumed load distribution in [Section 2.5.2.4, Tie-down Stresses Due to a Horizontal Compressive Load](#), the force on the welds attaching the tripler plate to the doubler plate is then one-half of 202,364 pounds, or 101,182 pounds. The tripler plate is welded with 3/8 inch fillet welds along three of its edges, and a 1/2 inch groove weld along the outer edge. The two side welds are approximately 8 inches long, and the back weld is 7 inches long, for a total, 3/8 inch fillet weld length of 23 inches. Four, 1½ inch diameter, 3/8 inch fillet welds supplement the peripheral 3/8 inch fillet welds, providing an additional $4 \times \pi(1.5) = 18.85$ inches of 3/8 inch fillet weld. Thus, the total 3/8 inch fillet weld length is 41.85 inches. In addition, the 10 inch long outer edge is welded with a 1/2 inch groove weld. The resulting weld shear area is:

$$A_s = (0.375)(\sin 45^\circ)(41.85) + (0.5)(10) = 16.1 \text{ in}^2$$

Thus, the shear stress in the tripler plate fillet welds is:

$$\tau = \frac{101,182}{16.1} = 6,285 \text{ psi}$$

The allowable shear stress for the tripler plate welds is 16,200 psi. Therefore, the margin of safety is:

$$MS = \frac{16,200}{6,285} - 1 = +1.58$$

As an option, the tripler plate may be one inch thick, and welded into a cutout through the 1/4 inch thick, lower OCA flat head and 1/4 inch thick, doubler plate in the same orientation and location as shown in [Figure 2.5-6](#). Full penetration groove welds are used around the periphery of the tripler plate (i.e., a one inch groove weld along the outside, 10 inch long edge, and 1/2 inch groove welds along the remaining three edges). The two side welds are approximately 8 inches long, and the back weld is 7 inches long, for a total weld length of 23 inches. The resulting weld shear area is:

$$A = (0.5)(23) + (1.0)(10) = 21.5 \text{ in}^2$$

Thus, the shear stress in the tripler plate groove welds is:

$$\tau = \frac{101,182}{21.5} = 4,706 \text{ psi}$$

The allowable shear stress for the tripler plate welds is 16,200 psi. Therefore, the margin of safety is:

$$MS = \frac{16,200}{4,706} - 1 = +2.44$$

2.5.2.4.3 Shear Stress in the Doubler Plate Welds

Based on the assumed load distribution in [Section 2.5.2.4, Tie-down Stresses Due to a Horizontal Compressive Load](#), the force on the welds attaching the doubler plate to the OCA flat head is then one-half plus one-quarter of 202,364 pounds, or 151,773 pounds. The doubler plate is welded with 1/4 inch fillet welds along its four inner edges, for a total 1/4 inch fillet weld length of approximately 35 inches. Eighteen, 1 inch diameter, 1/4 inch fillet welds supplement the peripheral 1/4 inch fillet welds, providing an additional $18 \times \pi(1.0) = 56$ inches of 1/4 inch fillet weld. Thus, the total 1/4 inch fillet weld length is 91 inches. In addition, the 20 inch long outer edge is welded with a 1/4 inch groove weld. The resulting weld shear area is:

$$A_s = (0.25)(\sin 45^\circ)(91) + (0.25)(20) = 21.1 \text{ in}^2$$

Thus, the shear stress in the doubler plate fillet welds is:

$$\tau = \frac{151,773}{21.1} = 7,193 \text{ psi}$$

The allowable shear stress for the doubler plate welds is 16,200 psi. Therefore, the margin of safety is:

$$MS = \frac{16,200}{7,193} - 1 = +1.25$$

2.5.2.5 Response of the Package if Treated as a Fixed Cantilever Beam

The preceding sections considered stresses in a localized region in and around the tie-down components. This section demonstrates that a more global response of the HalfPACT package to tie-down loads is also acceptable. For this assessment, the HalfPACT package is treated as a cantilever beam, fixed at its base. The 1/4 inch thick, OCA outer shell is conservatively assumed to be the only structural member resisting the applied 10g, 5g and 2g inertia loads. Stress intensity, SI, in the OCA outer shell is determined as follows:

$$SI = 2\sqrt{\left(\frac{\sigma}{2}\right)^2 + \tau^2} = \sqrt{\left(\frac{P}{A} + \frac{Mc}{I}\right)^2 + \left(\frac{2V}{A}\right)^2}$$

where, for 2g vertically, the axial force, $P = (2)(18,100) = 36,200$ pounds, the bending moment from [Section 2.5.2.1, Tie-down Forces](#), $M = HF_g = (45)(202,364) = 9,106,380$ in-lbs, the extreme fiber distance, $c = \frac{1}{2}(94\frac{3}{8}) = 47.2$ inches, the horizontal shear force, $V = F_g = 202,364$ inches, the OCA outer shell cross-sectional area, $A = (\pi/4)[(94.375)^2 - (93.875)^2] = 74$ in², and the OCA outer shell moment of inertia, $I = (\pi/64)[(94.375)^4 - (93.875)^4] = 81,869$ in⁴. The resulting stress intensity is:

$$SI = \sqrt{\left(\frac{36,200}{74} + \frac{(9,106,380)(47.2)}{81,869}\right)^2 + \left(\frac{2(202,364)}{74}\right)^2} = 7,928 \text{ psi}$$

The allowable stress intensity for the OCA outer shell is 27,000 psi. Therefore, the margin of safety is:

$$MS = \frac{27,000}{7,928} - 1 = +2.41$$

2.5.2.6 Summary

All margins of safety for tie-down loads, per 10 CFR §71.45(b)(1), are positive. The smallest tensile or shear margin of safety, $MS = +0.80$, is for failure of the welds attaching the tie-down lug to the doubler plate, indicating that this will be the mode of failure for the tie-downs under an excessive load condition. Note that compressive modes of failure are not considered relevant in the excessive load evaluation. In accordance with 10 CFR §71.45(b)(3), this failure mode does not compromise the performance capabilities of the HalfPACT package since no main shell is breached. Finally, it is noted that the fork lift pockets and OCA lifting sockets are not intended to be used as tie-down devices, and are appropriately disabled to prevent inadvertent use. The fork lift pockets and OCA lifting sockets are disabled by affixing a plate over each pocket and a cover over the each socket respectively (see the drawings in [Appendix 1.3.1, Packaging General Arrangement Drawings](#)).

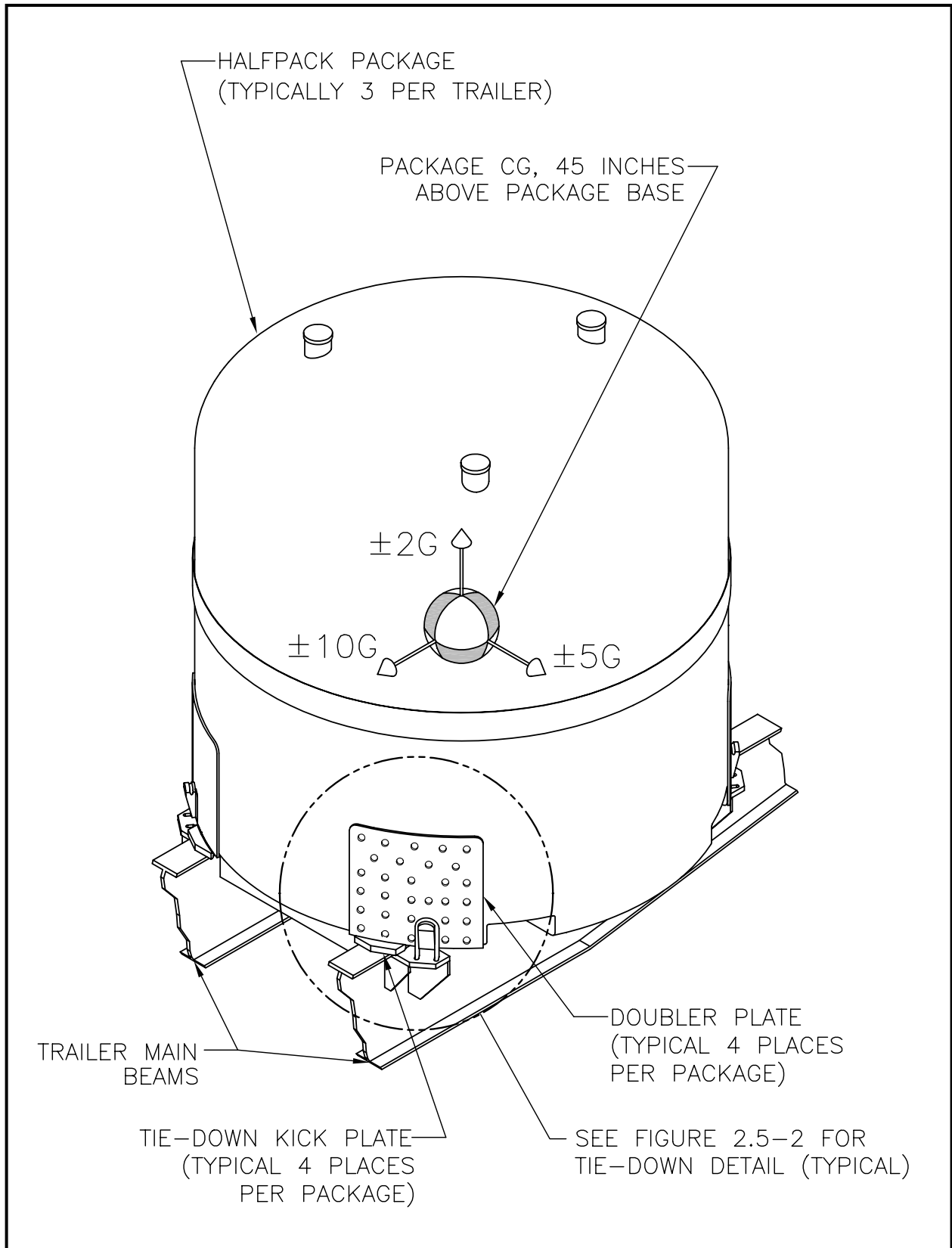


Figure 2.5-1 – Tie-down Device Layout

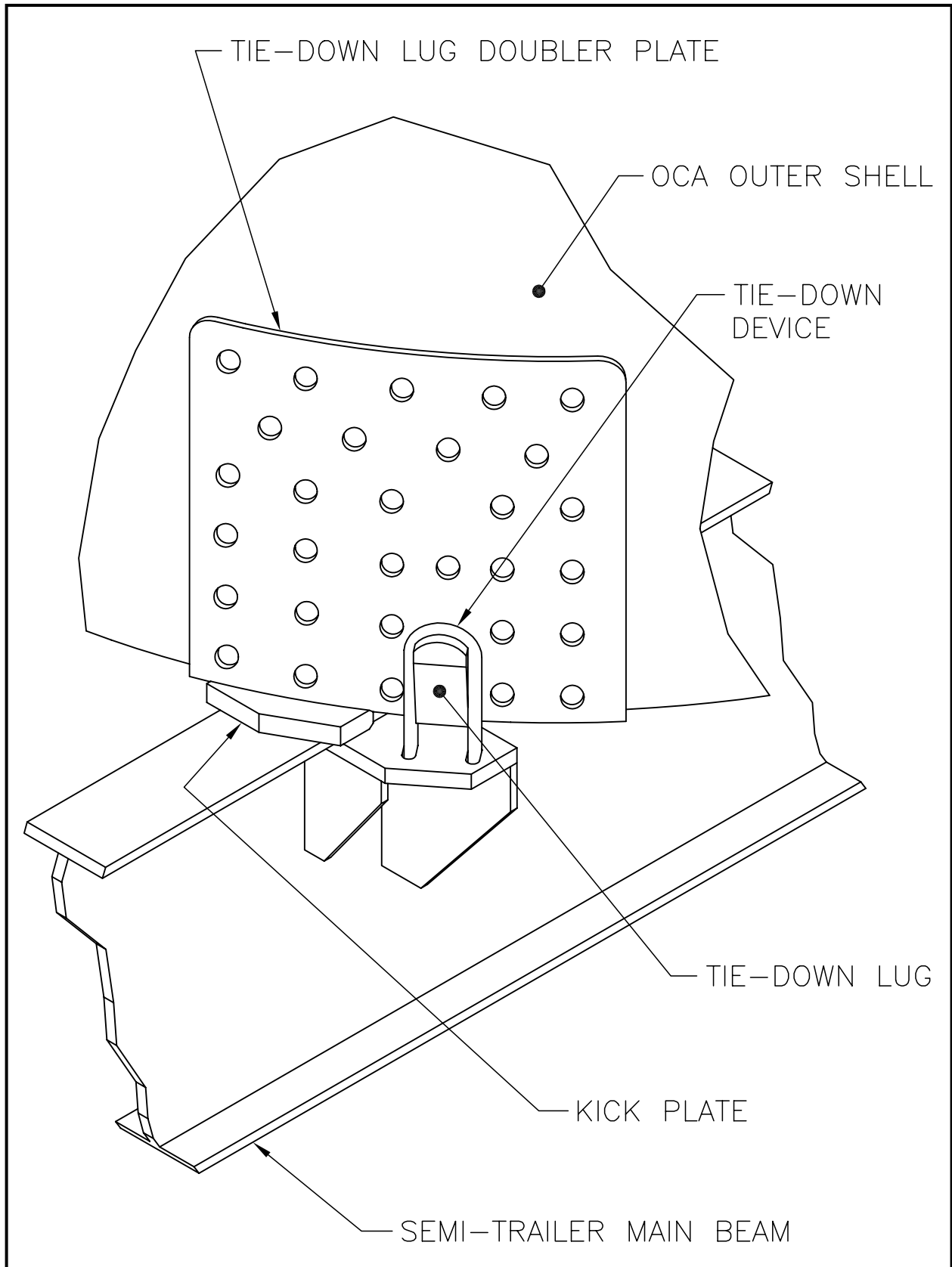


Figure 2.5-2 – Tie-down Device Detail

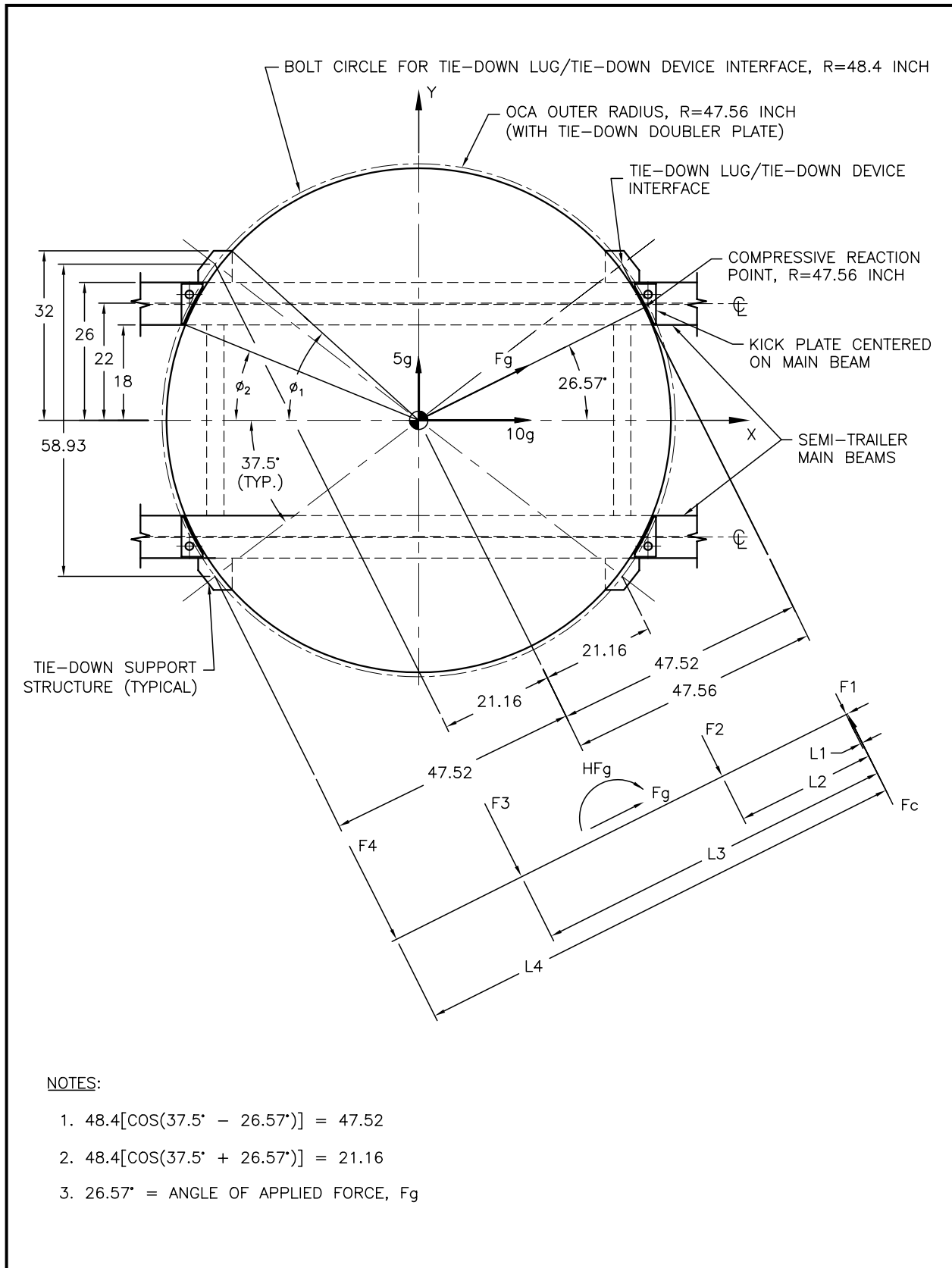


Figure 2.5-3 – Tie-down Plan View and Reaction Force Diagram

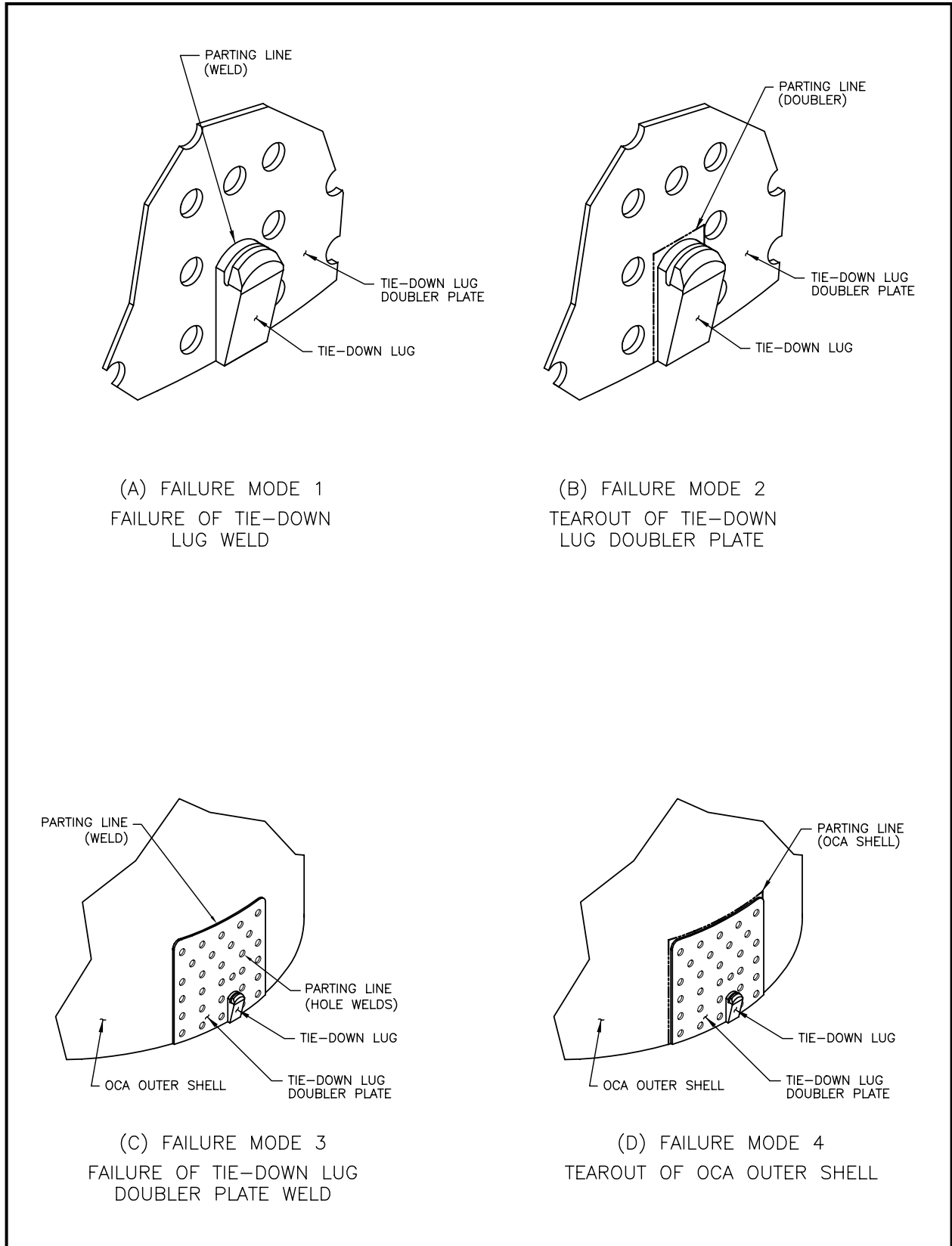


Figure 2.5-4 – Tie-down Tensile/Shear Failure Modes

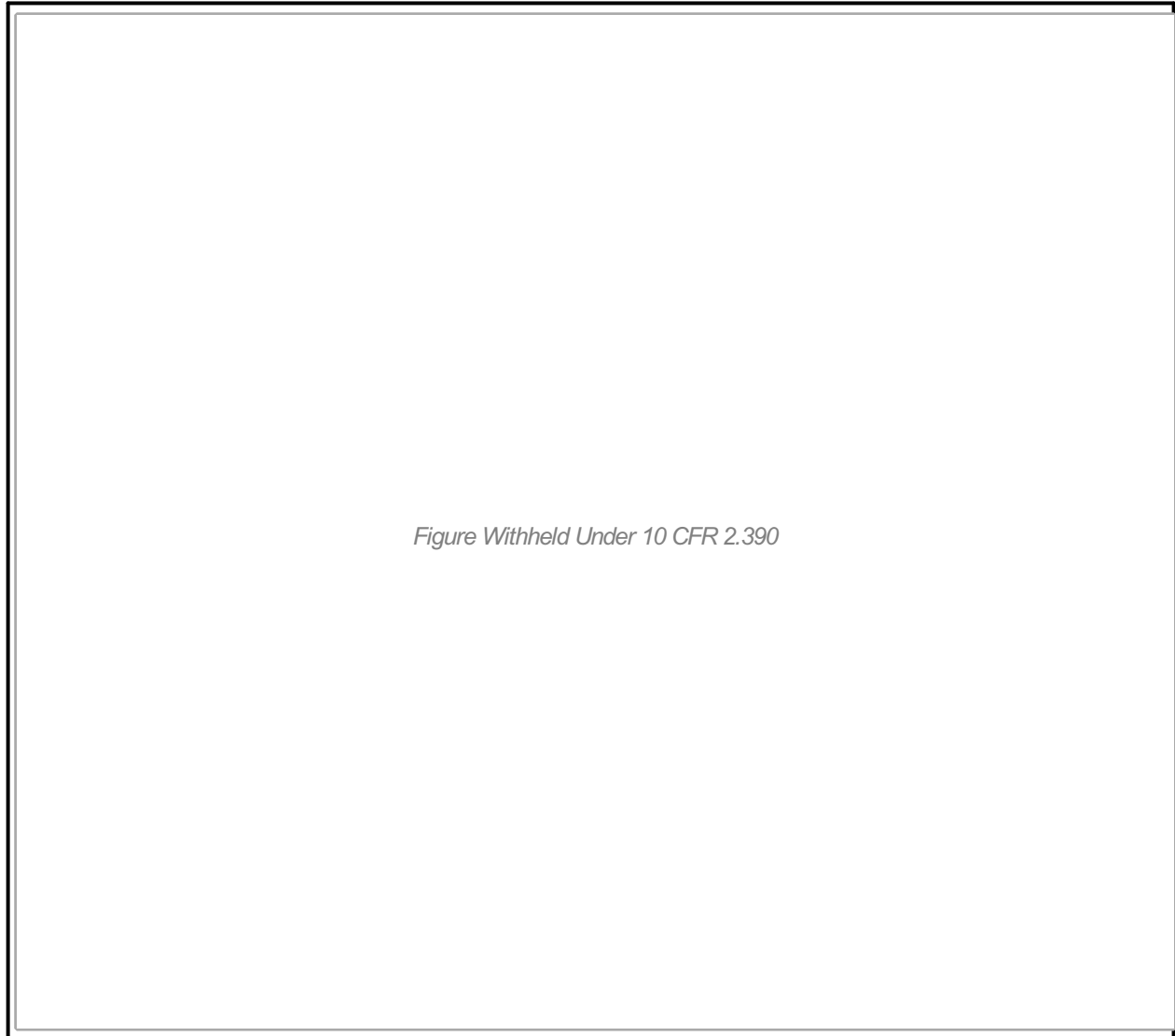


Figure 2.5-5 – Tie-down Lug Dimensions and Load Diagram

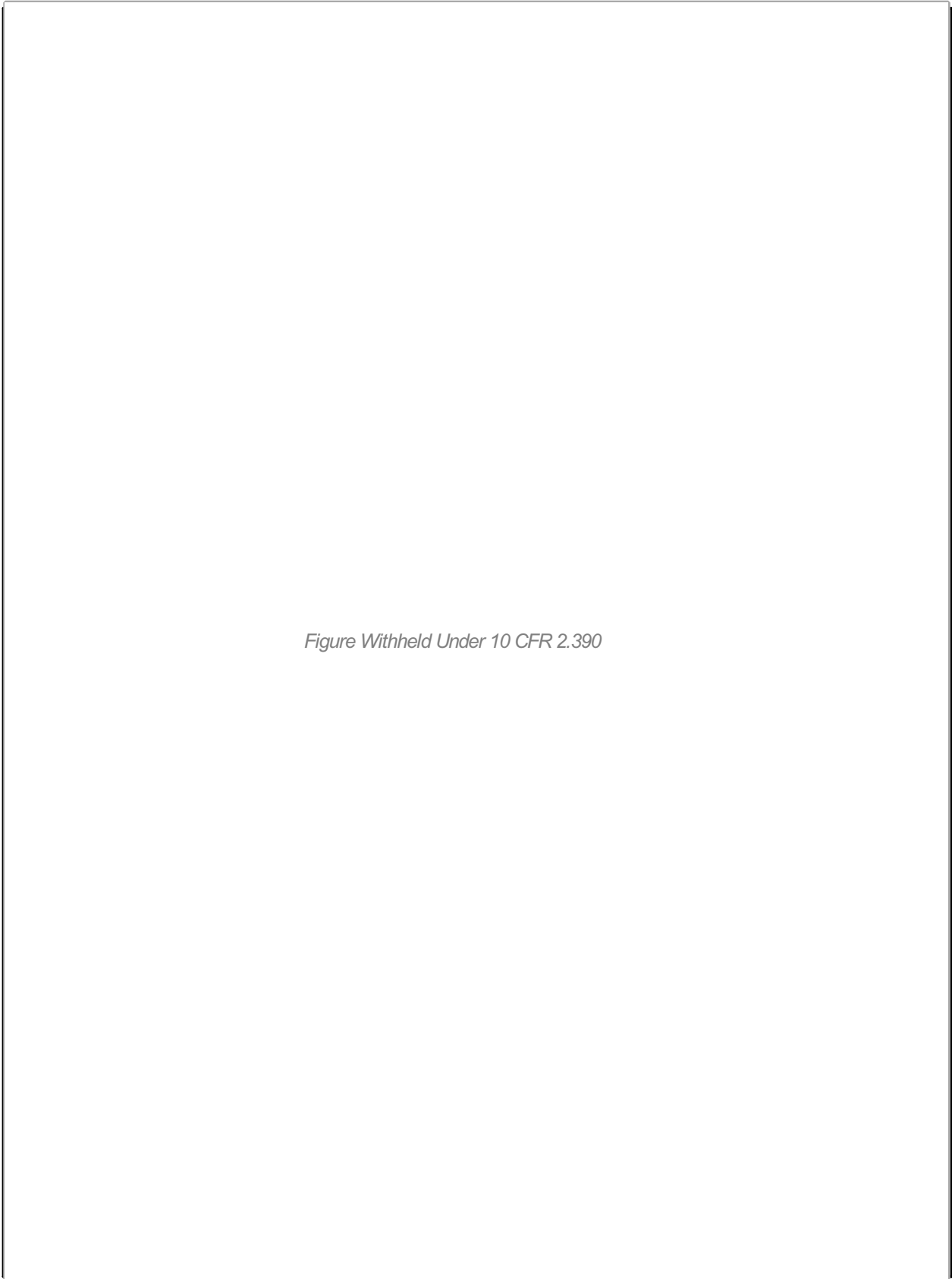


Figure Withheld Under 10 CFR 2.390

Figure 2.5-6 – Horizontal Doubler and Tripler Plate Details

This page intentionally left blank.

2.6 Normal Conditions of Transport

The HalfPACT package, when subjected to the normal conditions of transport (NCT) specified in 10 CFR §71.71¹, is shown to meet the performance requirements specified in Subpart E of 10 CFR 71. As discussed in the introduction to this chapter, with the exception of the NCT free drop, the primary proof of NCT performance is via analytic methods. Regulatory Guide 7.6² criteria are demonstrated as acceptable for all NCT analytic evaluations presented in this section. Specific discussions regarding brittle fracture and fatigue are presented in [Section 2.1.2.2, *Miscellaneous Structural Failure Modes*](#), and are shown not to be limiting cases for the HalfPACT package design. The ability of the butyl O-ring containment seals to remain leaktight is documented in [Appendix 2.10.2, *Elastomer O-ring Seal Performance Tests*](#).

With the exception of the NCT free drop evaluation, analyses for heat, cold, reduced external pressure, increased external pressure, and vibration are performed in this section. Allowable stress limits are consistent with [Table 2.1-1](#) and [Table 2.1-2](#) in [Section 2.1.2.1, *Analytic Design Criteria \(Allowable Stresses\)*](#), using temperature-adjusted material properties taken from [Table 2.3-1](#) in [Section 2.3.1, *Mechanical Properties Applied to Analytic Evaluations*](#).

For the analytic assessments performed within this section, properties for Type 304 stainless steel are based on data from [Table 2.3-1](#) from [Section 2.3.1, *Mechanical Properties Applied to Analytic Evaluations*](#). Similarly, the bounding values for polyurethane foam compressive strength are based on data from [Table 2.3-2](#) in [Section 2.3.1, *Mechanical Properties Applied to Analytic Evaluations*](#). Polyurethane foam compressive strength is further adjusted $\pm 15\%$ to account for manufacturing tolerance. At elevated NCT temperatures (i.e., 160 °F), the nominal compressive strength is reduced 25% for elevated temperature effects and reduced 15% for manufacturing tolerance. At reduced NCT temperatures (i.e., -40 °F), the nominal compressive strength is increased 50% for reduced temperature effects and increased 15% for manufacturing tolerance.

Properties of Type 304 stainless steel and polyurethane foam are summarized below.

Material Property	Material Property Value (psi)			Reference
	-40 °F	70 °F	160 °F	
Type 304 Stainless Steel				
Elastic Modulus, E	28.8×10^6	28.3×10^6	27.8×10^6	Table 2.3-1
Design Stress Intensity, S_m	20,000	20,000	20,000	
Yield Strength, S_m	30,000	30,000	27,000	
Polyurethane Foam Compressive Strength				
Parallel-to-Rise Direction, σ_c	405	235	150	Table 2.3-2
Perpendicular-to-Rise Direction, σ_c	336	195	124	

¹ Title 10, Code of Federal Regulations, Part 71 (10 CFR 71), *Packaging and Transportation of Radioactive Material*, 01-01-07 Edition.

² U. S. Nuclear Regulatory Commission, Regulatory Guide 7.6, *Design Criteria for the Structural Analysis of Shipping Cask Containment Vessels*, Revision 1, March 1978.

Finite element analysis methods are utilized to determine stresses in the HalfPACT packaging structure at various temperature extremes, including the effects of differential thermal expansion, when appropriate, and internal (I) and external (E) pressure combinations, as summarized below.

Load Case Number	Reference Section	Differential Expansion?	Pressure Differential	Temperature		Table Number	Figure Numbers
				Uniform	Reference		
OCA Case 1	§2.6.1	No	61.2 psig (I)	160 °F	160 °F	2.6-1	2.6-1/-2
OCA Case 2	§2.6.1	Yes	61.2 psig (I)	160 °F	70 °F	2.6-2	2.6-3/-4
OCA Case 3	§2.6.2	Yes	0 psig	-40 °F	70 °F	2.6-3	2.6-5/-6
OCA Case 4	§2.6.4	No	14.7 psig (E)	70 °F	70 °F	2.6-4	2.6-7/-8
ICV Case 1	§2.6.1	No	61.2 psig (I)	160 °F	160 °F	2.6-5	2.6-9/-10
ICV Case 2	§2.6.4	No	14.7 psig (E)	70 °F	70 °F	2.6-6	2.6-11/-12

For the NCT free drop evaluation, a certification test program was undertaken using a HalfPACT engineering and certification test unit (ETU and CTU, respectively). Results from certification testing demonstrated that under NCT free drop conditions, two leaktight levels of containment were maintained. NCT certification testing also demonstrated the HalfPACT package's ability to survive subsequent HAC, 30 foot free drop, puncture, and fire tests was not compromised. Analyses are performed, when appropriate, to supplement or expand on the available test results. This combination of analytic and test, structural evaluations provides an initial configuration for NCT thermal, shielding and criticality performance. In accordance with 10 CFR §71.43(f), the evaluations performed herein successfully demonstrate that under NCT tests the HalfPACT package experiences "no substantial reduction in the effectiveness of the packaging". Summaries of the more significant aspects of the full scale free drop testing are included in [Section 2.6.7, Free Drop](#), with details presented in [Appendix 2.10.3, Certification Tests](#).

2.6.1 Heat

The NCT thermal analyses presented in [Section 3.4, Thermal Evaluation for Normal Conditions of Transport](#), consists of exposing the HalfPACT package to direct sunlight and 100 °F still air per the requirements of 10 CFR §71.71(b). Although the actual internal heat load is a function of the particular payload configuration being transported, this section utilizes the maximum internal heat allowed within a HalfPACT package, or 30 thermal watts. The 30 thermal watt case results in maximum temperature gradients throughout the HalfPACT package.

2.6.1.1 Summary of Pressures and Temperatures

The maximum normal operating pressure (MNOP) is 50 psig, as determined in [Section 3.4.4, Maximum Internal Pressure](#). The pressure stress analyses within this section combine the internal pressure of 50 psig due to MNOP with a reduced external pressure, per 10 CFR §71.71(c)(3), of 3.5 psia (11.2 psig). The net resulting internal pressure utilized in all NCT structural analyses considering internal pressure is therefore 61.2 psig.

The NCT heat input results in modest temperatures and temperature gradients throughout the HalfPACT package. Maximum temperatures for the major packaging components are summarized

in [Table 3.4-1](#) from [Section 3.4.2, Maximum Temperatures](#). As shown in [Table 3.4-1](#), all packaging temperatures remain at or below 155 °F. For conservatism, structural analyses of the OCA and ICV utilize a uniform bounding temperature of 160 °F. Use of a uniform bounding temperature is also conservative since material strengths are lowest at the highest temperatures. In addition, in the case of the OCA, the main contributor to thermal stress is the result of differential expansion of the polyurethane foam and the surrounding stainless steel. Also shown by the temperatures presented in [Table 3.4-1](#), temperature gradients are modest for the NCT heat condition. Thus, temperature gradients are reasonably ignored in the analyses herein.

2.6.1.2 Differential Thermal Expansion

With NCT temperatures throughout the packaging being relatively uniform, (i.e., no significant temperature gradients), the concern with differential expansions is limited to regions of the HalfPACT packaging that employ adjacent materials with sufficiently different coefficients of thermal expansion. The OCA is a double-wall, composite construction of polyurethane foam between inner and outer shells of stainless steel. The polyurethane foam expands and contracts to a much greater degree than the surrounding stainless steel shells resulting in stresses due to differential thermal expansion. Finite element analyses presented in the following sections quantify these differential thermal expansion stresses. Differential thermal expansion stresses are negligible in the ICV for three reasons: 1) the temperature distribution throughout the entire ICV is relatively uniform, 2) the ICV is fabricated from only one type of structural material, and 3) the ICV is not radially or axially constrained within a tight-fitting structure (i.e., the OCV).

2.6.1.3 Stress Calculations

A finite element model of the OCA is used to determine the stresses due to the combined effects of pressure loads, and temperature loads due to differential thermal expansion. The details of this model are presented in [Appendix 2.10.1.1, Outer Containment Assembly \(OCA\) Structural Analysis](#). The ICV is also analyzed for the combined effects of pressure and temperature using a finite element model that is described in [Appendix 2.10.1.2, Inner Containment Assembly \(ICV\) Structural Analysis](#). For the NCT heat condition, evaluations include two load cases for the OCA and one load case for the ICV.

Maximum stress intensities are determined for each component, and classified according to primary or secondary, membrane or bending. Classification of stress intensities is per [Table NB-3217-1](#) of the ASME Boiler and Pressure Vessel Code³. Maximum stress intensities are presented for the maximum general primary membrane stress intensity, P_m , the maximum local primary membrane stress intensity, P_L , the maximum primary membrane (general or local) plus primary bending stress intensity, $P_m + P_b$ or $P_L + P_b$, and the maximum primary plus secondary stress intensity, $P_m + P_b + Q$ or $P_L + P_b + Q$.

OCA Load Case 1 (see [Table 2.6-1](#) and [Figure 2.6-1](#) and [Figure 2.6-2](#)): This analysis is performed at a uniform temperature of 160 °F, but with the reference temperature also set to 160 °F thereby eliminating any differential thermal expansion stresses. The internal pressure considers the effects of a maximum normal operating pressure (MNOP) of 50 psig, internal,

³ American Society of Mechanical Engineers (ASME) Boiler and Pressure Vessel Code, Section III, *Rules for Construction of Nuclear Power Plant Components*, 1995 Edition, 1997 Addenda.

coupled with a reduced external pressure of 3.5 psia (i.e., 11.2 psig, internal). The net result is an internal pressure of $50.0 + 11.2 = 61.2$ psig.

$P_m = 19,061$ psi, located in the OCV shell at the cylindrical/conical transition,

$P_L = 28,084$ psi, located in the knuckle region of the upper OCV torispherical head,

$P_L + P_b = 20,256$ psi, located in the OCV shell at the cylindrical/conical transition, and

$P_L + P_b + Q = 39,884$ psi, located in the knuckle region of the lower OCV torispherical head.

OCA Load Case 2 (see [Table 2.6-2](#) and [Figure 2.6-3](#) and [Figure 2.6-4](#)): This analysis is performed at a uniform temperature of 160 °F, but with the reference temperature set to 70 °F thereby including any differential thermal expansion stresses. As with OCA Load Case 1, the MNOP is coupled with the reduced external pressure for a net internal pressure of 61.2 psig. The use of these two cases allows primary stress intensities (from pressure loads) to be considered independently of secondary stress intensities (from differential thermal expansion loads).

$P_L + P_b + Q = 40,200$ psi, located in the knuckle region of the lower OCV torispherical head.

ICV Load Case 1 (see [Table 2.6-5](#) and [Figure 2.6-9](#) and [Figure 2.6-10](#)): This analysis is performed at a uniform temperature of 160 °F, but with the reference temperature also set to 160 °F thereby eliminating any differential thermal expansion stresses. As with OCA Load Cases 1 and 2, the MNOP is coupled with the reduced external pressure for a net internal pressure of 61.2 psig.

$P_m = 15,251$ psi, located in the upper ICV seal flange/shell transition,

$P_L = 26,968$ psi, located in the knuckle region of the upper ICV torispherical head,

$P_L + P_b = 22,336$ psi, located in the upper ICV seal flange/shell transition, and

$P_L + P_b + Q = 38,304$ psi, located in the knuckle region of the upper ICV torispherical head.

Polyurethane foam stress intensities are insignificant for OCA Load Case 1 (maximum stress intensity is 3 psi) and achieve a maximum value of 26 psi for OCA Load Case 2. Based on the perpendicular-to-rise direction at 160 °F, the minimum, polyurethane foam margin of safety is:

$$MS = \frac{124}{26} - 1 = +3.77$$

2.6.1.4 Comparison with Allowable Stresses

[Section 2.1.2, Design Criteria](#), presents the design criteria for structural evaluation of the HalfPACT packaging. The containment vessel design criteria for NCT analyses are in accordance with Regulatory Guide 7.6, which uses as a basis the criteria defined for Level A service limits in Section III of the ASME Boiler and Pressure Vessel Code⁴. Load combinations follow the guidelines of Regulatory Guide 7.8⁵.

⁴ American Society of Mechanical Engineers (ASME) Boiler and Pressure Vessel Code, Section III, *Rules for Construction of Nuclear Power Plant Components*, 1995 Edition, 1997 Addenda.

⁵ U. S. Nuclear Regulatory Commission, Regulatory Guide 7.8, *Load Combinations for the Structural Analysis of Shipping Casks for Radioactive Material*, Revision 1, March 1989.

From Table 2.3-1 in Section 2.3.1, *Mechanical Properties Applied to Analytic Evaluations*, the design stress intensity for Type 304 stainless steel used in the ICV and OCV is $S_m = 20,000$ psi at 160 °F. From Table 2.1-1 in Section 2.1.2.1.1, *Containment Structures*, the allowable stress intensities for the NCT hot condition is S_m for general primary membrane stress intensity (P_m), $1.5S_m$ for local primary membrane stress intensity (P_L), $1.5S_m$ for primary membrane (general or local) plus primary bending stress intensity ($P_m + P_b$ or $P_L + P_b$), and $3.0S_m$ for the range of primary plus secondary stress intensity ($P_m + P_b + Q$ or $P_L + P_b + Q$).

Maximum stress intensity, allowable stress intensity, and minimum margins of safety for each stress category and each load case are presented in Table 2.6-1, Table 2.6-2, and Table 2.6-5 for each of the cases discussed above. Since all margins of safety are positive, the design criteria are satisfied.

2.6.1.5 Range of Primary Plus Secondary Stress Intensities

Per Paragraph C.4 of Regulatory Guide 7.6, the maximum range of primary plus secondary stress intensity for NCT must be less than $3.0S_m$. This limitation on stress intensity range applies to the entire history of NCT loadings and not only to the stresses from each individual load transient.

2.6.1.5.1 Range of Primary Plus Secondary Stress Intensities for the OCA

The extreme ends of the stress range are determined from OCA Load Case 2 (from Section 2.6.1, *Heat*) and OCA Load Case 4 (from Section 2.6.4, *Increased External Pressure*). One extreme, OCA Load Case 2 represents the case of maximum internal pressure coupled with reduced external pressure, plus the effect of differential thermal expansion associated with heat-up from 70 °F to 160 °F. The other extreme, OCA Load Case 4, considers the effect of a minimum internal pressure at 70 °F. Note that combinations of other OCA load cases such as increased external pressure (20 psia, 5.3 psig) plus cool-down from 70 °F to -20 °F were also considered and found not to be bounding for the stress intensity range calculation.

The maximum range of primary plus secondary stress intensity occurs in the knuckle region of the lower OCV torispherical head (element 320). The extreme values of stress intensity are 40,200 psi and 9,641 psi from Table 2.6-2 and Table 2.6-4 for OCA Load Cases 2 and 4, respectively. Since OCA Load Cases 2 and 4 have opposite loads, the maximum range of primary plus secondary stress intensity is simply $40,200 + 9,641 = 49,841$ psi. The allowable stress intensity is $3.0S_m$, where $S_m = 20,000$ psi for Type 304 stainless steel at 160 °F. The margin of safety is:

$$MS = \frac{3(20,000)}{49,841} - 1 = +0.20$$

The positive margin of safety indicates that the design criterion is satisfied.

2.6.1.5.2 Range of Primary Plus Secondary Stress Intensities for the ICV

The extreme ends of the stress range are determined from ICV Load Case 1 (from Section 2.6.1, *Heat*) and ICV Load Case 2 (from Section 2.6.4, *Increased External Pressure*). One extreme, ICV Load Case 1 represents the case of maximum internal pressure coupled with reduced external pressure, plus the effect of differential thermal expansion associated with heat-up from 70 °F to 160 °F. The other extreme, ICV Load Case 2, considers the effect of a minimum internal pressure at 70 °F.

The extreme values of stress intensity are 38,304 psi and 9,104 psi from [Table 2.6-5](#) and [Table 2.6-6](#) for ICV Load Cases 1 and 2, respectively, conservatively ignoring the fact that the extreme values occur at locations remote from each other. Since ICV Load Cases 1 and 2 have opposite loads, the maximum range of primary plus secondary stress intensity is simply $38,304 + 9,104 = 47,408$ psi. The allowable stress intensity is $3.0S_m$, where $S_m = 20,000$ psi for Type 304 stainless steel at 160 °F. The margin of safety is:

$$MS = \frac{3(20,000)}{47,408} - 1 = +0.27$$

The positive margin of safety indicates that the design criterion is satisfied.

2.6.2 Cold

The NCT cold condition consists of exposing the HalfPACT packaging to a steady-state ambient temperature of -40 °F. Insolation and payload internal decay heat are assumed to be zero. These conditions will result in a uniform temperature throughout the package of -40 °F. With no internal heat load (i.e., no contents to produce heat and, therefore, pressure), the net pressure differential is assumed to be zero (14.7 psia internal, 14.7 psia external).

For the OCA, the principal structural concern due to the NCT cold condition is the effect of the differential expansion of the polyurethane foam relative to the surrounding stainless steel shells. During the cool-down from 70 °F to -40 °F, the foam material shrinks onto the OCV because thermal expansion coefficient for foam is greater than stainless steel. The resulting stresses are discussed in [Section 2.6.2.1, Stress Calculations](#).

Differential thermal expansion stresses are negligible in the ICV for three reasons: 1) the temperature distribution throughout the entire ICV is relatively uniform, 2) the ICV is fabricated from only one type of structural material, and 3) the ICV is not radially or axially constrained within a tight-fitting structure (i.e., the OCV).

Brittle fracture at -40 °F is addressed in [Section 2.1.2.2.1, Brittle Fracture](#). Performance of the O-ring seals at -40 °F is discussed in [Appendix 2.10.2, Elastomer O-ring Seal Performance Tests](#).

2.6.2.1 Stress Calculations

A finite element model of the OCA is used to determine the stresses due to the combined effects of pressure loads, and temperature loads due to differential thermal expansion. The details of this model are presented in [Appendix 2.10.1.1, Outer Containment Assembly \(OCA\) Structural Analysis](#). For the NCT cold condition, evaluations include one load case for the OCA.

Maximum stress intensities are determined for each component, and classified according to primary or secondary, membrane or bending. Classification of stress intensities is per Table NB-3217-1 of the ASME Boiler and Pressure Vessel Code. Membrane and membrane plus bending stresses due to differential thermal expansion are classified as secondary stresses (Q). Since there are no pressure loads, primary stresses (P_m , P_L , and $P_m + P_b$ or $P_L + P_b$) are equal to zero.

OCA Load Case 3 (see [Table 2.6-3](#) and [Figure 2.6-5](#) and [Figure 2.6-6](#)): This analysis is performed at a uniform temperature of -40 °F, but with the reference temperature set to 70 °F thereby including

differential thermal expansion stresses. For a uniform temperature cold case at -40 °F, both payload decay heat and solar heat are assumed to be zero. These conditions result in an internal pressure of 14.7 psia balanced with an external pressure of 14.7 psia, for a net pressure differential of zero.

$P_L + P_b + Q = 5,772$ psi, located in the lower OCV seal flange/Z-flange junction.

Polyurethane foam stress intensities are relatively small for OCA Load Case 3 (maximum stress intensity is 15 psi). Conservatively based on the perpendicular-to-rise direction at 160 °F, the minimum, polyurethane foam margin of safety is:

$$MS = \frac{124}{15} - 1 = +7.27$$

2.6.2.2 Comparison with Allowable Stresses

Section 2.1.2, *Design Criteria*, presents the design criteria for structural evaluation of the HalfPACT packaging. The containment vessel design criteria for NCT analyses are in accordance with Regulatory Guide 7.6, which uses as a basis the criteria defined for Level A service limits in Section III of the ASME Boiler and Pressure Vessel Code. Load combinations follow the guidelines of Regulatory Guide 7.8.

From Table 2.3-1 in Section 2.3.1, *Mechanical Properties Applied to Analytic Evaluations*, the design stress intensity for Type 304 stainless steel used in the ICV and OCV is $S_m = 20,000$ psi at -40 °F. From Table 2.1-1 in Section 2.1.2.1.1, *Containment Structures*, the allowable stress intensity for the NCT cold condition is $3.0S_m$ for the range of primary plus secondary stress intensity ($P_m + P_b + Q$ or $P_L + P_b + Q$).

Maximum stress intensity, allowable stress intensity, and minimum margins of safety for each stress category and each load case are presented in Table 2.6-3 for OCA Load Case 3. Since all margins of safety are positive, the design criteria are satisfied.

Since the NCT cold condition results in shrinking of the polyurethane foam onto the OCV shell, compressive stresses develop in the OCV shell. The buckling evaluation within Section 2.6.4, *Increased External Pressure*, demonstrates that the compressive stresses due to increased external pressure do not exceed the NCT allowable stresses. The compressive stresses generated during the NCT cold condition are bounded by the NCT increased external pressure condition, therefore no explicit buckling evaluation is required for the NCT cold condition.

2.6.3 Reduced External Pressure

The effect of a reduced external pressure of 3.5 psia (11.2 psig internal pressure), per 10 CFR §71.71(c)(3), is negligible for the HalfPACT packaging. This conclusion is based on the analyses presented in Section 2.6.1, *Heat*, addressing the ability of both containment vessels to independently withstand a maximum normal operating pressure (MNOP) of 50 psig, combined with a reduced external pressure of 3.5 psia, for a net effective internal pressure of 61.2 psig.

2.6.4 Increased External Pressure

The effect of an increased external pressure of 20 psia (5.3 psig external pressure), per 10 CFR §71.71(c)(4), is negligible for the HalfPACT packaging. Both containment vessels are designed to withstand a full vacuum equivalent to 14.7 psi external pressure during acceptance leakage

rate testing of the HalfPACT package, as described in [Section 8.1.3, Fabrication Leakage Rate Tests](#). Therefore, the worst case NCT external pressure loading is 14.7 psig.

The external pressure induces small compressive stresses in the containment boundaries that are limited by stability (buckling) requirements. Buckling assessments are performed for the OCV and ICV in [Section 2.6.4.3, Buckling Assessment of the Torispherical Heads](#), and [Section 2.6.4.4, Buckling Assessment of the Cylindrical Shells](#).

2.6.4.1 Stress Calculations

A finite element model of the OCA is used to determine the stresses due to the effect of a pressure load. The details of this model are presented in [Appendix 2.10.1.1, Outer Containment Assembly \(OCA\) Structural Analysis](#). The ICV is also analyzed for the effects of a pressure using a finite element model that is described in [Appendix 2.10.1.2, Inner Containment Assembly \(ICV\) Structural Analysis](#). For the NCT increased external pressure condition, evaluations include one load case for the OCA and one load case for the ICV.

Maximum stress intensities are determined for each component, and classified according to primary or secondary, membrane or bending. Classification of stress intensities is per Table NB-3217-1 of the ASME Boiler and Pressure Vessel Code. Maximum stress intensities are presented for the maximum general primary membrane stress intensity, P_m , the maximum local primary membrane stress intensity, P_L , the maximum primary membrane (general or local) plus primary bending stress intensity, $P_m + P_b$ or $P_L + P_b$, and the maximum primary plus secondary stress intensity, $P_m + P_b + Q$ or $P_L + P_b + Q$.

OCA Load Case 4 (see [Table 2.6-4](#) and [Figure 2.6-7](#) and [Figure 2.6-8](#)): This analysis is performed at a uniform temperature of 70 °F, and the reference temperature also set to 70 °F thereby eliminating any differential thermal expansion stresses. The external pressure is 14.7 psig.

$P_m = 4,748$ psi, located in the OCV shell at the cylindrical/conical transition,

$P_L = 6,852$ psi, located in the knuckle region of the upper OCV torispherical head,

$P_L + P_b = 5,087$ psi, located in the OCV shell at the cylindrical/conical transition, and

$P_L + P_b + Q = 9,641$ psi, located in the knuckle region of the lower OCV torispherical head.

ICV Load Case 2 (see [Table 2.6-6](#) and [Figure 2.6-11](#) and [Figure 2.6-12](#)): This analysis is performed at a uniform temperature of 70 °F, but with the reference temperature also set to 70 °F thereby eliminating any differential thermal expansion stresses. As with OCA Load Case 4, the external pressure is 14.7 psig.

$P_m = 3,635$ psi, located in the crown region of the upper ICV torispherical head,

$P_L = 6,384$ psi, located in the knuckle region of the upper ICV torispherical head,

$P_L + P_b = 4,656$ psi, located in the crown region of the upper ICV torispherical head, and

$P_L + P_b + Q = 9,104$ psi, located in the knuckle region of the upper ICV torispherical head.

Polyurethane foam stress intensities are insignificant for OCA Load Case 4.

2.6.4.2 Comparison with Allowable Stresses

[Section 2.1.2, Design Criteria](#), presents the design criteria for structural evaluation of the HalfPACT packaging. The containment vessel design criteria for NCT analyses are in accordance with Regulatory Guide 7.6, which uses as a basis the criteria defined for Level A service limits in Section III

of the ASME Boiler and Pressure Vessel Code. Load combinations follow the guidelines of Regulatory Guide 7.8.

From Table 2.3-1 in Section 2.3.1, *Mechanical Properties Applied to Analytic Evaluations*, the design stress intensity for Type 304 stainless steel used in the ICV and OCV is $S_m = 20,000$ psi at 160 °F. From Table 2.1-1 in Section 2.1.2.1.1, *Containment Structures*, the allowable stress intensities for the NCT increased external pressure condition is S_m for general primary membrane stress intensity (P_m), $1.5S_m$ for local primary membrane stress intensity (P_L), $1.5S_m$ for primary membrane (general or local) plus primary bending stress intensity ($P_m + P_b$ or $P_L + P_b$), and $3.0S_m$ for the range of primary plus secondary stress intensity ($P_m + P_b + Q$ or $P_L + P_b + Q$).

Maximum stress intensity, allowable stress intensity, and minimum margins of safety for each stress category and each load case are presented in Table 2.6-4 and Table 2.6-6 for each of the cases discussed above. Since all margins of safety are positive, the design criteria are satisfied.

2.6.4.3 Buckling Assessment of the Torispherical Heads

The buckling analysis of the torispherical heads is based on the methodology outlined in Paragraph NE-3133.4(e), *Torispherical Heads*, of the ASME Boiler and Pressure Vessel Code, Section III, Subsection NE. The results from following this methodology are summarized below.

Parameter	OCV Torispherical Head		ICV Torispherical Head	
	Upper	Lower	Upper	Lower
R	77.3125	74.1250	74.3750	73.1250
T	0.25	0.25	0.25	0.25
$A = \frac{0.125}{(R/T)}$	0.00040	0.00042	0.00042	0.00043
B^6	5,000	5,000	5,000	5,000
$P_a = \frac{B}{(R/T)}$	16.2	16.9	16.8	17.1

The smallest allowable pressure, P_a , is 16.2 psig for the OCV upper head. For an applied external pressure of 14.7 psig, the corresponding buckling margin of safety is:

$$MS = \frac{16.2}{14.7} - 1 = +0.10$$

⁶ Factor B is found from American Society of Mechanical Engineers (ASME) Boiler and Pressure Vessel Code, Section II, *Materials*, Part D, *Properties*, Subpart 3, *Charts and Tables for Determining the Shell Thickness of Components Under External Pressure*, Figure HA-1, *Chart for Determining Shell Thickness of Components Under External Pressure When Constructed of Austenitic Steel (18Cr-8Ni, Type 304)*, 1995 Edition, 1997 Addenda. Conservatively, the 400 °F temperature curve is used for each case.

Since the margin of safety in the worst case is positive, it is concluded that none of the OCV or ICV torispherical heads will buckle for an external pressure of 14.7 psig.

2.6.4.4 Buckling Assessment of the Cylindrical Shells

The cylindrical portions of the OCV and ICV are evaluated using ASME Boiler and Pressure Vessel Code Case N-284-1⁷. Consistent with Regulatory Guide 7.6 philosophy, a factor of safety of 2.0 is applied for NCT buckling evaluations per ASME Code Case N-284-1, corresponding to ASME Code, Service Level A conditions.

Buckling analysis geometry parameters are summarized in [Table 2.6-7](#), and loading parameters are summarized in [Table 2.6-8](#). The cylindrical shell buckling analysis conservatively utilizes an OCV and ICV temperature of 160 °F, consistent with [Section 2.6.1, Heat](#). The stresses are determined using an external pressure of 14.7 psig. The hoop stress, σ_{θ} , axial stress, σ_{ϕ} , and in-plane shear stress, $\sigma_{\phi\theta}$, are found from:

$$\sigma_{\theta} = \frac{Pr}{t} \quad \sigma_{\phi} = \frac{Pr}{2t} \quad \sigma_{\phi\theta} = \frac{Pr}{4t}$$

where P is the applied external pressure of 14.7 psi, r is the mean radius, and t is the cylindrical shell thickness. As shown in [Table 2.6-9](#), since all interaction check parameters are less than 1.0, as required, the design criteria are satisfied.

2.6.5 Vibration

By comparing the alternating stresses arising during NCT with the established endurance limits of the HalfPACT packaging materials of construction, the effects of vibration normally incident to transport are shown to be acceptable. These comparisons apply the methodology and limits of NRC Regulatory Guide 7.6. By conservatively comparing NCT stresses with endurance stress limits for an infinite service life, the development of accurate vibratory loading cycles is not required. The vibration evaluation is comprehensively addressed in the following sections.

2.6.5.1 Vibratory Loads Determination

ANSI N14.23⁸ provides a basis for estimating peak truck trailer vibration inputs. A summary of peak vibratory accelerations for a truck semi-trailer bed with light loads (less than 15 tons) is provided in Table 2 of ANSI N14.23. The component accelerations are given in Table 2 as 1.3g longitudinally, 0.5g laterally, and 2.0g vertically. Three fully loaded HalfPACT packages on a single trailer will exceed the light load limit, but acceleration magnitudes associated with light loads are conservative for heavy loads per Table 2 of ANSI N14.23. The commentary provided within Section 4.2, *Package Response*, of ANSI N14.23 states that recent “tests conducted by Sandia National Laboratories have shown that the *truck bed* accelerations provide an upper bound on *cask*

⁷ American Society of Mechanical Engineers (ASME) Boiler and Pressure Vessel Code, Section III, *Rules for Construction of Nuclear Power Plant Components*, Division 1, Class MC, Code Case N-284-1, *Metal Containment Shell Buckling Design Methods*, 1995 Edition, 1997 Addenda.

⁸ ANSI N14.23, *Design Basis for Resistance to Shock and Vibration of Radioactive Material Packages Greater than One Ton in Truck Transport* (Draft), 1980, American National Standards Institute, Inc, (ANSI).

(response) accelerations.” Based upon these data, conservatively assume the peak acceleration values from Table 2 are applied to the HalfPACT package in a continuously cycling fashion.

The compressive stress in the polyurethane foam for a 2g vertical acceleration is determined by conservatively ignoring the contributory effect of the OCA outer shell and dividing a maximum weight HalfPACT package (18,100 pounds) by the projected area of the package’s bottom. The projected area of a HalfPACT package is simply $(\pi/4)(94.375)^2 = 6,995 \text{ in}^2$. Therefore, the compressive stress is $(2)(18,100)/6,995 = 5 \text{ psi}$. This stress is negligible compared to the parallel-to-rise compressive strength of 150 psi for polyurethane foam at 160 °F, as discussed in [Section 2.6.1, Heat](#). Therefore, the remainder of the NCT vibration evaluation addresses only the structural steel portions of the HalfPACT packaging.

2.6.5.2 Calculation of Alternating Stresses

The HalfPACT package is a compact right circular cylinder. As such, the stresses developed as a result of transportation vibration become significant only where concentrated in the vicinity of the tie-downs and package interfaces with the transport vehicle. This fact allows the stress analyses of [Section 2.5.2, Tie-down Devices](#), to serve as the basis for derivation of alternating stress estimates.

The analyses of [Section 2.5.2, Tie-down Devices](#), identify three maximum stress locations of importance in the immediate vicinity of the tie-down lugs:

- 1. Tiedown lug weld shear stresses due to tensile tie-down forces.** Under a combined set of tie-down forces (i.e., 10g longitudinally, 5g laterally, and 2g vertically), the tie-down lug vertical tensile force is $F_{\text{tmax}} = 68,950$ pounds. The corresponding tie-down lug weld shear stress is $\tau = 8,997$ psi, from [Section 2.5.2.2.1, Failure of the Tie-down Lug Welds Due to Shear and Bending Loads](#). Weld shear stresses associated with unit accelerations (i.e., 1g) are derived from these values, as presented in [Table 2.6-10](#). Under unit horizontal and vertical accelerations, the maximum weld shear stresses are 699 psi and 590 psi, respectively, as shown in [Table 2.6-10](#).
- 2. OCA outer shell compressive membrane stresses due to vertical compressive loads.** Under a combined set of tie-down forces (i.e., 10g longitudinally, 5g laterally, and 2g vertically), the OCA outer shell and tie-down lug doubler plate vertical compressive load is $F_{\text{cmax}} = 128,901$ pounds. The corresponding compressive membrane stress is $\sigma_c = 12,394$ psi, from [Section 2.5.2.3.1, Bearing Stress in the OCA Outer Shell and Tie-down Lug Doubler Plate](#). Compressive membrane stresses associated with unit accelerations (i.e., 1g) are derived from these values, as presented in [Table 2.6-11](#). Under unit horizontal and vertical accelerations, the maximum membrane compression stresses are 1,031 psi and 435 psi, respectively, as shown in [Table 2.6-11](#).
- 3. OCA tie-down weldment compressive membrane stresses due to horizontal compressive loads.** Under a combined set of tie-down forces (i.e., 10g longitudinally, 5g laterally, and 2g vertically), the OCA tie-down weldment horizontal compressive load is $F_h = 202,364$ pounds. The corresponding compressive membrane stress is $\sigma_c = 25,296$ psi, from [Section 2.5.2.4.1, Bearing Stress in the Tie-down Weldment](#). Compressive membrane stresses associated with unit accelerations (i.e., 1g) are derived from these values, as presented in [Table 2.6-12](#). Under unit horizontal accelerations, the maximum membrane compression stress is 2,263 psi, as shown in [Table 2.6-12](#).

Alternating stress intensities, S_{alt} , due to 1g unit accelerations are calculated directly from the above values since there are no other measurable stresses acting on the package at the locations considered. Unit alternating stress intensities at the three evaluated locations are found as shown in [Table 2.6-13](#), making use of the definition of alternating stress intensity as one-half of the range of stress intensity at the location of interest, and the definition of stress intensity as twice the shear stress.

These maximum alternating stress intensity unit values correspond to stresses in the bevel-plus-fillet welds used to attach the tie-down lugs to the tie-down lug doubler plates. A stress concentration factor of four is conservatively applied in accordance with Paragraph C.3.d of Regulatory Guide 7.6. Normalizing the unit values to the peak acceleration estimates given in [Section 2.6.5.1, *Vibratory Loads Determination*](#), and including the stress concentration factor of four and assuming these worst cases occur at the same location, results in the following conservative estimates of alternating stress intensity associated with the vibratory environments.

For the maximum horizontal alternating stress intensity of 1,132 psi from [Table 2.6-13](#):

$$S_{alt} = 4(1,132)\sqrt{(1.3)^2 + (0.5)^2} = 6,307 \text{ psi}$$

and, for the maximum vertical alternating stress intensity of 590 psi from [Table 2.6-13](#):

$$S_{alt} = 4(590)(2.0) = 4,720 \text{ psi}$$

Assuming a simultaneous application of the above alternating stress intensities associated with horizontal and vertical loads yields a maximum alternating stress of $6,307 + 4,720 = 11,027$ psi.

2.6.5.3 Stress Limits and Results

The permissible alternating stress intensity, S_a , is given by conservatively using the minimum asymptotic value from the design fatigue curves in Table I-9.2.2 of the ASME Boiler and Pressure Vessel Code⁹. For design fatigue curve C at 10^{11} cycles, $S_a = 13,600$ psi, based on an elastic modulus of $28.3(10)^6$ psi. This value, when multiplied by the ratio of the elastic modulus at 160 °F of $27.8(10)^6$ psi to an elastic modulus at 70 °F of $28.3(10)^6$ psi results in an allowable alternating stress intensity amplitude at 160 °F of:

$$S_a = 13,600 \left(\frac{27.8}{28.3} \right) = 13,360 \text{ psi}$$

Finally, a conservative estimate of the margin of safety for vibratory effects becomes:

$$MS = \frac{S_a}{S_{alt}} - 1 = \frac{13,360}{11,027} - 1 = +0.21$$

⁹ American Society of Mechanical Engineers (ASME) Boiler and Pressure Vessel Code, Section III, *Rules for Construction of Nuclear Power Plant Components*, Appendix I, *Design Stress Intensity Values, Allowable Stresses, Material Properties, and Design Fatigue Curves*, 1995 Edition, 1997 Addenda.

2.6.6 Water Spray

The materials of construction utilized for the HalfPACT package are such that the water spray test identified in 10 CFR §71.71(c)(6) will have a negligible effect on the package.

2.6.7 Free Drop

Since the maximum gross weight of the HalfPACT package is 18,100 pounds, a three foot free drop is required per 10 CFR §71.71(c)(7). As discussed in [Appendix 2.10.3, *Certification Tests*](#), a NCT, three foot side drop, aligned over the OCV vent port, was performed on a HalfPACT package certification test unit (CTU) as an initial condition for subsequent hypothetical accident condition (HAC) tests. Leakage rate testing following certification testing demonstrated the ability of the HalfPACT package to maintain leaktight (i.e., 1.0×10^{-7} standard cubic centimeters per second (scc/sec), air) sealing integrity. Therefore, the requirements of 10 CFR §71.71(c)(7) are met.

2.6.8 Corner Drop

This test does not apply, since the package weight is in excess of 100 kg (220 pounds), and the materials do not include wood or fiberboard, as delineated in 10 CFR §71.71(c)(8).

2.6.9 Compression

This test does not apply, since the package weight is in excess of 5,000 kg (11,000 pounds), as delineated in 10 CFR §71.71(c)(9).

2.6.10 Penetration

The one meter (40 inch) drop of a 13 pound, hemispherically-headed, 1¼ inch diameter, steel cylinder, as delineated in 10 CFR §71.71(c)(10), is of negligible consequence to the HalfPACT package. This is due to the fact that the HalfPACT package is designed to minimize the consequences associated with the much more limiting case of a 40 inch drop of the entire package onto a puncture bar as discussed in [Section 2.7.3, *Puncture*](#). The 1/4 inch minimum thickness, OCA outer shell, the tie-down lugs and doubler plates, and the vent port and seal test port penetrations are not damaged by the penetration event.

Table 2.6-1 – Summary of Stress Results for OCA Load Case 1

Component	Location	Stress Intensity (psi)			
		General Primary Membrane (P_m)	Local Primary Membrane (P_L)	Primary Membrane + Bending ($P_{mL} + P_b$)	Primary plus Secondary ($P_{mL} + P_b + Q$)
OCV Shells	Cylindrical and Conical Shells	19,061 (Element 329)	-----	20,256 (Element 329)	-----
OCV Upper and Lower Torispherical Heads	Crown	13,366 (Element 339)	-----	18,739 (Element 340)	-----
	Knuckle	-----	28,084 (Element 337)	-----	39,884 (Element 320)
OCV Upper and Lower Seal Flanges	Shell side of the thickness transition	-----	-----	-----	32,358 (Node 2010)
	Flange side of the thickness transition	-----	-----	-----	20,129 (Node 2016)
OCV Locking Ring	Any location	-----	-----	-----	24,493 (Node 3050)
OCA Outer Shell and Z-flanges	Any location	9,114 (Element 414)	-----	14,215 (Element 414)	-----
Maximum Stress Intensity		19,061	28,084	20,256	39,884
Allowable Stress Intensity		20,000 (S_m)	30,000 ($1.5S_m$)	30,000 ($1.5S_m$)	60,000 ($3.0S_m$)
Minimum Margin of Safety		+0.05	+0.07	+0.48	+0.50

Table 2.6-2 – Summary of Stress Results for OCA Load Case 2

Component	Location	Stress Intensity (psi)			
		General Primary Membrane (P_m)	Local Primary Membrane (P_L)	Primary Membrane + Bending ($P_{mL} + P_b$)	Primary plus Secondary ($P_{mL} + P_b + Q$)
OCV Shells	Cylindrical and Conical Shells	-----	-----	-----	20,144 (Element 329)
OCV Upper and Lower Torispherical Heads	Crown	-----	-----	-----	18,831 (Element 340)
	Knuckle	-----	-----	-----	40,200 (Element 320)
OCV Upper and Lower Seal Flanges	Shell side of the thickness transition	-----	-----	-----	32,569 (Node 2010)
	Flange side of the thickness transition	-----	-----	-----	20,271 (Node 2016)
OCV Locking Ring	Any location	-----	-----	-----	24,503 (Node 3050)
OCA Outer Shell and Z-flanges	Any location	-----	-----	-----	12,385 (Element 399)
Maximum Stress Intensity		-----	-----	-----	40,200
Allowable Stress Intensity		20,000 (S_m)	30,000 ($1.5S_m$)	30,000 ($1.5S_m$)	60,000 ($3.0S_m$)
Minimum Margin of Safety		-----	-----	-----	+0.49

Table 2.6-3 – Summary of Stress Results for OCA Load Case 3

Component	Location	Stress Intensity (psi)			
		General Primary Membrane (P_m)	Local Primary Membrane (P_L)	Primary Membrane + Bending ($P_{mL} + P_b$)	Primary plus Secondary ($P_{mL} + P_b + Q$)
OCV Shells	Cylindrical and Conical Shells	-----	-----	-----	854 (Element 327)
OCV Upper and Lower Torispherical Heads	Crown	-----	-----	-----	538 (Element 309)
	Knuckle	-----	-----	-----	1,040 (Element 323)
OCV Upper and Lower Seal Flanges	Shell side of the thickness transition	-----	-----	-----	450 (Node 2001)
	Flange side of the thickness transition	-----	-----	-----	911 (Node 1040)
OCV Locking Ring	Any location	-----	-----	-----	0
OCA Outer Shell and Z-flanges	Any location	-----	-----	-----	5,772 (Element 393)
Maximum Stress Intensity		-----	-----	-----	5,772
Allowable Stress Intensity		20,000 (S_m)	30,000 ($1.5S_m$)	30,000 ($1.5S_m$)	60,000 ($3.0S_m$)
Minimum Margin of Safety		-----	-----	-----	+9.40

Table 2.6-4 – Summary of Stress Results for OCA Load Case 4

Component	Location	Stress Intensity (psi)			
		General Primary Membrane (P_m)	Local Primary Membrane (P_L)	Primary Membrane + Bending ($P_{mL} + P_b$)	Primary plus Secondary ($P_{mL} + P_b + Q$)
OCV Shells	Cylindrical and Conical Shells	4,748 (Element 329)	-----	5,087 (Element 329)	-----
OCV Upper and Lower Torispherical Heads	Crown	3,323 (Element 339)	-----	4,569 (Element 340)	-----
	Knuckle	-----	6,852 (Element 337)	-----	9,641 (Element 320)
OCV Upper and Lower Seal Flanges	Shell side of the thickness transition	-----	-----	-----	3,507 (Node 1016)
	Flange side of the thickness transition	-----	-----	-----	3,741 (Node 1164)
OCV Locking Ring	Any location	-----	-----	-----	4 (Node 3181)
OCA Outer Shell and Z-flanges	Any location	858 (Element 399)	-----	1,135 (Element 399)	-----
Maximum Stress Intensity		4,748	6,852	5,087	9,641
Allowable Stress Intensity		20,000 (S_m)	30,000 ($1.5S_m$)	30,000 ($1.5S_m$)	60,000 ($3.0S_m$)
Minimum Margin of Safety		+3.21	+3.38	+4.90	+5.22

Table 2.6-5 – Summary of Stress Results for ICV Load Case 1

Component	Location	Stress Intensity (psi)			
		General Primary Membrane (P_m)	Local Primary Membrane (P_L)	Primary Membrane + Bending ($P_{mL} + P_b$)	Primary plus Secondary ($P_{mL} + P_b + Q$)
ICV Shells	Cylindrical and Conical Shells	15,251 (Element 364)	-----	22,336 (Element 365)	-----
ICV Upper and Lower Torispherical Heads	Crown	15,242 (Element 376)	-----	19,519 (Element 377)	-----
	Knuckle	-----	26,968 (Element 373)	-----	38,304 (Element 374)
ICV Upper and Lower Seal Flanges	Shell side of the thickness transition	-----	-----	-----	34,042 (Node 2058)
	Flange side of the thickness transition	-----	-----	-----	27,922 (Node 2053)
ICV Locking Ring	Any location	-----	-----	-----	22,190 (Node 3046)
Maximum Stress Intensity		15,251	26,968	22,336	38,304
Allowable Stress Intensity		20,000 (S_m)	30,000 ($1.5S_m$)	30,000 ($1.5S_m$)	60,000 ($3.0S_m$)
Minimum Margin of Safety		+0.31	+0.11	+0.34	+0.57

Table 2.6-6 – Summary of Stress Results for ICV Load Case 2

Component	Location	Stress Intensity (psi)			
		General Primary Membrane (P_m)	Local Primary Membrane (P_L)	Primary Membrane + Bending ($P_{mL} + P_b$)	Primary plus Secondary ($P_{mL} + P_b + Q$)
ICV Shells	Cylindrical and Conical Shells	2,363 (Element 361)	-----	2,551 (Element 363)	-----
ICV Upper and Lower Torispherical Heads	Crown	3,635 (Element 376)	-----	4,656 (Element 377)	-----
	Knuckle	-----	6,382 (Element 373)	-----	9,104 (Element 374)
ICV Upper and Lower Seal Flanges	Shell side of the thickness transition	-----	-----	-----	2,706 (Node 2054)
	Flange side of the thickness transition	-----	-----	-----	3,640 (Node 1129)
ICV Locking Ring	Any location	-----	-----	-----	56 (Node 3046)
Maximum Stress Intensity		3,635	6,382	4,656	9,104
Allowable Stress Intensity		20,000 (S_m)	30,000 ($1.5S_m$)	30,000 ($1.5S_m$)	60,000 ($3.0S_m$)
Minimum Margin of Safety		+4.50	+3.70	+5.44	+5.59

Table 2.6-7 – Buckling Geometry Parameters per Code Case N-284-1

Geometry and Material Input		
	ICV	OCV
Mean Radius, inch	36.44	36.91
Shell Thickness, inch	0.25	0.188
Length, inch	36.0 ^①	32.0 ^②
Geometry Output (nomenclature consistent with ASME Code Case N-284-1)		
R =	36.44	36.91
t =	0.25	0.188
R/t =	145.76	196.85
ℓ_{ϕ} =	36.0	32.0
ℓ_{θ} =	228.94	231.89
M_{ϕ} =	11.93	12.16
M_{θ} =	75.85	88.15
M =	11.93	12.16

Notes:

- ① The ICV length is conservatively measured from five inches below the top of the lower ICV seal flange (at the beginning of the 1/4 inch wall thickness) to an assumed support point located one-third of the depth of the lower ICV torispherical head below the head-to-shell interface.
- ② The OCV length is conservatively measured from the top of the tapered wall portion (just below the lower OCV seal flange) to an assumed support point located one-third of the depth of the lower OCV torispherical head below the head-to-shell interface.

Table 2.6-8 – Stress Results for 14.7 psig External Pressure

ICV		OCV	
Axial Stress, σ_{ϕ}	1,071	Axial Stress, σ_{ϕ}	1,443
Hoop Stress, σ_{θ}	2,143	Hoop Stress, σ_{θ}	2,886
Shear Stress, $\sigma_{\phi\theta}$	536	Shear Stress, $\sigma_{\phi\theta}$	722

Table 2.6-9 – Buckling Summary for 14.7 psig External Pressure

Condition	ICV	OCV	Remarks
Capacity Reduction Factors (-1511)			
$\alpha_{\phi L} =$	0.2575	0.2575	
$\alpha_{\theta L} =$	0.8000	0.8000	
$\alpha_{\phi\theta L} =$	0.8000	0.8000	
Plasticity Reduction Factors (-1611)			
$\eta_{\phi} =$	0.5877	0.7307	
$\eta_{\theta} =$	1.0000	1.0000	
$\eta_{\phi\theta} =$	0.4474	0.5740	
Theoretical Buckling Values (-1712.1.1)			
$C_{\phi} =$	0.6050	0.6050	
$\sigma_{\phi eL} =$	115,720 psi	85,697 psi	
$C_{\theta r} =$	0.0855	0.0837	
$\sigma_{\theta eL} = \sigma_{reL} =$	16,354 psi	11,854 psi	
$C_{\theta h} =$	0.0815	0.0798	
$\sigma_{\theta eL} = \sigma_{heL} =$	15,581 psi	11,302 psi	
$C_{\phi\theta} =$	0.2184	0.2162	
$\sigma_{\phi\theta eL} =$	41,770 psi	30,615 psi	
Elastic Interaction Equations (-1713.1.1)			
$\sigma_{xa} =$	22,237 psi	16,466 psi	
$\sigma_{ha} =$	9,302 psi	6,748 psi	
$\sigma_{ra} =$	9,764 psi	7,077 psi	
$\sigma_{ra} =$	24,937 psi	18,278 psi	
Axial + Hoop \Rightarrow Check (a):	<i>N/A</i>	<i>N/A</i>	
Axial + Hoop \Rightarrow Check (b):	<i>N/A</i>	<i>N/A</i>	
Axial + Shear \Rightarrow Check (c):	<i>0.0697</i>	<i>0.1287</i>	<1 ∴ OK
Hoop + Shear \Rightarrow Check (d):	<i>0.3144</i>	<i>0.5873</i>	<1 ∴ OK
Axial + Hoop + Shear \Rightarrow Check (e,a):	<i>N/A</i>	<i>N/A</i>	
Axial + Hoop + Shear \Rightarrow Check (e,b):	<i>N/A</i>	<i>N/A</i>	
Inelastic Interaction Equations (-1713.2.1)			
$\sigma_{xc} =$	13,069 psi	12,032 psi	
$\sigma_{rc} =$	9,764 psi	7,077 psi	
$\sigma_{rc} =$	11,157 psi	10,492 psi	
Axial + Hoop \Rightarrow Check (a):	<i>0.3135</i>	<i>0.5841</i>	<1 ∴ OK
Axial + Shear \Rightarrow Check (b):	<i>0.1218</i>	<i>0.1750</i>	<1 ∴ OK
Hoop + Shear \Rightarrow Check (c):	<i>0.3182</i>	<i>0.5873</i>	<1 ∴ OK

Table 2.6-10 – Tie-down Lug Weld Shear Stresses

Case and Orientation	Load Factors (gs)	Load (pounds)	Shear Stress (psi)
Combined	10(x), 5(y), 2(z)	68,950	8,997
Horizontal	$[10^2 + 5^2]^{1/2} = 11.18$ (unit horizontal of 1g)	59,900 (5,358)	7,816 (699)
Vertical	2.00 (unit vertical of 1g)	9,050 (4,025)	1,181 (590)

Table 2.6-11 – OCA Outer Shell Compressive Membrane Stresses

Case and Orientation	Load Factors (gs)	Load (pounds)	Membrane Stress (psi)
Combined	10(x), 5(y), 2(z)	128,901	12,394
Horizontal	$[10^2 + 5^2]^{1/2} = 11.18$ (unit horizontal of 1g)	119,851 (10,720)	11,524 (1,031)
Vertical	2.00 (unit vertical of 1g)	9,050 (4,025)	870 (435)

Table 2.6-12 – OCA Tie-down Weldment Compressive Membrane Stresses

Case and Orientation	Load Factors (gs)	Load (pounds)	Membrane Stress (psi)
Horizontal	$[10^2 + 5^2]^{1/2} = 11.18$ (unit horizontal of 1g)	202,364 (18,100)	25,296 (2,263)

Table 2.6-13 – Maximum Unit Alternating Stress Intensities

Case and Orientation	Alternating Stress Intensity
Lug Weld Shear	$S_{alt} = \frac{2\tau_{max}}{2} = 699$ psi, Horizontal = 590 psi, Vertical
OCA Shell Compression	$S_{alt} = \frac{\sigma_{max}}{2} = 516$ psi, Horizontal = 218 psi, Vertical
OCA Base Compression	$S_{alt} = \frac{\sigma_{max}}{2} = 1,132$ psi, Horizontal
Maximum Unit Values	= 1,132 psi, Horizontal = 590 psi, Vertical

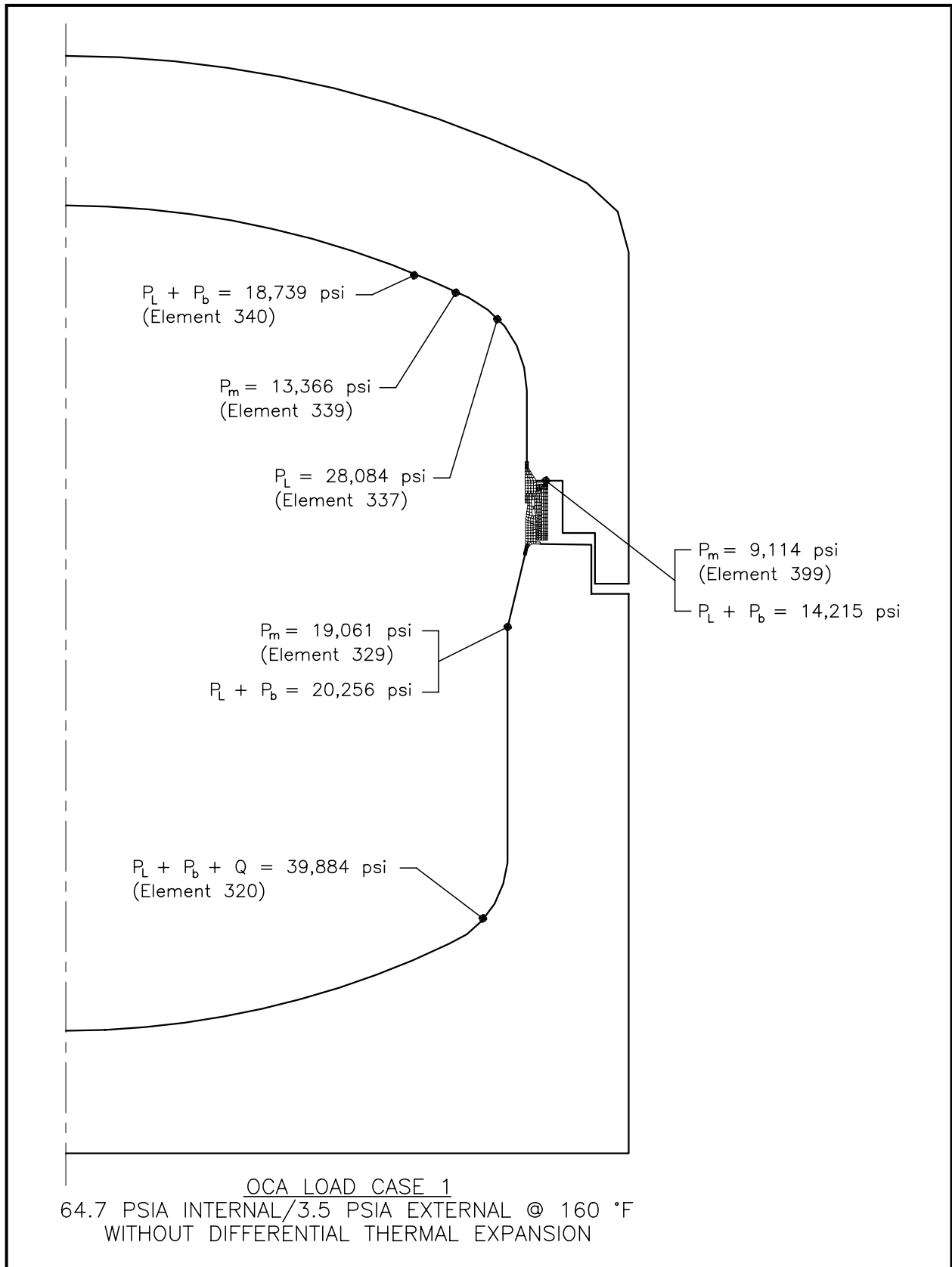


Figure 2.6-1 – OCA Load Case 1, Overall Model

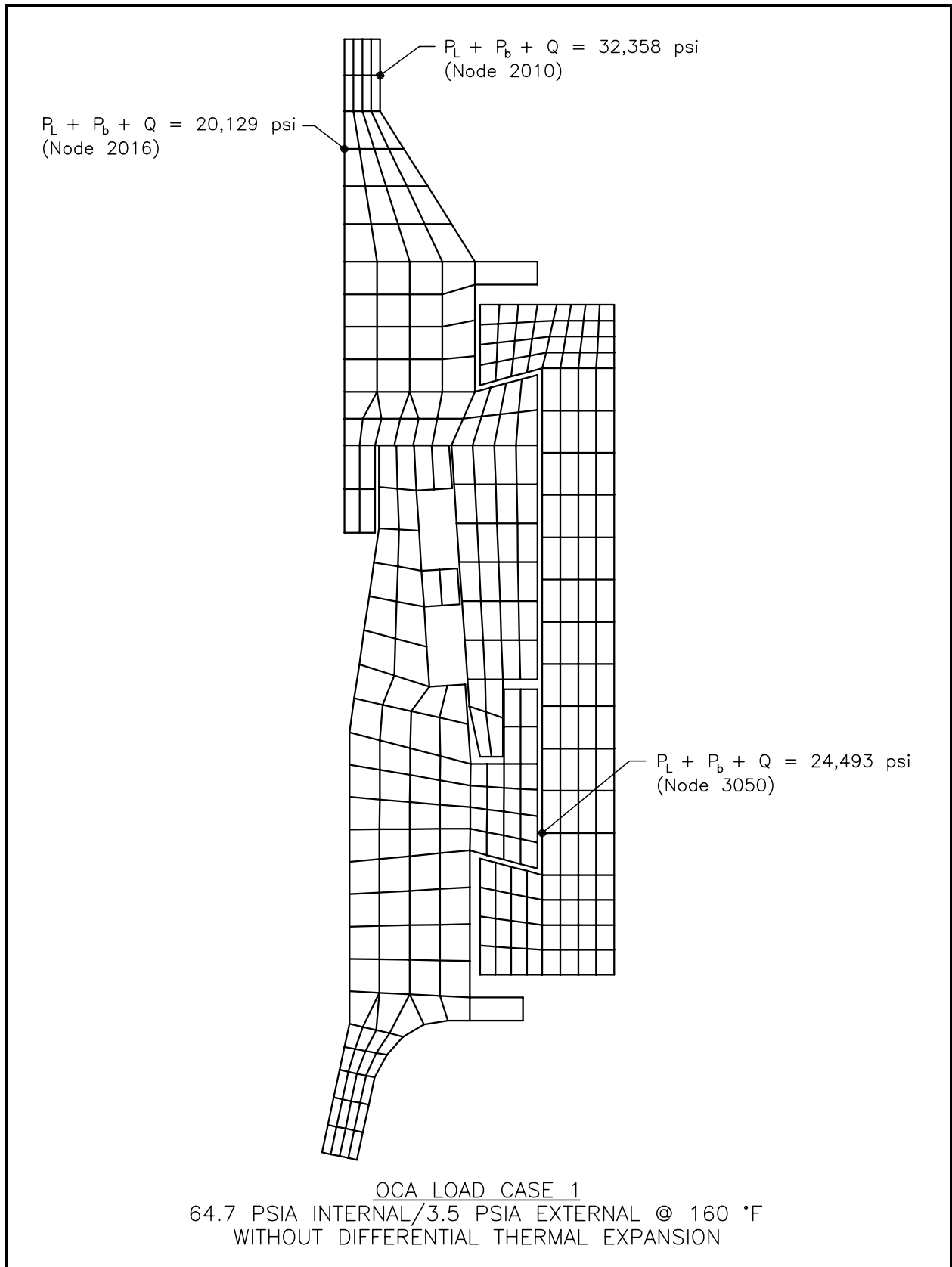


Figure 2.6-2 – OCA Load Case 1, Seal Region Detail

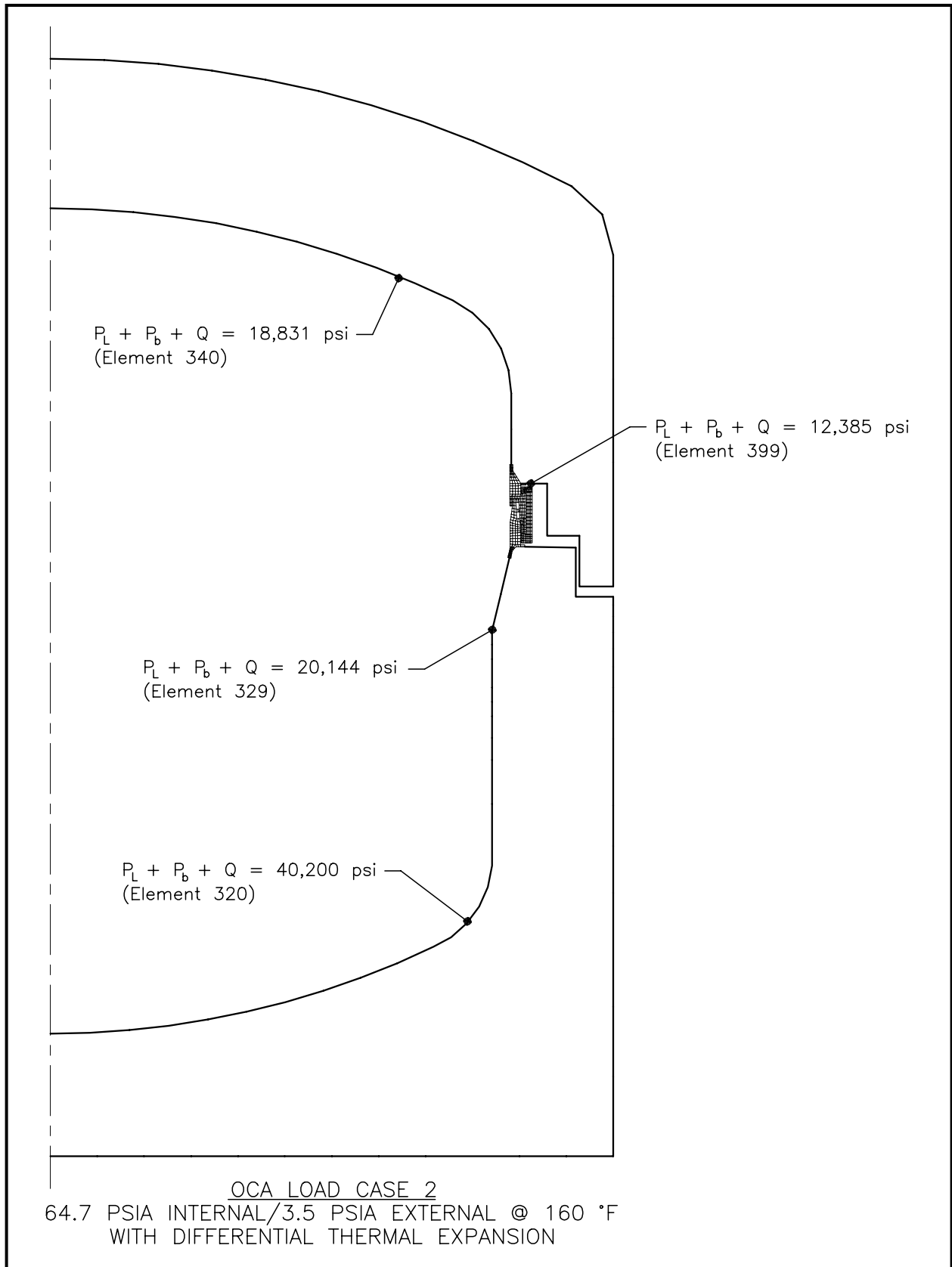


Figure 2.6-3 – OCA Load Case 2, Overall Model

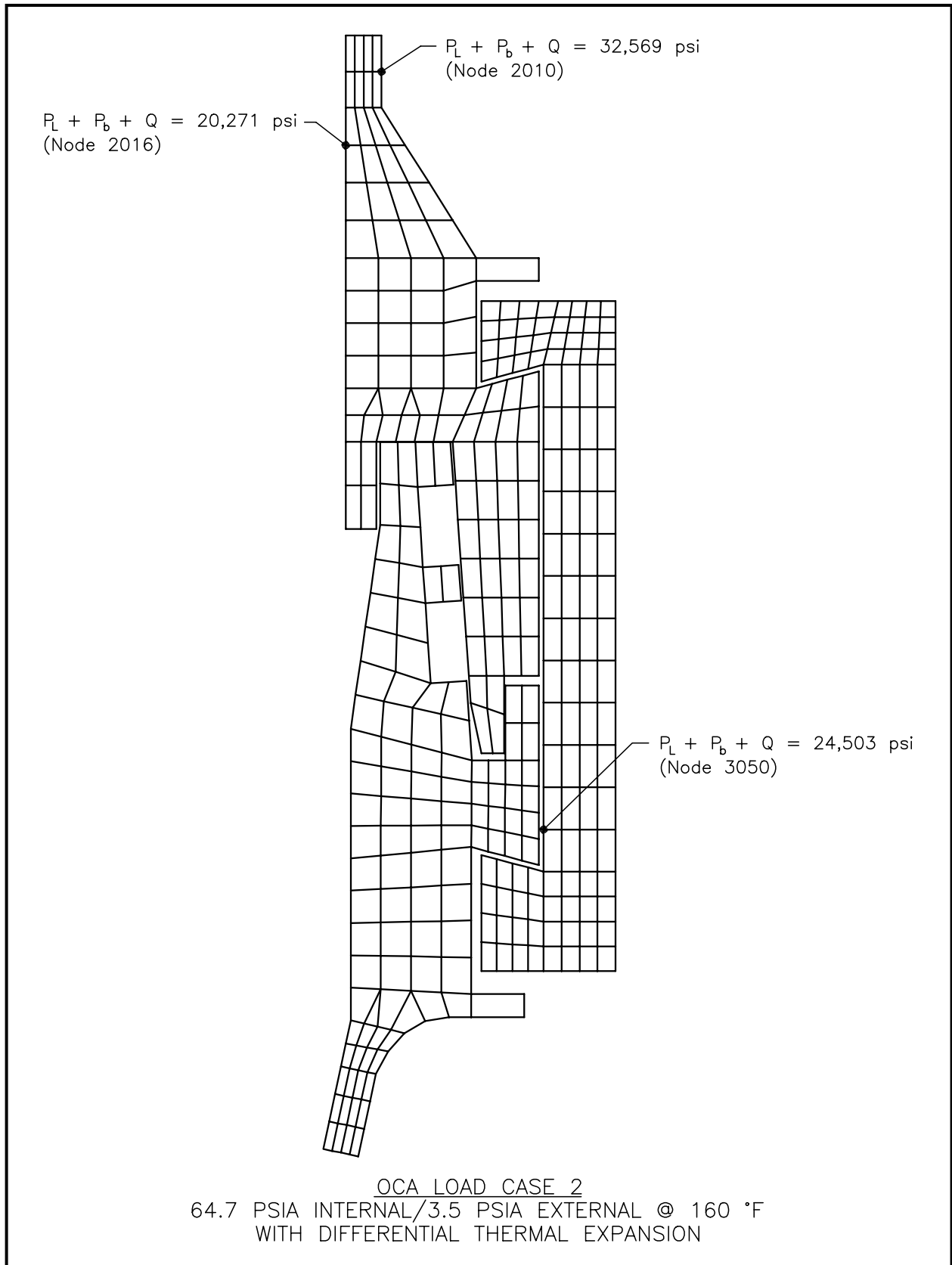


Figure 2.6-4 – OCA Load Case 2, Seal Region Detail

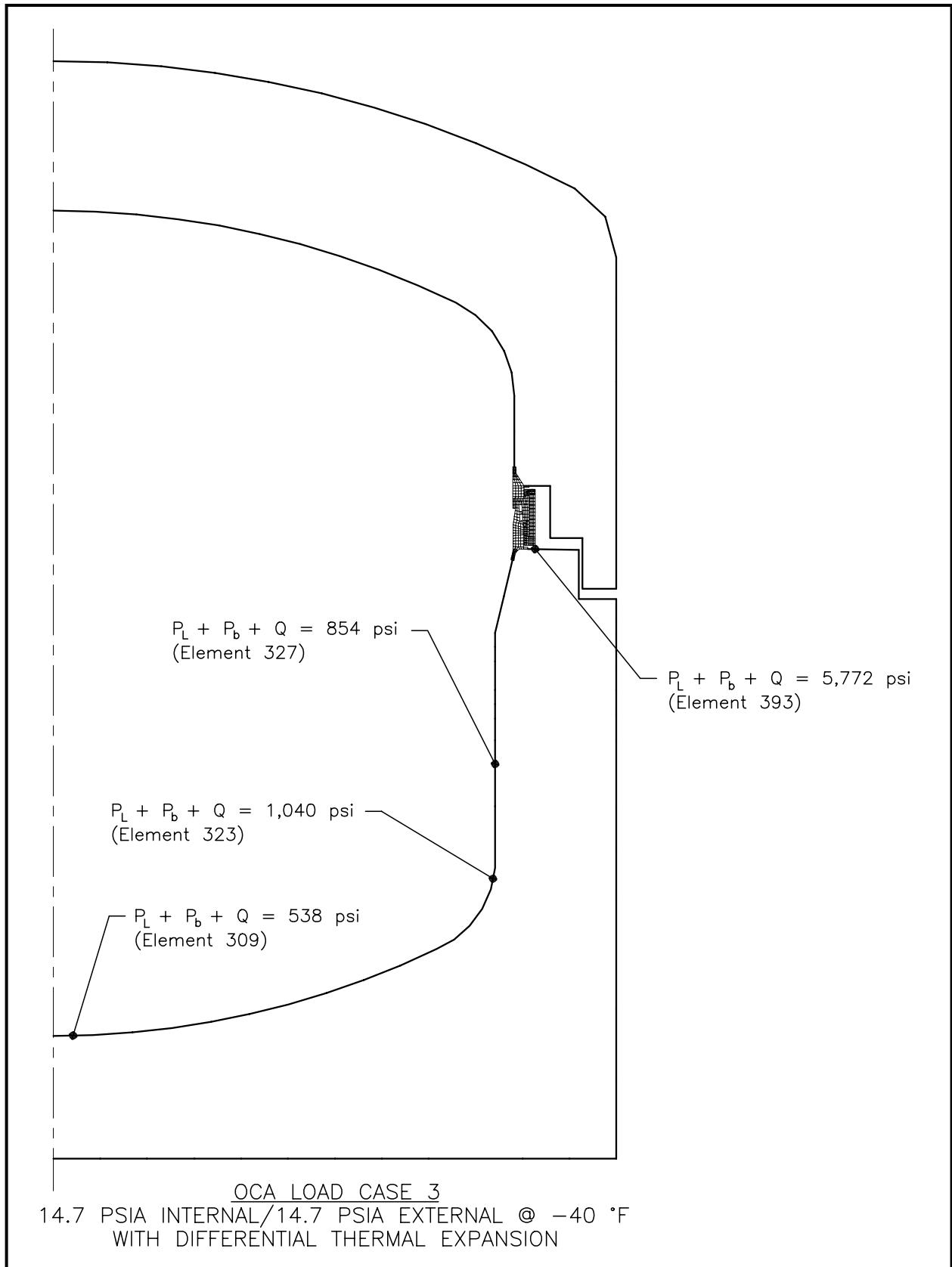


Figure 2.6-5 – OCA Load Case 3, Overall Model

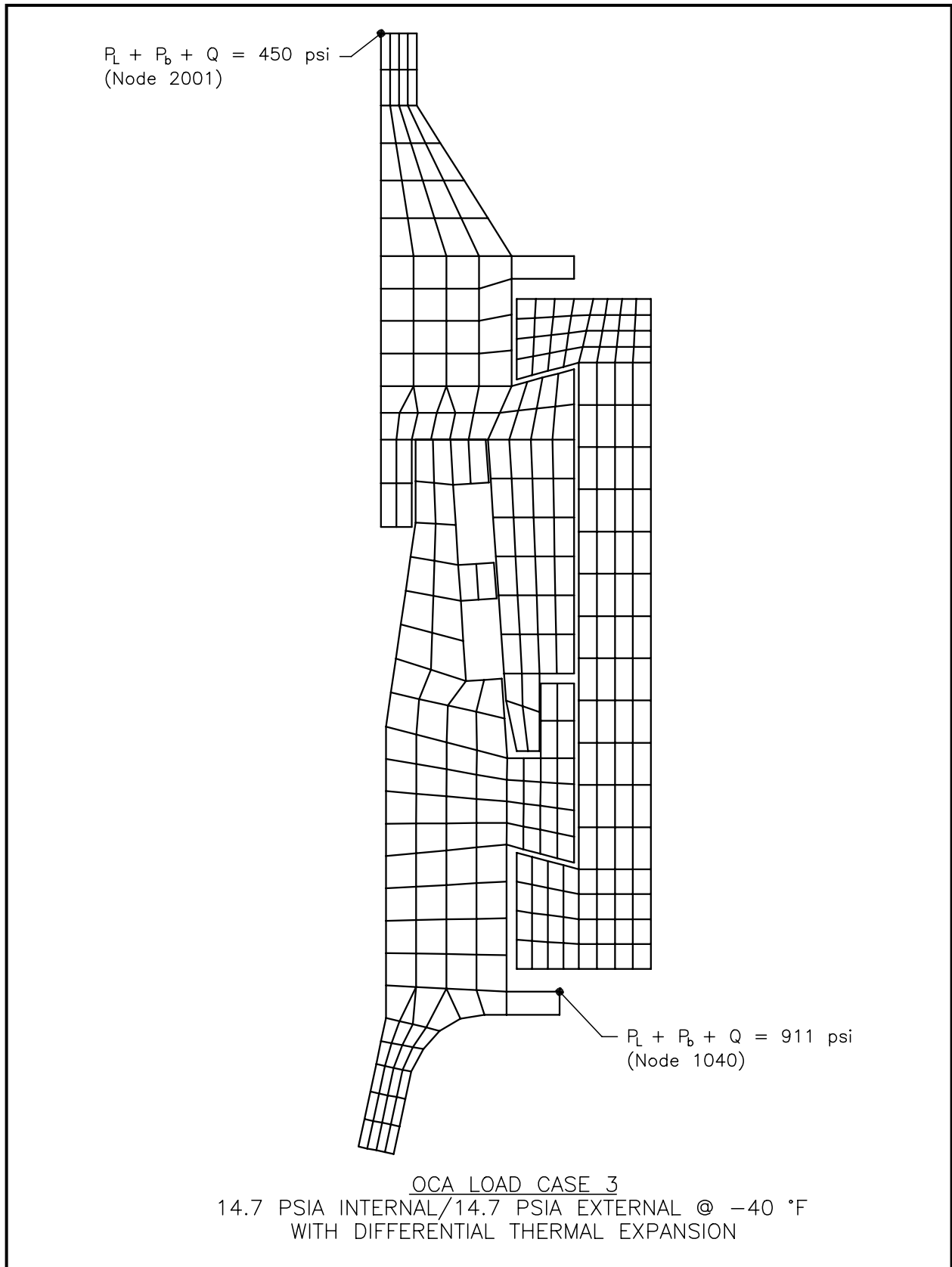


Figure 2.6-6 – OCA Load Case 3, Seal Region Detail

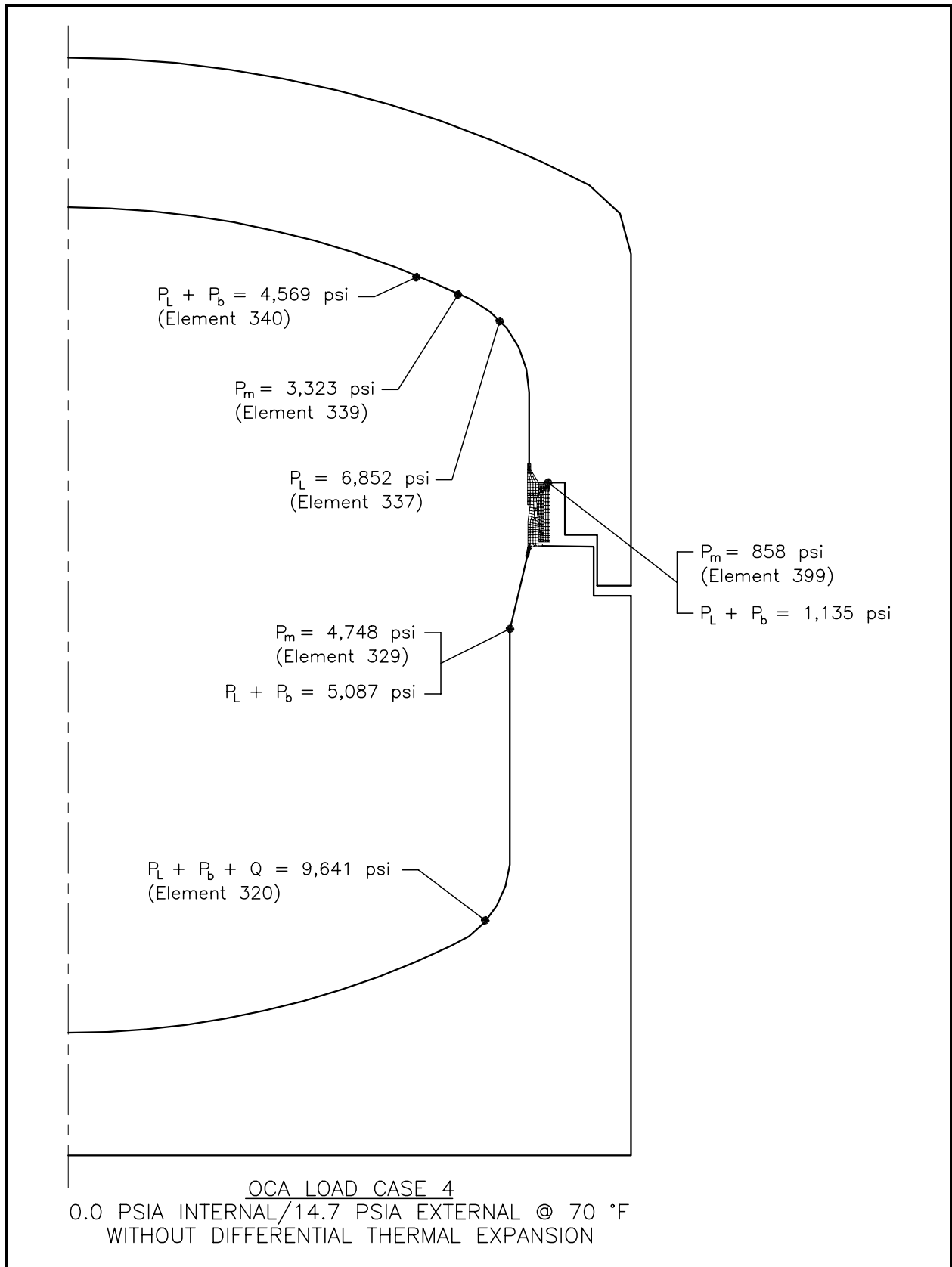


Figure 2.6-7 – OCA Load Case 4, Overall Model

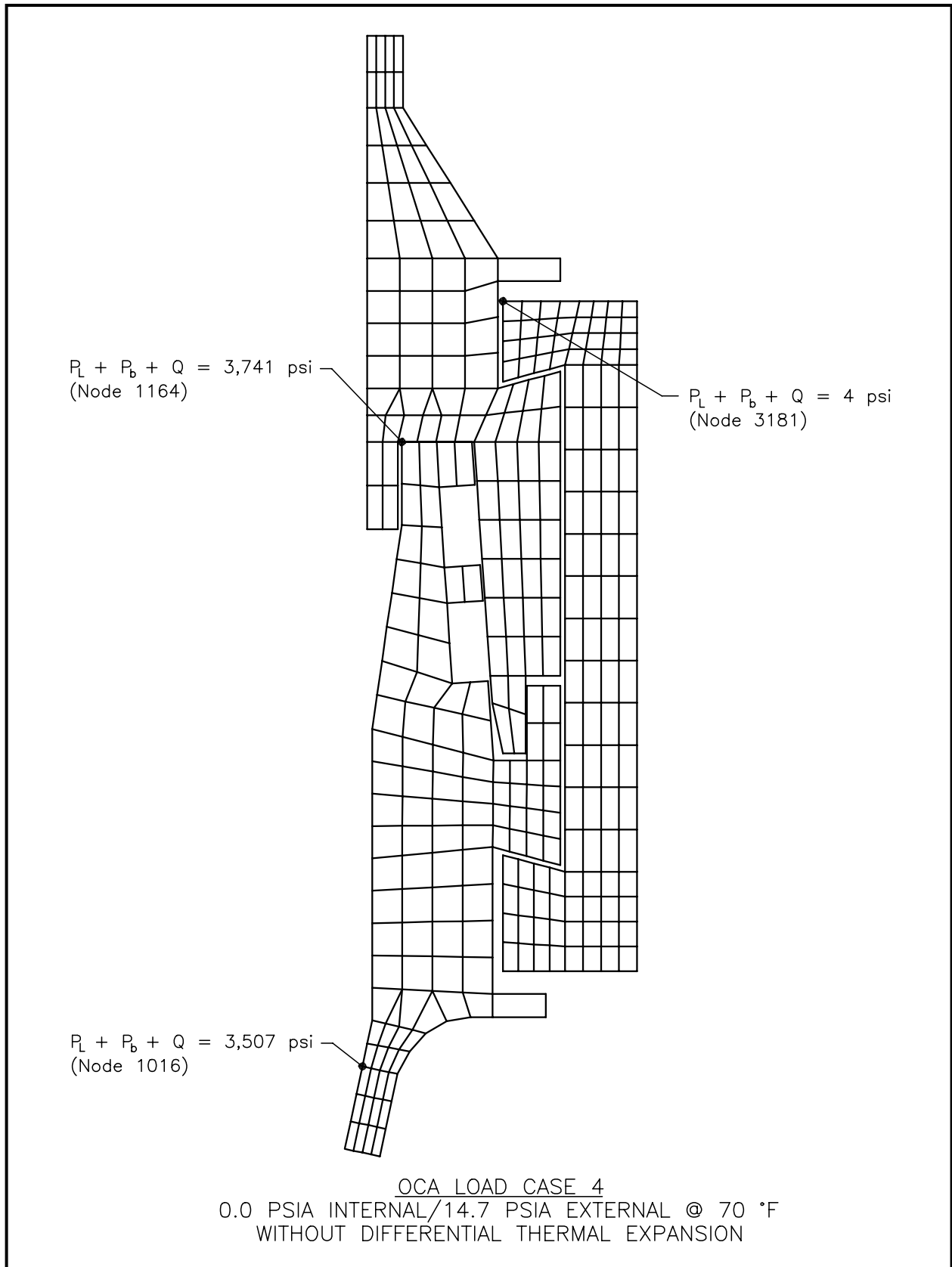


Figure 2.6-8 – OCA Load Case 4, Seal Region Detail

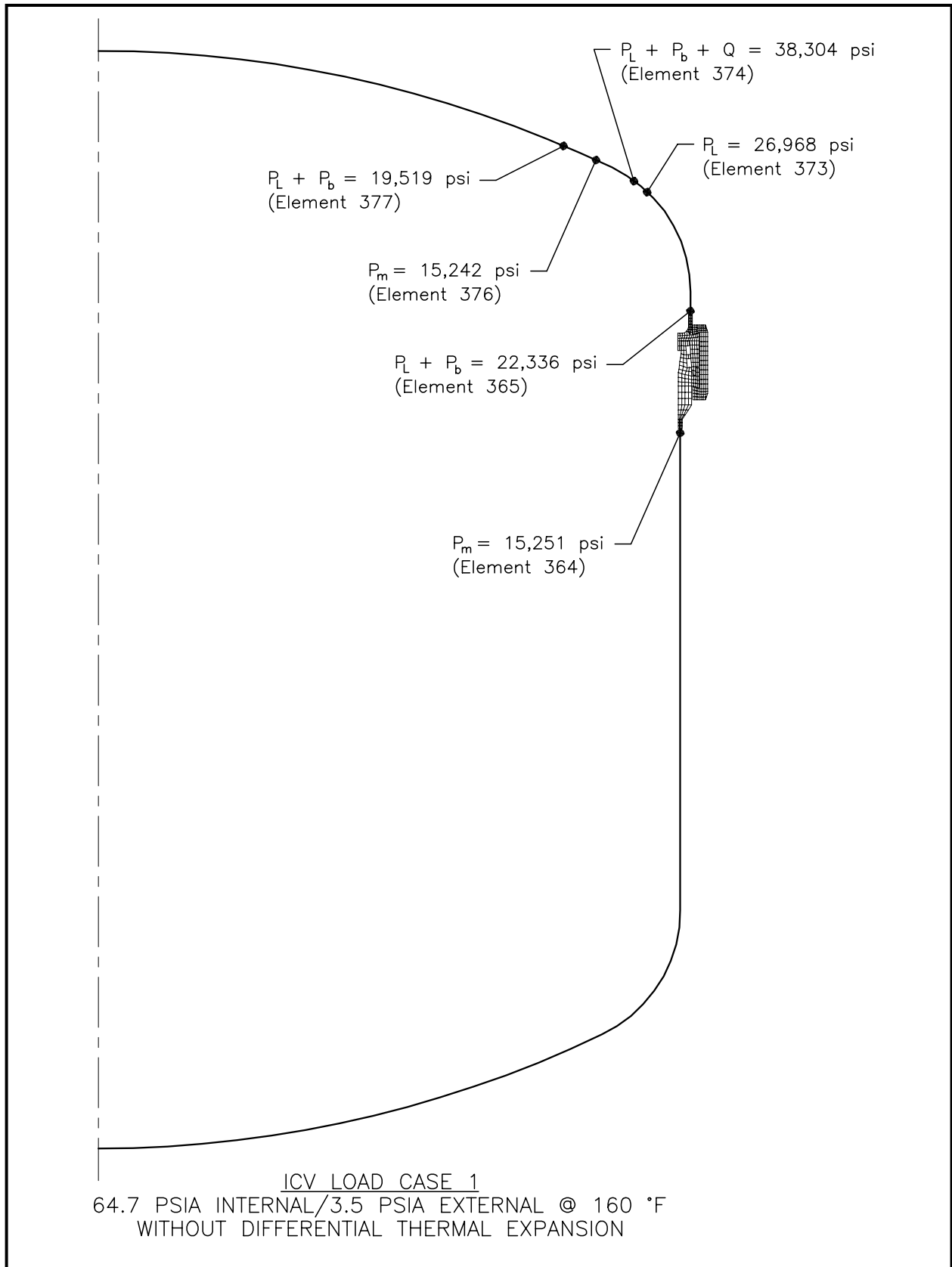


Figure 2.6-9 – ICV Load Case 1, Overall Model

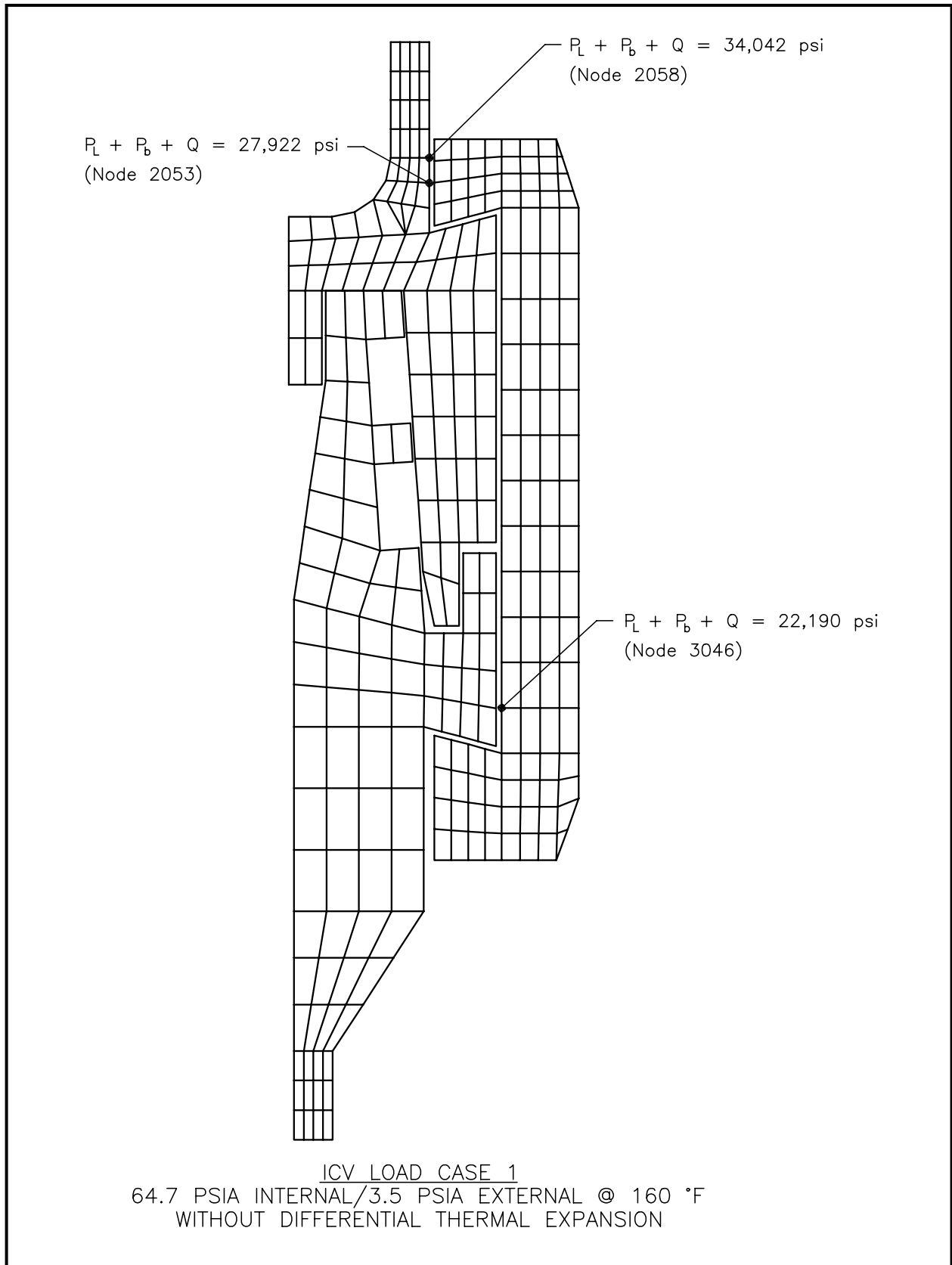


Figure 2.6-10 – ICV Load Case 1, Seal Region Detail

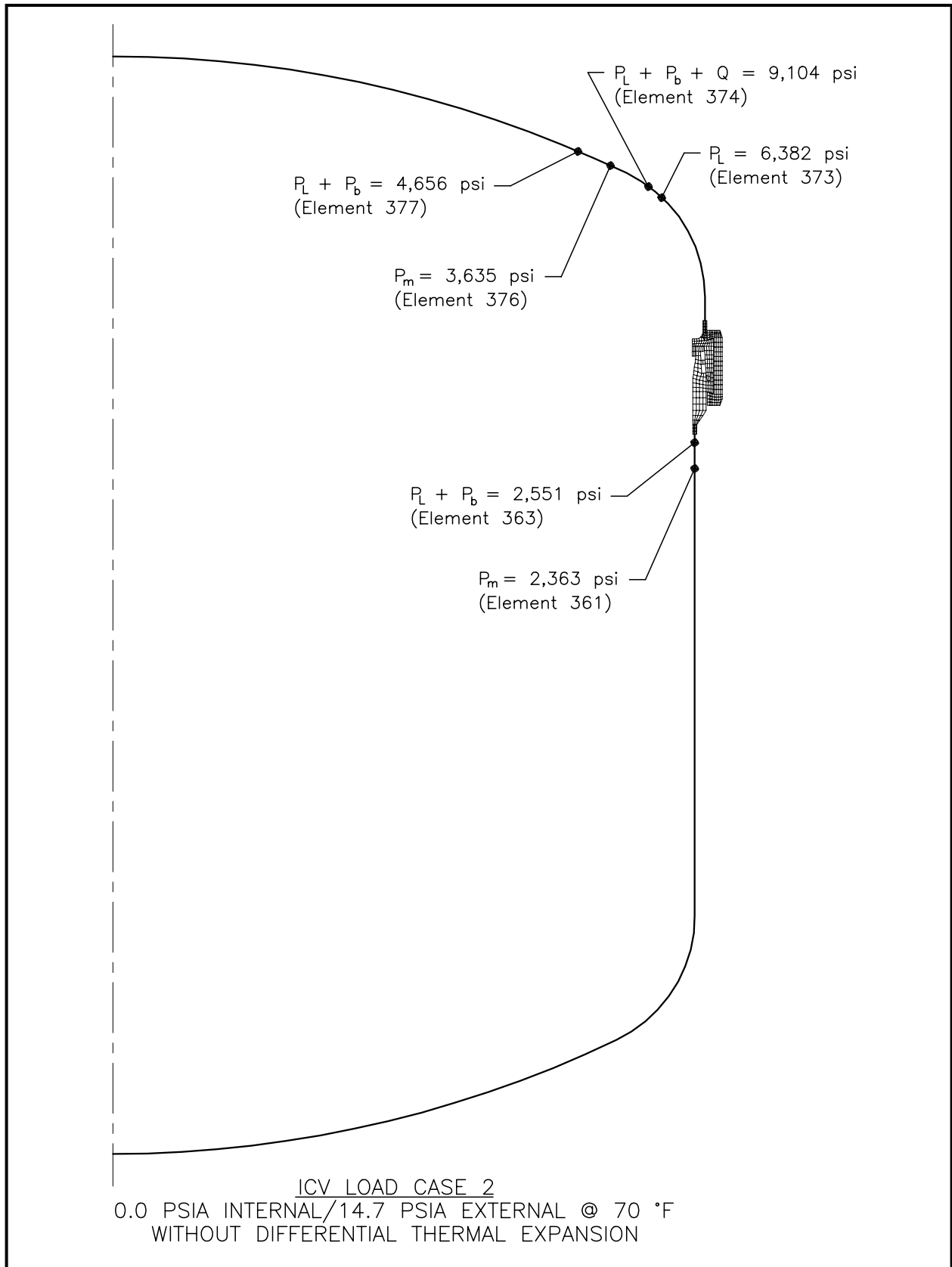


Figure 2.6-11 – ICV Load Case 2, Overall Model

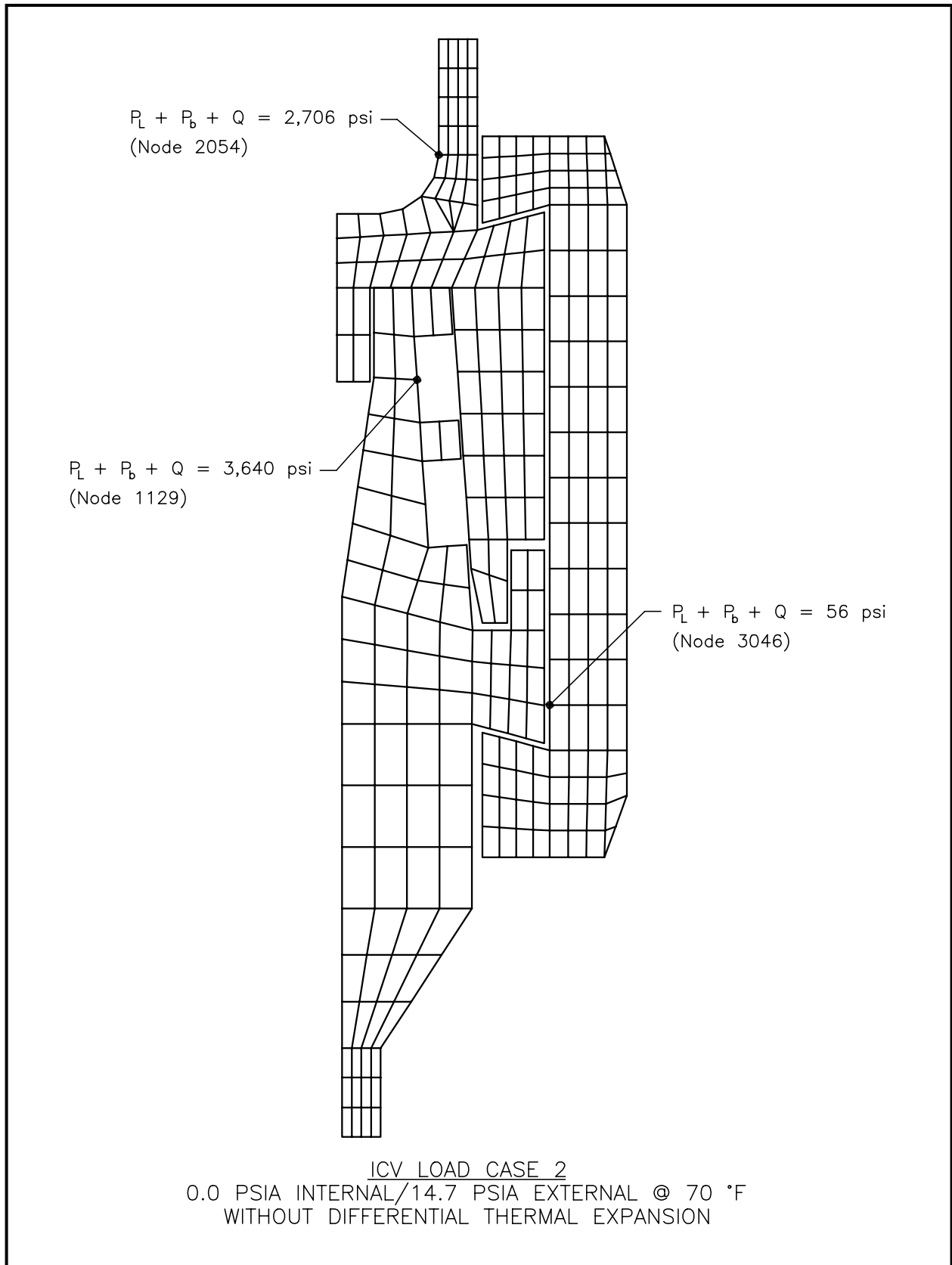


Figure 2.6-12 – ICV Load Case 2, Seal Region Detail

2.7 Hypothetical Accident Conditions

The HalfPACT package, when subjected to the sequence of hypothetical accident condition (HAC) tests specified in 10 CFR §71.73¹, subsequent to the sequence of normal conditions of transport (NCT) tests specified in 10 CFR §71.71, is shown to meet the performance requirements specified in Subpart E of 10 CFR 71. As indicated in the introduction to [Chapter 2.0, *Structural Evaluation*](#), with the exception of the immersion test, the primary proof of performance for the HAC tests is via the use of full scale testing. In particular, free drop, puncture, and fire testing of both a HalfPACT engineering test unit (ETU), and a HalfPACT certification test unit (CTU) confirms that both the inner and outer containment boundaries will remain leaktight after a worst case HAC sequence. Observations from testing of the ETU and CTU also confirm the conservative nature of deformed geometry assumptions used in the criticality assessment provided [Chapter 6.0, *Criticality Evaluation*](#), respectively.

Test results are summarized in [Section 2.7.8, *Summary of Damage*](#), with details provided in [Appendix 2.10.3, *Certification Tests*](#). Immersion is addressed by analysis, employing acceptance criteria consistent with NRC Regulatory Guide 7.6².

For the analytic assessments performed within this section, properties for Type 304 stainless steel are based on data from [Table 2.3-1](#) from [Section 2.3.1, *Mechanical Properties Applied to Analytic Evaluations*](#)). Similarly, the bounding values for the compressive strength of polyurethane foam are based on data from [Table 2.3-2](#) from [Section 2.3.1, *Mechanical Properties Applied to Analytic Evaluations*](#). Polyurethane foam compressive strength is further adjusted $\pm 15\%$ to account for manufacturing tolerance. At elevated HAC temperatures (i.e., 160 °F), the nominal compressive strength is reduced 25% for elevated temperature effects and reduced 15% for manufacturing tolerance. At reduced HAC temperatures (i.e., -20 °F), the nominal compressive strength is increased 40% for reduced temperature effects and increased 15% for manufacturing tolerance.

Properties of Type 304 stainless steel and polyurethane foam, as applied to analytic assessments within this section, are summarized below.

Material Property	Material Property Value (psi)			Reference
	-20 °F	70 °F	160 °F	
Type 304 Stainless Steel				
Elastic Modulus, E	28.8×10^6	28.3×10^6	27.8×10^6	Table 2.3-1
Design Stress Intensity, S_m	20,000	20,000	20,000	
Yield Strength, S_m	30,000	30,000	27,000	
Polyurethane Foam Compressive Strength				
Parallel-to-Rise Direction, σ_c	378	235	150	Table 2.3-2
Perpendicular-to-Rise Direction, σ_c	314	195	124	

¹ Title 10, Code of Federal Regulations, Part 71 (10 CFR 71), *Packaging and Transportation of Radioactive Material*, 01-01-07 Edition.

² U. S. Nuclear Regulatory Commission, Regulatory Guide 7.6, *Design Criteria for the Structural Analysis of Shipping Cask Containment Vessels*, Revision 1, March 1978.

2.7.1 Free Drop

Subpart F of 10 CFR 71 requires performing a free drop test in accordance with the requirements of 10 CFR §71.73(c)(1). The free drop test involves performing a 30 foot, HAC free drop onto a flat, essentially unyielding, horizontal surface, with the package striking the surface in a position (orientation) for which maximum damage is expected. The ability of the HalfPACT package to adequately withstand this specified free drop condition is demonstrated via testing of two full scale, HalfPACT test packages.

2.7.1.1 Technical Basis for the Free Drop Tests

To properly select a worst case package orientation for the 30 foot free drop event, items that could potentially compromise containment integrity, shielding integrity, and/or criticality safety of the HalfPACT package must be clearly identified. For the HalfPACT package design, the foremost item to be addressed is the ability of the containment seals to remain leaktight.

Shielding integrity is not a controlling case for the reasons described in [Chapter 5.0, *Shielding Evaluation*](#). Criticality safety is conservatively evaluated based on measured physical damage to the outer containment assembly (OCA) shells and polyurethane foam from certification testing, as described in [Chapter 6.0, *Criticality Evaluation*](#).

The leaktight capability of the containment seals may be compromised by two methods: 1) as a result of excessive sealing surface deformation leading to reduced seal compression, and/or 2) as a result of thermal degradation of the seal material itself in a subsequent fire event. Importantly, these methods require significant impact damage to the surrounding polyurethane foam. In other words, a significant reduction in polyurethane foam thickness or a gross exposure of the foam through splits or punctures in the OCA outer shell would have to occur near the main O-ring seal or vent port seal region.

Additional items for consideration include the possibility of separating the OCA lid from the OCA body (or significantly opening up the nominal 1/2 inch gap which exists between the upper and lower Z-flanges at the lid to body interface), and buckling of the outer containment vessel (OCV) or inner containment vessel (ICV) from a bottom end drop.

For the above reasons, testing must include impact orientations that affect the upper end of the HalfPACT package, with particularly emphasis in the closure region. Loads and resultant deformations occurring over the lower half of the package does not present a worst case regarding the leaktight capability of the seals or the separation of the OCA lid from the OCA body. However, as discussed above, a bottom end drop is of interest regarding the possibility of shell buckling because of the high axial acceleration forces imparted to the package.

In addition to package orientation, initial test conditions such as temperatures and pressures must be selected to complete the definition of the conditions existing at the time of a HAC free drop. In general, higher temperatures at the time of a drop test result in greater deformations and lesser acceleration loads than do lower temperatures. This is due primarily to the modest temperature sensitivity of the energy absorbing polyurethane foam used within the HalfPACT OCA.

[Appendix 2.10.3, *Certification Tests*](#), provides a comprehensive report of the certification test process and results. Discussions specific to the configuration of the test units are provided in [Appendix 2.10.3.4, *Test Unit Description*](#). Discussions specific to orientations of the test units for free drop, puncture, and fire tests, including initial test conditions, are provided in [Appendix](#)

2.10.3.5, *Technical Basis for Tests*. Discussions specific to test sequences for selected tests for the test units is provided in [Appendix 2.10.3.6, Test Sequence for Selected Free Drop, Puncture Drop, and Fire Tests](#).

2.7.1.2 Test Sequence for the Selected Tests

Based on the above general discussions, the ETU was tested for three specific, HAC 30 foot free drop conditions for inclusion in the engineering test program. Similarly, based on results from ETU testing, the CTU was tested for two specific, HAC 30 foot free drop conditions for inclusion in the certification test program. Although only a single “worst case” 30 foot drop is required by 10 CFR §71.73(c)(1), multiple tests were performed to ensure that the most vulnerable package features were subjected to “worst case” loads and deformations. The specific conditions selected for ETU and CTU free drop testing are summarized in [Table 2.7-1](#) and [Table 2.7-2](#), respectively.

2.7.1.3 Summary of Results from the Free Drop Tests

Successful HAC free drop testing of the ETU and CTU indicates that the various HalfPACT packaging design features are adequately designed to withstand the HAC 30 foot free drop event. The most important result of the testing program was the demonstrated ability of the OCV and ICV to remain leaktight³. Significant results of free drop testing common to both test units are as follows:

- There was no evidence of buckling of either containment boundary shell. Modest damage to the containment vessel shells did occur, an amount somewhat in excess of what was reported in the *TRUPACT-II package SAR*⁴. However, it is clear that the damage noted for the HalfPACT package corresponds to the much heavier payload drum’s interaction with the packaging wall.
- No excessive distortion of the seal flange regions occurred for either containment vessel, although some permanent deformation was noted.
- There was no rupture of the 3/8 inch thick, outer containment assembly (OCA) outer shell.
- Observed permanent deformations of the HalfPACT packaging were less than those assumed for the criticality evaluation.

A comprehensive summary of free drop test results is provided in [Appendix 2.10.3.7, Test Results](#).

2.7.2 Crush

Subpart F of 10 CFR 71 requires performing a dynamic crush test in accordance with the requirements of 10 CFR §71.73(c)(2). Since the HalfPACT package weight exceeds 1,100 pounds, the dynamic crush test is not required.

³ “Leaktight” is a leakage rate not exceeding 1×10^{-7} standard cubic centimeters per second (scc/sec), air, as defined in ANSI N14.5-1997, *American National Standard for Radioactive Materials – Leakage Tests on Packages for Shipment*, American National Standards Institute, Inc. (ANSI).

⁴ U.S. Department of Energy (DOE), *Safety Analysis Report for the TRUPACT-II Shipping Package*, USNRC Certificate of Compliance 71-9218, U.S. Department of Energy, Carlsbad Area Office, Carlsbad, New Mexico.

2.7.3 Puncture

Subpart F of 10 CFR 71 requires performing a puncture test in accordance with the requirements of 10 CFR §71.73(c)(3). The puncture test involves a 40 inch free drop of a package onto the upper end of a solid, vertical, cylindrical, mild steel bar mounted on an essentially unyielding, horizontal surface. The bar must be six inches in diameter, with the top surface horizontal and its edge rounded to a radius of not more than 1/4 inch. The package is to be oriented in a position for which maximum damage will occur. The minimum length of the bar is to be eight inches. The ability of the HalfPACT package to adequately withstand this specified puncture drop condition is demonstrated via testing of two full scale, HalfPACT test packages.

2.7.3.1 Technical Basis for the Puncture Drop Tests

To properly select a worst case package orientation for the puncture drop event, items that could potentially compromise containment integrity, shielding integrity, and/or criticality safety of the HalfPACT package must be clearly identified. For the HalfPACT package design, the foremost item to be addressed is the ability of the containment seals to remain leaktight. Shielding integrity is not a controlling case for the reasons described in [Chapter 5.0, *Shielding Evaluation*](#). Criticality safety is conservatively evaluated based on measured physical damage to the outer containment assembly (OCA) shells and polyurethane foam from certification testing, as described in [Chapter 6.0, *Criticality Evaluation*](#).

For the HalfPACT design, the primary item to be addressed for the puncture drop is the ability of the containment seals to remain leaktight. The leaktight capability of the O-ring seals would be most easily compromised by imposing gross deformations in the sealing region. These types of deformations are of concern from a mechanical viewpoint (i.e., leakage caused by excessive relative movement of the sealing surfaces). In addition, such deformations are of concern from a thermal viewpoint (i.e., leakage caused by thermal degradation of the butyl O-ring seals in a subsequent fire). Importantly, for mechanical damage to occur in the seal regions, the puncture event would have to result in a gross rupturing of the OCA outer shell near the O-ring seals. This could allow the puncture bar to reach and directly impact the OCA seal flanges or locking ring. Similarly, for thermal degradation of the butyl O-ring seals to occur in a subsequent fire, damage to the OCA outer shell near the O-ring seals would again have to occur as a result of the puncture event. Another item associated with the puncture event is the possibility of the puncture bar penetrating the OCA outer shell and rupturing the OCV containment boundary. Puncture is most likely to occur if the center of gravity of the package is directly in-line with the puncture bar, and the surface of the package is oriented at an angle to the bar axis. If the center of gravity of the package is not in-line with the puncture bar, puncture is less likely since package potential energy is transformed into rotational kinetic energy. Puncture is also more likely if the puncture bar impacts the package surface adjacent to a package shell weld seam. Observations from prior testing indicate that impacts with the package surface, normal to the axis of the puncture bar, will not lead to penetration of the OCA exterior shell. This is the primary reason for utilizing a torispherical head for the OCA lid. The torispherical head results in the puncture bar being oriented normal to the package surface when the center of gravity of the package is directly over the puncture bar. Further, a 3/8 inch thick, OCA outer shell is used near the closure region to ensure that no puncture will occur in this region, regardless of impact angle.

In addition to package orientation, initial test conditions such as temperatures and pressures must be selected to complete the definition of the conditions existing at the time of a HAC puncture drop. In general, higher temperatures at the time of a puncture test result in greater deformations and lesser acceleration loads than do lower temperatures. This is due primarily to the modest temperature sensitivity of the polyurethane foam used within the HalfPACT OCA.

[Appendix 2.10.3, *Certification Tests*](#), provides a comprehensive report of the certification test process and results. Discussions specific to the configuration of the test units are provided in [Appendix 2.10.3.4, *Test Unit Description*](#). Discussions specific to orientations of the test units for free drop, puncture, and fire tests, including initial test conditions, are provided in [Appendix 2.10.3.5, *Technical Basis for Tests*](#). Discussions specific to test sequences for selected tests for the test units is provided in [Appendix 2.10.3.6, *Test Sequence for Selected Free Drop, Puncture Drop, and Fire Tests*](#).

2.7.3.2 Test Sequence for the Selected Tests

Based on the above general discussions, the ETU was specifically tested for four HAC puncture drop conditions as part of the engineering test program. Similarly, based on results from ETU testing, the CTU was specifically tested for three HAC puncture drop conditions as part of the certification test program. Although only a single “worst case” puncture drop is required by 10 CFR §71.73(c)(3), multiple tests were performed to ensure that the most vulnerable package features were subjected to “worst case” loads and deformations. The specific conditions selected for ETU and CTU puncture drop testing are summarized in [Table 2.7-1](#) and [Table 2.7-2](#), respectively.

2.7.3.3 Summary of Results from the Puncture Drop Tests

Successful HAC puncture drop testing of the ETU and CTU indicates that the various HalfPACT packaging design features are adequately designed to withstand the HAC puncture drop event. As with the free drop test, the most important result of the testing program was the demonstrated ability of the OCV and ICV to remain leaktight. Significant results of puncture drop testing common to both test units are as follows:

- Besides the obvious permanent damage to the OCA outer shell at the location of the various puncture bar impacts, there was evidence of some permanent deformation of the OCV shell. The most significant damage occurred at the OCV vent port fitting during testing of the CTU. The cumulative effects of the NCT and HAC free drops, and the subsequent puncture drop caused successively greater permanent deformation to the region adjacent to the vent port fitting. A crack was noted in the inner weld of the CTU’s OCV vent port fitting, but not in the outer weld of the OCV vent port fitting. Subsequent helium leak testing determined that OCV containment integrity was maintained. Although essentially identical in configuration, the ETU did not have a similarly cracked weld. See [Appendix 2.10.3.7.2.8, *CTU Post-Test Disassembly*](#), for additional discussion regarding this result.
- Penetration of the OCA outer shell occurred below the 3/8-to-1/4 inch thick, OCA outer shell weld during testing of the ETU. The same test, repeated for certification testing, did not reproduce the hole. This result was due to lengthening the 3/8 inch thick, OCA outer shell from 12 to 18 inches, correspondingly changing the impact angle sufficiently to prevent penetration through the adjacent 1/4 inch thick shell.

- There was no rupture of the 3/8 inch thick, OCA outer shell. However, for both test units (ETU and CTU) a linear tear occurred along the weld at the 3/8-to-1/4 inch shell transition in the OCA body outer shell.

A comprehensive summary of test results is provided in [Appendix 2.10.3.7, Test Results](#).

2.7.4 Thermal

Subpart F of 10 CFR 71 requires performing a thermal test in accordance with the requirements of 10 CFR §71.73(c)(4). To demonstrate the performance capabilities of the HalfPACT package when subjected to the HAC thermal test specified in 10 CFR §71.73(c)(4), two full scale prototype test units were burned in two, separate, fully engulfing pool fires. Each test unit was subjected to a variety of HAC, 30 foot free drop and puncture tests prior to being burned, as discussed in [Section 2.7.1, Free Drop](#), and [Section 2.7.3, Puncture](#). Testing of the engineering test unit (ETU) preceded testing of the certification test unit (CTU), and was used for the purpose of accessing the effect of the various HAC tests. Planning to determine a worst case certification test scenario for the CTU was based ETU responses to a comprehensive set of HAC tests. Further, while the CTU had passive, temperature indicating labels to report post-test temperatures, the ETU did not. Thus, information reported herein considers only test results of the CTU.

As discussed further in [Appendix 2.10.3, Certification Tests](#), the CTU was oriented horizontally in a stand a distance one meter above the fuel per the requirements of 10 CFR §71.73(c)(4). The CTU was oriented circumferentially at an angle of 305° to position the damage from Drops 1, 2, and 4 (0°; aligned with the vent ports) and the damage from Drop 5 (250°) a distance 1/2 meter above the lowest part of the package while on the stand (i.e., 1½ meters above the fuel⁵). This particular arrangement put the maximum drop damage in the hottest part of the fire.

During the HAC fire test, the average wind speed was determined to be approximately 4 miles per hour. As discussed in [Appendix 2.10.3, Certification Tests](#), the duration of the fully engulfing, HAC fire test was approximately 33 minutes, and the ambient air temperature was 51 °F.

2.7.4.1 Summary of Pressures and Temperatures

Package pressures and temperatures due to the HAC fire test are presented in [Appendix 2.10.3, Certification Tests](#). Detailed discussions regarding measured temperatures are provided in [Section 3.5.3, Package Temperatures](#). Detailed discussions regarding calculated pressures are provided in [Section 3.5.4, Maximum Internal Pressure](#).

2.7.4.1.1 Summary of Temperatures

No active temperature measuring devices were employed prior to, during, or following the HAC fire test. Further, measurement of the outer containment assembly (OCA) outer shell temperature

⁵ M. E. Schneider and L. A. Kent, *Measurements of Gas Velocities and Temperatures in a Large Open Pool Fire*, Sandia National Laboratories (reprinted from *Heat and Mass Transfer in Fire*, A. K. Kulkarni and Y. Jaluria, Editors, HTD-Vol. 73 (Book No. H00392), American Society of Mechanical Engineers). Figure 3 shows that maximum temperatures occur at an elevation approximately 2.3 meters above the pool floor. The pool was initially filled with water and fuel to a level of 0.814 meters. The maximum temperatures therefore occur approximately 1½ meters above the level of the fuel, i.e., 1/2 meter above the lowest part of the package when set one meter above the fuel source per the requirements of 10 CFR §71.73(c)(4).

does not represent the outer containment vessel (OCV) or inner containment vessel (ICV) temperatures due to the large internal mass and thick, thermally insulating foam used within the OCA. As discussed in [Section 3.1.1, Packaging](#), the temperatures of the OCV, ICV, and payload are effectively decoupled from the OCA outer shell and polyurethane foam for short term thermal transients. Instead, the initial temperature of CTU No. 1 may be estimated based on the ambient temperature of the Sandia National Laboratory testing facilities in the six weeks prior to the HAC fire test⁶. Climatological data for Albuquerque, New Mexico, during the month of March and first two weeks of April 1998 shows an average temperature of 48 °F for those six weeks. Thus, when adjusting for the elevation difference between the testing facilities and Albuquerque, the initial temperature for HAC fire testing is taken as 43 °F.

Following completion of fire testing, the maximum measured OCV seal region temperature was 200 °F. Upwardly adjusting for the lower, pre-fire starting temperature by 90 °F results in a projected maximum OCV seal region temperature of 290 °F. The maximum measured ICV seal region temperature was 110 °F. Also, upwardly adjusting for the lower, pre-fire starting temperature by 90 °F results in a projected maximum ICV seal region temperature of 200 °F.

2.7.4.1.2 Summary of Pressures

The maximum internal pressure for the ICV is conservatively determined by assuming the air temperature within the ICV is at the maximum seal temperature of 200 °F. The ICV pressure increase, ΔP_{ICV} , using an initial maximum ICV wall temperature of 154 °F (from [Table 3.4-1](#)) at an initial pressure equal to the MNOP of 50 psig (64.7 psia), is determined using ideal gas relationships:

$$\frac{P_1}{T_1} = \frac{P_2}{T_2} \Rightarrow \frac{P_{154\text{ °F}}}{T_{154\text{ °F}}} = \frac{P_{200\text{ °F}}}{T_{200\text{ °F}}} \Rightarrow P_{200\text{ °F}} = P_{154\text{ °F}} \left(\frac{T_{200\text{ °F}}}{T_{154\text{ °F}}} \right)$$

$$P_{200\text{ °F}} = 64.7 \left(\frac{200 + 460}{154 + 460} \right) = 69.5 \text{ psia (54.8 psig)}$$

$$\Delta P_{ICV} = 54.8 - 50.0 = 4.8 \text{ psig}$$

Thus, the maximum internal pressure for the ICV for HAC is 54.8 psig, resulting in a net pressure increase of 4.8 psig.

The maximum internal pressure for the OCV is conservatively determined by assuming the air temperature within the OCV, 245 °F, is the average of the maximum ICV and OCV seal temperatures of 200 °F and 290 °F, respectively. The initial air temperature within the OCV, 152 °F, is the average of the maximum OCV and ICV wall temperatures of 150 °F and 154 °F, respectively (from [Table 3.4-1](#)). The OCV pressure increase, ΔP_{OCV} , using at an initial pressure equal to the MNOP of 50 psig (64.7 psia), is determined using ideal gas relationships:

⁶ CTU No. 1 was located at Sandia National Laboratories' Coyote Canyon drop test facility for the month of March, 1998, and the Lurance Canyon burn facility for the first two weeks of April, 1998. CTU No. 1 was burned on April 14, 1998. The elevation difference between the two test facilities and the city of Albuquerque results in an average ambient temperature approximately 5 °F cooler than Albuquerque.

$$\frac{P_1}{T_1} = \frac{P_2}{T_2} \Rightarrow \frac{P_{152\text{ }^\circ\text{F}}}{T_{152\text{ }^\circ\text{F}}} = \frac{P_{245\text{ }^\circ\text{F}}}{T_{245\text{ }^\circ\text{F}}} \Rightarrow P_{245\text{ }^\circ\text{F}} = P_{152\text{ }^\circ\text{F}} \left(\frac{T_{245\text{ }^\circ\text{F}}}{T_{152\text{ }^\circ\text{F}}} \right)$$

$$P_{245\text{ }^\circ\text{F}} = 64.7 \left(\frac{245 + 460}{152 + 460} \right) = 74.5 \text{ psia (59.8 psig)}$$

$$\Delta P = 59.8 - 50.0 = 9.8 \text{ psig}$$

Thus, the maximum internal pressure for the OCV for HAC is 59.8 psig, resulting in a net pressure increase of 9.8 psig.

2.7.4.2 Differential Thermal Expansion

Fire testing of two, full scale HalfPACT prototypes indicate that the effects associated with differential thermal expansion of the various packaging components are negligible. Subsequent to all NCT and HAC free drop, puncture drop, and fire tests, comprehensive helium leak testing of both containment vessels demonstrated that differential thermal expansion does not affect the capability of the containment boundaries to remain leaktight.

2.7.4.3 Stress Calculations

As shown in [Section 2.7.4.1.2, Summary of Pressures](#), the internal pressure within the ICV increases 4.8 psig (+10%), and within the OCV increases 9.8 psig (+20%) due to the HAC fire test. Pressure stresses due to the HAC fire test corresponding increase a maximum of 20%. With reference to [Table 2.1-1 in Section 2.1.2.1.1, Containment Structures](#), the HAC allowable stress intensity for general primary membrane stresses (applicable to pressure loads) is 240% of the NCT allowable stress intensity. Therefore, a HAC pressure stress increase of 20% will not exceed the HAC allowable stresses. Further, the pressure stresses in conjunction with stresses associated with differential thermal expansion are limited to an acceptable level since both containment vessels were shown to be leaktight after all NCT and HAC free drop, puncture drop, and fire tests (see [Appendix 2.10.3.7, Test Results](#)).

2.7.4.4 Comparison with Allowable Stresses

As discussed in [Section 2.7.4.3, Stress Calculations](#), further quantification of stresses in the various HalfPACT package components is not required.

2.7.5 Immersion – Fissile Material

Subpart F of 10 CFR 71 requires performing an immersion test for fissile material packages in accordance with the requirements of 10 CFR §71.73(c)(5). The criticality evaluation presented in [Chapter 6.0, Criticality Evaluation](#), assumes optimum homogeneous moderation of the contents, thereby conservatively addressing the effects and consequences of water in-leakage.

2.7.6 Immersion – All Packages

Subpart F of 10 CFR 71 requires performing an immersion test for all packages in accordance with the requirements of 10 CFR §71.73(c)(6). For the HalfPACT package design, the effect of a 21 psig external pressure due to immersion in 50 feet of water is applied to the OCV, since the

OCA outer shell is not designed as a pressure boundary. For conservatism, a buckling evaluation of the ICV is also performed.

The external pressure induces small compressive stresses in the containment boundaries that are limited by stability (buckling) requirements. Buckling assessments are performed for the OCV and ICV in [Section 2.7.6.1, *Buckling Assessment of the Torispherical Heads*](#), and [Section 2.7.6.2, *Buckling Assessment of the Cylindrical Shells*](#).

2.7.6.1 Buckling Assessment of the Torispherical Heads

The buckling analysis of the torispherical heads is based on the methodology outlined in Paragraph NE-3133.4(e), *Torispherical Heads*, of the ASME Boiler and Pressure Vessel Code, Section III⁷, Subsection NE. Since the external pressure loading due to immersion may be classified as Level D, the allowable buckling stress and, therefore, the allowable pressure, can be increased by 150% per paragraph NE-3222.2. The results from following this methodology are summarized below.

Parameter	OCV Torispherical Head		ICV Torispherical Head	
	Upper	Lower	Upper	Lower
R	77.3125	74.1250	74.3750	73.1250
T	0.25	0.25	0.25	0.25
$A = \frac{0.125}{(R/T)}$	0.00040	0.00042	0.00042	0.00043
B^8	5,000	5,000	5,000	5,000
$P_a = \frac{(1.5)B}{(R/T)}$	24.3	25.3	25.2	25.6

The smallest allowable pressure, P_a , is 24.3 psig for the OCV upper head. For an applied external pressure of 21 psig, the corresponding buckling margin of safety is:

$$MS = \frac{24.3}{21} - 1 = +0.16$$

Since the margin of safety in the worst case is positive, it is concluded that none of the OCV or ICV torispherical heads will buckle for an external pressure of 21 psig.

⁷ American Society of Mechanical Engineers (ASME) Boiler and Pressure Vessel Code, Section III, *Rules for Construction of Nuclear Power Plant Components*, 1995 Edition, 1997 Addenda.

⁸ Factor B is found from American Society of Mechanical Engineers (ASME) Boiler and Pressure Vessel Code, Section II, *Materials*, Part D, *Properties*, Subpart 3, *Charts and Tables for Determining the Shell Thickness of Components Under External Pressure*, Figure HA-1, *Chart for Determining Shell Thickness of Components Under External Pressure When Constructed of Austenitic Steel (18Cr-8Ni, Type 304)*, 1995 Edition, 1997 Addenda. Conservatively, the 400 °F temperature curve is used for each case.

2.7.6.2 Buckling Assessment of the Cylindrical Shells

The cylindrical portions of the OCV and ICV are evaluated using ASME Boiler and Pressure Vessel Code Case N-284-1⁹. Consistent with Regulatory Guide 7.6 philosophy, a factor of safety of 1.34 is applied for HAC buckling evaluations per ASME Code Case N-284-1, corresponding to ASME Code, Service Level D conditions.

Buckling analysis geometry parameters are summarized in Table 2.7-3, and loading parameters are summarized in Table 2.7-4. The cylindrical shell buckling analysis conservatively utilizes an OCV and ICV temperature of 160 °F, consistent with Section 2.6.1, *Heat*. The stresses are determined using an external pressure of 21 psig. The hoop stress, σ_{θ} , axial stress, σ_{ϕ} , and in-plane shear stress, $\sigma_{\phi\theta}$, are found from:

$$\sigma_{\theta} = \frac{Pr}{t} \quad \sigma_{\phi} = \frac{Pr}{2t} \quad \sigma_{\phi\theta} = \frac{Pr}{4t}$$

where P is the applied external pressure of 21 psi, r is the mean radius, and t is the cylindrical shell thickness. As shown in Table 2.7-5, since all interaction check parameters are less than 1.0, as required, the design criteria are satisfied.

2.7.7 Deep Water Immersion Test

Subpart E of 10 CFR 71 requires performing a deep water immersion test in accordance with 10 CFR §71.61. Since the HalfPACT does not transport payloads with an activity of greater than $10^5 A_2$, this requirement does not apply.

2.7.8 Summary of Damage

As discussed in the previous sections, the cumulative damaging effects of free drop, puncture drop, and fire tests were satisfactorily withstood by the HalfPACT packaging during both engineering and certification testing. Subsequent helium leak testing confirmed that containment integrity was maintained throughout the test series. Therefore, the requirements of 10 CFR §71.73 have been adequately met.

⁹ American Society of Mechanical Engineers (ASME) Boiler and Pressure Vessel Code, Section III, *Rules for Construction of Nuclear Power Plant Components*, Division 1, Class MC, Code Case N-284-1, *Metal Containment Shell Buckling Design Methods*, 1995 Edition, 1997 Addenda.

Table 2.7-1 – Summary of HalfPACT Engineering Test Unit (ETU) Tests and Results

Test No.	Test Description	Test Unit Angular Orientation		Remarks
		Axial (0° = horizontal)	Circumferential (0° = vent ports)	
1	NCT, 3 foot side drop opposite the OCV vent and seal test ports	0°	200°	NCT impact in region expected to produce worst case cumulative damage to package.
2	HAC, 30 foot side drop opposite the OCV vent and seal test ports	0°	200°	HAC impact in region expected to produce worst case cumulative damage to package.
3	NCT, 3 foot side drop on the OCV vent port	0°	0°	NCT impact in OCV vent port region.
4	HAC, 30 foot side drop on the OCV vent port	0°	0°	HAC impact in OCV vent port region.
5	NCT, 3 foot center-of-gravity-over-corner drop between tie-down doubler plates	43°	110°	NCT impact at location not tested during previous TRUPACT-II certification tests.
6	HAC, 30 foot center-of-gravity-over-corner drop between tie-down doubler plates	43°	110°	HAC impact at location not tested during previous TRUPACT-II certification tests.
7	HAC, puncture drop at the 1/4-to-3/8, OCA body shell weld (below weld)	20°	200°	Attempt to cause hole in shell below 1/4-to-3/8, OCA body shell weld.
8	HAC, puncture drop on OCV vent port	1°	0°	Puncture in region expected to produce worst case cumulative damage to package.
9	HAC, puncture drop at Test 6 damage	43°	110°	Attempt to cause hole in existing damage.
10	HAC, puncture drop at the 1/4-to-3/8, OCA body shell weld (above weld)	9°	290°	Attempt to cause linear tear in 1/4-to-3/8, OCA body shell weld.
11	HAC, fire test	0°	145°	Circumferential orientation places damage from Tests 4 and 8 in hottest part of fire.

Table 2.7-2 – Summary of Selected Certification Test Unit (CTU) Tests

Test No.	Test Description	Test Unit Angular Orientation		Remarks
		Axial (0° = horizontal)	Circumferential (0° = vent ports)	
1	NCT, 3 foot side drop on the OCV vent port	0°	0°	NCT impact in region expected to produce worst case cumulative damage to package.
2	HAC, 30 foot side drop on the OCV vent port	0°	0°	HAC impact in region expected to produce worst case cumulative damage to package.
3	HAC, 30 foot, 5° corner drop on the OCA top knuckle, slapdown on the tiedown lug	5°	147½°	Drop orientation producing maximum load on closure region.
4	HAC, puncture drop on the OCV vent port	1½°	0°	Puncture in region expected to produce worst case cumulative damage to package.
5	HAC, puncture drop at the 1/4-to-3/8, OCA body shell weld (below weld)	16°	110°	Attempt to cause hole in shell below 1/4-to-3/8, OCA body shell weld.
6	HAC, puncture drop at the 1/4-to-3/8, OCA body shell weld (above weld)	23°	250°	Attempt to cause linear tear in 1/4-to-3/8, OCA body shell weld.
7	HAC, fire test	0°	55° or 305° [Ⓢ] (max damage)	Circumferential orientation based on results of Tests 5 and 6.

Notes:

Ⓢ The 55° or 305° circumferential orientation is downward; package bottom is one meter above the fuel surface.

Table 2.7-3 – Buckling Geometry Parameters per Code Case N-284-1

Geometry and Material Input		
	ICV	OCV
Mean Radius, inch	36.44	36.91
Shell Thickness, inch	0.25	0.188
Length, inch	36.0 ^①	32.0 ^②
Geometry Output (nomenclature consistent with ASME Code Case N-284-1)		
R =	36.44	36.91
t =	0.25	0.188
R/t =	145.76	196.85
ℓ_{ϕ} =	36.0	32.0
ℓ_{θ} =	228.94	231.89
M_{ϕ} =	11.93	12.16
M_{θ} =	75.85	88.15
M =	11.93	12.16

Notes:

- ① The ICV length is conservatively measured from five inches below the top of the lower ICV seal flange (at the beginning of the 1/4 inch wall thickness) to an assumed support point located one-third of the depth of the lower ICV torispherical head below the head-to-shell interface.
- ② The OCV length is conservatively measured from the top of the tapered wall portion (just below the lower OCV seal flange) to an assumed support point located one-third of the depth of the lower OCV torispherical head below the head-to-shell interface.

Table 2.7-4 – Stress Results for 21 psig External Pressure

ICV		OCV	
Axial Stress, σ_{ϕ}	1,530	Axial Stress, σ_{ϕ}	2,067
Hoop Stress, σ_{θ}	3,061	Hoop Stress, σ_{θ}	4,133
Shear Stress, $\sigma_{\phi\theta}$	765	Shear Stress, $\sigma_{\phi\theta}$	1,031

Table 2.7-5 – Buckling Summary for 21 psig External Pressure

Condition	ICV	OCV	Remarks
Capacity Reduction Factors (-1511)			
$\alpha_{\phi L} =$	0.2575	0.2575	
$\alpha_{\theta L} =$	0.8000	0.8000	
$\alpha_{\phi\theta L} =$	0.8000	0.8000	
Plasticity Reduction Factors (-1611)			
$\eta_{\phi} =$	0.5877	0.7307	
$\eta_{\theta} =$	1.0000	1.0000	
$\eta_{\phi\theta} =$	0.4474	0.5740	
Theoretical Buckling Values (-1712.1.1)			
$C_{\phi} =$	0.6050	0.6050	
$\sigma_{\phi eL} =$	115,720 psi	85,687 psi	
$C_{\theta r} =$	0.0855	0.0837	
$\sigma_{\theta eL} = \sigma_{reL} =$	16,354 psi	11,854 psi	
$C_{\theta h} =$	0.0815	0.0798	
$\sigma_{\theta eL} = \sigma_{heL} =$	15,581 psi	11,302 psi	
$C_{\phi\theta} =$	0.2184	0.2162	
$\sigma_{\phi\theta eL} =$	41,770 psi	30,611 psi	
Elastic Interaction Equations (-1713.1.1)			
$\sigma_{xa} =$	14,899 psi	11,032 psi	
$\sigma_{ha} =$	6,232 psi	4,521 psi	
$\sigma_{ra} =$	6,542 psi	4,742 psi	
$\sigma_{\tau a} =$	16,708 psi	12,246 psi	
Axial + Hoop \Rightarrow Check (a):	<i>N/A</i>	<i>N/A</i>	
Axial + Hoop \Rightarrow Check (b):	<i>N/A</i>	<i>N/A</i>	
Axial + Shear \Rightarrow Check (c):	<i>0.0730</i>	<i>0.1343</i>	<1 ∴ OK
Hoop + Shear \Rightarrow Check (d):	<i>0.3290</i>	<i>0.6121</i>	<1 ∴ OK
Axial + Hoop + Shear \Rightarrow Check (e,a):	<i>N/A</i>	<i>N/A</i>	
Axial + Hoop + Shear \Rightarrow Check (e,b):	<i>N/A</i>	<i>N/A</i>	
Inelastic Interaction Equations (-1713.2.1)			
$\sigma_{xc} =$	8,756 psi	8,061 psi	
$\sigma_{rc} =$	6,542 psi	4,742 psi	
$\sigma_{\tau c} =$	7,475 psi	7,029 psi	
Axial + Hoop \Rightarrow Check (a):	<i>0.3276</i>	<i>0.6086</i>	<1 ∴ OK
Axial + Shear \Rightarrow Check (b):	<i>0.1282</i>	<i>0.1896</i>	<1 ∴ OK
Hoop + Shear \Rightarrow Check (c):	<i>0.3322</i>	<i>0.6192</i>	<1 ∴ OK

2.8 Special Form

This section does not apply for the HalfPACT package, since special form is not claimed.

This page intentionally left blank.

2.9 Fuel Rods

This section does not apply for the HalfPACT package, since fuel rods are not included as an approved payload configuration.

This page intentionally left blank.

2.10 Appendices

2.10.1 *Finite Element Analysis (FEA) Models*

2.10.2 *Elastomer O-ring Seal Performance Tests*

2.10.3 *Certification Tests*

This page intentionally left blank.

2.10.1 Finite Element Analysis (FEA) Models

2.10.1.1 Outer Containment Assembly (OCA) Structural Analysis

Finite element analyses (FEA) are performed on the OCA structure to determine the stress states of the various components under normal conditions of transport (NCT) loads. The FEA analyses are performed using ANSYS[®] 5.3¹. The OCA FEA model is comprised of six separate major structural components, modeled as shown in [Figure 2.10.1-1](#):

- upper OCV seal flange
- lower OCV seal flange
- OCV locking ring
- OCV shells
- OCA shells and Z-flanges
- polyurethane foam

The lower and upper seal flanges, locking ring and polyurethane foam are modeled using 2-D, isoparametric solid elements (PLANE42). The quadrilateral elements are defined by four nodal points (a triangular element may be formed by defining duplicate the 3rd and 4th node numbers), each having two degrees of freedom: translations in the nodal x-direction (radial) and y-direction (axial).

The upper and lower OCA shells (OCA lid and body shells, respectively) are modeled using 2-D, axisymmetric conical shell elements (SHELL51). The lineal elements are defined by two nodal points, each having three degrees of freedom: translations in the nodal x-direction (radial) and y-direction (axial), and rotation about the nodal z-axis (hoop). In addition, the axisymmetric conical shell element is biaxial, with membrane and bending capabilities. The OCA inner shell defines the outer containment vessel (OCV).

Relatively stiff, 2-D elastic beams (BEAM3) are utilized to maintain bending continuity between the three degree of freedom conical shell elements and two degree of freedom, isoparametric solid elements. Specifically, for both the lower and upper OCV seal flanges, four stiff beams are placed at each junction between the shell elements and the solid elements of the seal flanges. These elements are included to transmit the moment (i.e., to maintain slope continuity) between the shell and flange portions of the model, and have a negligible effect on the stress results.

Three sets of 2-D interface elements (CONTAC12) are utilized to connect the lower and upper OCV seal flanges to each other and to the OCV locking ring. The interface element is capable of supporting a load only in the direction normal to the surfaces, and is frictionless in the tangential direction. The interface element has two degrees of freedom at each node: translations in the nodal x-direction (radial) and y-direction (axial). A contact stiffness of 1×10^9 lb/in is chosen to reflect the relatively high interface stiffness when closed. Three sets of interface elements are used in these analyses: 1) between the lower OCV seal flange and the OCV locking ring, 2) between the upper OCV seal flange and the OCV locking ring, and 3) between the lower OCV seal flange and the upper OCV seal flange. Relatively flexible spring elements (COMBIN14) having a spring stiffness of 1×10^2 lb/in are also used at these same locations to improve model stability and to reduce interface element convergence time. The resulting forces in these springs are small, having a negligible effect on the stress results.

¹ ANSYS[®], Inc., *ANSYS Engineering Analysis System User's Manual for ANSYS[®] Revision 5.3*, Houston, PA.

Interface elements are also located along the entire shell-to-foam periphery to allow relative motion between the steel shells and the polyurethane foam. This approach effectively models the ceramic fiber paper by allowing compression-only forces, and assumes no shear continuity or tension effects. A contact stiffness of 1×10^5 lb/in is chosen to reflect the interface stiffness between the shells, ceramic fiber paper, and polyurethane foam. Stress results in the package shells and OCV seal flanges exhibit a negligible dependence on the actual magnitude of the gap contact stiffness.

To account for the tangential (hoop) direction slotting for the lower OCV seal flange and OCV locking ring in the axisymmetric model, the material properties in the directly affected regions are modified. Specifically, material properties for the shaded elements in the lower OCV seal flange and OCV locking ring, illustrated on [Figure 2.10.1-1](#), are modified to reflect only one-half the stainless steel being present for strength purposes. Specifically, the elastic modulus in the x- and y-directions is reduced to one-half their normal value (since only approximately one-half the material remains in the slotted regions), and the elastic modulus in the z-direction is set to a very low value to eliminate virtually all tangential (hoop) stiffness in the slotted regions. In addition, Poisson's ratio is set at the normal value of 0.3 for the x-y plane, but is set to zero in the y-z and x-z planes. In these ways, the analyses accurately depict the stress levels in all regions.

The global origin of the nodal coordinate system is located at the bottom center of the OCA body, as shown in [Figure 2.10.1-1](#). As such, the nodal x-axis corresponds to the radial direction, the nodal y-axis corresponds to the axial direction, and the nodal z-axis corresponds to the tangential (or hoop) direction. The model is constrained from translating in the radial direction and rotating about the hoop axis at the y-z symmetry plane at x equal zero. The model is also constrained from translating in the axial direction at a single node on the OCV locking ring.

2.10.1.1.1 OCA Structural Analysis – Load Case 1

For OCA Load Case 1, the OCA structural analysis uses a 50 psig (64.7 psia) internal pressure, corresponding to the maximum normal operating pressure (MNOP) from [Section 3.4.4, *Maximum Internal Pressure*](#), coupled with a reduced external pressure of 3.5 psia (equivalently an 11.2 psig internal pressure), per [Section 2.6.3, *Reduced External Pressure*](#), and 10 CFR §71.51(c)(3)². The net internal pressure for this case is 61.2 psig, applied throughout the inner periphery of the model. Relative to the upper and lower OCV seal flanges, the internal pressure does not extend beyond (below) the top of the upper main O-ring seal groove.

A uniform temperature of 160 °F, per [Section 2.6.1.1, *Summary of Pressures and Temperatures*](#), is utilized to determine the temperature-dependent, material property values. The only material properties affected by a temperature of 160 °F are the elastic modulus and the thermal expansion coefficient for the stainless steel. Consistent with [Table 2.3-1 in Section 2.3.1, *Mechanical Properties Applied to Analytic Evaluations*](#), the elastic modulus and thermal expansion coefficient for Type 304 stainless steel are $27.8(10)^6$ psi and $8.694(10)^{-6}$ inches/inch/°F, respectively, at a temperature of 160 °F.

The material properties for the polyurethane foam are consistent with those specified in [Section 2.3.1, *Mechanical Properties Applied to Analytic Evaluations*](#). The elastic modulus in the x- (radial) and z- (hoop) directions is based on the perpendicular-to-rise value of 4,773 psi.

² Title 10, Code of Federal Regulations, Part 71 (10 CFR 71), *Packaging and Transportation of Radioactive Material*, 01-01-07 Edition.

Young's modulus in the y- (axial) direction is based on the parallel-to-rise value of 6,810 psi. In addition, Poisson's ratio is 0.33, and the thermal expansion coefficient is $3.5(10)^{-5}$ inches/inch/°F for the polyurethane foam. Due to the relatively low stiffness of the polyurethane foam compared with the surrounding stainless steel structures, temperature adjusting the foam's elastic modulus and thermal expansion coefficient will have a negligible effect on component stresses.

Both the reference and uniform temperature are set to 160 °F, thereby excluding the effects of differential thermal expansion for this case. The effects of differential thermal expansion are considered in [Section 2.10.1.1.2, OCA Structural Analysis – Load Case 2](#).

For analysis model review, the ANSYS® input file is listed in [Table 2.10.1-1](#).

2.10.1.1.2 OCA Structural Analysis – Load Case 2

For OCA Load Case 2, the OCA structural analysis uses a 50 psig (64.7 psia) internal pressure, corresponding to the maximum normal operating pressure (MNOP) from [Section 3.4.4, Maximum Internal Pressure](#), coupled with a reduced external pressure of 3.5 psia (equivalently an 11.2 psig internal pressure), per [Section 2.6.3, Reduced External Pressure](#), and 10 CFR §71.51(c)(3). The net internal pressure for this case is 61.2 psig, applied throughout the inner periphery of the model. Relative to the upper and lower OCV seal flanges, the internal pressure does not extend beyond (below) the top of the upper main O-ring seal groove.

A uniform temperature of 160 °F, per [Section 2.6.1.1, Summary of Pressures and Temperatures](#), is utilized to determine the temperature-dependent, material property values. The only material properties affected by a temperature of 160 °F are the elastic modulus and the thermal expansion coefficient for the stainless steel. Consistent with [Table 2.3-1 in Section 2.3.1, Mechanical Properties Applied to Analytic Evaluations](#), the elastic modulus and thermal expansion coefficient for Type 304 stainless steel are $27.8(10)^6$ psi and $8.694(10)^{-6}$ inches/inch/°F, respectively, at a temperature of 160 °F.

The material properties for the polyurethane foam are consistent with those specified in [Section 2.3.1, Mechanical Properties Applied to Analytic Evaluations](#). The elastic modulus in the x- (radial) and z- (hoop) directions is based on the perpendicular-to-rise value of 4,773 psi. Young's modulus in the y- (axial) direction is based on the parallel-to-rise value of 6,810 psi. In addition, Poisson's ratio is 0.33, and the thermal expansion coefficient is $3.5(10)^{-5}$ inches/inch/°F for the polyurethane foam. Due to the relatively low stiffness of the polyurethane foam compared with the surrounding stainless steel structures, temperature adjusting the foam's elastic modulus and thermal expansion coefficient will have a negligible effect on component stresses.

The reference temperature is set to 70 °F, and the uniform temperature is set to 160 °F, thereby including the effects of differential thermal expansion for this case.

For analysis model review, the ANSYS® input file is listed in [Table 2.10.1-2](#).

2.10.1.1.3 OCA Structural Analysis – Load Case 3

For OCA Load Case 3, the OCA structural analysis uses a 0.0 psig (14.7 psia) internal pressure coupled with an external pressure of 0.0 psig (14.7 psia) for a net pressure differential of 0.0 psig.

A uniform temperature of -40 °F, per [Section 2.6.2, Cold](#), is utilized to determine the temperature-dependent, material property values. The only material properties affected by a temperature of

-40 °F are the elastic modulus and the thermal expansion coefficient for the stainless steel. Consistent with [Table 2.3-1](#) in [Section 2.3.1, *Mechanical Properties Applied to Analytic Evaluations*](#), the elastic modulus and thermal expansion coefficient for Type 304 stainless steel are $28.8(10)^6$ psi and $8.21(10)^{-6}$ inches/inch/°F, respectively, at a temperature of -40 °F.

The material properties for the polyurethane foam are consistent with those specified in [Section 2.3.1, *Mechanical Properties Applied to Analytic Evaluations*](#). The elastic modulus in the x- (radial) and z- (hoop) directions is based on the perpendicular-to-rise value of 4,773 psi. Young's modulus in the y- (axial) direction is based on the parallel-to-rise value of 6,810 psi. In addition, Poisson's ratio is 0.33, and the thermal expansion coefficient is $3.5(10)^{-5}$ inches/inch/°F for the polyurethane foam. Due to the relatively low stiffness of the polyurethane foam compared with the surrounding stainless steel structures, temperature adjusting the foam's elastic modulus and thermal expansion coefficient will have a negligible effect on component stresses.

The reference temperature is set to 70 °F, and the uniform temperature is set to -40 °F, thereby including the effects of differential thermal expansion for this case.

For analysis model review, the ANSYS® input file is listed in [Table 2.10.1-3](#).

2.10.1.1.4 OCA Structural Analysis – Load Case 4

For OCA Load Case 4, the OCA structural analysis uses a -14.7 psig (0.0 psia) internal pressure (i.e., full vacuum) coupled with a increased external pressure of 0.0 psig (14.7 psia), per [Section 2.6.4, *Increased External Pressure*](#). The net external pressure for this case is 14.7 psig, applied throughout the inner periphery of the model. Relative to the upper and lower OCV seal flanges, the internal pressure does not extend beyond (below) the top of the upper main O-ring seal groove.

A uniform temperature of 70 °F is utilized to determine the temperature-dependent, material property values. The only material properties affected by a temperature of 70 °F are the elastic modulus and the thermal expansion coefficient for the stainless steel. Consistent with [Table 2.3-1](#) in [Section 2.3.1, *Mechanical Properties Applied to Analytic Evaluations*](#), the elastic modulus and thermal expansion coefficient for Type 304 stainless steel are $28.3(10)^6$ psi and $8.46(10)^{-6}$ inches/inch/°F, respectively, at a temperature of 70 °F.

The material properties for the polyurethane foam are consistent with those specified in [Section 2.3.1, *Mechanical Properties Applied to Analytic Evaluations*](#). The elastic modulus in the x- (radial) and z- (hoop) directions is based on the perpendicular-to-rise value of 4,773 psi. Young's modulus in the y- (axial) direction is based on the parallel-to-rise value of 6,810 psi. In addition, Poisson's ratio is 0.33, and the thermal expansion coefficient is $3.5(10)^{-5}$ inches/inch/°F for the polyurethane foam. Due to the relatively low stiffness of the polyurethane foam compared with the surrounding stainless steel structures, temperature adjusting the foam's elastic modulus and thermal expansion coefficient will have a negligible effect on component stresses.

Both the reference and uniform temperature are set to 70 °F, thereby excluding the effects of differential thermal expansion for this case.

For analysis model review, the ANSYS® input file is listed in [Table 2.10.1-4](#).

2.10.1.2 Inner Containment Assembly (ICV) Structural Analysis

Finite element analyses (FEA) are performed on the ICV structure to determine the stress states of the various components under normal conditions of transport (NCT) loads. The FEA analyses are performed using ANSYS[®] 5.3. The ICV FEA model is comprised of four separate major structural components, modeled as shown in [Figure 2.10.1-2](#):

- upper ICV seal flange
- lower ICV seal flange
- ICV locking ring
- ICV shells

The lower and upper seal flanges, and locking ring are modeled using 2-D, isoparametric solid elements (PLANE42). The quadrilateral elements are defined by four nodal points (a triangular element may be formed by defining duplicate the 3rd and 4th node numbers), each having two degrees of freedom: translations in the nodal x-direction (radial) and y-direction (axial).

The upper and lower ICV shells (ICV lid and body shells, respectively) are modeled using 2-D, axisymmetric conical shell elements (SHELL51). The lineal elements are defined by two nodal points, each having three degrees of freedom: translations in the nodal x-direction (radial) and y-direction (axial), and rotation about the nodal z-axis (hoop). In addition, the axisymmetric conical shell element is biaxial, with membrane and bending capabilities.

Relatively stiff, 2-D elastic beams (BEAM3) are utilized to maintain bending continuity between the three degree of freedom conical shell elements and two degree of freedom, isoparametric solid elements. Specifically, for both the lower and upper ICV seal flanges, four stiff beams are placed at each junction between the shell elements and the solid elements of the seal flanges. These elements are included to transmit the moment (i.e., to maintain slope continuity) between the shell and flange portions of the model, and have a negligible effect on the stress results.

Three sets of 2-D interface elements (CONTAC12) are utilized to connect the lower and upper ICV seal flanges to each other and to the ICV locking ring. The interface element is capable of supporting a load only in the direction normal to the surfaces, and is frictionless in the tangential direction. The interface element has two degrees of freedom at each node: translations in the nodal x-direction (radial) and y-direction (axial). A contact stiffness of 1×10^9 lb/in is chosen to reflect the relatively high interface stiffness when closed. Three sets of interface elements are used in these analyses: 1) between the lower ICV seal flange and the ICV locking ring, 2) between the upper ICV seal flange and the ICV locking ring, and 3) between the lower ICV seal flange and the upper ICV seal flange.

To account for the tangential (hoop) direction slotting for the lower ICV seal flange and ICV locking ring in the axisymmetric model, the material properties in the directly affected regions are modified. Specifically, material properties for the shaded elements in the lower ICV seal flange and ICV locking ring, illustrated on [Figure 2.10.1-2](#), are modified to reflect only one-half the stainless steel being present for strength purposes. Specifically, the elastic modulus in the x- and y-directions is reduced to one-half their normal value (since only approximately one-half the material remains in the slotted regions), and the elastic modulus in the z-direction is set to a very low value to eliminate virtually all tangential (hoop) stiffness in the slotted regions. In addition, Poisson's ratio is set at the normal value of 0.3 for the x-y plane, but is set to zero in the y-z and x-z planes. In these ways, the analyses accurately depict the stress levels in all regions.

The global origin of the nodal coordinate system is located at the bottom center of the ICV body, as shown in [Figure 2.10.1-2](#). As such, the nodal x-axis corresponds to the radial direction, the nodal y-axis corresponds to the axial direction, and the nodal z-axis corresponds to the tangential (or hoop) direction. The model is constrained from translating in the radial direction and rotating about the hoop axis at the y-z symmetry plane at x equal zero. The model is also constrained from translating in the axial direction at a single node on the ICV locking ring.

2.10.1.2.1 ICV Structural Analysis – Load Case 1

For ICV Load Case 1, the ICV structural analysis uses a 50 psig (64.7 psia) internal pressure, corresponding to the maximum normal operating pressure (MNOP) from [Section 3.4.4, *Maximum Internal Pressure*](#), coupled with a reduced external pressure of 3.5 psia (equivalently an 11.2 psig internal pressure), per [Section 2.6.3, *Reduced External Pressure*](#), and 10 CFR §71.51(c)(3). The net internal pressure for this case is 61.2 psig, applied throughout the inner periphery of the model. Relative to the upper and lower ICV seal flanges, the internal pressure does not extend beyond (below) the top of the upper main O-ring seal groove.

A uniform temperature of 160 °F, per [Section 2.6.1.1, *Summary of Pressures and Temperatures*](#), is utilized to determine the temperature-dependent, material property values. The only material properties affected by a temperature of 160 °F are the elastic modulus and the thermal expansion coefficient for the stainless steel. Consistent with [Table 2.3-1 in Section 2.3.1, *Mechanical Properties Applied to Analytic Evaluations*](#), the elastic modulus and thermal expansion coefficient for Type 304 stainless steel are $27.8(10)^6$ psi and $8.694(10)^{-6}$ inches/inch/°F, respectively, at a temperature of 160 °F.

Both the reference and uniform temperature are set to 160 °F, thereby excluding the effects of differential thermal expansion for this case.

For analysis model review, the ANSYS® input file is listed in [Table 2.10.1-5](#).

2.10.1.2.2 ICV Structural Analysis – Load Case 2

For ICV Load Case 4, the OCA structural analysis uses a -14.7 psig (0.0 psia) internal pressure (i.e., full vacuum) coupled with a increased external pressure of 0.0 psig (14.7 psia), per [Section 2.6.4, *Increased External Pressure*](#). The net external pressure for this case is 14.7 psig, applied throughout the inner periphery of the model. Relative to the upper and lower ICV seal flanges, the internal pressure does not extend beyond (below) the top of the upper main O-ring seal groove.

A uniform temperature of 70 °F is utilized to determine the temperature-dependent, material property values. The only material properties affected by a temperature of 70 °F are the elastic modulus and the thermal expansion coefficient for the stainless steel. Consistent with [Table 2.3-1 in Section 2.3.1, *Mechanical Properties Applied to Analytic Evaluations*](#), the elastic modulus and thermal expansion coefficient for Type 304 stainless steel are $28.3(10)^6$ psi and $8.46(10)^{-6}$ inches/inch/°F, respectively, at a temperature of 70 °F.

Both the reference and uniform temperature are set to 70 °F, thereby excluding the effects of differential thermal expansion for this case.

For analysis model review, the ANSYS® input file is listed in [Table 2.10.1-6](#).

Table 2.10.1-1 – ANSYS® Input Listing for OCA Load Case 1

```

! initialize ANSYS
fini
/cle
/filename,oca_lcl,inp
/out,,txt

! start preprocessing the model
/prep7
/title, OCA Load Case 1: P=64.7/3.5 psia, T=160/160 F

! element types
et,1,42,,,1
et,2,51
et,3,42,,,1
et,4,12,,,,,,1
et,5,12,,,,,,1
et,6,3
et,7,14,,,2

! reference and uniform temperatures
tref,160
tunif,160

! material properties for non-slotted steel regions
ex,1,27.8e06
nuxy,1,.3
alpx,1,8.694e-06

! material properties for slotted steel regions
ex,2,13.9e06
ey,2,13.9e06
ez,2,1
nuxy,2,.3
nuxz,2,0
nuyz,2,0
alpx,2,8.694e-06
alpy,2,8.694e-06
alpz,2,8.694e-06

! material properties for the polyurethane foam
ex,3,4773
ey,3,6810
ez,3,4773
nuxy,3,.33
nuxz,3,.33
nuyz,3,.33
alpx,3,3.5e-5

! material properties for the rigid coupling elements
ex,4,27.8e06
nuxy,4,.3
alpx,4,8.694E-06

! element real constants
r,1,.25
r,2,.1875
r,3,.375
r,4,.075
r,5,1e9,.1
r,6,-15,1e9,-.036
r,7,15,1e9,-.036
r,8,0,1e9,.1
r,9,1,1,1
r,10,1e2
r,101,-180.000,1e5,,1
r,102,-177.444,1e5,,1
r,103,-174.888,1e5,,1
r,104,-172.333,1e5,,1
r,105,-169.777,1e5,,1
r,106,-167.221,1e5,,1
r,107,-164.665,1e5,,1
r,108,-162.109,1e5,,1
r,109,-159.553,1e5,,1
r,110,-156.998,1e5,,1
r,111,-154.442,1e5,,1
r,112,-141.553,1e5,,1
r,113,-128.665,1e5,,1
r,114,-115.777,1e5,,1
r,115,-102.888,1e5,,1
r,116,-90.0000,1e5,,1
r,130,-102.000,1e5,,1
r,136,-77.1520,1e5,,1

r,137,-64.3041,1e5,,1
r,138,-51.4561,1e5,,1
r,139,-38.6081,1e5,,1
r,140,-25.7602,1e5,,1
r,141,-23.1841,1e5,,1
r,142,-20.6081,1e5,,1
r,143,-18.0321,1e5,,1
r,144,-15.4561,1e5,,1
r,145,-12.8801,1e5,,1
r,146,-10.3041,1e5,,1
r,147,-7.72805,1e5,,1
r,148,-5.15203,1e5,,1
r,149,-2.57602,1e5,,1
r,150,,1e5,,1
r,639,-58.7238,1e5,,1
r,640,-27.4476,1e5,,1
r,641,-24.7029,1e5,,1
r,642,-21.9581,1e5,,1
r,643,-19.2133,1e5,,1
r,644,-16.4686,1e5,,1
r,645,-13.7238,1e5,,1
r,646,-10.9790,1e5,,1
r,647,-8.23429,1e5,,1
r,648,-5.48952,1e5,,1
r,649,-2.74476,1e5,,1

! nodes for the lower seal flange
local,11,,38.24941495,50.051977923,,-12
n,1001
n,1005,.25
fill
n,1016,,.58677836
n,1020,.25,.58677836
fill
fill,1001,1016,2,1006,5,5,1
n,1026,,.896632635
local,12,,38.505,50
move,1026,11,0,999,0,12,-.065,999,0
fill,1016,1026,1,1021
local,11,1,39.12699808,50.47
n,1025,.5,148.5
n,1030,.5,129
n,1031,.5,109.5
n,1032,.5,90
csys,12
fill,1021,1025,3,1022,1,2,5
n,1033,.775,.97
n,1034,1.145,.97
n,1076,-.065,2.98
fill,1026,1076,8,1035,5
fill,1035,1076,7,1041,5
n,1060,.775,2.15593612
ngen,2,6,1033,1034,1,,.16
fill,1039,1060,3,1045,5
fill,1035,1039
fill,1041,1045,3,1042,1,4,5
n,1064,1.245,2.03
fill,1060,1064
n,1092,-.065,2.98
n,1096,.77960172,2.76
fill
n,1100,1.245,2.76
fill,1096,1100
fill,1056,1092,3,1065,9,9,1
ngen,3,9,1098,1100,1,,.26
n,1146,.14020351,4.4
fill,1092,1146,5,1101,9
n,1164,.14020351,4.98
fill,1146,1164,1,1155
local,11,,39.13520351,54.98,, -86.15
n,1168
n,1159,.3
ngen,3,-1,1159,1159,, -.125
n,1148,.58,-.25
ngen,2,-18,1157,1159,1,.56
ngen,2,-9,1139,1141,1,.25
ngen,2,-27,1148,1148,,.81
ngen,2,-18,1130,1132,1,.56
fill,1096,1114,1,1105
csys,12
fill,1101,1105
fill,1110,1112,1,1111,,6,9

```

```

fill,1164,1168

! nodes for the upper seal flange
local,11,,38.405,52.81
n,2001,,5
n,2005,,25,5
fill
ngen,3,5,2001,2005,1,,-.25
n,2031,,3.45
n,2035,,.91,3.45
fill
fill,2011,2031,3,2016,5,5,1
n,2051,,2.543442101
n,2055,,.91,2.543442101
fill
fill,2031,2051,3,2036,5,4,1
n,2040,,.91,3.29
fill,2040,2055,2,2045,5
n,2059,1.345,2.66
fill,2055,2059
n,2071,,2.17
n,2073,,.21504507,2.17
fill
n,2077,,.74504507,2.17
fill,2073,2077
fill,2051,2071,1,2060
fill,2054,2076,1,2065
fill,2060,2065
n,2081,1.345,2.17
fill,2077,2081
fill,2055,2077,1,2066,,5,1
n,2107,,.85759646,,.54
n,2109,1.10488343,.54
fill
n,2111,1.345,.54
fill,2109,2111
fill,2077,2107,5,2082,5,5,1
n,2117,,.94488343
n,2119,1.10488343
fill
fill,2109,2119,1,2114
n,2112,,.870715847,.35
fill,2112,2114
n,2120,1.345,3.45
n,2121,1.345,3.29
ngen,2,51,2071,2073,1,,-.305
ngen,2,3,2122,2124,1,,-.305

! nodes for the locking ring
local,11,,39.35,51.29
n,3001
n,3005,,.435
fill
n,3009,,.935
fill,3005,3009
n,3037,,.81
n,3041,,.435,.693442101
fill
n,3045,,.935,.693442101
fill,3041,3045
fill,3001,3037,3,3010,9,9,1
n,3145,,.4.11
n,3149,,.435,4.226557899
fill
n,3153,,.935,4.226557899
fill,3149,3153
fill,3041,3149,11,3050,9,5,1
n,3181,,.4.67
n,3185,,.535,4.67
fill
n,3189,,.935,4.67
fill,3185,3189
fill,3145,3181,3,3154,9,9,1

! nodes for the OCA inner shell (OCV)
local,11,1,,84.5
n,101,74.25,-90
n,111,74.25,-64.44174492
fill
local,12,1,28.3125,24.29659664
n,116,8.625
fill,111,116
csys
!n,117,36.9375,25.79659664
n,122,36.9375,43.95292590
fill,116,122

ngen,2,-879,1003,1003
fill,122,124
ngen,2,-1870,2003,2003
n,135,38.53,63.78649751
fill,133,135
local,12,1,29.905,63.78649751
n,140,8.625,64.23984399
fill,135,140
local,14,1,,1.8125
n,150,77.4375,90
fill,140,150

! nodes for the OCA outer shell
csys
n,601
n,613,47.0625
fill
n,622,47.0625,46.7775
fill,613,622
n,630,47.0625,47.6325
n,638,47.0625,75.3440689
fill,630,638
local,15,1,40.5625,75.3440689
n,640,6.5,62.55238078
fill,638,640
local,16,1,,-2.75
n,650,94.5,90
fill,640,650

! nodes for the polyurethane foam inner surface
csys
ngen,2,100,101,150,1
n,125,38.58338729,50.9
n,232,38.53,56.26

! nodes for the polyurethane foam outer surface
ngen,2,-100,601,650,1

! intermediate polyurethane foam nodes
fill,201,501,2,301,100,22,1
n,300,43.9375,50.9
n,331,41.5375,51.8825
n,332,41.5375,56.26
n,422,43.9375,46.7775
n,430,44.2375,47.6375
n,431,44.2375,51.8825
fill,222,422,1,322
fill,223,300,1,323
fill,332,532,1,432
fill,233,533,2,333,100,18,1

! nodes for the z-flanges
ngen,2,279,422,422,0
ngen,2,402,300,300,0
ngen,2,273,430,430,0
rp2,,1,1
ngen,2,374,331,331,0
rp2,,1,1

! elements for the lower seal flange
type,1
mat,1
real,1
e,1001,1002,1007,1006
rp4,1,1,1,1
egen,5,5,1,4,1
e,1026,1027,1036,1035
e,1027,1028,1036
e,1028,1029,1037,1036
e,1029,1030,1031,1037
e,1031,1032,1038,1037
rp3,1,1,1,1
e,1035,1036,1042,1041
rp4,1,1,1,1
e,1041,1042,1047,1046
rp4,1,1,1,1
egen,3,5,32,35,1
e,1056,1057,1066,1065
rp4,1,1,1,1
egen,4,9,44,47,1
mat,2
e,1060,1061,1070,1069
rp4,1,1,1,1
egen,4,9,60,63,1
egen,3,9,74,75,1
egen,3,9,56,59,1

```

```

egen,7,9,84,85,1
egen,3,1,99,99
egen,3,1,93,93

! elements for the upper seal flange
type,1
mat,1
real,1
e,2006,2007,2002,2001
rp4,1,1,1,1
egen,10,5,104,107,1
e,2040,2121,2120,2035
e,2060,2061,2052,2051
e,2061,2062,2052
e,2062,2063,2053,2052
e,2063,2064,2053
e,2064,2065,2054,2053
rp6,1,1,1,1
e,2071,2072,2061,2060
rp10,1,1,1,1
e,2122,2123,2072,2071
rp2,1,1,1,1
e,2125,2126,2123,2122
rp2,1,1,1,1
e,2082,2083,2078,2077
rp4,1,1,1,1
egen,6,5,169,172,1
egen,3,5,189,190,1

! elements for the locking ring
type,1
mat,2
real,1
e,3001,3002,3011,3010
rp4,1,1,1,1
egen,4,9,197,200,1
mat,1
e,3005,3006,3015,3014
rp4,1,1,1,1
egen,20,9,213,216,1
e,3145,3146,3155,3154
rp4,1,1,1,1
egen,4,9,293,296,1

! elements for the OCA inner shell (OCV)
type,2
mat,1
real,1
e,101,102
rp16,1,1
real,2
e,117,118
rp5,1,1
real,1
e,122,123
e,123,1003
e,2003,134
e,134,135
rp16,1,1

! elements for the OCA outer shell
real,1
e,601,602
rp18,1,1
real,3
e,619,620
rp3,1,1
e,630,631
rp8,1,1
real,1
e,638,639
rp12,1,1

! elements for the Z-flanges
real,4
e,622,701
e,701,702
e,702,1034
e,1034,1033
e,630,703
e,703,704
rp3,1,1
e,706,2120
e,2120,2035

! polyurethane foam elements
type,3
mat,3
real,1
e,201,301,302,202
rp22,1,1,1,1
e,224,223,323
e,301,401,402,302
rp21,1,1,1,1
e,322,422,300,323
e,300,125,224,323
e,401,501,502,402
rp21,1,1,1,1
e,333,233,232,332
e,233,333,334,234
rp17,1,1,1,1
e,331,431,432,332
rp19,1,1,1,1
e,430,530,531,431
rp20,1,1,1,1

! interface elements between the steel shells
! and the polyurethane foam
type,5
mat,1
real,101
e,101,201
real,102
e,102,202
real,103
e,103,203
real,104
e,104,204
real,105
e,105,205
real,106
e,106,206
real,107
e,107,207
real,108
e,108,208
real,109
e,109,209
real,110
e,110,210
real,111
e,111,211
real,112
e,112,212
real,113
e,113,213
real,114
e,114,214
real,115
e,115,215
real,116
e,116,216
rp5,1,1
real,130
e,122,222
rp2,1,1
e,1003,224
real,101
e,702,300
e,701,422
e,622,522
real,150
e,706,332
e,705,331
e,704,431
e,703,430
e,630,530
real,116
e,300,702
e,422,701
e,706,332
e,705,331
e,704,431
e,703,430
e,2003,233
e,134,234
rp2,1,1
real,136
e,136,236
real,137
e,137,237
real,138

```

```

e,138,238
real,139
e,139,239
real,140
e,140,240
real,141
e,141,241
real,142
e,142,242
real,143
e,143,243
real,144
e,144,244
real,145
e,145,245
real,146
e,146,246
real,147
e,147,247
real,148
e,148,248
real,149
e,149,249
real,150
e,150,250
real,101
e,501,601
rp13,1,1
real,116
e,513,613
rp10,1,1
e,530,630
rp9,1,1
real,639
e,539,639
real,640
e,540,640
real,641
e,541,641
real,642
e,542,642
real,643
e,543,643
real,644
e,544,644
real,645
e,545,645
real,646
e,546,646
real,647
e,547,647
real,648
e,548,648
real,649
e,549,649
real,150
e,550,650

! interface elements between the lower seal flange
! and the locking ring
type,4
mat,1
real,6
e,3038,1061
rp3,1,1

! interface elements between the upper seal flange
! and the locking ring
type,4
mat,1
real,7
e,2056,3146
rp3,1,1

! interface elements between the lower seal flange
! and the upper seal flange
type,5
mat,1
real,8
e,1164,2073
rp5,1,1

! couple the lower shell to the lower seal flange
type,6
mat,4
real,9
e,1001,1002
rp4,1,1

! couple the upper shell to the upper seal flange
type,6
mat,4
real,9
e,2001,2002
rp4,1,1

! springs between the lower seal flange
! and the locking ring
type,7
mat,1
real,10
e,3038,1061
rp3,1,1

! springs between the upper seal flange
! and the locking ring
type,7
mat,1
real,10
e,2056,3146
rp3,1,1

! springs between the lower seal flange
! and the upper seal flange
type,7
mat,1
real,10
e,1164,2073
rp5,1,1

! displacement constraints
d,101,UX,0,,601,500,rotz
d,201,UX,0,,501,100
d,150,UX,0,,650,500,rotz
d,250,UX,0,,550,100
d,3099,UY,0
d,all,uz,0

! pressure loads
alls
pload=+(64.7-3.5)
p,101,102,pload,,122,1
p,123,1003,pload
p,1001,1006,pload,,1021,5
p,1026,1035,pload
p,1035,1041,pload
p,1041,1046,pload,,1051,5
p,1056,1065,pload,,1155,9
p,1164,1165,pload,,1167,1
p,1168,1159,pload
p,2077,2082,pload
p,2073,2074,pload,,2076,1
p,2127,2124,pload
p,2124,2073,pload
p,2125,2126,pload,,2126,1
p,2122,2125,pload
p,2071,2122,pload
p,2001,2006,pload,,2046,5
p,2051,2060,pload
p,2060,2071,pload
p,2003,134,pload
p,134,135,pload,,149,1

! delete unused nodes at seal flange interfaces
ndelete,124
ndelete,133

! solve the problem
fini
/solu
neqit,1000
alls
solv
fini
save

! post-process the problem
/post1
set
rsys,solu
ernorm,0

```



```

! table stress definitions for shell elements
nall
alls
esel,s,type,2
etab,sit,nmisc,4
etab,sim,nmisc,9
etab,sib,nmisc,14

/com,
/com,
/com,
/com,+++++
/com,+ lower seal flange +
/com,+++++
/com,
/com,
nall
eall
nset,s,node,,1000,1999,1
prns,prin

/com,
/com,
/com,
/com,+++++
/com,+ upper seal flange +
/com,+++++
/com,
/com,
nall
eall
nset,s,node,,2000,2999,1
prns,prin

/com,
/com,
/com,
/com,+++++
/com,+ locking ring +
/com,+++++
/com,
/com,
nall
eall
nset,s,node,,3000,3999,1
prns,prin

/com,
/com,
/com,
/com,+++++
/com,+ OCV cylindrical and conical shells +
/com,+++++
/com,
/com,
nall
eall
esel,s,elem,,324,331,1
pret

/com,
/com,
/com,
/com,+++++
/com,+ OCV torispherical head crown shells +
/com,+++++
/com,
/com,
nall
eall
esel,s,elem,,339,348,1 ! upper head
esel,a,elem,,309,318,1 ! lower head
pret

/com,
/com,
/com,
/com,+++++
/com,+ OCV torispherical head knuckle shells +
/com,+++++
/com,
/com,
nall
eall
esel,s,elem,,334,338,1 ! upper head
esel,a,elem,,319,323,1 ! lower head
pret

/com,
/com,
/com,
/com,+++++
/com,+ OCA outer shells and z-flanges +
/com,+++++
/com,
/com,
nall
eall
esel,s,elem,,349,399,1
pret

/com,
/com,
/com,
/com,+++++
/com,+ polyurethane foam elements +
/com,+++++
/com,
/com,
nall
eall
esel,s,elem,,415,559,1
prns,prin

! finalize ANSYS
nall
eall
save
/out,term
/eof

```

Table 2.10.1-2 – ANSYS® Input Listing for OCA Load Case 2

```

! initialize ANSYS
fini
/cle
/filename,oqa_lc2,inp
/out,,txt

! start preprocessing the model
/prep7
/title, OCA Load Case 2: P=64.7/3.5 psia, T=160/70 F

! element types
et,1,42,,,1
et,2,51
et,3,42,,,1
et,4,12,,,,,,1
et,5,12,,,,,,1
et,6,3
et,7,14,,,2

! reference and uniform temperatures
tref,70
tunif,160

! material properties for non-slotted steel regions
ex,1,27.8e06
nuxy,1,.3
alpx,1,8.694e-06

! material properties for slotted steel regions
ex,2,13.9e06
ey,2,13.9e06
ez,2,1
nuxy,2,.3
nuxz,2,0
nuyz,2,0
alpx,2,8.694e-06
alpy,2,8.694e-06
alpz,2,8.694e-06

! material properties for the polyurethane foam
ex,3,4773
ey,3,6810
ez,3,4773
nuxy,3,.33
nuxz,3,.33
nuyz,3,.33
alpx,3,3.5e-5

! material properties for the rigid coupling elements
ex,4,27.8e06
nuxy,4,.3
alpx,4,8.694E-06

! element real constants
r,1,.25
r,2,.1875
r,3,.375
r,4,.075
r,5,1e9,.1
r,6,-15,1e9,-.036
r,7,15,1e9,-.036
r,8,0,1e9,.1
r,9,1,1,1
r,10,1e2
r,101,-180.000,1e5,,1
r,102,-177.444,1e5,,1
r,103,-174.888,1e5,,1
r,104,-172.333,1e5,,1
r,105,-169.777,1e5,,1
r,106,-167.221,1e5,,1
r,107,-164.665,1e5,,1
r,108,-162.109,1e5,,1
r,109,-159.553,1e5,,1
r,110,-156.998,1e5,,1
r,111,-154.442,1e5,,1
r,112,-141.553,1e5,,1
r,113,-128.665,1e5,,1
r,114,-115.777,1e5,,1
r,115,-102.888,1e5,,1
r,116,-90.0000,1e5,,1
r,130,-102.000,1e5,,1
r,136,-77.1520,1e5,,1
r,137,-64.3041,1e5,,1
r,138,-51.4561,1e5,,1
r,139,-38.6081,1e5,,1
r,140,-25.7602,1e5,,1
r,141,-23.1841,1e5,,1
r,142,-20.6081,1e5,,1
r,143,-18.0321,1e5,,1
r,144,-15.4561,1e5,,1
r,145,-12.8801,1e5,,1
r,146,-10.3041,1e5,,1
r,147,-7.72805,1e5,,1
r,148,-5.15203,1e5,,1
r,149,-2.57602,1e5,,1
r,150,,1e5,,1
r,639,-58.7238,1e5,,1
r,640,-27.4476,1e5,,1
r,641,-24.7029,1e5,,1
r,642,-21.9581,1e5,,1
r,643,-19.2133,1e5,,1
r,644,-16.4686,1e5,,1
r,645,-13.7238,1e5,,1
r,646,-10.9790,1e5,,1
r,647,-8.23429,1e5,,1
r,648,-5.48952,1e5,,1
r,649,-2.74476,1e5,,1

! nodes for the lower seal flange
local,11,,38.24941495,50.051977923,,-12
n,1001
n,1005,.25
fill
n,1016,,.58677836
n,1020,.25,.58677836
fill
fill,1001,1016,2,1006,5,5,1
n,1026,,.896632635
local,12,,38.505,50
move,1026,11,0,999,0,12,-.065,999,0
fill,1016,1026,1,1021
local,11,1,39.12699808,50.47
n,1025,.5,148.5
n,1030,.5,129
n,1031,.5,109.5
n,1032,.5,90
csys,12
fill,1021,1025,3,1022,1,2,5
n,1033,.775,.97
n,1034,1.145,.97
n,1076,-.065,2.98
fill,1026,1076,8,1035,5
fill,1035,1076,7,1041,5
n,1060,.775,2.15593612
ngen,2,6,1033,1034,1,,.16
fill,1039,1060,3,1045,5
fill,1035,1039
fill,1041,1045,3,1042,1,4,5
n,1064,1.245,2.03
fill,1060,1064
n,1092,-.065,2.98
n,1096,.77960172,2.76
fill
n,1100,1.245,2.76
fill,1096,1100
fill,1056,1092,3,1065,9,9,1
ngen,3,9,1098,1100,1,,.26
n,1146,.14020351,4.4
fill,1092,1146,5,1101,9
n,1164,.14020351,4.98
fill,1146,1164,1,1155
local,11,,39.13520351,54.98,, -86.15
n,1168
n,1159,.3
ngen,3,-1,1159,1159,, -.125
n,1148,.58,-.25
ngen,2,-18,1157,1159,1,.56
ngen,2,-9,1139,1141,1,.25
ngen,2,-27,1148,1148,,.81
ngen,2,-18,1130,1132,1,.56
fill,1096,1114,1,1105
csys,12
fill,1101,1105
fill,1110,1112,1,1111,,6,9

```

```

fill,1164,1168

! nodes for the upper seal flange
local,11,,38.405,52.81
n,2001,,5
n,2005,,25,5
fill
ngen,3,5,2001,2005,1,,-.25
n,2031,,3.45
n,2035,,91,3.45
fill
fill,2011,2031,3,2016,5,5,1
n,2051,,2.543442101
n,2055,,91,2.543442101
fill
fill,2031,2051,3,2036,5,4,1
n,2040,,91,3.29
fill,2040,2055,2,2045,5
n,2059,1.345,2.66
fill,2055,2059
n,2071,,2.17
n,2073,,21504507,2.17
fill
n,2077,,74504507,2.17
fill,2073,2077
fill,2051,2071,1,2060
fill,2054,2076,1,2065
fill,2060,2065
n,2081,1.345,2.17
fill,2077,2081
fill,2055,2077,1,2066,,5,1
n,2107,,85759646,,54
n,2109,1.10488343,,54
fill
n,2111,1.345,,54
fill,2109,2111
fill,2077,2107,5,2082,5,5,1
n,2117,,94488343
n,2119,1.10488343
fill
fill,2109,2119,1,2114
n,2112,,870715847,,35
fill,2112,2114
n,2120,1.345,3.45
n,2121,1.345,3.29
ngen,2,51,2071,2073,1,,-.305
ngen,2,3,2122,2124,1,,-.305

! nodes for the locking ring
local,11,,39.35,51.29
n,3001
n,3005,,435
fill
n,3009,,935
fill,3005,3009
n,3037,,.81
n,3041,,435,,.693442101
fill
n,3045,,935,,.693442101
fill,3041,3045
fill,3001,3037,3,3010,9,9,1
n,3145,,4.11
n,3149,,435,4.226557899
fill
n,3153,,935,4.226557899
fill,3149,3153
fill,3041,3149,11,3050,9,5,1
n,3181,,4.67
n,3185,,535,4.67
fill
n,3189,,935,4.67
fill,3185,3189
fill,3145,3181,3,3154,9,9,1

! nodes for the OCA inner shell (OCV)
local,11,1,,84.5
n,101,74.25,-90
n,111,74.25,-64.44174492
fill
local,12,1,28.3125,24.29659664
n,116,8.625
fill,111,116
csys
!n,117,36.9375,25.79659664
n,122,36.9375,43.95292590
fill,116,122

ngen,2,-879,1003,1003
fill,122,124
ngen,2,-1870,2003,2003
n,135,38.53,63.78649751
fill,133,135
local,12,1,29.905,63.78649751
n,140,8.625,64.23984399
fill,135,140
local,14,1,,1.8125
n,150,77.4375,90
fill,140,150

! nodes for the OCA outer shell
csys
n,601
n,613,47.0625
fill
n,622,47.0625,46.7775
fill,613,622
n,630,47.0625,47.6325
n,638,47.0625,75.3440689
fill,630,638
local,15,1,40.5625,75.3440689
n,640,6.5,62.55238078
fill,638,640
local,16,1,,-2.75
n,650,94.5,90
fill,640,650

! nodes for the polyurethane foam inner surface
csys
ngen,2,100,101,150,1
n,125,38.58338729,50.9
n,232,38.53,56.26

! nodes for the polyurethane foam outer surface
ngen,2,-100,601,650,1

! intermediate polyurethane foam nodes
fill,201,501,2,301,100,22,1
n,300,43.9375,50.9
n,331,41.5375,51.8825
n,332,41.5375,56.26
n,422,43.9375,46.7775
n,430,44.2375,47.6375
n,431,44.2375,51.8825
fill,222,422,1,322
fill,223,300,1,323
fill,332,532,1,432
fill,233,533,2,333,100,18,1

! nodes for the z-flanges
ngen,2,279,422,422,0
ngen,2,402,300,300,0
ngen,2,273,430,430,0
rp2,,1,1
ngen,2,374,331,331,0
rp2,,1,1

! elements for the lower seal flange
type,1
mat,1
real,1
e,1001,1002,1007,1006
rp4,1,1,1,1
egen,5,5,1,4,1
e,1026,1027,1036,1035
e,1027,1028,1036
e,1028,1029,1037,1036
e,1029,1030,1031,1037
e,1031,1032,1038,1037
rp3,1,1,1,1
e,1035,1036,1042,1041
rp4,1,1,1,1
e,1041,1042,1047,1046
rp4,1,1,1,1
egen,3,5,32,35,1
e,1056,1057,1066,1065
rp4,1,1,1,1
egen,4,9,44,47,1
mat,2
e,1060,1061,1070,1069
rp4,1,1,1,1
egen,4,9,60,63,1
egen,3,9,74,75,1
egen,3,9,56,59,1

```

```

egen,7,9,84,85,1
egen,3,1,99,99
egen,3,1,93,93

! elements for the upper seal flange
type,1
mat,1
real,1
e,2006,2007,2002,2001
rp4,1,1,1,1
egen,10,5,104,107,1
e,2040,2121,2120,2035
e,2060,2061,2052,2051
e,2061,2062,2052
e,2062,2063,2053,2052
e,2063,2064,2053
e,2064,2065,2054,2053
rp6,1,1,1,1
e,2071,2072,2061,2060
rp10,1,1,1,1
e,2122,2123,2072,2071
rp2,1,1,1,1
e,2125,2126,2123,2122
rp2,1,1,1,1
e,2082,2083,2078,2077
rp4,1,1,1,1
egen,6,5,169,172,1
egen,3,5,189,190,1

! elements for the locking ring
type,1
mat,2
real,1
e,3001,3002,3011,3010
rp4,1,1,1,1
egen,4,9,197,200,1
mat,1
e,3005,3006,3015,3014
rp4,1,1,1,1
egen,20,9,213,216,1
e,3145,3146,3155,3154
rp4,1,1,1,1
egen,4,9,293,296,1

! elements for the OCA inner shell (OCV)
type,2
mat,1
real,1
e,101,102
rp16,1,1
real,2
e,117,118
rp5,1,1
real,1
e,122,123
e,123,1003
e,2003,134
e,134,135
rp16,1,1

! elements for the OCA outer shell
real,1
e,601,602
rp18,1,1
real,3
e,619,620
rp3,1,1
e,630,631
rp8,1,1
real,1
e,638,639
rp12,1,1

! elements for the Z-flanges
real,4
e,622,701
e,701,702
e,702,1034
e,1034,1033
e,630,703
e,703,704
rp3,1,1
e,706,2120
e,2120,2035

! polyurethane foam elements
type,3
mat,3
real,1
e,201,301,302,202
rp22,1,1,1,1
e,224,223,323
e,301,401,402,302
rp21,1,1,1,1
e,322,422,300,323
e,300,125,224,323
e,401,501,502,402
rp21,1,1,1,1
e,333,233,232,332
e,233,333,334,234
rp17,1,1,1,1
e,331,431,432,332
rp19,1,1,1,1
e,430,530,531,431
rp20,1,1,1,1

! interface elements between the steel shells
! and the polyurethane foam
type,5
mat,1
real,101
e,101,201
real,102
e,102,202
real,103
e,103,203
real,104
e,104,204
real,105
e,105,205
real,106
e,106,206
real,107
e,107,207
real,108
e,108,208
real,109
e,109,209
real,110
e,110,210
real,111
e,111,211
real,112
e,112,212
real,113
e,113,213
real,114
e,114,214
real,115
e,115,215
real,116
e,116,216
rp5,1,1
real,130
e,122,222
rp2,1,1
e,1003,224
real,101
e,702,300
e,701,422
e,622,522
real,150
e,706,332
e,705,331
e,704,431
e,703,430
e,630,530
real,116
e,300,702
e,422,701
e,706,332
e,705,331
e,704,431
e,703,430
e,2003,233
e,134,234
rp2,1,1
real,136
e,136,236
real,137
e,137,237
real,138

```

```

e,138,238
real,139
e,139,239
real,140
e,140,240
real,141
e,141,241
real,142
e,142,242
real,143
e,143,243
real,144
e,144,244
real,145
e,145,245
real,146
e,146,246
real,147
e,147,247
real,148
e,148,248
real,149
e,149,249
real,150
e,150,250
real,101
e,501,601
rp13,1,1
real,116
e,513,613
rp10,1,1
e,530,630
rp9,1,1
real,639
e,539,639
real,640
e,540,640
real,641
e,541,641
real,642
e,542,642
real,643
e,543,643
real,644
e,544,644
real,645
e,545,645
real,646
e,546,646
real,647
e,547,647
real,648
e,548,648
real,649
e,549,649
real,150
e,550,650

! interface elements between the lower seal flange
! and the locking ring
type,4
mat,1
real,6
e,3038,1061
rp3,1,1

! interface elements between the upper seal flange
! and the locking ring
type,4
mat,1
real,7
e,2056,3146
rp3,1,1

! interface elements between the lower seal flange
! and the upper seal flange
type,5
mat,1
real,8
e,1164,2073
rp5,1,1

! couple the lower shell to the lower seal flange
type,6
mat,4
real,9
e,1001,1002
rp4,1,1

! couple the upper shell to the upper seal flange
type,6
mat,4
real,9
e,2001,2002
rp4,1,1

! springs between the lower seal flange
! and the locking ring
type,7
mat,1
real,10
e,3038,1061
rp3,1,1

! springs between the upper seal flange
! and the locking ring
type,7
mat,1
real,10
e,2056,3146
rp3,1,1

! springs between the lower seal flange
! and the upper seal flange
type,7
mat,1
real,10
e,1164,2073
rp5,1,1

! displacement constraints
d,101,UX,0,,601,500,rotz
d,201,UX,0,,501,100
d,150,UX,0,,650,500,rotz
d,250,UX,0,,550,100
d,3099,UY,0
d,all,uz,0

! pressure loads
alls
pload=+(64.7-3.5)
p,101,102,pload,,122,1
p,123,1003,pload
p,1001,1006,pload,,1021,5
p,1026,1035,pload
p,1035,1041,pload
p,1041,1046,pload,,1051,5
p,1056,1065,pload,,1155,9
p,1164,1165,pload,,1167,1
p,1168,1159,pload
p,2077,2082,pload
p,2073,2074,pload,,2076,1
p,2127,2124,pload
p,2124,2073,pload
p,2125,2126,pload,,2126,1
p,2122,2125,pload
p,2071,2122,pload
p,2001,2006,pload,,2046,5
p,2051,2060,pload
p,2060,2071,pload
p,2003,134,pload
p,134,135,pload,,149,1

! delete unused nodes at seal flange interfaces
ndelete,124
ndelete,133

! solve the problem
fini
/solu
neqit,1000
alls
solv
fini
save

! post-process the problem
/post1
set
rsys,solu
ernorm,0

```

```

! table stress definitions for shell elements
nall
alls
esel,s,type,2
etab,sit,nmisc,4
etab,sim,nmisc,9
etab,sib,nmisc,14

/com,
/com,
/com,
/com,+++++
/com,+ lower seal flange +
/com,+++++
/com,
/com,
nall
eall
nset,s,node,,1000,1999,1
prns,prin

/com,
/com,
/com,
/com,+++++
/com,+ upper seal flange +
/com,+++++
/com,
/com,
nall
eall
nset,s,node,,2000,2999,1
prns,prin

/com,
/com,
/com,
/com,+++++
/com,+ locking ring +
/com,+++++
/com,
/com,
nall
eall
nset,s,node,,3000,3999,1
prns,prin

/com,
/com,
/com,
/com,+++++
/com,+ OCV cylindrical and conical shells +
/com,+++++
/com,
/com,
nall
eall
esel,s,elem,,324,331,1
pret

/com,
/com,
/com,

```

```

/com,+++++
/com,+ OCV torispherical head crown shells +
/com,+++++
/com,
/com,
nall
eall
esel,s,elem,,339,348,1 ! upper head
esel,a,elem,,309,318,1 ! lower head
pret

/com,
/com,
/com,
/com,+++++
/com,+ OCV torispherical head knuckle shells +
/com,+++++
/com,
/com,
nall
eall
esel,s,elem,,334,338,1 ! upper head
esel,a,elem,,319,323,1 ! lower head
pret

/com,
/com,
/com,
/com,+++++
/com,+ OCA outer shells and z-flanges +
/com,+++++
/com,
/com,
nall
eall
esel,s,elem,,349,399,1
pret

/com,
/com,
/com,
/com,+++++
/com,+ polyurethane foam elements +
/com,+++++
/com,
/com,
nall
eall
esel,s,elem,,415,559,1
prns,prin

! finalize ANSYS
nall
eall
save
/out,term
/eof

```

Table 2.10.1-3 – ANSYS® Input Listing for OCA Load Case 3

```

! initialize ANSYS
fini
/cle
/filename,oqa_lc3,inp
/out,,txt

! start preprocessing the model
/prep7
/title, OCA Load Case 3: P=14.7/14.7 psia, T=-40/70 F

! element types
et,1,42,,,1
et,2,51
et,3,42,,,1
et,4,12,,,,,,1
et,5,12,,,,,,1
et,6,3
et,7,14,,,2

! reference and uniform temperatures
tref,70
tunif,-40

! material properties for non-slotted steel regions
ex,1,28.8e06
nuxy,1,.3
alpx,1,8.21e-06

! material properties for slotted steel regions
ex,2,14.4e06
ey,2,14.4e06
ez,2,1
nuxy,2,.3
nuxz,2,0
nuyz,2,0
alpx,2,8.21e-06
alpy,2,8.21e-06
alpz,2,8.21e-06

! material properties for the polyurethane foam
ex,3,4773
ey,3,6810
ez,3,4773
nuxy,3,.33
nuxz,3,.33
nuyz,3,.33
alpx,3,3.5e-5

! material properties for the rigid coupling elements
ex,4,28.8e06
nuxy,4,.3
alpx,4,8.21E-06

! element real constants
r,1,.25
r,2,.1875
r,3,.375
r,4,.075
r,5,1e9,.1
r,6,-15,1e9,-.036
r,7,15,1e9,-.036
r,8,0,1e9,.1
r,9,1,1,1
r,10,1e2
r,101,-180.000,1e5,,1
r,102,-177.444,1e5,,1
r,103,-174.888,1e5,,1
r,104,-172.333,1e5,,1
r,105,-169.777,1e5,,1
r,106,-167.221,1e5,,1
r,107,-164.665,1e5,,1
r,108,-162.109,1e5,,1
r,109,-159.553,1e5,,1
r,110,-156.998,1e5,,1
r,111,-154.442,1e5,,1
r,112,-141.553,1e5,,1
r,113,-128.665,1e5,,1
r,114,-115.777,1e5,,1
r,115,-102.888,1e5,,1
r,116,-90.0000,1e5,,1
r,130,-102.000,1e5,,1
r,136,-77.1520,1e5,,1
r,137,-64.3041,1e5,,1
r,138,-51.4561,1e5,,1
r,139,-38.6081,1e5,,1
r,140,-25.7602,1e5,,1
r,141,-23.1841,1e5,,1
r,142,-20.6081,1e5,,1
r,143,-18.0321,1e5,,1
r,144,-15.4561,1e5,,1
r,145,-12.8801,1e5,,1
r,146,-10.3041,1e5,,1
r,147,-7.72805,1e5,,1
r,148,-5.15203,1e5,,1
r,149,-2.57602,1e5,,1
r,150,,1e5,,1
r,639,-58.7238,1e5,,1
r,640,-27.4476,1e5,,1
r,641,-24.7029,1e5,,1
r,642,-21.9581,1e5,,1
r,643,-19.2133,1e5,,1
r,644,-16.4686,1e5,,1
r,645,-13.7238,1e5,,1
r,646,-10.9790,1e5,,1
r,647,-8.23429,1e5,,1
r,648,-5.48952,1e5,,1
r,649,-2.74476,1e5,,1

! nodes for the lower seal flange
local,11,,38.24941495,50.051977923,,-12
n,1001
n,1005,.25
fill
n,1016,,.58677836
n,1020,.25,.58677836
fill
fill,1001,1016,2,1006,5,5,1
n,1026,,.896632635
local,12,,38.505,50
move,1026,11,0,999,0,12,-.065,999,0
fill,1016,1026,1,1021
local,11,1,39.12699808,50.47
n,1025,.5,148.5
n,1030,.5,129
n,1031,.5,109.5
n,1032,.5,90
csys,12
fill,1021,1025,3,1022,1,2,5
n,1033,.775,.97
n,1034,1.145,.97
n,1076,-.065,2.98
fill,1026,1076,8,1035,5
fill,1035,1076,7,1041,5
n,1060,.775,2.15593612
ngen,2,6,1033,1034,1,,.16
fill,1039,1060,3,1045,5
fill,1035,1039
fill,1041,1045,3,1042,1,4,5
n,1064,1.245,2.03
fill,1060,1064
n,1092,-.065,2.98
n,1096,.77960172,2.76
fill
n,1100,1.245,2.76
fill,1096,1100
fill,1056,1092,3,1065,9,9,1
ngen,3,9,1098,1100,1,,.26
n,1146,.14020351,4.4
fill,1092,1146,5,1101,9
n,1164,.14020351,4.98
fill,1146,1164,1,1155
local,11,,39.13520351,54.98,, -86.15
n,1168
n,1159,.3
ngen,3,-1,1159,1159,, -.125
n,1148,.58,-.25
ngen,2,-18,1157,1159,1,.56
ngen,2,-9,1139,1141,1,.25
ngen,2,-27,1148,1148,,.81
ngen,2,-18,1130,1132,1,.56
fill,1096,1114,1,1105
csys,12
fill,1101,1105
fill,1110,1112,1,1111,,6,9

```

```

fill,1164,1168

! nodes for the upper seal flange
local,11,,38.405,52.81
n,2001,,5
n,2005,,25,5
fill
ngen,3,5,2001,2005,1,,-.25
n,2031,,3.45
n,2035,,.91,3.45
fill
fill,2011,2031,3,2016,5,5,1
n,2051,,2.543442101
n,2055,,.91,2.543442101
fill
fill,2031,2051,3,2036,5,4,1
n,2040,,.91,3.29
fill,2040,2055,2,2045,5
n,2059,1.345,2.66
fill,2055,2059
n,2071,,2.17
n,2073,,.21504507,2.17
fill
n,2077,,.74504507,2.17
fill,2073,2077
fill,2051,2071,1,2060
fill,2054,2076,1,2065
fill,2060,2065
n,2081,1.345,2.17
fill,2077,2081
fill,2055,2077,1,2066,,5,1
n,2107,,.85759646,,.54
n,2109,1.10488343,.54
fill
n,2111,1.345,.54
fill,2109,2111
fill,2077,2107,5,2082,5,5,1
n,2117,,.94488343
n,2119,1.10488343
fill
fill,2109,2119,1,2114
n,2112,,.870715847,.35
fill,2112,2114
n,2120,1.345,3.45
n,2121,1.345,3.29
ngen,2,51,2071,2073,1,,-.305
ngen,2,3,2122,2124,1,,-.305

! nodes for the locking ring
local,11,,39.35,51.29
n,3001
n,3005,,.435
fill
n,3009,,.935
fill,3005,3009
n,3037,,.81
n,3041,,.435,.693442101
fill
n,3045,,.935,.693442101
fill,3041,3045
fill,3001,3037,3,3010,9,9,1
n,3145,,.4.11
n,3149,,.435,4.226557899
fill
n,3153,,.935,4.226557899
fill,3149,3153
fill,3041,3149,11,3050,9,5,1
n,3181,,.4.67
n,3185,,.535,4.67
fill
n,3189,,.935,4.67
fill,3185,3189
fill,3145,3181,3,3154,9,9,1

! nodes for the OCA inner shell (OCV)
local,11,1,,84.5
n,101,74.25,-90
n,111,74.25,-64.44174492
fill
local,12,1,28.3125,24.29659664
n,116,8.625
fill,111,116
csys
!n,117,36.9375,25.79659664
n,122,36.9375,43.95292590
fill,116,122

ngen,2,-879,1003,1003
fill,122,124
ngen,2,-1870,2003,2003
n,135,38.53,63.78649751
fill,133,135
local,12,1,29.905,63.78649751
n,140,8.625,64.23984399
fill,135,140
local,14,1,,1.8125
n,150,77.4375,90
fill,140,150

! nodes for the OCA outer shell
csys
n,601
n,613,47.0625
fill
n,622,47.0625,46.7775
fill,613,622
n,630,47.0625,47.6325
n,638,47.0625,75.3440689
fill,630,638
local,15,1,40.5625,75.3440689
n,640,6.5,62.55238078
fill,638,640
local,16,1,,-2.75
n,650,94.5,90
fill,640,650

! nodes for the polyurethane foam inner surface
csys
ngen,2,100,101,150,1
n,125,38.58338729,50.9
n,232,38.53,56.26

! nodes for the polyurethane foam outer surface
ngen,2,-100,601,650,1

! intermediate polyurethane foam nodes
fill,201,501,2,301,100,22,1
n,300,43.9375,50.9
n,331,41.5375,51.8825
n,332,41.5375,56.26
n,422,43.9375,46.7775
n,430,44.2375,47.6375
n,431,44.2375,51.8825
fill,222,422,1,322
fill,223,300,1,323
fill,332,532,1,432
fill,233,533,2,333,100,18,1

! nodes for the z-flanges
ngen,2,279,422,422,0
ngen,2,402,300,300,0
ngen,2,273,430,430,0
rp2,,1,1
ngen,2,374,331,331,0
rp2,,1,1

! elements for the lower seal flange
type,1
mat,1
real,1
e,1001,1002,1007,1006
rp4,1,1,1,1
egen,5,5,1,4,1
e,1026,1027,1036,1035
e,1027,1028,1036
e,1028,1029,1037,1036
e,1029,1030,1031,1037
e,1031,1032,1038,1037
rp3,1,1,1,1
e,1035,1036,1042,1041
rp4,1,1,1,1
e,1041,1042,1047,1046
rp4,1,1,1,1
egen,3,5,32,35,1
e,1056,1057,1066,1065
rp4,1,1,1,1
egen,4,9,44,47,1
mat,2
e,1060,1061,1070,1069
rp4,1,1,1,1
egen,4,9,60,63,1
egen,3,9,74,75,1
egen,3,9,56,59,1

```



```

egen,7,9,84,85,1
egen,3,1,99,99
egen,3,1,93,93

! elements for the upper seal flange
type,1
mat,1
real,1
e,2006,2007,2002,2001
rp4,1,1,1,1
egen,10,5,104,107,1
e,2040,2121,2120,2035
e,2060,2061,2052,2051
e,2061,2062,2052
e,2062,2063,2053,2052
e,2063,2064,2053
e,2064,2065,2054,2053
rp6,1,1,1,1
e,2071,2072,2061,2060
rp10,1,1,1,1
e,2122,2123,2072,2071
rp2,1,1,1,1
e,2125,2126,2123,2122
rp2,1,1,1,1
e,2082,2083,2078,2077
rp4,1,1,1,1
egen,6,5,169,172,1
egen,3,5,189,190,1

! elements for the locking ring
type,1
mat,2
real,1
e,3001,3002,3011,3010
rp4,1,1,1,1
egen,4,9,197,200,1
mat,1
e,3005,3006,3015,3014
rp4,1,1,1,1
egen,20,9,213,216,1
e,3145,3146,3155,3154
rp4,1,1,1,1
egen,4,9,293,296,1

! elements for the OCA inner shell (OCV)
type,2
mat,1
real,1
e,101,102
rp16,1,1
real,2
e,117,118
rp5,1,1
real,1
e,122,123
e,123,1003
e,2003,134
e,134,135
rp16,1,1

! elements for the OCA outer shell
real,1
e,601,602
rp18,1,1
real,3
e,619,620
rp3,1,1
e,630,631
rp8,1,1
real,1
e,638,639
rp12,1,1

! elements for the Z-flanges
real,4
e,622,701
e,701,702
e,702,1034
e,1034,1033
e,630,703
e,703,704
rp3,1,1
e,706,2120
e,2120,2035

! polyurethane foam elements
type,3
mat,3
real,1
e,201,301,302,202
rp22,1,1,1,1
e,224,223,323
e,301,401,402,302
rp21,1,1,1,1
e,322,422,300,323
e,300,125,224,323
e,401,501,502,402
rp21,1,1,1,1
e,333,233,232,332
e,233,333,334,234
rp17,1,1,1,1
e,331,431,432,332
rp19,1,1,1,1
e,430,530,531,431
rp20,1,1,1,1

! interface elements between the steel shells
! and the polyurethane foam
type,5
mat,1
real,101
e,101,201
real,102
e,102,202
real,103
e,103,203
real,104
e,104,204
real,105
e,105,205
real,106
e,106,206
real,107
e,107,207
real,108
e,108,208
real,109
e,109,209
real,110
e,110,210
real,111
e,111,211
real,112
e,112,212
real,113
e,113,213
real,114
e,114,214
real,115
e,115,215
real,116
e,116,216
rp5,1,1
real,130
e,122,222
rp2,1,1
e,1003,224
real,101
e,702,300
e,701,422
e,622,522
real,150
e,706,332
e,705,331
e,704,431
e,703,430
e,630,530
real,116
e,300,702
e,422,701
e,706,332
e,705,331
e,704,431
e,703,430
e,2003,233
e,134,234
rp2,1,1
real,136
e,136,236
real,137
e,137,237
real,138

```

```

e,138,238
real,139
e,139,239
real,140
e,140,240
real,141
e,141,241
real,142
e,142,242
real,143
e,143,243
real,144
e,144,244
real,145
e,145,245
real,146
e,146,246
real,147
e,147,247
real,148
e,148,248
real,149
e,149,249
real,150
e,150,250
real,101
e,501,601
rp13,1,1
real,116
e,513,613
rp10,1,1
e,530,630
rp9,1,1
real,639
e,539,639
real,640
e,540,640
real,641
e,541,641
real,642
e,542,642
real,643
e,543,643
real,644
e,544,644
real,645
e,545,645
real,646
e,546,646
real,647
e,547,647
real,648
e,548,648
real,649
e,549,649
real,150
e,550,650

! interface elements between the lower seal flange
! and the locking ring
type,4
mat,1
real,6
e,3038,1061
rp3,1,1

! interface elements between the upper seal flange
! and the locking ring
type,4
mat,1
real,7
e,2056,3146
rp3,1,1

! interface elements between the lower seal flange
! and the upper seal flange
type,5
mat,1
real,8
e,1164,2073
rp5,1,1

! couple the lower shell to the lower seal flange
type,6
mat,4
real,9
e,1001,1002
rp4,1,1

! couple the upper shell to the upper seal flange
type,6
mat,4
real,9
e,2001,2002
rp4,1,1

! springs between the lower seal flange
! and the locking ring
type,7
mat,1
real,10
e,3038,1061
rp3,1,1

! springs between the upper seal flange
! and the locking ring
type,7
mat,1
real,10
e,2056,3146
rp3,1,1

! springs between the lower seal flange
! and the upper seal flange
type,7
mat,1
real,10
e,1164,2073
rp5,1,1

! displacement constraints
d,101,UX,0,,601,500,rotz
d,201,UX,0,,501,100
d,150,UX,0,,650,500,rotz
d,250,UX,0,,550,100
d,3099,UY,0
d,all,uz,0

! pressure loads
alls
pload=+(14.7-14.7)
p,101,102,pload,,122,1
p,123,1003,pload
p,1001,1006,pload,,1021,5
p,1026,1035,pload
p,1035,1041,pload
p,1041,1046,pload,,1051,5
p,1056,1065,pload,,1155,9
p,1164,1165,pload,,1167,1
p,1168,1159,pload
p,2077,2082,pload
p,2073,2074,pload,,2076,1
p,2127,2124,pload
p,2124,2073,pload
p,2125,2126,pload,,2126,1
p,2122,2125,pload
p,2071,2122,pload
p,2001,2006,pload,,2046,5
p,2051,2060,pload
p,2060,2071,pload
p,2003,134,pload
p,134,135,pload,,149,1

! delete unused nodes at seal flange interfaces
ndelete,124
ndelete,133

! solve the problem
fini
/solu
neqit,1000
alls
solv
fini
save

! post-process the problem
/post1
set
rsys,solu
ernorm,0

```

```

! table stress definitions for shell elements
nall
alls
esel,s,type,2
etab,sit,nmisc,4
etab,sim,nmisc,9
etab,sib,nmisc,14

/com,
/com,
/com,
/com,+++++
/com,+ lower seal flange +
/com,+++++
/com,
/com,
nall
eall
nset,s,node,,1000,1999,1
prns,prin

/com,
/com,
/com,
/com,+++++
/com,+ upper seal flange +
/com,+++++
/com,
/com,
nall
eall
nset,s,node,,2000,2999,1
prns,prin

/com,
/com,
/com,
/com,+++++
/com,+ locking ring +
/com,+++++
/com,
/com,
nall
eall
nset,s,node,,3000,3999,1
prns,prin

/com,
/com,
/com,
/com,+++++
/com,+ OCV cylindrical and conical shells +
/com,+++++
/com,
/com,
nall
eall
esel,s,elem,,324,331,1
pret

/com,
/com,

```

```

/com,
/com,+++++
/com,+ OCV torispherical head crown shells +
/com,+++++
/com,
/com,
nall
eall
esel,s,elem,,339,348,1 ! upper head
esel,a,elem,,309,318,1 ! lower head
pret

/com,
/com,
/com,
/com,+++++
/com,+ OCV torispherical head knuckle shells +
/com,+++++
/com,
/com,
nall
eall
esel,s,elem,,334,338,1 ! upper head
esel,a,elem,,319,323,1 ! lower head
pret

/com,
/com,
/com,
/com,+++++
/com,+ OCA outer shells and z-flanges +
/com,+++++
/com,
/com,
nall
eall
esel,s,elem,,349,399,1
pret

/com,
/com,
/com,
/com,+++++
/com,+ polyurethane foam elements +
/com,+++++
/com,
/com,
nall
eall
esel,s,elem,,415,559,1
prns,prin

! finalize ANSYS
nall
eall
save
/out,term
/eof

```

Table 2.10.1-4 – ANSYS® Input Listing for OCA Load Case 4

```

! initialize ANSYS
fini
/cle
/filename,oqa_lc4,inp
/out,,txt

! start preprocessing the model
/prep7
/title, OCA Load Case 4: P=0.0/14.7 psia, T=70/70 F

! element types
et,1,42,,,1
et,2,51
et,3,42,,,1
et,4,12,,,,,,1
et,5,12,,,,,,1
et,6,3
et,7,14,,,2

! reference and uniform temperatures
tref,70
tunif,70

! material properties for non-slotted steel regions
ex,1,28.3e06
nuxy,1,.3
alpx,1,8.46e-06

! material properties for slotted steel regions
ex,2,14.15e06
ey,2,14.15e06
ez,2,1
nuxy,2,.3
nuxz,2,0
nuyz,2,0
alpx,2,8.46e-06
alpy,2,8.46e-06
alpz,2,8.46e-06

! material properties for the polyurethane foam
ex,3,4773
ey,3,6810
ez,3,4773
nuxy,3,.33
nuxz,3,.33
nuyz,3,.33
alpx,3,3.5e-5

! material properties for the rigid coupling elements
ex,4,28.3e06
nuxy,4,.3
alpx,4,8.46E-06

! element real constants
r,1,.25
r,2,.1875
r,3,.375
r,4,.075
r,5,1e9,.1
r,6,-15,1e9,-.036
r,7,15,1e9,-.036
r,8,0,1e9,.1
r,9,1,1,1
r,10,1e2
r,101,-180.000,1e5,,1
r,102,-177.444,1e5,,1
r,103,-174.888,1e5,,1
r,104,-172.333,1e5,,1
r,105,-169.777,1e5,,1
r,106,-167.221,1e5,,1
r,107,-164.665,1e5,,1
r,108,-162.109,1e5,,1
r,109,-159.553,1e5,,1
r,110,-156.998,1e5,,1
r,111,-154.442,1e5,,1
r,112,-141.553,1e5,,1
r,113,-128.665,1e5,,1
r,114,-115.777,1e5,,1
r,115,-102.888,1e5,,1
r,116,-90.0000,1e5,,1
r,130,-102.000,1e5,,1
r,136,-77.1520,1e5,,1

r,137,-64.3041,1e5,,1
r,138,-51.4561,1e5,,1
r,139,-38.6081,1e5,,1
r,140,-25.7602,1e5,,1
r,141,-23.1841,1e5,,1
r,142,-20.6081,1e5,,1
r,143,-18.0321,1e5,,1
r,144,-15.4561,1e5,,1
r,145,-12.8801,1e5,,1
r,146,-10.3041,1e5,,1
r,147,-7.72805,1e5,,1
r,148,-5.15203,1e5,,1
r,149,-2.57602,1e5,,1
r,150,,1e5,,1
r,639,-58.7238,1e5,,1
r,640,-27.4476,1e5,,1
r,641,-24.7029,1e5,,1
r,642,-21.9581,1e5,,1
r,643,-19.2133,1e5,,1
r,644,-16.4686,1e5,,1
r,645,-13.7238,1e5,,1
r,646,-10.9790,1e5,,1
r,647,-8.23429,1e5,,1
r,648,-5.48952,1e5,,1
r,649,-2.74476,1e5,,1

! nodes for the lower seal flange
local,11,,38.24941495,50.051977923,,-12
n,1001
n,1005,.25
fill
n,1016,,.58677836
n,1020,.25,.58677836
fill
fill,1001,1016,2,1006,5,5,1
n,1026,,.896632635
local,12,,38.505,50
move,1026,11,0,999,0,12,-.065,999,0
fill,1016,1026,1,1021
local,11,1,39.12699808,50.47
n,1025,.5,148.5
n,1030,.5,129
n,1031,.5,109.5
n,1032,.5,90
csys,12
fill,1021,1025,3,1022,1,2,5
n,1033,.775,.97
n,1034,1.145,.97
n,1076,-.065,2.98
fill,1026,1076,8,1035,5
fill,1035,1076,7,1041,5
n,1060,.775,2.15593612
ngen,2,6,1033,1034,1,,.16
fill,1039,1060,3,1045,5
fill,1035,1039
fill,1041,1045,3,1042,1,4,5
n,1064,1.245,2.03
fill,1060,1064
n,1092,-.065,2.98
n,1096,.77960172,2.76
fill
n,1100,1.245,2.76
fill,1096,1100
fill,1056,1092,3,1065,9,9,1
ngen,3,9,1098,1100,1,,.26
n,1146,.14020351,4.4
fill,1092,1146,5,1101,9
n,1164,.14020351,4.98
fill,1146,1164,1,1155
local,11,,39.13520351,54.98,,-86.15
n,1168
n,1159,.3
ngen,3,-1,1159,1159,,-.125
n,1148,.58,-.25
ngen,2,-18,1157,1159,1,.56
ngen,2,-9,1139,1141,1,.25
ngen,2,-27,1148,1148,,.81
ngen,2,-18,1130,1132,1,.56
fill,1096,1114,1,1105
csys,12
fill,1101,1105
fill,1110,1112,1,1111,,6,9

```

```

fill,1164,1168

! nodes for the upper seal flange
local,11,,38.405,52.81
n,2001,,5
n,2005,,25,5
fill
ngen,3,5,2001,2005,1,,-.25
n,2031,,3.45
n,2035,,.91,3.45
fill
fill,2011,2031,3,2016,5,5,1
n,2051,,2.543442101
n,2055,,.91,2.543442101
fill
fill,2031,2051,3,2036,5,4,1
n,2040,,.91,3.29
fill,2040,2055,2,2045,5
n,2059,1.345,2.66
fill,2055,2059
n,2071,,2.17
n,2073,,.21504507,2.17
fill
n,2077,,.74504507,2.17
fill,2073,2077
fill,2051,2071,1,2060
fill,2054,2076,1,2065
fill,2060,2065
n,2081,1.345,2.17
fill,2077,2081
fill,2055,2077,1,2066,,5,1
n,2107,,.85759646,,.54
n,2109,1.10488343,.54
fill
n,2111,1.345,.54
fill,2109,2111
fill,2077,2107,5,2082,5,5,1
n,2117,,.94488343
n,2119,1.10488343
fill
fill,2109,2119,1,2114
n,2112,,.870715847,.35
fill,2112,2114
n,2120,1.345,3.45
n,2121,1.345,3.29
ngen,2,51,2071,2073,1,,-.305
ngen,2,3,2122,2124,1,,-.305

! nodes for the locking ring
local,11,,39.35,51.29
n,3001
n,3005,,.435
fill
n,3009,,.935
fill,3005,3009
n,3037,,.81
n,3041,,.435,.693442101
fill
n,3045,,.935,.693442101
fill,3041,3045
fill,3001,3037,3,3010,9,9,1
n,3145,,.4.11
n,3149,,.435,4.226557899
fill
n,3153,,.935,4.226557899
fill,3149,3153
fill,3041,3149,11,3050,9,5,1
n,3181,,.4.67
n,3185,,.535,4.67
fill
n,3189,,.935,4.67
fill,3185,3189
fill,3145,3181,3,3154,9,9,1

! nodes for the OCA inner shell (OCV)
local,11,1,,84.5
n,101,74.25,-90
n,111,74.25,-64.44174492
fill
local,12,1,28.3125,24.29659664
n,116,8.625
fill,111,116
csys
!n,117,36.9375,25.79659664
n,122,36.9375,43.95292590
fill,116,122

ngen,2,-879,1003,1003
fill,122,124
ngen,2,-1870,2003,2003
n,135,38.53,63.78649751
fill,133,135
local,12,1,29.905,63.78649751
n,140,8.625,64.23984399
fill,135,140
local,14,1,,1.8125
n,150,77.4375,90
fill,140,150

! nodes for the OCA outer shell
csys
n,601
n,613,47.0625
fill
n,622,47.0625,46.7775
fill,613,622
n,630,47.0625,47.6325
n,638,47.0625,75.3440689
fill,630,638
local,15,1,40.5625,75.3440689
n,640,6.5,62.55238078
fill,638,640
local,16,1,,-2.75
n,650,94.5,90
fill,640,650

! nodes for the polyurethane foam inner surface
csys
ngen,2,100,101,150,1
n,125,38.58338729,50.9
n,232,38.53,56.26

! nodes for the polyurethane foam outer surface
ngen,2,-100,601,650,1

! intermediate polyurethane foam nodes
fill,201,501,2,301,100,22,1
n,300,43.9375,50.9
n,331,41.5375,51.8825
n,332,41.5375,56.26
n,422,43.9375,46.7775
n,430,44.2375,47.6375
n,431,44.2375,51.8825
fill,222,422,1,322
fill,223,300,1,323
fill,332,532,1,432
fill,233,533,2,333,100,18,1

! nodes for the z-flanges
ngen,2,279,422,422,0
ngen,2,402,300,300,0
ngen,2,273,430,430,0
rp2,,1,1
ngen,2,374,331,331,0
rp2,,1,1

! elements for the lower seal flange
type,1
mat,1
real,1
e,1001,1002,1007,1006
rp4,1,1,1,1
egen,5,5,1,4,1
e,1026,1027,1036,1035
e,1027,1028,1036
e,1028,1029,1037,1036
e,1029,1030,1031,1037
e,1031,1032,1038,1037
rp3,1,1,1,1
e,1035,1036,1042,1041
rp4,1,1,1,1
e,1041,1042,1047,1046
rp4,1,1,1,1
egen,3,5,32,35,1
e,1056,1057,1066,1065
rp4,1,1,1,1
egen,4,9,44,47,1
mat,2
e,1060,1061,1070,1069
rp4,1,1,1,1
egen,4,9,60,63,1
egen,3,9,74,75,1
egen,3,9,56,59,1

```

```

egen,7,9,84,85,1
egen,3,1,99,99
egen,3,1,93,93

! elements for the upper seal flange
type,1
mat,1
real,1
e,2006,2007,2002,2001
rp4,1,1,1,1
egen,10,5,104,107,1
e,2040,2121,2120,2035
e,2060,2061,2052,2051
e,2061,2062,2052
e,2062,2063,2053,2052
e,2063,2064,2053
e,2064,2065,2054,2053
rp6,1,1,1,1
e,2071,2072,2061,2060
rp10,1,1,1,1
e,2122,2123,2072,2071
rp2,1,1,1,1
e,2125,2126,2123,2122
rp2,1,1,1,1
e,2082,2083,2078,2077
rp4,1,1,1,1
egen,6,5,169,172,1
egen,3,5,189,190,1

! elements for the locking ring
type,1
mat,2
real,1
e,3001,3002,3011,3010
rp4,1,1,1,1
egen,4,9,197,200,1
mat,1
e,3005,3006,3015,3014
rp4,1,1,1,1
egen,20,9,213,216,1
e,3145,3146,3155,3154
rp4,1,1,1,1
egen,4,9,293,296,1

! elements for the OCA inner shell (OCV)
type,2
mat,1
real,1
e,101,102
rp16,1,1
real,2
e,117,118
rp5,1,1
real,1
e,122,123
e,123,1003
e,2003,134
e,134,135
rp16,1,1

! elements for the OCA outer shell
real,1
e,601,602
rp18,1,1
real,3
e,619,620
rp3,1,1
e,630,631
rp8,1,1
real,1
e,638,639
rp12,1,1

! elements for the Z-flanges
real,4
e,622,701
e,701,702
e,702,1034
e,1034,1033
e,630,703
e,703,704
rp3,1,1
e,706,2120
e,2120,2035

! polyurethane foam elements
type,3
mat,3
real,1
e,201,301,302,202
rp22,1,1,1,1
e,224,223,323
e,301,401,402,302
rp21,1,1,1,1
e,322,422,300,323
e,300,125,224,323
e,401,501,502,402
rp21,1,1,1,1
e,333,233,232,332
e,233,333,334,234
rp17,1,1,1,1
e,331,431,432,332
rp19,1,1,1,1
e,430,530,531,431
rp20,1,1,1,1

! interface elements between the steel shells
! and the polyurethane foam
type,5
mat,1
real,101
e,101,201
real,102
e,102,202
real,103
e,103,203
real,104
e,104,204
real,105
e,105,205
real,106
e,106,206
real,107
e,107,207
real,108
e,108,208
real,109
e,109,209
real,110
e,110,210
real,111
e,111,211
real,112
e,112,212
real,113
e,113,213
real,114
e,114,214
real,115
e,115,215
real,116
e,116,216
rp5,1,1
real,130
e,122,222
rp2,1,1
e,1003,224
real,101
e,702,300
e,701,422
e,622,522
real,150
e,706,332
e,705,331
e,704,431
e,703,430
e,630,530
real,116
e,300,702
e,422,701
e,706,332
e,705,331
e,704,431
e,703,430
e,2003,233
e,134,234
rp2,1,1
real,136
e,136,236
real,137
e,137,237
real,138

```

```

e,138,238
real,139
e,139,239
real,140
e,140,240
real,141
e,141,241
real,142
e,142,242
real,143
e,143,243
real,144
e,144,244
real,145
e,145,245
real,146
e,146,246
real,147
e,147,247
real,148
e,148,248
real,149
e,149,249
real,150
e,150,250
real,101
e,501,601
rp13,1,1
real,116
e,513,613
rp10,1,1
e,530,630
rp9,1,1
real,639
e,539,639
real,640
e,540,640
real,641
e,541,641
real,642
e,542,642
real,643
e,543,643
real,644
e,544,644
real,645
e,545,645
real,646
e,546,646
real,647
e,547,647
real,648
e,548,648
real,649
e,549,649
real,150
e,550,650

! interface elements between the lower seal flange
! and the locking ring
type,4
mat,1
real,6
e,3038,1061
rp3,1,1

! interface elements between the upper seal flange
! and the locking ring
type,4
mat,1
real,7
e,2056,3146
rp3,1,1

! interface elements between the lower seal flange
! and the upper seal flange
type,5
mat,1
real,8
e,1164,2073
rp5,1,1

! couple the lower shell to the lower seal flange
type,6
mat,4
real,9
e,1001,1002
rp4,1,1

! couple the upper shell to the upper seal flange
type,6
mat,4
real,9
e,2001,2002
rp4,1,1

! springs between the lower seal flange
! and the locking ring
type,7
mat,1
real,10
e,3038,1061
rp3,1,1

! springs between the upper seal flange
! and the locking ring
type,7
mat,1
real,10
e,2056,3146
rp3,1,1

! springs between the lower seal flange
! and the upper seal flange
type,7
mat,1
real,10
e,1164,2073
rp5,1,1

! displacement constraints
d,101,UX,0,,601,500,rotz
d,201,UX,0,,501,100
d,150,UX,0,,650,500,rotz
d,250,UX,0,,550,100
d,3099,UY,0
d,all,uz,0

! pressure loads
alls
pload=+(0.0-14.7)
p,101,102,pload,,122,1
p,123,1003,pload
p,1001,1006,pload,,1021,5
p,1026,1035,pload
p,1035,1041,pload
p,1041,1046,pload,,1051,5
p,1056,1065,pload,,1155,9
p,1164,1165,pload,,1167,1
p,1168,1159,pload
p,2077,2082,pload
p,2073,2074,pload,,2076,1
p,2127,2124,pload
p,2124,2073,pload
p,2125,2126,pload,,2126,1
p,2122,2125,pload
p,2071,2122,pload
p,2001,2006,pload,,2046,5
p,2051,2060,pload
p,2060,2071,pload
p,2003,134,pload
p,134,135,pload,,149,1

! delete unused nodes at seal flange interfaces
ndelete,124
ndelete,133

! solve the problem
fini
/solu
nequit,1000
alls
solv
fini
save

! post-process the problem
/post1
set
rsys,solu
ernorm,0

```

```

! table stress definitions for shell elements
nall
alls
esel,s,type,,2
etab,sit,nmisc,4
etab,sim,nmisc,9
etab,sib,nmisc,14

/com,
/com,
/com,
/com,+++++
/com,+ lower seal flange +
/com,+++++
/com,
/com,
nall
eall
nset,s,node,,1000,1999,1
prns,prin

/com,
/com,
/com,
/com,+++++
/com,+ upper seal flange +
/com,+++++
/com,
/com,
nall
eall
nset,s,node,,2000,2999,1
prns,prin

/com,
/com,
/com,
/com,+++++
/com,+ locking ring +
/com,+++++
/com,
/com,
nall
eall
nset,s,node,,3000,3999,1
prns,prin

/com,
/com,
/com,
/com,+++++
/com,+ OCV cylindrical and conical shells +
/com,+++++
/com,
/com,
nall
eall
esel,s,elem,,324,331,1
pret

/com,

```

```

/com,
/com,
/com,+++++
/com,+ OCV torispherical head crown shells +
/com,+++++
/com,
/com,
nall
eall
esel,s,elem,,339,348,1 ! upper head
esel,a,elem,,309,318,1 ! lower head
pret

/com,
/com,
/com,
/com,+++++
/com,+ OCV torispherical head knuckle shells +
/com,+++++
/com,
/com,
nall
eall
esel,s,elem,,334,338,1 ! upper head
esel,a,elem,,319,323,1 ! lower head
pret

/com,
/com,
/com,
/com,+++++
/com,+ OCA outer shells and z-flanges +
/com,+++++
/com,
/com,
nall
eall
esel,s,elem,,349,399,1
pret

/com,
/com,
/com,
/com,+++++
/com,+ polyurethane foam elements +
/com,+++++
/com,
/com,
nall
eall
esel,s,elem,,415,559,1
prns,prin

! finalize ANSYS
nall
eall
save
/out,term
/eof

```


Table 2.10.1-5 – ANSYS® Input Listing for ICV Load Case 1

```

! initialize ANSYS
fini
/cle
/filename,icv_lcl,inp
/out,,txt

! start preprocessing the model
/prep7
/title, ICV Load Case 1: P=64.7/3.5 psia, T=160/160 F

! element types
et,1,42,,,1
et,2,51
et,3,12,,,,,,1
et,4,12,,,,,,1
et,5,3
et,6,14,,,2

! reference and uniform temperatures
tref,160
tunif,160

! material properties for non-slotted steel regions
ex,1,27.8e6
nuxy,1,.3
alpx,1,8.694e-6

! material properties for slotted steel regions
ex,2,13.9e6
ey,2,13.9e6
ez,2,1
nuxy,2,.3
nuyz,2,0
nuxz,2,0
alpx,2,8.694e-6
alpy,2,8.694e-6
alpz,2,8.694e-6

! material properties for the rigid coupling elements
ex,3,27.8e6
nuxy,3,.3
alpx,3,8.694e-6

! element real constants
r,1,.25
r,2,-15,1e9,-.036
r,3,15,1e9,-.036
r,4,0,1e9,-.01
r,5,1,1,1
r,10,1e2

! nodes for the lower seal ring
local,11,0,36.315,45.08954245
n,1001
n,1005,.25
fill
n,1016,.575
n,1020,.25,.575
fill
fill,1001,1016,2,1006,5,5,1
n,1031,1.48
n,1035,.84,1.48
fill
fill,1016,1031,2,1021,5,5,1
n,1046,2.6759361
n,1050,.84,2.67593612
fill
fill,1031,1046,2,1036,5,5,1
n,1054,1.31,2.55
fill,1050,1054
n,1073,.3.5
n,1077,.844601720,3.28
fill
n,1079,1.095,3.28
fill,1077,1079
n,1081,1.31,3.28
fill,1079,1081
fill,1046,1073,2,1055,9,9,1
n,1127,.205,4.92
fill,1073,1127,5,1082,9
local,12,,37.01020351,50.58954246,, -86.15
n,1140,.3
n,1138,.3,-.25
fill
n,1122,.86
n,1120,.86,-.25
fill
n,1113,1.11
n,1111,1.11,-.25
fill
n,1095,1.67
n,1093,1.67,-.25
fill
csys,11
n,1145,.205,5.5
fill,1127,1145,1,1136
n,1149,.695,5.5
fill,1145,1149
fill,1120,1138,1,1129
fill,1093,1111,1,1102
fill,1077,1095,1,1086
fill,1091,1093,,,6,9
fill,1073,1091,1,1082,,5,1
ngen,3,9,1079,1081,1,,.26

! nodes for the upper seal ring
n,2001,-.035,4.89
n,2003,.180045070,4.89
fill
n,2007,-0.035,5.5
n,2009,.180045070,5.5
fill
fill,2001,2007,1,2004,,3,1
n,2013,.710045070,5.5
fill,2009,2013
n,2017,1.31,5.5
fill,2013,2017
n,2040,-0.035,5.98
fill,2007,2040,2,2018,11
n,2035,0.875,5.873442101
fill,2029,2035
n,2039,1.31,5.99
fill,2035,2039
fill,2008,2030,1,2019,,10,1
n,2042,.245,5.98
fill,2040,2042
n,2043,.390419704,6.008925778
n,2044,.513700577,6.091299423
n,2049,.596074222,6.214580296
n,2054,.625,6.36
n,2058,.875,6.36
fill
fill,2035,2058,2,2048,5
fill,2044,2048
fill,2049,2053
ngen,5,5,2054,2058,1,,.1875
n,2104,.822596460,3.87
n,2106,1.07,3.87
fill
n,2116,1.07,3.33
fill,2106,2116,1,2111
n,2108,1.31,3.87
fill,2106,2108
fill,2013,2104,5,2079,5,5,1
n,2109,.835715950,3.68
fill,2109,2111
n,2114,.909883430,3.33
fill,2114,2116

! nodes for the locking ring
local,13,0,37.225,46.89954245
n,3001
n,3005,.435
fill
n,3008,.789412
fill,3005,3008
n,3037,.81
n,3041,.435,.693442101
fill
n,3045,.935,.693442101
fill,3041,3045
fill,3001,3037,3,3010,9,8,1
n,3027,.935,.4
fill,3008,3027,1,3018

```

```

fill,3027,3045,1,3036
n,3101,,4.11
n,3105,.435,4.226557898
fill
n,3109,.935,4.226557899
fill,3105,3109
fill,3041,3105,11,3046,5,5,1
n,3137,,4.67
n,3141,.435,4.67
fill
n,3144,.789412,4.67
fill,3141,3144
fill,3101,3137,3,3110,9,8,1
fill,3109,3144,3,3118,9

! nodes for the lower shell
local,14,1,,73.25
n,4001,73.25,-90
n,4016,73.25,-64.50665929
fill
local,15,1,27.815,14.9171927
n,4025,8.625
fill,4016,4025
csys,0
n,4081,36.44,45.08954245
fill,4025,4081
n,4001,0,0

! nodes for the upper shell
local,16,1,,-5.75
n,5001,74.5,90
n,5016,74.5,64.42280563
fill
local,17,1,28.44,53.66954245
n,5025,8.625
fill,5016,5025
csys,0
n,5027,37.065,52.16954245
fill,5025,5027
n,5001,0,68.75

! elements for the lower seal ring
type,1
mat,1
real,1
e,1001,1002,1007,1006
rp4,1,1,1,1
egen,9,5,1,4,1
e,1046,1047,1056,1055
rp4,1,1,1,1
egen,5,9,37,40,1
egen,7,9,53,54,1
egen,3,27,55,56,1
mat,2
e,1050,1051,1060,1059
rp4,1,1,1,1
egen,3,9,73,76,1
egen,3,9,83,84,1

! elements for the upper seal ring
type,1
mat,1
real,1
e,2001,2002,2005,2004
rp2,1,1,1,1
egen,2,3,89,90,1
e,2007,2008,2019,2018
rp10,1,1,1,1
egen,2,11,93,102,1
egen,2,11,103,107,1
e,2046,2045,2034
rp2,1,1,0
e,2034,2035,2048,2047
e,2044,2045,2050,2049
rp4,1,1,1,1
egen,6,5,121,124,1
e,2079,2080,2014,2013
rp4,1,1,1,1
e,2084,2085,2080,2079
rp4,1,1,1,1
egen,5,5,149,152,1
egen,3,5,165,166,1

! elements for the locking ring
type,1
mat,2
real,1
e,3001,3002,3011,3010
rp4,1,1,1,1
egen,4,9,173,176,1
mat,1
e,3005,3006,3015,3014
rp3,1,1,1,1
e,3018,3017,3008
e,3014,3015,3024,3023
rp4,1,1,1,1
egen,3,9,193,196,1
e,3041,3042,3047,3046
rp4,1,1,1,1
egen,11,5,205,208,1
e,3096,3097,3106,3105
rp4,1,1,1,1
e,3101,3102,3111,3110
rp8,1,1,1,1
egen,4,9,253,259,1
e,3117,3118,3127,3126
e,3126,3127,3136,3135
e,3135,3136,3144,3144

! elements for the lower shell
type,2
mat,1
real,1
e,4001,4002
rp79,1,1
e,4080,1003

! elements for the upper shell
type,2
mat,1
real,1
e,2076,5026
e,5026,5025
rp25,-1,-1

! interface elements between the lower seal flange
! and the locking ring
type,3
mat,1
real,2
e,3038,1051
rp3,1,1

! interface elements between the upper seal flange
! and the locking ring
type,3
mat,1
real,3
e,2036,3102
rp3,1,1

! interface elements between the lower seal flange
! and the upper seal flange
type,4
mat,1
real,4
e,1145,2009
rp5,1,1

! couple the lower shell to the lower seal flange
type,5
mat,3
real,5
e,1001,1002
rp4,1,1

! couple the upper shell to the upper seal flange
type,5
mat,3
real,5
e,2074,2075
rp4,1,1

! springs between the lower seal flange
! and the locking ring
type,6
mat,1
real,10
e,3038,1051
rp3,1,1

! springs between the upper seal flange

```

```

! and the locking ring
type,6
mat,1
real,10
e,2036,3102
rp3,1,1

! springs between the lower seal flange
! and the upper seal flange
type,6
mat,1
real,10
e,1145,2009
rp5,1,1

! displacement constraints
d,4001,ux,0,,5001,1000,rotz
d,3075,uy,0

! pressure loads
pload=(64.7-3.5)
alls
p,4001,4002,pload,,4079,1
p,4080,1003,pload
p,1001,1006,pload,,1041,5
p,1046,1055,pload,,1136,9
p,1145,1146,pload,,1148,9
p,1140,1149,pload
p,2001,2002,pload,,2002,1
p,2003,2006,pload,,2006,3
p,2009,2010,pload,,2012,1
p,2013,2079,pload
p,2001,2004,pload,,2004,3
p,2007,2018,pload,,2029,11
p,2040,2041,pload,,2043,1
p,2044,2049,pload,,2069,5
p,5001,5002,pload,,5025,1
p,5026,2076,pload

! solve the problem
fini
/solu
neqit,1000
alls
solv
fini
save

! post-process the problem
/post1
set
rsys,solu
ernorm,0

! table stress definitions for shell elements
nall
alls
esel,s,type,2
etab,sit,nmisc,4
etab,sim,nmisc,9
etab,sib,nmisc,14

/com,
/com,
/com,
/com,+++++++
/com,+ lower seal flange +
/com,+++++++
/com,
/com,
nall
eall
nset,s,node,,1000,1999,1
esln
prns,prin

/com,
/com,
/com,
/com,+++++++
/com,+ upper seal flange +
/com,+++++++
/com,
/com,
nall
eall
nset,s,node,,2000,2999,1
esln
prns,prin

/com,
/com,
/com,
/com,+++++++
/com,+ locking ring +
/com,+++++++
/com,
/com,
nall
eall
nset,s,node,,3000,3999,1
esln
prns,prin

/com,
/com,
/com,
/com,+++++++
/com,+ cylindrical shells +
/com,+++++++
/com,
/com,
esel,s,elem,,309,366,1
pret

/com,
/com,
/com,
/com,+++++++
/com,+ torispherical head crown shells +
/com,+++++++
/com,
/com,
esel,s,elem,,376,390,1 ! upper head
esel,a,elem,,285,299,1 ! lower head
pret

/com,
/com,
/com,
/com,+++++++
/com,+ torispherical head knuckle shells +
/com,+++++++
/com,
/com,
esel,s,elem,,367,375,1 ! upper head
esel,a,elem,,300,308,1 ! lower head
pret

! finalize ANSYS
nall
eall
save
/out,term
/eof

```

Table 2.10.1-6 – ANSYS® Input Listing for ICV Load Case 2

```

! initialize ANSYS
fini
/cle
/filename,icv_lc2,inp
/out,,txt

! start preprocessing the model
/prep7
/title, ICV Load Case 2: P=0.0/14.7 psia, T=70/70 F

! element types
et,1,42,,,1
et,2,51
et,3,12,,,,,,1
et,4,12,,,,,,1
et,5,3
et,6,14,,,2

! reference and uniform temperatures
tref,70
tuniF,70

! material properties for non-slotted steel regions
ex,1,28.3e6
nuxy,1,.3
alpx,1,8.46e-6

! material properties for slotted steel regions
ex,2,14.15e6
ey,2,14.15e6
ez,2,1
nuxy,2,.3
nuyz,2,0
nuxz,2,0
alpx,2,8.46e-6
alpy,2,8.46e-6
alpz,2,8.46e-6

! material properties for the rigid coupling elements
ex,3,28.3e6
nuxy,3,.3
alpx,3,8.46e-6

! element real constants
r,1,.25
r,2,-15,1e9,-.036
r,3,15,1e9,-.036
r,4,0,1e9,-.01
r,5,1,1,1
r,10,1e2

! nodes for the lower seal ring
local,11,0,36.315,45.08954245
n,1001
n,1005,.25
fill
n,1016,.575
n,1020,.25,.575
fill
fill,1001,1016,2,1006,5,5,1
n,1031,1.48
n,1035,.84,1.48
fill
fill,1016,1031,2,1021,5,5,1
n,1046,2.6759361
n,1050,.84,2.67593612
fill
fill,1031,1046,2,1036,5,5,1
n,1054,1.31,2.55
fill,1050,1054
n,1073,.3.5
n,1077,.844601720,3.28
fill
n,1079,1.095,3.28
fill,1077,1079
n,1081,1.31,3.28
fill,1079,1081
fill,1046,1073,2,1055,9,9,1
n,1127,.205,4.92
fill,1073,1127,5,1082,9
local,12,,37.01020351,50.58954246,, -86.15
n,1140,.3
n,1138,.3,-.25
fill
n,1122,.86
n,1120,.86,-.25
fill
n,1113,1.11
n,1111,1.11,-.25
fill
n,1095,1.67
n,1093,1.67,-.25
fill
csys,11
n,1145,.205,5.5
fill,1127,1145,1,1136
n,1149,.695,5.5
fill,1145,1149
fill,1120,1138,1,1129
fill,1093,1111,1,1102
fill,1077,1095,1,1086
fill,1091,1093,,,6,9
fill,1073,1091,1,1082,,5,1
ngen,3,9,1079,1081,1,,.26

! nodes for the upper seal ring
n,2001,-.035,4.89
n,2003,.180045070,4.89
fill
n,2007,-0.035,5.5
n,2009,.180045070,5.5
fill
fill,2001,2007,1,2004,,3,1
n,2013,.710045070,5.5
fill,2009,2013
n,2017,1.31,5.5
fill,2013,2017
n,2040,-0.035,5.98
fill,2007,2040,2,2018,11
n,2035,0.875,5.873442101
fill,2029,2035
n,2039,1.31,5.99
fill,2035,2039
fill,2008,2030,1,2019,,10,1
n,2042,.245,5.98
fill,2040,2042
n,2043,.390419704,6.008925778
n,2044,.513700577,6.091299423
n,2049,.596074222,6.214580296
n,2054,.625,6.36
n,2058,.875,6.36
fill
fill,2035,2058,2,2048,5
fill,2044,2048
fill,2049,2053
ngen,5,5,2054,2058,1,,.1875
n,2104,.822596460,3.87
n,2106,1.07,3.87
fill
n,2116,1.07,3.33
fill,2106,2116,1,2111
n,2108,1.31,3.87
fill,2106,2108
fill,2013,2104,5,2079,5,5,1
n,2109,.835715950,3.68
fill,2109,2111
n,2114,.909883430,3.33
fill,2114,2116

! nodes for the locking ring
local,13,0,37.225,46.89954245
n,3001
n,3005,.435
fill
n,3008,.789412
fill,3005,3008
n,3037,.81
n,3041,.435,.693442101
fill
n,3045,.935,.693442101
fill,3041,3045
fill,3001,3037,3,3010,9,8,1
n,3027,.935,.4
fill,3008,3027,1,3018

```

```

fill,3027,3045,1,3036
n,3101,,4.11
n,3105,,.435,4.226557898
fill
n,3109,,.935,4.226557899
fill,3105,3109
fill,3041,3105,11,3046,5,5,1
n,3137,,4.67
n,3141,,.435,4.67
fill
n,3144,,.789412,4.67
fill,3141,3144
fill,3101,3137,3,3110,9,8,1
fill,3109,3144,3,3118,9

! nodes for the lower shell
local,14,1,,73.25
n,4001,73.25,-90
n,4016,73.25,-64.50665929
fill
local,15,1,27.815,14.9171927
n,4025,8.625
fill,4016,4025
csys,0
n,4081,36.44,45.08954245
fill,4025,4081
n,4001,0,0

! nodes for the upper shell
local,16,1,,-5.75
n,5001,74.5,90
n,5016,74.5,64.42280563
fill
local,17,1,28.44,53.66954245
n,5025,8.625
fill,5016,5025
csys,0
n,5027,37.065,52.16954245
fill,5025,5027
n,5001,0,68.75

! elements for the lower seal ring
type,1
mat,1
real,1
e,1001,1002,1007,1006
rp4,1,1,1,1
egen,9,5,1,4,1
e,1046,1047,1056,1055
rp4,1,1,1,1
egen,5,9,37,40,1
egen,7,9,53,54,1
egen,3,27,55,56,1
mat,2
e,1050,1051,1060,1059
rp4,1,1,1,1
egen,3,9,73,76,1
egen,3,9,83,84,1

! elements for the upper seal ring
type,1
mat,1
real,1
e,2001,2002,2005,2004
rp2,1,1,1,1
egen,2,3,89,90,1
e,2007,2008,2019,2018
rp10,1,1,1,1
egen,2,11,93,102,1
egen,2,11,103,107,1
e,2046,2045,2034
rp2,1,1,0
e,2034,2035,2048,2047
e,2044,2045,2050,2049
rp4,1,1,1,1
egen,6,5,121,124,1
e,2079,2080,2014,2013
rp4,1,1,1,1
e,2084,2085,2080,2079
rp4,1,1,1,1
egen,5,5,149,152,1
egen,3,5,165,166,1

! elements for the locking ring
type,1
mat,2
real,1
e,3001,3002,3011,3010
rp4,1,1,1,1
egen,4,9,173,176,1
mat,1
e,3005,3006,3015,3014
rp3,1,1,1,1
e,3018,3017,3008
e,3014,3015,3024,3023
rp4,1,1,1,1
egen,3,9,193,196,1
e,3041,3042,3047,3046
rp4,1,1,1,1
egen,11,5,205,208,1
e,3096,3097,3106,3105
rp4,1,1,1,1
e,3101,3102,3111,3110
rp8,1,1,1,1
egen,4,9,253,259,1
e,3117,3118,3127,3126
e,3126,3127,3136,3135
e,3135,3136,3144,3144

! elements for the lower shell
type,2
mat,1
real,1
e,4001,4002
rp79,1,1
e,4080,1003

! elements for the upper shell
type,2
mat,1
real,1
e,2076,5026
e,5026,5025
rp25,-1,-1

! interface elements between the lower seal flange
! and the locking ring
type,3
mat,1
real,2
e,3038,1051
rp3,1,1

! interface elements between the upper seal flange
! and the locking ring
type,3
mat,1
real,3
e,2036,3102
rp3,1,1

! interface elements between the lower seal flange
! and the upper seal flange
type,4
mat,1
real,4
e,1145,2009
rp5,1,1

! couple the lower shell to the lower seal flange
type,5
mat,3
real,5
e,1001,1002
rp4,1,1

! couple the upper shell to the upper seal flange
type,5
mat,3
real,5
e,2074,2075
rp4,1,1

! springs between the lower seal flange
! and the locking ring
type,6
mat,1
real,10
e,3038,1051
rp3,1,1

! springs between the upper seal flange

```

```

! and the locking ring
type,6
mat,1
real,10
e,2036,3102
rp3,1,1

! springs between the lower seal flange
! and the upper seal flange
type,6
mat,1
real,10
e,1145,2009
rp5,1,1

! displacement constraints
d,4001,ux,0,,5001,1000,rotz
d,3075,uy,0

! pressure loads
pload=+(0.0-14.7)
alls
p,4001,4002,pload,,4079,1
p,4080,1003,pload
p,1001,1006,pload,,1041,5
p,1046,1055,pload,,1136,9
p,1145,1146,pload,,1148,9
p,1140,1149,pload
p,2001,2002,pload,,2002,1
p,2003,2006,pload,,2006,3
p,2009,2010,pload,,2012,1
p,2013,2079,pload
p,2001,2004,pload,,2004,3
p,2007,2018,pload,,2029,11
p,2040,2041,pload,,2043,1
p,2044,2049,pload,,2069,5
p,5001,5002,pload,,5025,1
p,5026,2076,pload

! solve the problem
fini
/solu
neqit,1000
alls
solv
fini
save

! post-process the problem
/post1
set
rsys,solu
ernorm,0

! table stress definitions for shell elements
nall
alls
esel,s,type,,2
etab,sit,nmisc,4
etab,sim,nmisc,9
etab,sib,nmisc,14

/com,
/com,
/com,
/com,+++++
/com,+ lower seal flange +
/com,+++++
/com,
/com,
nall
eall
nset,s,node,,1000,1999,1
esln
prns,prin

/com,
/com,
/com,
/com,+++++
/com,+ upper seal flange +
/com,+++++
/com,
/com,
nall
eall
    
```

```

nset,s,node,,2000,2999,1
esln
prns,prin

/com,
/com,
/com,
/com,+++++
/com,+ locking ring +
/com,+++++
/com,
/com,
nall
eall
nset,s,node,,3000,3999,1
esln
prns,prin

/com,
/com,
/com,
/com,+++++
/com,+ cylindrical shells +
/com,+++++
/com,
/com,
esel,s,elem,,309,366,1
pret

/com,
/com,
/com,
/com,+++++
/com,+ torispherical head crown shells +
/com,+++++
/com,
/com,
esel,s,elem,,376,390,1 ! upper head
esel,a,elem,,285,299,1 ! lower head
pret

/com,
/com,
/com,
/com,+++++
/com,+ torispherical head knuckle shells +
/com,+++++
/com,
/com,
esel,s,elem,,367,375,1 ! upper head
esel,a,elem,,300,308,1 ! lower head
pret

! finalize ANSYS
nall
eall
save
/out,term
/eof
    
```

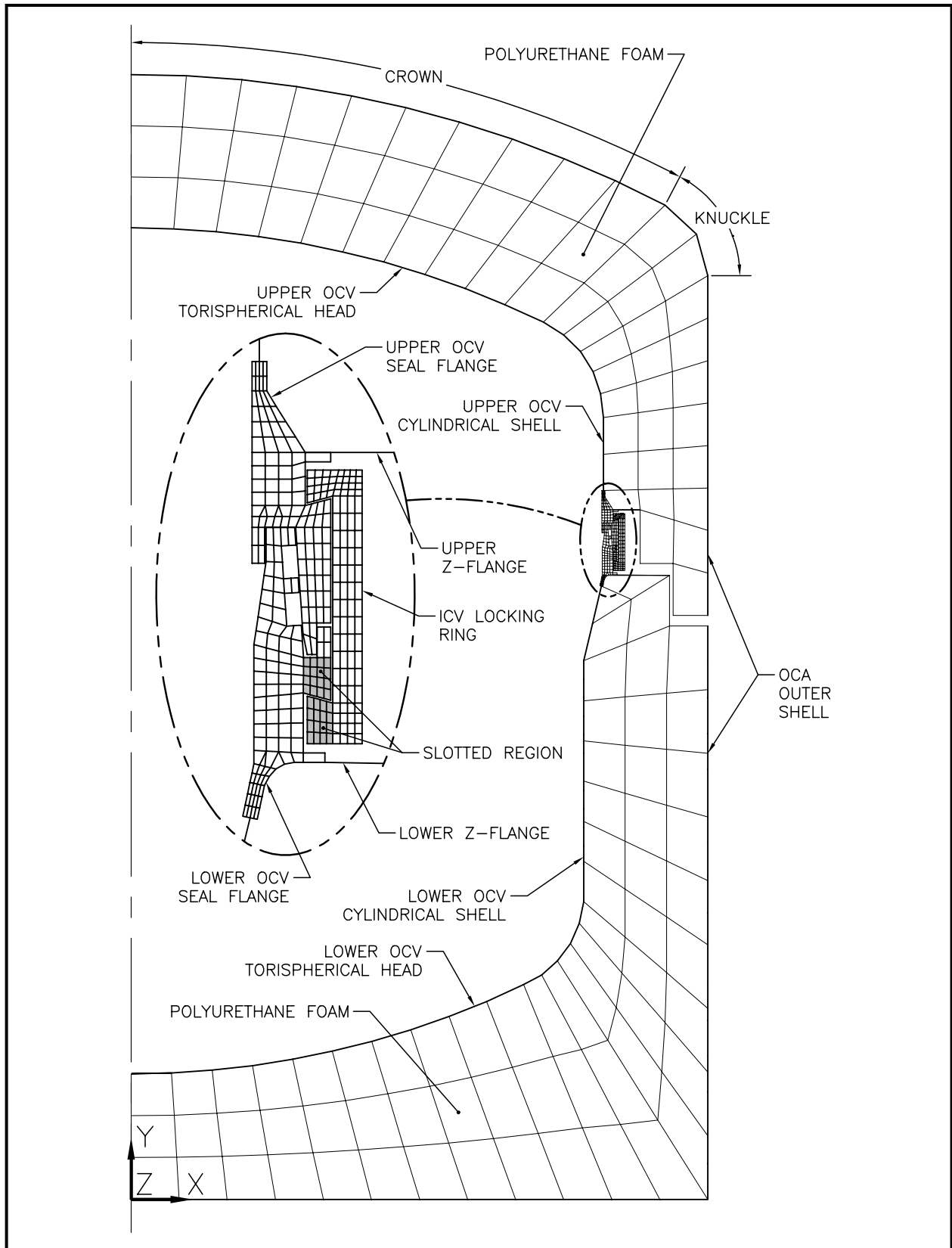


Figure 2.10.1-1 – OCA FEA Model Element Plot

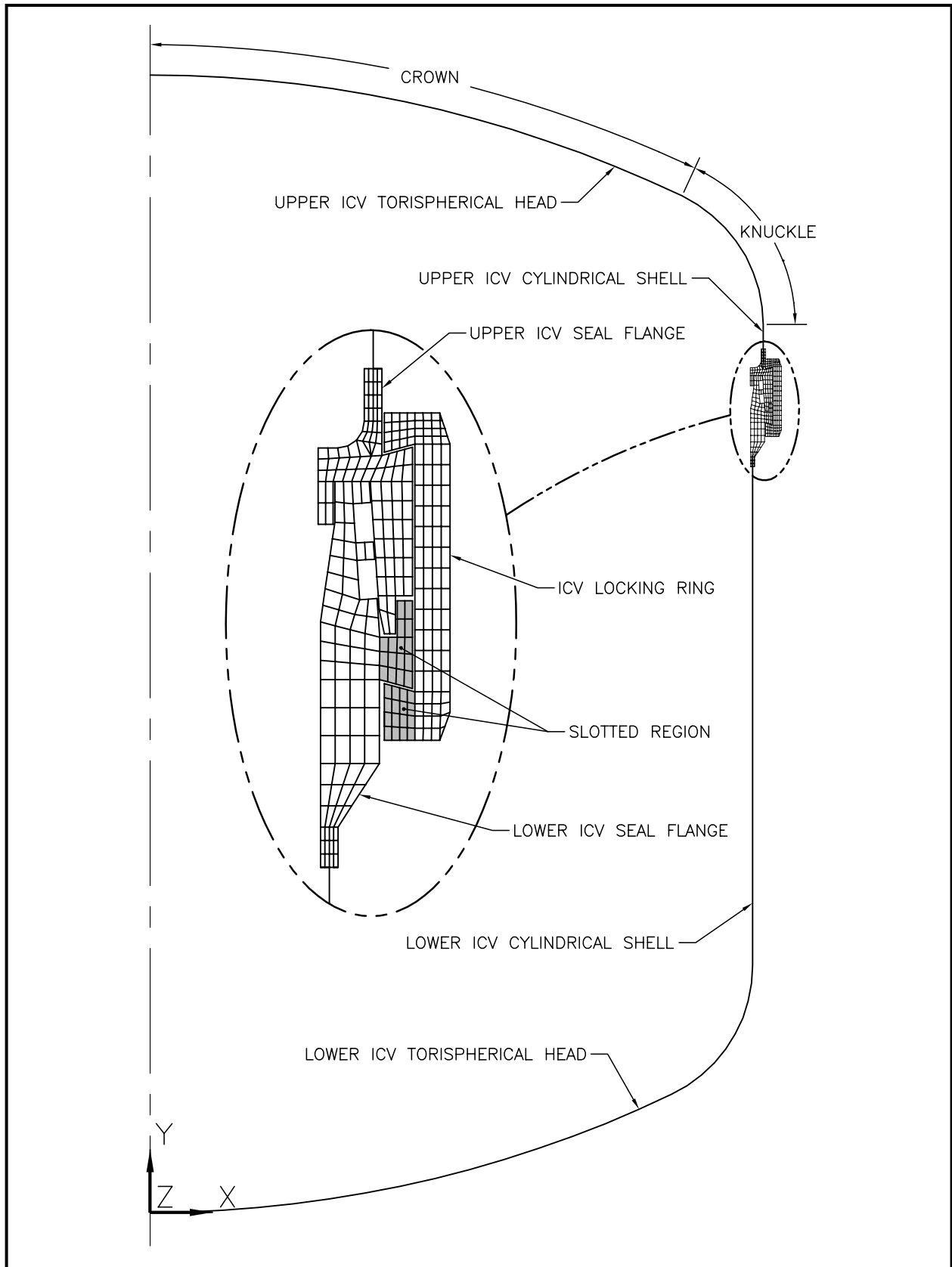


Figure 2.10.1-2 – ICV FEA Model Element Plot

2.10.2 Elastomer O-ring Seal Performance Tests

2.10.2.1 Introduction

Elastomer O-ring seal testing was performed in support of the certification of the TRUPACT-II package. Since the HalfPACT packaging is identical to the TRUPACT-II packaging with respect to closure region design, the result of these performance tests is directly applicable.

The elastomer O-ring seal tests demonstrated the ability of Rainier Rubber's butyl compound RR0405-70¹, used for the main O-ring (containment) seal, to maintain a leaktight² containment boundary under the worst-case conditions of temperature, duration, and minimum compression. An identical closure region design for the TRUPACT-II and HalfPACT packages assures that minimum compression possible for the HalfPACT main O-ring seal is also identical. In addition, the normal conditions of transport (NCT) and hypothetical accident condition (HAC) O-ring seal temperatures are nearly the same as those determined for the TRUPACT-II package, as shown in [Chapter 3.0, Thermal Evaluation](#). Thus, O-ring seal testing that was performed for TRUPACT-II package certification is directly applicable to HalfPACT package conditions. This section is a summary of the test conditions, procedures, and results, first documented in the [TRUPACT-II Safety Analysis Report \(SAR\)](#)³. Therefore, no additional O-ring seal performance testing is necessary.

2.10.2.2 Test Specimens and Equipment

A bore-type test fixture was used to test the O-ring seals. The fixture included an inner disk containing two, side-by-side O-ring seal grooves. An O-ring seal of prototypic cross-section and butyl material, as delineated on the drawings in [Appendix 1.3.1, Packaging General Arrangement Drawings](#), was placed into each seal groove, and the assembly was placed within a mating bore component. In this test fixture, the compression direction is radial and special jacking screws were utilized to displace the disk radially relative to the bore, resulting in decreased O-ring compression on one side of the test fixture. This decreased compression bounds the minimum compression that is possible in the HalfPACT package main O-ring seal under NCT or HAC. Therefore, the test fixture was capable of duplicating the worst-case conditions of minimum compression that could occur in a prototypic HalfPACT package. [Figure 2.10.2-1](#) illustrates the O-ring seal test fixture.

The size and surface finish of the test fixture's O-ring seal grooves is prototypic of the main O-ring seal design used for the TRUPACT-II and HalfPACT packages. However, to ensure a worst case O-ring seal compression for testing, the O-ring seal grooves and bore component were sized to ensure less compression than provided in a prototypic HalfPACT package. Worst case compression of the O-ring seal in the test fixture occurs when the inner disk is radially displaced to achieve metal-to-metal contact on one side thereby resulting in minimum O-ring

¹ Rainier Rubber Company, Seattle, WA.

² Leaktight is defined as leakage of 1×10^{-7} standard cubic centimeters per second (scc/sec), air, or less, per Section 5.4(3), *Reference Air Leakage Rate*, of ANSI N14.5-1997, *American National Standard for Radioactive Materials – Leakage Tests on Packages for Shipment*, American National Standards Institute, Inc. (ANSI).

³ U.S. Department of Energy (DOE), *Safety Analysis Report for the TRUPACT-II Shipping Package*, USNRC Docket No. 71-9218, U.S. Department of Energy, Carlsbad Field Office, Carlsbad, New Mexico.

seal compression at the diametrically opposite location (180° away). As expected, the minimum O-ring seal compression in a prototypic HalfPACT package occurs when the upper and lower seal flanges are at their extreme dimensional tolerances.

The test fixture was designed with O-ring seal grooves to accommodate prototypically full-sized O-ring seals of 0.400 ± 0.010 inch diameter, as delineated on the drawings in [Appendix 1.3.1, *Packaging General Arrangement Drawings*](#). However, the test fixture's overall diameter was reduced relative to a full-scale TRUPACT-II/HalfPACT package to achieve a practical size for testing, with the gland having a bore diameter of 12.74 inches. A reduction in relative diameter is acceptable since the cross-sectional configuration and corresponding O-ring seal compression are the parameters of primary importance relative to maintaining a leaktight seal. Additionally, the cross-sectional diameter of the actual test O-ring seals were on the low side of the tolerance range specified for HalfPACT O-ring seals of $\text{Ø}0.400 \pm 0.010$ inches. The test specimens were all in the range of $\text{Ø}0.387$ to $\text{Ø}0.400$ inches, thus minimizing the test compression. Actual minimum compressions are recorded in [Appendix 2.10.2.6, *Test Results*](#). All test specimens were coated lightly with vacuum grease prior to installation into the test fixture. The fully assembled test fixture was placed within an environmental test chamber for both heating and cooling. Thermocouples attached to the fixture were used to confirm the O-ring seal temperature.

The region between the two O-ring seals, corresponding to the annulus between the upper main (containment) O-ring seal and lower main (test) O-ring seal on a HalfPACT packaging, constitutes a test volume. To perform a leak test, the test volume was connected to a helium mass spectrometer leak detector and the outside tented and flooded with helium gas, consistent with the guidelines of Section A3.10.2, *Helium Mass Spectrometer Envelope, Pressurized Envelope*, of ANSI N14.5⁴. An O-ring seal test was successful if the leakage between the seals was 1×10^{-7} standard cubic centimeters per second (scc/sec), air, or less (i.e., "leaktight").

2.10.2.3 Test Conditions

Test conditions were selected to simulate conditions of worst case temperature and worst case minimum compression for the prototypic O-ring seals. Tests were performed at -40 °F, with the inner disk centered, to simulate NCT cold conditions. Tests were also performed at -20 °F, with the inner disk fully offset, to simulate a cold temperature, HAC free drop or puncture event. Tests were further performed at elevated temperatures for 8 hour durations, with the inner disk fully offset, to simulate a HAC fire following the free drop and puncture events. A range of elevated temperatures was investigated to demonstrate the large margin of safety that exists for a leaktight seal in a prototypic HalfPACT package, based on temperatures measured from HAC fire testing as reported in [Appendix 2.10.3, *Certification Tests*](#).

All helium leak tests were performed at cold temperatures, either at -40 °F for the NCT cold condition case, or at -20 °F for all other cases. No attempt was made to perform leak testing at elevated temperatures due to the rapid helium gas permeation and saturation of the elastomeric material at high temperatures. A fully saturated O-ring seal test specimen results in a measured leakage in excess of 1×10^{-7} scc/sec, air. The ability of the test fixture to establish a rapid, hard

⁴ ANSI N14.5-1997, *American National Standard for Radioactive Materials – Leakage Tests on Packages for Shipment*, American National Standards Institute, Inc. (ANSI).

vacuum between the O-ring seals was used as the basis for acceptance at elevated temperatures, with leaktightness proven subsequent to the elevated temperature phase by leak testing at -20 °F.

2.10.2.4 Test Procedure

The process of leak testing an O-ring seal is given below. Specific steps included for each test are provided in more detail in [Table 2.10.2-1](#).

1. Assemble the test fixture, with O-ring seals, at ambient temperature conditions.
2. Perform a helium leak test with the disk centered in the bore.
3. Cool the test fixture to -40 °F.
4. Perform a helium leak test with the test fixture temperature at -40 °F.
5. Warm the test fixture to -20 °F.
6. Radially shift the disk inside the bore to establish metal-to-metal contact on one side, and minimum O-ring seal compression on the diametrically opposite side.
7. Perform a helium leak test with the test fixture temperature at -20 °F.
8. Warm the test fixture to the elevated test temperature (i.e., 350 °F, 400 °F, or 450 °F, according to the particular test), continuing to restrain the disk in the fully offset position relative to the bore.
9. Maintain the elevated temperature for an 8 hour duration.
10. At the end of the 8 hour period, confirm that a rapid, hard vacuum can be achieved and maintained in the test volume between the two, test O-ring seals at the elevated temperature.
11. Cool the test fixture to -20 °F, continuing to restrain the disk in the fully offset position relative to the bore.
12. Perform a helium leak test with the test fixture temperature at -20 °F.

2.10.2.5 Example O-ring Seal Compression Calculation

The minimum compression in the test specimens was calculated based on measured test fixture dimensions and the measured cross-sectional diameter of the test O-ring seal. The procedure for the calculation of minimum compression is now illustrated using Test No. 3 as an example (see [Table 2.10.2-1](#) for applicable data). The same procedure was used for all tests.

Four quantities are needed for the compression calculation: 1) the cross-sectional diameter, W , of the O-ring seal, 2) stretch, S , of the O-ring seal, 3) groove depth, D , of the test fixture, and 4) the diametrical clearance or gap, G , between the test fixture gland and bore diameters. The minimum O-ring seal compression for Test No. 3 is found as follows:

1. Extract pertinent data from [Table 2.10.2-1](#).

W_{\min} = 0.387 inches, the minimum O-ring seal cross-sectional diameter

W_{\max} = 0.399 inches, the maximum O-ring seal cross-sectional diameter

G = 0.052 inches, the maximum gap (offset) between the outside diameter of the disk and the inside diameter of the bore for the test fixture

$D = 0.265 \pm 0.001$, the test fixture groove depth

2. Determine the reduction in O-ring seal cross-sectional diameter due to stretch.

From Table 2.10.2-1, the stretch of the O-ring seal diameter over the groove diameter was from 2.0% to 4.1% for all tests. The resulting reduction in O-ring seal cross-sectional diameter is 1.7% and 3.1%, respectively, from Figure A4-9 of the Parker O-ring Handbook⁵. The reduced cross-sectional diameters, W_{Rmax} and W_{Rmin} , are thus 1.7% and 3.1%, respectively, less than the non-stretched diameters, W_{max} and W_{min} , or:

$$W_{Rmax} = (1 - 0.017)W_{max} = 0.392 \text{ inches}$$

$$W_{Rmin} = (1 - 0.031)W_{min} = 0.375 \text{ inches}$$

3. Calculate the O-ring Seal Compression.

Using the quantities that are determined in (1) and (2), above, the compression is calculated as:

$$C_{min} = W_{Rmin} - D_{max} - G = 0.057 \text{ inches}$$

$$C_{max} = W_{Rmax} - D_{min} - G = 0.076 \text{ inches}$$

Expressing these values as a percent of the cross-section gives:

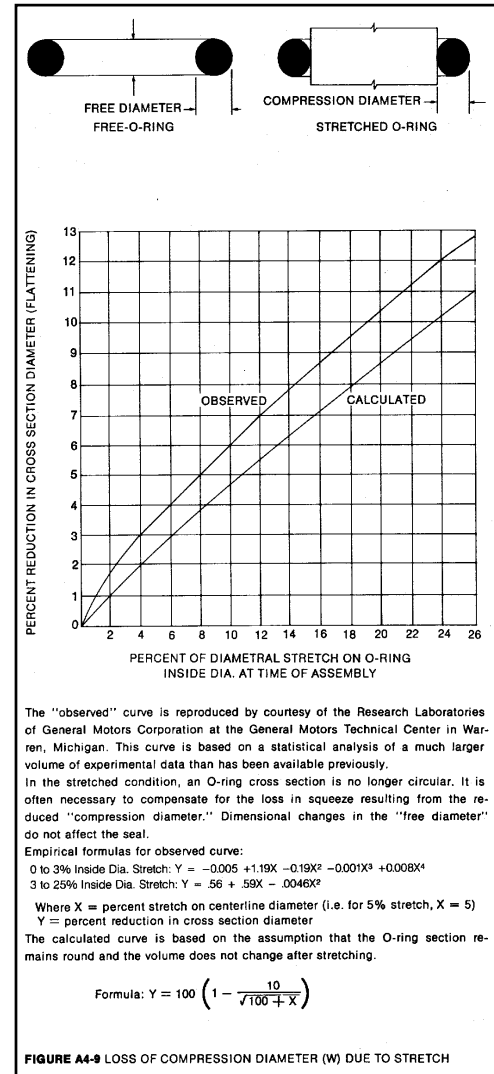
$$\%C_{min} = \left(\frac{C_{min}}{W_{Rmin}} \right) \times 100 = \left(\frac{0.057}{0.375} \right) \times 100 = 15.2\%$$

$$\%C_{max} = \left(\frac{C_{max}}{W_{Rmax}} \right) \times 100 = \left(\frac{0.076}{0.392} \right) \times 100 = 19.4\%$$

Note that the minimum and maximum O-ring seal compression values determined above represent a range of minimum compression. Following the procedure used above, the minimum O-ring seal compressions are calculated for all tests. The results are summarized in Table 2.10.2-1. Corresponding minimum compression ranges for a prototypic HalfPACT packaging are 23.6% to 37.7% for the initially centered configuration, and 17.0% to 31.5% for the worst case offset configuration.

2.10.2.6 Test Results

Test results are summarized in Table 2.10.2-1. As shown in the table, using worst case, minimum O-ring seal compression at extreme operating temperatures, the butyl rubber material is capable of maintaining a leaktight seal when used for the HalfPACT package. These results confirm that the O-ring seals used in the HalfPACT package will remain leaktight if subjected to worst-case seal



⁵ ORD 5700, *Parker O-ring Handbook*, 1992, Parker Hannifin Corporation, Cleveland, OH.

compressions over the range of NCT and HAC cold and hot temperatures. Additionally, following a HAC fire, the O-ring seals will remain leaktight when cooled to a temperature of -20 °F.

An additional test using a maximum elevated temperature of 450 °F was performed (see Test 2 in Table 2.10.2-1). In this case, the O-ring seals were not leaktight during the final, post-heat, -20 °F leak test, a vacuum at the high temperature could not be rapidly achieved, and the seals evidenced loss of elasticity and visible cracking was evident. Such was not the case for tests where the maximum temperature was 400 °F. It is therefore concluded that the upper limit for this butyl compound is somewhere between 400 °F and 450 °F, but an upper limit of 400 °F is conservatively utilized.

Of final note, further developmental O-ring seal testing of Rainier Rubber's butyl compound RR0405-70 was conducted as part of the design effort for the Radioisotope Thermoelectric Generator (RTG) Transportation System Packaging⁶. This testing demonstrated that this specific butyl rubber compound has a peak temperature rating of 380 °F, minimum, for durations of 24 hours or less. Continuous operation at temperatures between 350 °F and 380 °F may be allowed for longer durations, decreasing as a function of increasing temperature.

2.10.2.7 Designating an Alternative Seal Material

As discussed previously, Rainier Rubber RR0405-70 butyl rubber compound was selected for qualification testing that closely simulated the required performance characterized by package performance testing. The actual ability of the O-ring seals to meet these requirements is based on the seal material's basic characteristics.

Qualification testing identified certain key parameters that are important to seal performance. Of these, two important parameters for this application are resistance to helium permeation and acceptable resiliency at cold temperatures. Butyl rubber performs very well resisting helium permeation, and the TR-10 test in ASTM D1329⁷ provides an acceptable method for determining cold temperature material resiliency, with the properties of the RR0405-70 acting as a baseline for the required resiliency.

The ability of the compound to withstand elevated temperatures while not having significant reduction in material properties is also required to maintain seal integrity after the hypothetical accident condition thermal event. Material properties in elastomers are reduced through the process of de-polymerization, an aging phenomenon. Elastomer aging can be accelerated by the application of energy (heat). The effect of aging can be quantified by measuring the reduction of

⁶ DOE Docket No. 94-6-9904, *Radioisotope Thermoelectric Generator Transportation System Safety Analysis Report for Packaging*, WHC-SD-RTG-SARP-001, prepared for the U.S. Department of Energy Office of Nuclear Energy under Contract No. DE-AC06-87RL10930 by Westinghouse Hanford Company, Richland, WA. Per Appendix 2.10.6, elevated temperature tests were performed on Rainier Rubber Company butyl rubber compound No. RR-0405-70 O-ring seals with seal compressions as low as 10%. The specific time-temperature test parameters evaluated were 380 °F for 24 hours followed by 350 °F for 144 hours, for a total of 168 hours (1 week). At these temperatures, all elastomeric compounds are susceptible to relatively high helium permeability; thus, helium leak testing was not performed. Instead, a hard vacuum of less than 0.0029 psia (20 Pa) was maintained on the test O-ring seals with no measurable pressure loss that would indicate leakage. At the end of the entire test sequence, the test O-ring seals were stabilized at -20 °F and shown, via helium leak testing, to be leaktight (i.e., a leakage rate less than 1×10^{-7} standard cubic centimeters per second (scc/s), air leakage).

⁷ ASTM D1329-88 (re-approved 1998), *Standard Test Method for Evaluating Rubber Property – Retraction at Lower Temperatures (TR Test)*, American Society for Testing and Materials, Philadelphia, PA, Volume 09.01, 2001.

physical properties after maintaining the seal material at an elevated temperature for a specific length of time. For the same amount of reduction in properties, a shorter time can be used at a higher temperature, or a longer time can be used at a lower temperature. ASTM D573⁸ provides an acceptable method for determining the effects of temperature aging on elastomeric compounds.

ASTM D395⁹ provides an acceptable method for determining the effects of compression set. RR0405-70 butyl rubber compound uses an acceptance criteria of less than 25% compression set for 22 hours at an elevated temperature of 70 °C.

ASTM D2137¹⁰ provides an acceptable method for determining an elastomeric material's ability to withstand cold temperatures and remain pliable. Although the TR-10 test in ASTM D1329 demonstrates the seal material's resiliency at a much lower temperature, this test verifies the seal material's lack of brittleness at the minimum regulatory temperature of -40 °C.

Hardness or durometer along with tensile strength and elongation are defined and checked to ensure durability of the seal material during operation. ASTM D2240¹¹ provides an acceptable method for determining the required 70 ±5 durometer, and ASTM D412¹² provides an acceptable method for determining the required minimum 10 MPa (1,450 psi) tensile strength and minimum 250% elongation, with the properties of the RR0405-70 acting as a baseline for the required hardness, tensile strength, and elongation.

For proprietary seal materials that have fairly demanding requirements such as the RR0405-70 butyl rubber compound, the compound is commonly specified by a company designator and subsequently checked against exacting performance standards. Specifying an elastomeric compound by its chemistry alone is difficult considering the shear number of parameters that affect seal performance. However, by applying the above nationally recognized standards to a material batch, the important parameters are defined for verifying the performance of the seal material.

ASTM D1414¹³ is the standard method for testing O-ring seals, and covers most, but not all, of the required testing delineated above. However, due to the overall size of the O-ring seals and the additional testing specified, ASTM D2000¹⁴ provides a better standard classification system.

⁸ ASTM D573-99, *Standard Test Method for Rubber – Deterioration in an Air Oven*, American Society for Testing and Materials, Philadelphia, PA, Volume 09.01, 2001.

⁹ ASTM D395-01, *Standard Test Methods for Rubber Property – Compression Set*, American Society for Testing and Materials, Philadelphia, PA, Volume 09.01, 2001.

¹⁰ ASTM D2137-94 (re-approved 2000), *Standard Test Methods for Rubber Property – Brittleness Point of Flexible Polymers and Coated Fabrics*, American Society for Testing and Materials, Philadelphia, PA, Volume 09.02, 2001.

¹¹ ASTM D2240-00, *Standard Test Method for Rubber Property – Durometer Hardness*, American Society for Testing and Materials, Philadelphia, PA, Volume 09.01, 2002.

¹² ASTM D412-98a, *Standard Test Methods for Vulcanized Rubber and Thermoplastic Rubbers and Thermoplastic Elastomers – Tension*, American Society for Testing and Materials, Philadelphia, PA, Volume 09.01, 2001.

¹³ ASTM D1414-94 (re-approved 1999), *Standard Test Methods for Rubber O-Rings*, American Society for Testing and Materials, Philadelphia, PA, Volume 09.02, 2001.

¹⁴ ASTM D2000-01, *Standard Classification System for Rubber Products in Automotive Applications*, American Society for Testing and Materials, Philadelphia, PA, Volume 09.02, 2001.

Each batch of compounded material requires testing, where a “batch” represents the chemical compounding of the material before vulcanizing and a “lot” refers to the quantity of finished product made at any one time.

Using the ASTM D2000 designator, O-ring seals with properties equivalent to RR0405-70 butyl rubber material are classified as follows; this designator callout is currently being specified for the RR0405-70 butyl rubber material, as discussed above, and summarized in the table below:

M4AA710 A13 B13 F17 F48 Z Trace Element

Designator	Condition
M	Metric units designator (default condition)
4	Grade 4 acceptance criteria for the tests specified
AA	Butyl rubber compound
7	70 Shore A durometer hardness per ASTM D2240
10	Tensile strength and elongation per ASTM D 412; acceptance criteria are a minimum 10 MPa (1,450 psi) tensile strength and a minimum 250% elongation
A13	Heat resistance test per ASTM D573; the acceptance criteria are a maximum 10 Shore A durometer hardness increase, a maximum reduction in tensile strength of 25%, and a maximum reduction in ultimate elongation of 25% at 70 °C
B13	Compression set per Method B of ASTM D395; acceptance criterion is a maximum 25% compression set after 22 hours at 70 °C
F17	Cold temperature resistance specifying low temperature brittleness per Method A, 9.3.2, of ASTM D2137; non-brittle after 3 minutes at -40 °C
F48	Cold temperature resiliency, where F is for cold temperature resistance, and 4 specifies testing to the TR-10 test of ASTM D1329; 8 indicates a TR-10 temperature of -50 °C (-58 °F), or less
Z Trace Element	Z designator allows specific notes to be added; “Z Trace Element” allows trace elements to be added to the elastomeric compound to meet the seal material requirements

Using the above seal material designator, the acceptable seal material for the HalfPACT package are O-ring seals meeting the SAR drawing requirements and specified as:

“Butyl rubber material per Rainier Rubber RR0405-70, or equivalent meeting the requirements of ASTM D2000 M4AA710 A13 B13 F17 F48 Z Trace Element”

This page intentionally left blank.

Table 2.10.2-1 – O-ring Seal Performance Test Results

Test Number	O-ring Seal Cross-Sectional Diameter (inches) ^①				Stretch (%)		Maximum Gap (inches)		Minimum Compression (%)				Temperature for “Leaktight” Leak Test (Leakage $\leq 2.0 \times 10^{-8}$ scc/sec, He)				
	O-ring Seal No. 1		O-ring Seal No. 2		Min	Max	Center Disk	Offset Disk	Center Disk		Offset Disk		Center Disk ^④		Offset Disk ^④		
	Min	Max	Min	Max					Min	Max	Min	Max	Min	Max	Ambient	-40 °F	-20 °F
1	0.387	0.397	0.387	0.396	2.0	4.1	0.026	③	22.1	25.6	14.9	20.0	Yes	Yes	Yes	350 °F	Yes
2	0.388	0.398	0.387	0.398	2.0	4.1	0.029	0.050	21.3	25.1	15.7	19.7	Yes	Yes	⑥	450 °F	No
3	0.387	0.397	0.387	0.399	2.0	4.1	0.027	0.052	21.9	25.8	15.2	19.4	Yes	Yes	Yes	400 °F	Yes
4	②	②	②	②	2.0	4.1	0.027	0.053	21.9	25.8	14.9	19.1	Yes	Yes	Yes	400 °F	Yes
5	②	②	②	②	2.0	4.1	0.026	0.050	22.1	26.0	15.7	19.9	Yes	Yes	Yes	400 °F	Yes

Notes:

- ① Material for all O-ring seal test specimens is butyl rubber compound RR0405-70, Rainier Rubber Co., Seattle, WA.
- ② Not measured; calculations assume the worst case range as taken from Tests Numbers 1 - 3 (i.e., Ø0.387 minimum to Ø0.399 maximum).
- ③ Range of values is 0.048 minimum to 0.053 maximum due to an indirect method of gap measurement (used for this test only).
- ④ A “Yes” response indicates that helium leakage testing demonstrated that the leakage rate was $\leq 1.0 \times 10^{-7}$ scc/sec, air (i.e., “leaktight” per ANSI N14.5). In all cases, measured leakage rates were $\leq 2.0 \times 10^{-8}$ scc/sec, helium, for tests with a “Yes” response.
- ⑤ No helium leak tests were performed at elevated temperatures due to O-ring seal permeation and saturation by helium gas. The ability of the test fixture to establish a rapid, hard vacuum between the O-ring seals was used as the basis for leak test acceptance at elevated temperatures. All tests rapidly developed a hard vacuum, with the exception of Test Number 2 at an elevated temperature of 450 °F, that slowly developed a vacuum.
- ⑥ Initial leakage of 1.0×10^{-5} scc/sec, helium; became leaktight ($\leq 2.0 \times 10^{-8}$ scc/sec, He) approximately one minute later.

This page intentionally left blank.

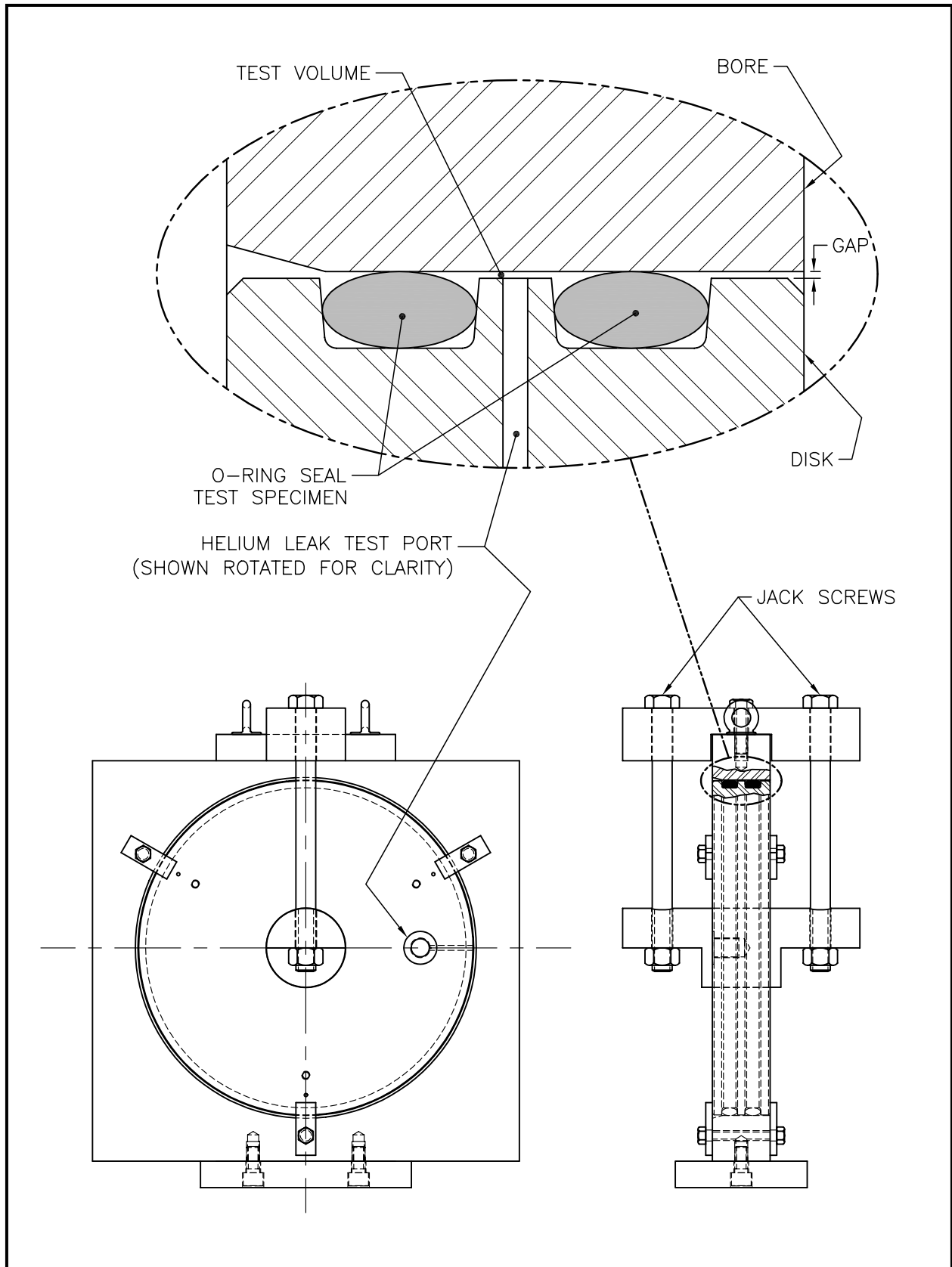


Figure 2.10.2-1 – Test Fixture for O-ring Seal Performance Testing

This page intentionally left blank.

2.10.3 Certification Tests

Presented herein are the results of normal conditions of transport (NCT) and hypothetical accident condition (HAC) tests that address the free drop, puncture, and fire test performance requirements of 10 CFR 71¹. This appendix summarizes the information presented in the test reports for the HalfPACT engineering test unit (ETU)² and certification test unit (CTU)³.

2.10.3.1 Introduction

The HalfPACT package, when subjected to the sequence of hypothetical accident condition (HAC) tests specified in 10 CFR §71.73, subsequent to the sequence of normal conditions of transport (NCT) tests specified in 10 CFR §71.71, is shown to meet the performance requirements specified in Subpart E of 10 CFR 71. As indicated in the introduction to [Chapter 2.0, Structural Evaluation](#), with the exception of the immersion test, the primary proof of performance for the HAC tests is via the use of full scale testing. In particular, free drop, puncture, and fire testing of both a HalfPACT ETU and CTU confirms that both the outer and inner containment boundaries will remain leaktight after a worst case HAC sequence. Observations from testing of the two test units also confirm the conservative nature of deformed geometry assumptions used in the criticality assessment provided in [Chapter 6.0, Criticality Evaluation](#).

Since the HalfPACT package is essentially a “cut-down” version of the TRUPACT-II package, this appendix provides a number of comparative discussions between the HalfPACT and TRUPACT-II certification testing programs. Where appropriate, these comparisons are useful for providing an additional level of confidence in the HalfPACT testing programs by illustrating test results similar to the comprehensive TRUPACT-II certification testing program. As discussed in [Appendix 2.10.3.5, Technical Basis for Tests](#), the selection of HalfPACT test conditions was determined based on the various TRUPACT-II certification tests.

2.10.3.2 Summary

As seen in the figures presented in [Appendix 2.10.3.7, Test Results](#), successful testing of the ETU and CTU indicates that the various HalfPACT packaging design features are adequately designed to withstand the HAC tests specified in 10 CFR §71.73. The most important result of the testing program was the demonstrated ability of the outer containment vessel (OCV) and inner containment vessel (ICV) to remain leaktight⁴.

¹ Title 10, Code of Federal Regulations, Part 71 (10 CFR 71), *Packaging and Transportation of Radioactive Material*, 01-01-07 Edition.

² Packaging Technology, Inc. (PacTec), *HalfPACT Packaging Engineering Prototype Test Report*, PacTec Engineering Document ED-019, Tacoma, Washington.

³ S. A. Porter, et al, *Certification Test Report for the HalfPACT Package*, TR-001, Packaging Technology, Inc. (PacTec), Tacoma, Washington.

⁴ “Leaktight” is a leakage rate not exceeding 1×10^{-7} standard cubic centimeters per second (scc/sec), air, as defined in ANSI N14.5-1997, *American National Standard for Radioactive Materials – Leakage Tests on Packages for Shipment*, American National Standards Institute, Inc. (ANSI).

Significant results of free drop testing common to both test units (ETU and CTU) are as follows:

- There was no evidence of buckling of either containment boundary shell. Modest damage to the inner containment vessel shells did occur, an amount somewhat in excess of what was reported in [Appendix 2.10.3, Certification Tests](#), in the *TRUPACT-II package SAR*⁵. However, it is clear that the damage noted for the HalfPACT package corresponds to the much heavier payload drum's interaction with the packaging wall.
- No excessive distortion of the seal flange regions occurred for either containment vessel, although some permanent deformation was noted.
- There was no rupture of the 3/8 inch thick, outer containment assembly (OCA) outer shell.
- Observed permanent deformations of the HalfPACT packaging were less than those assumed for the criticality evaluation.

Significant results of puncture drop testing common to both test units (ETU and CTU) are as follows:

- Besides the obvious permanent damage to the OCA outer shell at the location of the various puncture bar impacts, there was evidence of some permanent deformation of the OCV shell. The most significant damage occurred at the OCV vent port fitting during testing of the CTU. The cumulative effects of the NCT and HAC free drops, and the subsequent puncture drop caused successively greater permanent deformation to the region adjacent to the vent port fitting. A crack was noted in the inner weld of the CTU's OCV vent port fitting, but not in the outer weld of the OCV vent port fitting. Subsequent helium leakage rate testing determined that OCV containment integrity was maintained. Although essentially identical in configuration, the ETU did not have a similarly cracked weld. See [Appendix 2.10.3.7.2.8, CTU Post-Test Disassembly](#), for additional discussion regarding this result.
- Penetration of the OCA outer shell occurred below the 3/8-to-1/4 inch thick, OCA outer shell weld during testing of the ETU. The same test, repeated for certification testing, did not reproduce the hole. This result was due to lengthening the 3/8 inch thick, OCA outer shell from 12 to 18 inches, correspondingly changing the impact angle sufficiently to prevent penetration through the adjacent 1/4 inch thick shell.
- There was no rupture of the 3/8 inch thick, OCA outer shell. However, for both test units (ETU and CTU) a linear tear occurred along the weld at the 3/8-to-1/4 inch shell transition in the OCA body outer shell.

Significant results of fire testing common to both test units (ETU and CTU) are as follows:

- The fire tests met or exceeded the minimum flame temperature of 1,475 °F for 30 minutes as required by 10 CFR §71.73(c)(4).
- Gases formed by thermal degradation of the polyurethane foam were safely vented out the OCA fire vents located in the OCA lid and body.
- The polyurethane foam self-extinguished shortly after the end of the fire.

⁵ U.S. Department of Energy (DOE), *Safety Analysis Report for the TRUPACT-II Shipping Package*, USNRC Docket No. 71-9218, U.S. Department of Energy, Carlsbad Field Office, Carlsbad, New Mexico.

- The average residual thickness of unburned polyurethane foam in the OCA side wall was approximately five inches in regions undamaged by free drop tests, and approximately three inches in regions damaged by free drop tests. In regions of multiple free drop and puncture drop tests (e.g., at the OCV vent port), only charred foam and ceramic fiber paper remained.
- None of the containment seals sustained extensive degradation due to excessive temperature.

2.10.3.3 Test Facilities

Drop testing of the HalfPACT package prototype test unit was performed at Sandia National Laboratories' Coyote Canyon Aerial Cable Facility in Albuquerque, New Mexico. The drop test facility utilizes free fall and, if needed, rocket power to attain closely controlled impact velocities as defined by a particular testing program. The drop test facility consists of a 5,000 foot long wire cable suspended across a mountain canyon. The cable can support proportionally heavier package weights at lower elevations, with a package weight in excess of 50,000 pounds for the regulatory defined, hypothetical accident condition 30 foot free drop test. The "unyielding" target consists of a highly reinforced, armor steel plated concrete block as illustrated in [Figure 2.10.3-1](#). The target is designed to accommodate test packages weighing up to 100 tons.

In accordance with the requirements of 10 CFR §71.73(c)(3), the puncture bar was fabricated from solid, six inch diameter mild steel, approximately 36 inches long. The puncture bar was welded perpendicularly to a 1½ inch thick, mild steel plate having an outside diameter of approximately 24 inches. The top edge of the puncture bar was finished to a 1/4 inch radius. When utilized, the puncture bar was securely welded (mounted) to the impact surface.

Fire testing of the HalfPACT package prototype test unit was performed at Sandia National Laboratories' Lurance Canyon Burn Site in Albuquerque, New Mexico. The open pool fire facility can be adjusted to a maximum size of 30 by 60 feet for performing free-burning fires for a duration of 2 hours, maximum. Packages weighing up to 149 tons can be supported at heights up to a few meters above the pool surface. During fire testing, thermocouples and calorimeters that are strategically placed measure and record fire temperatures and heat flux, respectively. The pool is enclosed by a 20 foot high wind screen deployed in a nominal 50 foot radius from the pool center. The wind screen is constructed of chain link fencing fitted with aluminum slats resulting in a screen porosity of 50%. The wind screen demonstrates a 3-to-1 reduction in wind velocity in high wind conditions, and a 2-to-1 reduction in low wind conditions.

2.10.3.4 Test Unit Description

The HalfPACT package is essentially a 30 inch shorter version of the TRUPACT-II package, being identical in almost all respects, the few exceptions noted in later discussions. Both the HalfPACT and TRUPACT-II packages are designed to transport payloads of contact-handled transuranic (CH-TRU) waste. The HalfPACT package is designed to carry five different payload configurations: 1) seven 55-gallon drums, 2) one standard waste box (SWB), 3) four 85-gallon drums, 4) three 100-gallon drums, or 5) three shielded containers for its payload. The HalfPACT package height is based on the need to carry oversized 85-gallon drums used as overpacks for 55-gallon drums. Drums may weigh 1,000 pounds each, for a maximum weight of 7,000 pounds for seven 55-gallon drums, 4,000 pounds for four 85-gallon drums, and 3,000

pounds for three 100-gallon drums. The maximum SWB weight is 4,000 pounds and the maximum weight of three shielded containers is 6,780 pounds.

For purposes of comparison, the primary design differences between the HalfPACT package and TRUPACT-II package are summarized as follows (see [Figure 2.10.3-2](#) and [Figure 2.10.3-3](#) for the differences between the packaging design and 55-gallon drum payload configuration for the TRUPACT-II and HalfPACT packages, respectively):

- maximum package weight: 18,100 pounds for HalfPACT; 19,250 pounds for TRUPACT-II,
- maximum payload assembly weight (including pallet, spacer, guide tubes, and slipsheets): 7,600 pounds for HalfPACT; 7,265 pounds for TRUPACT-II,
- payload assembly configurations (comparing current TRUPACT-II package certification):
 - 55-gallon drums: seven for HalfPACT; fourteen for TRUPACT-II (includes pipe overpacks),
 - SWBs: one for HalfPACT; two for TRUPACT-II,
 - 85-gallon drums: four for HalfPACT; eight for TRUPACT-II,
 - 100-gallon drums: three for the HalfPACT; six for the TRUPACT-II,
 - ten drum overpack (TDOP): none for HalfPACT; one for TRUPACT-II,
 - shielded containers: three for HalfPACT with radial and axial dunnage; none for TRUPACT-II
- overall height: 91½ inches for HalfPACT; 121½ inches for TRUPACT-II,
- ICV payload cavity length: 44¹⁵/₁₆ inches for HalfPACT; 74⁵/₈ inches for TRUPACT-II,
- OCV cylindrical shell stiffening ring: removed for HalfPACT; included for TRUPACT-II,
- OCA body fire vent locations changed between HalfPACT and TRUPACT-II,
- OCA body, 3/8 inch thick outer shell length: 18 inches for HalfPACT; 12 inches for TRUPACT-II,
- Payload spacer: A payload spacer is used to reduce excess axial clearance for HalfPACT payloads consisting of 55-gallon drums, 100-gallon drums, short 85-gallon drums, and SWBs; no payload spacer is used for TRUPACT-II

The following sections expand on the individual details relating to the ETU and CTU configurations. Both HalfPACT packaging engineering test units were fabricated from TRUPACT-II packaging training units⁶, as discussed below.

2.10.3.4.1 Engineering Test Unit (ETU)

The HalfPACT packaging engineering test unit (ETU) was fabricated from TRUPACT-II unit number 104, a TRUPACT-II packaging training unit. As illustrated in [Figure 2.10.3-4](#), the OCA

⁶ Early TRUPACT-II production units have shells of insufficient thickness per TRUPACT-II SAR requirements. Designated “training units”, excessive grinding of some welds in localized regions reduced shell thicknesses below the minimum allowed by the TRUPACT-II (and HalfPACT) SAR packaging general arrangement drawings.

body for the HalfPACT ETU was created by removing 30 inches from the OCV cylindrical shell above the torispherical head, and 30 inches from the OCA outer shell below the 3/8-to-1/4 inch shell transition from TRUPACT-II unit number 104. All polyurethane foam and ceramic fiber paper below the parting line was removed. New ceramic fiber paper was installed, the shells welded closed, and new polyurethane foam installed. Polyurethane foam compressive strength properties were tested to be consistent with the requirements of [Table 8.1-1](#) in [Section 8.1.4.1, Polyurethane Foam](#). Similarly, as illustrated in [Figure 2.10.3-5](#), the ICV body for the HalfPACT ETU was created by removing 30 inches of the cylindrical region above the torispherical head from TRUPACT-II unit number 104. Both the OCA and ICV lid assemblies remained unchanged.

Tested differences between the HalfPACT ETU and TRUPACT-II CTUs (i.e., components or parameters used during TRUPACT-II certification testing that were not used during HalfPACT certification testing) are summarized as follows:

- Seal flange O-ring seal region tolerances: carefully controlled fabrication procedures to arrive at worst case (minimum) O-ring seal compression and worst case (maximum) axial free play were used for the TRUPACT-II CTUs; the HalfPACT ETU used unmodified, as-built production unit tolerances,
- Loose debris outside the payload drums: additional cement and sand was used outside the payload drums for the TRUPACT-II CTUs, but not for the HalfPACT CTU (both test programs used additional loose sand inside the payload drums),
- Active and passive test instrumentation (e.g., thermocouples, accelerometers, pressure transducers, and/or temperature indicating labels): active and passive test instrumentation was used for the TRUPACT-II CTUs, but no instrumentation was used for the HalfPACT ETU,
- Internal pressure: pressurization of the containment vessels to the maximum normal operating pressure (MNOP) for some of the free drop, puncture drop, and fire tests was performed for the TRUPACT-II CTUs, but not for the HalfPACT ETU,
- Cooling before drop testing: cooling to -20 °F prior to some of the free drop and puncture drop tests was performed for the TRUPACT-II CTUs, but not for the HalfPACT ETU,
- Pre-heating before the fire test: pre-heating prior to fire testing was performed for the TRUPACT-II CTUs, but not for the HalfPACT ETU, and
- Cooling before leakage rate testing: cooling to -20 °F prior to post-test, helium leakage rate testing was performed for the TRUPACT-II CTUs, but not for the HalfPACT ETU.

In addition to the tested differences between the HalfPACT ETU and TRUPACT-II CTUs, the difference between the HalfPACT ETU and the HalfPACT packaging design depicted in [Appendix 1.3.1, Packaging General Arrangement Drawings](#), are summarized as follows:

- Minimum shell material thickness: HalfPACT packaging design requires minimum shell material thicknesses per ASTM A480⁷; HalfPACT ETU was fabricated from a cut-down

⁷ ASTM A480/A480M, *Standard Specification for General Requirements for Flat-Rolled Stainless and Heat-Resisting Steel Plate, Sheet, and Strip*, American Society for Testing and Materials (ASTM), West Conshohocken, PA.

TRUPACT-II training unit (number 104) with localized regions not meeting ASTM A480 because of excessive grinding of some welds,

- OCA body, 3/8 inch thick outer shell length: HalfPACT packaging design is 18 inches long; HalfPACT ETU was 12 inches long,
- Painting of OCA exterior surfaces: HalfPACT packaging design allows optional painting; HalfPACT ETU was not painted,
- OCV vent and seal test port thermal plugs: HalfPACT packaging design specifies foam or ceramic fiber paper thermal plugs; HalfPACT ETU used polyurethane foam thermal plugs,
- Optional catalyst assembly recess in ICV aluminum honeycomb spacers: HalfPACT packaging design specifies Ø18 inches × 1½ inches deep; HalfPACT ETU used recesses Ø15 inches × 11/16 inches deep,
- Aluminum honeycomb spacer assembly attachment bracket: HalfPACT packaging design specifies right-angled brackets; HalfPACT ETU used obtuse-angled brackets,
- Locking ring stop tabs: HalfPACT packaging design specifies up to three stop tabs per locking ring; HalfPACT ETU used one stop tab per locking ring,
- OCA exterior welds: HalfPACT packaging design specifies 3/32 inch maximum weld reinforcement for OCA exterior welds; HalfPACT ETU used 3/32 inch maximum weld reinforcement only on new 3/8-to-1/4 inch, outer shell weld, and
- External handling features were added to the exterior surfaces of the HalfPACT ETU to facilitate lifting and handling the package during testing.

The following table summarizes a comparison of major component weights for the HalfPACT ETU and TRUPACT-II CTUs:

Packaging Component	TRUPACT-II Certification Test Units			HalfPACT ETU
	CTU No. 1	CTU No. 2	CTU No. 3	
Empty Package				
• ICV Assembly	2,614	2,773	2,570	2,025
• OCA Assembly	9,450	9,400	9,196	8,100
• Total	12,064	12,173	11,766	10,125
Payload				
• 55-Gallon Drums	7,000	7,000	7,000	7,350
• Pallet, Slipsheets, etc.	315	269	375	160
• Total	7,315	7,269	7,375	7,510
Loaded Package Total	19,379	19,442	19,141	17,635

2.10.3.4.2 Certification Test Unit (CTU)

Similar to the HalfPACT ETU, the HalfPACT packaging certification test unit (CTU) was fabricated from TRUPACT-II unit number 107, a TRUPACT-II packaging training unit. As illustrated in [Figure 2.10.3-6](#), the OCA body for the HalfPACT CTU was created by removing 30 inches from the OCV cylindrical shell above the torispherical head, and 36 inches from the OCA outer shell below the 3/8-to-1/4 inch shell transition from TRUPACT-II unit number 107. All polyurethane foam and ceramic fiber paper below the parting line was removed. Six inches of 3/8 inch thick, OCA outer shell was added below the existing 12 inch length to extend the shell length to 18 inches per the HalfPACT packaging design. New ceramic fiber paper was installed, the shells welded closed, and new polyurethane foam installed. Polyurethane foam compressive strength properties were tested to be consistent with the requirements of [Table 8.1-1](#) in [Section 8.1.4.1, Polyurethane Foam](#). Similarly, as illustrated in [Figure 2.10.3-7](#), the ICV body for the HalfPACT CTU was created by removing 30 inches of the cylindrical region above the torispherical head from TRUPACT-II unit number 107. Both the OCA and ICV lid assemblies remained unchanged. All OCA exterior surfaces were painted gray.

Tested differences between the HalfPACT CTU and TRUPACT-II CTUs (i.e., components or parameters used during TRUPACT-II certification testing that were not used during HalfPACT certification testing) are summarized as follows:

- Seal flange O-ring seal region tolerances: carefully controlled fabrication procedures to arrive at worst case (minimum) O-ring seal compression and worst case (maximum) axial free play were used for the TRUPACT-II CTUs; the HalfPACT CTU used unmodified, as-built production unit tolerances,
- Loose debris outside the payload drums: additional cement and sand was used outside the payload drums for the TRUPACT-II CTUs, but not for the HalfPACT CTU (both test programs used additional loose sand inside the payload drums),
- Active and passive test instrumentation (e.g., thermocouples, accelerometers, pressure transducers, and/or temperature indicating labels): active and passive test instrumentation was used for the TRUPACT-II CTUs, but only temperature indicating labels were used for the HalfPACT CTU,
- Internal pressure: pressurization of the containment vessels to the maximum normal operating pressure (MNOP) for some of the free drop, puncture drop, and fire tests was performed for the TRUPACT-II CTUs, but not for the HalfPACT CTU,
- Cooling before drop testing: cooling to -20 °F prior to some of the free drop and puncture drop tests was performed for the TRUPACT-II CTUs, but not for the HalfPACT CTU,
- Pre-heating before the fire test: pre-heating prior to fire testing was performed for the TRUPACT-II CTUs, but not for the HalfPACT CTU, and
- Cooling before leakage rate testing: cooling to -20 °F prior to post-test, helium leakage rate testing was performed for the TRUPACT-II CTUs, but not for the HalfPACT CTU.

In addition to the tested differences between the HalfPACT CTU and TRUPACT-II CTUs, the difference between the HalfPACT CTU and the HalfPACT packaging design depicted in [Appendix 1.3.1, Packaging General Arrangement Drawings](#), are summarized as follows:

- Minimum shell material thickness: HalfPACT packaging design requires minimum shell material thicknesses per ASTM A480; HalfPACT CTU was fabricated from a cut-down TRUPACT-II training unit (number 107) with localized regions not meeting ASTM A480 because of excessive grinding of some welds,
- Optional catalyst assembly recess in ICV aluminum honeycomb spacers: HalfPACT packaging design specifies Ø18 inches × 1½ inches deep; HalfPACT CTU used recesses Ø15 inches × 11/16 inches deep,
- Aluminum honeycomb spacer assembly attachment bracket: HalfPACT packaging design specifies right-angled brackets; HalfPACT CTU used obtuse-angled brackets,
- Locking ring stop tabs: HalfPACT packaging design specifies up to three stop tabs per locking ring; HalfPACT CTU used one stop tab per locking ring,
- OCA exterior welds: HalfPACT packaging design specifies 3/32 inch maximum weld reinforcement for OCA exterior welds; HalfPACT CTU used 3/32 inch maximum weld reinforcement only on new 3/8-to-3/8 inch and 3/8-to-1/4 inch, outer shell welds, and
- Payload Spacer: To accommodate a single layer of 55-gallon drums for the test payload, a 5-inch high wooden payload spacer was utilized,
- External handling features were added to the exterior surfaces of the HalfPACT CTU to facilitate lifting and handling the package during testing.

The following table summarizes a comparison of major component weights for the HalfPACT ETU and CTU, and TRUPACT-II CTUs:

Packaging Component	TRUPACT-II			HalfPACT	
	CTU No. 1	CTU No. 2	CTU No. 3	ETU	CTU
Empty Package					
• ICV Assembly	2,614	2,773	2,570	2,025	2,120
• OCA Assembly	9,450	9,400	9,196	8,100	7,950
• Total	12,064	12,173	11,766	10,125	10,070
Payload					
• 55-Gallon Drums	7,000	7,000	7,000	7,350	7,410
• Pallet, Payload Spacer, etc.	315	269	375	160	590
• Total	7,315	7,269	7,375	7,510	8,000
Loaded Package Total	19,379	19,442	19,141	17,635	18,070

2.10.3.5 Technical Basis for Tests

The following sections supply the technical basis for the chosen test orientations and sequences for both the HalfPACT ETU and CTU as presented in [Section 2.10.3.6, Test Sequence for Selected Free Drop, Puncture Drop, and Fire Tests.](#)

2.10.3.5.1 Initial Test Conditions

2.10.3.5.1.1 Internal Pressure

Internal pressure could affect the certification test results in two ways. First, it imparts primary stress to the containment vessels, and second, it could affect the leaktight condition of the seals in a HAC fire. In the first case, containment vessel stress due to internal pressure is $pr/t = 7,288$ psi, where p , the internal design pressure, is 50 psi, the ICV mean radius, r , is 36.44 inches, and the thickness, t , is 0.25 inches. Per Regulatory Guide 7.6, this stress is compared to the design stress intensity, $S_m = 20,000$ psi at NCT temperatures. The result is that pressure-related membrane stress that is only 36% of the allowable stress. Pressure would normally be present only in the ICV, and due to the presence of the OCA, the polyurethane foam, and the OCV, the relative deformation of the ICV due to any free drop or puncture event is insignificant. Further, during TRUPACT-II testing, no pressure spikes as a result of impact were recorded. Thus, the addition of pressure membrane stress would be insignificant to the outcome of HalfPACT free drop and puncture drop testing.

In the second case, the pressure sealing capacity of the containment seals is significantly greater than the maximum normal operating pressure (MNOP) of 50 psig. For the HAC fire test, O-ring seal compression is expected to increase as a result of differential expansion between the seal and the surrounding metal, thus increasing the pressure capacity of the seal. Certification testing of the TRUPACT-II demonstrated that no pressure was lost for any of the fire tests. Therefore, as long as temperatures in the O-ring seal regions are similar to the temperatures measured during TRUPACT-II fire testing, pressurizing either the ICV or OCV is considered unnecessary for HalfPACT certification fire testing.

2.10.3.5.1.2 Temperature

Ambient temperature will be used at the time of HalfPACT certification testing. Results might differ if the two extremes (NCT maximum temperature, or minimum, -20 °F, temperature) were employed. However, it can be shown that these differences are not significant as follows.

As discussed in [Section 2.7, Hypothetical Accident Conditions](#), polyurethane foam compressive strength at an NCT temperature of 160 °F is approximately 75% of the compressive strength at 75 °F, and at -20 °F is approximately 140% of the crush strength at 75 °F. In contrast, the minimum strength of the Type 304 stainless steel varies to a much lesser extent, decreasing from 35,000 psi at -20 °F⁸ to 30,000 psi at 100 °F, and to 27,000 psi at 160 °F. Thus, for drop orientations where stresses in structural steel members are of concern, the worst case temperature is -20 °F since this is the temperature where the ratio of impact induced acceleration load to steel strength is the greatest. For drop orientations where deformations are of concern, elevated temperatures would result in a worst-case condition.

Deformations will be greater if the polyurethane foam is at NCT warm temperatures during free and puncture drops. The greater the deformation, the less residual foam thickness to protect the O-ring seals from thermal degradation in the subsequent fire. The elastomer seal material short-term

⁸ For the purposes of this discussion, yield strength at -20 °F is extrapolated from data in [Table 2.3-1](#) using a curve shape for Type 304 stainless steel in the -80 °F to 800 °F range in *Engineering Properties of Steel*, Philip D. Harvey, Editor, American Society for Metals, 1982.

temperature limit is 400 °F per [Appendix 2.10.2, Elastomer O-ring Seal Performance Tests](#). Considering a maximum O-ring seal region temperature of 260 °F for TRUPACT-II fire testing and the relatively large amount of unburned foam following fire testing (~5 inches, average), the margin against O-ring seal failure is relatively large. In view of this, a reasonable limit for the average maximum O-ring seal region temperature for HalfPACT fire testing is 300 °F. In this case, the margin will be virtually as great as for the TRUPACT-II, and drop testing at warm temperatures is considered unnecessary.

Impact forces will be greater if the polyurethane foam is at NCT cold temperatures (-20 °F) during free and puncture drops. However, the bounding free drop where impact severity is a factor is a side slapdown. As discussed in [Section 2.10.3.5.2.4, Closure \(Lid\) Separation](#), the results indicate that all HalfPACT slapdown drops are enveloped by TRUPACT-II slapdown drops. Therefore, reduction of the foam temperature would still not create a governing impact severity condition, and drop testing at cold temperatures is considered unnecessary.

2.10.3.5.2 Free Drop Tests

The HalfPACT package is qualified primarily by full scale testing, with the acceptance criterion being the ability to demonstrate leaktight containment for both the outer containment vessel (OCV; primary containment), and the inner containment vessel (ICV; secondary containment).

Per 10 CFR §71.73(c)(1), the package is required to “strike an essentially unyielding surface *in a position for which maximum damage is expected.*” Therefore, for determining the drop orientations that satisfy the regulatory “maximum damage” requirement, attention is focused predominantly on the issue of containment. Loss of containment could potentially occur one of two ways: 1) directly, as a result of free drop impact damage, or 2) indirectly, as a result of normal conditions of transport (NCT) or hypothetical accident condition (HAC) impact damage that could lead to degradation of sealing capability in the subsequent puncture and/or fire events.

Direct damage would take the form of one of the following:

1. Rupture of a containment vessel,
2. Buckling of a containment vessel,
3. Excessive deformation in the main O-ring sealing region resulting in the loss of a leaktight seal, and/or
4. Separation of one of the containment vessel lids from its corresponding body.

Indirect damage would require significant impact damage to the surrounding polyurethane foam leading to thermal degradation of the seal material. A significant reduction in polyurethane foam thickness or a gross exposure of the foam through splits or punctures in the outer containment assembly (OCA) outer shell would have to occur near the main O-ring seal or vent port seal region. In a free drop event, such damage could occur as follows:

5. Deformation of the polyurethane foam due to impact could result in an inadequate remaining thickness to prevent seal thermal degradation in the fire event, and/or
6. Deformation of the OCA outer shell could lead to a fissure in the shell material or in a weld, or a puncture through the shell material, thereby exposing foam.

These six issues will now be discussed in detail in the following sections.

2.10.3.5.2.1 Containment Vessel Rupture

Rupture of a containment vessel as a result of the HAC free drop is not credible for the HalfPACT package. In comparison, the TRUPACT-II package was certified utilizing three different certification test packages that were subjected to a large number of 3 foot NCT free drops, and 30 foot HAC free drops. Post-test examination of the TRUPACT-II CTUs revealed no indication of impending rupture of either the OCV or ICV, either as a result of impact forces with the ground or as a result of interaction with the maximum-weight payload. The HalfPACT package is both 25% shorter and 6% lighter than the TRUPACT-II package. Otherwise, construction, including shell thicknesses and foam strength, is essentially identical⁹. Therefore, behavior of the HalfPACT package with regards to containment vessel rupture will be the same, and rupture will not occur as demonstrated during TRUPACT-II package certification testing.

2.10.3.5.2.2 Containment Vessel Buckling

Buckling of a containment vessel as a result of the HAC free drop is also not of concern. As mentioned above, the similar TRUPACT-II package was tested extensively as a part of its certification process. TRUPACT-II testing included a flat bottom impact with cold, -20 °F, polyurethane foam to impose maximum axial impact forces. In these drops, no indication of containment vessel buckling was observed. The HalfPACT package is, however, 6% less gross weight than the TRUPACT-II package, and the OCV body shell ring stiffener is not included. It will now be shown that these differences are insignificant relative to buckling.

Impact acceleration is a function of the crush force and of the package weight, as follows:

$$g = \frac{F}{W}$$

where g is the impact level in units of g s, F is the crush force, and W is the package weight. If weight is reduced and the force is conservatively assumed to remain constant¹⁰, it is possible to determine an impact level for a lighter package based on results for a heavier one. From the TRUPACT-II SAR, the impact for the governing, bottom-down drop, with -20 °F foam, was 385 g . Using the above relation, the maximum bottom-down impact would therefore be $385g \times W_T / W_H = 409g$, where the TRUPACT-II package weight, $W_T = 19,250$ pounds, and the HalfPACT package weight, $W_H = 18,100$ pounds.

The compressive stress in the ICV shell is a function of both the impact load and the weight of the shell. The weight conservatively includes ICV assembly and upper aluminum honeycomb spacer assembly, but does not include the weight of the lower ICV torispherical head. Therefore, the total weight on the ICV shell is approximately 1,722 pounds, resulting in a corresponding compressive stress in the ICV shell of:

⁹ With the exception of the overall reduction in packaging height of 30 inches, the HalfPACT and TRUPACT-II packages differ in only a few minor aspects. The two most notable aspects are removal of the OCV stiffener ring, and beneficially lengthening of the 3/8 inch thick portion of the OCA outer shell, just below the OCA closure joint.

¹⁰ This simplifying assumption is based on an equivalent impact “footprint” for the HalfPACT and TRUPACT-II packages. Due to lower deformation, strain hardening, and geometric considerations, the impact force is somewhat less for the lighter weight HalfPACT package, but is never greater than the TRUPACT-II package.

$$\sigma = \frac{P}{A} = \frac{Wg}{\pi dt} = \frac{(1,722)(409g)}{\pi(72.875)(0.25)} = 12,305 \text{ psi}$$

where the mean diameter of the ICV shell, $d = 72.875$ inches, and the shell thickness, $t = 0.25$ inches. Note that the stress calculated above is less than the equivalent value of 14,192 psi determined in the TRUPACT-II SAR. This result is because, even though the HalfPACT impact is 6% greater than the TRUPACT-II impact, the weight used is 18% less due to a 30 inch shorter OCV body shell length for the HalfPACT package. Therefore, since the governing stress in the HalfPACT ICV shells under worst case cold end drop conditions is lower than for the TRUPACT-II, buckling of the HalfPACT is not of concern.

Similarly, buckling of the OCV is not of concern. As for the TRUPACT-II, the HalfPACT OCV is surrounded by supporting polyurethane foam. And, even though the OCV body ring stiffener is not used on the HalfPACT package as for the TRUPACT-II package, the longest unsupported length for each package is almost identical. Therefore, buckling of the HalfPACT package OCV shell will not occur, and a cold, bottom end drop is not a bounding test.

2.10.3.5.2.3 Excessive Deformation in the Main O-ring Sealing Region

Excessive deformation in the main O-ring sealing region would be most likely to occur in a drop orientation where the seal region is in the impact zone. For the HalfPACT package, where the seal flanges are located approximately halfway along its length, the seal region can experience local impact only in a horizontal side drop. In addition, payload interaction forces between the payload and the ICV are maximized in a side drop since the entire payload inertia force must be carried through the ICV sidewall, and proportionally through the ICV seal region. Excessive deformation of the sealing surfaces could relieve O-ring seal compression and potentially affect leaktight containment. Therefore, a side drop orientation should be tested.

2.10.3.5.2.4 Closure (Lid) Separation

A lid could become partially separated from the body if tensile or moment forces on the lid are high enough to cause permanent deformation of the seal flanges or locking ring. Due to the shape of the HalfPACT package, direct tensile forces separating the lid from the body are not possible for primary impact in a free drop event. For the same reason, moment forces also do not occur at the joint in a horizontal side drop. However, in a near-horizontal orientation, it is possible for moment forces to occur at the lid joint for secondary impact in a slapdown event.

Since lid and closure design for both the TRUPACT-II and HalfPACT packages are identical, and since the TRUPACT-II package was subjected to two different slapdown drop orientations, the lid closure has previously been successfully subjected to such moment forces. It remains to be shown, however, that the moments experienced during TRUPACT-II package certification testing envelop or bound those of the HalfPACT package. Bounding analyses can be done using the methods outlined in NUREG/CR-3966¹¹.

Section 2.2 of NUREG/CR-3966 presents a method for evaluating the axial force, shear force, and bending moment in a package as it undergoes impact, including primary and secondary

¹¹ T. A. Nelson, R. C. Chun, *Methods for Impact Analysis of Shipping Containers*, NUREG/CR-3966, UCID-20639, U.S. Nuclear Regulatory Commission, November 1987.

(slapdown) impacts. The analysis consists of two parts. First, the portion of the total energy that is absorbed by a given impact (say, primary) is determined. Realizing that this energy is equivalent to the area beneath the force-deflection curve for a given drop height and orientation, the maximum force acting on that end of the cask is established. Then, using this force and a quasi-static analysis, the axial, shear, and moment forces in the cask can be determined. These internal force distributions are plotted as a function of force, F , and cask length, L , in Figure 2.7 (primary impact) and Figure 2.10 (secondary impact) of NUREG/CR-3966. Using these relationships, the response of the TRUPACT-II and HalfPACT packages can be compared.

The relevant parameters of each package are defined as follows. The impact limiter in both cases is fully enveloping, and, for simplicity, the nose (primary) and tail (secondary) impact limiters are defined as meeting at the geometric center of the package. The length of the equivalent cask is defined in each case as equal to the length of the payload cavity, plus 2/3 of the length of each aluminum honeycomb spacer. The resulting length is 90.34 inches for the TRUPACT-II package model, and 60.34 inches for the HalfPACT package model, since the length of the HalfPACT package is 30 inches less than the TRUPACT-II package. In both cases, the package inside diameter is $73\frac{5}{8}$ inches at the lower end is the OCV body, and is $76\frac{13}{16}$ inches at the upper end is the OCV lid. In both cases, the outer diameter of the impact limiters is the outside diameter of the OCA outer shell, or $94\frac{3}{8}$ inches. The weight (including the maximum weight payload) is 19,250 pounds for the TRUPACT-II package and 18,100 pounds for the HalfPACT package. The corresponding rotational mass moment of inertia is $89,487 \text{ in-lb-s}^2$ for the TRUPACT-II package and $59,239 \text{ in-lb-s}^2$ for the HalfPACT package.

The method described requires the use of impact limiter, force-deflection curves. These are generated by means of the Packaging Technology computer code, *CASKDROP*¹². Once impact limiter geometry is defined, this program calculates crush force as a function of impact limiter deformation using simple geometry and a foam stress-strain curve. A foam stress-strain curve is used that, for a horizontal side drop of 30 feet, gives the same deformation distance as for the TRUPACT-II certification tests ($3\frac{5}{8}$ inches for CTU No. 1, Test No. 2). An illustration of each package, along with the corresponding *CASKDROP* representation, is given in Figure 2.10.3-8. The forces and moments in the cask are evaluated at a distance “ x ” from the lid end, which is equivalent to the location of the axial center of the OCV locking ring, or 20.0 inches in each case. A drop height of 30 feet is used.

Given the package mass, rotational moment of inertia about its center of gravity, cask length, and angle of primary impact, the energy absorbed by the primary impact limiter can be found from Equation 2.2-10 of NUREG/CR-3966. From the force-deflection curve of the primary impact limiter at the same orientation the maximum force reached in the crush event can be found. Then, given the crush force and the distance, x , the resulting axial force, shear force, and bending moment in the cask at the location of interest (the OCV locking ring) can be found from Equations 2.2-1 through 2.2-3 of NUREG/CR-3966. Similarly, the forces and moments at the OCV locking ring due to the secondary impact can be found as follows: Equation 2.2-11 for the energy absorbed by the secondary impact limiter, the force-deflection curve for the secondary impact from *CASKDROP* (secondary impact is assumed to be horizontal), and Equations 2.2-12

¹² S. A. Porter, *CASKDROP v2.31 – A Computer Program to Determine Cask Force-Deflection Response to a Free Drop*, Packaging Technology, Inc. (PacTec), Tacoma, Washington.

and 2.2-13 for axial, shear, and moment forces. Note that the force-deflection curves are identical for TRUPACT-II and HalfPACT packages.

Since the lid force-deflection curves differ slightly from the body end force-deflection curves (because the cask diameter is $76\frac{13}{16}$ inches at the lid and $73\frac{5}{8}$ inches at the body end), two complete sets of results are obtained for each package: one set is lid primary, body secondary, and the other is body primary, and lid secondary. Primary impact angles of 5° , 10° , and 15° are investigated, plus two special cases for the TRUPACT-II based on orientations used during actual testing. The results are summarized in [Table 2.10.3-1](#). Also included in the table are lid primary impacts with the package's center of gravity over the impacted corner. Results are compared primarily based on shear and moment forces.

Note that for the TRUPACT-II, the forces due to the secondary impact are always greater than for the primary impact, whereas for the HalfPACT, this is not always the case. This outcome is a function of the different relationships between the cask length, L , and the locking ring location, x . Also, note that the worst overall case is for the TRUPACT-II, primary impact angle of 5° , body primary. The worst case actually tested (body primary, impact angle 18°) is within 2% of this maximum value. Importantly, note that none of the HalfPACT results approach these values. The worst case HalfPACT result (lid primary, impact angle 5°) has a shear load and moment of 7,431 pounds and $1.760(10)^7$ in-lb, respectively, which is much less than the actual TRUPACT-II certification test values (body primary, impact angle 18° ; CTU No. 2, Test No. 1) of 477,148 pounds and $2.212(10)^7$ in-lb, respectively. Therefore, the worst case HalfPACT slakedown lid closure forces and moments are bounded by TRUPACT-II certification testing.

2.10.3.5.2.5 Insufficient Residual Foam Thickness for Fire Protection

The package deformations which result from free drop impacts will reduce the thickness of polyurethane foam in the region of damage, with a consequent reduction in the ability of the foam layer to insulate the seal regions during the fire event. If deformation is excessive, thermal degradation of the elastomeric O-rings could occur and the leaktightness of the ICV and/or OCV could be affected. The worst case reduction in thermal resistance would occur where free drop and puncture damage are combined at the most vulnerable location on the package.

Of the two vessels, the OCV is most vulnerable, since as the outermost vessel it is nearest the fire. There are two penetrations in the OCV: the main closure (lid) and the vent port. Since the main seal flanges have considerably more thermal mass than the vent port fitting, the vent port fitting is the more critical location. Puncture damage is discussed in the next section, but for the purposes of choosing the most damaging free drop orientation relative to thermal degradation of the seals in the subsequent fire, the horizontal side drop, with the OCV vent port located in the center of the impact, is the worst case. The only other orientation in which greater local deformation might occur is at the lid knuckle, due to a center of gravity over corner drop. However, this location is relatively far from the sealing regions, and is therefore not as vulnerable in the subsequent fire.

2.10.3.5.2.6 OCA Outer Shell Fracture/Tearing

Deformation of the OCA shell, if it caused a fracture or tear in the base material or weld, would expose foam directly to the fire conditions. The polyurethane foam used in the HalfPACT is intumescent, such that relatively small holes or tears are filled with an expansive char under fire

conditions. Depending on size, fractures or tears are therefore self-healing and do not result in significantly higher temperatures on the inside surface of the foam (i.e., in sealing regions). However, extensive testing of the TRUPACT-II certification packages exhibited no tendency to develop such openings, however, as a result of NCT or HAC free drops, regardless of orientation. This behavior is due to the highly ductile nature of Type 304 stainless steel and the use of full penetration welds for OCA shell construction. Therefore, substantial foam exposure as a result of a free drop is not credible.

2.10.3.5.3 Puncture Drop Tests

10 CFR §71.73(c)(3) requires a free drop of the specimen through a distance of 40 inches onto a puncture bar “in a position for which maximum damage is expected.” As in [Section 2.10.3.5.2, Free Drop Tests](#), the “maximum damage” criterion is evaluated primarily in terms of loss of containment. Loss of containment could occur directly, due to actual puncture bar impact on the package components, or indirectly, by inducing damage which might lead to degradation of sealing capability in the subsequent fire event.

Direct damage would take the form of one of the following:

1. Rupture of one of the containment vessels (ICV or OCV),
2. Separation of the OCV lid from its body,
3. Loss of leaktight capability of the OCV seals due to excessive local deformation of the sealing region, and/or
4. Loss of sealing capability of an ICV or OCV vent port plug.

For seal degradation to occur in a subsequent fire, significant exposure or loss of polyurethane foam would have to occur in the vicinity of the O-ring seals as a result of puncture damage. Such damage might occur as follows:

5. Deformation of the OCA shell due to puncture bar impact, when added to the deformation arising from the free drop, could result in inadequate remaining thickness to prevent local seal thermal degradation in the fire event, and/or
6. Puncture bar impact could result in a fissure in the OCA material or weld, exposing significant foam to the fire event.

These issues will now be discussed in detail in the following sections.

2.10.3.5.3.1 Containment Vessel Rupture

Rupture of one of the containment vessels is not a likely failure mode. The TRUPACT-II certification test packages were subjected to a number of puncture drops where the bar axis was aligned with the package center of gravity. The worst damage to the containment vessels was a relatively insignificant denting of the OCV in a region well removed from the seal regions. Due to its similar geometry but lighter weight, the HalfPACT package is slightly less susceptible to puncture bar damage than the TRUPACT-II. Therefore, direct rupture of the containment vessels will not occur for the HalfPACT.

2.10.3.5.3.2 Closure (Lid) Separation

Separation of the OCV lid due to puncture bar impact is extremely unlikely. To rip the OCV lid off of the OCV body would require failure of the OCV locking ring, which cannot occur due to puncture bar impact. The potential energy available in a 40 inch puncture drop is equal to $40/(12 \times 30) = 11.1\%$ of the energy available in the 30 foot free drop. As shown in [Section 2.10.3.5.2.4, Closure \(Lid\) Separation](#), the greatest lid separation loads that are to be applied in the near-horizontal slapdown drop are not able to separate the OCV lid. Therefore, separation of the lid in a 40 inch puncture drop is not credible. To make such an event even more unlikely, the orientation of the puncture bar that is necessary to apply a separating load on the lid joint is such that it diverges from the package center of gravity, thus reducing the energy available to apply to the joint. Therefore, separation of the OCV lid due to puncture bar impact will not occur for the HalfPACT package. Local puncture bar damage is discussed below.

2.10.3.5.3.3 Loss of Lid Sealing Integrity

Loss of leaktight capability of the OCV seals due to local puncture bar deformation is not likely. This behavior is because, due to the presence of increased thickness (3/8 inch) OCA shells in the sealing region, of Z-flanges, and of polyurethane foam, virtually all of the puncture drop energy is absorbed before significant deformation of the OCV sealing area has taken place. This behavior was demonstrated during TRUPACT-II certification testing, by means of drops where the puncture bar axis was aligned with the OCV sealing area and the package center of gravity (TRUPACT-II CTU No. 2, Test No. 8, and CTU No. 3, Test No. 8). Therefore, loss of leaktight capability of the OCV seals due to local puncture bar deformation will not occur for the HalfPACT package. However, for reasons discussed below, a puncture bar impact is planned which will be located very near the OCV sealing area, with the axis passing through the package center of gravity, and which will simultaneously demonstrate the ability of the HalfPACT package to sustain such damage without loss of its leaktight capability.

2.10.3.5.3.4 Loss of Vent Port Sealing Integrity

Loss of sealing capability of an ICV or OCV vent port plug is unlikely for the same reasons cited in [Section 2.10.3.5.3.3, Loss of Lid Sealing Integrity](#). Since deformation of the OCV in any puncture drop is minimal, only the OCV vent port plug could possibly be affected by a puncture impact. Due to the small size of the plug, and to protection by surrounding structure, deformations do not reach the level at which the seal could be affected. This behavior was well demonstrated during TRUPACT-II certification testing (CTU No. 1, Test No. 5; CTU No. 2, Test No. 7; and CTU No. 3, Test No. 7). Again, for reasons discussed below, a puncture bar impact is planned to occur directly over the OCV vent port, in alignment with the package center of gravity, and in combination with compounded NCT and HAC side drop damage. This test will amply demonstrate the ability of the HalfPACT package to sustain such damage without loss of OCV vent port leaktight capability.

2.10.3.5.3.5 Insufficient Residual Foam Thickness for Fire Protection

Deformation of the OCA shell due to puncture bar impact, when added to the deformation arising from the free drop, could result in inadequate remaining thickness to prevent local seal thermal degradation in the fire event. Therefore, a puncture drop is planned in which damage from free drop and puncture are combined, with the puncture located directly over the OCV vent

port, as discussed above in [Section 2.10.3.5.2, Free Drop Tests](#), and [Section 2.10.3.5.3.4, Loss of Vent Port Sealing Integrity](#).

2.10.3.5.3.6 OCA Outer Shell Fracture/Tearing

Puncture bar impact could result in a fracture or tear of the OCA outer shell base material or weld, exposing significant foam to the fire event. The polyurethane foam used in the HalfPACT is intumescent, such that holes (such as puncture bar holes) or relatively small tears are filled with an expansive char under fire conditions. Depending on size, holes or tears are therefore self-healing and do not result in significantly higher temperatures on the inside surface of the foam, i.e., near sealing regions.

The likelihood of creating significant damage is increased by use of an oblique angle between the puncture bar and the package surface. It is also increased by the presence of a transition in package outer shell thickness. In the case of the HalfPACT package, the OCA outer shell experiences a transition in thickness from 1/4 inch to 3/8 inch, located approximately 19 inches below the lid-to-body interface joint. The 3/8 inch thickness is located above the transition. The angle of the package to the horizontal is approximately 20°. A puncture drop at this location is the most likely to produce relevant damage, since:

- a transition in shell thickness, including a full penetration weld, is located there,
- the puncture bar axis, aligned with the package center of gravity, has an oblique orientation to the package surface, increasing its likelihood to “bite” and rip the shell, and
- the location is close to the sealing region, relative to thermal degradation in the fire event.

Further down the package, even though the puncture bar orientation would be more oblique, there is no comparable shell thickness transition, and additionally, would be farther away from the vulnerable seal region. Farther up the package (closer to the lid-to-body joint), even though the puncture damage would be closer to the seals, the outer shell thickness has no transition, is thicker (3/8 inch), and the puncture bar orientation is nearer to perpendicular to the package, thus minimizing its potential to “bite” and rip the shell. As described in the next section, in order to fully explore the potential of this puncture orientation, two separate puncture events are planned.

The circumferential location for the impact is chosen such that the worst-case damage at the OCV vent port and the worst case damage from one of the two punctures discussed here can both be simultaneously placed in the hottest part of the fire in the subsequent fire test. The hottest part of the fire is located approximately 1½ meters above the fuel surface¹³. Since the lowest part of the package is located one meter above the fuel surface (per 10 CFR §71.73(c)(4)), the damage must be 1/2 meter, or approximately 20 inches, above the lowest part of the package. If two damage locations are to be thus placed, they must be separated by approximately 110°, based on the HalfPACT package outside diameter. Thus, since either of the two puncture events

¹³ M. E. Schneider and L. A. Kent, *Measurements of Gas Velocities and Temperatures in a Large Open Pool Fire*, Sandia National Laboratories (reprinted from *Heat and Mass Transfer in Fire*, A. K. Kulkarni and Y. Jaluria, Editors, HTD-Vol. 73 (Book No. H00392), American Society of Mechanical Engineers). Figure 3 shows that maximum temperatures occur at an elevation approximately 2.3 meters above the pool floor. The pool was initially filled with water and fuel to a level of 0.814 meters. The maximum temperatures therefore occur approximately 1½ meters above the level of the fuel, i.e., 1/2 meter above the lowest part of the package when set one meter above the fuel source per the requirements of 10 CFR §71.73(c)(4).

discussed here most likely create the maximum damage in conjunction with the OCV vent port side drop/puncture drop damage, one is placed 110° counter-clockwise and the other 110° clockwise from the OCV vent port. In the fire, the OCV vent port damage, plus the worst one of the other two puncture damage sites, will therefore be placed in the hottest part of the fire.

2.10.3.5.4 Fire Test

At the conclusion of free drop and puncture drop testing, the HalfPACT test units will be subjected to a fully engulfing pool fire test in accordance with 10 CFR §71.73(c)(4). The package will be oriented horizontally in the flames and minimally supported to least impede the heat flow into the package. The combined damage due to the free and puncture drops on the OCV vent port region will be located in the hottest portion of the fire, i.e., 1½ meters above the fuel surface, i.e., 1/2 meter above the lowest part of the package. The damage due to other puncture drops will be evaluated, and the most damaging puncture test oriented similarly at 1/2 meter above the lowest part of the package.

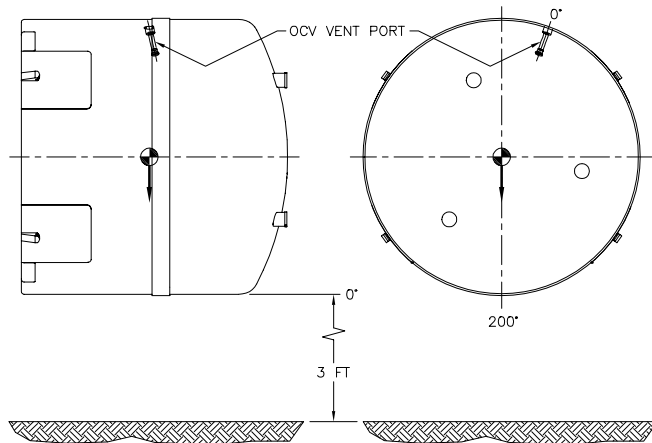
Justification is provided in [Section 2.10.3.5.1, *Initial Test Conditions*](#), for using ambient pressure and temperature in the HalfPACT test units. Temperature indicating labels will be used with the HalfPACT CTU to determine the maximum temperature in the O-ring seal region during the HAC fire test. Determination of the maximum O-ring seal region temperature must account for ambient temperature conditions starting below the HAC fire test initial temperatures predicted in [Section 3.5.3, *Package Temperatures*](#). This will be accomplished by adding the temperature differential between the actual ambient temperature and the analytically predicted O-ring seal region starting temperature to the average measured O-ring seal region temperature. Although conservative, the result will be directly comparable to measured TRUPACT-II certification fire test temperatures in the O-ring seal regions. As discussed in [Section 2.10.3.5.1, *Initial Test Conditions*](#), a maximum O-ring seal region temperature of 300 °F for HalfPACT fire testing shall be considered acceptable.

2.10.3.6 Test Sequence for Selected Free Drop, Puncture Drop, and Fire Tests

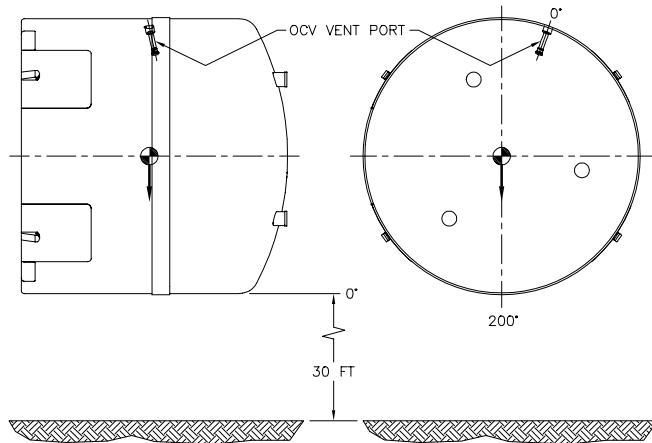
The following sections establish the selected free drop, puncture drop, and fire test sequence for both the HalfPACT engineering test unit (ETU) and HalfPACT certification test unit (CTU) based on the discussions provided in [Section 2.10.3.5, *Technical Basis for Tests*](#). The test sequences are summarized in [Table 2.10.3-2](#) and [Table 2.10.3-3](#), and illustrated in [Figure 2.10.3-9](#) and [Figure 2.10.3-10](#) for the ETU and CTU, respectively.

2.10.3.6.1 Engineering Test Unit (ETU)

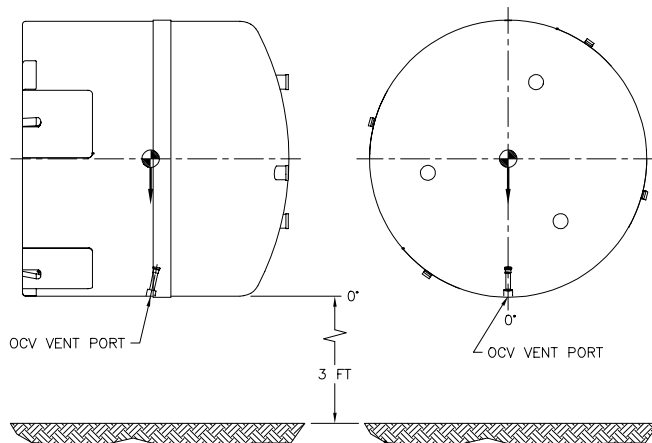
Free Drop No. 1 is a NCT free drop from a height of three feet, impacting horizontally on the ETU side, parallel to the forklift pockets, nearly opposite the OCV vent port. The three foot drop height is based on the requirements of 10 CFR §71.71(c)(7) for a package weight between 11,000 and 22,000 pounds. The purpose of this drop test is to demonstrate that the NCT free drop does not compromise the ability of the HalfPACT package to successfully sustain subsequent HAC test events in the same or other orientations.



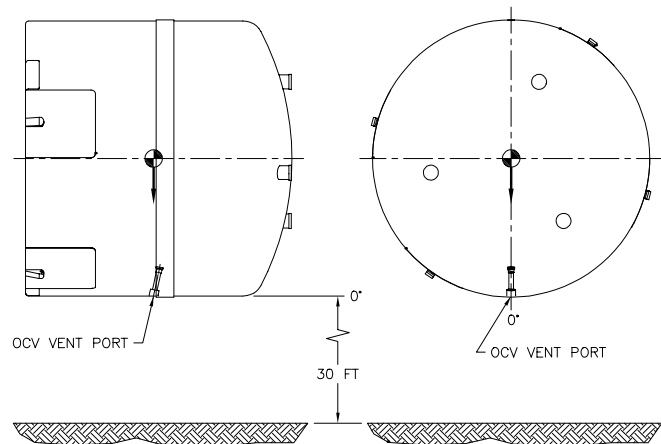
Free Drop No. 2 is a HAC free drop from a height of 30 feet, impacting horizontally on the ETU side, parallel to the forklift pockets, nearly opposite the OCV vent port. In this way, NCT and HAC free drop damage is cumulative. The 30 foot drop height is based on the requirements of 10 CFR §71.73(c)(1). The purpose of Free Drops Nos. 1 and 2, combined with Puncture Drop No. 7, is to create the greatest possible cumulative damage (i.e., the greatest reduction in foam thickness) in a region punctured through the OCA outer shell.



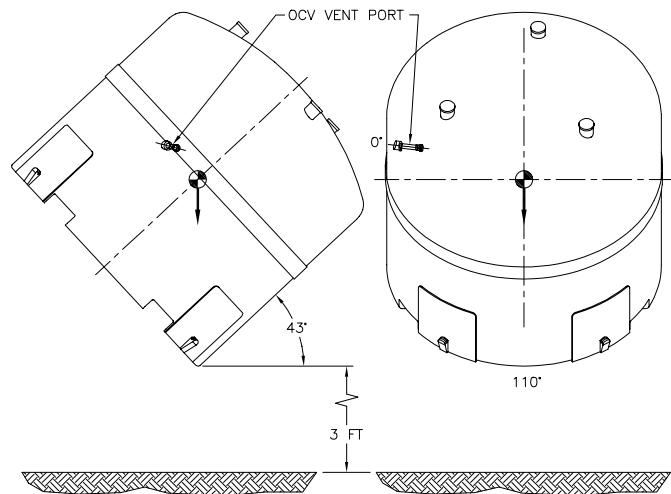
Free Drop No. 3 is a NCT free drop from a height of three feet, impacting horizontally on the ETU side, with the OCV vent port oriented downward. The three foot drop height is based on the requirements of 10 CFR §71.71(c)(7) for a package weight between 11,000 and 22,000 pounds. The purpose of this drop test is to demonstrate that the NCT free drop does not compromise the ability of the HalfPACT package to successfully sustain subsequent HAC test events in the same or other orientations.



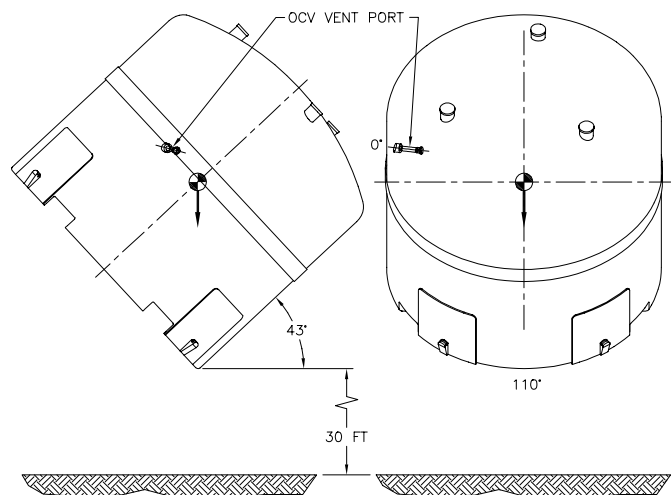
Free Drop No. 4 is a HAC free drop from a height of 30 feet, impacting horizontally on the ETU side, with the OCV vent port oriented downward. In this way, NCT and HAC free drop damage is cumulative. The 30 foot drop height is based on the requirements of 10 CFR §71.73(c)(1). The purpose of Free Drops Nos. 3 and 4, combined with Puncture Drop No. 8, is to create the greatest possible cumulative damage (i.e., the greatest reduction in foam thickness) over the OCV vent port.



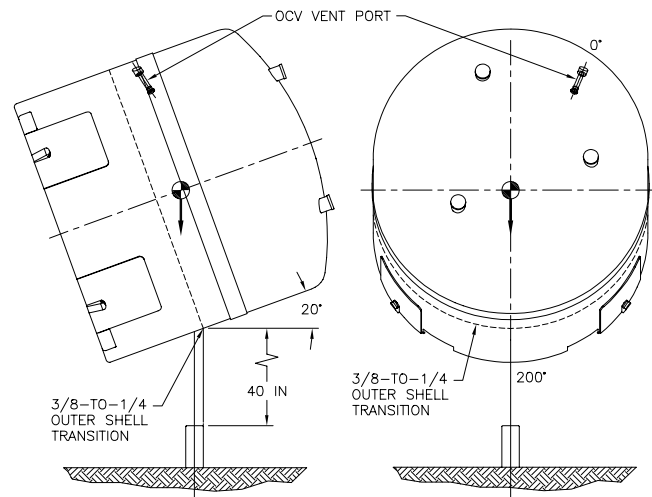
Free Drop No. 5 is a NCT free drop from a height of three feet, impacting the ETU bottom corner perpendicular to the forklift pockets, with the package's center of gravity over the impact point. The three foot drop height is based on the requirements of 10 CFR §71.71(c)(7) for a package weight between 11,000 and 22,000 pounds. The purpose of this drop test is to demonstrate that the NCT free drop does not compromise the ability of the HalfPACT package to successfully sustain subsequent HAC test events in the same or other orientations.



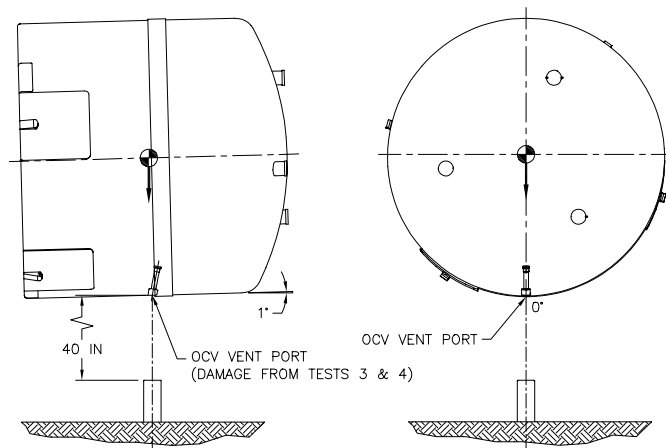
Free Drop No. 6 is a HAC free drop from a height of 30 feet, impacting the ETU bottom corner perpendicular to the forklift pockets, with the package's center of gravity over the impact point. In this way, NCT and HAC free drop damage is cumulative. The 30 foot drop height is based on the requirements of 10 CFR §71.73(c)(1). The purpose of Free Drops Nos. 5 and 6, combined with Puncture Drop No. 9, is to create the greatest possible cumulative damage in a region not tested during TRUPACT-II testing.



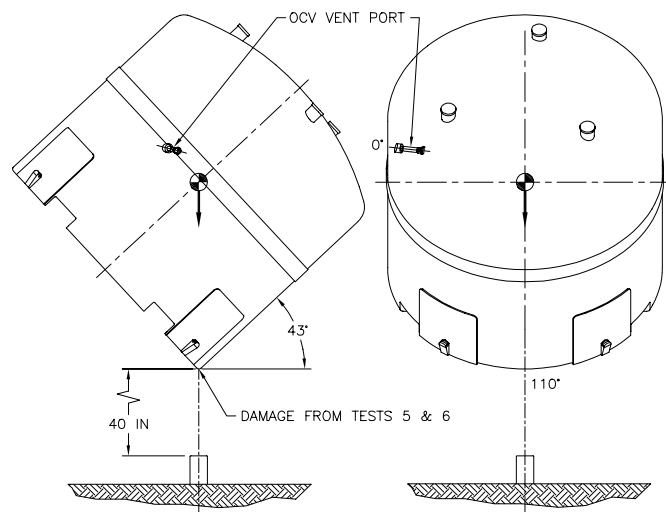
Puncture Drop No. 7 impacts directly onto the damage created by Free Drop Tests 1 and 2, directly below the 3/8-to-1/4 inch, OCA outer shell transition. The puncture drop height is based on the requirements of 10 CFR §71.73(c)(3). The purpose of Puncture Drop No. 7 is to breach the 1/4 inch thick OCA outer shell. Testing of this package region, when cumulatively damaged from the free drops, puncture drop, and fire testing demonstrate that containment integrity is maintained for the main OCV O-ring seal.



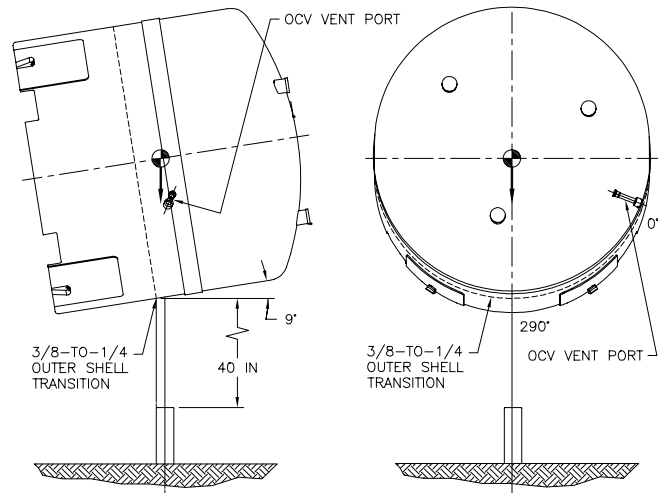
Puncture Drop No. 8 impacts directly onto the OCV vent port opening, compounding the cumulative damage created by Free Drop Tests 3 and 4. The puncture drop height is based on the requirements of 10 CFR §71.73(c)(3). The purpose of Puncture Drop No. 8 is to create the greatest cumulative damage (i.e., greatest reduction in foam thickness) over the OCV vent port region. Testing of this package region, when cumulatively damaged from the free drops, puncture drop, and fire testing, demonstrate that containment integrity is maintained for the OCV vent port O-ring seal.



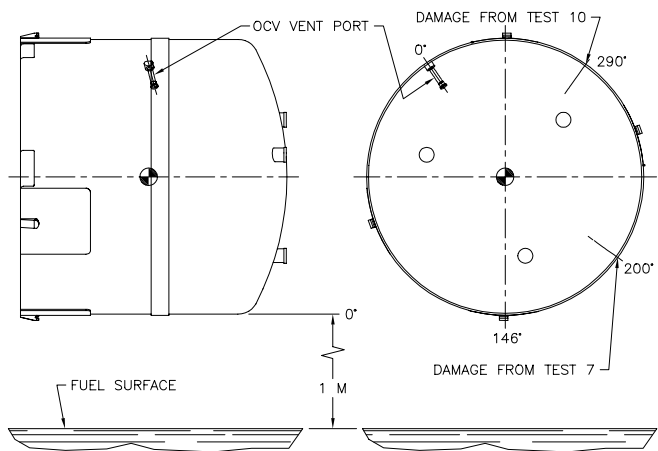
Puncture Drop No. 9 impacts directly onto the cumulative damage created by Free Drop Tests 5 and 6. The puncture drop height is based on the requirements of 10 CFR §71.73(c)(3). The purpose of Puncture Drop No. 9 is to create the greatest possible cumulative damage in a region not tested during TRUPACT-II testing. Testing of this package region, when cumulatively damaged from the free drops, puncture drop, and fire testing, demonstrates that containment integrity is maintained for the main OCV O-ring containment seal.



Puncture Drop No. 10 impacts directly above the 3/8-to-1/4 inch transition in the OCA body outer shell. The puncture drop height is based on the requirements of 10 CFR §71.73(c)(3). The purpose of Puncture Drop No. 10 is to attempt to break the circumferential weld at the 3/8-to-1/4 inch transition in the OCA body outer shell. Testing of this package region, when cumulatively damaged from the puncture drop and fire tests, demonstrates that containment integrity is maintained for the OCV vent port and main O-ring containment seals.

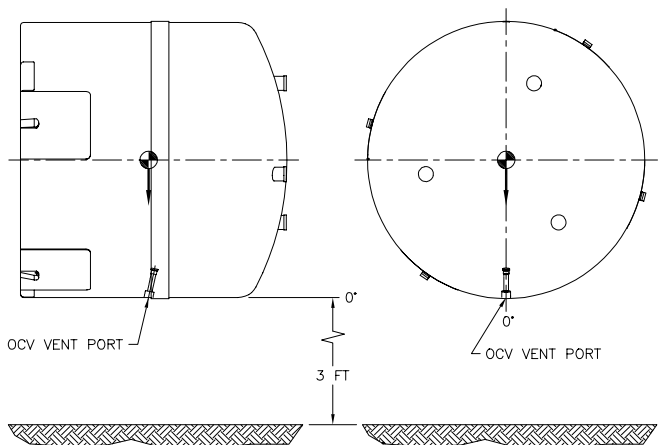


Fire No. 11 is performed by orienting the cumulative damage from Free Drop Tests 1 and 2, and Puncture Drop Test 7 at the hottest location in the fire (i.e., one meter above the fuel surface). The puncture damage from Puncture Drop No. 10 is oriented above the hole created by Puncture Drop No. 7 in an attempt to create a “chimney” through the foam cavity inside the OCA body.

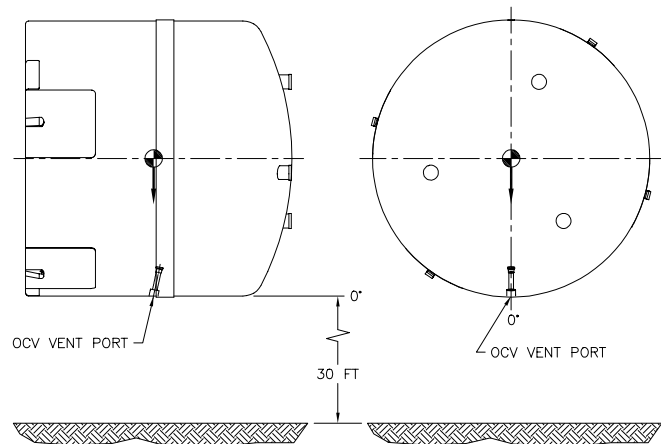


2.10.3.6.2 Certification Test Unit (CTU)

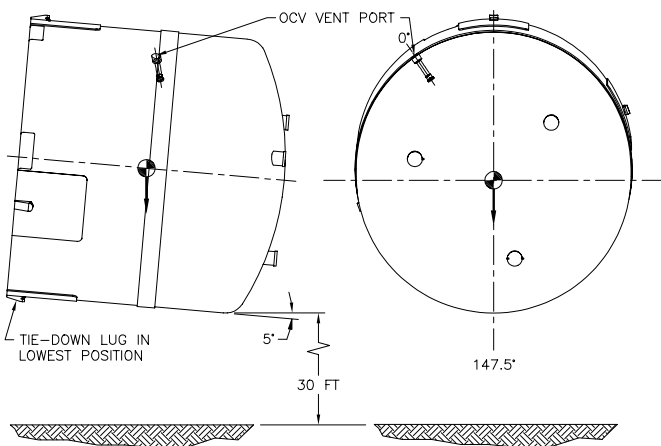
Free Drop No. 1 is a NCT free drop from a height of three feet, impacting horizontally on the CTU side, with the OCV vent port oriented downward. The three foot drop height is based on 10 CFR §71.71(c)(7) for a package weight between 11,000 and 22,000 pounds. The purpose of this drop test is to demonstrate that the NCT free drop does not compromise the ability of the HalfPACT package to successfully sustain the subsequent HAC test events in the same or other orientations.



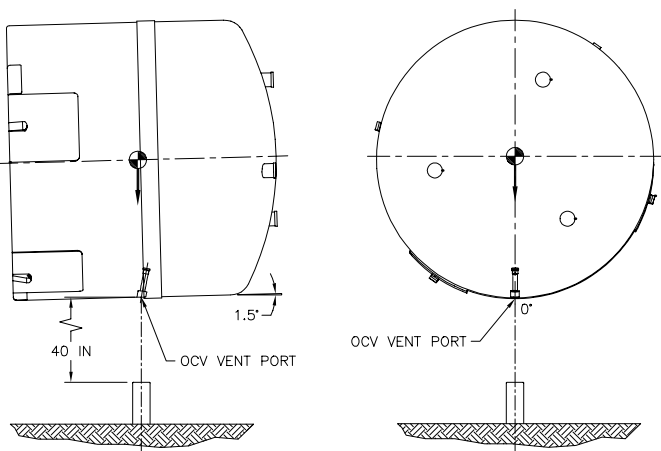
Free Drop No. 2 is a HAC free drop from a height of 30 feet, impacting horizontally on the CTU side, with the OCV vent port oriented downward. In this way, NCT and HAC free drop damage is cumulative. The 30 foot drop height is based on the requirements of 10 CFR §71.73(c)(1). The purpose of Free Drops Nos. 1 and 2, combined with Puncture Drop No. 4, is to create the greatest possible cumulative damage (i.e., the greatest reduction in foam thickness) over the OCV vent port.



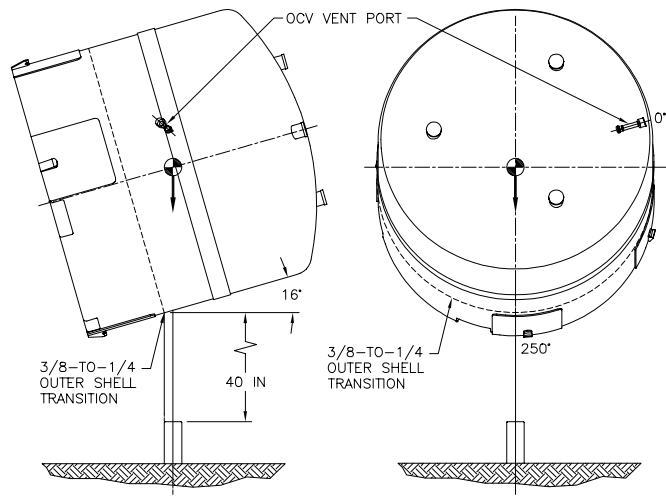
Free Drop No. 3 is a HAC free drop from a height of 30 feet, impacting 5° from horizontal with primary impact on the lid and secondary impact on a body tie-down lug. Although shown in [Section 2.10.3.5.2.4, Closure \(Lid\) Separation](#), to be bounded by TRUPACT-II certification testing, the purpose of this drop is to apply the greatest separation forces to the closures. This test demonstrates retention of the lids, and that containment integrity is not compromised by this worst-case slapdown condition.



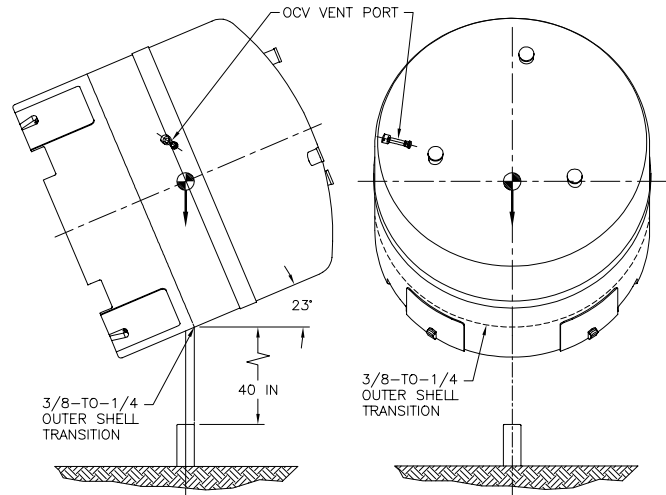
Puncture Drop No. 4 impacts directly onto the OCV vent port opening, compounding the damage created by Free Drop Tests 1 and 2. The puncture drop height is based on the requirements of 10 CFR §71.73(c)(3). The purpose of Puncture Drop No. 4 is to create the greatest cumulative damage (i.e., greatest reduction in foam thickness) over the OCV vent port region, thereby demonstrating that containment integrity is maintained for the OCV vent port O-ring seal.



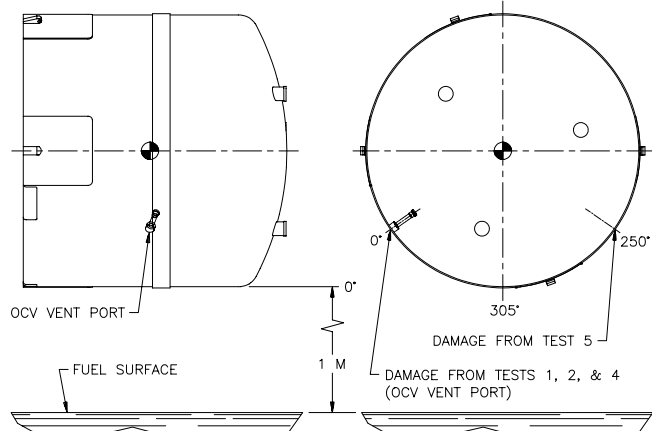
Puncture Drop No. 5 impacts directly above the 3/8-to-1/4 inch transition in the OCA body outer shell. The puncture drop height is based on the requirements of 10 CFR §71.73(c)(3). The purpose of Puncture Drop No. 5 is to attempt to break the circumferential weld at the 3/8-to-1/4 inch transition in the OCA body outer shell. Testing of this package region, when cumulatively damaged from the puncture drop and fire tests, demonstrates that containment integrity is maintained for the OCV vent port and main O-ring containment seals.



Puncture Drop No. 6 impacts directly onto the damage created by Free Drop Tests 1 and 2, directly below the 3/8-to-1/4 inch, OCA outer shell transition. The puncture drop height is based on the requirements of 10 CFR §71.73(c)(3). The purpose of Puncture Drop No. 6 is to breach the 1/4 inch thick OCA outer shell. Testing of this package region, when cumulatively damaged from the free drops, puncture drop, and fire testing demonstrate that containment integrity is maintained for the main OCV O-ring seal.



Fire No. 7 is performed by orienting the cumulative damage from Free Drop Tests 1 and 2, and Puncture Drop Test 4, at the hottest location in the fire (i.e., one meter above the fuel surface). In addition, the package is oriented to include the puncture damage from Puncture Drop No. 5 at the hottest location in the fire, directly opposite the damage from Free Drop Tests 1 and 2, and Puncture Drop Test 4.



2.10.3.7 Test Results

The following sections report the results of free drop, puncture drop, and fire tests following the sequence provided in [Section 2.10.3.6, *Test Sequence for Selected Free Drop, Puncture Drop, and Fire Tests*](#). Results are summarized in [Table 2.10.3-2](#) and [Table 2.10.3-3](#) for the ETU and CTU, respectively (also, see [Figure 2.10.3-9](#) and [Figure 2.10.3-10](#), respectively).

As can be seen in the subsequent sections, overall deformation and temperature results agree closely with those reported in the TRUPACT-II SAR.

[Figure 2.10.3-12](#) through [Figure 2.10.3-95](#) sequentially photo-document the engineering and certification testing process for the HalfPACT ETU and CTU, respectively.

2.10.3.7.1 Engineering Test Unit (ETU)

2.10.3.7.1.1 ETU Free Drop Test No. 1

Free Drop No. 1 was a NCT free drop from a height of three feet, impacting horizontally on the ETU side, parallel to the forklift pockets, nearly opposite the OCV vent port. As shown in [Figure 2.10.3-9](#), the HalfPACT ETU was oriented horizontal to the impact surface (meridional angle (i.e., pitch) = 0°), and circumferentially aligned to impact 200° from the OCA vent port (between the tie-down lugs, with the forklift pockets oriented vertically). The following list summarizes the test parameters:

- verified meridional angle as 0° ±1°
- verified circumferential angle to be 200° ±1°
- verified free drop height as 3 feet, +1/-0 inches (actual drop height 3 feet, 1/2 inches)
- measured temperature at 53 °F at time of test
- conducted test at 9:54 a.m. on Tuesday, 2/18/97

A very slight rebound (bounce) occurred upon impact. The measured permanent deformations of the ETU were flats 16 inches wide at the OCA top, and 18 inches wide at the OCA bottom, corresponding to a crush depth of approximately 3/4 inches. In comparison, from the TRUPACT-II SAR for CTU No. 1, Test 1, the measured permanent deformations were flats 18 inches wide at both the OCA top and bottom.

2.10.3.7.1.2 ETU Free Drop Test No. 2

Free Drop No. 2 was a HAC free drop from a height of 30 feet, impacting horizontally on the ETU side, parallel to the forklift pockets, nearly opposite the OCV vent port. As shown in [Figure 2.10.3-9](#), the HalfPACT ETU was oriented horizontal to the impact surface (meridional angle (i.e., pitch) = 0°), and circumferentially aligned to impact 200° from the OCA vent port (between the tie-down lugs, with the forklift pockets oriented vertically). The following list summarizes the test parameters:

- verified meridional angle as 0° ±1°
- verified circumferential angle to be 200° ±1°

- verified free drop height as 30 feet, +3/-0 inches (actual drop height 30 feet, 1 inch)
- measured temperature at 57 °F at time of test
- conducted test at 1:10 p.m. on Tuesday, 2/18/97

A small rebound (bounce) occurred upon impact. The measured permanent deformations of the ETU were flats 36 inches wide at the OCA top, and 33 inches wide at the OCA bottom, corresponding to a crush depth of approximately 3¼ inches. In comparison, from the TRUPACT-II SAR for CTU No. 1, Test 2, the measured permanent deformation were flats 37 inches wide at the OCA top, and 35 inches wide at the OCA bottom.

2.10.3.7.1.3 ETU Free Drop Test No. 3

Free Drop No. 3 was a NCT free drop from a height of three feet, impacting horizontally on the ETU side, with the OCV vent port oriented downward. As shown in [Figure 2.10.3-9](#), the ETU was oriented horizontal to the impact surface (meridional angle (i.e., pitch) = 0°), and circumferentially aligned to impact directly onto the OCV vent port. The following list summarizes the test parameters:

- verified meridional angle as 0° ±1°
- verified circumferential angle to be 0° ±1°
- verified free drop height as 3 feet, +1/-0 inches (actual drop height 3 feet, 3/4 inches)
- measured temperature at 40 °F at time of test
- conducted test at 10:20 a.m. on Wednesday, 2/19/97

A very slight rebound (bounce) occurred upon impact. The measured permanent deformation of the ETU were flats 18 inches wide at both the OCA top and bottom, corresponding to a crush depth of approximately 3/4 inches. In comparison, from the TRUPACT-II SAR for CTU No. 1, Test 1, the measured permanent deformations were flats 18 inches wide at both the OCA top and bottom.

2.10.3.7.1.4 ETU Free Drop Test No. 4

Free Drop No. 4 was a HAC free drop from a height of 30 feet, impacting horizontally on the ETU side, with the OCV vent port oriented downward. As shown in [Figure 2.10.3-9](#), the ETU was oriented horizontal to the impact surface (meridional angle (i.e., pitch) = 0°), and circumferentially aligned to impact directly onto the OCV vent port. The following list summarizes the test parameters:

- verified meridional angle as 0° ±1°
- verified circumferential angle to be 0° ±1°
- verified drop height as 30 feet, +3/-0 inches (actual drop height 30 feet, 2 inches)
- measured temperature at 48 °F at time of test
- conducted test at 1:47 p.m. on Wednesday, 2/19/97

A small rebound (bounce) occurred upon impact. The measured permanent deformations of the ETU were flats 34 inches wide at both the OCA top and bottom, corresponding to a crush depth of approximately 3¼ inches. In comparison, from the TRUPACT-II SAR for CTU No. 1, Test 2,

the measured permanent deformation were flats 37 inches wide at the OCA top, and 35 inches wide at the OCA bottom.

2.10.3.7.1.5 ETU Free Drop Test No. 5

Free Drop No. 5 was a NCT free drop from a height of three feet, impacting the ETU bottom corner perpendicular to the forklift pockets, with the package's center of gravity over the impact point. As shown in [Figure 2.10.3-9](#), the ETU was oriented at an angle 43° from horizontal relative to the impact surface (meridional angle (i.e., pitch) = 43°), and circumferentially aligned to impact 110° from the OCA vent port (between the tie-down lugs, with the forklift pockets oriented horizontally). The following list summarizes the test parameters:

- verified meridional angle as 43° ±1°
- verified circumferential angle to be 110° ±1°
- verified free drop height as 3 feet, +1/-0 inches (actual drop height 3 feet, 5/8 inches)
- measured temperature at 53 °F at time of test
- conducted test at 10:14 a.m. on Thursday, 2/20/97

A very slight rebound (bounce) occurred upon impact. The measured permanent deformation of the ETU was a flat 26 inches long and 5½ inches wide at the bottom corner, corresponding to a crush depth of approximately 1¾ inches. No applicable comparison is available from the TRUPACT-II SAR.

2.10.3.7.1.6 ETU Free Drop Test No. 6

Free Drop No. 6 was a HAC free drop from a height of 30 feet, impacting the ETU bottom corner perpendicular to the forklift pockets, with the package's center of gravity over the impact point. As shown in [Figure 2.10.3-9](#), the ETU was oriented at an angle 43° from horizontal relative to the impact surface (meridional angle (i.e., pitch) = 43°), and circumferentially aligned to impact 110° from the OCA vent port (between the tie-down lugs, with the forklift pockets oriented horizontally). The following list summarizes the test parameters:

- verified meridional angle as 43° ±1°
- verified circumferential angle to be 110° ±1°
- verified free drop height as 30 feet, +1/-0 inches (actual drop height 30 feet, 1 inch)
- measured temperature at 55 °F at time of test
- conducted test at 1:53 p.m. on Thursday, 2/20/97

A small rebound (bounce) occurred upon impact. The measured permanent deformation of the ETU was a flat 40 inches long and 12 inches wide at the bottom corner, corresponding to a crush depth of approximately 3¼ inches. In comparison, from the TRUPACT-II SAR for CTU No. 1, Test 3, the measured permanent deformation was a flat 53 inches long and 30 inches wide at the top corner (on the knuckle radius of the torispherical head), corresponding to a crush depth of approximately 3¾ inches.

2.10.3.7.1.7 ETU Puncture Drop Test No. 7

Puncture Drop No. 7 impacted directly onto the damage created by Free Drop Tests 1 and 2, directly below the 3/8-to-1/4 inch, OCA outer shell transition. As shown in [Figure 2.10.3-9](#), the ETU was oriented at an angle 20° from horizontal relative to the impact surface (meridional angle (i.e., pitch) = 20°), and circumferentially aligned to impact 200° from the OCA vent port (between the tie-down lugs, with the forklift pockets oriented vertically). This orientation placed the puncture bar impact directly adjacent to and below the 3/8-to-1/4 inch thick transition in the OCA body outer shell (i.e., on the 1/4 inch thick shell). The following list summarizes the test parameters:

- verified meridional angle as $20^\circ \pm 1^\circ$
- verified circumferential angle to be $200^\circ \pm 1^\circ$
- verified puncture drop height as 40 +1/-0 inches (actual drop height 40¼ inches)
- measured temperature at 38 °F at time of test
- conducted test at 11:04 a.m. on Friday, 2/21/97

The puncture drop penetrated the OCA outer shell in the region damaged by Free Drop Tests 1 and 2. The measured permanent deformation of the ETU was a hole 10½ inches long and 11½ inches wide, measuring 8 inches deep radially and 11 inches deep along the axis of the puncture bar. Although no direct comparison is available, similar results may be obtained from the TRUPACT-II SAR. As shown in the TRUPACT-II SAR for CTU No. 1, Test 7, a similar hole occurred in the CTU body approximately 12 inches long. Further, as shown in the TRUPACT-II SAR for CTU No. 2, Test R, a similar hole occurred in the CTU body approximately 9½ inches deep along the axis of the puncture bar. From the TRUPACT-II SAR for CTU No. 2, Test 4, a similar hole occurred in the CTU head approximately 7 inches deep along the axis of the puncture bar. From the TRUPACT-II SAR for CTU No. 3, Test 4, a similar hole occurred in the CTU body approximately 8 inches deep along the axis of the puncture bar. Of final note, from the TRUPACT-II SAR for CTU No. 2, Test 4, similar puncture bar damage occurred at approximately the same distance from the main OCV containment O-ring seal as the damage produced on the HalfPACT ETU for this test.

2.10.3.7.1.8 ETU Puncture Drop Test No. 8

Puncture Drop No. 8 impacted directly onto the OCV vent port opening, compounding the cumulative damage created by Free Drop Tests 3 and 4. As shown in [Figure 2.10.3-9](#), the ETU was oriented at an angle 1° from horizontal relative to the impact surface (meridional angle (i.e., pitch) = 1°), and circumferentially aligned to impact directly onto the OCV vent port. The following list summarizes the test parameters:

- verified meridional angle as $1^\circ \pm 1^\circ$ (i.e., package top-end slightly raised)
- verified circumferential angle to be $0^\circ \pm 1^\circ$
- verified puncture drop height as 40 +1/-0 inches (actual drop height 40⅜ inches)
- measured temperature at 40 °F at time of test
- conducted test at 2:42 p.m. on Friday, 2/21/97

The puncture drop impacted the OCA outer shell in the region damaged by Free Drop Tests 3 and 4, and was offset approximately six inches from the OCV vent port due to high crosswinds. The measured permanent deformation of the ETU was a non-penetrating radial dent 2½ inches deep. In comparison, from the TRUPACT-II SAR for CTU No. 1, Test 5, the measured permanent deformation was a non-penetrating radial dent 3 inches deep.

2.10.3.7.1.9 ETU Puncture Drop Test No. 9

Puncture Drop No. 9 impacts directly onto the cumulative damage created by Free Drop Tests 5 and 6. As shown in [Figure 2.10.3-9](#), the ETU was oriented at an angle 43° from horizontal relative to the impact surface (meridional angle (i.e., pitch) = 43°), and circumferentially aligned to impact 110° from the OCA vent port (between the tie-down lugs, with the forklift pockets oriented horizontally). This orientation placed the puncture bar impact directly over the OCA bottom corner onto the damage created by Free Drop Tests 5 and 6. The following list summarizes the test parameters:

- verified meridional angle as 43° ±1°
- verified circumferential angle to be 110° ±1°
- verified puncture drop height as 40 +1/-0 inches (actual drop height 40¼ inches)
- measured temperature at 28 °F at time of test
- conducted test at 12:26 p.m. on Monday, 2/24/97

The puncture drop impacted the OCA outer shell, centered on the corner drop damage created by drop tests 5 and 6. The measured permanent deformation of the ETU was a dent 3 inches deep along the axis of the puncture bar, with no penetration. In comparison, from the TRUPACT-II SAR for CTU No. 2, Test 5, resulted in a measured permanent deformation as a dent approximately 5 inches deep along the axis of the puncture bar.

2.10.3.7.1.10 ETU Puncture Drop Test No. 10

Puncture Drop No. 10 impacted directly above the 3/8-to-1/4 inch transition in the OCA body outer shell. As shown in [Figure 2.10.3-9](#), the ETU was oriented at an angle 9° from horizontal relative to the impact surface (meridional angle (i.e., pitch) = 9°), and circumferentially aligned to impact 290° from the OCA vent port (between the tie-down lugs, with the forklift pockets oriented horizontally). This orientation placed the puncture bar impact directly adjacent to and above the 3/8-to-1/4 inch thick transition in the OCA body outer shell (i.e., on the 3/8 inch thick shell). The following list summarizes the test parameters:

- verified meridional angle as 9° ±1°
- verified circumferential angle to be 290° ±1°
- verified puncture drop height as 40 +1/-0 inches (actual drop height 40¼ inches)
- measured temperature at 29 °F at time of test
- conducted test at 11:43 a.m. on Tuesday, 2/25/97

The puncture drop impacted the OCA outer shell in a region with no previous damage. The measured permanent deformation of the ETU was a circumferential tear along the 3/8-to-1/4

transition weld, approximately 27 inches long and 5½ inches deep radially. No applicable comparison is available from the TRUPACT-II SAR.

2.10.3.7.1.11 ETU Fire Test No. 11

Fire No. 11 was performed to demonstrate packaging compliance with the requirements of 10 CFR 71, and followed the guidelines set forth in IAEA Safety Series No. 37¹⁴. The following list summarizes the test parameters:

- Consistent with the TRUPACT-II SAR, the HalfPACT ETU was oriented on an insulated test stand (identical to the test stand used for TRUPACT-II fire testing) such that the most severe damage was approximately 1½ meters above the fuel surface. With a circumferential orientation of 146° (see Figure 2.10.3-9), the most severe damage was determined to be from the cumulative effects of free drop tests 1 and 2, and puncture drop test 7, followed by additional damage due to puncture drop test 10. Thus, the hole caused by puncture drop test 7 was located 1½ meters above the fuel surface, and the damage from puncture drop test 10 was located above the hole, approximately 3 meters above the fuel surface. Orienting the HalfPACT ETU this way maximized the potential for a “chimney”¹⁵ to form between the penetrating damage from puncture drop tests 7 and 10.
- Consistent with Paragraph A-628.4 of IAEA Safety Series No. 37, the HalfPACT ETU was installed onto the insulated test stand at an elevation to place the lowest part of the package one meter above the fuel surface. The ETU was oriented horizontally on the test stand to maximize heat input.
- Consistent with Paragraph A-628.4 of IAEA Safety Series No. 37, requiring the test pool to extend 1 to 3 meters beyond the package edges, the test pool size extended approximately 1½ meters beyond each side of the ETU.
- Consistent with Paragraph A-628.5 of IAEA Safety Series No. 37, requiring wind speeds not to exceed 2 m/s (4.5 mph), a balloon was released that demonstrated both ground level and 1,000 feet altitude wind speeds under 5 mph. Weather conditions included a high altitude overcast, without precipitation for the duration of the fire test. Further, wind baffles were erected to surround the test pool to reduce the possible effects of wind gusts. The time-averaged wind speed during the fire test was approximately 1 mph both outside and inside the test area.
- Consistent with Paragraphs A-628.6 and A-628.8 of IAEA Safety Series No. 37, a JP4-type fuel was used for the fire test, and the amount of fuel was controlled to ensure the fire duration exceeded 30 minutes. The fuel was floated on a pool of water approximately 1/2 meter deep to ensure even distribution during burning. The fire test lasted approximately 33 minutes, and burning continued for approximately 45 minutes after the end of the fire.
- Consistent with Paragraphs A-628.7 and A-628.9 of IAEA Safety Series No. 37, the test pool was instrumented to measure fire temperatures and heat fluxes at various locations around

¹⁴ IAEA Safety Series No. 37, *Advisory Material for the IAEA Regulations for the Safe Transport of Radioactive Material (1985 Edition)*, Third Edition (As Amended 1990), International Atomic Energy Agency, Vienna, 1990.

¹⁵ A “chimney” is characterized as a preferentially burning, convective flow channel from one opening to another. The formation of a chimney can cause severe erosion of the underlying insulating polyurethane foam thereby creating localized “hot spots” that could, in-turn, prevent the packaging from performing as intended.

the ETU. Temperatures and heat fluxes were monitored before, during, and following the fire test until magnitudes stabilized back to ambient conditions. The average and standard deviation of the measured flame temperature was $1,575 \pm 191$ °F, and the average and standard deviation of the measured heat flux was 8.2 ± 3.8 Btu/ft²-s.

- Consistent with Paragraph A-628.10 of IAEA Safety Series No. 37, the ETU containment O-ring seals were leakage rate tested following performance testing to verify containment integrity. Discussions regarding post-test leakage rate testing are provided in [Section 2.10.3.7.1.12, ETU Post-Test Disassembly](#).
- Commenced fire testing (fire ignition) at 7:50 a.m. on Tuesday, 3/4/97. The ambient temperature was 43 °F at the start of the fire test.

Similar observations and results were noted in the TRUPACT-II SAR for fire testing. Since no instrumentation was utilized to measure HalfPACT ETU temperatures from fire testing, no direct comparison can be made to the reported TRUPACT-II CTU temperatures.

2.10.3.7.1.12 ETU Post-Test Disassembly

Post-test disassembly of the HalfPACT ETU was performed during the week of Monday, 3/10/97, through Friday, 3/14/97. Both abrasive cutting and gas plasma cutting methods were utilized, depending on their potential affect on subsequent post-test seal testing, to enable opening the ETU.

Upon removal of the OCA lid and body outer shells, the presence of several inches of very light density foam char that showed the intumescent behavior of the polyurethane foam. An average of 11 inches of undamaged foam was measured throughout the torispherical head region in the OCA lid. In regions remote from side drop damage, an average of 5 inches of undamaged foam was measured through the OCA lid side. In regions of side drop damage, an average of 3 inches of undamaged foam was measured through the OCA lid side. On a per-volume basis estimate, more than 80% of the polyurethane foam in the OCA lid remained undamaged.

Similarly, approximately 5 inches of undamaged foam was measured at the bottom center of the OCA body. In regions remote from side drop damage, an average of 6 inches of undamaged foam was measured through the OCA body side. In regions of side drop damage, an average of 3 inches of undamaged foam was measured through the OCA body side. On a per-volume basis estimate, more than 50% of the polyurethane foam in the OCA body remained undamaged.

In comparison, the TRUPACT-II packaging certification test units exhibited nearly identical amounts of undamaged polyurethane foam with a minimum of 5 inches remaining around the OCV except in localized regions damaged by free and puncture drops.

Upon removal of all the remaining polyurethane foam and ceramic fiber paper material, the OCV lid and body appeared lightly damaged. Some minor flattening was noted along the axes of the three sets of free drops (i.e., free drop tests 1 and 2, 3 and 4, and 5 and 6). Thus, damage to the OCV was mostly due to external application of force (i.e., due to the free drop and puncture drop tests). The ICV, however, appeared to have greater deformation coinciding with the axes of the 55-gallon payload drums. In contrast to the OCV, damage to the ICV was mostly due to an internal application of force caused by the greater weight capacity of the HalfPACT payload drums compared to that of the TRUPACT-II payload drums. The result was that the HalfPACT ETU ICV exhibited larger permanent deformation than compared to that of the TRUPACT-II CTUs. Several of the 55-gallon payload drums were distorted sufficiently to cause loss of their

lids, as similarly noted for TRUPACT-II certification testing. Of final note, additional damage to the ETU ICV may have been caused by the 5+ inches of excess axial gap above the payload drums, since a payload spacer was not used for the HalfPACT ETU. This surplus axial gap could have allowed the non-immobilized payload drums to bounce excessively thereby compounding the effect of increased payload drum weight.

Demonstration of containment vessel leaktightness was accomplished by installing 3/8 NPT ports through the knuckle region of the OCV and ICV lid torispherical heads to allow evacuation and subsequent backfill of each corresponding containment vessel cavity with helium gas. This method ensured helium gas was present behind each containment seal, thereby validating the testing process. Although performed prior to beginning the ETU testing program, helium leakage rate testing was not performed on either of the metallic containment boundaries following testing of the ETU. Results of successful mass spectrometer helium leakage rate testing are summarized below:

Sealing Component	OCV	ICV
Main O-ring Seal	$<1.0 \times 10^{-8}$ cc/s, helium	7.8×10^{-8} cc/s, helium
Vent Port Plug O-ring Seal	3.6×10^{-8} cc/s, helium	3.0×10^{-8} cc/s, helium

When accounting for the conversion between air leakage (per ANSI N14.5) and helium leakage, a 2.6 factor applies for standard temperatures and pressures. Thus, a reported helium leakage rate of 7.8×10^{-8} cc/s, helium, is equivalently 3.9×10^{-8} cc/s, air, a magnitude well below the “leaktight” criterion of 1×10^{-7} cc/s, air, per ANSI N14.5.

The ICV wiper O-ring seal ring was damaged somewhat (buckled) in two locations due to failure of several adjacent drive screws. Thus, some of the payload drum filler material appeared to be forced into the region above the wiper O-ring seal. Both the damage to the wiper seal ring and presence of residual material in the wiper seal region were identically noted for the TRUPACT-II CTUs. As noted earlier, however, all containment O-ring seals successfully passed subsequent helium leakage rate testing thereby clearly demonstrating that containment integrity was maintained.

In conclusion, overall damage to the HalfPACT ETU paralleled the measured damage from TRUPACT-II certification testing. This was expected due to the close overall similarities between packages.

2.10.3.7.2 Certification Test Unit (CTU)

Performance testing in accordance with the requirements of 10 CFR §71.71 and §71.73 for free drops, puncture drops, and fire testing was performed based on a certification test plan prepared specifically for the HalfPACT certification testing program¹⁶.

2.10.3.7.2.1 CTU Free Drop Test No. 1

Free Drop No. 1 was a NCT free drop from a height of three feet, impacting horizontally on the CTU side, with the OCV vent port oriented downward. As shown in [Figure 2.10.3-10](#), the CTU

¹⁶ S. A. Porter, et al, *Certification Test Plan for the HALFPACK Package*, TP-005, Rev. 1, March 6, 1998, Packaging Technology, Inc. (PacTec), Tacoma, Washington.

was oriented horizontal to the impact surface (meridional angle (i.e., pitch) = 0°), and circumferentially aligned to impact directly onto the OCV vent port. The following list summarizes the test parameters:

- verified meridional angle as $0^\circ \pm 1^\circ$
- verified circumferential angle to be $0^\circ \pm 1^\circ$
- verified free drop height as 3 feet, +1/-0 inches (actual drop height 3 feet, 1/2 inches)
- measured temperature at 52 °F at time of test
- conducted test at 4:54 p.m. on Monday, 3/16/98

A very slight rebound (bounce) occurred upon impact. The measured permanent deformation of the CTU were flats 13 inches wide at both the OCA top and bottom, corresponding to a crush depth of approximately 1/2 inches. In comparison, from the TRUPACT-II SAR for CTU No. 1, Test 1, the measured permanent deformations were flats 18 inches wide at both the OCA top and bottom. Further, for HalfPACT ETU, Free Drop Test 1, presented in [Table 2.10.3-2](#), the measured permanent deformations were flats 16 inches wide at the OCA top, and 18 inches wide at the OCA bottom. Finally, for HalfPACT ETU, Free Drop Test 3, also presented in [Table 2.10.3-2](#), the measured permanent deformations were flats 18 inches wide at both the OCA top and bottom.

2.10.3.7.2.2 CTU Free Drop Test No. 2

Free Drop No. 2 was a HAC free drop from a height of 30 feet, impacting horizontally on the CTU side, with the OCV vent port oriented downward. As shown in [Figure 2.10.3-10](#), the CTU was oriented horizontal to the impact surface (meridional angle (i.e., pitch) = 0°), and circumferentially aligned to impact directly onto the OCV vent port. The following list summarizes the test parameters:

- verified meridional angle as $0^\circ \pm 1^\circ$
- verified circumferential angle to be $0^\circ \pm 1^\circ$
- verified free drop height as 30 feet, +3/-0 inches (actual drop height 30 feet, 1 inch)
- measured temperature at 50 °F at time of test
- conducted test at 11:32 a.m. on Tuesday, 3/17/98

A small rebound (bounce) occurred upon impact. The measured permanent deformation of the CTU were flats 37 inches wide at both the OCA top and bottom, corresponding to a crush depth of approximately 3¾ inches. In comparison, from the TRUPACT-II SAR for CTU No. 1, Test 2, the measured permanent deformation were flats 37 inches wide at the OCA top, and 35 inches wide at the OCA bottom. Further, for HalfPACT ETU, Free Drop Test 2, presented in [Table 2.10.3-2](#), the measured permanent deformations were flats 36 inches wide at the OCA top, and 33 inches wide at the OCA bottom. Finally, for HalfPACT ETU, Free Drop Test 3, also presented in [Table 2.10.3-2](#), the measured permanent deformations were flats 34 inches wide at both the OCA top and bottom.

2.10.3.7.2.3 CTU Free Drop Test No. 3

Free Drop No. 4 was a HAC free drop from a height of 30 feet, impacting 5° from horizontal with primary impact on the lid and secondary impact on a body tie-down lug. As shown in [Figure 2.10.3-10](#), the CTU was oriented at an angle 5° from horizontal relative to the impact surface (meridional angle (i.e., pitch) = 5°), and circumferentially aligned to impact $147\frac{1}{2}^\circ$ from the OCA vent port (aligned with a tie-down lug). The following list summarizes the test parameters:

- verified meridional angle as $5^\circ \pm 1^\circ$
- verified circumferential angle to be $147\frac{1}{2}^\circ \pm 1^\circ$
- verified drop height as 30 feet, +3/-0 inches (actual drop height 30 feet, 1 inch)
- measured temperature at 41 °F at time of test
- conducted test at 11:50 a.m. on Wednesday, 3/18/98

A small rebound (bounce) occurred upon impact. The measured permanent deformation of the CTU was a flat $41\frac{1}{2}$ inches wide at the OCA top, corresponding to a crush depth at the OCA lid of approximately $4\frac{1}{4}$ inches. In comparison, from the TRUPACT-II SAR for CTU No. 2, Test 1, the measured permanent deformation was a flat 45 inches wide at the OCA top. Also, from the TRUPACT-II SAR for CTU No. 3, Test 1, the measured permanent deformation was a flat 48 inches wide at the OCA top. Note that Tests 1 for TRUPACT-II CTU Nos. 2 and 3 were performed at cold temperature conditions (-20°F). Had the TRUPACT-II slapdown drops been performed at ambient temperature conditions such as the case for HalfPACT CTU, Free Drop Test 3, the corresponding TRUPACT-II deformations would have been greater. These results correspond with the discussions from [Section 2.10.3.5.2.4, Closure \(Lid\) Separation](#), where it is shown that TRUPACT-II slapdown drop testing bounds HalfPACT slapdown drop testing.

Of final note, approximately two inches of separation of the OCA Z-flanges was measured. The magnitude of this separation corresponds to the amount observed during TRUPACT-II slapdown testing. Regardless, the generous overlap of the OCA outer thermal shield provided sufficient protection of the OCA Z-flange gap for the subsequent fire test.

2.10.3.7.2.4 CTU Puncture Drop Test No. 4

Puncture Drop No. 4 impacted directly onto the OCV vent port opening, compounding the cumulative damage created by Free Drop Tests 1 and 2. As shown in [Figure 2.10.3-10](#), the CTU was oriented at an angle $1\frac{1}{2}^\circ$ from horizontal relative to the impact surface (meridional angle (i.e., pitch) = $1\frac{1}{2}^\circ$), and circumferentially aligned to impact directly onto the OCV vent port. The following list summarizes the test parameters:

- verified meridional angle as $1\frac{1}{2}^\circ \pm 1^\circ$ (i.e., package top-end slightly raised)
- verified circumferential angle to be $0^\circ \pm 1^\circ$
- verified puncture drop height as 40 +1/-0 inches (actual drop height $40\frac{1}{2}$ inches)
- measured temperature at 42 °F at time of test
- conducted test at 10:24 a.m. on Thursday, 3/19/98

The puncture drop impacted the OCA outer shell in the region damaged by Free Drop Tests 1 and 2, directly onto the OCV vent port. The measured permanent deformation of the CTU was a non-penetrating radial dent 3¾ inches deep. In comparison, from the TRUPACT-II SAR for CTU No. 1, Test 5, the measured permanent deformation was a non-penetrating radial dent 3 inches deep. Further, for HalfPACT ETU, Free Drop Test 8, presented in [Table 2.10.3-2](#), the measured permanent deformation was a non-penetrating radial dent 2½ inches deep. Regardless of the greater radial deformation noted for the HalfPACT CTU, OCV vent port region, subsequent fire and helium leakage rate testing demonstrated that containment integrity was maintained.

2.10.3.7.2.5 CTU Puncture Drop Test No. 5

Puncture Drop No. 5 impacted directly above the 3/8-to-1/4 inch transition in the OCA body outer shell. As shown in [Figure 2.10.3-10](#), the CTU was oriented at an angle 16° from horizontal relative to the impact surface (meridional angle (i.e., pitch) = 16°), and circumferentially aligned to impact 250° from the OCA vent port. This orientation placed the puncture bar impact directly adjacent to and above the 3/8-to-1/4 inch thick transition in the OCA body outer shell (i.e., on the 3/8 inch thick shell). The following list summarizes the test parameters:

- verified meridional angle as 16° ±1°
- verified circumferential angle to be 250° ±1°
- verified puncture drop height as 40 +1/-0 inches (actual drop height 40⅞ inches)
- measured temperature at 52 °F at time of test
- conducted test at 3:48 p.m. on Thursday, 3/19/98

The puncture drop impacted the OCA outer shell in a region with no previous damage. The measured permanent deformation of the CTU was a circumferential tear along the 3/8-to-1/4 transition weld, approximately 23 inches long and 4 inches deep radially. In comparison, the measured permanent deformation of the ETU was a circumferential tear along the 3/8-to-1/4 transition weld, approximately 27 inches long and 5½ inches deep radially. No applicable comparison is available from the TRUPACT-II SAR.

2.10.3.7.2.6 CTU Puncture Drop Test No. 6

Puncture Drop No. 6 impacted directly below the 3/8-to-1/4 inch transition in the OCA body outer shell. As shown in [Figure 2.10.3-10](#), the CTU was oriented at an angle 23° from horizontal relative to the impact surface (meridional angle (i.e., pitch) = 23°), and circumferentially aligned to impact 110° from the OCA vent port (between the tie-down lugs, with the forklift pockets oriented horizontally). This orientation placed the puncture bar impact directly adjacent to and below the 3/8-to-1/4 inch thick transition in the OCA body outer shell (i.e., on the 1/4 inch thick shell). The following list summarizes the test parameters:

- verified meridional angle as 23° ±1°
- verified circumferential angle to be 110° ±1°
- verified puncture drop height as 40 +1/-0 inches (actual drop height 40¼ inches)
- measured temperature at 52 °F at time of test
- conducted test at 12:19 p.m. on Friday, 3/20/97

The puncture drop impacted the OCA outer shell in a region with no previous damage. The measured permanent deformation of the CTU was a non-penetrating radial dent 3½ inches deep. In comparison, the measured permanent deformation of the HalfPACT ETU was a hole 10½ inches long and 11½ inches wide, measuring 8 inches deep radially and 11 inches deep along the axis of the puncture bar. Rather than penetrating, the puncture bar slid on the surface of the OCA outer shell until sufficient offset was achieved to allow the HalfPACT CTU to roll off the puncture bar. This result was due to lengthening the 3/8 inch thick, OCA outer shell from 12 to 18 inches, correspondingly changing the impact angle sufficiently to prevent penetration through the adjacent 1/4 inch thick shell.

2.10.3.7.2.7 CTU Fire Test No. 7

Fire No. 7 was performed to demonstrate packaging compliance with the requirements of 10 CFR 71, and followed the guidelines set forth in IAEA Safety Series No. 37. The following list summarizes the test parameters:

- Consistent with the TRUPACT-II SAR and the HalfPACT ETU, the HalfPACT CTU was oriented on an insulated test stand (identical to the test stand used for TRUPACT-II and HalfPACT ETU fire testing) such that the most severe damage was approximately 1½ meters above the fuel surface. The most severe damage was determined to be from the cumulative effects of free drop tests 1 and 2, and puncture drop test 4, followed by additional damage due to puncture drop test 5. With a circumferential orientation of 305° (see [Figure 2.10.3-10](#)), the damage from the two sets of tests were located 1½ meters above the fuel surface.
- Consistent with Paragraph A-628.4 of IAEA Safety Series No. 37, the HalfPACT CTU was installed onto the insulated test stand at an elevation to place the lowest part of the package one meter above the fuel surface. The CTU was oriented horizontally on the test stand to maximize heat input.
- Consistent with Paragraph A-628.4 of IAEA Safety Series No. 37, requiring the test pool to extend 1 to 3 meters beyond the package edges, the test pool size extended approximately 1½ meters beyond each side of the CTU.
- Consistent with Paragraph A-628.5 of IAEA Safety Series No. 37, requiring wind speeds not to exceed 2 m/s (4.5 mph), a balloon was released that demonstrated both ground level and 1,000 feet altitude wind speeds under 5 mph at the start of the fire test. Weather conditions included relatively clear skies, without precipitation for the duration of the fire test. Further, wind baffles were erected to surround the test pool to reduce the possible effects of wind gusts. The time-averaged wind speed during the fire test was approximately 8 mph outside the test area, corresponding to approximately 4 mph inside the test area.
- Consistent with Paragraphs A-628.6 and A-628.8 of IAEA Safety Series No. 37, a JP4-type fuel was used for the fire test, and the amount of fuel was controlled to ensure the fire duration exceeded 30 minutes. The fuel was floated on a pool of water approximately 1/2 meter deep to ensure even distribution during burning. The fire test lasted approximately 33 minutes, and burning continued for approximately 30 minutes after the end of the fire.
- Consistent with Paragraphs A-628.7 and A-628.9 of IAEA Safety Series No. 37, the test pool was instrumented to measure fire temperatures and heat fluxes at various locations around the CTU. Temperatures and heat fluxes were monitored before, during, and following the

fire test until magnitudes stabilized back to ambient conditions. The average measured flame temperature was 1,486 °F.

- Consistent with Paragraph A-628.10 of IAEA Safety Series No. 37, the CTU containment O-ring seals were leakage rate tested following performance testing to verify containment integrity. Discussions regarding post-test leakage rate testing are provided in [Section 2.10.3.7.2.8, CTU Post-Test Disassembly](#).
- Commenced fire testing (fire ignition) at 7:54 a.m. on Tuesday, 4/14/98. The ambient temperature was 51 °F at the start of the fire test.

No active temperature measuring devices were employed prior to, during, or following the HAC fire test. Further, measurement of the outer containment assembly (OCA) outer shell temperature does not represent the outer containment vessel (OCV) or inner containment vessel (ICV) temperatures due to the large internal mass and thick, thermally insulating foam used within the OCA. As discussed in [Section 3.1.1, Packaging](#), the temperatures of the OCV, ICV, and payload are effectively decoupled from the OCA outer shell and polyurethane foam for short term thermal transients. Instead, the initial temperature of the CTU may be estimated based on the ambient temperature of the Sandia National Laboratory testing facilities in the six weeks prior to the HAC fire test¹⁷. Climatological data for Albuquerque, New Mexico, during the month of March and first two weeks of April 1998 shows an average temperature of 48 °F for those six weeks. Thus, when adjusting for the elevation difference between the testing facilities and Albuquerque, the initial temperature for fire testing is taken as 43 °F.

As stated in [Section 3.5.1.1, Analytical Model](#), the initial condition temperatures for the HAC fire test are presented in [Table 3.5-1](#). Accordingly, the average temperature of the ICV wall and OCV wall is 133 °F and 131 °F, respectively. Therefore, the difference between the theoretical pre-fire package temperature and actual adjusted starting temperature is conservatively taken as $133\text{ °F} - 43\text{ °F} = 90\text{ °F}$.

The CTU utilized passive, non-reversible temperature indicating labels at various locations near each containment vessel's seal flanges to record temperatures from the HAC fire test. Each set of temperature indicating labels recorded temperatures in 40 steps from 105 °F to 500 °F. As illustrated in [Figure 2.10.3-11](#), some locations used redundant sets of temperature labels to ensure comprehensive results at critical regions.

A summary of temperature indicating label temperatures is presented in [Table 2.10.3-4](#). The maximum measured OCV seal region temperature was 200 °F. Upwardly adjusting for the lower, pre-fire starting temperature by 90 °F results in a projected maximum OCV seal region temperature of 290 °F. The maximum measured ICV seal region temperature was 110 °F. Similarly adjusting for the lower, pre-fire starting temperature by 90 °F results in a projected maximum ICV seal region temperature of 200 °F. In comparison, certification testing of the TRUPACT-II package showed a maximum OCV seal region temperature of 260 °F, and a maximum ICV seal region temperature of 200 °F (see the TRUPACT-II SAR). As with the

¹⁷ CTU was located at Sandia National Laboratories' Coyote Canyon drop test facility for the month of March, 1998, and the Lurance Canyon burn facility for the first two weeks of April, 1998. CTU was burned on April 14, 1998. The elevation difference between the two test facilities and the city of Albuquerque results in an average ambient temperature approximately 5 °F cooler than Albuquerque.

comparison of measurements of drop damage, fire temperatures between the two similar package designs agree very well.

Two final observations are notable regarding fire testing. First, changing the OCV vent and seal test port thermal plugs from polyurethane foam to ceramic fiber paper material appears to have benefited the corresponding port plugs (compare ETU [Figure 2.10.3-45](#), [Figure 2.10.3-46](#), and [Figure 2.10.3-47](#) to CTU [Figure 2.10.3-84](#), [Figure 2.10.3-86](#), and [Figure 2.10.3-87](#)). Second, with reference to [Table 2.10.3-4](#), the temperature indicating labels (Nos. 3 and 7) at circumferential angle $\phi = 250^\circ$ read substantially lower temperatures than all other OCV locations. The reason is not known since the 250° location was positioned in the hottest location in the fire (i.e., 1½ meters above the fuel surface).

2.10.3.7.2.8 CTU Post-Test Disassembly

Post-test disassembly of the HalfPACT CTU was performed during the week of Monday, 4/26/98, through Friday, 5/8/98. To limit potentially misleading peripheral damage to the CTU during post-test disassembly, only abrasive cutting methods were utilized.

As with the ETU, upon removal of the OCA lid and body outer shells, the presence of several inches of very light density foam char that showed the intumescent behavior of the polyurethane foam. Undamaged foam thicknesses in the OCA lid closely paralleled those measured for the HalfPACT ETU. An average of 11 inches of undamaged foam was measured throughout the crown region of the OCA lid torispherical head, and 9 inches of undamaged foam in the knuckle region. In regions remote from side drop damage, an average of 5 inches of undamaged foam was measured through the OCA lid side. In regions of side drop damage, an average of 3 inches of undamaged foam was measured through the OCA lid side. On a per-volume basis estimate, more than 80% of the polyurethane foam in the OCA lid remained undamaged.

Similarly, approximately 6½ inches of undamaged foam was measured at the bottom center of the OCA body. In regions remote from side drop damage, an average of 8 inches of undamaged foam was measured through the OCA body side. In regions of side drop damage, an average of 4½ inches of undamaged foam was measured through the OCA body side. On a per-volume basis estimate, more than 70% of the polyurethane foam in the OCA body remained undamaged. More undamaged foam remained in the OCA body for the CTU than for the ETU. This effect was most likely due to the presence of more wind during the CTU fire test, blowing from the package bottom toward the top. Regardless, the package closure region remained fully engulfed in the fire for the duration of the fire test.

In comparison, the TRUPACT-II packaging certification test units exhibited nearly identical amounts of undamaged polyurethane foam with a minimum of 5 inches remaining around the OCV except in localized regions damaged by free and puncture drops.

Upon removal of all the remaining polyurethane foam and ceramic fiber paper material, the OCV lid and body appeared lightly damaged. Some minor flattening was noted along the axes of the three free drops (i.e., free drop tests 1, 2, and 3). Thus, as with the ETU, damage to the OCV was mostly due to external application of force (i.e., due to the free drop and puncture drop tests). As with the ETU, the ICV, however, appeared to have greater deformation coinciding with the axes of the 55-gallon payload drums. In contrast to the OCV, damage to the ICV was mostly due to an internal application of force caused by the greater weight capacity of the

HalfPACT payload drums compared to that of the TRUPACT-II payload drums. The result was that the HalfPACT CTU ICV exhibited larger permanent deformation than compared to that of the TRUPACT-II CTUs. Several of the 55-gallon payload drums were distorted sufficiently to cause loss of their lids, as similarly noted for TRUPACT-II certification testing.

Demonstration of containment vessel leaktightness was accomplished by installing 1/2 NPT ports through the knuckle region of the OCV and ICV lid torispherical heads to allow evacuation and subsequent backfill of each corresponding containment vessel cavity with helium gas. This method ensured helium gas was present behind each containment seal, thereby validating the testing process. Helium leakage rate testing was also performed on the metallic containment boundaries following testing of the CTU. Helium leakage rate testing of each containment boundary was accomplished by welding each containment component (i.e., lid and body structure) to a flat steel plate. Each containment component was evacuated, tented with helium gas, and helium leakage rate tested to demonstrate containment integrity. Results of successful mass spectrometer helium leakage rate testing are summarized below:

Sealing Component	OCV	ICV
Main O-ring Seal	$<1.0 \times 10^{-8}$ cc/s, helium	$<1.0 \times 10^{-8}$ cc/s, helium
Vent Port Plug O-ring Seal	$<1.0 \times 10^{-8}$ cc/s, helium	$<1.0 \times 10^{-8}$ cc/s, helium
Lid Structure	3.5×10^{-8} cc/s, helium	$<1.0 \times 10^{-8}$ cc/s, helium
Body Structure	4.2×10^{-8} cc/s, helium	1.3×10^{-7} cc/s, helium

When accounting for the conversion between air leakage (per ANSI N14.5) and helium leakage, a 2.6 factor applies for standard temperatures and pressures. Thus, a reported helium leakage rate of 1.3×10^{-7} cc/s, helium, is equivalently 5×10^{-8} cc/s, air, a magnitude well below the “leaktight” criterion of 1×10^{-7} cc/s, air, per ANSI N14.5.

As with the ETU, the ICV wiper O-ring seal ring was damaged somewhat (buckled) in several locations due to failure of several drive screws. Thus, some of the payload drum filler material appeared to be forced into the region above the wiper O-ring seal. Both the damage to the wiper seal ring and presence of residual material in the wiper seal region were identically noted for the TRUPACT-II CTUs. As noted earlier, however, all containment O-ring seals successfully passed subsequent helium leakage rate testing due to the beneficial presence of the foam debris seal, thereby clearly demonstrating that containment integrity was maintained.

In general, damage to the CTU closely paralleled damage to the ETU. The only exception noted was for the OCV vent port region. Visual inspection of the OCV vent port fitting determined that the inner groove weld was cracked approximately 1/3 of its circumferential length. Upon closer visual inspection of the 5/16 inch inner groove weld, the weld size appeared below nominal size, possible due to excessive grinding of welded regions during fabrication. As noted earlier, both the ETU and CTU were fabricated from TRUPACT-II training units, i.e., production units with undersized welds in localized regions where excessive “flush” grinding sometimes significantly reduced the shell thickness. The only way to determine actual, as-tested, OCV vent port fitting weld sizes would be to “section” the fitting region, a process that was not performed. Of significance is that helium leakage rate testing determined that containment

integrity was maintained due to the presence of the outer fillet weld. Therefore, although damaged during testing, the OCV vent port region nevertheless remained acceptably leaktight because of the double weld configuration.

In conclusion, with the aforementioned exception, overall damage to the HalfPACT CTU paralleled the measured damage from both HalfPACT ETU and TRUPACT-II certification testing, as expected.

Table 2.10.3-1 – TRUPACT-II / HalfPACT Comparison Using NUREG/CR-3966

Impact Angle (with respect to horizontal)	Axial, Shear, and Moment Forces at the OCV Locking Ring					
	Due to Primary Impact			Due to Secondary Impact		
	Axial Force, lb	Shear Force, lb	Moment, in-lb	Axial Force, lb	Shear Force, lb	Moment, in-lb
TRUPACT-II, Primary Impact on OCA Lid						
5°	121,225	465,347	2.158(10) ⁷	0	471,554	2.186(10) ⁷
10°	195,504	372,368	1.727(10) ⁷	0	471,036	2.184(10) ⁷
15°	251,344	315,030	1.461(10) ⁷	0	467,404	2.167(10) ⁷
20° (CTU Test, -20 °F)	302,679	279,288	1.295(10) ⁷	0	461,178	2.138(10) ⁷
47.7° (c.g. over corner)	738,279	223,251	1.035(10) ⁷			
TRUPACT-II, Primary Impact on OCA Body						
5°	118,730	455,768	2.113(10) ⁷	0	485,900	2.253(10) ⁷
10°	189,342	360,631	1.672(10) ⁷	0	485,275	2.250(10) ⁷
15°	244,441	306,378	1.421(10) ⁷	0	480,899	2.230(10) ⁷
18° (CTU Test, Ambient)	274,975	284,218	1.318(10) ⁷	0	477,148	2.212(10) ⁷
HalfPACT, Primary Impact on OCA Lid						
5°	115,380	7,431	1.760(10) ⁷	0	4,876	1.157(10) ⁷
10°	185,532	5,929	1.407(10) ⁷	0	4,866	1.155(10) ⁷
15°	235,898	4,961	1.177(10) ⁷	0	4,822	1.144(10) ⁷
37° (c.g. over corner)	451,020	3,373	0.800(10) ⁷			
HalfPACT, Primary Impact on OCA Body						
5°	112,409	7,240	1.718 (10) ⁷	0	5,035	1.195(10) ⁷
10°	178,914	5,717	1.357 (10) ⁷	0	5,022	1.192(10) ⁷
15°	227,810	4,791	1.137 (10) ⁷	0	4,971	1.180(10) ⁷

Table 2.10.3-2 – Summary of HalfPACT ETU Test Results in Sequential Order^①

Test No.	Test Description	Orientation		Test Temperature	Observations and Results
		θ°	ϕ°		
1	NCT 3' side drop opposite OCV vent port	0°	200°	53 °F	16"/18" flat at top/bottom; ~3/4" deep
2	HAC 30' side drop opposite OCV vent port	0°	200°	57 °F	36"/33" flat at top/bottom; ~3/4" deep
3	NCT 3' side drop on OCV vent port	0°	0°	40 °F	18"/18" flat at top/bottom; ~3/4" deep
4	HAC 30' side drop on OCV vent port	0°	0°	48 °F	34"/34" flat at top/bottom; ~3/4" deep
5	NCT 3' corner drop between tie-down lugs	43°	110°	53 °F	26" long × 5½" wide flat; ~1⅜" deep
6	HAC 30' corner drop between tie-down lugs	43°	110°	55 °F	40" long × 12" wide flat; ~3/4" deep
7	Puncture drop below 3/8-to-1/4 inch transition	20°	200°	38 °F	10½" long × 11½" wide hole; ~8" deep
8	Puncture drop on OCV vent port	1°	0°	40 °F	~2½" deep dent
9	Puncture drop on damaged bottom corner	43°	110°	28 °F	~3" deep dent
10	Puncture drop above 3/8-to-1/4 inch transition	9°	290°	29 °F	~5½" deep dent; ~27" long weld tear
11	Fire with Test 1, 2, & 4 damage at hottest location	0°	146°	43 °F	~1,575 °F temperature; ~33 minutes

Notes:

- ① Tested 2/18/97 – 3/10/97.
- ② Meridional angle, θ , is relative to horizontal (i.e., side drop orientation).
- ③ Circumferential angle, ϕ , is relative to OCV vent port.

Table 2.10.3-3 – Summary of HalfPACT CTU Test Results in Sequential Order^①

Test No.	Test Description	Orientation		Test Temperature	Observations and Results
		θ°	ϕ°		
1	NCT 3' side drop on OCV vent port	0°	0°	52 °F	13"/13" flat at top/bottom; ~1/2" deep
2	HAC 30' side drop on OCV vent port	0°	0°	50 °F	37"/37" flat at top/bottom; ~3¾" deep
3	HAC 30' slapdown drop on OCA lid/tie-down lug	5°	147½°	41 °F	41½" flat at top; ~4¾" deep at top
4	Puncture drop on OCV vent port	1½°	0°	42 °F	~3¾" deep dent
5	Puncture drop above 3/8-to-1/4 inch transition	16°	250°	52 °F	~4" deep dent; ~23" long weld tear
6	Puncture drop below 3/8-to-1/4 inch transition	23°	110°	52 °F	~3½" deep dent (no penetration)
7	Fire with Test 1, 2, & 4 damage at hottest location	0°	146°	43 °F	~1,485 °F temperature; ~33 minutes

Notes:

- ① Tested 3/16/98 – 4/14/98.
- ② Meridional angle, θ , is relative to horizontal (i.e., side drop orientation).
- ③ Circumferential angle, ϕ , is relative to OCV vent port.

Table 2.10.3-4 – Summary of HalfPACT CTU Temperature Indicating Label Readings

Temperature Indicating Label Location and Circumferential Angle, ϕ	Label Number	Temperature
OCV Conical Shell at 0° (OCV Vent Port Seal) – Free Drop Tests 1 & 2, and Puncture Drop Test 4	1a, 1b	180 °F, 170 °F
OCV Conical Shell at 110° – Puncture Drop Test 6	2	180 °F
OCV Conical Shell at 250° – Puncture Drop Test 5	3	130 °F
OCV Seal Flange at 0° (Main OCV Seals) – Free Drop Tests 1 & 2, and Puncture Drop Test 4	4a, 4b	200 °F, 200 °F
OCV Seal Flange at 110° (Main OCV Seals) – Puncture Drop Test 6	5	200 °F
OCV Seal Flange at 147½° (Main OCV Seals) – Free Drop Test 3	6	180 °F
OCV Seal Flange at 250° (Main OCV Seals) – Puncture Drop Test 5	7	140 °F
ICV Seal Flange at 0° (ICV Vent Port Seal) – Free Drop Tests 1 & 2, and Puncture Drop Test 4	8	105 °F
ICV Seal Flange at 0° (Main ICV Seals) – Free Drop Tests 1 & 2, and Puncture Drop Test 4	9	105 °F
ICV Seal Flange at 110° (Main ICV Seals) – Puncture Drop Test 6	10	105 °F
ICV Seal Flange at 147½° (Main ICV Seals) – Free Drop Test 3	11	110 °F
ICV Seal Flange at 250° (Main ICV Seals) – Puncture Drop Test 5	12	110 °F

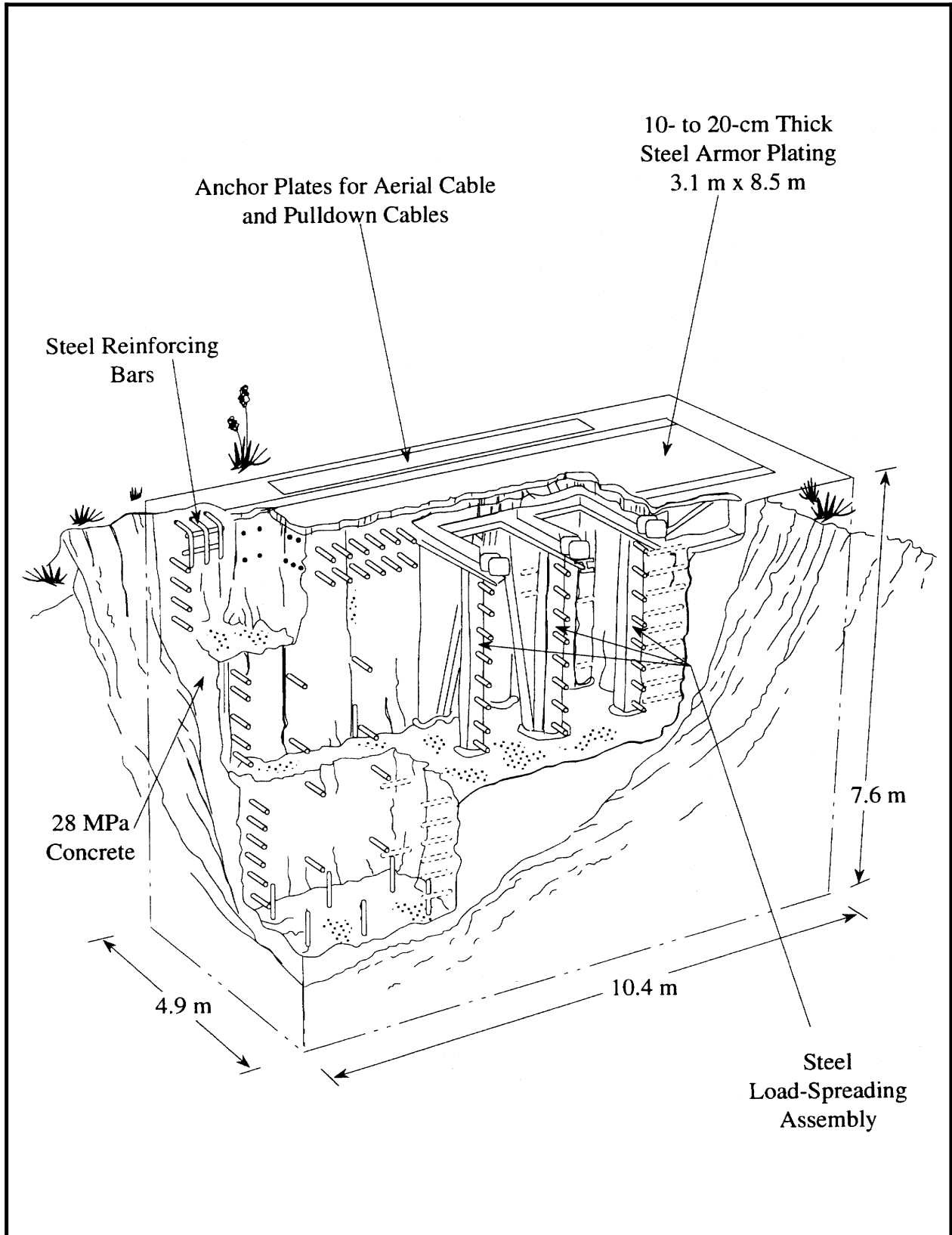


Figure 2.10.3-1 – Drop Pad at the Coyote Canyon Aerial Cable Facility

This page intentionally left blank.

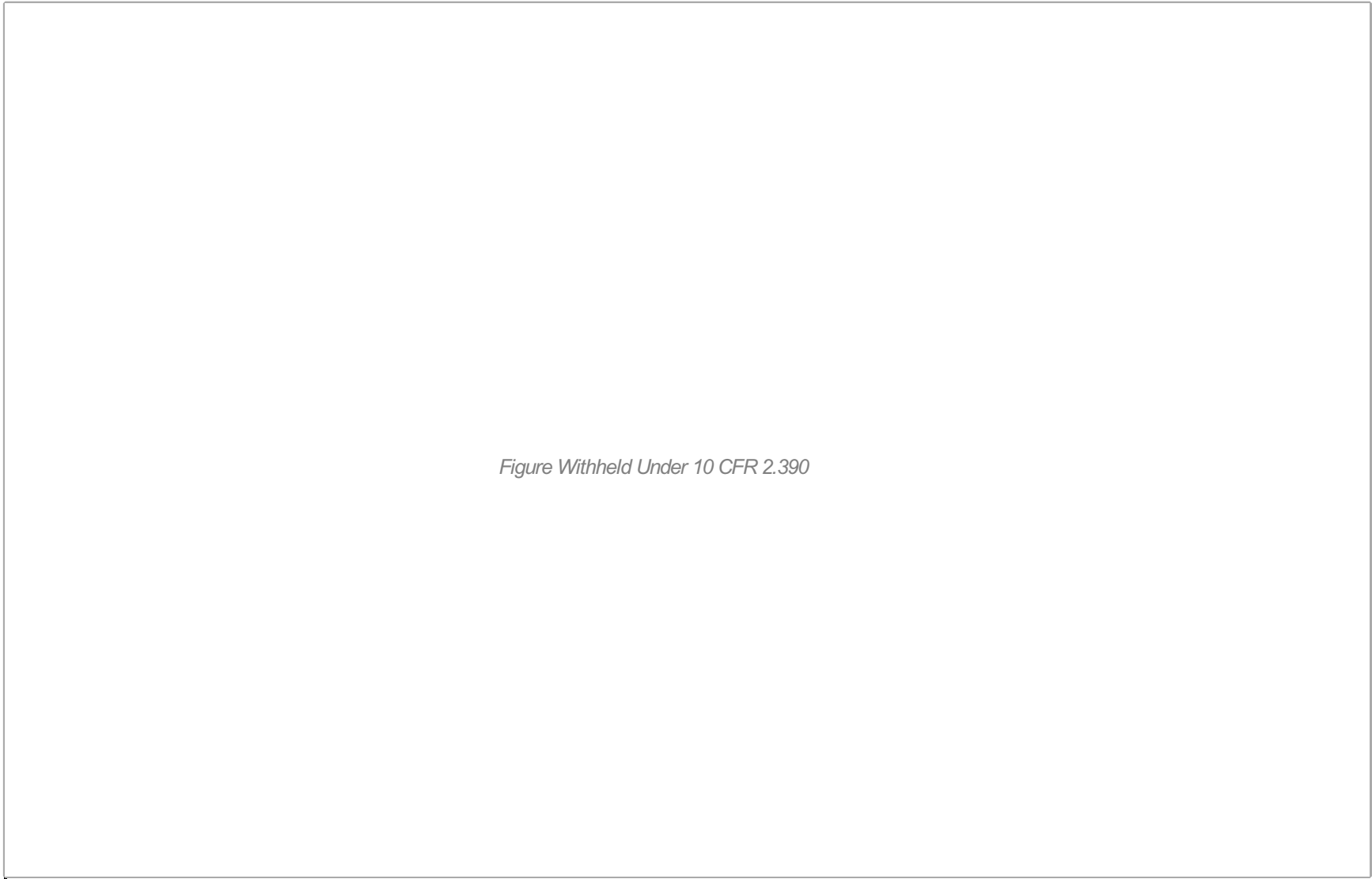


Figure Withheld Under 10 CFR 2.390

Figure 2.10.3-2 – Design Comparison between a TRUPACT-II Packaging and a HalfPACT Packaging

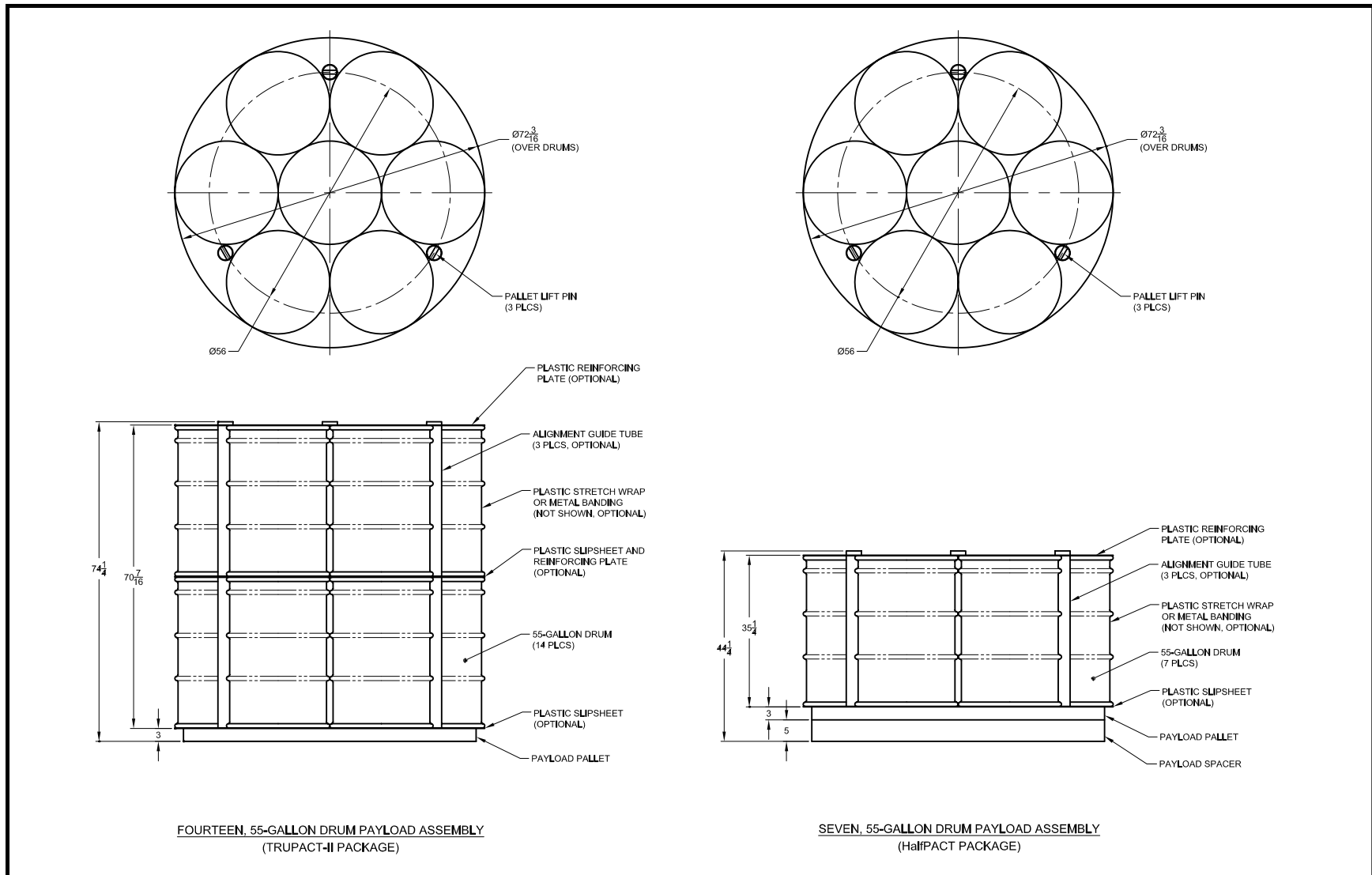


Figure 2.10.3-3 – Design Comparison between 55-Gallon Drum Payload Assemblies

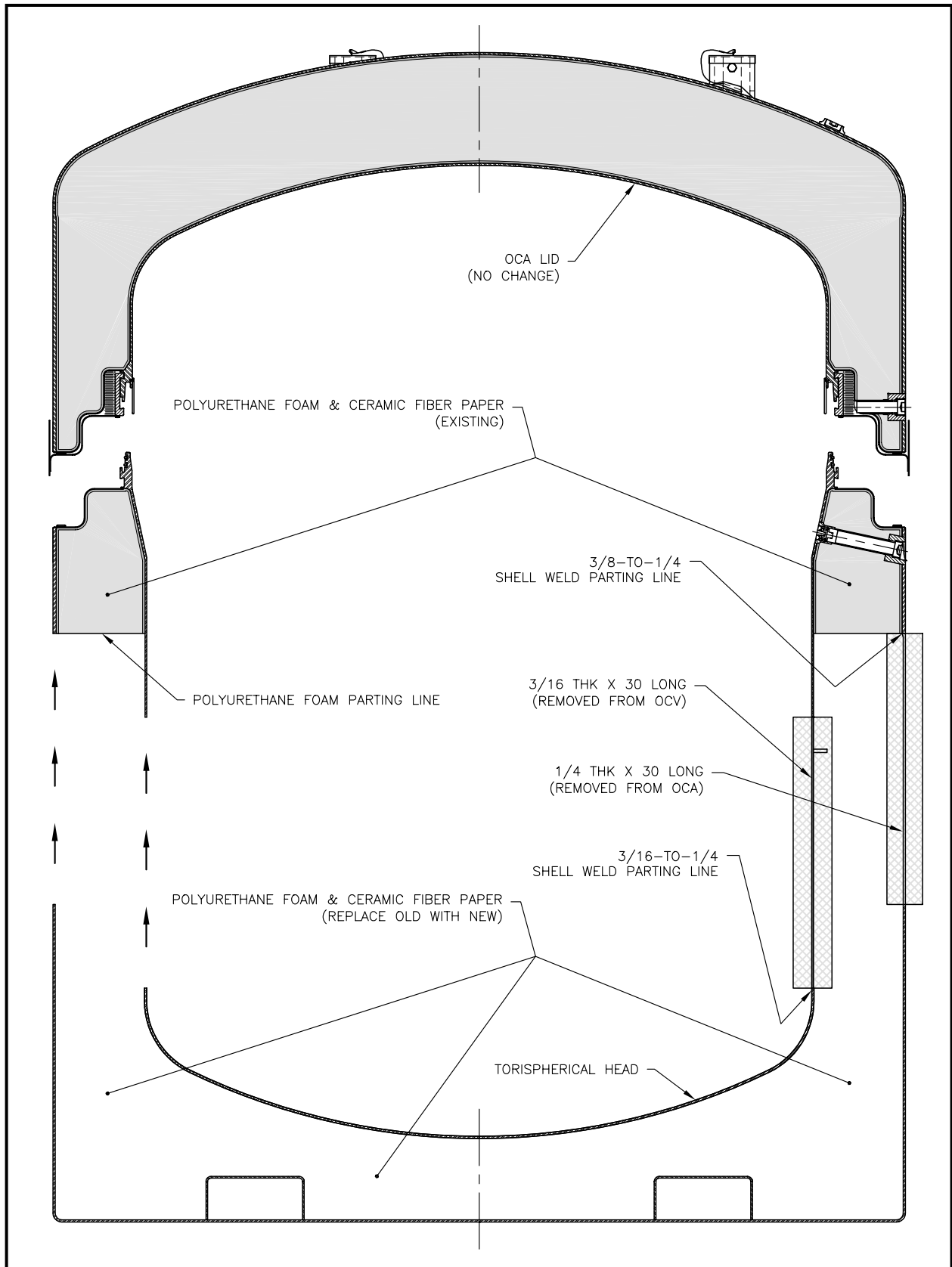


Figure 2.10.3-4 – Making the HalfPACT ETU OCA from TRUPACT-II Unit 104

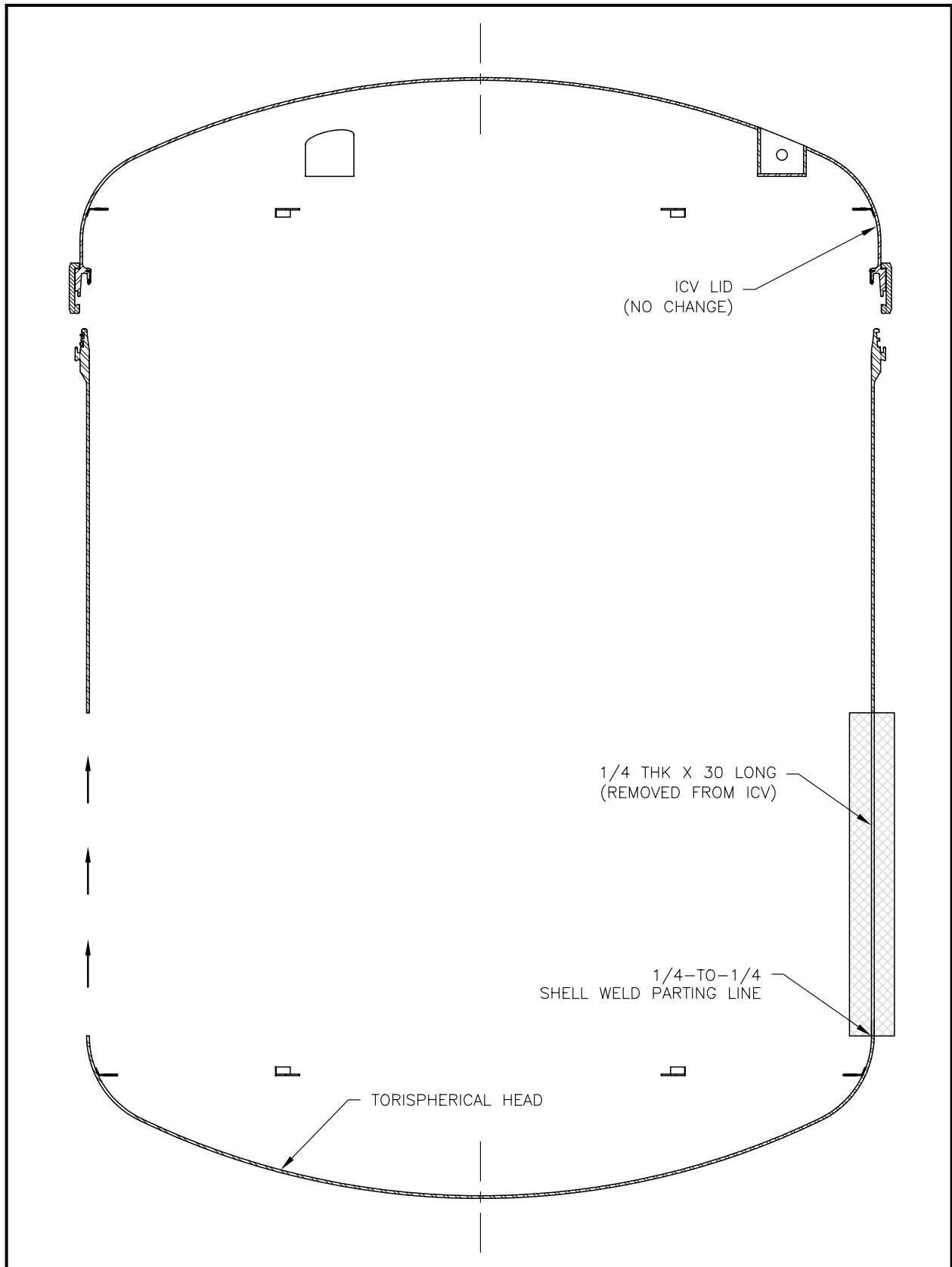


Figure 2.10.3-5 – Making the HalfPACT ETU OCA from TRUPACT-II Unit 104

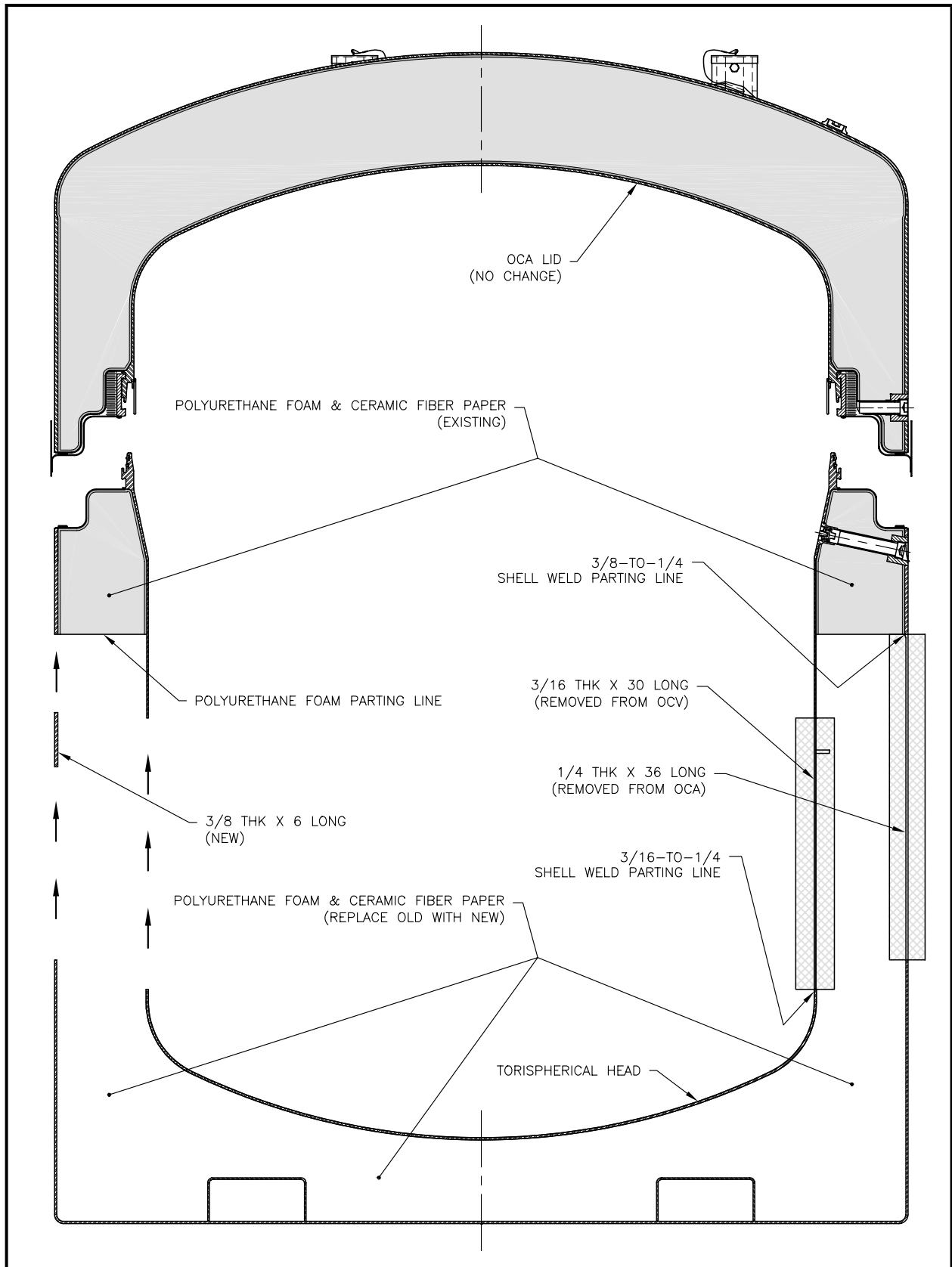


Figure 2.10.3-6 – Making the HalfPACT CTU OCA from TRUPACT-II Unit 107

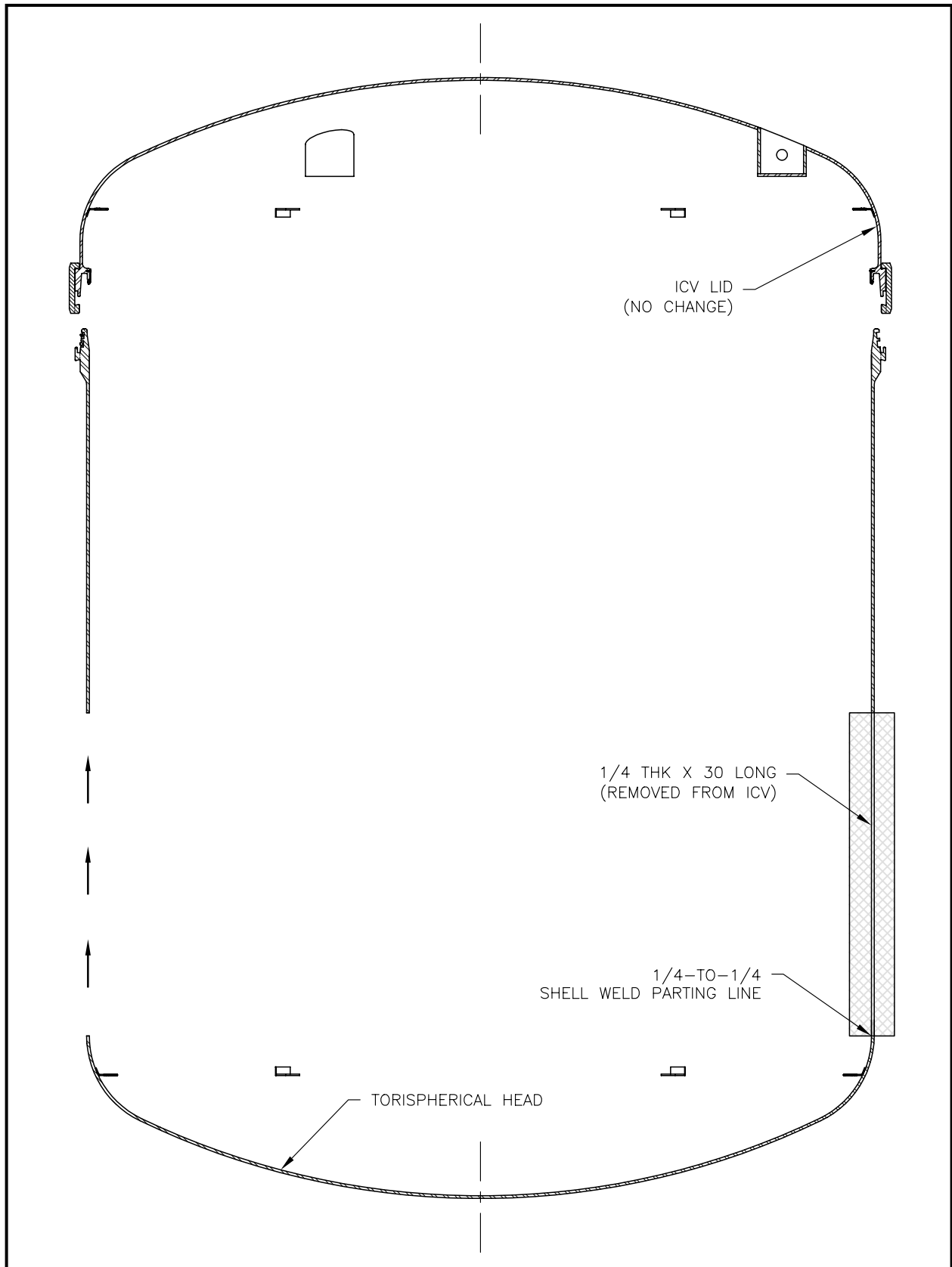


Figure 2.10.3-7 – Making the HalfPACT CTU ICV from TRUPACT-II Unit 107

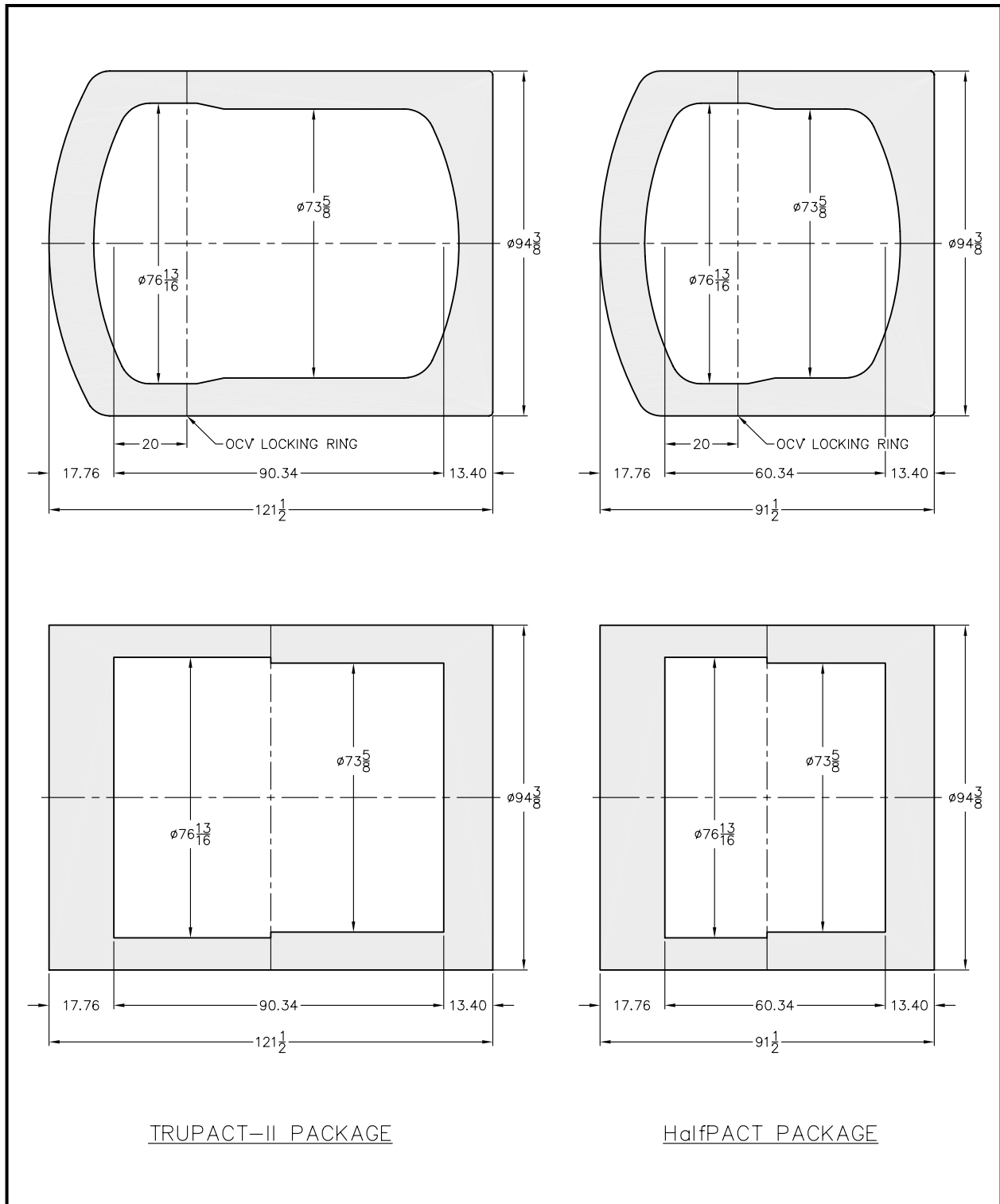


Figure 2.10.3-8 – Dimensional Comparison of TRUPACT-II and HalfPACT for NUREG/CR-3966 (Lower Figures are Simplifying Representations Used in CASKDROP)

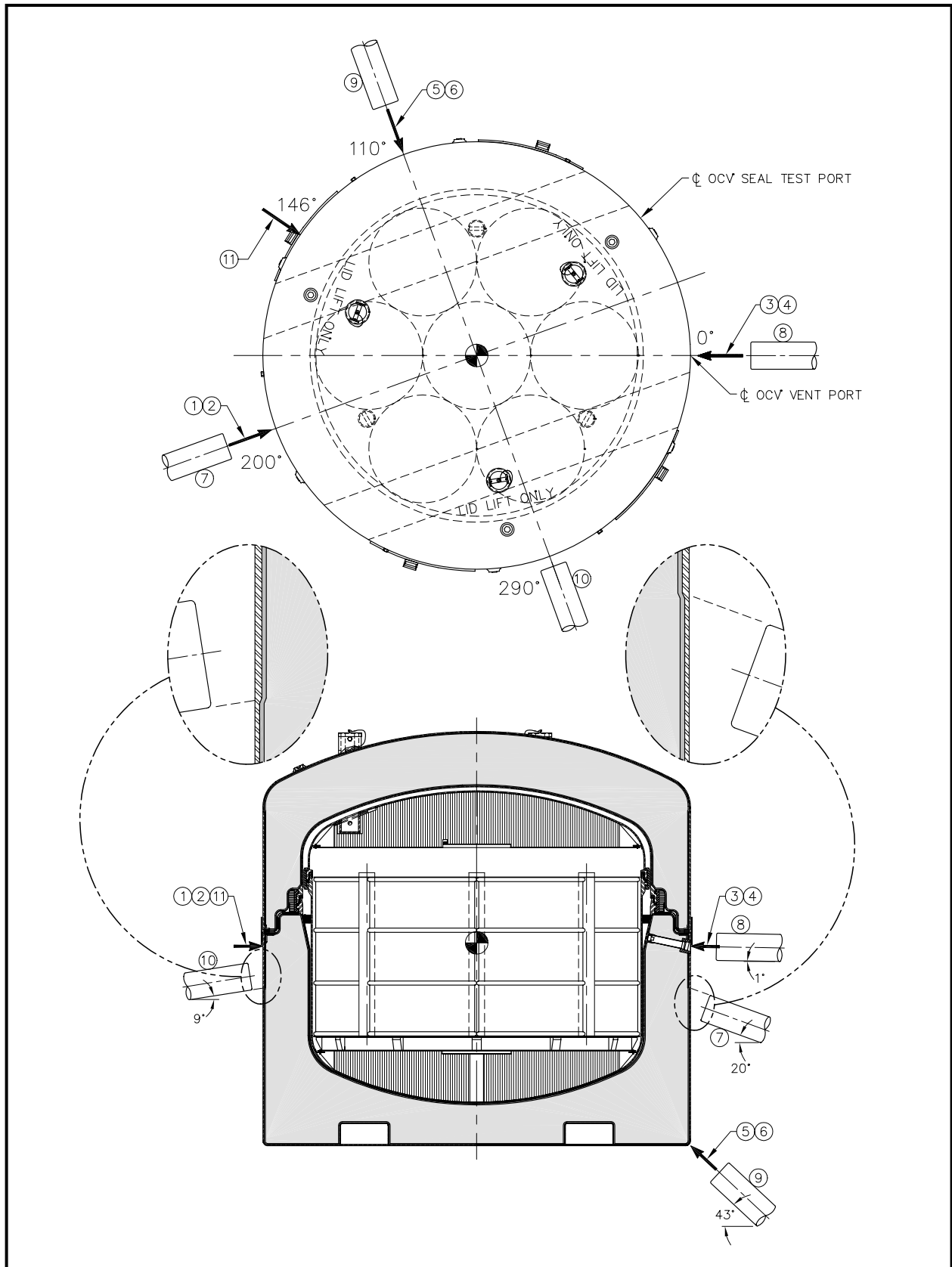


Figure 2.10.3-9 – Schematic of HalfPACT ETU Test Orientations

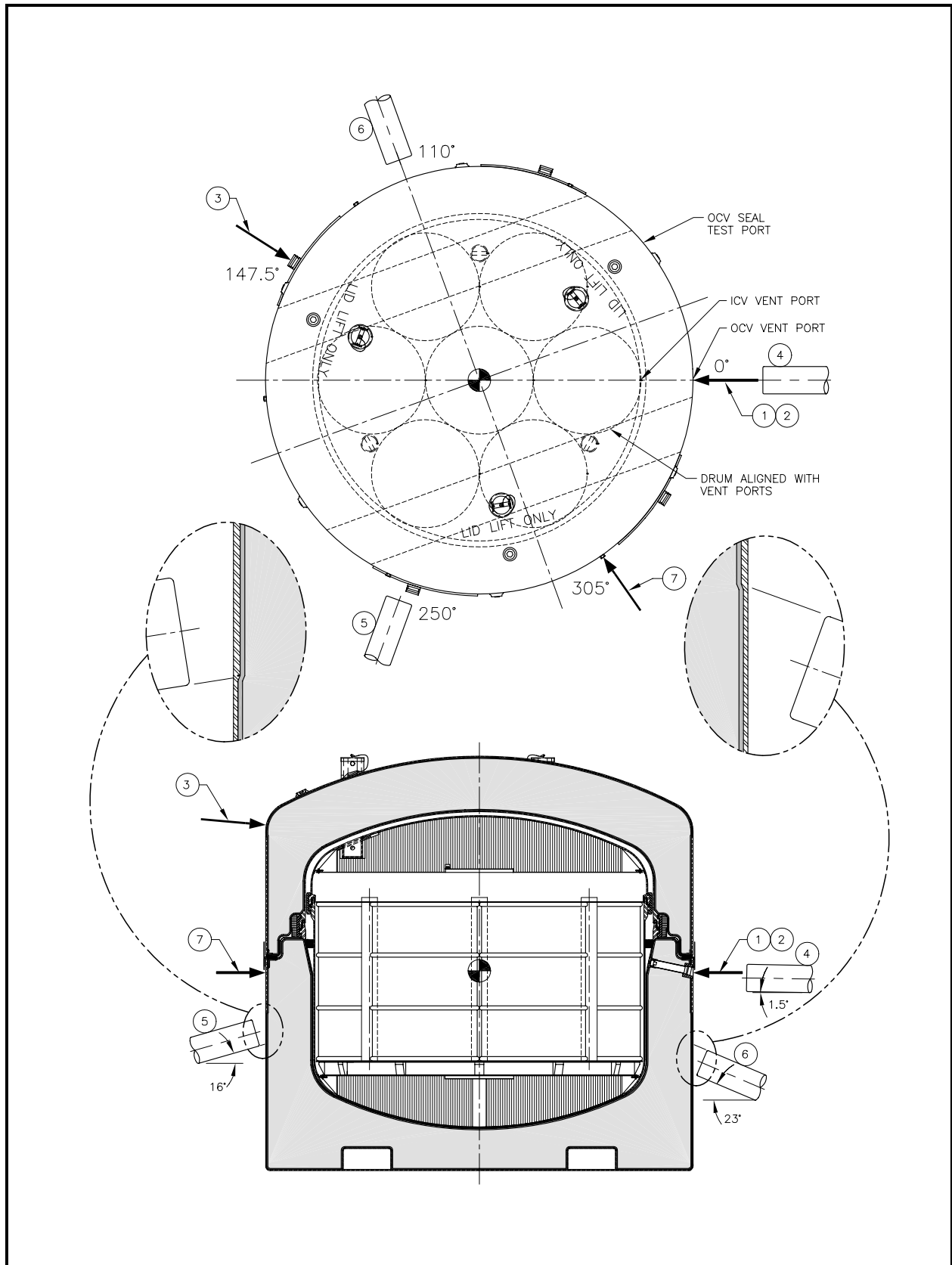


Figure 2.10.3-10 – Schematic of HalfPACT CTU Test Orientations

This page intentionally left blank.

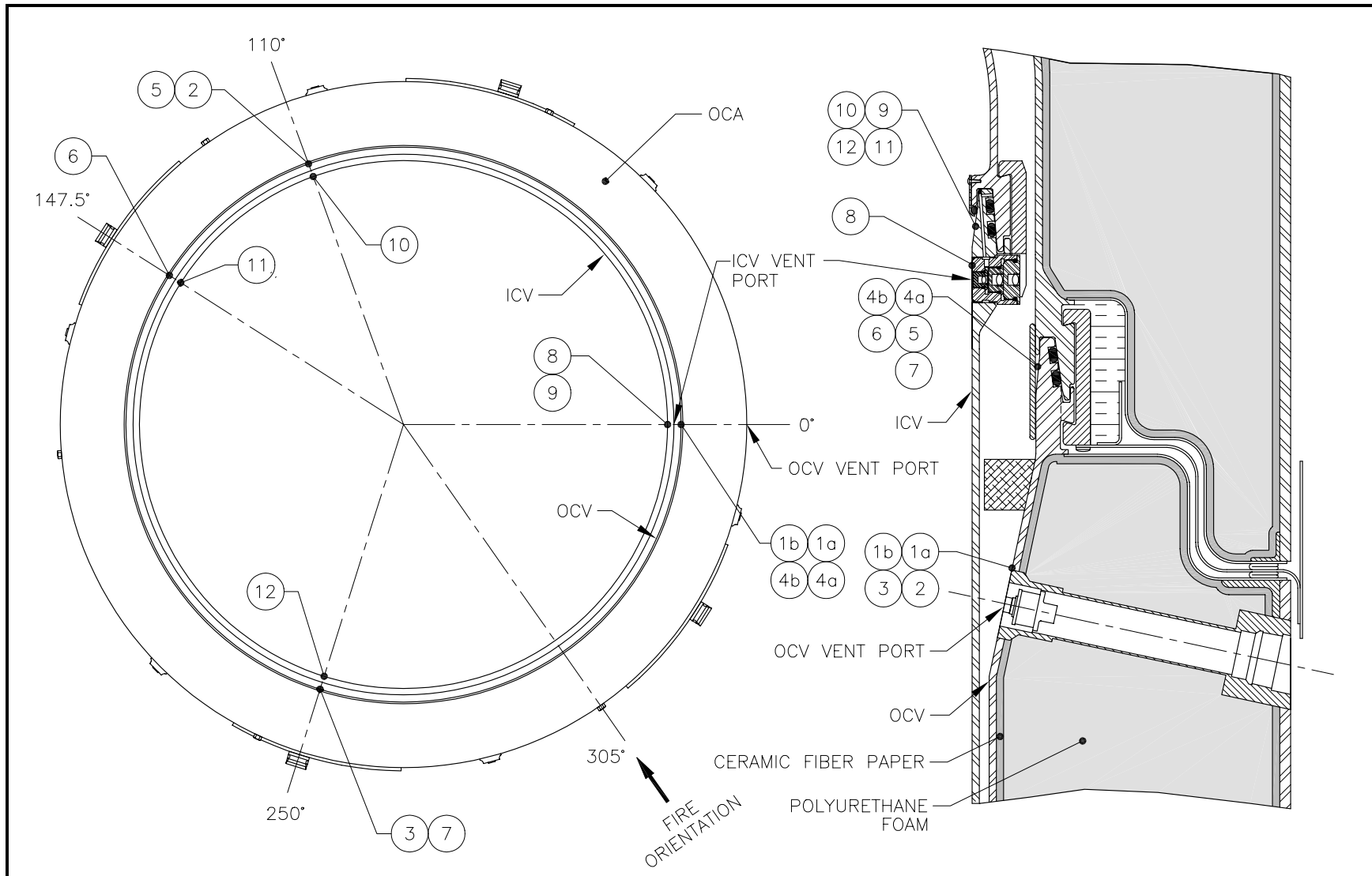


Figure 2.10.3-11 – Schematic of HalfPACT CTU Temperature Indicating Label Location

This page intentionally left blank.

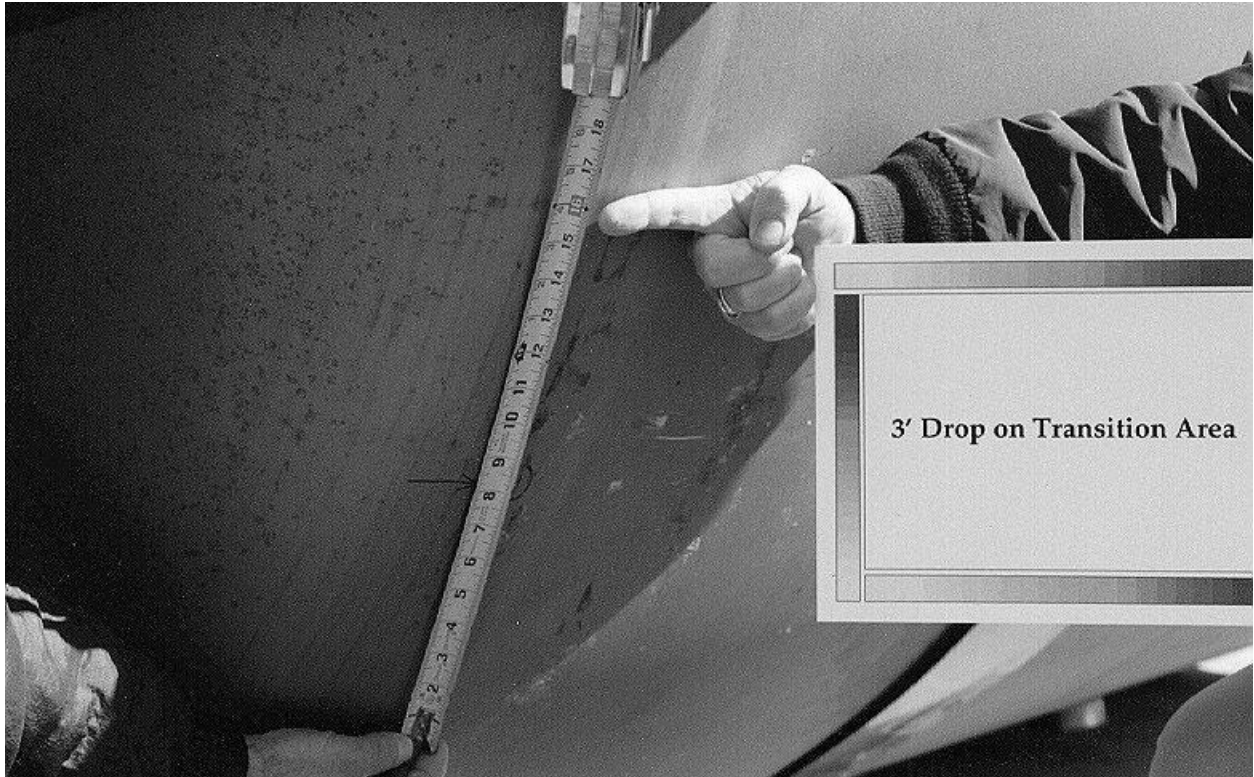


Figure 2.10.3-12 – ETU Free Drop Test 1; Top-End Damage; ~16" Wide Flat

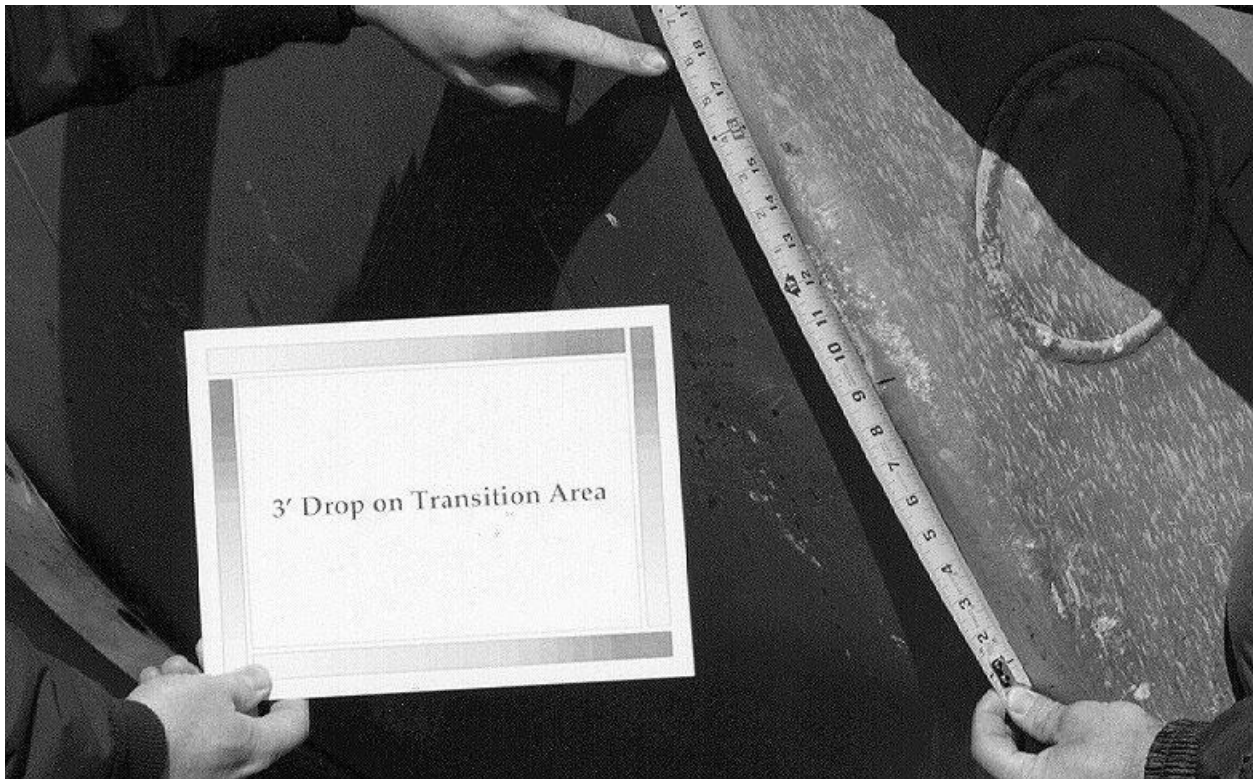


Figure 2.10.3-13 – ETU Free Drop Test 1; Bottom-End Damage; ~18" Wide Flat

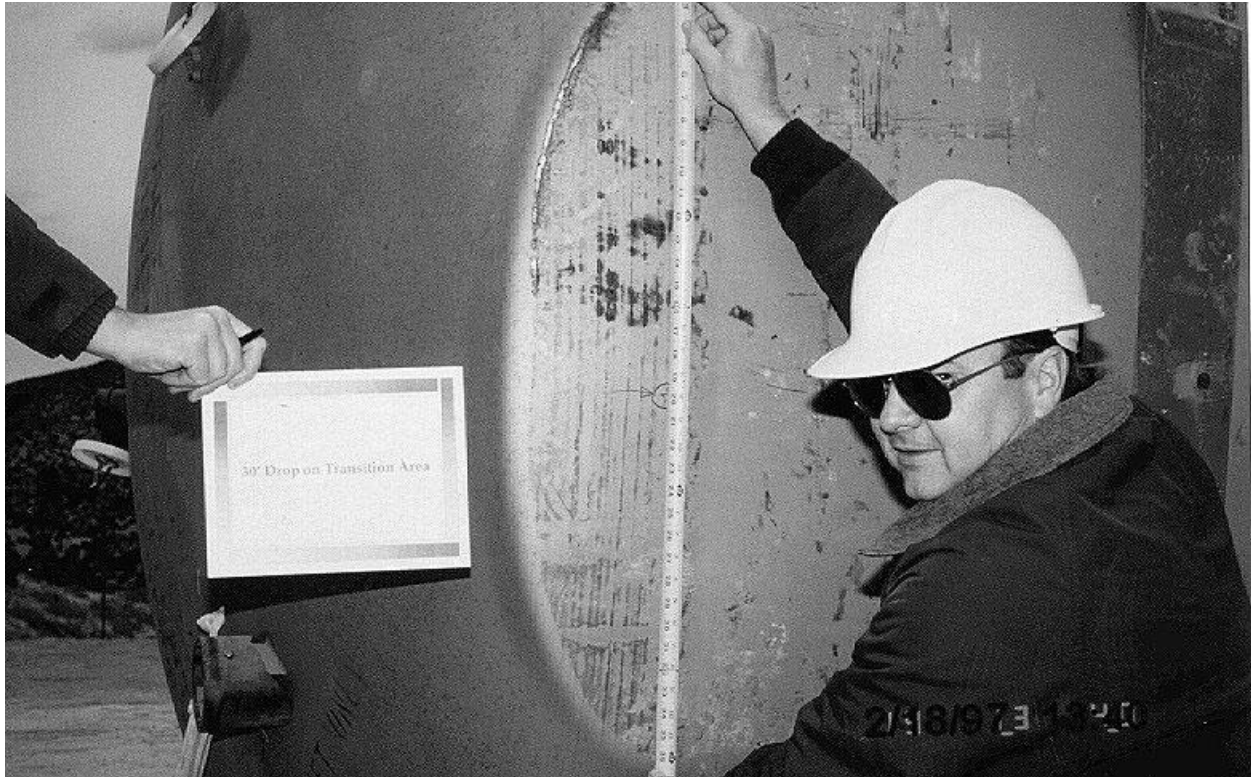


Figure 2.10.3-14 – ETU Free Drop Test 2; Top-End Damage; ~36" Wide Flat



Figure 2.10.3-15 – ETU Free Drop Test 2; Bottom-End Damage; ~33" Wide Flat



Figure 2.10.3-16 – ETU Free Drop Test 3; View Just Prior to NCT Free Drop Test

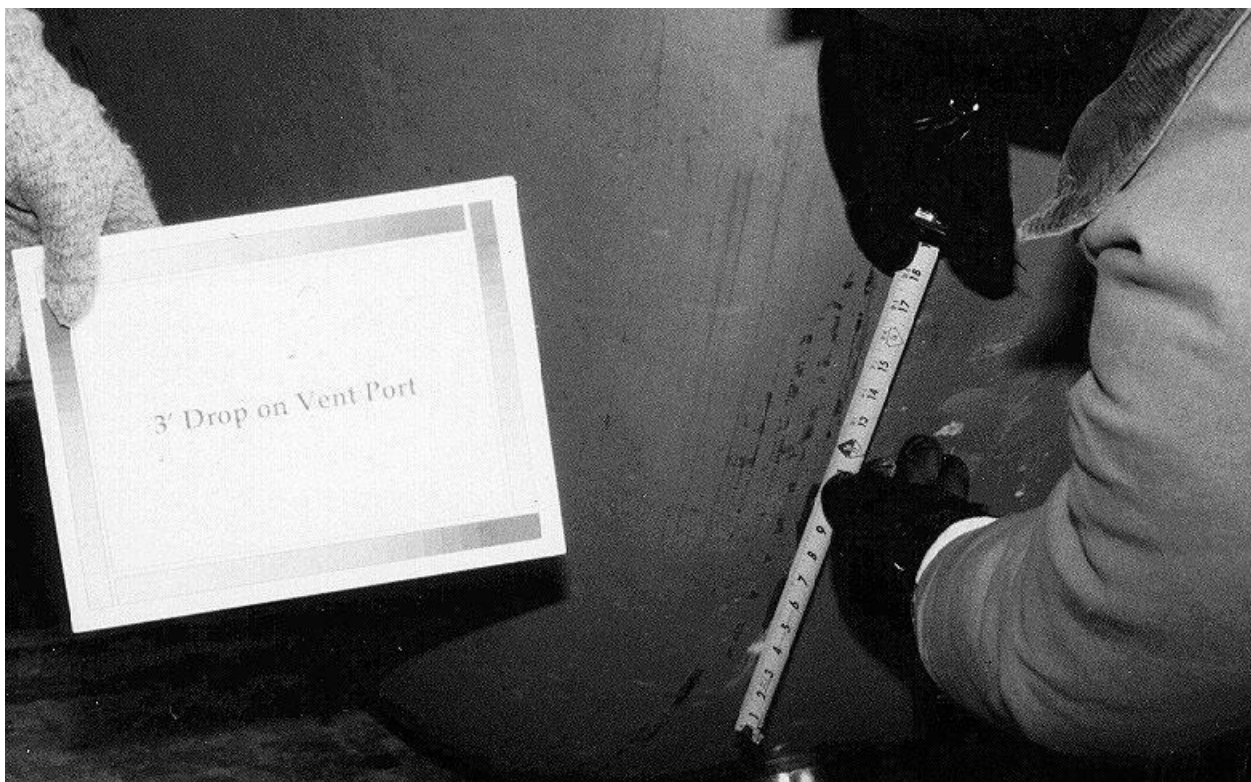


Figure 2.10.3-17 – ETU Free Drop Test 3; Top-End Damage; ~18" Wide Flat



Figure 2.10.3-18 – ETU Free Drop Test 4; Top-End Damage; ~34" Wide Flat



Figure 2.10.3-19 – ETU Free Drop Test 4; Bottom-End Damage; ~34" Wide Flat

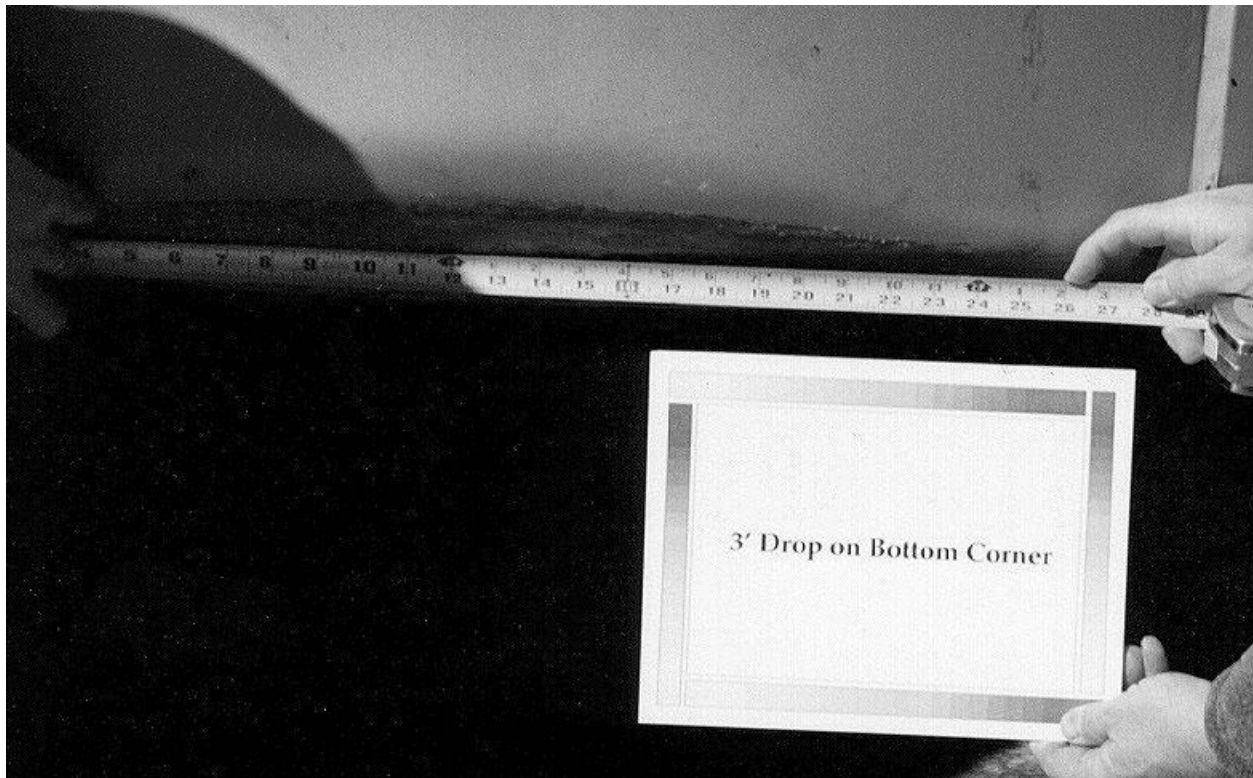


Figure 2.10.3-20 – ETU Free Drop Test 5; Bottom Corner Damage; ~26" Wide Flat



Figure 2.10.3-21 – ETU Free Drop Test 5; Bottom Corner Damage; ~5½" Deep Flat

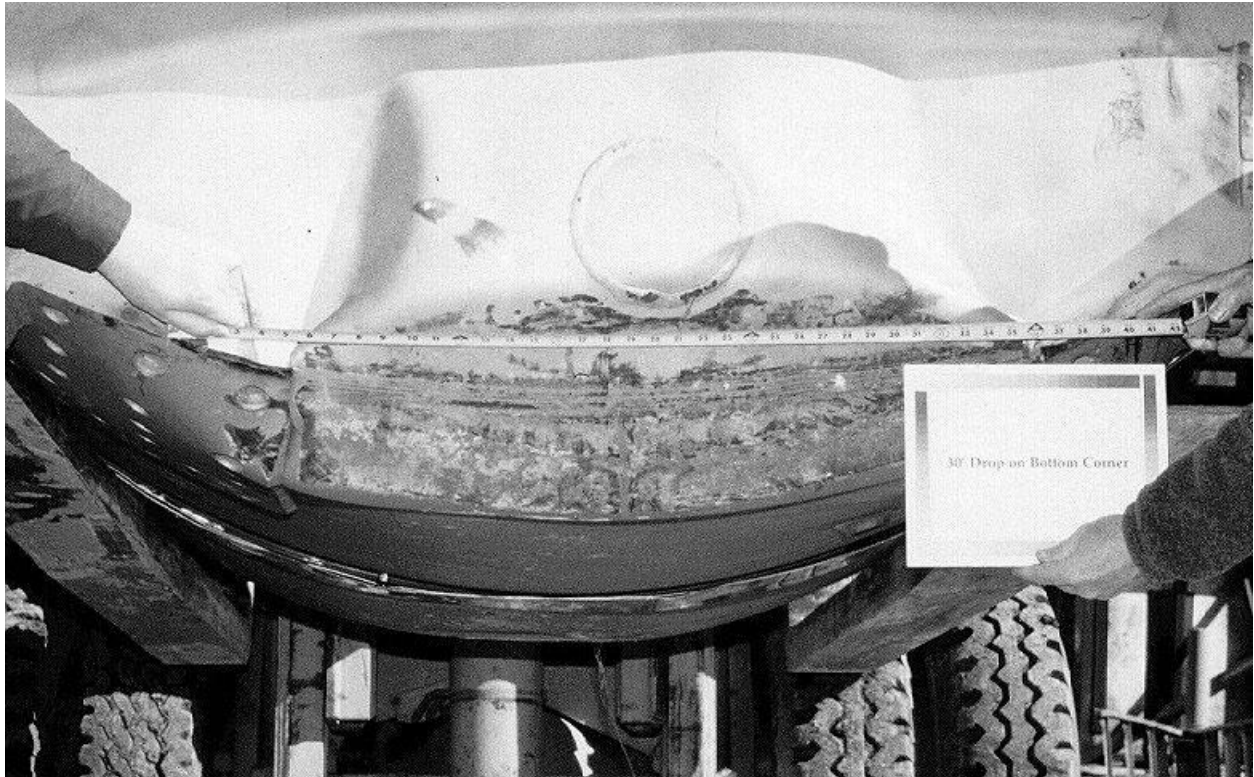


Figure 2.10.3-22 – ETU Free Drop Test 6; Bottom Corner Damage; ~40" Wide Flat



Figure 2.10.3-23 – ETU Free Drop Test 6; Bottom Corner Damage; ~12" Deep Flat



Figure 2.10.3-24 – ETU Puncture Drop Test 7; ~10½" High × ~11½" Wide Hole

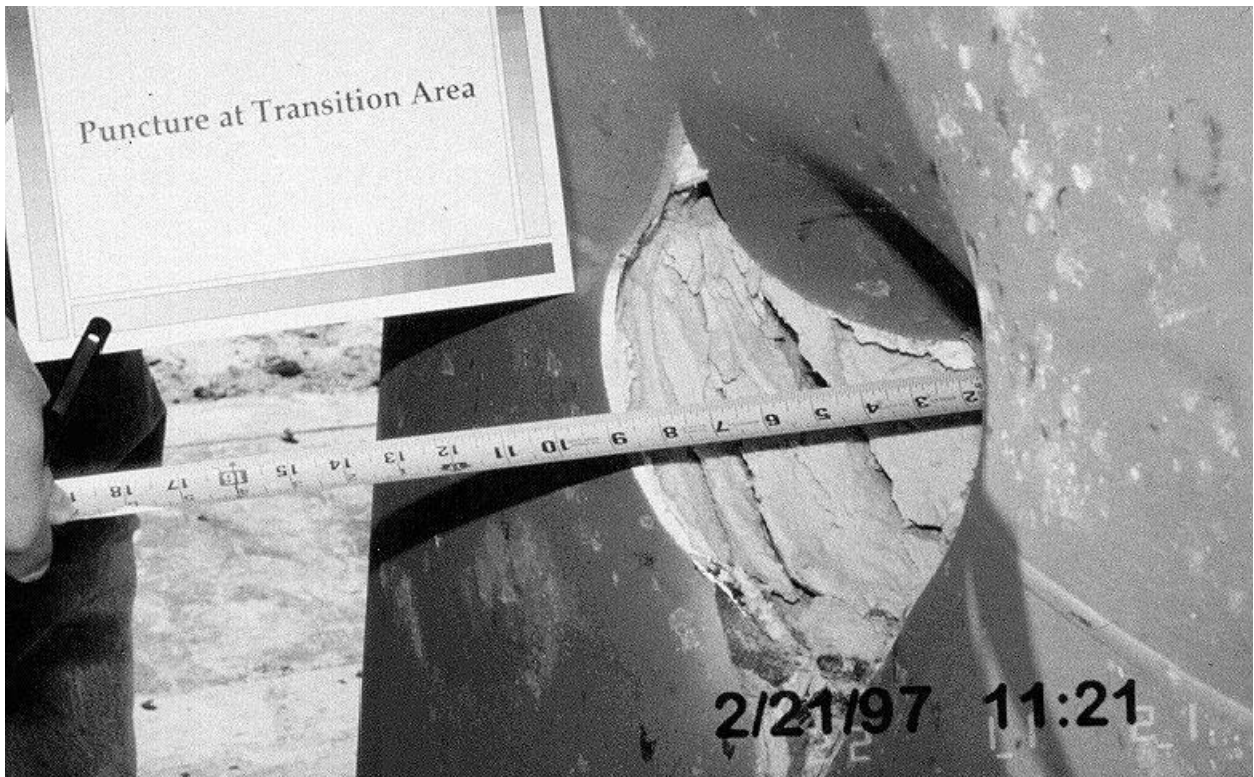


Figure 2.10.3-25 – ETU Puncture Drop Test 7; Radial Penetration ~8" Deep

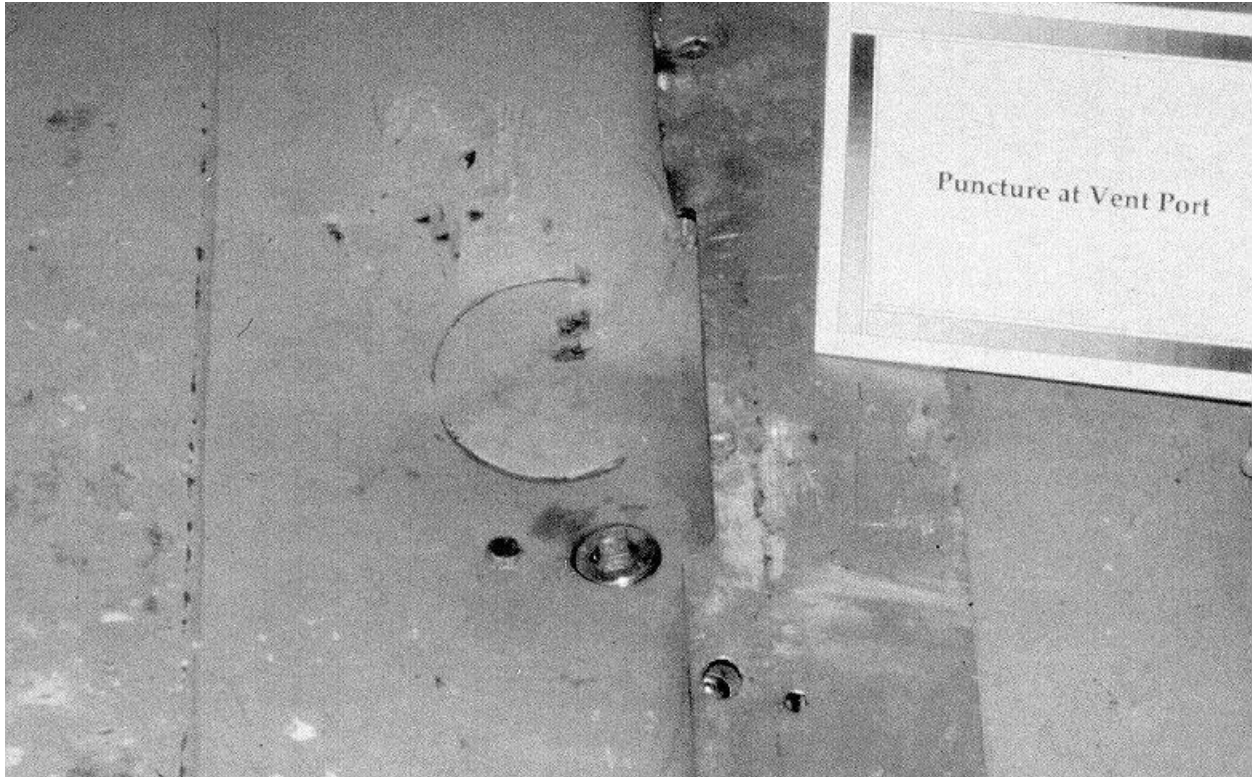


Figure 2.10.3-26 – ETU Puncture Drop Test 8; View of Damage; ~2½" Deep Dent



Figure 2.10.3-27 – ETU Puncture Drop Test 8; Close-up View of Damage; ~2½" Deep Dent

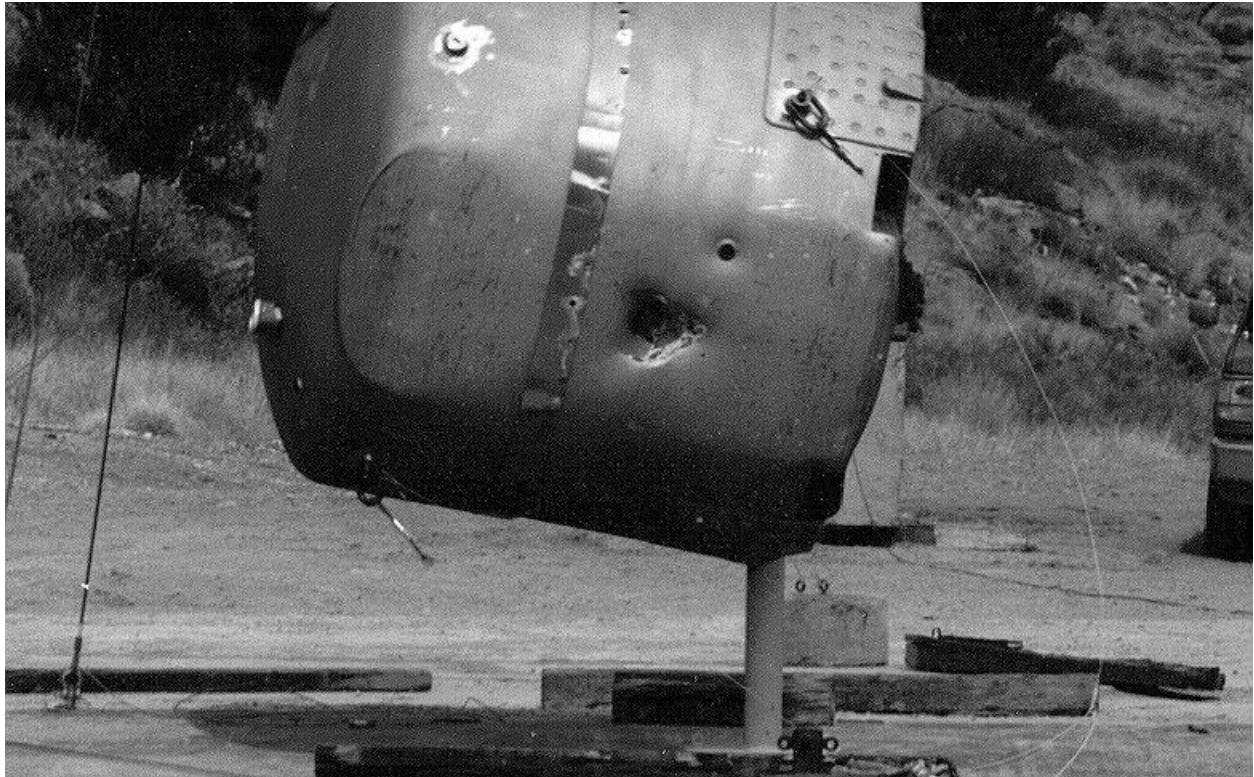


Figure 2.10.3-28 – ETU Puncture Drop Test 9; View of Impact on Puncture Bar



Figure 2.10.3-29 – ETU Puncture Drop Test 9; Bottom Corner Damage; ~3" Deep Dent

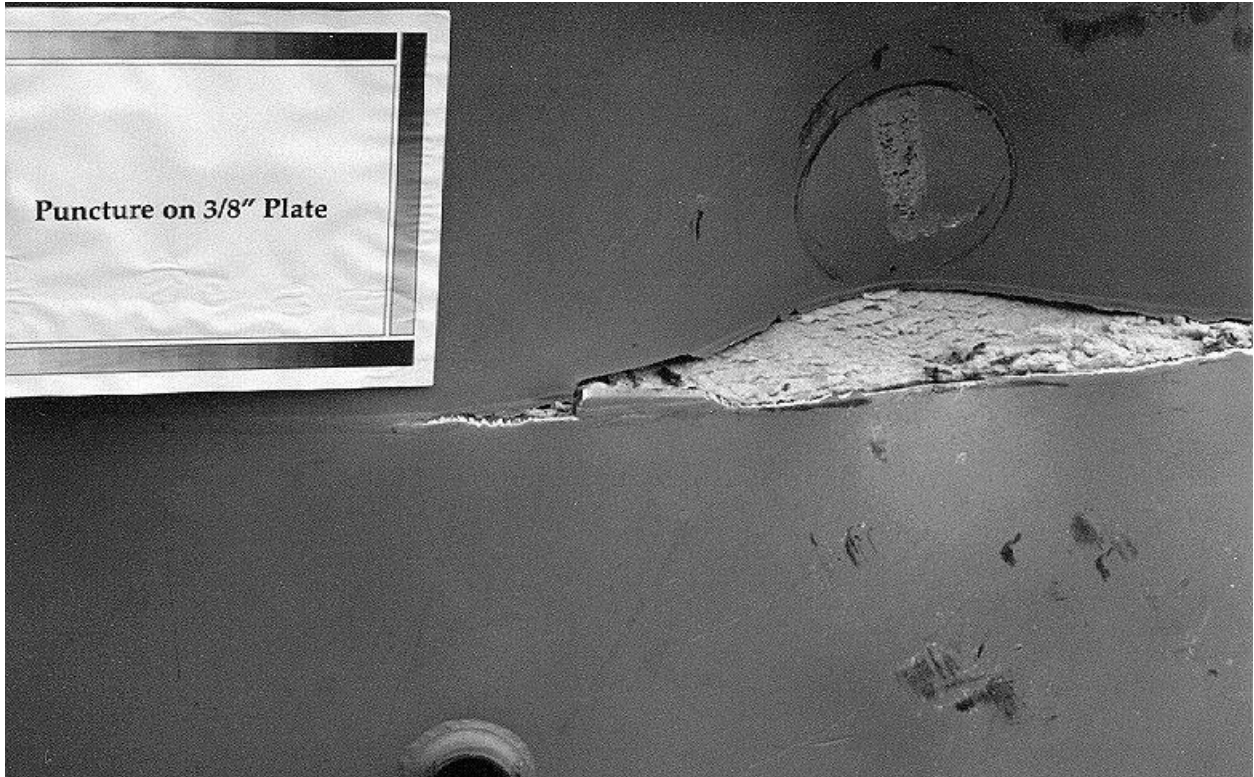


Figure 2.10.3-30 – ETU Puncture Drop Test 10; 3/8–to-1/4 Transition; ~27" Long Tear

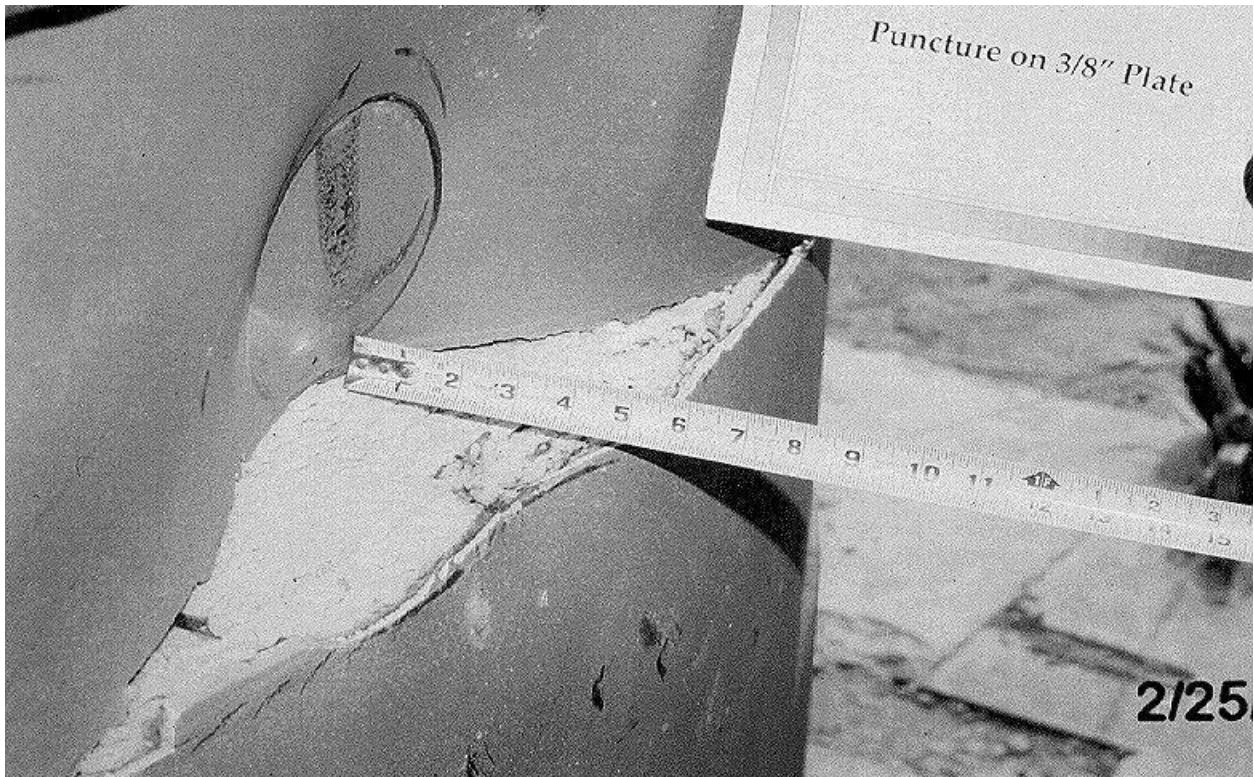


Figure 2.10.3-31 – ETU Puncture Drop Test 10; 3/8–to-1/4 Transition; ~5½" Deep Dent

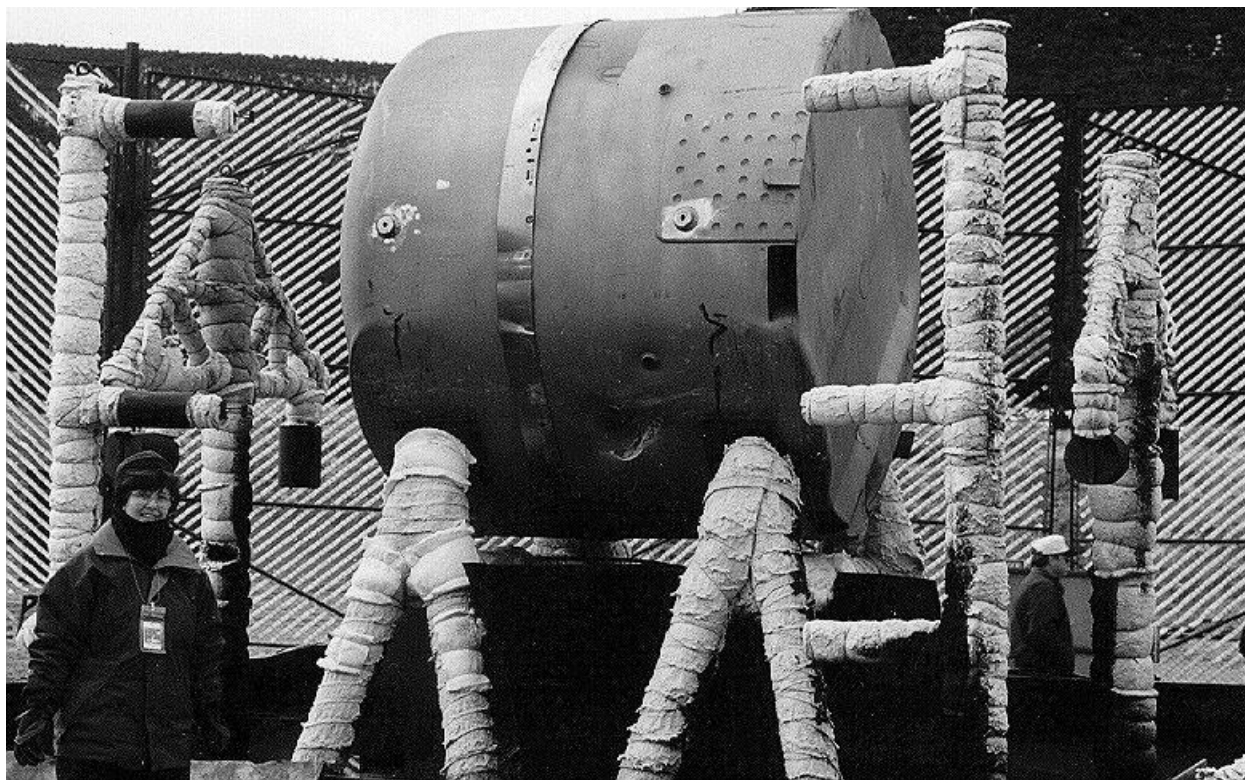


Figure 2.10.3-32 – ETU Fire Test 11; Side 1 View Showing Tests 1, 2, 7, & 10 Damage



Figure 2.10.3-33 – ETU Fire Test 11; Side 2 View Showing Tests 3, 4, 5, 6, 8, & 9 Damage

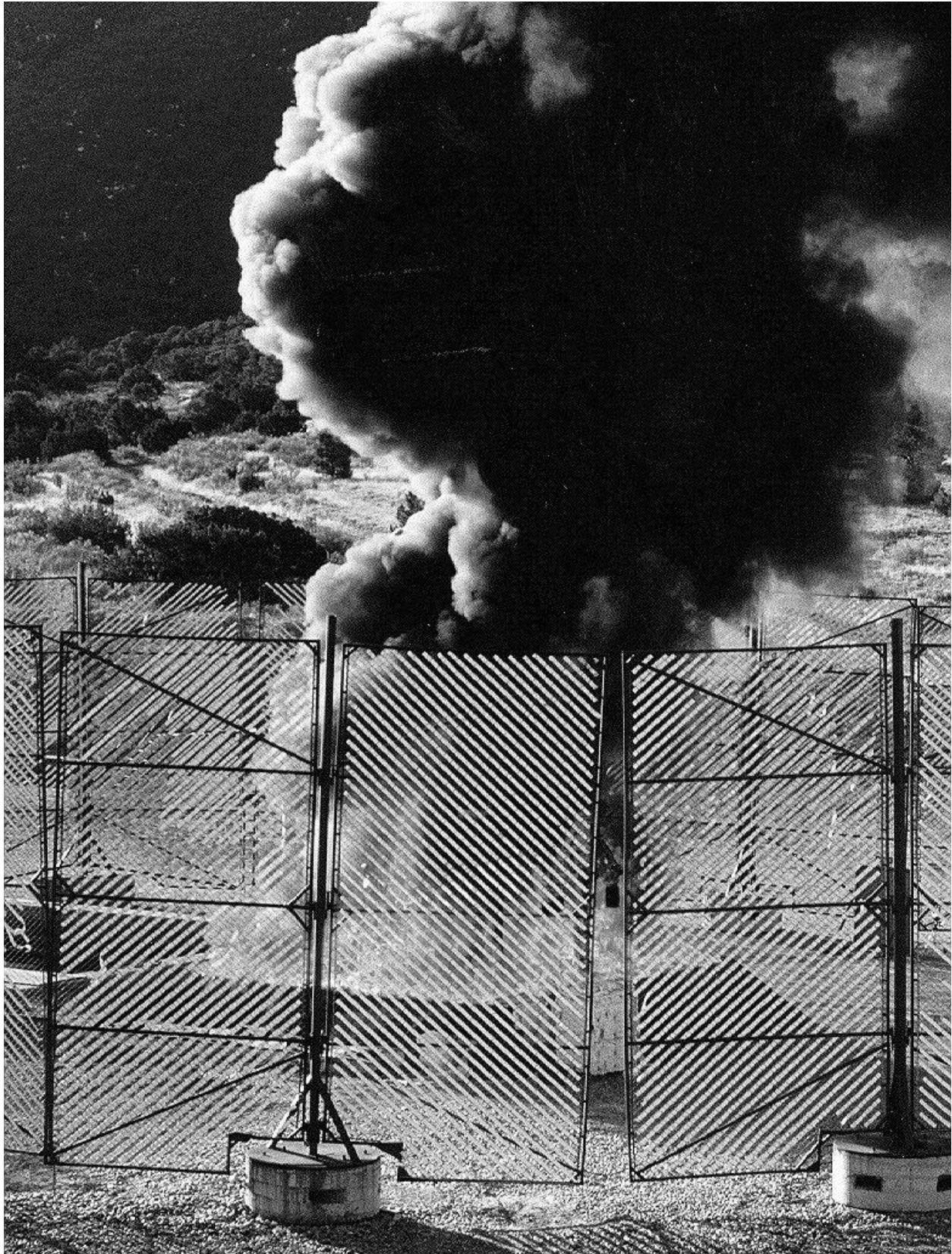


Figure 2.10.3-34 – ETU Fire Test 11; Overall View ~5 Minutes after Start of Fire

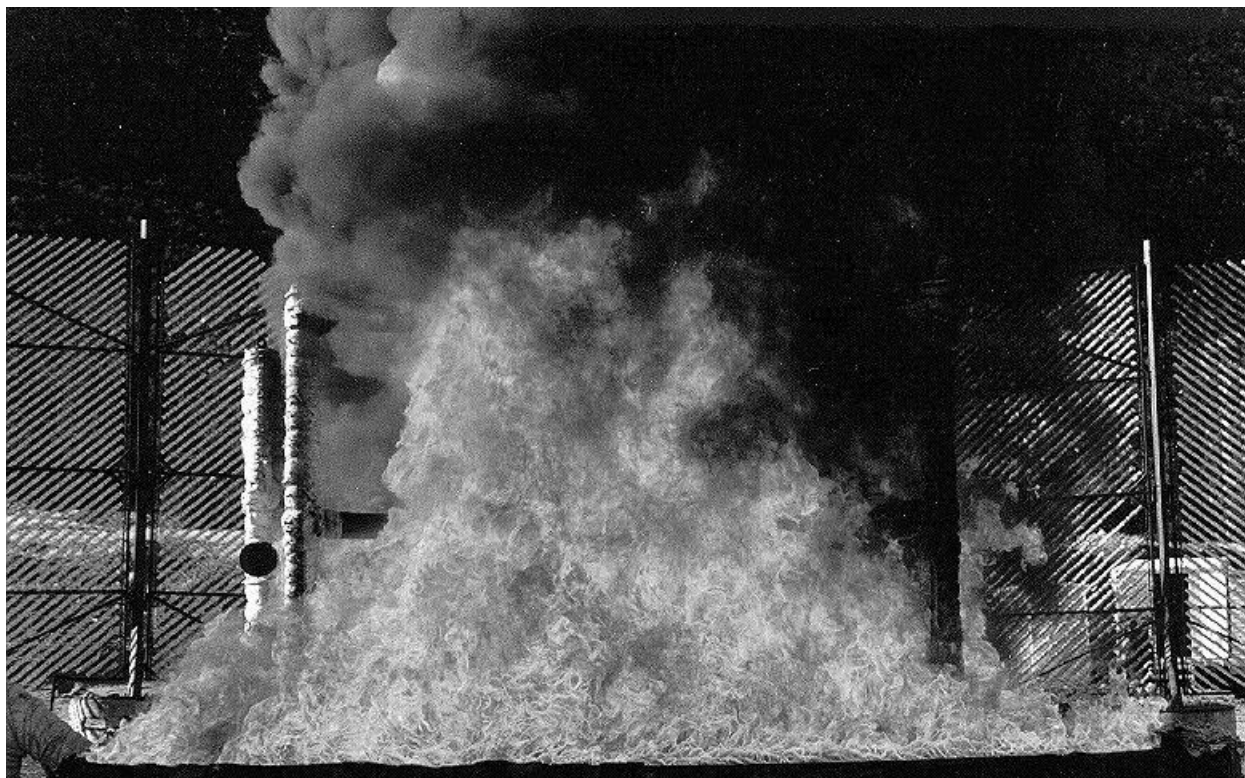


Figure 2.10.3-35 – ETU Fire Test 11; View ~12 Minutes after Start of Fire

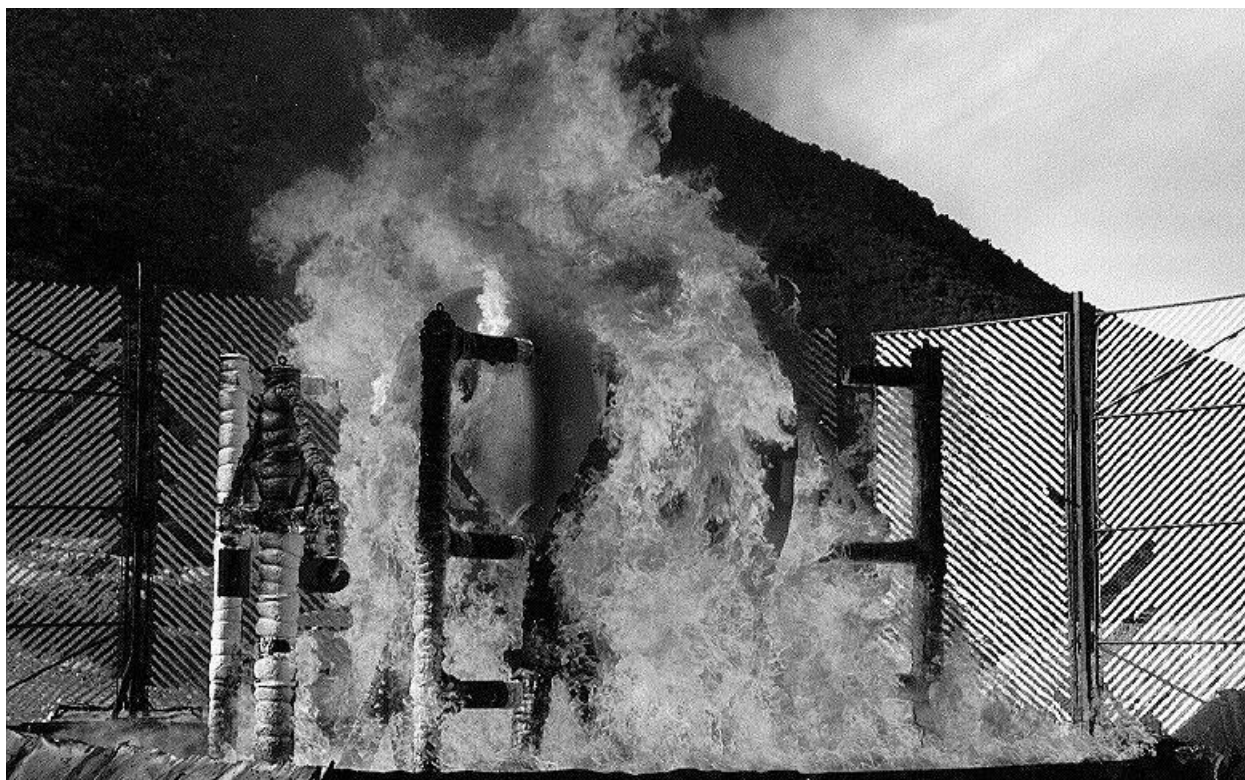


Figure 2.10.3-36 – ETU Fire Test 11; View ~25 Minutes after Start of Fire

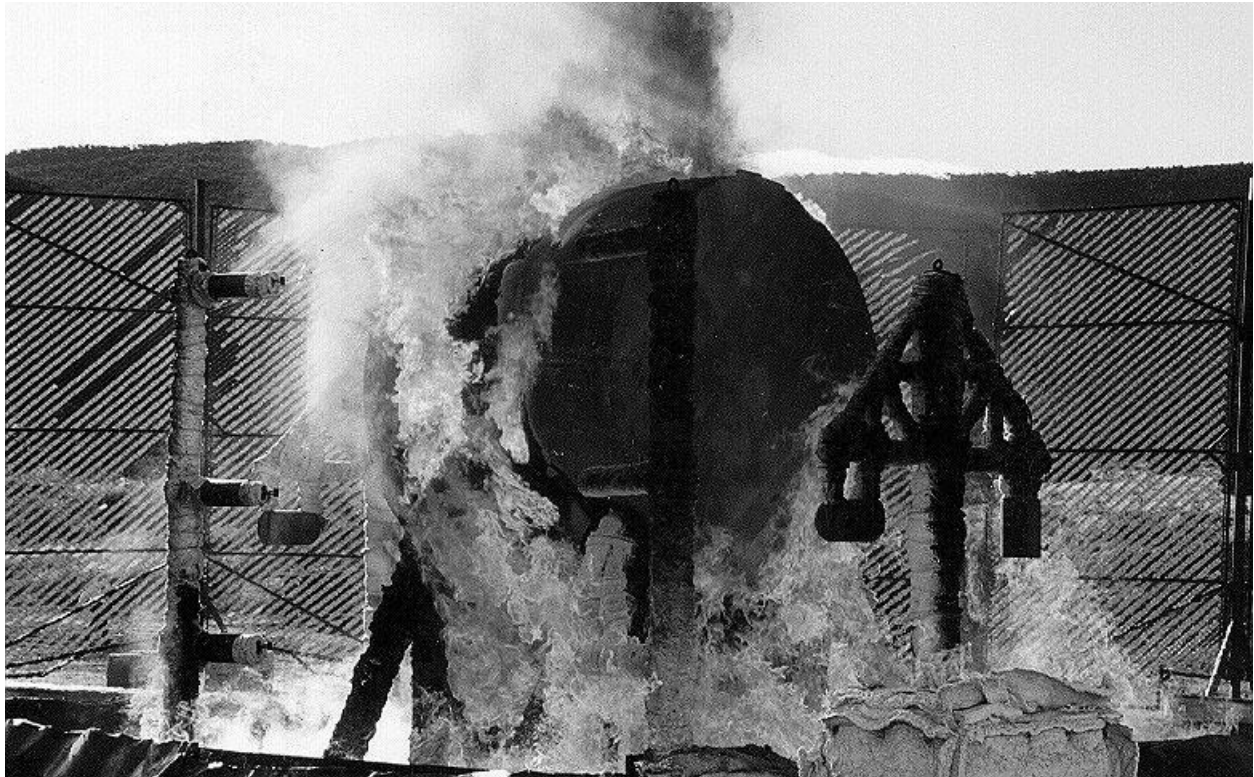


Figure 2.10.3-37 – ETU Fire Test 11; View ~32 Minutes after Start of Fire



Figure 2.10.3-38 – ETU Fire Test 11; View ~17 Minutes after End of Fire

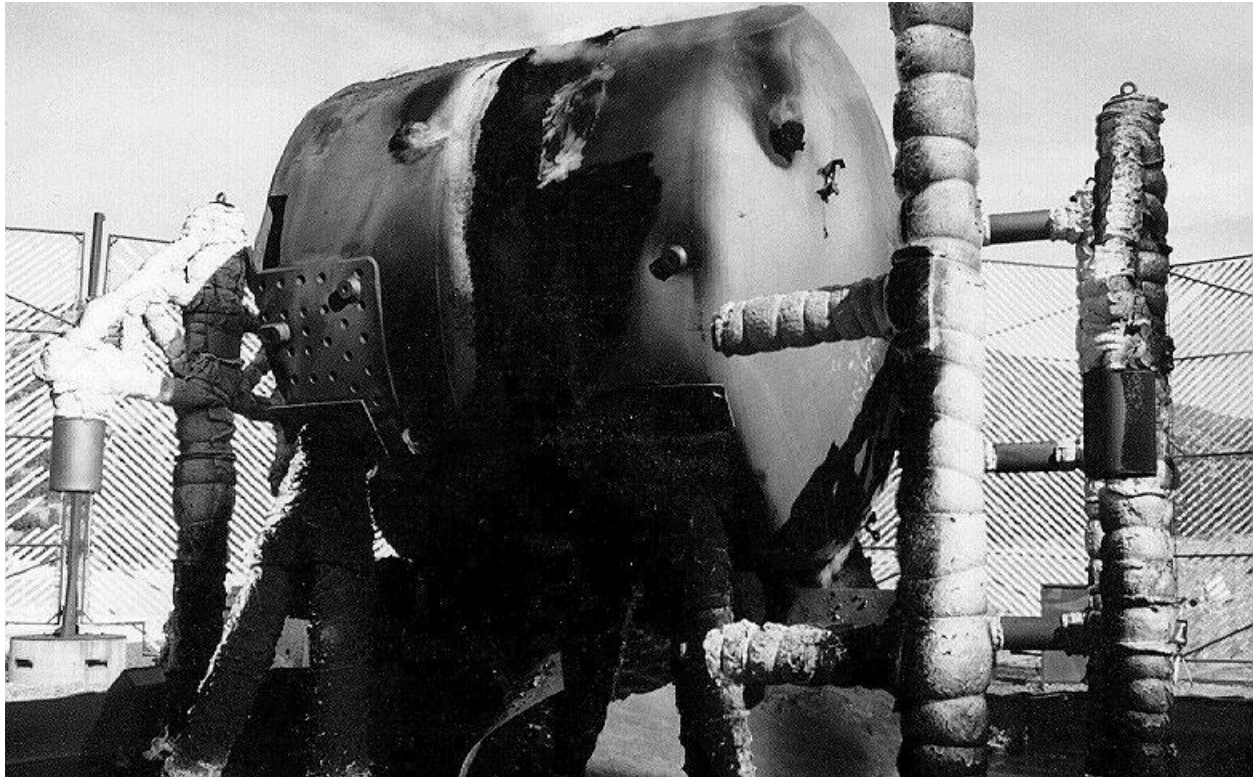


Figure 2.10.3-39 – ETU Fire Test 11; View ~37 Minutes after End of Fire

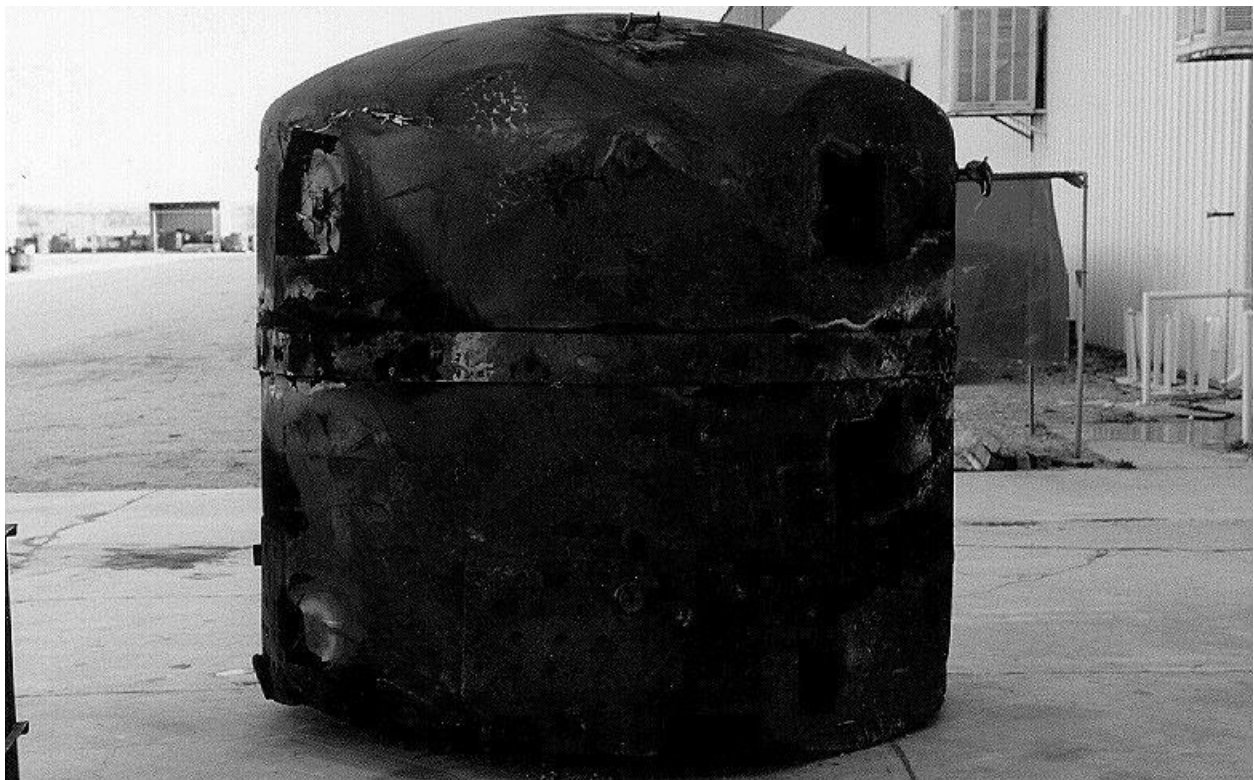


Figure 2.10.3-40 – ETU; View Before Disassembly



Figure 2.10.3-41 – ETU; Removal of the OCA Lid Outer Shell (Note Crumbling Foam Char)

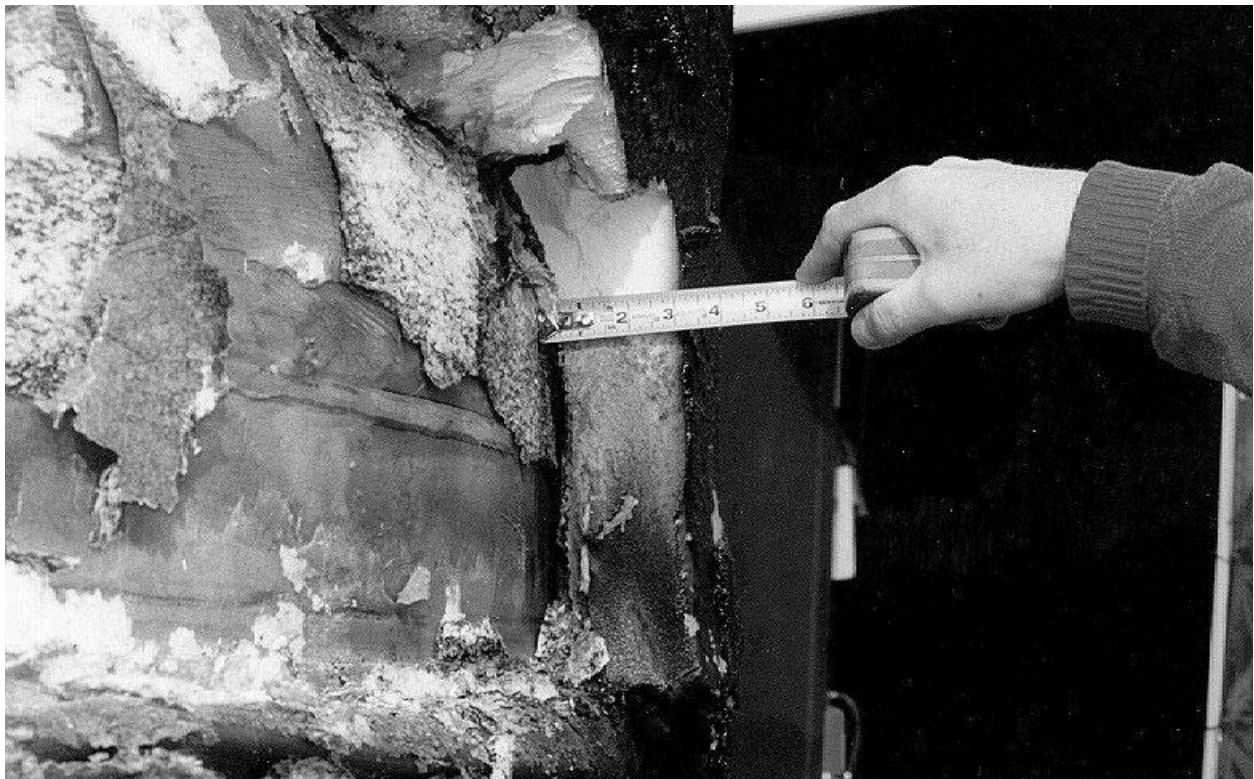


Figure 2.10.3-42 – ETU; Residual Foam in OCA Lid Side; Aligned with Test 1, 2, & 7 Damage



Figure 2.10.3-43 – ETU; Residual Foam in OCA Lid Side; Remote From Test Damage



Figure 2.10.3-44 – ETU; Residual Foam in OCA Lid Top (~11")



Figure 2.10.3-45 – ETU; View of OCV Seal Test Port Plug (As Removed; Not Cleaned)



Figure 2.10.3-46 – ETU; View of OCV Vent Port Cover (As Removed; Not Cleaned)



Figure 2.10.3-47 – ETU; View of OCV Vent Port Plug (As Removed; Not Cleaned)



Figure 2.10.3-48 – ETU; View of 55-Gallon Payload Drums Following ICV Lid Removal



Figure 2.10.3-49 – ETU; View of ICV Body Cavity Following Payload Drum Removal



Figure 2.10.3-50 – ETU; View of Debris Inside ICV Body Cavity After Payload Drum Removal

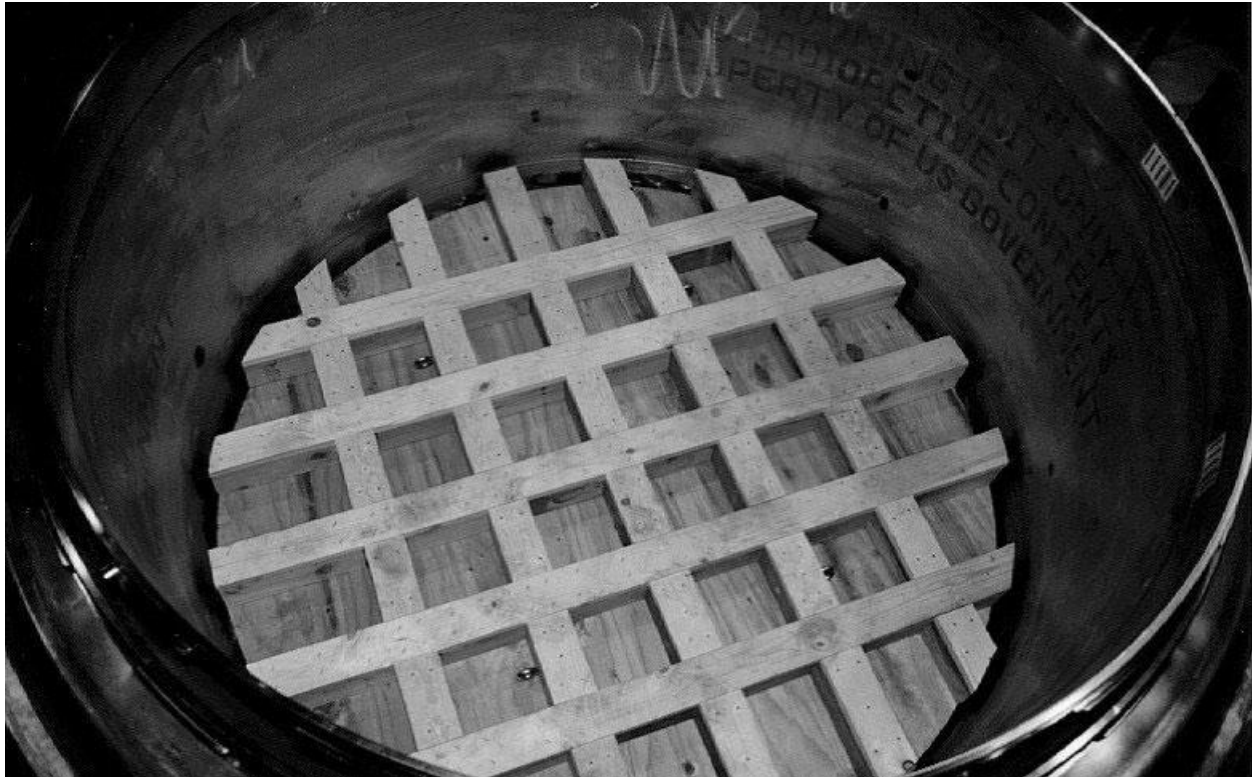


Figure 2.10.3-51 – CTU; 5 Inch Thick Payload Spacer (Wood Simulation) in Bottom of ICV

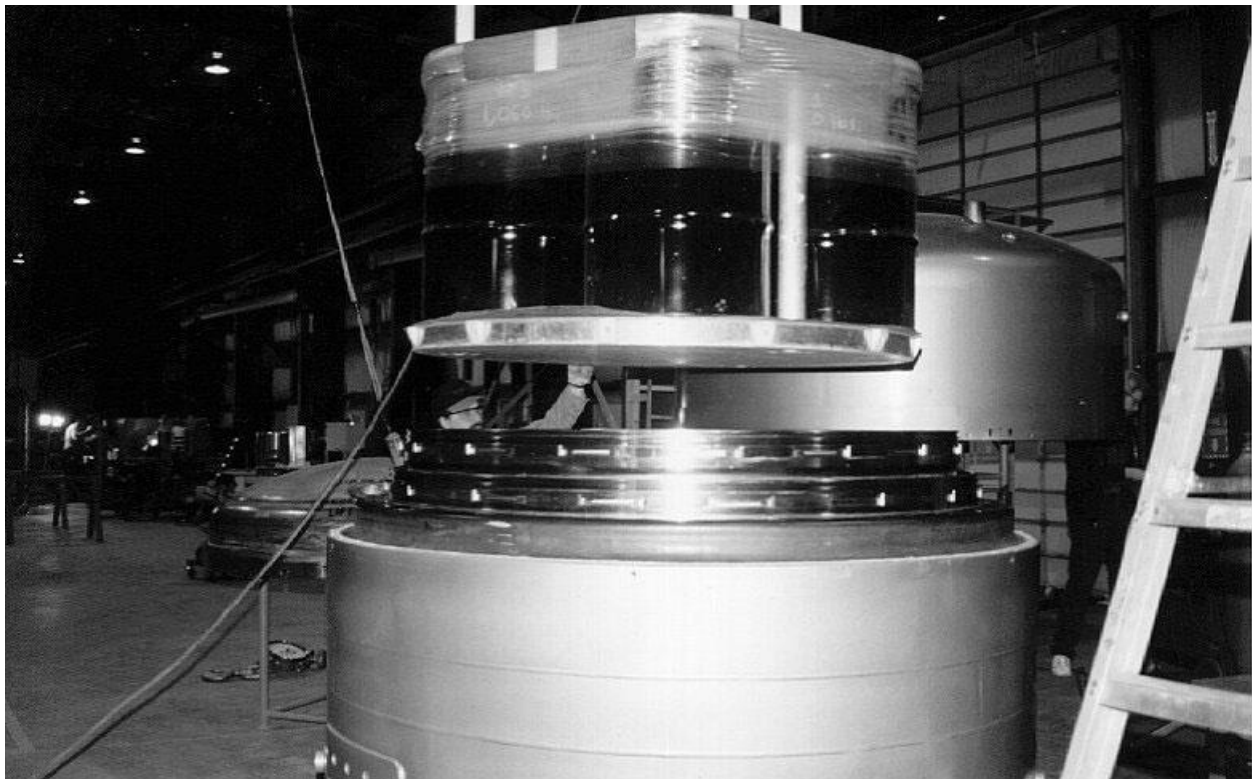


Figure 2.10.3-52 – CTU; Aligning 55-Gallon Drum Payload Assembly for Installation into ICV



Figure 2.10.3-53 – CTU; Final ICV Lid Alignment During ICV Lid Installation

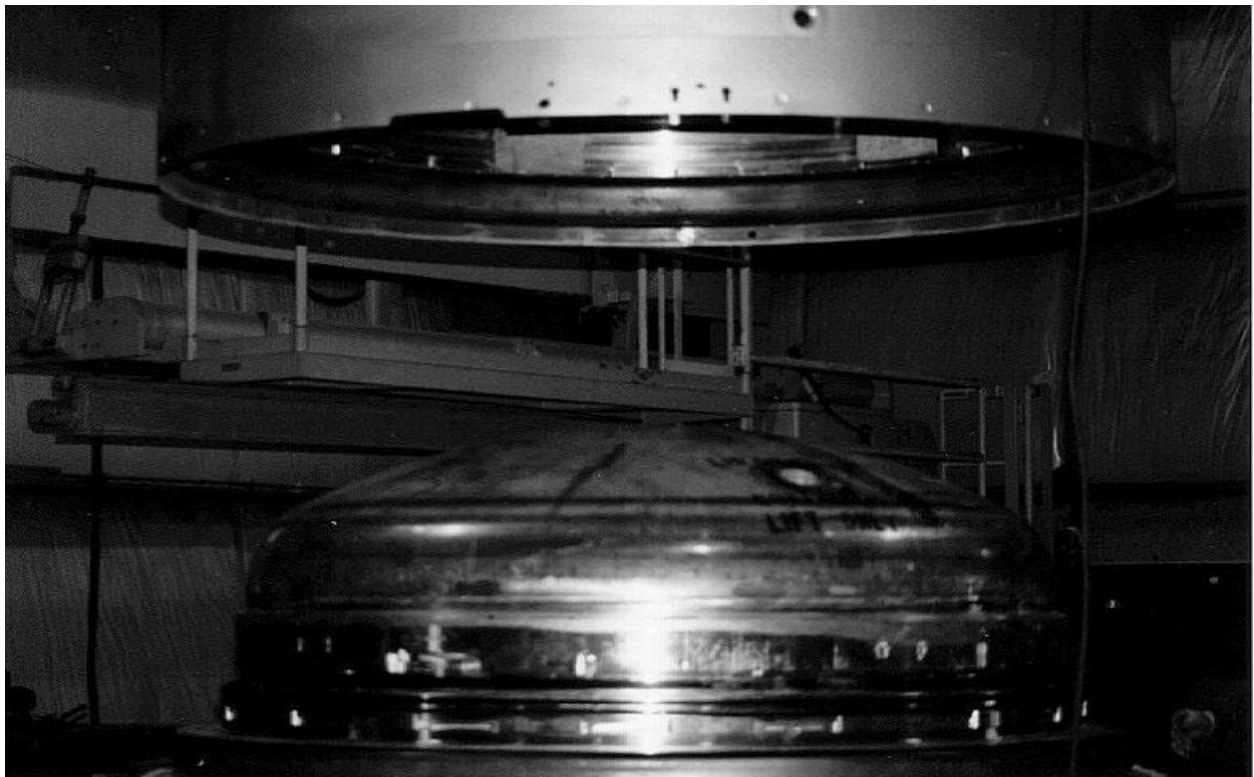


Figure 2.10.3-54 – CTU; Final OCA Lid Alignment During OCA Lid Installation



Figure 2.10.3-55 – CTU; Certification Test Unit (TRUPACT-II Unit 107) After Final Assembly

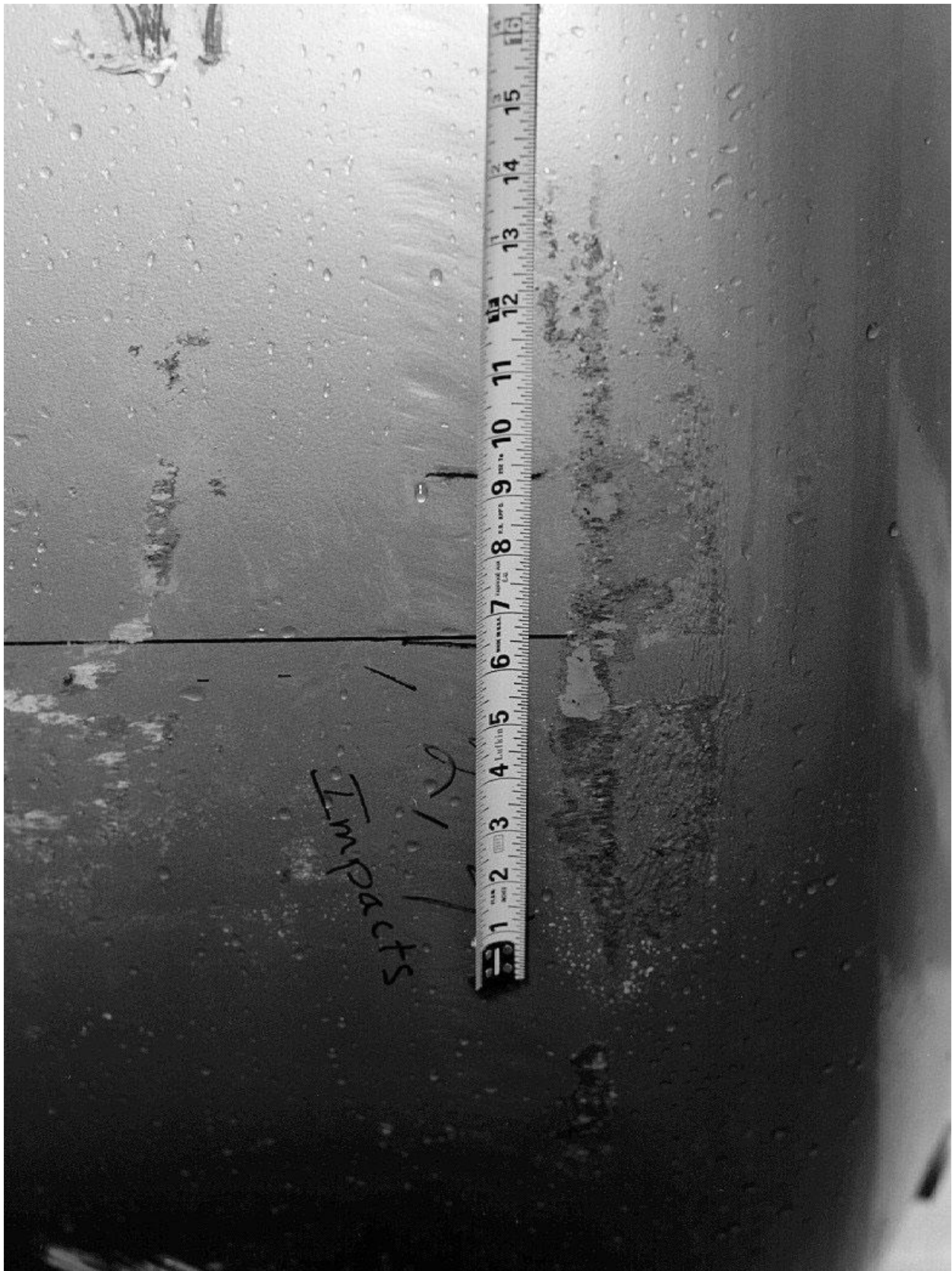


Figure 2.10.3-56 – CTU Free Drop Test 1; Lid-End Damage; ~13" Wide Flat



Figure 2.10.3-57 – CTU Free Drop Test 1; Bottom-End Damage; ~13" Wide Flat



Figure 2.10.3-58 – CTU Free Drop Test 2; Lid-End Damage; ~37” Wide Flat



Figure 2.10.3-59 – CTU Free Drop Test 2; Bottom-End Damage; ~37" Wide Flat

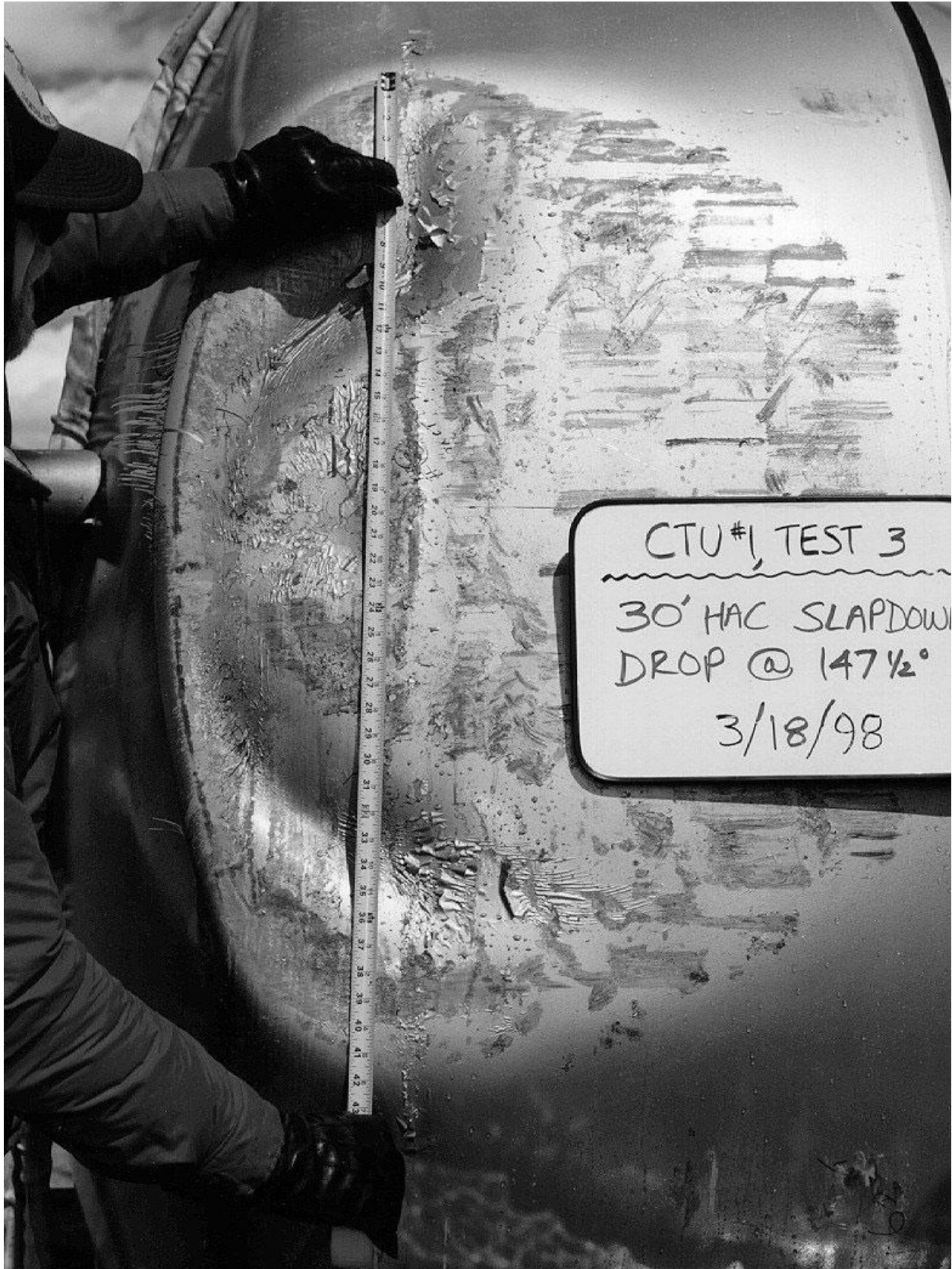


Figure 2.10.3-60 – CTU Free Drop Test 3; Lid-End Damage; ~41½" Wide Flat



Figure 2.10.3-61 – CTU Free Drop Test 3; Bottom-End Damage

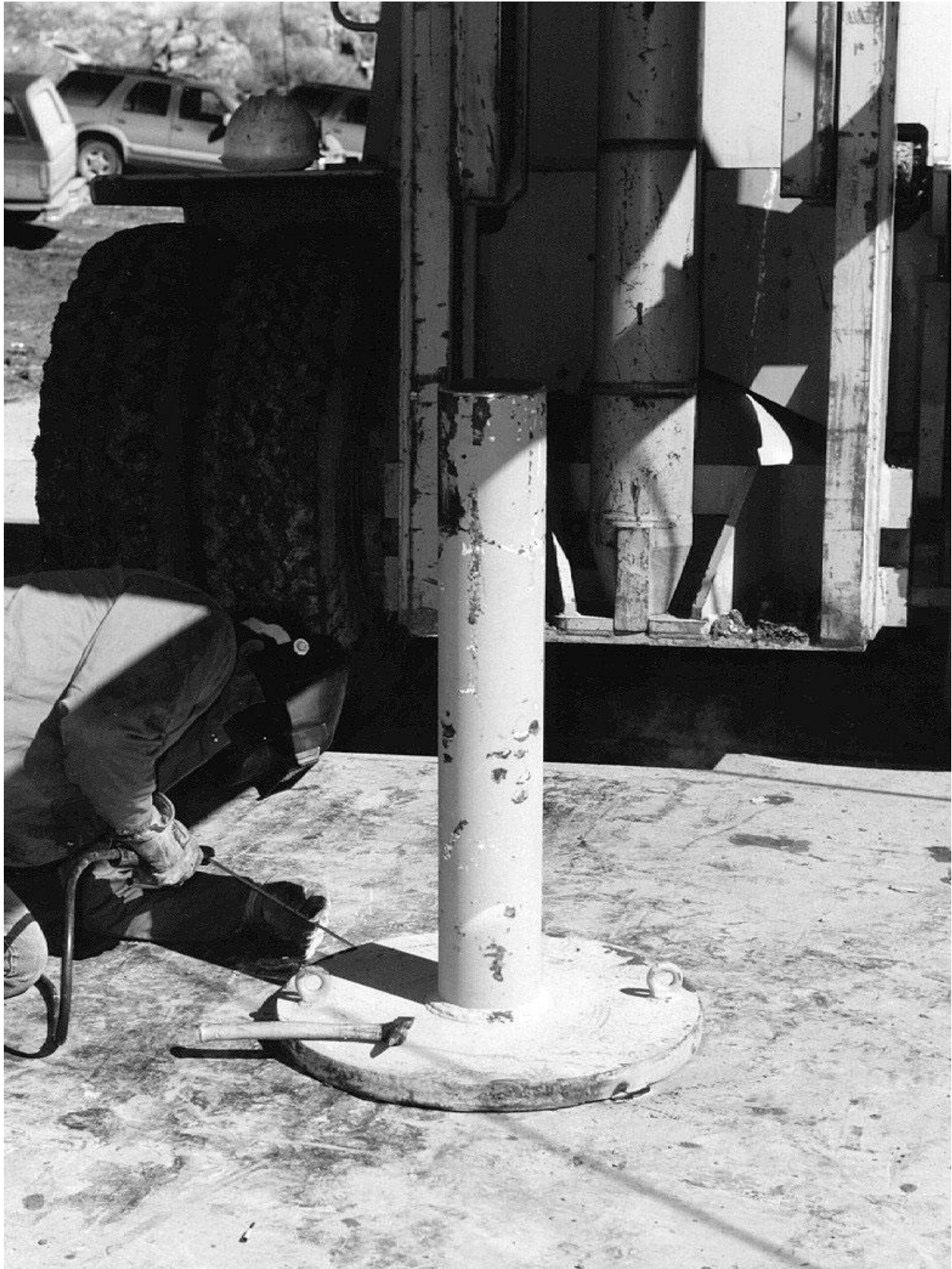


Figure 2.10.3-62 – CTU Puncture Drop Test 4; Mounting the Puncture Bar



Figure 2.10.3-63 – CTU Puncture Drop Test 4; Close-up View of Damage



Figure 2.10.3-64 – CTU Puncture Drop Test 4; Close-up Profile View of Damage; ~3³/₄" Deep

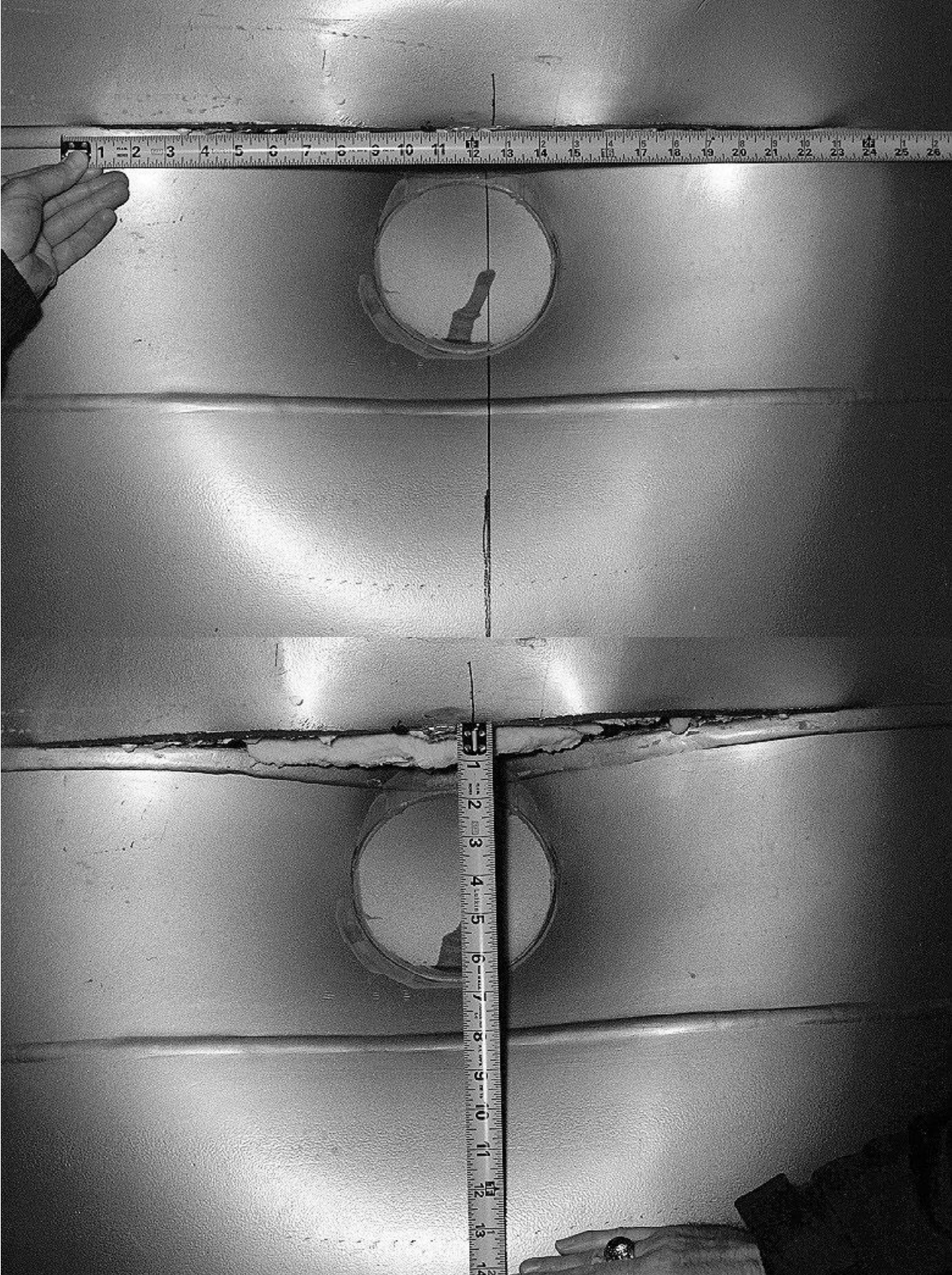


Figure 2.10.3-65 – CTU Puncture Drop Test 5; Close-up View of Damage

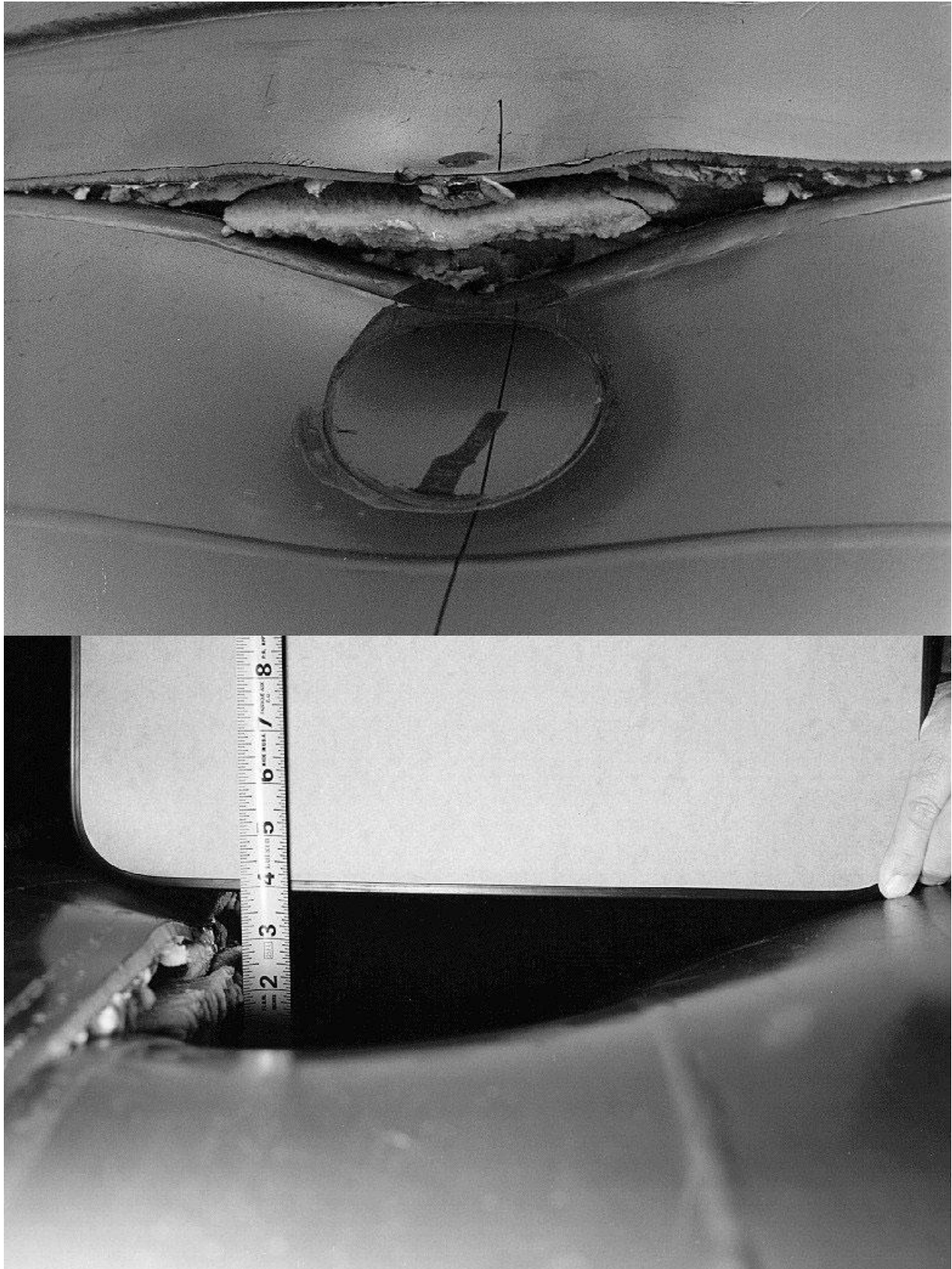


Figure 2.10.3-66 – CTU Puncture Drop Test 5; Profile Views of Damage; ~4" Deep



Figure 2.10.3-67 – CTU Puncture Drop Test 6; Overall View of Damage

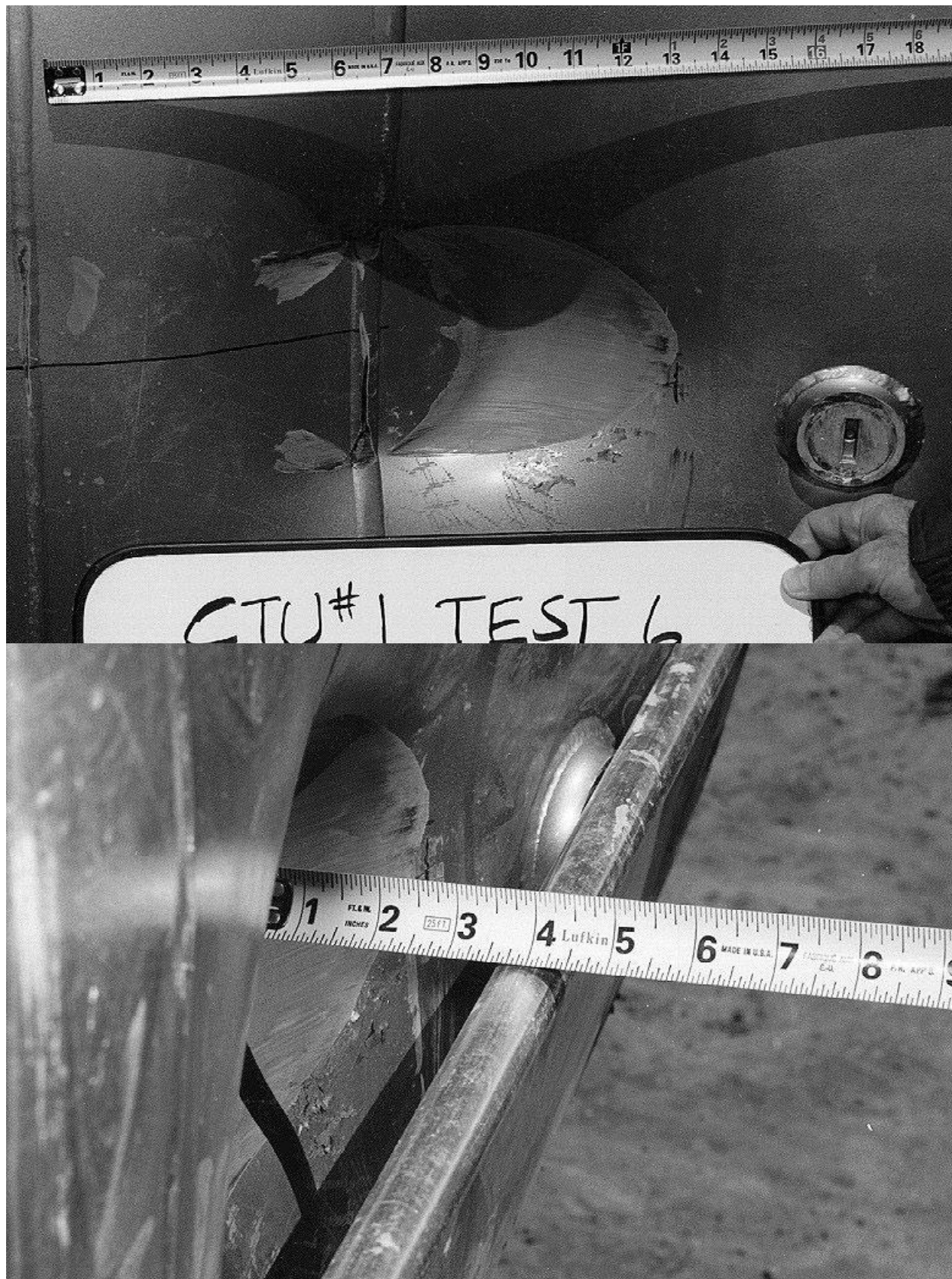


Figure 2.10.3-68 – CTU Puncture Drop Test 6; Close-up Views of Damage; ~3½" Deep

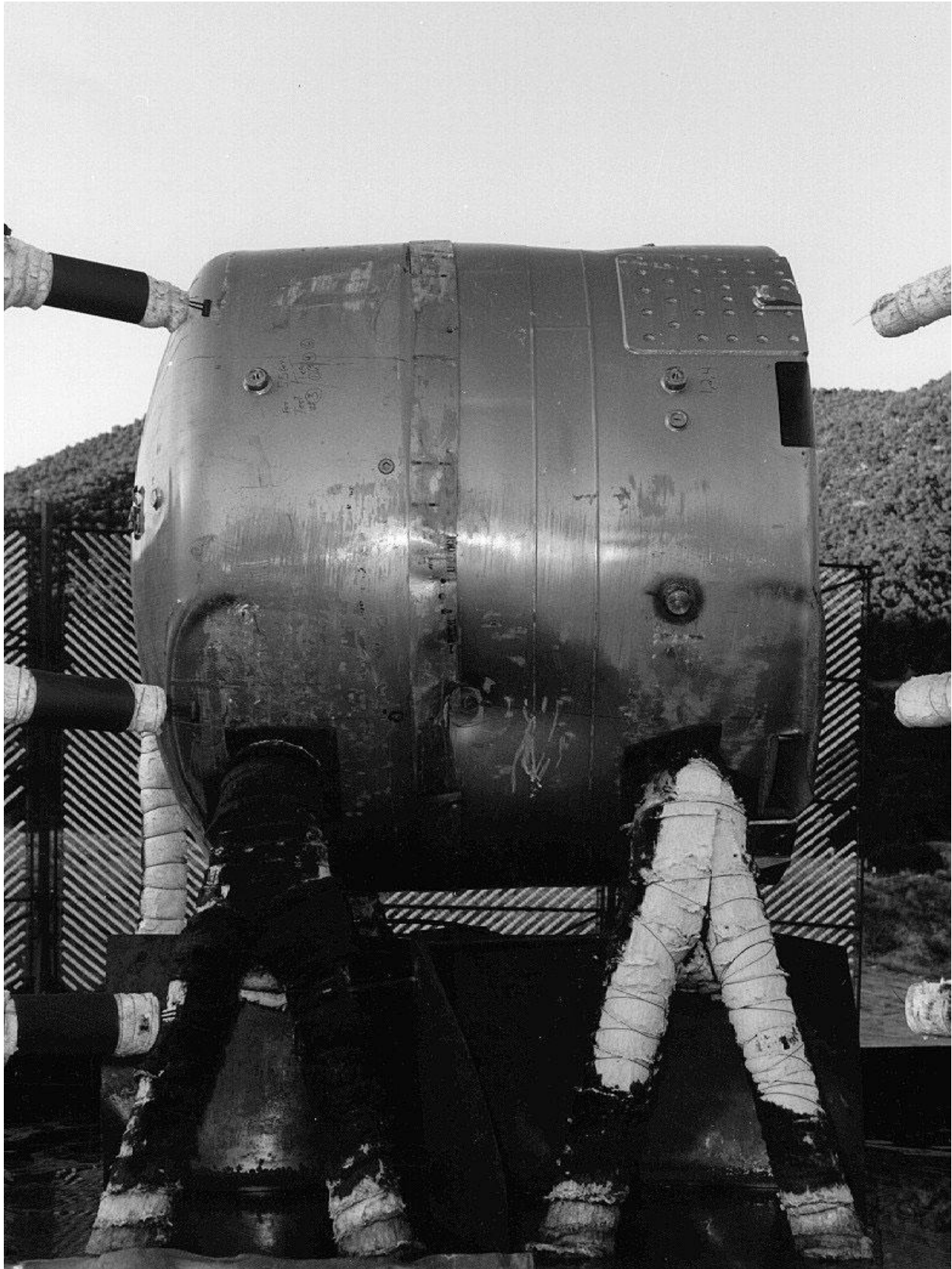


Figure 2.10.3-69 – CTU Fire Test 7; Side 1 View Before Fire Showing Tests 1, 2, & 4 Damage



Figure 2.10.3-70 – CTU Fire Test 7; Side 2 View Before Fire Showing Test 5 Damage

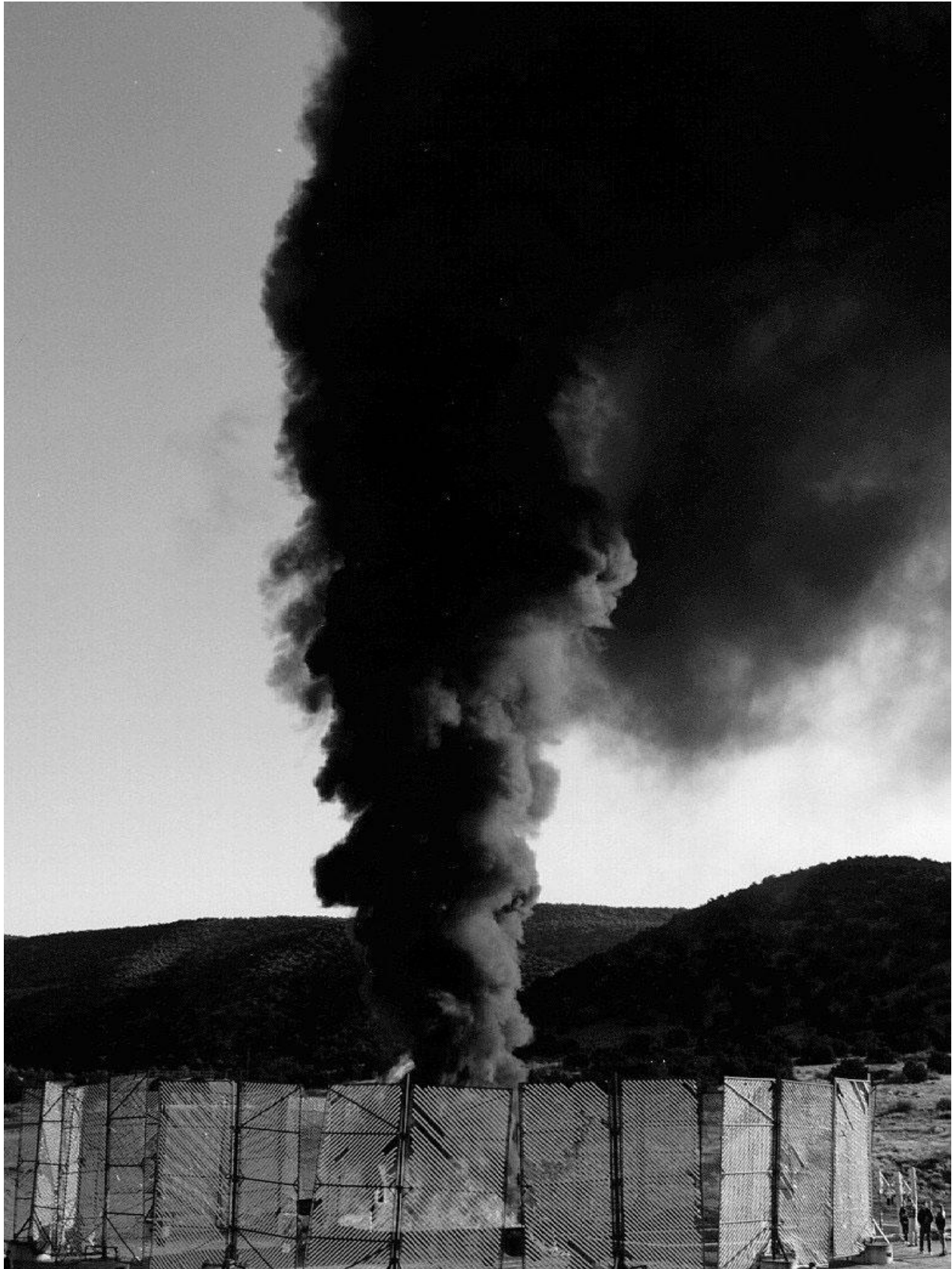


Figure 2.10.3-71 – CTU Fire Test 7; Overall View ~5 Minutes after Start

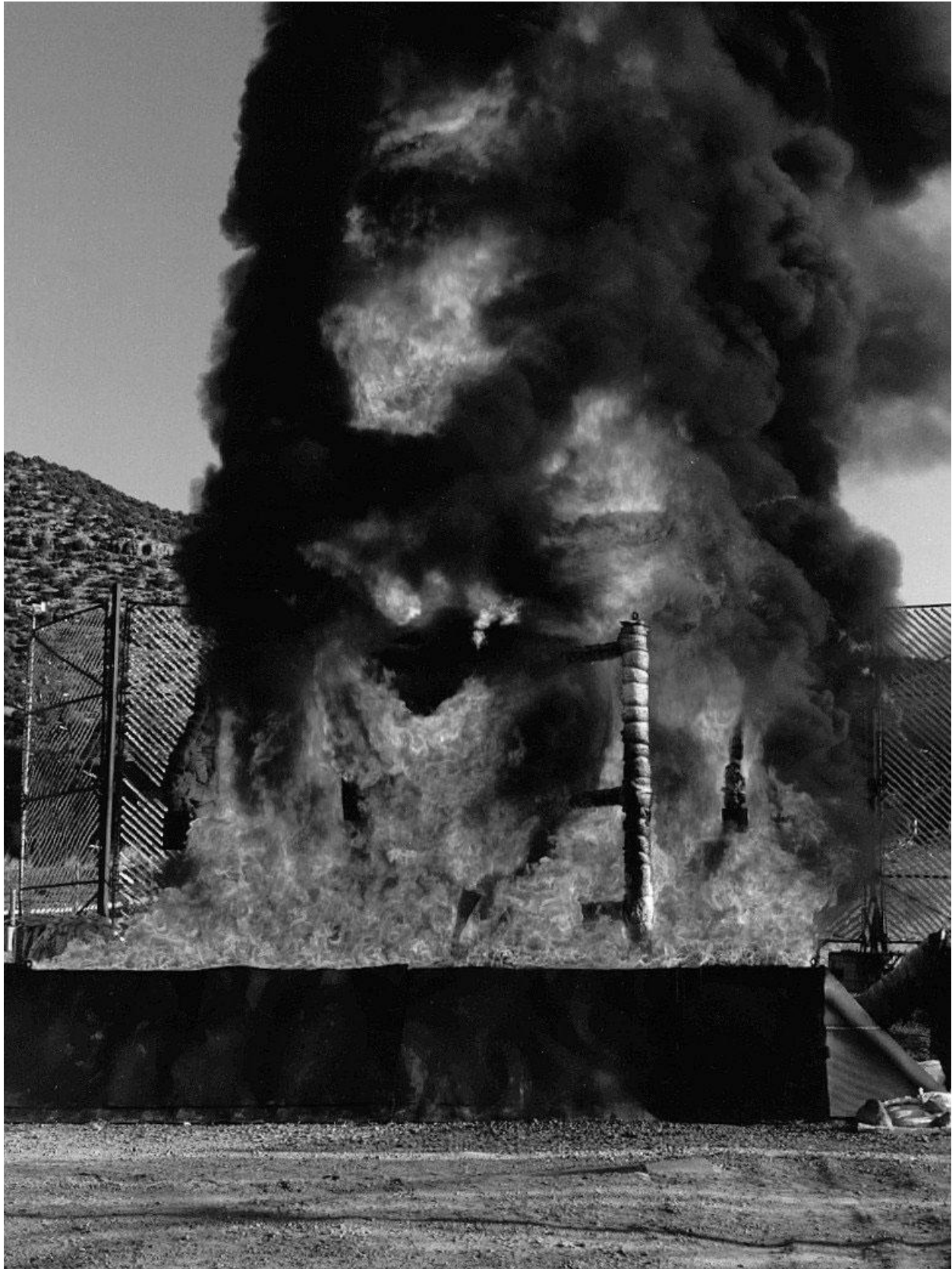


Figure 2.10.3-72 – CTU Fire Test 7; View ~10 Minutes after Start



Figure 2.10.3-73 – CTU Fire Test 7; View ~15 Minutes after Start (Showing Wind Effects)



Figure 2.10.3-74 – CTU Fire Test 7; View ~28 Minutes after Start (Note Flares at Vents)



Figure 2.10.3-75 – CTU Fire Test 7; Side 1 View ~33 Minutes after Start (End of Fire)



Figure 2.10.3-76 – CTU Fire Test 7; Side 2 View ~33 Minutes after Start (End of Fire)

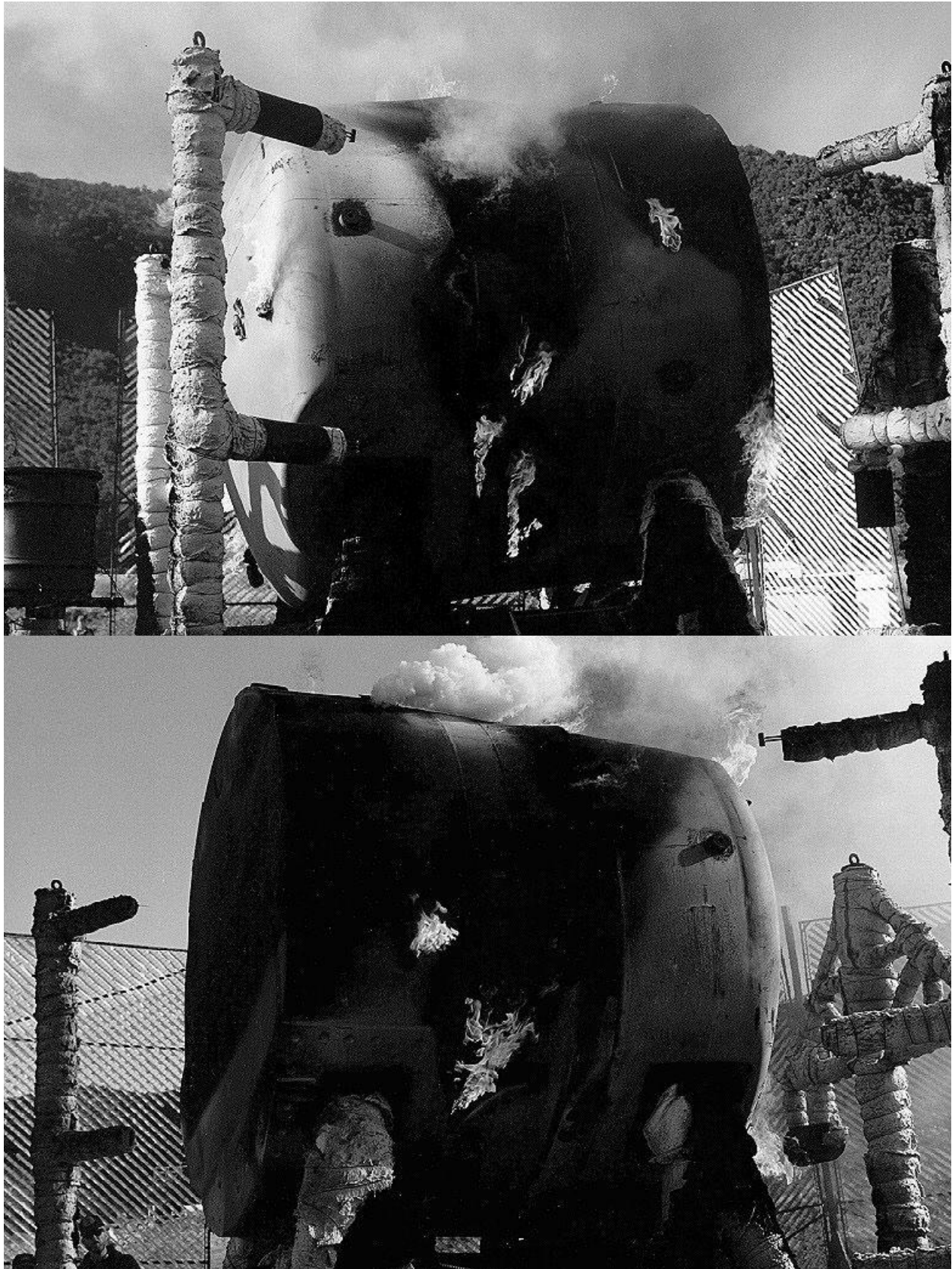


Figure 2.10.3-77 – CTU Fire Test 7; Side 1/2 Views ~10 Minutes after End of Fire



Figure 2.10.3-78 – CTU; View Before Disassembly (OCV Seal Test Port in Foreground)



Figure 2.10.3-79 – CTU; Removal of the OCA Lid Outer Shell (Note Crumbling Foam Char)



Figure 2.10.3-80 – CTU; Residual Foam in OCA Lid Side; Aligned with Test 1, 2, & 4 Damage



Figure 2.10.3-81 – CTU; Residual Foam in OCA Lid Knuckle; Aligned with Test 1, 2, & 4 Damage

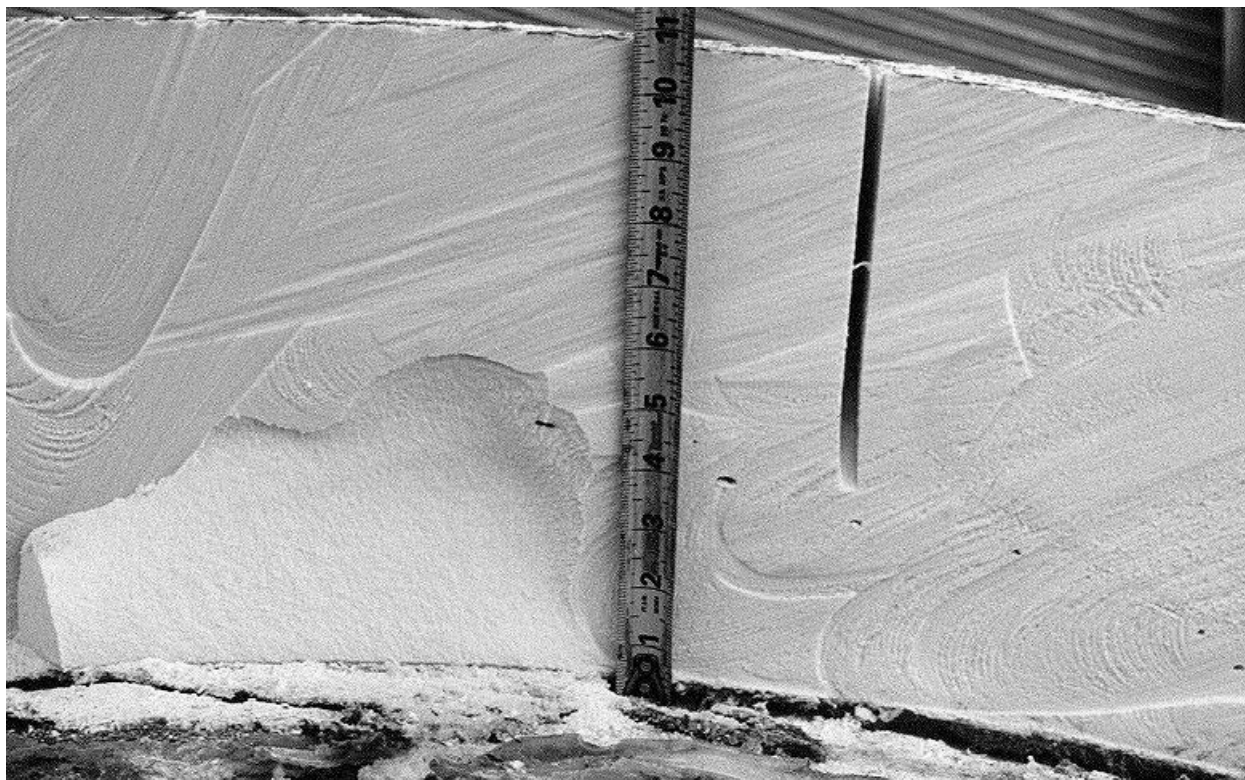


Figure 2.10.3-82 – CTU; Residual Foam in OCA Lid Top (~11")



Figure 2.10.3-83 – CTU; Residual Foam in OCA Lid Side; Remote from Test Damage



Figure 2.10.3-84 – CTU; Close-up of OCV Seal Test Port Plug (As Removed/Not Cleaned)



Figure 2.10.3-85 – CTU; OCV Vent Port Region After Removing Excess Foam Char

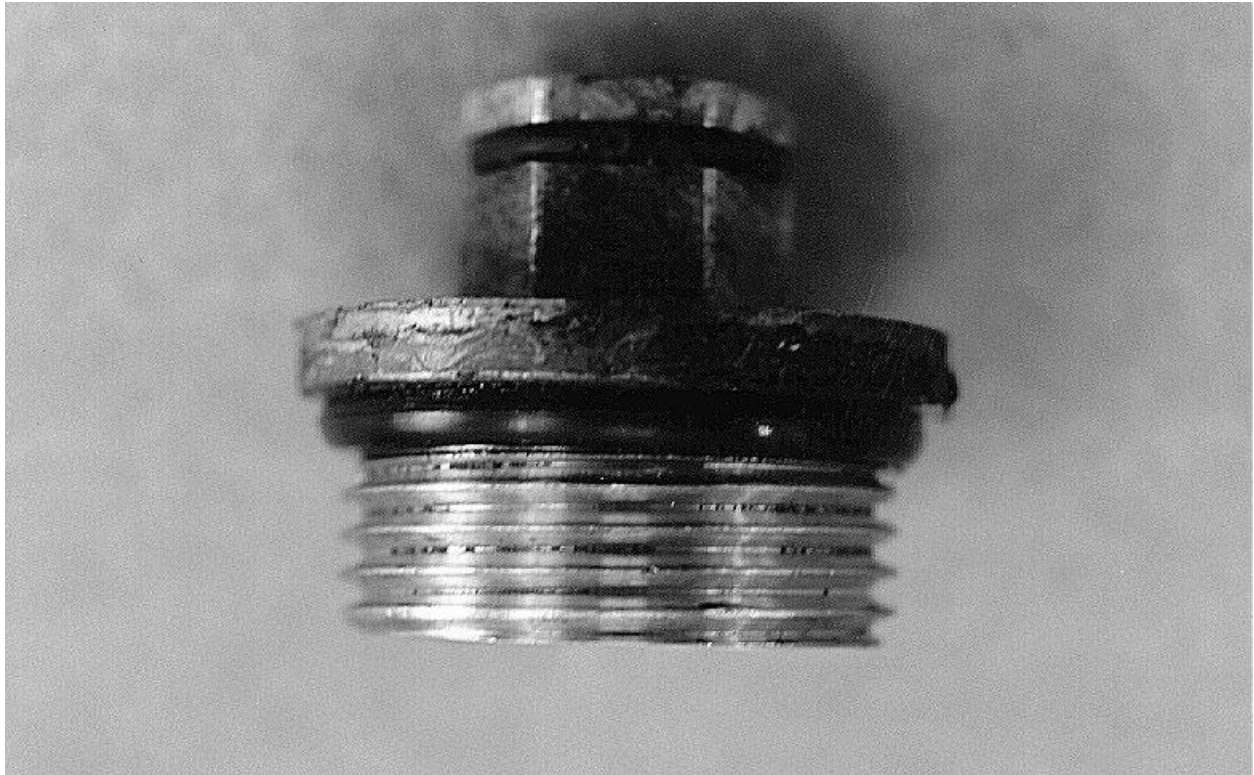


Figure 2.10.3-86 – CTU; Close-up of OCV Vent Port Cover (As Removed/Not Cleaned)

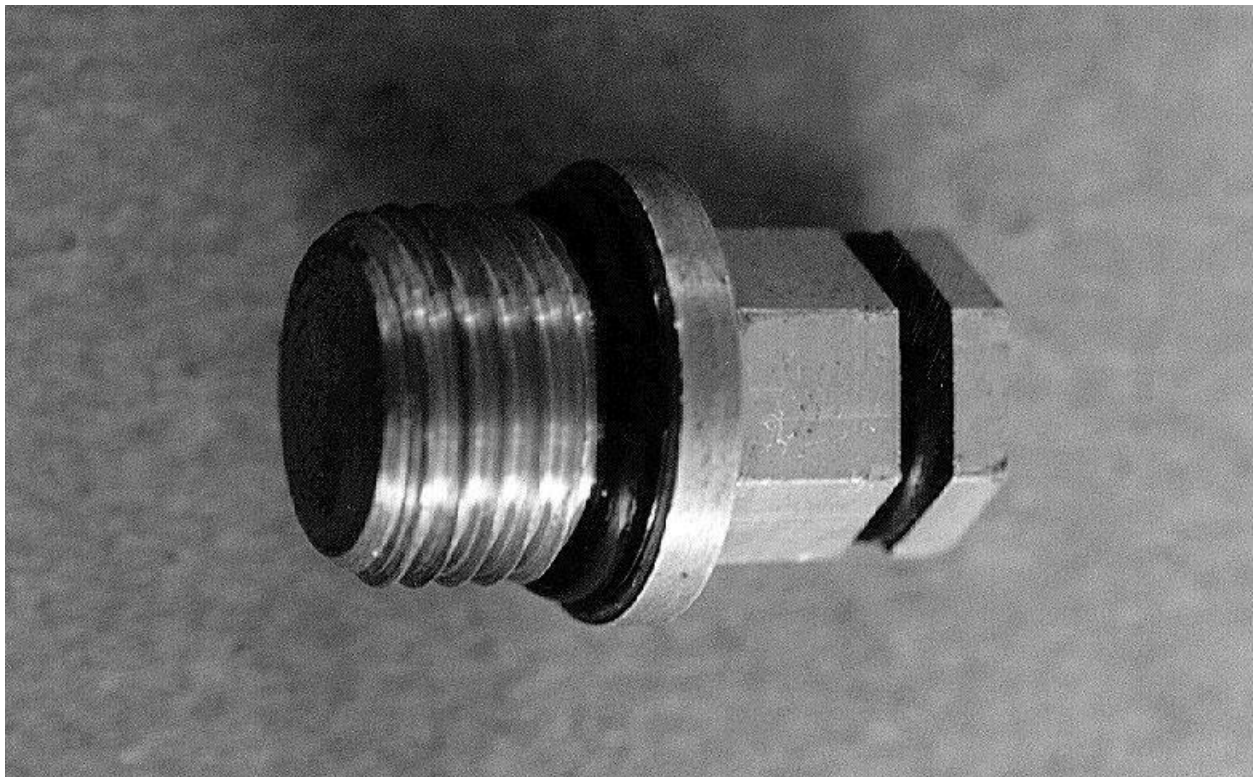


Figure 2.10.3-87 – CTU; Close-up of OCV Vent Port Plug (As Removed/Not Cleaned)



Figure 2.10.3-88 – CTU; Close-up of Damage to ICV Locking Ring



Figure 2.10.3-89 – CTU; End View of OCV Cavity Showing Deformed Lower Seal Flange



Figure 2.10.3-90 – CTU; Residual Foam in OCA Lid Side; Aligned with Test 1, 2, & 4 Damage



Figure 2.10.3-91 – CTU; Residual Foam in OCA Body Side; Remote from Test Damage



Figure 2.10.3-92 – CTU; Helium Leakage Rate Testing the ICV Lid Structure

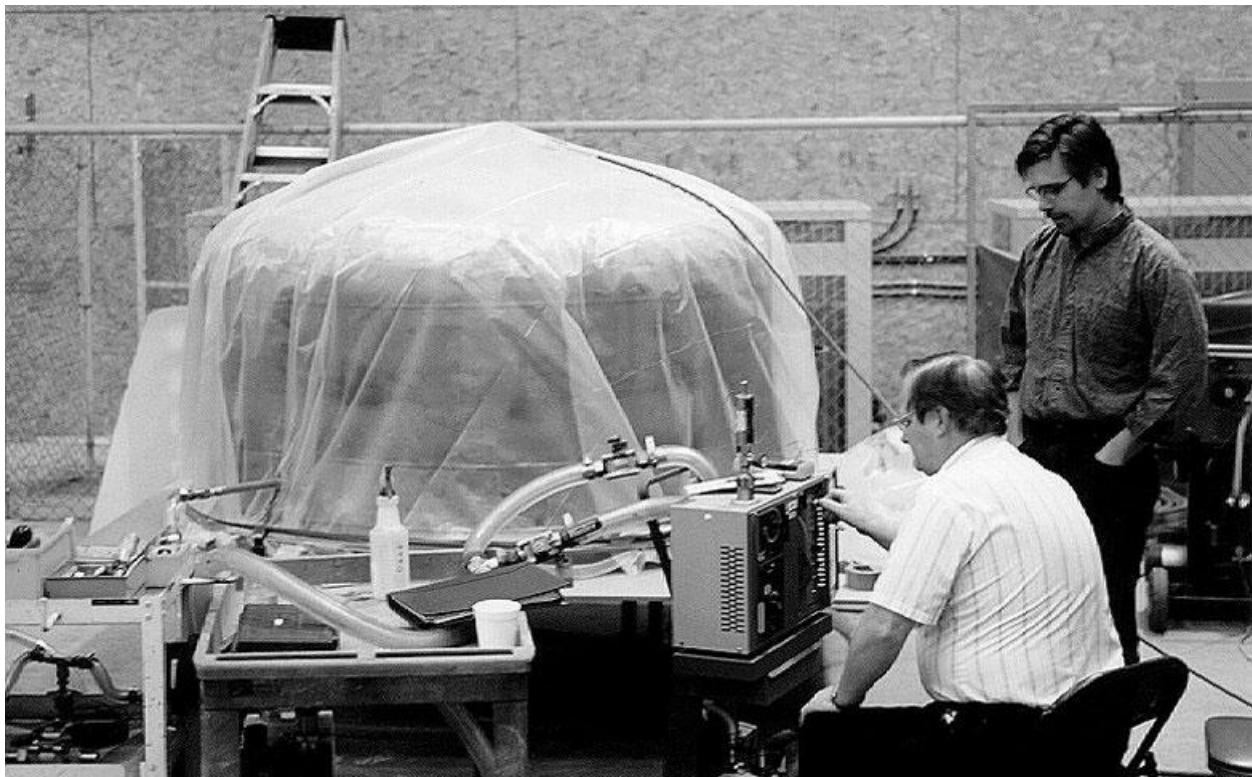


Figure 2.10.3-93 – CTU; Helium Leakage Rate Testing the OCV Body Structure



Figure 2.10.3-94 – CTU; Close-up View of Cracked OCV Vent Port Coupling Inner Weld

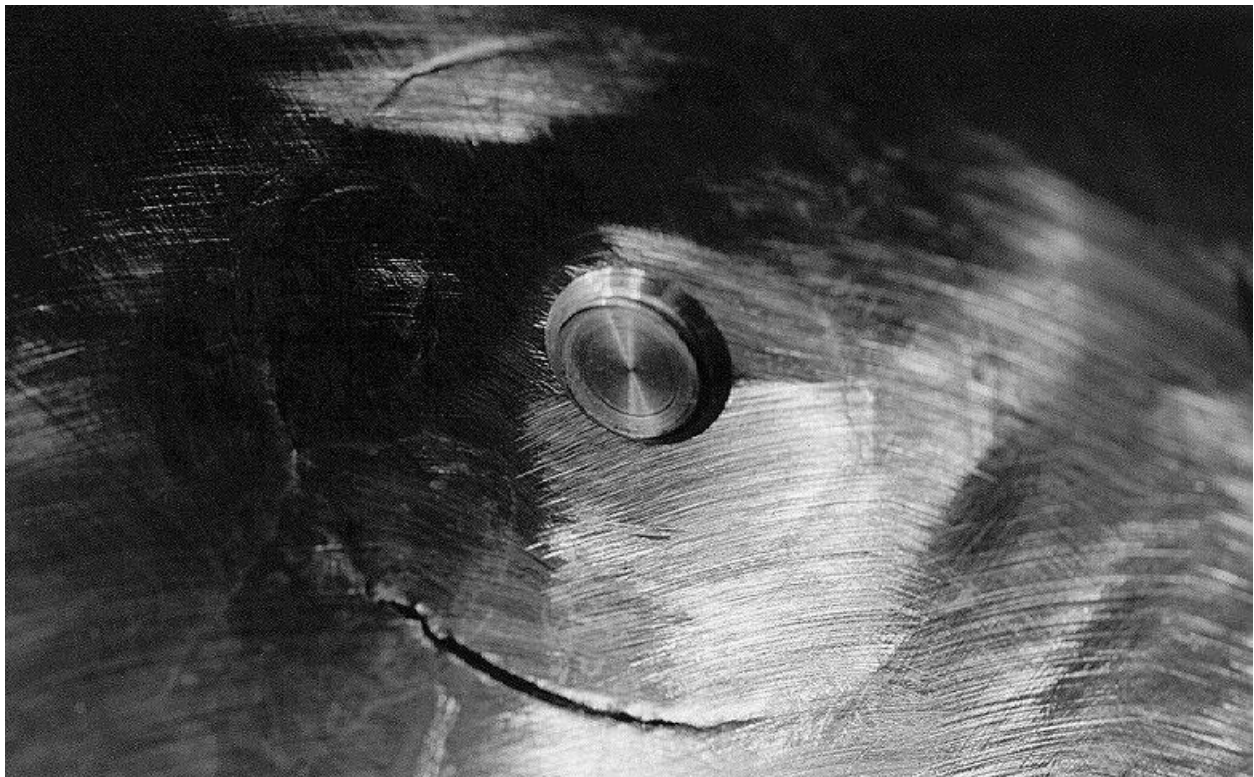


Figure 2.10.3-95 – CTU; Close-up View of Cracked OCV Vent Port Coupling Inner Weld

This page intentionally left blank.

3.0 THERMAL EVALUATION

This chapter identifies and describes the principal thermal design aspects of the HalfPACT package. This chapter further demonstrates the thermal safety of the system and compliance with the thermal requirements of 10 CFR 71¹ when transporting a payload generating a maximum of 30 watts decay heat. Specifically, per 10 CFR §71.43(g), the maximum accessible package surface temperature is shown to be less than 122 °F during normal conditions of transport (NCT). The bulk temperature of the impact absorbing, polyurethane foam is shown to be less than 160 °F based on NCT maximum temperature conditions thereby retaining sufficient structural integrity to protect the payload during the subsequent hypothetical accident condition (HAC) drop scenarios described in [Chapter 2.0, *Structural Evaluation*](#). Finally, the maximum HAC containment seal temperature of 290 °F is sufficiently below the seal material limit to ensure containment integrity.

All details relating to payloads and payload preparation for shipment in a HalfPACT package are presented in the [Contact-Handled Transuranic Waste Authorized Methods for Payload Control \(CH-TRAMPAC\)](#)².

3.1 Discussion

3.1.1 Packaging

The HalfPACT packaging is designed with a totally passive thermal system. As illustrated in [Figure 1.1-1](#) and [Figure 1.1-2](#) from [Section 1.1, *Introduction*](#), the principal thermal characteristic of the HalfPACT package is that it does not contain the relatively thick steel shells and lead shielding typical of other shipping packages. Instead, the HalfPACT packaging utilizes two, relatively thin containment vessels with shell thicknesses of 3/16 and 1/4 inch. Use of the thin shells means that the thermal response of the packaging shells to transient heat input is more rapid than for conventional, heavy walled packages. This characteristic is significantly offset by the unusually large, insulating capability of the polyurethane foam tending to isolate, or decouple, interior responses from temperature variations due to exterior transients. The outer surface of these shells may be painted. The analyses herein use unpainted surface (i.e., bare stainless steel) thermal properties. Since painted surfaces have higher emissivities that allow for better decay heat rejection than unpainted surfaces, the use of unpainted surface thermal properties is conservative.

Both the inner containment vessel (ICV) and the outer containment vessel (OCV) are constructed of Type 304 stainless steel. As discussed in [Section 1.2, *Package Description*](#), the ICV has a 72⁵/₈ inch inside diameter, and the OCV has a 73⁵/₈ inch inside diameter and is completely encased in polyurethane foam with a density of approximately 8¹/₄ lb/ft³. The foam provides impact protection for the NCT and HAC drop events, and thermal protection during the subsequent HAC thermal event. The 1/4-to-3/8 inch thick outer shell of the outer containment

¹ Title 10, Code of Federal Regulations, Part 71 (10 CFR 71), *Packaging and Transportation of Radioactive Material*, 01-01-07 Edition.

² U.S. Department of Energy (DOE), [Contact-Handled Transuranic Waste Authorized Methods for Payload Control \(CH-TRAMPAC\)](#), U.S. Department of Energy, Carlsbad Field Office, Carlsbad, New Mexico.

assembly (OCA) is comprised of Type 304 stainless steel that serves to protect the polyurethane foam from damage encountered during normal handling and shipping operations.

3.1.2 Payload Configuration

As described in [Section 1.1, Introduction](#), the HalfPACT packaging is designed to carry five different payload configurations. The first payload configuration consists of seven 55-gallon drums arranged on one pallet. The drums are arranged by placing six drums symmetrically around a seventh, center drum. [Figure 2.9-3](#) of the [CH-TRAMPAC](#) illustrates the arrangement of the seven, 55-gallon drums. This seven drum configuration represents the bounding thermal case for the HalfPACT package due to the center drum being insulated from the package side wall by six peripheral drums, and due to their smaller relative size, a higher volumetric heat generation than the other payload configurations described below.

Two polyethylene sheets (a molded, bottom slip sheet, and a flat, top reinforcing plate for the set of seven drums) may be used for handling operations (as an option, the bottom slip sheet may be of cardboard). In addition, optional polyethylene plastic wrap may be used to provide greater stability for the payload drums once loaded on the pallet. Calculations show that as many as eighteen layers of the clear-to-translucent plastic wrap (each 0.002 inches thick) may be installed around the outside of the drums without having a significant thermal effect (see [Appendix 3.6.2.3, Polyethylene Plastic Wrap Transmittance Calculation](#)). The plastic wrap may also overlap the top of the drums by a few inches. As an option, steel banding straps may be used around the outside of the payload drums instead of the polyethylene stretch wrap to maintain drum stability.

The second payload configuration consists of one 37-inch tall standard waste box (SWB) designed specifically for this type of packaging. [Figure 2.9-18](#) of the [CH-TRAMPAC](#) illustrates a SWB assembly. This configuration does not represent a bounding thermal condition due to its relatively large size corresponding to a lower volumetric heat generation rate in comparison to the seven 55-gallon drum payload configuration. Thus, presentation of the SWB evaluation is not explicitly included herein.

The third payload configuration consists of four 85-gallon drums, which range in dimensions to yield 75 to 88 gallons. [Figure 2.9-11](#) of the [CH-TRAMPAC](#) illustrates the arrangement of four short 85-gallon drums, which includes the additional payload spacer, and [Figure 2.9-12](#) of the [CH-TRAMPAC](#) illustrates the arrangement of four tall 85-gallon drums. As with the 55-gallon drums, both top and bottom polyethylene sheets may be used for handling operations. In addition, the 85-gallon drums may be banded together with either polyethylene plastic wrap or steel banding straps. Similarly, this configuration does not represent a bounding thermal condition since all of the drums are adjacent to the package side wall resulting in cooler payload drum temperatures. Thus, presentation of the 85-gallon drum payload evaluation is not explicitly included herein.

The fourth payload configuration consists of three 100-gallon drums. [Figure 2.9-15](#) of the [CH-TRAMPAC](#) illustrates the arrangement of the three 100-gallon drums. As with the 55-gallon drums, both top and bottom polyethylene sheets may be used for handling operations. In addition, the 100-gallon drums may be banded together with either polyethylene plastic wrap or steel banding straps. Similarly, this configuration does not represent a bounding thermal condition since all of the drums are adjacent to the package side wall resulting in cooler payload

drum temperatures. Thus, presentation of the 100-gallon drum payload evaluation is not explicitly included herein.

The fifth payload configuration consists of three shielded containers. [Figure 2.9-22](#) of the [CH-TRAMPAC](#) illustrates the arrangement of the three shielded containers. Presentation of the shielded container payload evaluation is provided in [Appendix 4.5](#) of the [CH-TRU Payload Appendices](#).

Based on the wide variety of payloads for the HalfPACT, the analyses presented herein use a bounding thermal payload of 30 thermal watts per package³ uniformly distributed in one or more payload container(s) combined with a conservatively low payload conductivity commensurate with that of loosely packed paper. Actual payload decay heat is typically far less than 30 watts. Additionally, high heat payloads typically have correspondingly higher thermal conductivities than loosely packed paper, so a combination of low conductivity with a uniform heat generation will lead to conservatively upper bounded temperature predictions. Two steady-state thermal analysis cases are presented based on decay heat distributions as follows:

1. Seven 55-gallon drums with all the decay heat distributed uniformly in all seven drums, and
2. Seven 55-gallon drums with all the decay heat distributed uniformly within the center drum.

3.1.3 Boundary Conditions

The heat transfer characteristics of the HalfPACT packaging are evaluated for the bounding payload configuration under two thermal boundary conditions. These conditions are:

- A. Steady-state conditions at an ambient temperature of 100 °F, with insolation as defined in 10 CFR §71.71(c)(1), and
- B. Steady-state conditions at an ambient temperature of -40 °F, without insolation as described in 10 CFR §71.71(c)(2).

Note that 10 CFR §71.43(g) stipulates that for non-exclusive use packages, maximum accessible surface temperatures must be less than 122 °F for a package under 100 °F ambient conditions without insolation. Package temperatures prior to the start of the HAC thermal event are based on this condition, and are presented in [Table 3.5-1](#) from [Section 3.5.3, Package Temperatures](#).

Maximum steady-state package temperatures with insolation are determined by using a combination of solar heating values. An analysis is made using the insolation values delineated in 10 CFR §71.71(c)(1), averaged over 24 hours. This action is intended to simulate the slow thermal response that the payload and internal package components have to a varying (i.e., cyclic) solar load. The relatively large thermal mass on the inside of the polyurethane foam insulation isolates (i.e., decouples) the “12 hour on / 12 hour off” solar step function cycle applied to the outside of the foam insulation. Thus, components on the inside of the polyurethane foam use the insolation values of 10 CFR §71.71(c)(1), averaged over 24 hours.

³ U.S. Department of Energy (DOE), [Contact-Handled Transuranic Waste Authorized Methods for Payload Control \(CH-TRAMPAC\)](#), U.S. Department of Energy, Carlsbad Field Office, Carlsbad, New Mexico, Section 5.0, [Gas Generation Requirements](#).

In contrast, the outer sections of the polyurethane foam and the OCA outer shell will respond much more quickly to varying external solar loads. As such, the maximum steady-state temperatures of the polyurethane foam and OCA outer shell are estimated using the 10 CFR §71.71(c)(1) insolation values averaged over 12 hours thereby resulting in a more accurate estimate of the maximum external temperature during the “12 hour on” solar cycle. [Table 3.1-1](#) presents results from both analyses, depending on the packaging component being considered.

Package performance and resulting component temperatures, when subjected to the hypothetical accident thermal event as described in 10 CFR §71.73(c)(4), are determined via full scale fire testing of the HalfPACT packaging, and are discussed in [Section 3.5, *Thermal Evaluation for Hypothetical Accident Conditions*](#).

3.1.4 Analysis Summary

The primary heat transfer mechanisms utilized in the thermal analyses are conduction and radiation from component to component within the HalfPACT packaging, and convection and radiation from the exterior of the packaging to the ambient. Due to the relatively close coupling of the bodies within the package, convective heat transfer within the payload cavity is conservatively neglected. As discussed in [Section 3.1.2, *Payload Configuration*](#), the thermal conductivity of the material inside the drums is conservatively chosen to be that of still air, based on the assumption of loosely packed paper. The following sections present these analyses in greater detail.

In all cases, the steady-state heat transfer analyses are performed using the thermal network analyzer computer program, SINDA’85/FLUINT, Version 3.1⁴.

[Table 3.1-1](#) presents a summary of the temperatures determined by the steady-state heat transfer analyses for the major components of the HalfPACT packaging for the two bounding payload configurations with the maximum internal decay heat of 30 thermal watts. Temperatures denoted as “average” use volume-based weighting of the nodal temperatures to determine the average. Further details of these analyses are presented in [Section 3.4, *Thermal Evaluation for Normal Conditions of Transport*](#).

Discussion of HAC fire testing is provided in [Section 3.5, *Thermal Evaluation for Hypothetical Accident Conditions*](#). Adjusting for the difference between the calculated initial condition temperatures and actual test temperatures, the maximum containment seal temperatures are 290 °F for the OCV seals and 200 °F for the ICV seals. All seal temperatures are shown to be well below the 350 °F temperature limit for short term exposure.

⁴ *Systems Improved Numerical Differencing Analyzer and Fluid Integrator* (SINDA/FLUINT), Version 3.1, Cullimore and Ring Technologies, Inc., 1996.

Table 3.1-1 – NCT Steady-State Temperatures with 30 Watts Decay Heat Load and Insolation; Seven, 55-Gallon Drums

Location	Solar Loading	Temperature (°F)		
		Case 1 (Uniform Heat in All Seven Drums)	Case 2 (Uniform Heat in Center Drum Only)	Maximum Allowable
Center Drum Centerline				
• Maximum	24 hr avg	183.8	340.4	N/A
• Average	24 hr avg	169.5	251.9	N/A
Center Drum Wall				
• Maximum	24 hr avg	156.9	164.4	N/A
• Average	24 hr avg	156.4	162.7	N/A
Outer Drum Centerline				
• Maximum	24 hr avg	181.4	152.9	N/A
• Average	24 hr avg	167.7	152.7	N/A
Outer Drum Wall				
• Maximum	24 hr avg	156.7	162.0	N/A
• Average	24 hr avg	153.0	152.6	N/A
Average All Drums				
• Centerline	24 hr avg	168.0	166.9	N/A
• Wall	24 hr avg	153.5	154.0	N/A
ICV Wall				
• Maximum	24 hr avg	152.8	153.8	N/A
• Average	24 hr avg	148.7	147.7	N/A
• Minimum	24 hr avg	146.3	144.9	N/A
ICV Air				
• Average	24 hr avg	151.1	150.9	N/A
ICV Main O-ring Seal				
• Maximum	24 hr avg	147.1	145.4	225
OCV Wall				
• Maximum	24 hr avg	150.1	149.6	N/A
• Average	24 hr avg	147.0	145.5	N/A
OCV Main O-ring Seal				
• Maximum	24 hr avg	145.5	143.9	225
Polyurethane Foam				
• Maximum	12 hr avg	155.0	155.0	N/A
• Average	24 hr avg	128.9	128.4	N/A
OCA Outer Shell				
• Maximum	12 hr avg	155.0	155.0	N/A

This page intentionally left blank.

3.2 Summary of Thermal Properties of Materials

The HalfPACT packaging is fabricated primarily of Type 304 stainless steel, 6061-T6 aluminum, polyurethane foam, and ceramic fiber paper insulation. The payload containers (i.e., the 55-gallon drums, 85-gallon drums, 100-gallon drums, and SWB) are constructed of carbon steel, and may be painted or galvanized.

The payload is expected to consist of a combination of low decay heat, non-solidified organically-based material, and higher decay heat, solidified organic or inorganically-based material as described in [Section 1.2.3, *Contents of Packaging*](#), and [Section 5.0 of the *Contact-Handled Transuranic Waste Authorized Methods for Payload Control \(CH-TRAMPAC\)*](#)¹. Analyses presented herein assume a thermally conservative (i.e., very low thermal conductivity; analyzed as still air) payload of loosely packed paper with a maximum total decay heat of 30 watts. This assumption combines the low conductivity of a paper-based payload with the highest decay heat load expected from an all-metallic payload to yield the highest and, therefore, the most conservative payload temperatures. For the purposes of the thermal model, the space between the payload containers is conservatively assumed to be still air.

[Table 3.2-1](#) presents the thermal properties used in the heat transfer model and the references from which they are obtained. Properties between the reported values are calculated via linear interpolation by the heat transfer code. The thermal conductivity of the ceramic paper insulation used as a liner between the polyurethane foam and the outer containment assembly (OCA) inner and outer shell surfaces is 0.0028 Btu/hr-in-°F. The thermal analysis model ignores the relatively small effect that the ceramic paper insulation would have on the overall conductivity through the package wall. This assumption is valid because the relatively small thickness of the ceramic fiber paper insulation (1/4 inch thick on both the inside and outside shell surfaces) coupled with a thermal conductivity comparable to that of the polyurethane foam (i.e., 0.0028 Btu/hr-in-°F versus 0.0016 Btu/hr-in-°F, respectively) tends to minimize the overall effect. Also, using the lower conductivity of the polyurethane foam bounds the temperatures in the NCT steady-state thermal analyses.

[Table 3.2-2](#) presents the material properties for the 3.5 lb/ft³ aluminum honeycomb used in the inner containment vessel (ICV). Due to the orthotropic nature of the honeycomb structure, thermal conductivity varies in both the radial and axial directions. [Appendix 3.6.2.2, *Aluminum Honeycomb Conductivity Calculation*](#), presents the calculational methodology utilized to determine aluminum honeycomb thermal conductivity based on the honeycomb geometry.

[Table 3.2-3](#) presents the thermal conductivity of air. Because the thermal conductivity of air varies significantly with temperature, the computer model calculates the thermal conductivity across air spaces as a function of the mean film temperature. The void spaces within the ICV, and between the ICV and OCV are conservatively assumed filled with one atmosphere air.

[Table 3.2-4](#) presents the important parameters in radiative heat transfer, emissivity (ϵ) for each radiating surface and solar absorptivity (α) value for the exterior surfaces. The outer shell of the containment assembly (OCA) conservatively uses the lower value of emissivity ($\epsilon = 0.25$) for the NCT steady-state analyses lower bounding heat transmission in the outward direction thereby

¹ U.S. Department of Energy (DOE), [Contact-Handled Transuranic Waste Authorized Methods for Payload Control \(CH-TRAMPAC\)](#), U.S. Department of Energy, Carlsbad Field Office, Carlsbad, New Mexico.

conservatively upper bounding the package internal temperatures. Optionally painting the OCA outer surface significantly increases the emissivity; therefore, use of the lower value of emissivity of $\epsilon = 0.25$ is conservative². Transmittance (τ) of the optional drum polyethylene plastic wrap is discussed in [Appendix 3.6.2.3, Polyethylene Plastic Wrap Transmittance Calculation](#).

Table 3.2-1 – Thermal Properties of Homogenous Materials

Material	Temperature (°F)	Thermal Conductivity (Btu/hr-in-°F)	Specific Heat (Btu/lb-°F)	Density (lb/in ³)
Stainless Steel [Ⓞ] Type 304	-200	0.516	0.080	0.289
	0	0.633	0.111	
	100	0.675	---	
	200	0.716	0.124	
	400	0.816	0.130	
	600	0.916	0.134	
	800	1.000	0.140	
	1,000	1.100	---	
	1,200	1.200	0.158	
	1,600	1.400	---	
Carbon Steel [Ⓞ] A36	-40	2.750	---	0.283
	32	---	0.102	
	212	2.750	0.115	
	392	2.520	0.126	
	572	2.280	0.134	
	752	2.040	0.145	
	932	1.820	0.159	
	1,112	---	0.179	
	1,472	1.820 [Ⓞ]	0.203	
Polyurethane Foam [Ⓞ]	---	0.0016	0.300	0.005
Fiberglass Insulation [Ⓞ]	---	0.0019	0.160	---

² Rohsenow, W. M. and J. P. Hartnett, *Handbook of Heat Transfer*, McGraw-Hill, New York, 1973, Section 15, Table 5. This provides an effective emissivity for painted surfaces from 0.81 for oil based paint on polished iron to 0.95 for enamel based paints. Per Table 3.2-4, the package surface emissivity used in this analysis is 0.25.

Notes for [Table 3.2-1](#):

- ① *Aerospace Structural Metals Handbook*, 1989, Metals and Ceramics Information Center, Battelle Memorial Institute, Columbus, Ohio.
- ② *Properties of Solids, Thermal Conductivity, Metallic Materials*, General Electric, Heat Transfer Division, July 1974.
- ③ Thermal conductivity and specific heat for 8¼ pcf polyurethane foam are documented in [Section 8.1.4.1.2.1.5, *Thermal Conductivity*](#), and [Section 8.1.4.1.2.1.6, *Specific Heat*](#).
- ④ W. M. Rohsenow and J. P. Hartnett, *Handbook of Heat Transfer*, McGraw-Hill, New York, 1973. Properties for glass wool were used.
- ⑤ Bounding property value used to ensure model stability.

Table 3.2-2 – Thermal Properties of Non-Homogenous Materials

Material	Temperature (°F)	Thermal Conductivity ^{①②③} (Btu/hr-in-°F)		Specific Heat ^② (Btu/lb-°F)	Density ^③ (lb/in ³)
		Axial	Radial		
Aluminum Honeycomb (3.5 lb/ft ³)	-40	0.053	0.142	0.225	0.002
	68	0.053	0.142		
	212	0.055	0.146		
	752	0.067	0.178		
	1,500	0.067 ^④	0.178 ^④		

Notes:

- ① *Properties of Solids, Thermal Conductivity, Metallic Materials*, General Electric, Heat Transfer Division, July 1974.
- ② D. G. Gilmore, Editor, *Satellite Thermal Control Handbook*, The Aerospace Corporation Press, El Segundo, CA, 1994, ppC-12 to C-16.
- ③ *Mechanical Properties of Hexcel Honeycomb Materials*, TSB-120 (Technical Service Bulletin 120), Hexcel, 1992 (see also [Appendix 3.6.2.2, *Aluminum Honeycomb Conductivity Calculation*](#)).
- ④ Bounding property value used to ensure model stability.

Table 3.2-3 – Thermal Properties of Air

Temperature (°F)	Thermal Conductivity ^① (Btu/hr-in-°F)	Specific Heat ^② (Btu/lb-°F)	Density ^③ (lb/in ³)	Prandtl Number ^③	Viscosity ^① (in ² /s)
-99	0.0013 ^④	0.239	Use ideal gas law with STP density of 4.4(10) ⁻⁵ lb/in ³	0.739	0.01161
81	0.0013	---		---	0.02610
170	---	---		0.697	---
261	---	0.242		---	0.04015
350	---	---		0.683	---
441	0.0019	0.246		---	0.05875
530	---	---		0.680	---
621	0.0022	0.251		---	0.07958
710	---	---		0.682	---
801	0.0025	0.257		---	0.10269
890	---	---		0.686	---
981	0.0028	0.262		---	---
1,070	---	---		0.692	0.14066
1,161	---	0.267		---	---
1,250	---	---		0.699	0.16771
1,341	0.0033	0.272		---	---
1,500	0.0033 ^④	0.280		---	---
1,520	---	---	0.704	0.21483	

Notes:

- ① E. R. Eckert, R. M. Drake, *Analysis of Heat Mass Transfer*, 3rd Edition, McGraw-Hill Publishers, 1972.
- ② Y.S. Touloukian and C.Y. Ho, Editors, *Specific Heat – Nonmetallic Liquids and Gases*, Thermophysical Properties Research Center Data Series, Volume 6, Purdue University, 1970.
- ③ Rohsenow, Hartnett, and Ganic, *Handbook of Heat Transfer Fundamentals*, 2nd Edition, McGraw-Hill Publishers, 1973.
- ④ Bounding property value used to ensure model stability.

Table 3.2-4 – Thermal Radiative Properties

Material	Emissivity	Absorptivity
Stainless Steel ^①	0.25	0.50
Carbon Steel ^②	0.80	N/A
Aluminum Honeycomb ^③	0.25	N/A
Ambient Environment	1.00	N/A

Notes:

- ① W. D. Wood, et al., *Thermal Radiation Properties of Selected Materials, Volume I*, p56. The emissivity of 0.25 is a conservative lower-bound value for clean and smooth stainless steel, leading to conservatively higher temperatures for NCT.
- ② Frank Kreith, *Principles of Heat Transfer*, 3rd Edition, Intext Press, Inc., 1973, Table 5-2, p237.
- ③ A defined surface emissivity is unavailable from the aluminum honeycomb manufacturer. However, F. F. Gubareff, J. E. Janssen, and R. H. Torborg, *Thermal Radiation Properties Survey*, Honeywell Research Center, Minneapolis, Minnesota, p23, 1960, gives an emissivity of 0.31 for oxidized aluminum; 0.25 is conservatively used as a bounding value.

This page intentionally left blank.

3.3 Technical Specifications of Components

The materials used in the HalfPACT packaging that are considered to be temperature sensitive are the butyl O-ring seals and the polyurethane foam.

The butyl rubber O-ring seals are fabricated of Rainier Rubber compound RR0405-70¹, or equivalent meeting the requirements of ASTM D2000 M4AA710 A13 B13 F17 F48 Z Trace Element. Butyl rubber sealing material has a working temperature range of -65 °F to 225 °F². Developmental O-ring seal testing, conducted as part of the TRUPACT-II packaging program and presented in [Appendix 2.10.2, *Elastomer O-ring Seal Performance Tests*](#), discusses the butyl rubber O-ring seal's performance at reduced and elevated temperatures. Further developmental O-ring seal testing was conducted as part of the Radioisotope Thermoelectric Generator (RTG) Transportation System Packaging³ design effort. This testing demonstrated that this specific butyl rubber compound has a peak temperature rating of 380 °F, minimum, for durations of 24 hours or less. Operation at temperatures between 350 °F and 380 °F may be allowed for longer durations, decreasing as a function of increasing temperature.

The NCT temperature range for the polyurethane foam material is -40 °F to 300 °F, per the foam manufacturer's recommendations⁴. Polyurethane foam is not subject to degradation with age when encased within the stainless steel shells of the OCA. Foam strength sensitivity to temperatures is addressed in [Section 2.5, *Lifting and Tie-down Standards for All Packages*](#), [Section 2.6, *Normal Conditions of Transport*](#), and [Section 2.7, *Hypothetical Accident Conditions*](#).

The ceramic fiber paper, comprised almost entirely (>99%) of Al₂O₃ and SiO₂ in approximately 50/50 proportions, has a maximum use temperature of 2,300 °F and a melting point of 3,260 °F. Like the polyurethane foam, this essentially inert material is not subject to degradation with age when encased within the stainless steel shells of the OCA.

The other primary packaging materials are stainless steel and aluminum. The melting point for each of these materials is 2,600 °F and 1,100 °F, respectively. Carbon steel used for the payload containers has a melting temperature of approximately 2,750 °F. Polyethylene plastic wrap has a

¹ Rainier Rubber Company, Seattle, WA.

² Rainier Rubber Company, Company Standard Compounds, <http://www.rainierrubber.com>, Seattle, WA.

³ DOE Docket No. 94-6-9904, *Radioisotope Thermoelectric Generator Transportation System Safety Analysis Report for Packaging*, WHC-SD-RTG-SARP-001, prepared for the U.S. Department of Energy Office of Nuclear Energy under Contract No. DE-AC06-87RL10930 by Westinghouse Hanford Company, Richland, WA. Per Appendix 2.10.6, elevated temperature tests were performed on Rainier Rubber Company butyl rubber compound No. RR-0405-70 O-ring seals with seal compressions as low as 10%. The specific time-temperature test parameters evaluated were 380 °F for 24 hours followed by 350 °F for 144 hours, for a total of 168 hours (1 week). At these temperatures, all elastomeric compounds are susceptible to relatively high helium permeability; thus, helium leakage rate testing was not performed. Instead, a hard vacuum of less than 0.0029 psia (20 Pa) was maintained on the test O-ring seals with no measurable pressure loss that would indicate leakage. At the end of the entire test sequence, the test O-ring seals were stabilized at -20 °F and shown, via helium leakage rate testing, to be leaktight (i.e., a leakage rate less than 1×10^{-7} standard cubic centimeters per second (scc/s), air leakage).

⁴ *LAST-A-FOAM FR-3700 for Crash and Fire Protection of Nuclear Material Shipping Containers*, General Plastics Manufacturing Company, P.O. Box 9097, Tacoma, WA.

melting temperature of approximately 250 °F. Loss of the plastic wrap is of no consequence to the safety of the HalfPACT package since its effect on conductive and radiative heat transfer is negligible, as discussed in [Appendix 3.6.2.3, *Polyethylene Plastic Wrap Transmittance Calculation*](#). Similarly, the loss of items such as foam rubber padding or plastic sheets have negligible impact on the package thermal performance.

3.4 Thermal Evaluation for Normal Conditions of Transport

This section presents the steady-state thermal analyses of the HalfPACT package for normal conditions of transport (NCT). Under NCT, the package is mounted in an upright position on its transport trailer or railcar. This establishes the orientation of the exterior surfaces of the package for determining the free convection heat transfer coefficients and insolation loading. In addition, the bottom of the dedicated transport trailer is open to free air. Thus, the bottom of the HalfPACT package would be exposed to ambient air instead of resting on the ground or some other semi-adiabatic, conducting surface.

The thermal conditions that are considered for NCT are those specified in 10 CFR §71.71(c)(1)¹. Accordingly, a 100 °F ambient temperature with the following insolation values are used for heat input to the exterior package surfaces. Note that the flat base of the package has no insolation; all other surfaces, since they are curved, have an insolation value of 400 gcal/cm² (10.24 Btu/in²).

Form and Location of Surface	Total Insolation for a 12-Hour Period	
	(gcal/cm ²)	(Btu/in ²)
Flat surfaces transported horizontally:		
• Base	None	none
• Other surfaces	800	20.49
Flat surfaces not transported horizontally	200	5.12
Curved surfaces	400	10.24

3.4.1 Thermal Model

3.4.1.1 Analytical Model

Figure 3.4-1 and Figure 3.4-2 illustrate the location of the thermal nodes used in the analytical model of the HalfPACT packaging and the 55-gallon drum payload configuration, respectively. The location and the number of thermal nodes are chosen to achieve an accurate determination of the temperature distribution within the major package components.

The analysis model was constructed using SINDA/FLUINT, Version 3.1², and utilizes the thermal properties presented in Section 3.2, *Summary of Thermal Properties of Materials*. To enhance the accuracy of the model, the material properties of the package steel and aluminum, as well as the air within the package cavity, are computed as a function of temperature. In the case of the polyurethane foam, material properties change little over the NCT temperature range of interest; therefore, constant thermal property values are used.

¹ Title 10, Code of Federal Regulations, Part 71 (10 CFR 71), *Packaging and Transportation of Radioactive Material*, 01-01-07 Edition.

² *Systems Improved Numerical Differencing Analyzer and Fluid Integrator* (SINDA/FLUINT), Version 3.1, Cullimore and Ring Technologies, Inc., 1996.

The thermal model represents a two-dimensional axisymmetric model of the packaging and its payload. The bounding payload, described in [Section 3.1.2, *Payload Configuration*](#), consists of a uniform payload of low conductivity and uniform heat distribution. Sensitivity studies have shown that, with a total decay heat load of 30 watts, the placement of the payload within the HalfPACT packaging cavity has a negligible effect on component maximum temperatures.

As seen from [Figure 3.4-1](#), a two-dimensional, axisymmetric model consisting of just under 100 nodes is used to represent the HalfPACT packaging. Increased resolution is utilized in the outer containment vessel (OCV) and inner containment vessel (ICV) sealing regions to enhance the accuracy of seal temperature predictions.

[Figure 3.4-2](#) illustrates the thermal model used for the 55-gallon drum payload configuration. To account for the non-symmetric effects that occur within the drum-based payload configuration, a quasi-three-dimensional model (i.e., a three-dimensional model with symmetry planes along adiabatic boundaries) of the drums is used. Using the quasi-three-dimensional model with the drum-based payload configuration provides a simplified, yet accurate representation of the packaging as each analysis assumes the heat is either uniformly distributed in all seven drums or in the center drum. The configuration with seven 55-gallon drums with all the decay heat in the center drum represents the bounding case. This is because this particular payload configuration has the highest heat concentration within a single drum and six surrounding drums adding an additional insulating barrier. Therefore, the SWB, four 85-gallon drum, and three 100-gallon drum payload configurations, although evaluated, are not specifically included herein.

Heat transfer across air gaps is calculated using a combination of conduction and radiation heat transfer. Since any offset of the ICV within OCV would be relatively small, and would tend to decrease the net thermal resistance across the shells, the ICV and OCV are assumed to be concentric cylinders. Thus, the air gaps separating the side and top of these components are assumed to be uniform with no contacting surfaces. The bottom ICV/OCV interface is separated by a 1/8 inch thick rubber pad. To maximize the insulating properties of this interface, the pad is assumed to behave as a layer of still air without radiative heat transfer (air conduction only).

The bounding payload configuration is assumed loaded in the ICV cavity with uniform and symmetrical separation from the ICV walls. Again, any eccentricity in the placement of the payload in the package would result in reduced thermal resistance between the payload and cask. Due to the relatively low decay heat load and the narrowness of most gaps and the blockage provided by the pallets, stretch wrap, etc., the model also assumes that no significant internal natural convection paths exist. Free convection of decay heat and solar radiation from the exterior surfaces of the package is computed as a function of temperature and orientation of the surface using standard equations for free convection from vertical and horizontal surfaces. Methodology for calculating convection coefficients is presented in [Appendix 3.6.2.1, *Convection Coefficient Calculation*](#).

The optional polyethylene plastic wrap around the payload drums has a small effect on the radiative heat transfer between the drums and the ICV wall. As discussed in [Appendix 3.6.2.3, *Polyethylene Plastic Wrap Transmittance Calculation*](#), the interaction of the plastic wrap with regard to the heat transfer process is determined to have a negligible effect and, therefore, is ignored.

3.4.1.2 Test Model

This section is not applicable since NCT thermal tests are not performed for the HalfPACT package.

3.4.2 Maximum Temperatures

The maximum temperatures for NCT hot conditions (i.e., 100 °F ambient temperature and insolation per 10 CFR §71.71(c)(1)) and 30 watts decay heat are reported in [Table 3.4-1](#) for the major components of the HalfPACT package. Average drum wall temperatures, ICV wall temperatures, and ICV air temperatures are determined using the area-weighted nodal temperatures. A complete listing of nodal temperatures for the evaluated cases is also provided in the [Appendix 3.6.1, Computer Analysis Results](#).

3.4.3 Minimum Temperatures

The minimum temperature distribution for the HalfPACT packaging occurs with a zero decay heat load and an ambient air temperature of -40 °F per 10 CFR §71.71(c)(2). Since the steady-state analysis of this condition represents a trivial case, no thermal calculations are performed. Instead, it is assumed that all package components achieve the -40 °F temperature under steady-state conditions. As discussed in [Section 3.3, Technical Specifications of Components](#), the -40 °F temperature is within the allowable range of all HalfPACT packaging components. As a potential initial condition for all normal or accident events, a minimum uniform temperature of -20 °F must be considered per 10 CFR §71.71(b) and §71.73(b). Detailed structural analyses considering the effects of minimum temperatures are presented in [Section 2.6.2, Cold](#).

3.4.4 Maximum Internal Pressure

The evaluation of the maximum internal pressure for the HalfPACT packaging considers the factors that affect pressure to demonstrate that the pressure increases are below the allowable pressure for the package.

3.4.4.1 Design Pressure

The HalfPACT packaging has a design pressure of 50 psig. [Chapter 2.0, Structural Evaluation](#), discusses the ability of the package to withstand 50 psig for both normal conditions of transport and hypothetical accident conditions. The ICV or both the OCV and ICV were pressurized to 50 psig in many of the full-scale tests for hypothetical accident conditions as described in [Appendix 2.10.3, Certification Tests](#). The maximum normal operating pressure (MNOP) is discussed in [Section 3.4.4.3, Maximum Normal Operating Pressure](#).

3.4.4.2 Maximum Pressure for Normal Conditions of Transport

The maximum pressure in the ICV under normal conditions of transport is less than the 50 psig design pressure, as shown by the following analysis. The major factors affecting the ICV internal pressure are radiolytic gas generation, thermal expansion of gases, and the vapor pressure of water within the ICV cavity. Barometric changes that affect the external pressure, and hence the gauge pressure of the HalfPACT packaging containment vessels, are bounded by the regulatory condition of a 3.5 psia external pressure and considered in the use of the 50 psig

pressure increase limit. ICV internal pressure would not increase significantly due to chemical reactions, biological gas generation, or thermal decomposition in the payload. For the payload shipping categories qualified for transport by gas generation testing, the maximum pressure increase allowed in the ICV for normal conditions is the 50 psig pressure increase limit.

The maximum pressure in the ICV for all categories is calculated for the maximum shipping period of 60 days. The use of a 60-day shipping period in the calculation of maximum normal operating pressure is consistent with 10 CFR 71.41(c). As specified by 10 CFR 71.41(c), this section shows that the "...controls proposed to be exercised by the shipper are demonstrated to be adequate to provide equivalent safety of the shipment." The use of this shipping period is consistent with the analysis presented in [Appendix 3.4](#) of the *CH-TRU Payload Appendices*³, which shows that the maximum normal shipping period will be less than 60 days by a large margin of safety. As described in [Appendix 3.4](#) of the *CH-TRU Payload Appendices*, routine monitoring of shipments includes the use of the TRANSCOM system at the Waste Isolation Pilot Plant, which provides continuous tracking of shipments from the shipping site to its destination.

Calculation of maximum pressure in the ICV for all categories considers immediate release of gases from the innermost layer of confinement around the waste to the available void volume of the ICV cavity. The available void volume for accumulation of gas in the ICV is conservatively estimated. The available ICV void volume is the ICV void volume less the volume occupied by the payload assembly. The ICV void volume is the internal volume within the ICV containment boundary less the volume occupied by the materials of construction of the end spacers. Since the end spacers were purposely designed to use perforated aluminum honeycomb, each has a large void volume for gas accumulation.

The volume occupied by the payload assembly is the volume of the payload containers plus the volume occupied by the pallet, slipsheets, reinforcing plates, and guide tubes, if applicable. The estimate of the void volume of the ICV considers only the volume in the ICV outside of the payload containers with no credit for the void volume present within the payload containers except for SWBs overpacking four 55-gallon drums. Since drum payload containers have a significant void volume that has historically averaged over 50% of the internal volume, neglecting the void volume in the payload containers will overestimate the pressure increase in the ICV.

The void volume between the SWB and four overpacked 55-gallon drums is included in the ICV volume for pressure analyses because this SWB overpack configuration is not sealed and the internal void volume is quantifiable. The external volume of a single, steel 55-gallon drum can be calculated based on its internal dimensions, tare weight, and the density of steel as follows:

$$V_{\text{drum}} = \left(\frac{\pi}{4} \times D^2 \times H + \frac{W}{\rho} \right) \times \frac{0.01639 \text{ liters}}{\text{inches}^3}$$

³ U.S. Department of Energy (DOE), *CH-TRU Payload Appendices*, U.S. Department of Energy, Carlsbad Field Office, Carlsbad, New Mexico.

where:

D = Internal diameter of a 55-gallon drum (cubic inches)

H = Internal height of a 55-gallon drum (cubic inches)

W = Tare weight (empty) of a 55-gallon drum (pounds)

ρ = Density of steel (pounds per cubic inch)

Therefore, the external volume of a 55-gallon drum is:

$$V_{\text{drum}} = \left(\frac{\pi}{4} \times 22.5^2 \times 33.25 + \frac{60}{0.285} \right) \times \frac{0.01639 \text{ liters}}{\text{inches}^3} = 220 \text{ liters}$$

As shown in [Appendix 2.4](#) of the *CH-TRU Payload Appendices*, the internal void volume of an empty SWB is conservatively taken as 1,750 liters. Subtracting the volume of four overpacked 55-gallon drums from the empty SWB void volume results in an internal void volume of approximately 870 liters per SWB overpack.

The net void volume in the ICV is assumed filled with air at 70 °F and 14.7 psia when the ICV is sealed for transport. Sufficient water is assumed present for saturated water vapor at any temperature. The pressure increase due to water vapor is obtained from the tabulated thermodynamic properties of saturated water and steam.

The maximum pressure increase analysis for HalfPACT payloads can be categorized as follows:

- Analytical category payloads have decay heat limits based on conservative theoretical analyses of flammable gas generation as shown in [Section 5.0](#) of the *Contact-Handled Transuranic Waste Authorized Methods for Payload Control (CH-TRAMPAC)*⁴. These limits are lower than applicable limits for test category wastes and the pressure increase for all analytical category payloads is bound by the test category payloads.
- Test category payloads for which the MNOP can be shown to be below the design pressure by analysis. This analysis is presented in [Section 3.4.4.2.1](#), *MNOP Determination by Analysis*.
- Test category payloads for which the MNOP is limited to the design pressure and compliance is shown by measurement. Derivation of gas generation rates for these cases in compliance with the pressure limit is presented in [Section 3.4.4.2.2](#), *MNOP Determination by Measurement*.

In addition, the following conditions govern the pressure analysis for HalfPACT package payloads:

- Waste Material Types I.2, I.3, II.3, III.2, and III.3 have lower G values compared to Waste Material Types I.1, II.1, and III.1, respectively, and will therefore have lower pressure increases.
- The case of the decay heat uniformly distributed in all containers in a payload (versus all decay heat in one container) results in the lowest void volume and bounds the pressure increase calculations (Note that to meet flammable gas generation requirements, the decay

⁴ U.S. Department of Energy (DOE), *Contact-Handled Transuranic Waste Authorized Methods for Payload Control (CH-TRAMPAC)*, U.S. Department of Energy, Carlsbad Field Office, Carlsbad, New Mexico.

heat in a HalfPACT with a single drum will be less than the decay heat in a HalfPACT with 7 drums.)

- The normal condition, steady state temperatures for decay heat values from 0 to 40 watts for SWBs in the TRUPACT-II bound the steady state temperatures for HalfPACT payload configurations with decay heat values from 0 to 20 watts. This relationship was derived from the temperature profile for 55-gallon drum payload assemblies in the TRUPACT-II and the HalfPACT where the temperature at 20 watts in the HalfPACT is less than the temperature at 40 watts in the TRUPACT-II.

3.4.4.2.1 MNOP Determination by Analysis

The method used to calculate the maximum ICV pressure is provided below for an example payload shipping category. The number of moles per second of total gas generated by radiolysis is calculated from the following equation:

$$n_{\text{gen}} = G_{\text{eff}(T)} \times W \times C$$

where n_{gen} is the rate of radiolytic gas generation (moles/sec), $G_{\text{eff}(T)}$ is the temperature-corrected effective G value (the total number of molecules of gas generated per 100 eV of energy emitted (molecules/100 eV) at the temperature of the target material), W is the total decay heat (watts), and the conversion constant for the units used is $C = 1.04(10)^{-5}$ (g-moles)(eV)/(molecule)(watt-sec).

The effective G values are provided in [Appendix 3.2](#) of the *CH-TRU Payload Appendices* for the payload shipping categories. The maximum decay heat for each category determines the average contents temperature for that category. As discussed in [Appendix 3.2](#) of the *CH-TRU Payload Appendices*, the effective G values provided at room temperature (RT) are a function of temperature based on the activation energy (E_a) for the material. The effective G values used in the calculation for pressure increase in the ICV are corrected to the average contents temperature for each category using the activation energy of the material in the category that is provided in [Appendix 3.2](#) of the *CH-TRU Payload Appendices*.

For example, the effective G value (total gas) at room temperature for Waste Material Type I.1 is 2.4 (from [Appendix 3.2](#) of the *CH-TRU Payload Appendices*). The temperature-corrected effective G value is calculated using the following equation:

$$G_{(\text{Total}, T)} = G_{(\text{Total}, \text{RT})} e^{\left(\frac{E_a}{R}\right) \left(\frac{T - T_{\text{RT}}}{T(T_{\text{RT}})}\right)}$$

where $G_{(\text{Total}, \text{RT})}$ is the effective G value at room temperature (the number of molecules of gas generated per 100 eV of energy (molecules/100 eV) for target material at room temperature), E_a is the activation energy for the target material, kcal/g-mole, the ideal gas constant $R = 1.99(10)^{-3}$ kcal/g-mole-K, T is the temperature of the target material (the average contents temperature), and the room temperature is $T_{\text{RT}} = 25 \text{ }^\circ\text{C} = 298 \text{ K}$.

The temperature-corrected effective G value for Waste Material Type I.1 is calculated at the average contents temperature based on the maximum decay heat for that waste material type. [Table 3.4-2](#) provides the summary of normal condition, steady state temperatures for decay heat values from 0 to 30 watts for package temperatures of interest including average contents temperatures. From [Table 3.4-2](#), the average contents temperature for a total payload decay heat of 30 watts is 169.5 °F. From

Appendix 3.2 of the *CH-TRU Payload Appendices*, the activation energy is zero ($E_a = 0$) for water, which is the target material. The temperature corrected effective G-value is:

$$G_{(\text{eff}, 169.5^\circ \text{F})} = (2.4 \text{ molecules}/100 \text{ eV}) e^{\left(\frac{0 \text{ kcal/g-mole}}{1.99(10)^{-23} \text{ kcal/g-mole-K}} \right) \left(\frac{349.5 \text{ K} - 298 \text{ K}}{(349.5 \text{ K})(298 \text{ K})} \right)}$$

$$= 2.4 \text{ molecules}/100 \text{ eV}$$

Using this temperature-corrected effective G value, the radiolytic gas generation rate, n_{gen} , is:

$$n_{\text{gen}} = (2.4 \text{ molecules}/100 \text{ eV})(30 \text{ watts})[1.04(10)^{-5} \text{ (g - moles)(eV)/(molecule)(watt - sec)}]$$

$$= 7.49(10)^{-6} \text{ moles/sec}$$

The total number of liters of radiolytic gases that is generated, V_R , when corrected from moles to liters at STP (32 °F and 1 atmosphere pressure) after 60 days would be:

$$V_R = [n_{\text{gen}}](60 \text{ days})\{\text{conversion factors}\}$$

$$= [7.49(10)^{-6}](60)\{(86,400 \text{ sec/day})(22.4 \text{ liters/mole})\} = 869.75 \text{ liters @ STP}$$

The generated volume of radiolytic gases (corrected to STP) is heated to the average ICV gas temperature for normal conditions of transport. The average ICV gas temperature is also available from the HalfPACT package temperatures given in Table 3.4-2. For Waste Material Type I.1, the average gas temperature is 151.1 °F. The radiolytic gas would occupy a volume, V_{rg} of:

$$V_{\text{rg}} = (869.75) \left(\frac{151.1^\circ \text{F} + 460^\circ \text{R}}{32^\circ \text{F} + 460^\circ \text{R}} \right) = 1,080.29 \text{ liters @ } 151.1^\circ \text{F}$$

For a payload of seven 55-gallon drums and an available void volume in the ICV of 1,846 liters, this gas contributes a pressure, p_{rg} , of:

$$p_{\text{rg}} = \frac{1,080.29}{1,846} = 0.59 \text{ atm (8.67 psia) @ } 151.1^\circ \text{F}$$

The initial volume of gas present in the ICV at 70 °F and 14.7 psia is also heated to 151.1 °F for a decay heat of 30 watts. The increased pressure associated with this heat-up, p_{hu} , is:

$$p_{\text{hu}} = (14.7 \text{ psia}) \left(\frac{151.1^\circ \text{F} + 460^\circ \text{R}}{70^\circ \text{F} + 460^\circ \text{R}} \right) = 16.95 \text{ psia}$$

The water vapor pressure is based on the temperature of the coolest or condensing surface of the ICV. From Table 3.4-2, the minimum ICV wall temperature is 146.3 °F for a decay heat of 30 watts. The corresponding water vapor pressure, p_{wv} , at this temperature is 3.39 psia.

The maximum ICV pressure after 60 days for Waste Material Type I.1, p_{max} , is the sum of the three pressure components less an assumed atmospheric pressure, p_a , of 14.7 psia, or:

$$p_{\text{max}} = p_{\text{rg}} + p_{\text{hu}} + p_{\text{wv}} - p_a = 8.67 \text{ psia} + 16.95 \text{ psia} + 3.39 \text{ psia} - 14.7 \text{ psia} = 14.32 \text{ psig}$$

After 60 days, the maximum ICV pressure would be 14.32 psig for a payload of seven 55-gallon drums of Waste Material Type I.1 with a total payload decay heat of 30 watts. Thus, the

pressure increase for any such payload with a decay heat less than 30 watts is below the allowable pressure increase limit of 50 psig.

Waste Material Types I.2 and I.3 have lower G values and will therefore have lower total gas generation rates. This means that the pressure increase will be lower than that of Waste Material Type I.1. Hence, the pressure increase for Waste Material Type I.1 is the bounding value for Waste Type I. Similar logic applies for Waste Types II and III and hence [Table 3.4-3](#) provides pressure increase values for Waste Material Types I.1, II.1 and III.1 only. In addition to the above-stated decay heat limit for a payload of seven 55-gallon drums for Waste Type I, compliance with the 50 psig pressure limit can be demonstrated for other container types and Waste Material Types as shown in [Table 3.4-3](#) through [Table 3.4-8](#). Maximum allowable decay heat limits for analytical shipping categories are below the associated test category values shown in [Table 3.4-3](#) through [Table 3.4-8](#), and will therefore have lower pressure increase values.

For all payloads satisfying the applicable container decay heat limits specified in [Table 3.4-3](#) through [Table 3.4-8](#), there is no need to perform total gas generation testing to determine compliance with the 50 psig pressure limit.

For cases where the wattage limits specified in [Table 3.4-3](#) through [Table 3.4-8](#) are exceeded but the packaging design limit of 30 watts per HalfPACT is met, compliance with the container flammable gas generation can be used to evaluate compliance with the total gas generation rate limit. Because the primary mechanism for gas generation for both flammable and total gas for Waste Types I, II, and III is radiolysis, compliance with the flammable gas generation rate limit implies actual G values (both flammable and total) that are much lower than those used to derive the limits in [Table 3.4-3](#) through [Table 3.4-8](#). Therefore, as described in [Section 5.2.5.3.3](#) of the [CH-TRAMPAC](#), compliance with the flammable gas generation rate limits will ensure compliance with the total gas generation rate limits for these cases (e.g., SWBs of Waste Type III greater than 17 watts). Note that, as shown below, Waste Type IV containers compliance with the total gas generation rate limit will be evaluated by measurement.

3.4.4.2.2 MNOP Determination by Measurement

For all containers of Waste Type IV, the total gas generation rate must be measured by testing and shown to comply with the applicable limits as described below. (Note: Payloads must also comply with the HalfPACT decay heat limit of 30 watts.)

For containers requiring total gas generation testing as specified above, the allowable number of moles per second of gases (excluding water vapor) released may not exceed a specified limit (see [Table 5.2-11](#), [Section 5.2.5](#) of the [CH-TRAMPAC](#)). The calculation is based on the maximum decay heat for each test category. This decay heat provides the minimum ICV wall temperature for determining the vapor pressure of water, and the average ICV gas temperature for determining the pressure rise due to heating the gases initially present when the ICV is sealed. Assuming that atmospheric pressure is 14.7 psia, the allowable absolute pressure in the ICV, p_{abs} , is:

$$p_{abs} = 50 \text{ psig} + 14.7 \text{ psia} = 64.7 \text{ psia}$$

This absolute pressure is decreased by the water vapor pressure and the increased pressure of the gas initially present in the ICV.

The maximum gas release rate in moles/sec per payload container for containers subjected to total gas generation testing is provided in [Section 5.2.5](#) of the [CH-TRAMPAC](#). The method used to calculate the maximum gas release rate is provided below with an example for Waste Type IV.

The maximum decay heat for Waste Type IV in 55-gallon drums is 7 watts (see [Section 5.2.5](#) of the [CH-TRAMPAC](#)). Interpolating from the data in [Table 3.4-2](#), the minimum ICV wall temperature is 122.6 °F and the average ICV gas temperature is 123.4 °F. The corresponding water vapor pressure at the ICV wall temperature is 1.82 psia. The increased pressure of the ICV gas initially present (assuming air at 70 °F and 14.7 psia), p_{ini} , is then:

$$p_{ini} = (14.7 \text{ psia}) \left(\frac{123.4 \text{ °F} + 460 \text{ °R}}{70 \text{ °F} + 460 \text{ °R}} \right) = 16.2 \text{ psia}$$

The allowable absolute pressure in the ICV available for accumulation of gas released from the payload containers, p_{all} , is:

$$p_{all} = 64.7 \text{ psia} - 1.82 \text{ psia} - 16.2 \text{ psia} = 46.7 \text{ psia} (3.18 \text{ atm})$$

For a payload of seven 55-gallon drums and an available void volume in the ICV of 1,846 liters, the amount of gas that may be released from the payload containers at 123.4 °F, V_g , is:

$$V_g = (3.18 \text{ atm})(1,846 \text{ liters}) = 5,870 \text{ liters @ } 123.4 \text{ °F and } 1 \text{ atm pressure}$$

Thus, the number of moles per second at STP allowed for 60 days from all seven (7) 55-gallon drums for Waste Type IV, n_g , is:

$$\begin{aligned} n_g &= (5,870 \text{ liters}) \left(\frac{32 \text{ °F} + 460 \text{ °R}}{123.4 \text{ °F} + 460 \text{ °R}} \right) \left(\frac{1 \text{ mole}}{22.4 \text{ liters}} \right) \left(\frac{1}{60 \text{ days}} \right) \left(\frac{1 \text{ day}}{86,400 \text{ sec}} \right) \\ &= 4.26(10)^{-5} \text{ moles/sec} \end{aligned}$$

The number of moles/sec per 55-gallon drum, n_p , would be:

$$n_p = \frac{4.26(10)^{-5} \text{ moles/sec}}{7 \text{ drums}} = 6.09(10)^{-6} \text{ moles/sec per drum}$$

The maximum allowable gas release rate for 60 days for 55-gallon drums from Waste Type IV is $6.09(10)^{-6}$ moles/sec per payload container. However, the applicable TRUPACT-II limit of $3.97(10)^{-6}$ (lower limit of the two packages) is used to qualify payload containers for either package. The limit for moles/sec per payload container for Waste Type IV is provided in [Section 5.2.5](#) of the [CH-TRAMPAC](#). Compliance with these limits will be evaluated for 55-gallon drums of Waste Type IV less than or equal to a decay heat of 7 watts per payload container and per HalfPACT and for other payload containers of Waste Type IV less than or equal to a decay heat of 3.5 watts per payload container and per HalfPACT. The maximum allowable gas release rates provided ensure that the maximum pressure increase in 60 days under normal conditions of transport will not exceed the 50 psig design limit.

The maximum allowable internal pressure in the OCV is also 50 psig. The OCV would only experience significant internal pressure if the ICV had such a pressure and the gases were free to communicate with

the OCV. In this case, the maximum internal pressure is 50 psig in the ICV and the additional void volume in the OCV would result in a maximum pressure in the OCV of less than 50 psig.

3.4.4.3 Maximum Normal Operating Pressure

The HalfPACT package was designed to withstand 50 psig of internal pressure to accommodate the transport of payload materials with the potential to generate gases and increase pressure within the ICV. For the analytical payload shipping categories, the pressure increase in 60 days is less than that for test category waste due to the decay heat limits imposed on analytical category waste. Therefore, the MNOP for the ICV for the analytical categories is not the limiting MNOP for the ICV since a higher value is established by the test payload shipping categories. As discussed in [Section 3.4.4.2, *Maximum Pressure for Normal Conditions of Transport*](#), the maximum pressure increase in the ICV in 60 days for a test category is allowed to be 50 psig. Since the ICV pressure is allowed to increase to the design pressure of 50 psig, the MNOP for the ICV in the HalfPACT package is 50 psig.

The MNOP for the OCV is low and the pressure increase is due to the temperature increase of the air in the OCV cavity and the vapor pressure of water within the OCV cavity when the HalfPACT package reaches the maximum normal operating temperature. Per [Table 3.4-1](#), the normal condition steady state temperature of the ICV and OCV walls with 30 watts of decay heat is less than 154 °F. Conservatively assuming that the initial volume of gas present in the OCV at 70 °F and 14.7 psia is heated to 154 °F, the increased pressure associated with this heat-up, p_{hu} , is:

$$p_{hu} = (14.7 \text{ psia}) \left(\frac{154 \text{ °F} + 460 \text{ °R}}{70 \text{ °F} + 460 \text{ °R}} \right) = 17.03 \text{ psia}$$

Also, conservatively assuming a condensing OCV surface temperature of 154 °F, the water vapor pressure, p_{wv} , at this temperature is 4.10 psia.

Thus, for normal conditions of transport, the MNOP for the OCV is the sum of the two pressure components less an assumed atmospheric pressure, p_a , of 14.7 psia, or:

$$p_{max} = p_{hu} + p_{wv} - p_a = 17.03 \text{ psia} + 4.10 \text{ psia} - 14.7 \text{ psia} = 6.43 \text{ psig}$$

The design pressure for the OCV is the same as that for the ICV or 50 psig and ensures pressure retention by the OCV in a non-normal situation in which the ICV cavity communicates with the OCV cavity.

3.4.5 Maximum Thermal Stresses

Maximum thermal stresses for NCT are determined using the temperature results from [Section 3.4.2, *Maximum Temperatures*](#), and [Section 3.4.3, *Minimum Temperatures*](#). NCT thermal stresses are discussed in [Section 2.6.1, *Heat*](#), and [Section 2.6.2, *Cold*](#). Corresponding structural analyses utilize a minimum temperature of -40 °F (-20 °F when combined with any other load cases), and a maximum temperature of 170 °F for any HalfPACT packaging component.

3.4.6 Evaluation of Package Performance for Normal Conditions of Transport

The component temperatures and the internal decay heat distributions presented in [Section 3.4.2, *Maximum Temperatures*](#), and [Section 3.4.3, *Minimum Temperatures*](#), are all within the allowable limits for the materials of construction delineated in [Section 3.3, *Technical Specifications of Components*](#).

Table 3.4-1 – NCT Steady-State Temperatures with 30 Watts Decay Heat Load and Insolation; Seven 55-Gallon Drums

Location	Solar Loading	Temperature (°F)		
		Case 1 (Uniform Heat in All Seven Drums)	Case 2 (Uniform Heat in Center Drum Only)	Maximum Allowable
Center Drum Centerline				
• Maximum	24 hr avg	183.8	340.4	N/A
• Average	24 hr avg	169.5	251.9	N/A
Center Drum Wall				
• Maximum	24 hr avg	156.9	164.4	N/A
• Average	24 hr avg	156.4	162.7	N/A
Outer Drum Centerline				
• Maximum	24 hr avg	181.4	152.9	N/A
• Average	24 hr avg	167.7	152.7	N/A
Outer Drum Wall				
• Maximum	24 hr avg	156.7	162.0	N/A
• Average	24 hr avg	153.0	152.6	N/A
Average All Drums				
• Centerline	24 hr avg	168.0	166.9	N/A
• Wall	24 hr avg	153.5	154.0	N/A
ICV Wall				
• Maximum	24 hr avg	152.8	153.8	N/A
• Average	24 hr avg	148.7	147.7	N/A
• Minimum	24 hr avg	146.3	144.9	N/A
ICV Air				
• Average	24 hr avg	151.1	150.9	N/A
ICV Main O-ring Seal				
• Maximum	24 hr avg	147.1	145.4	225
OCV Wall				
• Maximum	24 hr avg	150.1	149.6	N/A
• Average	24 hr avg	147.0	145.5	N/A
OCV Main O-ring Seal				
• Maximum	24 hr avg	145.5	143.9	225
Polyurethane Foam				
• Maximum	12 hr avg	155.0	155.0	N/A
• Average	24 hr avg	128.9	128.4	N/A
OCA Outer Shell				
• Maximum	12 hr avg	155.0	155.0	N/A

Table 3.4-2 – Summary of Temperatures for Determining MNOP for the ICV

Location	Temperature (°F) with Internal Decay Heat (watts)			
	0	10	20	30
Case 1 – Seven 55-Gallon Drums, Uniform Decay Heat in All Seven Drums				
Average Center Drum Centerline	115.2	133.1	151.2	169.5
Average ICV Air	115.2	126.9	140.4	151.1
Minimum ICV Wall	115.2	125.8	135.8	146.3
Case 2 – Seven 55-Gallon Drums, Uniform Decay Heat in Center Drum Only				
Average Center Drum Centerline	115.2	163.9	209.5	251.9
Average ICV Air	115.2	127.4	139.5	150.9
Minimum ICV Wall	115.2	125.8	135.7	144.9

This page intentionally left blank.

Table 3.4-3 – HalfPACT Pressure Increase with a 7-Drum Payload, 60-Day Duration*

Waste Material Type	Decay Heat per Drum (watts)	Total Decay Heat per Package (watts)	Average Contents Temperature (°F)	Total Gas Value, G_{eff} (molecules/100eV)	Activation Energy (kcal/g-mole)	Temperature Correlation Value, G_{eff} (molecules/100eV)	Radiolytic Gas Generation Rate (moles/sec)	Radiolytic Gas Generation STP/60 days (liters)	Average ICV Gas Temperature (°F)	Radiolytic Gas Pressure Increase (psia)	Initial Gas Pressure Increase (psia)	Minimum ICV Wall Temperature (°F)	Water Vapor Pressure (psia)	Pressure Increase @ 60 days (psig)
I.1	4.2857	30.00	169.5	2.4	0	2.4	$7.49(10)^{-6}$	869.75	151.1	8.67	16.95	146.3	3.39	14.32
II.1	4.2857	30.00	169.5	1.7	0.8	2.1	$6.47(10)^{-6}$	751.31	151.1	7.50	16.95	146.3	3.39	13.14
III.1	3.8571	27.00	164.0	8.4	2.1	13.8	$3.87(10)^{-5}$	4496.23	147.9	44.25	16.86	143.2	3.13	49.54

* void volume in the HalfPACT with 7 55-gallon drums is 1,846 liters

Table 3.4-4 – HalfPACT Pressure Increase with a 1 SWB Payload, 60-Day Duration*

Waste Material Type	Decay Heat per SWB (watts)	Total Decay Heat per Package (watts)	Average Contents Temperature (°F)	Total Gas Value, G_{eff} (molecules/100eV)	Activation Energy (kcal/g-mole)	Temperature Correlation Value, G_{eff} (molecules/100eV)	Radiolytic Gas Generation Rate (moles/sec)	Radiolytic Gas Generation STP/60 days (liters)	Average ICV Gas Temperature (°F)	Radiolytic Gas Pressure Increase (psia)	Initial Gas Pressure Increase (psia)	Minimum ICV Wall Temperature (°F)	Water Vapor Pressure (psia)	Pressure Increase @ 60 days (psig)
I.1	20.0000	20.00	238.0	2.4	0	2.4	$4.99(10)^{-6}$	579.45	148.0	7.06	16.86	144.0	3.20	12.42
II.1	20.0000	20.00	238.0	1.7	0.8	2.3	$4.83(10)^{-6}$	560.87	148.0	6.76	16.86	144.0	3.20	12.13
III.1	17.0000	17.00	221.2	8.4	2.1	17.8	$3.15(10)^{-5}$	3655.51	144.4	44.10	16.76	140.4	2.92	49.09

* void volume in the HalfPACT with one direct load SWB is 1,496 liters

Table 3.4-5 – HalfPACT Pressure Increase with 4 Drums Overpacked in 1 SWB, 60-Day Duration*

Waste Material Type	Decay Heat per Drum (watts)	Total Decay Heat per Package (watts)	Average Contents Temperature (°F)	Total Gas Value, G_{eff} (molecules/100eV)	Activation Energy (kcal/g-mole)	Temperature Correlation Value, G_{eff} (molecules/100eV)	Radiolytic Gas Generation Rate (moles/sec)	Radiolytic Gas Generation STP/60 days (liters)	Average ICV Gas Temperature (°F)	Radiolytic Gas Pressure Increase (psia)	Initial Gas Pressure Increase (psia)	Minimum ICV Wall Temperature (°F)	Water Vapor Pressure (psia)	Pressure Increase @ 60 days (psig)
I.1	5.0000	20.00	238.0	2.4	0	2.4	$4.99(10)^{-6}$	579.45	148.0	4.41	16.86	144.0	3.20	9.78
II.1	5.0000	20.00	238.0	1.7	0.8	2.3	$4.83(10)^{-6}$	560.87	148.0	4.26	16.86	144.0	3.20	9.63
III.1	5.0000	20.00	238.0	8.4	2.1	19.0	$3.96(10)^{-5}$	4599.58	148.0	35.28	16.86	144.0	3.20	40.65

* void volume in the HalfPACT with four 55-gallon drums in one SWB overpack is 2,366 liters

Table 3.4-6 – HalfPACT Pressure Increase with 4 85-Gallon Drums or 4 55-Gallon Drums Overpacked in 4 85-Gallon Drums, 60-Day Duration*

Waste Material Type	Decay Heat per Drum (watts)	Total Decay Heat per Package (watts)	Average Contents Temperature (°F)	Total Gas Value, G _{eff} (molecules/100eV)	Activation Energy (kcal/g-mole)	Temperature Correlation Value, G _{eff} (molecules/100eV)	Radiolytic Gas Generation Rate (moles/sec)	Radiolytic Gas Generation STP/60 days (liters)	Average ICV Gas Temperature (°F)	Radiolytic Gas Pressure Increase (psia)	Initial Gas Pressure Increase (psia)	Minimum ICV Wall Temperature (°F)	Water Vapor Pressure (psia)	Pressure Increase @ 60 days (psig)
I.1	5.0000	20.00	238.0	2.4	0	2.4	4.99(10) ⁻⁶	579.45	148.0	6.32	16.86	144.0	3.20	11.69
II.1	5.0000	20.00	238.0	1.7	0.8	2.3	4.83(10) ⁻⁶	560.87	148.0	6.17	16.86	144.0	3.20	11.54
III.1	4.5000	18.00	226.8	8.4	2.1	18.2	3.41(10) ⁻⁵	3959.75	145.6	43.07	16.80	141.6	3.01	48.18

* void volume in the HalfPACT with four 85-gallon drums is 1,664 liters

Table 3.4-7 – HalfPACT Pressure Increase with 3 100-Gallon Drums, 60-Day Duration*

Waste Material Type	Decay Heat per Drum (watts)	Total Decay Heat per Package (watts)	Average Contents Temperature (°F)	Total Gas Value, G _{eff} (molecules/100eV)	Activation Energy (kcal/g-mole)	Temperature Correlation Value, G _{eff} (molecules/100eV)	Radiolytic Gas Generation Rate (moles/sec)	Radiolytic Gas Generation STP/60 days (liters)	Average ICV Gas Temperature (°F)	Radiolytic Gas Pressure Increase (psia)	Initial Gas Pressure Increase (psia)	Minimum ICV Wall Temperature (°F)	Water Vapor Pressure (psia)	Pressure Increase @ 60 days (psig)
I.1	6.6667	20.00	238.0	2.4	0	2.4	4.99(10) ⁻⁶	579.45	148.0	5.29	16.86	144.0	3.20	10.66
II.1	6.6667	20.00	238.0	1.7	0.8	2.3	4.83(10) ⁻⁶	560.87	148.0	5.15	16.86	144.0	3.20	10.51
III.1	6.6667	20.00	238.0	8.4	2.1	19.0	3.96(10) ⁻⁵	4599.58	148.0	42.19	16.86	144.0	3.20	47.56

* void volume in the HalfPACT with three 100-gallon drums is 1,978 liters

Table 3.4-8 – HalfPACT Pressure Increase with 3 Shielded Containers, 60-Day Duration*

Waste Material Type	Decay Heat per Drum (watts)	Total Decay Heat per Package (watts)	Average Contents Temperature (°F)	Total Gas Value, G _{eff} (molecules/100eV)	Activation Energy (kcal/g-mole)	Temperature Correlation Value, G _{eff} (molecules/100eV)	Radiolytic Gas Generation Rate (moles/sec)	Radiolytic Gas Generation STP/60 days (liters)	Average ICV Gas Temperature (°F)	Radiolytic Gas Pressure Increase (psia)	Initial Gas Pressure Increase (psia)	Minimum ICV Wall Temperature (°F)	Water Vapor Pressure (psia)	Pressure Increase @ 60 days (psig)
I.1	10.0000	30.00	178.3	2.4	0	2.4	7.49(10) ⁻⁶	869.75	154.0	7.64	17.03	148.0	3.53	13.50
II.1	10.0000	30.00	178.3	1.7	0.8	2.1	6.58(10) ⁻⁶	764.08	154.0	6.62	17.03	148.0	3.53	12.48
III.1	9.3333	28.00	174.1	8.4	2.1	14.5	4.22(10) ⁻⁵	4894.53	151.4	42.63	16.96	145.8	3.35	48.24

* void volume in the HalfPACT with three shielded containers is 2,100 liters

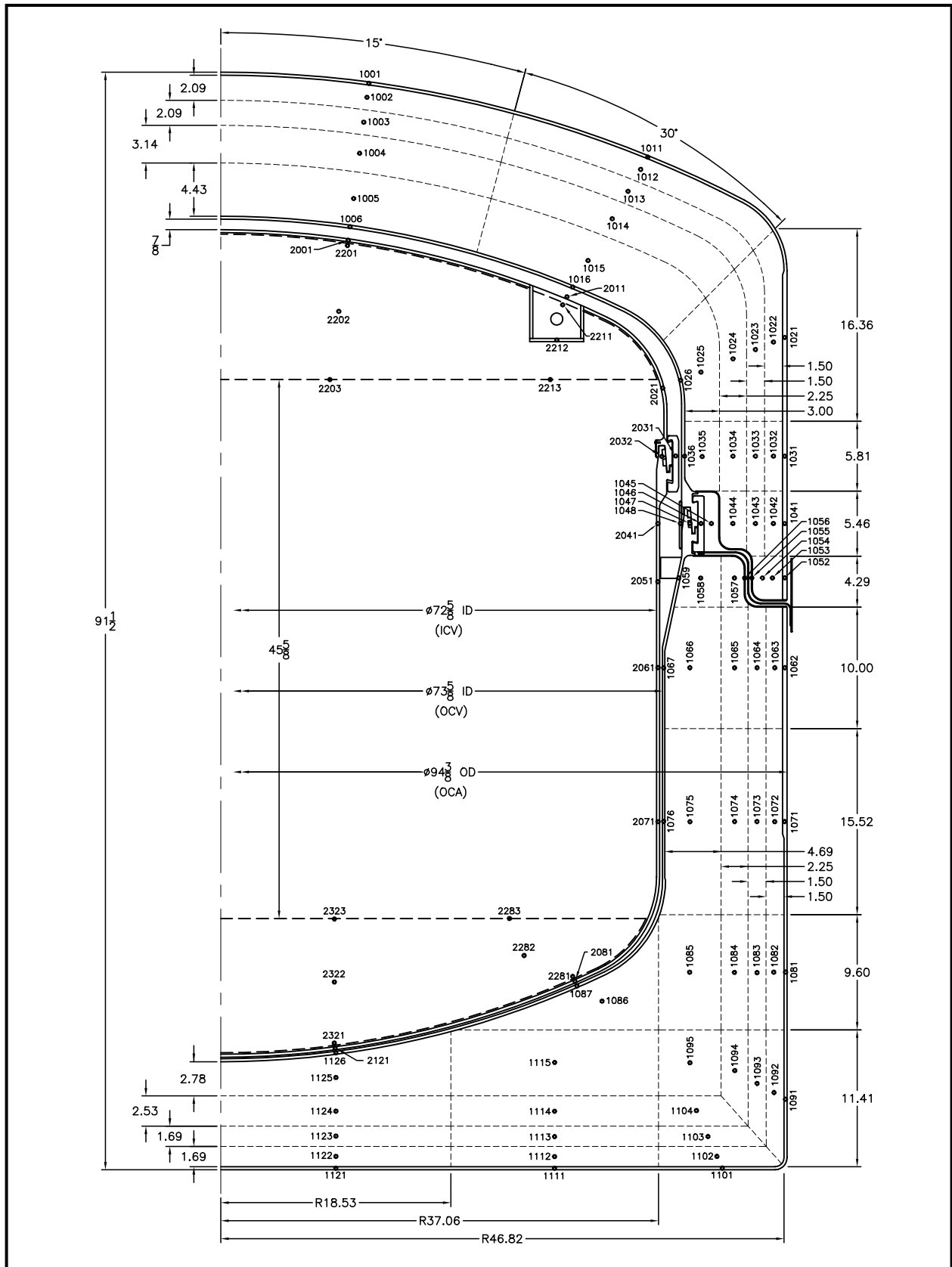


Figure 3.4-1 – HalfPACT Packaging Thermal Model Node Layout

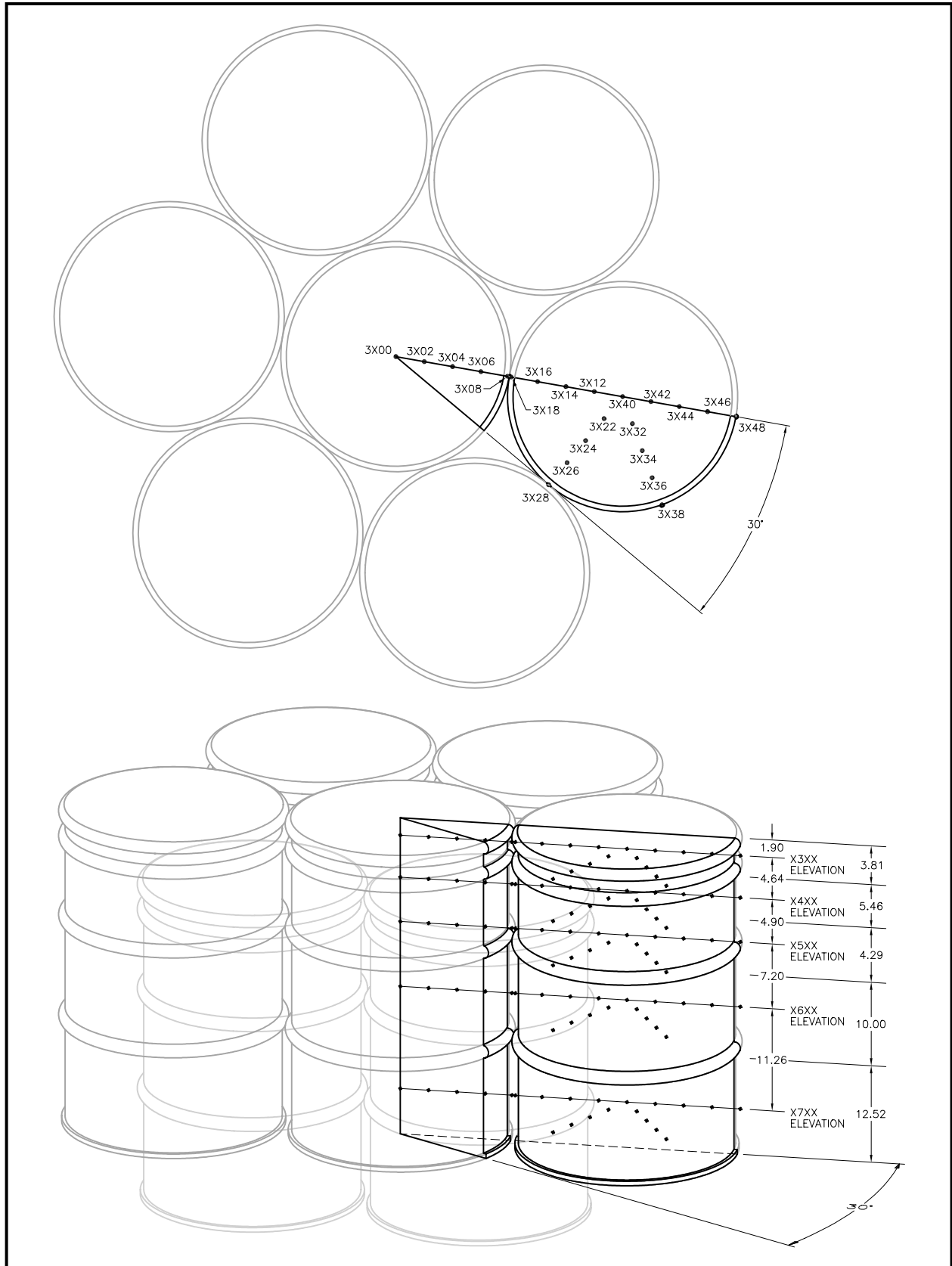


Figure 3.4-2 – Seven 55-Gallon Drum Payload Thermal Node Layout

3.5 Thermal Evaluation for Hypothetical Accident Conditions

This section presents the results of thermal testing of the HalfPACT package for the hypothetical accident condition (HAC) specified in 10 CFR §71.73(c)(4)¹.

3.5.1 Thermal Model

3.5.1.1 Analytical Model

Consistent with the *Summary and Resolution of Public Comments* relating to §71.73, "...the effects of solar radiation may be neglected before and during the thermal test...", the initial conditions for the HAC thermal event ignore insolation. [Table 3.5-1](#) summarizes component temperatures with the maximum decay heat load of 30 watts, but ignoring insolation. These analyses utilize the NCT model as described in [Section 3.4.1, Thermal Model](#), and provide a basis for adjusting temperatures to compensate for an ambient starting temperature for the HAC fire test that was under 100 °F.

3.5.1.2 Test Model

HAC thermal event (fire) testing was performed on two prototypical HalfPACT packages, identified as the HalfPACT engineering test unit (ETU) and certification test unit (CTU). A full description of the ETU and CTU, the test facilities, the pre-fire damage and initial orientation in the fire, and the test results is presented in [Appendix 2.10.3, Certification Tests](#).

Unlike the ETU that did not use any temperature measuring devices, the CTU utilized passive, non-reversible temperature indicating labels at various locations near each containment vessel's seal flanges to record temperatures from the HAC fire test. Each set of temperature indicating labels recorded temperatures in 40 steps from 105 °F to 500 °F. As illustrated in [Figure 3.5-1](#), some locations used redundant sets of labels to ensure comprehensive results at critical regions.

3.5.2 Package Conditions and Environment

As discussed further in [Appendix 2.10.3, Certification Tests](#), the CTU was oriented horizontally in a stand a distance one meter above the fuel per the requirements of 10 CFR §71.73(c)(4). With reference to [Figure 3.5-1](#), the CTU was oriented circumferentially at an angle of 305° to position the damage from Drops 1, 2, and 4 (0°) and the damage from Drop 5 (250°) a distance 1/2 meter above the lowest part of the package on the stand (i.e., 1½ meters above the fuel²). This particular arrangement put the maximum drop damage in the hottest part of the fire.

¹ Title 10, Code of Federal Regulations, Part 71 (10 CFR 71), *Packaging and Transportation of Radioactive Material*, 01-01-07 Edition.

² M. E. Schneider and L. A. Kent, *Measurements of Gas Velocities and Temperatures in a Large Open Pool Fire*, Sandia National Laboratories (reprinted from *Heat and Mass Transfer in Fire*, A. K. Kulkarni and Y. Jaluria, Editors, HTD-Vol. 73 (Book No. H00392), American Society of Mechanical Engineers). Figure 3 shows that maximum temperatures occur at an elevation approximately 2.3 meters above the pool floor. The pool was initially filled with water and fuel to a level of 0.814 meters. The maximum temperatures therefore occur approximately 1½ meters above the level of the fuel, i.e., 1/2 meter above the lowest part of the package when set one meter above the fuel source per the requirements of 10 CFR §71.73(c)(4).

As discussed earlier, no active temperature measuring devices were employed prior to, during, or following the HAC fire test. Further, measurement of the outer containment assembly (OCA) outer shell temperature does not represent the outer containment vessel (OCV) or inner containment vessel (ICV) temperatures due to the large internal mass and thick, thermally insulating foam used within the OCA. As discussed earlier in [Section 3.1.1, *Packaging*](#), the temperatures of the OCV, ICV, and payload are effectively decoupled from the OCA outer shell and polyurethane foam for short term thermal transients. Instead, the initial temperature of the CTU may be estimated based on the ambient temperature of the Sandia National Laboratory testing facilities in the six weeks prior to the HAC fire test³. Climatological data for Albuquerque, New Mexico, during the month of March and first two weeks of April 1998 shows an average temperature of 48 °F for those six weeks. Thus, when adjusting for the elevation difference between the testing facilities and Albuquerque, the initial temperature for HAC fire testing is taken as 43 °F.

The exterior surface of the CTU was painted, an option allowed on the drawings in [Appendix 1.3.1, *Packaging General Arrangement Drawings*](#). Having paint present on the OCA exterior surface is conservative for the HAC fire test because of the relatively high emissivity of paint ($\epsilon > 0.90$) compared to that of bare stainless steel ($\epsilon = 0.25$). The higher emissivity results in higher heat flow into the CTU during the HAC fire test, but the net affect is small since the paint burns away shortly after the start of the fire.

Prior to the beginning of the HAC fire test, average wind speed was determined to be below 10 miles per hour. As discussed in [Appendix 2.10.3, *Certification Tests*](#), the length of time of the fully engulfing, HAC fire test was approximately 33 minutes, and the ambient air temperature was 51 °F.

3.5.3 Package Temperatures

As stated in [Section 3.5.1.1, *Analytical Model*](#), initial condition temperatures for the HAC fire test are presented in [Table 3.5-1](#). Accordingly, the average temperature of the ICV wall and OCV wall is 133 °F and 131 °F, respectively. As stated in [Section 3.5.2, *Package Conditions and Environment*](#), the actual starting temperature of the CTU was 51 °F. Therefore, the difference between the actual and theoretical pre-fire package temperature is conservatively taken as $133\text{ °F} - 43\text{ °F} = 90\text{ °F}$.

As discussed in [Appendix 2.10.3, *Certification Tests*](#), the duration of the HAC fire test was 33 minutes. In addition, the time-averaged temperature of the HAC fire was 1,486 °F. Both the test duration and fire temperature exceeded the requirements of 10 CFR §71.73(c)(4).

A summary of temperature indicating label temperatures is presented in [Table 3.5-2](#). The maximum measured OCV seal region temperature was 200 °F. Upwardly adjusting for the lower, pre-fire starting temperature by 90 °F results in a projected maximum OCV seal region temperature of 290 °F. The maximum measured ICV seal region temperature was 110 °F. Also, upwardly adjusting for the lower, pre-fire starting temperature by 90 °F results in a projected maximum ICV seal region temperature of 200 °F. In comparison, certification testing of the

³ CTU was located at Sandia National Laboratories' Coyote Canyon drop test facility for the month of March, 1998, and the Lurance Canyon burn facility for the first two weeks of April, 1998. CTU was burned on April 14, 1998. The elevation difference between the two test facilities and the city of Albuquerque results in an average ambient temperature approximately 5 °F cooler than Albuquerque.

TRUPACT-II package showed a maximum OCV seal region temperature of 260 °F, and a maximum ICV seal region temperature of 200 °F (see [Table 3.5-5](#) from [Section 3.5.3, Package Temperatures](#), of the *TRUPACT-II SAR*⁴). As with the comparison of measurements of drop damage, fire temperatures between the two similar package designs agree very well.

3.5.4 Maximum Internal Pressure

The maximum internal pressure for the ICV may be conservatively determined by assuming the air temperature within the ICV is at the maximum seal temperature of 200 °F. The ICV pressure increase, ΔP_{ICV} , using an initial maximum ICV wall temperature of 154 °F (from [Table 3.4-1](#)) at an initial pressure equal to the MNOP of 50 psig (64.7 psia), is determined using ideal gas relationships:

$$\frac{P_1}{T_1} = \frac{P_2}{T_2} \Rightarrow \frac{P_{154\text{ °F}}}{T_{154\text{ °F}}} = \frac{P_{200\text{ °F}}}{T_{200\text{ °F}}} \Rightarrow P_{200\text{ °F}} = P_{154\text{ °F}} \left(\frac{T_{200\text{ °F}}}{T_{154\text{ °F}}} \right)$$

$$P_{200\text{ °F}} = 64.7 \left(\frac{200 + 460}{154 + 460} \right) = 69.5 \text{ psia (54.8 psig)}$$

$$\Delta P_{ICV} = 54.8 - 50.0 = 4.8 \text{ psig}$$

Thus, the maximum internal pressure for the ICV for HAC is 54.8 psig, resulting in a net pressure increase of 4.8 psig. In comparison, certification testing of the TRUPACT-II package showed a ICV pressure increase of 2.6 psig (see [Section 3.5.4, Maximum Internal Pressure](#), of the *TRUPACT-II SAR*). The difference in ΔP_{ICV} is due to the conservative assumption of using *maximum* seal region temperature rather than *average* air temperature for determining the pressure increase. Unlike TRUPACT-II certification testing, actual measurement of internal pressure was not performed for HalfPACT certification testing, hence, the conservatism.

The maximum internal pressure for the OCV may be conservatively determined by assuming the air temperature within the OCV, 245 °F, is the average of the maximum ICV and OCV seal temperatures of 200 °F and 290 °F, respectively. The initial air temperature within the OCV, 152 °F, is the average of the maximum OCV and ICV wall temperatures of 150 °F and 154 °F, respectively (from [Table 3.4-1](#)). The OCV pressure increase, ΔP_{OCV} , using at an initial pressure equal to the MNOP of 50 psig (64.7 psia), is determined using ideal gas relationships:

$$\frac{P_1}{T_1} = \frac{P_2}{T_2} \Rightarrow \frac{P_{152\text{ °F}}}{T_{152\text{ °F}}} = \frac{P_{245\text{ °F}}}{T_{245\text{ °F}}} \Rightarrow P_{245\text{ °F}} = P_{152\text{ °F}} \left(\frac{T_{245\text{ °F}}}{T_{152\text{ °F}}} \right)$$

$$P_{245\text{ °F}} = 64.7 \left(\frac{245 + 460}{152 + 460} \right) = 74.5 \text{ psia (59.8 psig)}$$

$$\Delta P = 59.8 - 50.0 = 9.8 \text{ psig}$$

⁴ U.S. Department of Energy (DOE), *Safety Analysis Report for the TRUPACT-II Shipping Package*, USNRC Docket No. 71-9218, U.S. Department of Energy, Carlsbad Field Office, Carlsbad, New Mexico.

Thus, the maximum internal pressure for the OCV for HAC is 59.8 psig, resulting in a net pressure increase of 9.8 psig. In comparison, certification testing of the TRUPACT-II package showed a maximum OCV pressure increase of 4.6 psig (see [Section 3.5.4, *Maximum Internal Pressure*](#), of the *TRUPACT-II SAR*). As is the case for the ICV, the difference in ΔP_{OCV} is due to the conservative assumption of using *maximum* seal region temperature rather than *average* air temperature for determining the pressure increase. Unlike TRUPACT-II certification testing, actual measurement of internal pressure was not performed for HalfPACT certification testing, hence, the conservatism.

3.5.5 Maximum Thermal Stresses

As shown in [Section 3.5.4, *Maximum Internal Pressure*](#), the internal pressure within the ICV increases 4.8 psig (+10%), and within the OCV increases 9.8 psig (+20%) due to the HAC fire test. Pressure stresses due to the HAC fire test corresponding increase a maximum of 20%. With reference to [Table 2.1-1 in Section 2.1.2.1.1, *Containment Structures*](#), the HAC allowable stress intensity for general primary membrane stresses (applicable to pressure loads) is 240% of the NCT allowable stress intensity. Therefore, a HAC pressure stress increase of 20% will not exceed the HAC allowable stresses. Further discussion regarding HAC thermal stresses is presented in [Section 2.7.4, *Thermal*](#).

3.5.6 Evaluation of Package Performance for the Hypothetical Accident Thermal Conditions

The most temperature sensitive material in the HalfPACT package containment boundaries is the butyl rubber used for the containment O-ring seals. The certification test unit (CTU), when subjected to the rigors of the HAC free drops, puncture drops, and fire testing, was shown to be leaktight (i.e., demonstrating a leakage rate of 1×10^{-7} standard cubic centimeters per second (scc/s), air, or better) for both the OCV and ICV. Following testing, the maximum OCV and ICV seal temperatures were recorded as 290 °F and 200 °F, respectively, temperatures well below the 350 °F O-ring seal material limit.

With regard to the criticality analyses of [Chapter 6.0, *Criticality Evaluation*](#), the minimum remaining polyurethane foam for the CTU averaged approximately five inches. Sufficient polyurethane foam material remained to validate modeling assumptions used in the criticality analyses.

Table 3.5-1 – NCT Steady-State Temperatures with 30 Watts Decay Heat Load and Zero Insolation; Seven 55-Gallon Drums

Location	Solar Loading	Temperature (°F)		
		Case 1 (Uniform Heat in All Seven Drums)	Case 2 (Uniform Heat in Center Drum Only)	Maximum Allowable
Center Drum Centerline				
• Maximum	N/A	169.0	328.9	N/A
• Average	N/A	154.4	239.2	N/A
Center Drum Wall				
• Maximum	N/A	141.6	150.4	N/A
• Average	N/A	141.0	148.8	N/A
Outer Drum Centerline				
• Maximum	N/A	166.5	138.8	N/A
• Average	N/A	152.6	138.6	N/A
Outer Drum Wall				
• Maximum	N/A	141.4	147.9	N/A
• Average	N/A	137.4	138.2	N/A
Average All Drums				
• Centerline	N/A	152.9	153.0	N/A
• Wall	N/A	137.9	139.7	N/A
ICV Wall				
• Maximum	N/A	138.0	140.4	N/A
• Average	N/A	133.1	133.2	N/A
• Minimum	N/A	129.8	129.6	N/A
ICV Air				
• Average	N/A	135.5	136.5	N/A
ICV Main O-ring Seal				
• Maximum	N/A	130.8	130.3	225
OCV Wall				
• Maximum	N/A	133.7	134.5	N/A
• Average	N/A	130.4	131.1	N/A
OCV Main O-ring Seal				
• Maximum	N/A	129.0	128.6	225
Polyurethane Foam				
• Maximum	N/A	125.8	126.3	N/A
• Average	N/A	112.3	112.3	N/A
OCA Outer Shell				
• Maximum	N/A	101.6	101.6	N/A

Table 3.5-2 – HAC Thermal Event Temperature Readings

Location	Number	Temperature
OCV Conical Shell at 0° (near Vent Port) – Drop Tests 1, 2, 4	1a, 1b	180 °F, 170 °F
OCV Conical Shell at 110° – Drop Test 6	2	180 °F
OCV Conical Shell at 250° – Drop Test 5	3	130 °F
OCV Seal Flange at 0° (near Main Seals) – Drop Tests 1, 2, 4	4a, 4b	200 °F, 200 °F
OCV Seal Flange at 110° (near Main Seals) – Drop Test 6	5	200 °F
OCV Seal Flange at 147½° (near Main Seals) – Drop Test 3	6	180 °F
OCV Seal Flange at 250° (near Main Seals) – Drop Test 5	7	140 °F
ICV Seal Flange at 0° (near Vent Port) – Drop Tests 1, 2, 4	8	105 °F
ICV Seal Flange at 0° (near Main Seals) – Drop Tests 1, 2, 4	9	105 °F
ICV Seal Flange at 110° (near Main Seals) – Drop Test 6	10	105 °F
ICV Seal Flange at 147½° (near Main Seals) – Drop Test 3	11	110 °F
ICV Seal Flange at 250° (near Main Seals) – Drop Test 5	12	110 °F

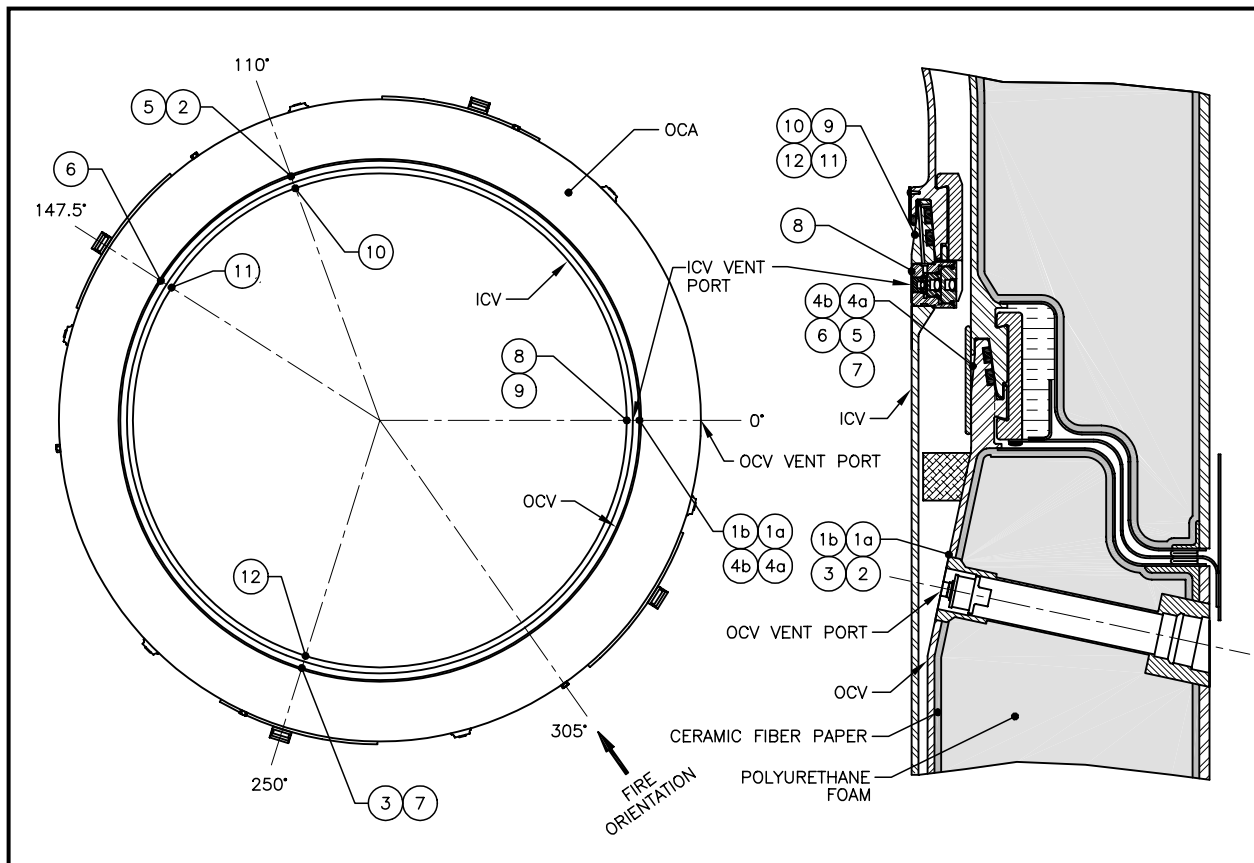


Figure 3.5-1 – HAC Thermal Event Temperature Indicating Label Locations

3.6 Appendices

3.6.1 *Computer Analysis Results*

3.6.2 *Thermal Model Details*

This page intentionally left blank.

3.6.1 Computer Analysis Results

3.6.1.1 Seven 55-Gallon Drum Payload with 100 °F Ambient and Full Solar Loading, Uniformly Distributed Decay Heat Load (Case 1)

SYSTEMS IMPROVED NUMERICAL DIFFERENCING ANALYZER WITH FLUID INTEGRATOR PAGE 8

MODEL = WHOLE HALF PACK w/7 55G Drums, 30W Uniform Heat Dist +100F w/solar 10/20
 STDSTL
 SINDA/FLUINT v3.1 Runtime: 7/13/98 13:47
 SUBMODEL NAME = HalfPACT

	CALCULATED	ALLOWED
MAX DIFF DELTA T PER ITER	DRLXCC(HalfPACT 2202) = 4.882812E-04	VS. DRLXCA= 5.000000E-04
MAX ARITH DELTA T PER ITER	ARLXCC(HalfPACT 2203) = 9.765625E-04	VS. ARLXCA= 1.000000E-02
MAX SYSTEM ENERGY BALANCE	EBALSC = 2.209933E-02	VS. EBALSA * ESUMIS = 0.341709
ENERGY INTO AND OUT OF SYS	ESUMIS = 341.709	ESUMOS= 350.215
MAX NODAL ENERGY BALANCE	EBALNC(HalfPACT 2212) = 6.202337E-03	VS. EBALNA= 0.000000E+00
NUMBER OF ITERATIONS	LOOPCT = 648	VS. NLOOPS= 20000
PROBLEM TIME	TIMEN = 0.500000	VS. TIMEND= 3.00000

DIFFUSION NODES IN ASCENDING NODE NUMBER ORDER

T 1001= 129.88	T 1002= 130.76	T 1003= 132.83	T 1004= 136.29	T 1005= 143.51	T 1006= 150.14
T 1011= 129.33	T 1012= 129.80	T 1013= 131.60	T 1014= 135.00	T 1015= 142.27	T 1016= 148.66
T 1021= 119.70	T 1022= 121.18	T 1023= 124.56	T 1024= 129.69	T 1025= 138.72	T 1026= 145.66
T 1031= 119.28	T 1032= 121.35	T 1033= 125.78	T 1034= 131.71	T 1035= 140.19	T 1036= 145.41
T 1041= 119.22	T 1042= 122.18	T 1043= 127.26	T 1044= 134.38	T 1045= 141.90	T 1046= 144.74
T 1047= 145.49	T 1052= 119.18	T 1053= 121.86	T 1054= 126.41	T 1058= 141.39	T 1059= 145.55
T 1062= 119.00	T 1063= 120.81	T 1064= 124.70	T 1065= 129.92	T 1066= 139.86	T 1067= 147.35
T 1071= 118.91	T 1072= 120.57	T 1073= 124.18	T 1074= 129.10	T 1075= 138.94	T 1076= 147.17
T 1081= 118.29	T 1082= 118.88	T 1083= 120.17	T 1084= 121.93	T 1085= 125.46	T 1086= 135.89
T 1087= 146.36	T 1091= 116.53	T 1092= 116.45	T 1093= 116.43	T 1094= 116.60	T 1095= 117.09
T 1101= 105.68	T 1102= 106.80	T 1103= 109.20	T 1104= 112.71	T 1111= 102.56	T 1112= 104.60
T 1113= 108.64	T 1114= 113.63	T 1115= 122.48	T 1121= 102.60	T 1122= 106.50	T 1123= 114.35
T 1124= 124.29	T 1125= 137.32	T 1126= 144.83	T 2001= 151.35	T 2011= 150.83	T 2021= 146.33
T 2031= 146.87	T 2032= 147.10	T 2041= 147.62	T 2051= 147.91	T 2061= 148.12	T 2071= 148.06
T 2081= 149.43	T 2121= 148.96	T 2202= 153.14	T 2212= 152.89	T 2282= 152.94	T 2322= 153.17

ARITHMETIC NODES IN ASCENDING NODE NUMBER ORDER

T 1055= 128.07	T 1056= 129.38	T 1057= 132.68	T 2201= 152.87	T 2203= 153.60	T 2211= 152.70
T 2213= 153.04	T 2281= 152.64	T 2283= 153.20	T 2321= 152.55	T 2323= 153.88	

HEATER NODES IN ASCENDING NODE NUMBER ORDER
 ++NONE++

BOUNDARY NODES IN ASCENDING NODE NUMBER ORDER

T 1= 100.00

SYSTEMS IMPROVED NUMERICAL DIFFERENCING ANALYZER WITH FLUID INTEGRATOR PAGE 11

MODEL = WHOLE HALF PACK w/7 55G Drums, 30W Uniform Heat Dist +100F w/solar 10/20
 STDSTL
 SUBMODEL NAME = DRUMS
 SINDA/FLUINT v3.1 Runtime: 7/13/98 13:47

	CALCULATED	ALLOWED
MAX DIFF DELTA T PER ITER	DRLXCC(DRUMS 3540) = 3.662109E-04	VS. DRLXCA= 5.000000E-04
MAX ARITH DELTA T PER ITER	ARLXCC(0) = 0.000000E+00	VS. ARLXCA= 1.000000E-02
MAX SYSTEM ENERGY BALANCE	EBALSC = 4.037903E-03	VS. EBALSA * ESUMIS = 8.532419E-03
ENERGY INTO AND OUT OF SYS	ESUMIS = 8.53242	ESUMOS= 0.000000E+00
MAX NODAL ENERGY BALANCE	EBALNC(DRUMS 2413) = 6.148017E-04	VS. EBALNA= 0.000000E+00
NUMBER OF ITERATIONS	LOOPCT = 648	VS. NLOOPS= 20000
PROBLEM TIME	TIMEN = 0.500000	VS. TIMEND= 3.00000

DIFFUSION NODES IN ASCENDING NODE NUMBER ORDER

T 2403= 155.17	T 2404= 154.66	T 2413= 153.96	T 2414= 153.66	T 3300= 155.53	T 3302= 155.53
T 3304= 155.54	T 3306= 155.57	T 3308= 156.03	T 3312= 154.44	T 3314= 154.63	T 3316= 155.39
T 3318= 155.87	T 3322= 154.30	T 3324= 154.30	T 3326= 154.32	T 3328= 154.61	T 3332= 154.24
T 3334= 154.17	T 3336= 153.90	T 3338= 152.26	T 3340= 154.29	T 3342= 154.20	T 3344= 154.07
T 3346= 153.58	T 3348= 150.47	T 3400= 173.96	T 3402= 173.70	T 3404= 172.43	T 3406= 168.61
T 3408= 156.51	T 3412= 172.11	T 3414= 171.17	T 3416= 167.87	T 3418= 156.33	T 3422= 171.91
T 3424= 170.74	T 3426= 167.01	T 3428= 154.95	T 3432= 171.57	T 3434= 170.03	T 3436= 165.60
T 3438= 151.86	T 3440= 172.02	T 3442= 171.38	T 3444= 169.61	T 3446= 164.73	T 3448= 149.80
T 3500= 181.87	T 3502= 181.47	T 3504= 179.53	T 3506= 173.80	T 3508= 156.87	T 3512= 179.57
T 3514= 178.02	T 3516= 172.85	T 3518= 156.68	T 3522= 179.35	T 3524= 177.55	T 3526= 171.99
T 3528= 155.21	T 3532= 178.89	T 3534= 176.61	T 3536= 170.22	T 3538= 151.81	T 3540= 179.53
T 3542= 178.64	T 3544= 176.08	T 3546= 169.18	T 3548= 149.72	T 3600= 184.00	T 3602= 183.55
T 3604= 181.39	T 3606= 175.11	T 3608= 157.07	T 3612= 181.53	T 3614= 179.79	T 3616= 174.09
T 3618= 156.87	T 3622= 181.28	T 3624= 179.30	T 3626= 173.21	T 3628= 155.36	T 3632= 180.77
T 3634= 178.26	T 3636= 171.30	T 3638= 151.82	T 3640= 181.49	T 3642= 180.51	T 3644= 177.69
T 3646= 170.22	T 3648= 149.78	T 3700= 156.39	T 3702= 156.39	T 3704= 156.35	T 3706= 156.26
T 3708= 156.08	T 3712= 155.59	T 3714= 155.78	T 3716= 155.98	T 3718= 155.91	T 3722= 155.35
T 3724= 155.36	T 3726= 155.21	T 3728= 154.67	T 3732= 154.96	T 3734= 154.68	T 3736= 153.97
T 3738= 151.76	T 3740= 155.19	T 3742= 154.73	T 3744= 154.26	T 3746= 153.20	T 3748= 149.94

ARITHMETIC NODES IN ASCENDING NODE NUMBER ORDER
 ++NONE++

HEATER NODES IN ASCENDING NODE NUMBER ORDER
 ++NONE++

BOUNDARY NODES IN ASCENDING NODE NUMBER ORDER
 ++NONE++

3.6.1.2 Seven 55-Gallon Drum Payload with 100 °F Ambient and Full Solar Loading, All Decay Heat Load in Center Drum Only (Case 2)

SYSTEMS IMPROVED NUMERICAL DIFFERENCING ANALYZER WITH FLUID INTEGRATOR PAGE 4

MODEL = WHOLE HALF PACK w/7 55G Drums, One Drum Heat +100F w/solar 7/8/98
STDSTL
SINDA/FLUINT v3.1 Runtime: 7/13/98 16:56
SUBMODEL NAME = HalfPACT

Table with columns for calculated vs allowed values for various parameters like MAX DIFF DELTA T PER ITER, ENERGY INTO AND OUT OF SYS, and node temperatures (T 1001= to T 2322=).

SYSTEMS IMPROVED NUMERICAL DIFFERENCING ANALYZER WITH FLUID INTEGRATOR PAGE 5

MODEL = WHOLE HALF PACK w/7 55G Drums, One Drum Heat +100F w/solar 7/8/98
STDSTL
SINDA/FLUINT v3.1 Runtime: 7/13/98 16:56
SUBMODEL NAME = DRUMS

Table with columns for calculated vs allowed values for various parameters like MAX DIFF DELTA T PER ITER, ENERGY INTO AND OUT OF SYS, and node temperatures (T 2403= to T 3748=).

3.6.1.3 Seven 55-Gallon Drum Payload with 100 °F Ambient and No Solar Loading, Uniformly Distributed Decay Heat Load (Case 1)

SYSTEMS IMPROVED NUMERICAL DIFFERENCING ANALYZER WITH FLUID INTEGRATOR PAGE 8
MODEL = WHOLE HALF PACK w/7 55G Drums, 30W Uniform Heat Dist +100F w/o solar 10/

STDSTL
SINDA/FLUINT v3.1 Runtime: 7/7/98 16:49
SUBMODEL NAME = HalfPACT
MAX DIFF DELTA T PER ITER
MAX ARITH DELTA T PER ITER
MAX SYSTEM ENERGY BALANCE
ENERGY INTO AND OUT OF SYS
MAX NODAL ENERGY BALANCE
NUMBER OF ITERATIONS
PROBLEM TIME
CALCULATED
DRLXCC(HalfPACT 2202)= 4.272461E-04 VS.
ARLXCC(HalfPACT 2211)= 4.272461E-04 VS.
EBALSC = 1.493508E-02 VS.
ESUMIS = 0.000000E+00
EBALNC(HalfPACT 2212)= 3.714838E-03 VS.
LOOPCT = 731 VS.
TIMEN = 0.500000 VS.
ALLOWED
DRLXCA= 5.000000E-04
ARLXCA= 1.000000E-02
EBALSA * ESUMIS = 0.000000E+00
ESUMOS= 8.51318
EBALNA= 0.000000E+00
NLOOPS= 20000
TIMEND= 3.00000
DIFFUSION NODES IN ASCENDING NODE NUMBER ORDER
T 1001= 100.09 T 1002= 102.70 T 1003= 107.56 T 1004= 114.07 T 1005= 124.94 T 1006= 133.68
T 1011= 100.24 T 1012= 102.70 T 1013= 107.32 T 1014= 113.55 T 1015= 123.98 T 1016= 132.12
T 1021= 100.97 T 1022= 102.50 T 1023= 106.07 T 1024= 111.57 T 1025= 121.40 T 1026= 129.02
T 1031= 101.28 T 1032= 103.45 T 1033= 108.08 T 1034= 114.33 T 1035= 123.31 T 1036= 128.87
T 1041= 101.37 T 1042= 104.48 T 1043= 109.80 T 1044= 117.28 T 1045= 125.19 T 1046= 128.17
T 1047= 128.97 T 1052= 101.38 T 1053= 104.19 T 1054= 108.97 T 1058= 124.73 T 1059= 129.08
T 1062= 101.21 T 1063= 103.15 T 1064= 107.30 T 1065= 112.88 T 1066= 123.51 T 1067= 131.53
T 1071= 101.12 T 1072= 102.94 T 1073= 106.88 T 1074= 112.24 T 1075= 122.92 T 1076= 131.72
T 1081= 100.66 T 1082= 101.53 T 1083= 103.40 T 1084= 105.91 T 1085= 110.72 T 1086= 123.00
T 1087= 131.75 T 1091= 100.38 T 1092= 100.68 T 1093= 101.46 T 1094= 102.65 T 1095= 105.26
T 1101= 100.44 T 1102= 100.84 T 1103= 101.78 T 1104= 103.27 T 1111= 100.85 T 1112= 102.10
T 1113= 104.61 T 1114= 107.77 T 1115= 113.52 T 1121= 101.56 T 1122= 104.26 T 1123= 109.70
T 1124= 116.62 T 1125= 125.76 T 1126= 131.11 T 2001= 135.11 T 2011= 134.58 T 2021= 129.85
T 2031= 130.50 T 2032= 130.76 T 2041= 131.41 T 2051= 131.84 T 2061= 132.32 T 2071= 132.65
T 2081= 134.66 T 2121= 134.63 T 2202= 137.15 T 2212= 136.89 T 2282= 138.21 T 2322= 138.49
ARITHMETIC NODES IN ASCENDING NODE NUMBER ORDER
T 1055= 110.70 T 1056= 112.14 T 1057= 115.60 T 2201= 136.86 T 2203= 137.62 T 2211= 136.68
T 2213= 137.05 T 2281= 137.92 T 2283= 138.45 T 2321= 137.96 T 2323= 139.18
HEATER NODES IN ASCENDING NODE NUMBER ORDER
++NONE++
BOUNDARY NODES IN ASCENDING NODE NUMBER ORDER
T 1= 100.00

SYSTEMS IMPROVED NUMERICAL DIFFERENCING ANALYZER WITH FLUID INTEGRATOR PAGE 9

MODEL = WHOLE HALF PACK w/7 55G Drums, 30W Uniform Heat Dist +100F w/o solar 10/
STDSTL
SINDA/FLUINT v3.1 Runtime: 7/7/98 16:49
SUBMODEL NAME = DRUMS

CALCULATED
DRLXCC(DRUMS 2404)= 3.662109E-04 VS.
ARLXCC(0)= 0.000000E+00 VS.
EBALSC = 4.457929E-03 VS.
ESUMIS = 8.53242
EBALNC(DRUMS 2413)= 1.191008E-03 VS.
LOOPCT = 731 VS.
TIMEN = 0.500000 VS.
ALLOWED
DRLXCA= 5.000000E-04
ARLXCA= 1.000000E-02
EBALSA * ESUMIS = 8.532419E-03
ESUMOS= 0.000000E+00
EBALNA= 0.000000E+00
NLOOPS= 20000
TIMEND= 3.00000
DIFFUSION NODES IN ASCENDING NODE NUMBER ORDER
T 2403= 139.33 T 2404= 138.79 T 2413= 138.05 T 2414= 137.73 T 3300= 139.70 T 3302= 139.70
T 3304= 139.70 T 3306= 139.75 T 3308= 140.30 T 3312= 138.55 T 3314= 138.76 T 3316= 139.56
T 3318= 140.12 T 3322= 138.41 T 3324= 138.41 T 3326= 138.44 T 3328= 138.83 T 3332= 138.35
T 3334= 138.27 T 3336= 138.00 T 3338= 136.41 T 3340= 138.40 T 3342= 138.30 T 3344= 138.16
T 3346= 137.66 T 3348= 134.49 T 3400= 158.56 T 3402= 158.30 T 3404= 157.01 T 3406= 153.14
T 3408= 140.84 T 3412= 156.66 T 3414= 155.72 T 3416= 152.36 T 3418= 140.64 T 3422= 156.46
T 3424= 155.28 T 3426= 151.49 T 3428= 139.23 T 3432= 156.11 T 3434= 154.54 T 3436= 150.04
T 3438= 136.07 T 3440= 156.57 T 3442= 155.92 T 3444= 154.10 T 3446= 149.11 T 3448= 133.85
T 3500= 166.72 T 3502= 166.31 T 3504= 164.33 T 3506= 158.51 T 3508= 141.27 T 3512= 164.37
T 3514= 162.80 T 3516= 157.53 T 3518= 141.06 T 3522= 164.14 T 3524= 162.32 T 3526= 156.65
T 3528= 139.57 T 3532= 163.68 T 3534= 161.36 T 3536= 154.85 T 3538= 136.10 T 3540= 164.33
T 3542= 163.42 T 3544= 160.81 T 3546= 153.76 T 3548= 133.87 T 3600= 169.01 T 3602= 168.56
T 3604= 166.36 T 3606= 159.96 T 3608= 141.58 T 3612= 166.52 T 3614= 164.75 T 3616= 158.93
T 3618= 141.36 T 3622= 166.28 T 3624= 164.26 T 3626= 158.05 T 3628= 139.85 T 3632= 165.77
T 3634= 163.22 T 3636= 156.13 T 3638= 136.28 T 3640= 166.49 T 3642= 165.50 T 3644= 162.63
T 3646= 155.01 T 3648= 134.13 T 3700= 141.18 T 3702= 141.17 T 3704= 141.13 T 3706= 141.03
T 3708= 140.76 T 3712= 140.40 T 3714= 140.57 T 3716= 140.77 T 3718= 140.58 T 3722= 140.19
T 3724= 140.17 T 3726= 140.00 T 3728= 139.36 T 3732= 139.87 T 3734= 139.60 T 3736= 138.89
T 3738= 136.52 T 3740= 140.06 T 3742= 139.67 T 3744= 139.23 T 3746= 138.19 T 3748= 134.66
ARITHMETIC NODES IN ASCENDING NODE NUMBER ORDER
++NONE++
HEATER NODES IN ASCENDING NODE NUMBER ORDER
++NONE++
BOUNDARY NODES IN ASCENDING NODE NUMBER ORDER
++NONE++

3.6.1.4 Seven 55-Gallon Drum Payload with 100 °F Ambient and No Solar Loading, All Decay Heat Load in Center Drum Only (Case 2)

SYSTEMS IMPROVED NUMERICAL DIFFERENCING ANALYZER WITH FLUID INTEGRATOR PAGE 4
MODEL = WHOLE HALF PACK w/7 55G Drums, One Drum Heat +100F w/o solar 8/12/97

STDSTL
SINDA/FLUINT v3.1 Runtime: 7/8/98 9:51
SUBMODEL NAME = HalfPACT
MAX DIFF DELTA T PER ITER DRLXCC(HalfPACT 1066)=-2.685547E-03 VS. DRLXCA= 1.000000E-02
MAX ARITH DELTA T PER ITER ARLXCC(HalfPACT 2321)= 2.258301E-03 VS. ARLXCA= 1.000000E-02
MAX SYSTEM ENERGY BALANCE EBALSC = 5.408887E-02 VS. EBALSA * ESUMIS = 0.000000E+00
ENERGY INTO AND OUT OF SYS ESUMIS = 0.000000E+00
MAX NODAL ENERGY BALANCE EBALNC(HalfPACT 2212)= 1.684309E-02 VS. EBALNA= 0.000000E+00
NUMBER OF ITERATIONS LOOPCT = 507 VS. NLOOPS= 20000
PROBLEM TIME TIMEN = 0.500000 VS. TIMEND= 3.00000
DIFFUSION NODES IN ASCENDING NODE NUMBER ORDER
T 1001= 100.09 T 1002= 102.72 T 1003= 107.64 T 1004= 114.24 T 1005= 125.34 T 1006= 134.50
T 1011= 100.24 T 1012= 102.71 T 1013= 107.36 T 1014= 113.65 T 1015= 124.19 T 1016= 132.52
T 1021= 100.97 T 1022= 102.49 T 1023= 106.04 T 1024= 111.52 T 1025= 121.31 T 1026= 128.90
T 1031= 101.26 T 1032= 103.41 T 1033= 107.99 T 1034= 114.16 T 1035= 123.02 T 1036= 128.49
T 1041= 101.36 T 1042= 104.42 T 1043= 109.67 T 1044= 117.04 T 1045= 124.84 T 1046= 127.78
T 1047= 128.56 T 1052= 101.36 T 1053= 104.13 T 1054= 108.83 T 1058= 124.34 T 1059= 128.61
T 1062= 101.19 T 1063= 103.09 T 1064= 107.16 T 1065= 112.62 T 1066= 123.00 T 1067= 130.80
T 1071= 101.11 T 1072= 102.90 T 1073= 106.78 T 1074= 112.07 T 1075= 122.60 T 1076= 131.29
T 1081= 100.66 T 1082= 101.53 T 1083= 103.40 T 1084= 105.91 T 1085= 110.72 T 1086= 123.09
T 1087= 131.89 T 1091= 100.38 T 1092= 100.69 T 1093= 101.47 T 1094= 102.66 T 1095= 105.27
T 1101= 100.45 T 1102= 100.85 T 1103= 101.79 T 1104= 103.28 T 1111= 100.85 T 1112= 102.12
T 1113= 104.65 T 1114= 107.82 T 1115= 113.59 T 1121= 101.59 T 1122= 104.35 T 1123= 109.90
T 1124= 116.97 T 1125= 126.32 T 1126= 131.79 T 2001= 136.26 T 2011= 135.29 T 2021= 129.55
T 2031= 130.02 T 2032= 130.25 T 2041= 130.78 T 2051= 131.12 T 2061= 131.53 T 2071= 132.18
T 2081= 134.92 T 2121= 135.85 T 2202= 139.02 T 2212= 137.81 T 2282= 138.68 T 2322= 141.12
ARITHMETIC NODES IN ASCENDING NODE NUMBER ORDER
T 1055= 110.53 T 1056= 111.95 T 1057= 115.36 T 2201= 138.63 T 2203= 140.43 T 2211= 137.58
T 2213= 137.82 T 2281= 138.38 T 2283= 138.63 T 2321= 140.38 T 2323= 143.70
HEATER NODES IN ASCENDING NODE NUMBER ORDER
++NONE++
BOUNDARY NODES IN ASCENDING NODE NUMBER ORDER
T 1= 100.00

SYSTEMS IMPROVED NUMERICAL DIFFERENCING ANALYZER WITH FLUID INTEGRATOR PAGE 5
MODEL = WHOLE HALF PACK w/7 55G Drums, One Drum Heat +100F w/o solar 8/12/97

STDSTL
SINDA/FLUINT v3.1 Runtime: 7/8/98 9:51
SUBMODEL NAME = DRUMS
MAX DIFF DELTA T PER ITER DRLXCC(DRUMS 3740)= 2.441406E-03 VS. DRLXCA= 1.000000E-02
MAX ARITH DELTA T PER ITER ARLXCC(0)= 0.000000E+00 VS. ARLXCA= 1.000000E-02
MAX SYSTEM ENERGY BALANCE EBALSC = 2.541827E-02 VS. EBALSA * ESUMIS = 8.532490E-02
ENERGY INTO AND OUT OF SYS ESUMIS = 8.53249
MAX NODAL ENERGY BALANCE EBALNC(DRUMS 2413)= 2.466544E-03 VS. EBALNA= 0.000000E+00
NUMBER OF ITERATIONS LOOPCT = 507 VS. NLOOPS= 20000
PROBLEM TIME TIMEN = 0.500000 VS. TIMEND= 3.00000
DIFFUSION NODES IN ASCENDING NODE NUMBER ORDER
T 2403= 145.46 T 2404= 143.86 T 2413= 137.86 T 2414= 137.85 T 3300= 147.88 T 3302= 147.86
T 3304= 147.77 T 3306= 147.53 T 3308= 147.35 T 3312= 138.76 T 3314= 139.94 T 3316= 144.57
T 3318= 145.80 T 3322= 137.95 T 3324= 137.98 T 3326= 138.17 T 3328= 139.49 T 3332= 137.84
T 3334= 137.75 T 3336= 137.49 T 3338= 135.79 T 3340= 137.99 T 3342= 137.79 T 3344= 137.64
T 3346= 137.13 T 3348= 133.79 T 3400= 268.41 T 3402= 266.71 T 3404= 258.39 T 3406= 233.04
T 3408= 148.64 T 3412= 139.41 T 3414= 140.77 T 3416= 143.37 T 3418= 146.68 T 3422= 138.68
T 3424= 138.93 T 3426= 139.33 T 3428= 140.10 T 3432= 137.96 T 3434= 137.54 T 3436= 136.82
T 3438= 135.21 T 3440= 138.38 T 3442= 137.66 T 3444= 136.96 T 3446= 135.73 T 3448= 132.89
T 3500= 316.28 T 3502= 313.79 T 3504= 301.60 T 3506= 265.06 T 3508= 149.75 T 3512= 139.69
T 3514= 141.05 T 3516= 143.42 T 3518= 147.43 T 3522= 138.96 T 3524= 139.31 T 3526= 139.79
T 3528= 140.49 T 3532= 138.05 T 3534= 137.51 T 3536= 136.65 T 3538= 135.06 T 3540= 138.55
T 3542= 137.65 T 3544= 136.76 T 3546= 135.33 T 3548= 132.71 T 3600= 328.87 T 3602= 326.12
T 3604= 312.71 T 3606= 272.92 T 3608= 150.43 T 3612= 139.91 T 3614= 141.29 T 3616= 143.66
T 3618= 147.91 T 3622= 139.16 T 3624= 139.55 T 3626= 140.07 T 3628= 140.79 T 3632= 138.18
T 3634= 137.62 T 3636= 136.72 T 3638= 135.14 T 3640= 138.72 T 3642= 137.76 T 3644= 136.81
T 3646= 135.35 T 3648= 132.86 T 3700= 156.32 T 3702= 156.19 T 3704= 155.58 T 3706= 153.72
T 3708= 147.69 T 3712= 140.05 T 3714= 141.15 T 3716= 143.53 T 3718= 145.94 T 3722= 138.95
T 3724= 139.06 T 3726= 139.34 T 3728= 140.31 T 3732= 138.40 T 3734= 138.11 T 3736= 137.58
T 3738= 135.88 T 3740= 138.81 T 3742= 138.18 T 3744= 137.72 T 3746= 136.82 T 3748= 133.90
ARITHMETIC NODES IN ASCENDING NODE NUMBER ORDER
++NONE++
HEATER NODES IN ASCENDING NODE NUMBER ORDER
++NONE++
BOUNDARY NODES IN ASCENDING NODE NUMBER ORDER
++NONE++

3.6.2 Thermal Model Details

3.6.2.1 Convection Coefficient Calculation

Heat transfer coefficients from the OCA outer surface are calculated as follows. From *Elements of Heat Transfer*¹, the convective heat transfer coefficient, h , is:

$$h = \text{Nu} \frac{k}{L} \text{ Btu/hr-in}^2\text{-}^\circ\text{F}$$

where k is the conductivity of gas at film temperature (Btu/hr-in-°F) and L is the effective length of the vertical surface or cylinder diameter for the horizontal surface.

The Nusselt number, Nu , for horizontally heated surfaces facing upward is:

$$\begin{aligned} \text{Nu} &= 0.54(\text{Gr Pr})^{1/4} && \text{for } 10^5 < \text{GrPr} < 2 \times 10^7 \\ \text{Nu} &= 0.14(\text{Gr Pr})^{1/3} && \text{for } 2 \times 10^7 < \text{GrPr} < 3 \times 10^{10} \end{aligned}$$

and, for horizontally heated surfaces facing downward:

$$\text{Nu} = 0.27(\text{Gr Pr})^{1/4} \quad \text{for } 3 \times 10^5 < \text{GrPr} < 3 \times 10^{10}$$

The Nusselt number, Nu , for vertically heated surfaces is:

$$\text{Nu} = \left(0.825 + \frac{0.387(\text{Gr Pr})^{1/6}}{\left[1 + (0.492/\text{Pr})^{9/16} \right]^{8/27}} \right)^2 \quad \text{for } 10^{-1} < \text{GrPr} < 10^{12}$$

For both horizontally and vertically heated surfaces, the Grashof number, Gr , is:

$$\text{Gr} = \frac{g\beta\Delta TL^3}{\nu^2}$$

where g is the gravitational acceleration constant (in/s²), β is the gas coefficient of thermal expansion (°F⁻¹), where $\beta = (T_{\text{abs}})^{-1}$ for an ideal gas, ΔT is the differential temperature (°F), where $\Delta T = |T_{\text{wall}} - T_{\infty}|$, ν is the kinematic viscosity of gas at the film temperature (in²/s), and Pr is the Prandtl number. Note that k , Gr , and Pr are each a function of air temperature per [Table 3.2-3](#).

3.6.2.2 Aluminum Honeycomb Conductivity Calculation

The thermal conductivity of aluminum honeycomb reported by Hexcel in TSB-120² provides little or no supporting information for how those values were obtained, or for what honeycomb orientation they are valid. The *Satellite Thermal Control Handbook*³ provides a computationally derived method for determining the effective thermal conductivity of honeycomb structures

¹ Y. Bayazitoglu and M. Ozisik, *Elements of Heat Transfer*, McGraw-Hill Publishing, New York, 1988, pp180-181.

² Hexcel, *Mechanical Properties of Hexcel Honeycomb Materials*, TSB-120 (Technical Service Bulletin 120), 1992.

³ D. G. Gilmore, Editor, *Satellite Thermal Control Handbook*, The Aerospace Corporation Press, El Segundo, CA, 1994.

based on cell size, material thickness, and orientation. Thermal conductivity calculated by this method is lower than the value reported by Hexcel, and is therefore conservatively used in the thermal model. The following figure, derived from the *Satellite Thermal Control Handbook*, serves to illustrate the dimensional parameters considered.

The effective conductivity for the x, y and z directions (W, L and T directions, respectively, on above drawing) are calculated as follows:

$$k_x = \frac{3 k_{Al} \delta}{2 S}, \quad k_y = \frac{k_{Al} \delta}{S}, \quad k_z = \frac{8 k_{Al} \delta}{3 S}$$

Note that for the HalfPACT calculations, k_y and k_z represent axial and radial conductivity, respectively. The aluminum honeycomb spacers used in the ICV torispherical heads have a foil thickness, δ , of 0.003 inches, and a nominal cell dimension, S , of 0.375 inches. Therefore,

$$k_x = (0.0120)k_{Al}, \quad k_y = (0.0080)k_{Al}, \quad k_z = (0.0213)k_{Al}$$

From Section 515.29, Page 2, of *Properties of Solids, Thermal Conductivity, Metallic Materials*⁴, the thermal conductivity of 5052 aluminum, k_{Al} , is 79.7 Btu/hr-ft-°F at 68 °F, 82.2 Btu/hr-ft-°F at 212 °F, and 100.0 Btu/hr-ft-°F at 752 °F. Table 3.6.2-1 summarizes the thermal conductivities for the aluminum honeycomb used in the analyses. Thermal conductivities are provided at -40 °F and 1,500 °F are provided to ensure computational stability.

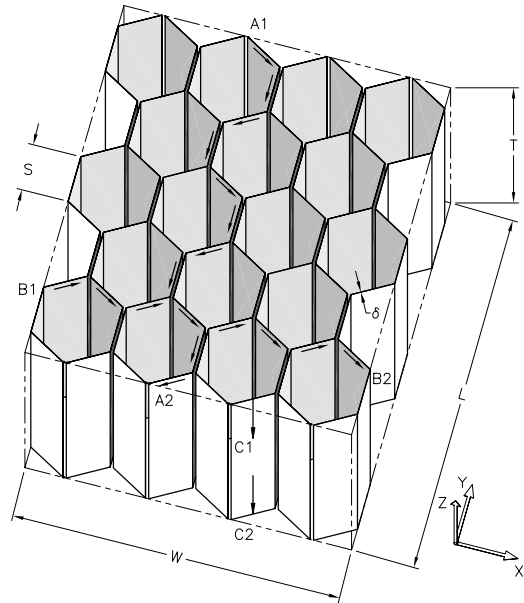


Table 3.6.2-1– Effective Thermal Conductivity of Aluminum Honeycomb

Temperature, °F	k_{axial} , Btu/hr-in-°F	k_{radial} , Btu/hr-in-°F
-40	0.053	0.142
68	0.053	0.142
212	0.055	0.146
752	0.067	0.178
1,500	0.067	0.178

⁴ General Electric, *Properties of Solids, Thermal Conductivity, Metallic Materials*, Heat Transfer Division, July 1974.

3.6.2.3 Polyethylene Plastic Wrap Transmittance Calculation

As many as 18 layers of the optional, 0.002 inch thick, polyethylene plastic wrap is used to restrain the payload drums during transport. Data on the transmittance of polyethylene is available from Figure 659 of *Thermophysical Properties of Matter*⁵. Assuming a plastic wrap temperature of 200 °F to 250 °F, Curves 1 through 4 from Figure 659 of *Thermophysical Properties of Matter* are applicable. Wien's displacement law states:

$$\lambda_{\max} T = 5215.6 \mu\text{m}\cdot\text{R}$$

Thus, at 250 °F, the wavelength of maximum intensity is:

$$\lambda_{\max} = \frac{5215.6}{(250 + 460)} = 7.436 \mu\text{m}$$

The number of wraps is of secondary importance to the overall transmittance, since the first few layers perform essentially all of the filtering. The maximum monochromatic radiation is near 10 μm, and since the low end of the transmittance curves is near $\tau = 0.75$, an overall transmittance of 0.75 is applicable.

From Case 1 (see the computer analysis results in [Appendix 3.6.1.1, Seven 55-Gallon Drum Payload with 100 °F Ambient and Full Solar Loading, Uniformly Distributed Decay Heat Load \(Case 1\)](#)), the maximum temperature differential between the drum surface and the ICV wall surface is between drum node 3348 and ICV node 2032. With drum node 3348 at 153.3 °F, and ICV node 2032 at 150.2 °F, the temperature difference is only 3.1 °F. Extracting heat flow at these nodes from the computer run, approximately 14% of the decay heat is transferred from the drum surface to the ICV wall via radiative heat transfer. Therefore, the inclusion of the 0.75 transmittance would have a negligible impact on maximum drum temperatures.

⁵ Y.S. Touloukian and C.Y. Ho, Editors, *Thermophysical Properties of Matter*, Thermophysical Properties Research Center (TPRC) Data Series, Purdue University, 1970, IFI/Plenum, New York.

This page intentionally left blank.

4.0 CONTAINMENT

4.1 Containment Boundary

4.1.1 Containment Vessel

Two independent levels of containment are established within the HalfPACT package. In general, each containment vessel is constructed primarily of ASTM A240, Type 304, austenitic stainless steel. The exceptions to the use of ASTM A240, Type 304, stainless steel are so noted in the following detailed descriptions.

4.1.1.1 Outer Containment Assembly (Primary Level of Containment)

The containment boundary of the Outer Containment Vessel (OCV), provided as part of the Outer Containment Assembly (OCA), consists of the inner stainless steel vessel comprised of a mating lid and body, plus the uppermost (innermost) of two main O-ring seals between them. In addition, the containment boundary includes an ASTM B16, Alloy 360, brass OCV vent port plug with a mating butyl O-ring seal. A more detailed description of the OCV containment boundary is provided in [Section 1.2.1.1.1, *Outer Containment Assembly \(OCA\)*](#), and in [Appendix 1.3.1, *Packaging General Arrangement Drawings*](#).

The non-stainless steel components utilized in the OCV containment boundary are the upper (inner) butyl O-ring seal, the brass vent port plug, and the butyl O-ring seal on the vent port plug.

4.1.1.2 Inner Containment Vessel (Secondary Level of Containment)

The containment boundary of the Inner Containment Vessel (ICV) consists of a stainless steel vessel comprised of a mating lid and body, plus the uppermost (innermost) of the two main O-ring seals between them. In addition, the containment boundary includes an ASTM B16, Alloy 360, brass ICV outer vent port plug with a mating butyl O-ring seal. A more detailed description of the ICV containment boundary is provided in [Section 1.2.1.1.2, *Inner Containment Vessel \(ICV\) Assembly*](#), and in [Appendix 1.3.1, *Packaging General Arrangement Drawings*](#).

The non-stainless steel components utilized in the ICV containment boundary are the upper (inner) butyl O-ring seal, the brass outer vent port plug, and the butyl O-ring seal on the vent port plug.

4.1.2 Containment Penetrations

The only containment boundary penetrations into each of the two containment vessels (OCV and ICV) are the lids themselves, and the corresponding vent ports. Each penetration is designed to demonstrate “leaktight” sealing integrity, i.e., a leakage rate not to exceed 1×10^{-7} standard cubic centimeters per second (scc/sec), air, as defined in ANSI N14.5¹.

¹ ANSI N14.5-1997, *American National Standard for Radioactive Materials – Leakage Tests on Packages for Shipment*, American National Standards Institute, Inc. (ANSI).

4.1.3 Seals and Welds

4.1.3.1 Seals

Seals affecting containment are described above. A summary of seal testing prior to first use, during routine maintenance, and upon assembly for transportation is as follows.

4.1.3.1.1 Fabrication Leakage Rate Tests

During fabrication and following the pressure testing per [Section 8.1.2.2, Containment Vessel Pressure Testing](#), both the OCV and ICV (primary and secondary containment, respectively) shall be individually leakage rate tested as delineated in [Section 8.1.3, Fabrication Leakage Rate Tests](#). The fabrication leakage rate tests are consistent with the guidelines of Section 7.3 of ANSI N14.5. This leakage rate test verifies the containment integrity of the HalfPACT package's OCV and ICV to a leakage rate not to exceed 1×10^{-7} scc/sec, air.

4.1.3.1.2 Maintenance/Periodic Leakage Rate Tests

Annually, or at the time of damaged containment seal replacement or sealing surface repair, the OCV and/or ICV O-ring seals shall be leakage rate tested as delineated in [Section 8.2.2, Maintenance/Periodic Leakage Rate Tests](#). The maintenance/periodic leakage rate tests are consistent with the guidelines of Section 7.4 of ANSI N14.5. This test verifies the sealing integrity of the HalfPACT package's ICV and OCV lid and vent port containment seals to a leakage rate not to exceed 1×10^{-7} scc/sec, air.

4.1.3.1.3 Preshipment Leakage Rate Tests

Prior to shipment of the loaded HalfPACT package, the main O-ring seal and vent port plug O-ring seal for both the OCV and ICV shall be leakage rate tested per [Section 7.4, Preshipment Leakage Rate Test](#). The preshipment leakage rate tests are consistent with the guidelines of Section 7.6 of ANSI N14.5. This test verifies the sealing integrity of the HalfPACT package's OCV and ICV lid and vent port containment seals to a leakage rate sensitivity of 1×10^{-3} scc/sec, air, or less.

As an option, the maintenance/periodic leakage rate tests, delineated in [Section 8.2.2, Maintenance/Periodic Leakage Rate Tests](#), may be performed in lieu of the preshipment leakage rate tests.

4.1.3.2 Welds

All containment vessel body welds are full penetration welds that have been radiographed to ensure structural and containment integrity. Non-radiographed, safety related welds such as those that attach the OCV vent port coupling and the ICV vent port insert to their respective containment shells are examined using liquid penetrant testing on the final pass or both the root and final passes, as applicable. All containment boundary welds are confirmed to be leaktight as delineated in [Section 8.1.3, Fabrication Leakage Rate Tests](#).

4.1.4 Closure

4.1.4.1 Outer Containment Assembly (OCA) Closure

With reference to [Figure 1.1-1](#) and [Figure 1.1-2](#) in [Chapter 1.0, *General Information*](#), the OCA lid is secured to the OCA body via an OCV locking ring assembly located at the outer diameter of the OCV upper (lid) and lower (body) seal flanges. The upper end of the OCV locking ring is a continuous ring that mates with the OCV upper seal flange (also a continuous ring). The lower end of the OCV locking ring is comprised of 18 tabs that mate with a corresponding set of 18 tabs on the OCV lower seal flange. The OCV locking ring and OCV upper seal flange are an assembly that normally does not disassemble.

[Figure 1.2-1](#) in [Chapter 1.0, *General Information*](#), illustrates OCA lid installation in five steps:

1. As an option, lightly lubricate the main O-ring seals with vacuum grease; install the main O-ring seals into the O-ring seal grooves located in the OCV lower seal flange.
2. Using external alignment stripes as a guide, align the OCA lid's OCV locking ring tabs with the OCV lower seal flange tab spaces.
3. Install the OCA lid; if necessary, evacuate the OCV cavity through the OCV vent port to fully seat the OCA lid and allow free movement of the OCV locking ring.
4. Rotate the OCV locking ring to the "locked" position, again using external alignment stripes as a guide. The locked position aligns the OCV locking ring's tabs with the OCV lower seal flange's tabs. A locking "Z-flange" is bolted to the bottom end of the OCV locking ring and extends radially outward to the exterior of the HalfPACT package. The exterior flange of the locking Z-flange is attached to an outer thermal shield. This Z-flange/thermal shield assembly allows external operation of the OCV locking ring.
5. Install six 1/2 inch diameter lock bolts (socket head cap screws) through the outer thermal shield and into the exterior surface of the OCA to secure the OCV locking ring assembly in the locked position.

4.1.4.2 Inner Containment Vessel (ICV) Closure

With the exception of the locking Z-flange/outer thermal shield assembly, and the use of three rather than six locking ring lock bolts, ICV lid installation is identical to OCA lid installation as described in [Section 4.1.4.1, *Outer Containment Assembly \(OCA\) Closure*](#).

This page intentionally left blank.

4.2 Containment Requirements for Normal Conditions of Transport

4.2.1 Containment of Radioactive Material

The results of the normal conditions of transport (NCT) structural and thermal evaluations performed in [Section 2.6, *Normal Conditions of Transport*](#), and [Section 3.4, *Thermal Evaluation for Normal Conditions of Transport*](#), respectively, and the results of the full-scale, structural testing presented in [Appendix 2.10.3, *Certification Tests*](#), verify that there will be no release of radioactive materials per the “leaktight” definition of ANSI N14.5¹ under any of the NCT tests described in 10 CFR §71.71².

4.2.2 Pressurization of Containment Vessel

The maximum normal operating pressure (MNOP) of both the OCV and ICV is 50 psig per [Section 3.4.4, *Maximum Internal Pressure*](#). The design pressure of both the OCV and ICV is 50 psig. Based on the structural evaluations performed in [Chapter 2.0, *Structural Evaluation*](#), pressure increases to 50 psig will not reduce the effectiveness of the HalfPACT package to maintain containment integrity per [Section 4.2.1, *Containment of Radioactive Material*](#).

4.2.3 Containment Criterion

At the completion of fabrication, both the OCV and ICV shall be leakage rate tested as described in [Section 4.1.3.1.1, *Fabrication Leakage Rate Tests*](#). For annual maintenance, both the OCV and ICV shall be leakage rate tested as described in [Section 4.1.3.1.2, *Maintenance/Periodic Leakage Rate Tests*](#). In addition, at the time of seal replacement if other than during routine maintenance (e.g., if damage during assembly necessitates seal replacement), maintenance/periodic leakage rate testing shall be performed for that seal. For verification of proper assembly prior to shipment, both the OCV and ICV shall be leakage rate tested as described in [Section 4.1.3.1.3, *Preshipment Leakage Rate Tests*](#).

¹ ANSI N14.5-1997, *American National Standard for Radioactive Materials – Leakage Tests on Packages for Shipment*, American National Standards Institute, Inc. (ANSI).

² Title 10, Code of Federal Regulations, Part 71 (10 CFR 71), *Packaging and Transportation of Radioactive Material*, 01-01-07 Edition.

This page intentionally left blank.

4.3 Containment Requirements for Hypothetical Accident Conditions

4.3.1 Fission Gas Products

There are no fission gas products in the HalfPACT package payload.

4.3.2 Containment of Radioactive Material

The results of the hypothetical accident condition (HAC) structural and thermal evaluations performed in [Section 2.7, *Hypothetical Accident Conditions*](#), and [Section 3.5, *Thermal Evaluation for Hypothetical Accident Conditions*](#), respectively, and the results of the full-scale, structural and thermal testing presented in [Appendix 2.10.3, *Certification Tests*](#), verify that there will be no release of radioactive materials per the “leaktight” definition of ANSI N14.5¹ under any of the HAC tests described in 10 CFR §71.73².

4.3.3 Containment Criterion

The HalfPACT package has been designed, and has been verified by leakage rate testing both prior to and following structural and thermal certification testing as presented in [Appendix 2.10.3, *Certification Tests*](#), to meet the “leaktight” definition of ANSI N14.5.

¹ ANSI N14.5-1997, *American National Standard for Radioactive Materials – Leakage Tests on Packages for Shipment*, American National Standards Institute, Inc. (ANSI).

² Title 10, Code of Federal Regulations, Part 71 (10 CFR 71), *Packaging and Transportation of Radioactive Material*, 01-01-07 Edition.

This page intentionally left blank.

4.4 Special Requirements

4.4.1 Plutonium Shipments

The HalfPACT package is designed and has been structurally and thermally tested as a Type B(U), double containment package meeting the requirements of 10 CFR §71.63¹ for plutonium shipments. Both containment vessels (i.e., the OCV and ICV) are shown on the drawings in [Appendix 1.3.1, *Packaging General Arrangement Drawings*](#), and described in [Section 4.1.1.1, *Outer Containment Assembly \(Primary Level of Containment\)*](#), and [Section 4.1.1.2, *Inner Containment Vessel \(Secondary Level of Containment\)*](#). Further, the HalfPACT package has been designed, and has been verified by leakage rate testing both prior to and following structural and thermal certification testing as presented in [Appendix 2.10.3, *Certification Tests*](#), to meet the “leaktight” definition of ANSI N14.5.²

4.4.2 Interchangeability

The HalfPACT package is designed and fabricated so that both the OCV lid assembly and the ICV lid assembly are interchangeable between OCV body assemblies and ICV body assemblies, respectively. Each combination of a particular lid assembly and body assembly becomes a containment system that shall be maintained in accordance with [Section 4.1.3.1.2, *Maintenance/Periodic Leakage Rate Tests*](#), and used in accordance with [Section 4.1.3.1.3, *Preshipment Leakage Rate Tests*](#). When the interchangeability option has been exercised, newly combining a lid and a body, measure the axial play per the requirements of [Section 8.2.3.3.2.3, *Axial Play*](#), to determine acceptability.

¹ Title 10, Code of Federal Regulations, Part 71 (10 CFR 71), *Packaging and Transportation of Radioactive Material*, 01-01-07 Edition.

² ANSI N14.5-1997, *American National Standard for Radioactive Materials – Leakage Tests on Packages for Shipment*, American National Standards Institute, Inc. (ANSI).

This page intentionally left blank.

5.0 SHIELDING EVALUATION

The compliance evaluations of the HalfPACT packaging with respect to the dose rate limits established by 10 CFR §71.47(a)¹ for normal conditions of transport (NCT) or 10 CFR §71.51(a)(2) for hypothetical accident conditions (HAC) are based on two categories. The first category does not permit the use of shielding materials to meet the NCT or HAC dose rate limits and is evaluated for compliance in this section. The second category permits the use of shielding materials in the standard, S100, S200, and S300 pipe overpack payload containers and the shielded container as evaluated in [Appendices 4.1 through 4.5](#) of the *CH-TRU Payload Appendices*.²

Each contact-handled transuranic (CH-TRU) waste payload container (i.e., 55-gallon drum, 85-gallon drum, 100-gallon drum, or standard waste box [SWB]), as prepared for transport in a HalfPACT package, is limited such that the external radiation field, both gamma and neutron, shall be less than or equal to 200 millirem per hour (mrem/hr) at the package surface. This dose rate limit is for payload containers prior to addition of any lead, steel or other shielding material to the payload containers for *as-low-as-reasonably-achievable* (ALARA) dose reduction purposes during non-transport handling operations.

The HalfPACT packaging is not designed to provide significant gamma or neutron shielding. Three shells, the inner containment vessel (ICV), outer containment vessel (OCV), and outer containment assembly (OCA) outer shell are composed of stainless steel having minimum thicknesses of 1/4 inch, 3/16 inch, and 1/4 inch, respectively. Approximately ten inches of polyurethane foam occupies the annular cavity between the OCV and OCA outer shell.

Prior to transport, the HalfPACT package shall be monitored on the semi-trailer or railcar for both gamma and neutron radiation to demonstrate compliance with 10 CFR §71.47. Since the HalfPACT package is not significantly deformed under NCT, the package will meet the dose rate limits for NCT if the measurements demonstrate compliance with the allowable dose rate levels in 10 CFR §71.47. The shielding Transport Index (TI), as defined in 10 CFR §71.4, will be determined by measuring the dose rate a distance of one meter from the package surface per the requirements of 49 CFR §173.403.³

Shielding materials are not specifically provided by the HalfPACT packaging, and none are permitted in the payload containers to meet the dose rate limits of 10 CFR §71.47 for NCT. Therefore, shielding provided by the stainless steel shells and polyurethane foam of the packaging is not needed to meet the higher dose rate limits after the HAC tests delineated in 10 CFR §71.73. This ensures that the post-HAC, allowable dose rate of one rem per hour (rem/hr) a distance of one meter from the package surface per 10 CFR §71.51(a)(2) will be met.

¹ Title 10, Code of Federal Regulations, Part 71 (10 CFR 71), *Packaging and Transportation of Radioactive Material*, 01-01-07 Edition.

² U.S. Department of Energy (DOE), *CH-TRU Payload Appendices*, current revision, U.S. Department of Energy, Carlsbad Field Office, Carlsbad, New Mexico.

³ Title 49, Code of Federal Regulations, Part 173 (49 CFR 173), *Shippers—General Requirements for Shipments and Packagings*, 10-01-06 Edition.

Even if payload material is released from a payload container during a HAC event, the post-HAC dose rate limit of one rem/hr at one meter from the package surface will always be met. This is because each CH-TRU waste payload container must have a dose rate less than or equal to 200 mrem/hr on contact prior to the addition of any ALARA dose reduction shielding for non-transport handling operations prior to being loaded into the HalfPACT packaging. Since shielding within the payload containers is not permitted to meet the transportation dose rate limits for NCT, release of the materials from the payload containers during a HAC event will not increase the dose rate significantly or cause it to exceed the dose rate limit for the HAC.

6.0 CRITICALITY EVALUATION

The following analyses demonstrate that the HalfPACT package complies with the requirements of 10 CFR §71.55¹ and §71.59. The analyses show that the criticality requirements are satisfied when limiting the payload containers and the HalfPACT package to fissile gram equivalent (FGE) of Pu-239 limits given in [Table 6.1-1](#) and [Table 6.1-2](#), respectively for the payloads described in the *Contact-Handled Transuranic Waste Authorized Methods for Payload Control (CH-TRAMPAC)*². In summary, Case A is applicable to waste that is not machine compacted and contains less than or equal to 1% by weight quantities of special reflector materials and Case B is applicable to waste that is not machine compacted and contains greater than 1% by weight quantities of special reflector materials. For Case A, package limits were calculated for various Pu-240 contents in the package. Case C is applicable to machine compacted waste that contains less than or equal to 1% by weight quantities of special reflector materials. Case D is specifically applicable to machine compacted waste in the form of “puck” drums overpacked in 55-, 85-, or 100-gallon drums with less than or equal to 1% by weight quantities of special reflector materials. Case E is applicable to waste that is not machine compacted in the standard, S100, S200, and S300 pipe overpacks with less than or equal to 1% by weight quantities of special reflector materials and Case F is applicable to waste that is not machine compacted in the standard, S100, S200, and S300 pipe overpacks with greater than 1% by weight quantities of special reflector materials. Case G is applicable to waste that is not machine compacted in the shielded container with less than or equal to 1% by weight quantities of special reflector materials. Case H is applicable to machine compacted waste in the shielded container with less than or equal to 1% by weight quantities of special reflector materials. However, if the quantity of special reflector material in the payload is greater than 1% by weight but the form of the payload is such that the thickness and/or packing fraction of the special reflector material is less than the reference poly/water reflector or the special reflector material (excluding beryllium in non-pipe overpack configurations) is mechanically or chemically bound to the fissile material, then Case A and Case E limits apply in lieu of Case B and Case F limits, respectively. Also, the Case G limit is applicable to waste that is not machine compacted with greater than 1% by weight quantities of special reflectors in the above stated forms. Similarly, Case C, Case D, and Case H limits are applicable to machine compacted waste with greater than 1% by weight quantities of special reflectors in the above stated forms.

The criticality evaluations for Cases E and F are presented in [Appendices 4.1, 4.2, 4.3, and 4.4](#) in the *CH-TRU Payload Appendices*³ and Cases G and H are presented in [Appendix 4.5](#) of the *CH-TRU Payload Appendices* whereas the analyses for Cases A through D are presented in this chapter. Based on an unlimited array of undamaged or damaged HalfPACT packages, the Criticality Safety Index (CSI), per 10 CFR §71.59, is 0.0.

¹ Title 10, Code of Federal Regulations, Part 71 (10 CFR 71), *Packaging and Transportation of Radioactive Material*, 01-01-07 Edition.

² U.S. Department of Energy (DOE), *Contact-Handled Transuranic Waste Authorized Methods for Payload Control (CH-TRAMPAC)*, U.S. Department of Energy, Carlsbad Field Office, Carlsbad, New Mexico.

³ U.S. Department of Energy (DOE), *CH-TRU Payload Appendices*, current revision, U.S. Department of Energy, Carlsbad Field Office, Carlsbad, New Mexico.

6.1 Discussion and Results

The criticality analyses presented herein are identical to the analyses presented in [Chapter 6.0, Criticality Evaluation](#), of the *TRUPACT-II Shipping Package Safety Analysis Report*¹. Since the height of a HalfPACT package is 30 inches shorter than a TRUPACT-II package, resulting in a closer axial packaging in the infinite arrays, the criticality analyses utilizing the HalfPACT package geometry are considered conservative for Cases A through D. A comprehensive description of the HalfPACT packaging is provided in [Section 1.2, Package Description](#), and in the packaging drawings in [Appendix 1.3.1, Packaging General Arrangement Drawings](#).

For the contents of the HalfPACT package specified in [Section 6.2, Package Contents](#), no special features are required to maintain criticality safety for any number of HalfPACT packages for both normal conditions of transport (NCT) and hypothetical accident conditions (HAC). The presence and location of the stainless steel, inner and outer containment vessel shells (ICV and OCV, respectively) and outer containment assembly (OCA) outer shell are all that are required to maintain criticality safety.

The criteria for ensuring that a package (or package array) is safely subcritical is:

$$k_s = k_{\text{eff}} + 2\sigma < \text{USL}$$

where the quantity k_s is the multiplication factor computed for a given configuration plus twice the uncertainty in the computed result, σ . This quantity is computed and reported in order to permit a direct comparison of results against the upper subcriticality limit, USL, determined in [Section 6.5, Critical Benchmark Experiments](#). The USL is determined on the basis of a benchmark analysis and incorporates the combined effects of code computational bias, the uncertainty in the bias based on both experimental and computational uncertainties, and an administrative margin. Further discussion regarding the USL is provided in Chapter 4, *Determination of Bias and Subcritical Limits*, of NUREG/CR-6361².

The results of the criticality calculations are summarized in [Table 6.1-3](#). Calculations performed for Case A for a HalfPACT single unit and infinite arrays of damaged HalfPACT packages indicate that the maximum reactivity of the package arrays are essentially the same as that of the NCT single-unit to within the calculated uncertainty of the Monte Carlo analysis. This occurs because:

- When the ICV and OCA regions are filled with reflecting material, the size of these regions allows the presence of enough material to isolate the fissile material region of each HalfPACT packages from each other, and
- When the fissile material region of each damaged or undamaged HalfPACT package is unreflected, interaction among HalfPACT packages is maximized. However, interactive effects are not as great as the effect of full reflection.

¹ U.S. Department of Energy (DOE), *TRUPACT-II Shipping Package Safety Analysis Report*, USNRC Certificate of Compliance 71-9218, U.S. Department of Energy, Carlsbad Area Office, Carlsbad, New Mexico.

² J. J. Lichtenwalter, S. M. Bowman, M. D. DeHart, C. M. Hopper, *Criticality Benchmark Guide for Light-Water-Reactor Fuel in Transportation and Storage Packages*, NUREG/CR-6361, ORNL/TM-13211, March 1997.

As discussed below, all k_s values are less than the USL of 0.9382. For all cases, the modeled conditions are considered to be extremely conservative, nevertheless, they provide an upper limit on k_s . Therefore, the requirements of 10 CFR §71.55 are met when the contents of a single HalfPACT package are limited in accordance with [Table 6.1-1](#) and [Table 6.1-2](#). The application of these limits to the HalfPACT payload described in the [CH-TRAMPAC](#)³ is discussed, in summary, in [Section 6.4.3.5](#), *Applicable Criticality Limits for CH-TRU Waste*.

Infinite arrays of both damaged and undamaged HalfPACT packages, as defined in [Section 6.3.4](#), *Array Models*, are also safely subcritical ($k_s < \text{USL}$). The post-accident geometry used in the model of the damaged HalfPACT packages conservatively bounds the damage experienced from certification testing described in [Appendix 2.10.3](#), *Certification Tests*. Based on the results of the HAC 30 foot drops, the criticality model conservatively assumes that the OCA outer shell is deformed inward on the side, top, and bottom to a distance of 5 inches from the OCV. Further, the criticality model conservatively models the region between the ICV and the OCA as containing a mixture of 25% polyethylene, 74% water and 1% beryllium in all bounding cases to bound the presence of polyurethane foam in this region. After the HAC thermal event (fire), actual post-test measurements show 3 inches of foam, minimum, remains in impact regions, and 5 inches, minimum, remains elsewhere.

For an infinite array of damaged HalfPACT packages, the maximum calculated k_s values for each case occurred for optimal internal moderation and maximum reflection within the ICV, OCA and interspersed regions. Of all calculations performed and summarized in [Table 6.1-3](#), the maximum neutron multiplication factor, adjusted for code bias and uncertainty, of $k_s = 0.9359$ occurs in Case A at the 360 FGE limit with 15 g of Pu-240 for an infinite array of HAC packages when optimally moderated and reflected. All results are detailed in [Section 6.4.3](#), *Criticality Results*. As with the single-unit cases, the calculations contain conservatism in the geometry and material assumptions (as identified in [Section 6.2](#), *Package Contents*, and [Section 6.4.2](#), *Fuel Loading or Other Contents Loading Optimization*). At maximum reflection, the packages in the array are isolated from each other. An investigation of array reactivity when array interaction effects become significant as a result of decreased reflector volume fraction is provided in [Section 6.4.3.2](#), *Criticality Results for Infinite Arrays of HalfPACT Packages*. Therefore, the requirements of 10 CFR §71.59 are met as arrays of HalfPACT packages will remain subcritical when the contents of a single HalfPACT package is limited as indicated in [Table 6.1-1](#) and [Table 6.1-2](#). Furthermore, a CSI of zero (0.0) is justified.

³ U.S. Department of Energy (DOE), *Contact-Handled Transuranic Waste Authorized Methods for Payload Control (CH-TRAMPAC)*, U.S. Department of Energy, Carlsbad Field Office, Carlsbad, New Mexico.

Table 6.1-1 – Fissile Material Limit per Payload Container

Payload Configuration	Fissile Material Limit per Payload Container (Pu-239 FGE)							
	Case A ^①	Case B	Case C	Case D	Case E	Case F	Case G	Case H
55-gallon drums	200	100	200	200	-	-	-	-
Pipe overpacks	-	-	-	-	200	140	-	-
SWB	325	100	250	-	-	-	-	-
85-gallon drums	200	100	200	200	-	-	-	-
100-gallon drums	200	100	200	200	-	-	-	-
Shielded containers	-	-	-	-	-	-	200	200

Note:

- ① The FGE limit given applies to the payload container regardless of Pu-240 content in the package.

Table 6.1-2 – Fissile Material Limit per HalfPACT Package

Minimum Pu-240 Content in Package	Fissile Material Limit per HalfPACT Package (Pu-239 FGE)							
	Case A	Case B	Case C	Case D	Case E	Case F	Case G	Case H
0 g	325	100	250	325	1400	980	325	245
5 g	340	-	-	-	-	-	-	-
15 g	360	-	-	-	-	-	-	-
25 g	380	-	-	-	-	-	-	-

Table 6.1-3 – Summary of Criticality Analysis Results

	Case A	Case B	Case C	Case D
Normal Conditions of Transport (NCT)				
Number of undamaged packages calculated to be subcritical	∞	∞	∞	∞
Single Unit Maximum k_s	0.9339	Same as HAC Infinite Array k_s		
Infinite Array Maximum k_s	Same as HAC Infinite Array k_s			
Hypothetical Accident Conditions (HAC)				
Number of damaged packages calculated to be subcritical	∞	∞	∞	∞
Single Unit Maximum k_s (0 g Pu-240)	0.9331	Same as HAC Infinite Array k_s		
Infinite Array Maximum k_s (0 g Pu-240)	0.9331	0.9184	0.9345	0.9349
Infinite Array Maximum k_s (with Pu-240)	0.9359	-	-	-
Upper Subcriticality Limit (USL)	0.9382			

This page intentionally left blank.

6.2 Package Contents

The payload cavity of a HalfPACT package can accommodate seven 55-gallon drums, four 85-gallon drums, three 100-gallon drums, or one standard waste boxes (SWB). Different fissile gram equivalent (FGE) limits are available depending on the contents of the shipment as described in the subsections below.

The quantities of all fissile isotopes other than Pu-239 present in the CH-TRU waste material and other authorized payloads may be converted to a FGE using the conversion factors outlined in the [CH-TRAMPAC](#)¹. For modeling purposes, the package is assumed to contain Pu-239 at the FGE limit. The fissile composition of the payload will typically be as follows:

Nuclide	Weight-Percent
Pu-238	Trace
Pu-239	93.0
Pu-240	5.8
Pu-241	0.4
Pu-242	Trace
Am-241	Trace
All other fissile isotopes	0.7

Except for Cases A and D, no credit is taken for parasitic neutron absorption in CH-TRU waste materials and other authorized payloads, dunnage, or package contents. The entire contents of a HalfPACT package are conservatively modeled as an optimally moderated sphere of Pu-239 as determined by varying the H/Pu atom ratio. The size of the sphere is calculated based on the H/Pu ratio and the Pu mass. Case A takes credit for the presence of varying amounts of Pu-240 in the package, see [Table 6.1-2](#). Case D is applicable to a very specific case where drums and their contents are machine compacted and then overpacked in 55-, 85-, or 100-gallon drums. Due to the machine compaction, a higher polyethylene packing fraction is achieved and the fissile material is in a more reactive state within the pucks than if it reconfigured outside of the pucks and homogenized at a lower polyethylene packing fraction within the inner containment vessel (ICV). Thus, in this case, some of structural materials are credited and a cylindrical fissile region is modeled as discussed in [Section 6.3.1.4, Case D Contents Model](#). The HalfPACT package meets the criticality safety requirements as specified in 10 CFR §71.55² and §71.59, provided the limits specified in [Table 6.1-1](#) and [Table 6.1-2](#) are not exceeded.

¹ U.S. Department of Energy (DOE), *Contact-Handled Transuranic Waste Authorized Methods for Payload Control (CH-TRAMPAC)*, U.S. Department of Energy, Carlsbad Field Office, Carlsbad, New Mexico.

² Title 10, Code of Federal Regulations, Part 71 (10 CFR 71), *Packaging and Transportation of Radioactive Material*, 01-01-07 Edition.

6.2.1 Applicability of Case A Limit

The Case A limit is applicable provided the contents are manually compacted (i.e., not machine compacted) and contain less than or equal to 1% by weight quantities of special reflector materials. These requirements drive the assumptions regarding the appropriately bounding moderator and reflector materials that are utilized in the analyses to bound the presence of all materials that are authorized for shipment under the Case A FGE limits. The contents model assumptions are provided in [Section 6.3.1.1, Case A Contents Model](#).

The utilization of polyethylene as the bounding hydrogenous moderating material is justified by the SAIC-1322-001³ study which concludes that polyethylene is the most reactive moderator that could credibly moderate CH-TRU waste in a pure form. A 25% volumetric packing fraction for polyethylene is used as a conservative value which is based on physical testing that bounds the packing fraction of polyethylene in manually compacted CH-TRU waste of 13.36%⁴.

Materials that can credibly provide better than 25% polyethylene/75% water equivalent reflection are termed “special reflectors” and not authorized for shipment under Case A in quantities that exceed 1% by weight except in specific configurations discussed below. Based on the results from SAIC-1322-001³, Be, BeO, C, D₂O, MgO and depleted U ($\geq 0.3\%$ ²³⁵U) are the only materials that can provide reflection equivalent to a 2 ft thickness of 25% polyethylene and 75% water mixture under any of the following conditions and are therefore the only materials considered as special reflectors:

- Less than 5/8 inch thick at 100% of theoretical density⁵ in the form of large solids
- Less than 11/16 inch thick at 70% of theoretical density in the form of tightly-packed particulate solids
- Less than 20% packing fraction at 24 inches thick in the form of randomly dispersed particulate solids

The utilization of 1% by volume beryllium in the reflector material filling the ICV bounds the presence of up to 1% by weight quantities of special reflectors that are randomly dispersed in the payload containers based on the volume of the ICV and the maximum allowed weight of the payload containers in the package. SAIC-1322-001 found that beryllium is the bounding special reflector as it provides the best reflection of the system resulting in the highest reactivity.

If the fissile material is bound to the special reflector material, these materials will provide moderation of the fissile material but will not be available to reflect the fissile region. The reference study, SAIC-1322-001, found that adding special reflector materials, with the exception of beryllium, to the fissile region reduced the reactivity of a single 325 FGE 25% polyethylene/75% water reflected sphere. The moderating effect of heavy water was not studied,

³ Neeley, G. W., D. L. Newell, S. L. Larson, and R. J. Green, *Reactivity Effects of Moderator and Reflector Materials on a Finite Plutonium System*, SAIC-1322-001, Revision 1, Science Applications International Corporation, Oak Ridge, Tennessee, May 2004.

⁴ WP 08-PT.09, *Test Plan to Determine the TRU Waste Polyethylene Packing Fraction*, Washington TRU Solutions, LLC., Revision 0, June 2003.

⁵ Theoretical densities used in the study are 1.85 g/cm³ for Be, 2.69 g/cm³ for BeO, 2.1 g/cm³ for C, 1.1054 g/cm³ for D₂O, 3.22 g/cm³ for MgO, and 19.05 g/cm³ for U.

but the quantity of liquid allowed in the HalfPACT is limited such that heavy water would not be present in greater than 1% by weight quantities. Thus, if the special reflector, excluding beryllium, is chemically or mechanically bound to the fissile material, Case A limits apply even in the presence of greater than 1% by weight quantities of the special reflector. Chemically bound means that the special reflector materials are chemically reacted with the fissile material such that the reflector materials and the fissile materials are chemically interacted and are stable. Mechanically bound means the fissile material is mechanically bound to the reflector such that the reflector material will not disengage from the fissile material because it is topographically imbedded, topographically interlocked, or surface contaminated. A summary discussion of special reflectors is provided in [Section 6.4.3.3](#).

6.2.2 Applicability of Case B Limit

The Case B limit is applicable for contents containing greater than 1% by weight quantities of special reflector materials provided the contents are manually compacted (i.e., not machine compacted). These requirements drive the assumptions regarding the appropriately bounding moderator and reflector materials that are utilized in the analyses to bound the presence of all materials that are authorized for shipment under the Case B FGE limits. However, if the special reflector materials can be demonstrated to be in thicknesses and/or packing fractions that are less than the 25% polyethylene/ 75% water equivalent parameters given in [Table 6.2-1](#), then Case A limits can be used. Note that equivalent thicknesses for Be and BeO are not given as, for thin reflectors of these materials, 100% packing fraction does not result in the highest reactivity and the equivalent thickness increases inversely with the packing fraction; thus, only a packing fraction comparison can be used for Be and BeO. The contents model assumptions are provided in [Section 6.3.1.2, Case B Contents Model](#).

The utilization of polyethylene as the bounding hydrogenous moderating material at a 25% packing fraction is consistent with the justification provided in [Section 6.2.1, Applicability of Case A Limit](#). However, the fissile sphere is moderated with varying volume fractions of beryllium as beryllium was also found in SAIC-1322-001 to increase reactivity when significant quantities are included in the moderator. The use of a 100% dense thick Be reflector in the model bounds the presence of other special reflector materials.

6.2.3 Applicability of Case C Limit

The Case C limit is applicable provided the contents are machine compacted and contain less than or equal to 1% by weight quantities of special reflector materials. These requirements drive the assumptions regarding the appropriately bounding moderator and reflector materials that are utilized in the analyses to bound the presence of all materials that are authorized for shipment under the Case C FGE limits. The contents model assumptions are provided in [Section 6.3.1.3, Case C Contents Model](#).

The utilization of polyethylene as the bounding hydrogenous moderating material at a 100% packing fraction is consistent with the justification provided in [Section 6.2.1, Applicability of Case A Limit](#). Additionally, SAIC-1322-001 concluded no material, that could credibly moderate a fissile sphere in a pure form, resulted in a higher reactivity than the 100% polyethylene moderated system. Thus, compared to Case A, the packing fraction of the moderator is the dominant factor that results in an increase in reactivity. The only inorganic

material that increased reactivity when added to the fissile mixture was beryllium. The effect of more than 1% by weight quantities of beryllium in the moderator is studied under Case B as beryllium is also the leading special reflector. The use of 99% polyethylene and 1% beryllium (by volume) in the reflector region is an appropriately bounding reflector material as it is consistent with the moderator assumption and accounts for the less than or equal to 1% by weight quantities of special reflector materials allowed in the package.

Again, if the special reflector material, excluding beryllium, is chemically or mechanically bound to the fissile material or if the special reflector materials can be demonstrated to be in thicknesses and/or packing fractions that are less than the 25% polyethylene/ 75% water equivalent parameters given in [Table 6.2-1](#), then Case C limits apply even in the presence of greater than 1% by weight quantities of the special reflector.

6.2.4 Applicability of Case D Limit

The Case D limit is specifically applicable provided the contents are machine compacted in the form of “puck” drums overpacked in 55-, 85-, or 100-gallon drums with less than or equal to 1% by weight quantities of special reflector materials and either of the following two controls: a) the packing fraction of polyethylene in the pucks is not greater than 70% or b) the separation between pucks in two axially adjacent overpack drums is maintained at greater than or equal to 0.50 inch through the use of a compacted puck drum spacer placed in the bottom of each overpack drum. These requirements drive the assumptions regarding the appropriately bounding moderator and reflector materials that are utilized in the analyses to bound the presence of all materials that are authorized for shipment under the Case D FGE limits. The contents model assumptions are provided in [Section 6.3.1.4, Case D Contents Model](#).

The utilization of polyethylene as the bounding hydrogenous moderating material is consistent with the justification provided in [Section 6.2.1, Applicability of Case A Limit](#). The use of a 70% packing fraction is applicable provided that controls are implemented to ensure the packing fraction is limited during machine compaction. The use of 70% polyethylene, 29% water and 1% beryllium (by volume) in the reflector region is an appropriately bounding reflector material as it is consistent with the moderator assumption, again provided that controls are implemented to ensure the packing fraction is limited during machine compaction, and accounts for the less than or equal to 1% by weight quantities of special reflector materials allowed in the package. Otherwise, the use of 99% polyethylene and 1% beryllium (by volume) in the reflector region is an appropriately bounding reflector material as it is consistent with the moderator assumption and accounts for the less than or equal to 1% by weight quantities of special reflector materials allowed in the package.

The compacted puck drum spacers have been demonstrated to maintain the minimum required axial spacing between pucks in axially adjacent overpack drums under Hypothetical Accident Conditions (HAC) and are described in [Appendix 1.3.1, Packaging General Arrangement Drawings⁶](#).

⁶ Packaging Technology, Inc., *Test Report for Compacted Drums*, TR-017, Revision 0, Packaging Technology, Inc., Tacoma, Washington, March 2004.

Again, if the special reflector material, excluding beryllium, is chemically or mechanically bound to the fissile material or if the special reflector materials can be demonstrated to be in thicknesses and/or packing fractions that are less than the 25% polyethylene/ 75% water equivalent parameters given in [Table 6.2-1](#), then Case D limits apply even in the presence of greater than 1% by weight quantities of the special reflector.

6.2.5 Applicability of Case E Limit

The Case E limit is specifically applicable provided the contents are manually compacted and shipped in the standard, S100, S200, or S300 pipe overpacks with less than or equal to 1% by weight quantities of special reflector materials. Following the logic presented in [Section 6.2.1, *Applicability of Case A Limit*](#), the presence of greater than 1% by weight quantities of special reflectors may be authorized for shipment under the Case E FGE limits if the fissile material is chemically and/or mechanically bound to the special reflector material. Due to the fact that beryllium was also specifically evaluated as a moderator in the pipe overpacks, this applies to all special reflector materials except heavy water, which is restricted based on the free liquid requirements for the package. The contents model assumptions and analysis results are provided in [Appendices 4.1, 4.2, 4.3, and 4.4](#) in the *CH-TRU Payload Appendices*.

6.2.6 Applicability of Case F Limit

The Case F limit is specifically applicable provided the contents are manually compacted and shipped in the standard, S100, S200, or S300 pipe overpacks with greater than 1% by weight quantities of special reflector materials. However, if the special reflector materials can be demonstrated to be in thicknesses and/or packing fractions that are less than the 25% polyethylene/ 75% water equivalent parameters given in [Table 6.2-1](#), then Case E limits can be used. The contents model assumptions and analysis results are provided in [Appendices 4.1, 4.2, 4.3, and 4.4](#) in the *CH-TRU Payload Appendices*.

6.2.7 Applicability of Case G Limit

The Case G limit is specifically applicable provided the contents are manually compacted and shipped in the shielded container with less than or equal to 1% by weight quantities of special reflector materials. However, if the quantity of special reflector material in the payload is greater than 1% by weight but the form of the payload is such that the thickness and/or packing fraction of the special reflector material is less than the reference poly/water reflector or the special reflector material (excluding beryllium) is mechanically or chemically bound to the fissile material, then the Case G limit is applicable to waste meeting these form requirements. The contents model assumptions and analysis results are provided in [Appendix 4.5](#) of the *CH-TRU Payload Appendices*.

6.2.8 Applicability of Case H Limit

The Case H limit is specifically applicable provided the contents are machine compacted and shipped in the shielded container with less than or equal to 1% by weight quantities of special reflector materials. However, if the quantity of special reflector material in the payload is greater than 1% by weight but the form of the payload is such that the thickness and/or packing fraction of the special reflector material is less than the reference poly/water reflector or the

special reflector material (excluding beryllium) is mechanically or chemically bound to the fissile material, then the Case H limit is applicable to waste meeting these form requirements. The contents model assumptions and analysis results are provided in [Appendix 4.5](#) of the *CH-TRU Payload Appendices*.

Table 6.2-1 – Special Reflector Material Parameters that Achieve the Reactivity of a 25%/75% Polyethylene/Water Mixture Reflector

Special Reflector Material	Equivalent Thickness at 100% of Theoretical Density (inch)	Equivalent Thickness at 70% of Theoretical Density (inch)	Equivalent Packing Fraction at 24 in. Thickness (%)
Be	N/A	N/A	7
BeO	N/A	N/A	7
C	0.18	0.25	9
D ₂ O	0.24	0.27	14
MgO	0.26	0.33	15
U(Natural)	0.08	0.10	1
U(0.6% ²³⁵ U)	0.14	0.18	1
U(0.5% ²³⁵ U)	0.18	0.28	2
U(0.4% ²³⁵ U)	0.33	0.51	3
U(0.3% ²³⁵ U)	0.56	0.73	5

6.3 Model Specification

Criticality calculations for the HalfPACT package are performed using the three-dimensional Monte Carlo computer code KENO-V.a¹, executed as part of the SCALE-PC v4.4a system² using the CSAS25 driver utility³. Descriptions of the calculational models are given in [Section 6.3.1, Contents Model](#), [Section 6.3.2, Packaging Model](#), [Section 6.3.3, Single-Unit Models](#), [Section 6.3.4, Array Models](#) for all cases except Cases E and F, which are discussed in [Appendices 4.1, 4.2, 4.3, and 4.4 in the CH-TRU Payload Appendices](#)⁴. A summary of materials and atom densities that are used in the evaluation of the HalfPACT package is given in [Section 6.3.5, Package Regional Densities](#).

The limiting mass of fissile material that may be transported in a single HalfPACT package is shown to provide adequate subcritical margin based on detailed KENO-V.a analyses. These calculations are performed for an optimally moderated single-unit model and an infinite array model of HalfPACT packages under both normal conditions of transport (NCT) and hypothetical accident conditions (HAC).

In all cases, the computational model consists of a contents model and a packaging model. The contents model conservatively represents the package contents, including all payload material, dunnage, fissile and moderating material. The packaging model represents the remaining structural materials comprising the HalfPACT packaging. The amount of moderating and reflecting material assumed to be present in the packaging model is varied to maximize reactivity.

6.3.1 Contents Model

6.3.1.1 Case A Contents Model

The Case A contents are represented as an optimally moderated homogeneous sphere of Pu-239 and a 25% polyethylene and 75% water mixture (by volume). The radius of the model sphere is determined based on the modeled mass of plutonium and a specified H/Pu ratio. In each case, the H/Pu ratio is varied until the most reactive configuration is identified. FGE limits with 0 g, 5 g, 15 g, and 25 g Pu-240 present are calculated. When Pu-240 is present, the H/Pu ratio specified represents the H/Pu-239 atom ratio.

The remainder of the inner containment vessel (ICV) around the fissile sphere is filled with a 25% polyethylene, 74% water and 1% beryllium mixture (by volume). (Henceforward, unless otherwise specified, any reference to a polyethylene/water/beryllium mixture implies this particular

¹ L. M. Petrie and N. F. Landers, *KENO-V.a: An Improved Monte Carlo Criticality Program with Supergrouping*, ORNL/NUREG/CSD-2/V2/R6, Volume 2, Section F11, March 2000.

² Oak Ridge National Laboratory (ORNL), *SCALE 4.4a: Modular Code System for Performing Standardized Computer Analyses for Licensing Evaluation for Workstations and Personal Computers*, ORNL/NUREG/CSD-2/R6, March 2000.

³ N. F. Landers and L. M. Petrie, *CSAS: Control Module for Enhanced Criticality Safety Analysis Sequences*, ORNL/NUREG/CSD-2/V1/R6, Volume 1, Section C4, March 2000.

⁴ U.S. Department of Energy (DOE), *CH-TRU Payload Appendices*, current revision, U.S. Department of Energy, Carlsbad Field Office, Carlsbad, New Mexico.

25% polyethylene, 74% water and 1% beryllium reflector composition.) The beryllium is added to represent less than or equal to 1% by weight quantities of special reflectors that are allowed under the Case A loading limits. Based on the volume of the ICV and the maximum allowed weight of the payload containers in the package, modeling 1% beryllium by volume bounds the limit of 1% by weight. The reactivity effect of the addition of the 1% beryllium is shown to be very slight but positive. The KENO-V.a representation of the Case A single-unit contents model is illustrated in [Figure 6.3-1](#).

The fissile sphere is nominally positioned in the center of the packaging model. In the array analyses, the effect of displacing the contents model within the packaging model in directions likely to increase reactivity is investigated. These array models are further described in [Section 6.3.4, Array Models](#).

6.3.1.2 Case B Contents Model

The fissile sphere composition in the Case B model is identical to the Case A fissile sphere composition. Unlimited quantities of beryllium in the fissile sphere are also studied but shown to reduce reactivity with the beryllium reflector. The difference in the Case A and B model lies in the reflector material filling the ICV. In the Case B model, the ICV is filled with beryllium and the volume fraction is varied from 10% to 100% to determine the point of maximum reactivity. The KENO-V.a representation of the Case B single-unit contents model is illustrated in [Figure 6.3-2](#).

6.3.1.3 Case C Contents Model

The fissile sphere composition in the Case C model is moderated with 100% polyethylene and the reflector material filling the ICV is 99% polyethylene and 1% beryllium (by volume). The 1% beryllium in the ICV accounts for the reactivity increase provided by less than or equal to 1% by weight quantities of special reflector materials allowed in the package. The KENO-V.a representation of the Case C single-unit contents model is illustrated in [Figure 6.3-3](#).

6.3.1.4 Case D Contents Model

The Case D model is an extension of Case C applied to compacted “puck” drums overpacked in 55-, 85-, or 100-gallon drums where either the packing fraction of the contents is limited to 70% through the use of process controls implemented during machine compaction or the separation between pucks in two axially adjacent overpack drums is maintained at greater than or equal to 0.50 inch through the use of a compacted puck drum spacer placed in the bottom of each overpack drum. The HalfPACT package can accommodate only a single tier of overpack drums whereas two tiers of overpack drums can be loaded into a TRUPACT-II package. Reconfiguration of the fissile material from within each compacted puck is bounded by the Case A analysis since the reconfiguration would reduce the polyethylene packing fraction to below 25% as the material with the ICV is homogenized. Because of the axial separation between the overpack drums in a single tier and the 200 FGE limit per overpack drum, the most reactive scenario occurs in the TRUPACT-II package instead of in the HalfPACT package.

The most reactive, credible scenario consists of 325 FGE in two overpack drums that are stacked on top of one another. The fissile material will be separated by the steel of the compacted puck and overpack drum (or steel of the compacted puck drum spacer) and the polyethylene slip-sheet

and reinforcing plate placed between the layers of overpack drums in the package. Thus, the contents model includes two cylinders of fissile material with 0.06 inch (0.1524 cm) thick steel representing a conservative lower bound of the thickness of the steel in the lid of the lower puck and overpack drum (or steel in the compacted puck drum spacer), 0.15 inch (0.3810 cm) thick polyethylene representing 50% of the thickness of the slip-sheet and reinforcing plate, and another 0.06 inch (0.1524 cm) thick layer of steel representing a conservative lower bound of the thickness of steel in the bottom of the upper puck and overpack drum (or steel in the compacted puck drum spacer). Where applicable due to the use of a compacted puck drum spacer, the contents model includes an additional 0.50 inch of separation between the pucks, modeled filled with polyethylene or water to determine which is most reactive.

A 325 FGE fissile cylinder is modeled with an optimum height to diameter ratio of 0.924 to maximize reactivity and then split in two to represent the material in each overpack drum. The bottom half of the cylinder contains 200 FGE to represent the FGE limit in an overpack payload container and the top half of the cylinder contains 125 FGE. Modeling of the polyethylene in the slip-sheet and reinforcing plate is more reactive than modeling a water gap. The moderator is modeled either as 70% polyethylene and 30% water by volume or as 100% polyethylene. The material filling the ICV is either 70% polyethylene, 29% water and 1% beryllium or 99% polyethylene and 1% beryllium. The 1% beryllium is included to account for less than or equal to 1% by weight quantities of special reflector materials. Filling the ICV with this material is conservative as the void space around the overpack drums is filled with the better reflecting polyethylene/water/beryllium or polyethylene/beryllium mixture. The results of calculations performed for Case A as discussed in [Section 6.4.3.1.1, Case A Single Unit Results](#), showed that including 1% beryllium in the ICV region but not in the moderator was the most reactive placement and thus this configuration was modeled in the Case D calculations.

Even though only the TRUPACT-II package would allow the stacked drum configuration modeled, the packaging model representing the HalfPACT configuration is used to increase interaction between packages as discussed in the following section. The KENO-V.a representation of the Case D single-unit contents model is illustrated in [Figure 6.3-4](#).

6.3.2 Packaging Model

The criticality analyses presented herein are identical to the analyses presented in [Chapter 6.0, Criticality Evaluation](#), of the *TRUPACT-II Shipping Package Safety Analysis Report*⁵. With the exception of removing 30 inches from the package's height, all other post-test aspects (i.e., the package's configuration following free drop, puncture, and fire testing) between the HalfPACT and TRUPACT-II packages are essentially identical, especially with regard to the amount of remaining polyurethane foam. Also, the ICV region of the HalfPACT is large enough to provide full reflection of the fissile contents by the material contained therein. Therefore, due to the closer axial packaging in the infinite arrays, the criticality analyses utilizing the HalfPACT package geometry are considered conservative.

The packaging model represents the package structural materials, including the stainless steel shells and polyurethane foam. The model consists of nested, right circular cylindrical shells of

⁵ U.S. Department of Energy (DOE), *TRUPACT-II Shipping Package Safety Analysis Report*, USNRC Certificate of Compliance 71-9218, U.S. Department of Energy, Carlsbad Area Office, Carlsbad, New Mexico.

Type 304 stainless steel (SS304). The right cylindrical geometry of the model conservatively neglects the torispherical shape of the inner and outer containment vessel ends. The model's inner shell represents the combined ICV and outer containment vessel (OCV) components of the actual package. The narrow gap between the ICV and OCV shells is neglected, and the two components are modeled as a single shell of thickness $\frac{1}{4} + \frac{3}{16} = \frac{7}{16}$ inches thick (1.1113 cm) on the side, and $\frac{1}{4} + \frac{1}{4} = \frac{1}{2}$ inches thick (1.2700 cm) on the top and bottom. The outside radius of the cylindrical shell representing the combined ICV and OCV components is $38 \frac{2}{32}$ inches (98.1869 cm), preserving the outer radius of OCV lid shell. The height of the cylinder, $44 \frac{15}{16}$ inches (114.1413 cm), preserves the distance between the upper and lower aluminum honeycomb spacer assemblies within the ICV.

The second, outermost, cylindrical shell is $\frac{1}{4}$ inches (0.6350 cm) thick, also of Type 304 stainless steel, and represents the outer containment assembly (OCA) outer shell. The $\frac{3}{8}$ inch thick portion of the OCA outer shell is conservatively ignored. Under NCT, the inside radius and inside height of the OCA outer shell are $46 \frac{15}{16}$ inches (119.2213 cm) and 70 inches (177.8000 cm), respectively and the outer radius and height are $47 \frac{3}{16}$ inches (119.8563 cm) and $70 \frac{1}{2}$ inches (179.0700 cm), respectively. Under HAC, the inner radius and height of the OCA outer shell are based on the observed maximum deformation of the OCA following certification testing. At the conclusion of testing, approximately 5 inches of foam remained in the certification test units, except for local areas damaged by puncture bar drops. Hence, the inside of the OCA outer shell is set a distance of 5 inches (12.7000 cm) from the outside of the combined ICV and OCV shell and the $\frac{1}{4}$ inches (0.6350 cm) thick OCA shell is modeled. Under both NCT and HAC, no credit is taken for parasitic neutron absorption properties of the polyurethane foam. Instead, the foam is replaced with the 25% polyethylene/ 74% water/1% beryllium mixture used in Case A as a bounding reflecting material at a volume fraction that maximizes reactivity. Consideration is made for the structural properties of the foam by assuming that the inner cylindrical shell is maintained in its central position subsequent to all HAC tests. The KENO-V.a representation of single-unit undamaged and damaged HalfPACT packages are illustrated in [Figure 6.3-5](#) and [Figure 6.3-6](#), respectively.

The following simplifying assumptions tend to decrease the amount of structural material represented in the calculational model and decrease the center-to-center separation between HalfPACT packages in the array analyses and are, therefore, conservative.

- The domed surfaces of the torispherical heads are represented as flat surfaces and are positioned such that the overall height of the HalfPACT packaging is reduced.
- Under HAC, the thickness of the polyurethane foam region is reduced to 5 inches (12.7000 cm) throughout the entire OCA. In all cases, polyurethane foam is ignored and replaced with a polyethylene/water/beryllium mixture that fills the space at a volume fraction that optimizes reactivity.

6.3.3 Single-Unit Models

Compliance with the requirements of 10 CFR §71.55⁶ is demonstrated by analyzing optimally moderated damaged and undamaged, single-unit HalfPACT packages. In the NCT single-unit model, the packaging and contents models described above are employed, and water is conservatively assumed to leak into the containment vessel to an extent that optimizes reactivity. In Case A, the ICV is filled with the same polyethylene/water/beryllium mixture employed in the contents model. In Case B, the ICV is filled with beryllium to represent the bounding special reflector material and in Case C, the ICV is filled with 99% polyethylene and 1% beryllium to represent machine compacted waste with no limitations on compaction. In Case D, the ICV is filled with either a mixture of 70% polyethylene, 29% water and 1% beryllium to represent machine compacted waste that is controlled to a 70% packing fraction or 99% polyethylene and 1% beryllium to represent machine compacted waste without packing fraction controls. In all cases, the area between the ICV/OCV shells and the OCA outer shell, simply termed the OCA, is filled with the 25% polyethylene/ 74% water/1% beryllium mixture employed in the ICV of Case A. This material is a bounding reflector for the low density foam normally present and the water that could leak into this area. These reflectors are assumed to occupy all void space within the packaging model at full theoretical density to maximize reflection of the fissile material and thus maximize reactivity. In addition, a 30 cm thick, close-fitting water reflector is placed around the outside of the packaging model to ensure full reflection is achieved.

The single-unit, HAC model is identical to the single-unit, NCT model, except the HAC packaging model assumes the model's outer shell is displaced to within 5 inches (12.7000 cm) of the model's inner shell.

6.3.4 Array Models

Calculations are performed for an infinite array of damaged HalfPACT packages in a close-packed, square-pitch configuration. Triangular-pitched array configurations are not considered because the square-pitch array analyses demonstrate that array interaction effects are of minor consequence. A specularly reflective boundary condition is applied to all six faces of the unit cell defining the array configuration in order to represent an infinite array of HalfPACT packages. Displacement of the contents models within the ICV/OCV shell is considered in a manner that maximizes interaction of the fissile material between packages. [Table 6.3-1](#) describes the configurations considered, with reference to KENO-generated plots that graphically illustrate each variation.

In the HAC array analysis, reflection of the fissile sphere by a 25% polyethylene/74% water/1% beryllium mixture filling the ICV is considered in Case A. Case B considers beryllium filling the ICV as the bounding special reflector material and Case C considers full density polyethylene in the ICV to represent machine compacted waste. Case D is specific to machine compacted waste compacted in puck drums and then placed in 55-, 85-, or 100-gallon overpack drums with either a 70% packing fraction or puck separation controls modeled with either 70% polyethylene/29% water/1% beryllium or 99% polyethylene/1% beryllium reflection filling the ICV, respectively. In all cases, water is considered between the packages in addition to a 25%

⁶ Title 10, Code of Federal Regulations, Part 71 (10 CFR 71), *Packaging and Transportation of Radioactive Material*, 01-01-07 Edition.

polyethylene/74% water/1% beryllium mixture in the OCA region. The volume fraction of all of these materials is varied to ensure the most reactive conditions are analyzed.

As a result of the explicit optimization of reactivity against interspersed moderator volume fraction, and because of the closer spacing between packages achieved in the accident geometry, the result of the HAC array calculations bound the NCT array cases.

6.3.5 Package Regional Densities

A summary of all material compositions used in the HalfPACT package contents models is given in [Table 6.3-2](#) for various H/Pu ratios. The parameters are computed based on SCALE Standard Composition Library⁷ values of a plutonium density of 19.84 g/cm³, a polyethylene density of 0.923 g/cm³ and a water density of 0.9982 g/cm³. The material used to represent the HalfPACT package is Type 304 stainless steel (SS304) with a density of 7.94 g/cm³ and carbon steel, with a density of 7.82 g/cm³, was used to represent the drum lid/bottom modeled in Case D. Number densities of the SS304 and carbon steel constituent nuclides are also based on the SCALE Standard Composition Library composition as presented in [Table 6.3-3](#). The number densities for the various polyethylene, water and beryllium reflector mixtures are given in [Table 6.3-4](#). The SCALE standard composition identifier “BEBOUND”, nuclide identifier 4309, was used to model the beryllium reflector. The theoretical density of this material is 1.85 g/cm³ and the number density is 1.23621E-01 a/b-cm. The cross-section for BEBOUND is based on a beryllium metal whereas the cross-section for standard material BE is based on a free gas representation. BEBOUND is also used to model beryllium in the benchmark cases discussed in [Section 6.5, Critical Benchmark Experiments](#).

Table 6.3-1 – Description of Contents Displacement in Array Models

Variation	Replicated Array Size	Description	Reference
0	1×1×1	Contents centered in packaging model	Figure 6.3-7
1	2×2×2	All contents models displaced toward center	Figure 6.3-8

⁷ L.M. Petrie, P.B. Fox and K. Lucius, *Standard Composition Library*, ORNL/NUREG/CSD-2/V3/R6, Volume 3, Section M8, March 2000.

Table 6.3-2 – Fissile Contents Model Properties for Various H/Pu Ratios

		Number Density			
		Pu (a/b-cm)	H (a/b-cm)	O (a/b-cm)	C (a/b-cm)
25% Polyethylene/75% Water Moderator used in Cases A and B					
500	55.32	1.39374E-04	6.96904E-02	2.49700E-02	9.88730E-03
600	46.12	1.16199E-04	6.97198E-02	2.49802E-02	9.89131E-03
700	39.55	9.96359E-05	6.97470E-02	2.49901E-02	9.89517E-03
800	34.61	8.71898E-05	6.97634E-02	2.49958E-02	9.89720E-03
900	30.77	7.75285E-05	6.97805E-02	2.50019E-02	9.89996E-03
1,000	27.70	6.97733E-05	6.97894E-02	2.50040E-02	9.90030E-03
1,100	25.19	6.34398E-05	6.97967E-02	2.50067E-02	9.90185E-03
1,200	23.09	5.81675E-05	6.98011E-02	2.50093E-02	9.90271E-03
1,300	21.31	5.36925E-05	6.98150E-02	2.50137E-02	9.90445E-03
1,400	19.79	4.98652E-05	6.98177E-02	2.50142E-02	9.90461E-03
1,500	18.48	4.65401E-05	6.98231E-02	2.50171E-02	9.90571E-03
100% Polyethylene Moderator used in Cases C and D					
500	62.76	1.58107E-04	7.90648E-02	---	3.95315E-02
600	52.33	1.31834E-04	7.91113E-02	---	3.95542E-02
700	44.87	1.13038E-04	7.91400E-02	---	3.95699E-02
800	39.27	9.89296E-05	7.91566E-02	---	3.95785E-02
900	34.92	8.79796E-05	7.91787E-02	---	3.95891E-02
1,000	31.43	7.91773E-05	7.91959E-02	---	3.95974E-02
1,100	28.58	7.20029E-05	7.92017E-02	---	3.95998E-02
1,200	26.20	6.60091E-05	7.92166E-02	---	3.96070E-02
1,300	24.19	6.09431E-05	7.92274E-02	---	3.96122E-02
70% Polyethylene/30% Water Moderator used in Case D					
500	59.79	1.50619E-04	7.53181E-02	9.98572E-03	2.76775E-02
600	49.85	1.25577E-04	7.53520E-02	9.99020E-03	2.76903E-02
700	42.75	1.07685E-04	7.53858E-02	9.99448E-03	2.77024E-02
800	37.41	9.42500E-05	7.54065E-02	9.99712E-03	2.77094E-02
900	33.26	8.37973E-05	7.54144E-02	9.99869E-03	2.77136E-02
1,000	29.94	7.54335E-05	7.54312E-02	1.00011E-02	2.77201E-02
1,100	27.22	6.85754E-05	7.54447E-02	1.00022E-02	2.77236E-02
1,200	24.96	6.28771E-05	7.54476E-02	1.00029E-02	2.77255E-02

Table 6.3-3 – Composition of Modeled Steels

Component	SCALE Nuclide ID	Number Density (a/b-cm)
Type 304 Stainless Steel for HalfPACT Package		
Cr	24304	1.74726E-02
Mn	25055	1.74071E-03
Fe	26304	5.85446E-02
Ni	28304	7.74020E-03
P	15031	6.94680E-05
Si	14000	1.70252E-03
C	6012	3.18772E-04
Carbon Steel used in Case D		
Fe	26000	8.34982E-02
C	6012	3.92503E-03

Table 6.3-4 – Composition of the Polyethylene/Water/Beryllium Reflector

Component	SCALE Nuclide ID	Number Density (a/b-cm)
25% Polyethylene/ 74% Water/ 1% Beryllium Reflector used in Case A		
C	6012	9.91472E-03
H	1001	6.92387E-02
O	8016	2.47046E-02
Be	4309	1.23621E-03
99% Polyethylene/ 1% Beryllium used in Cases C and D		
C	6012	3.92623E-02
H	1001	7.85246E-02
Be	4309	1.23621E-03
70% Polyethylene/ 29% Water/ 1% Beryllium used in Case D		
C	6012	2.77612E-02
H	1001	7.48855E-02
O	8016	9.68153E-03
Be	4309	1.23621E-03

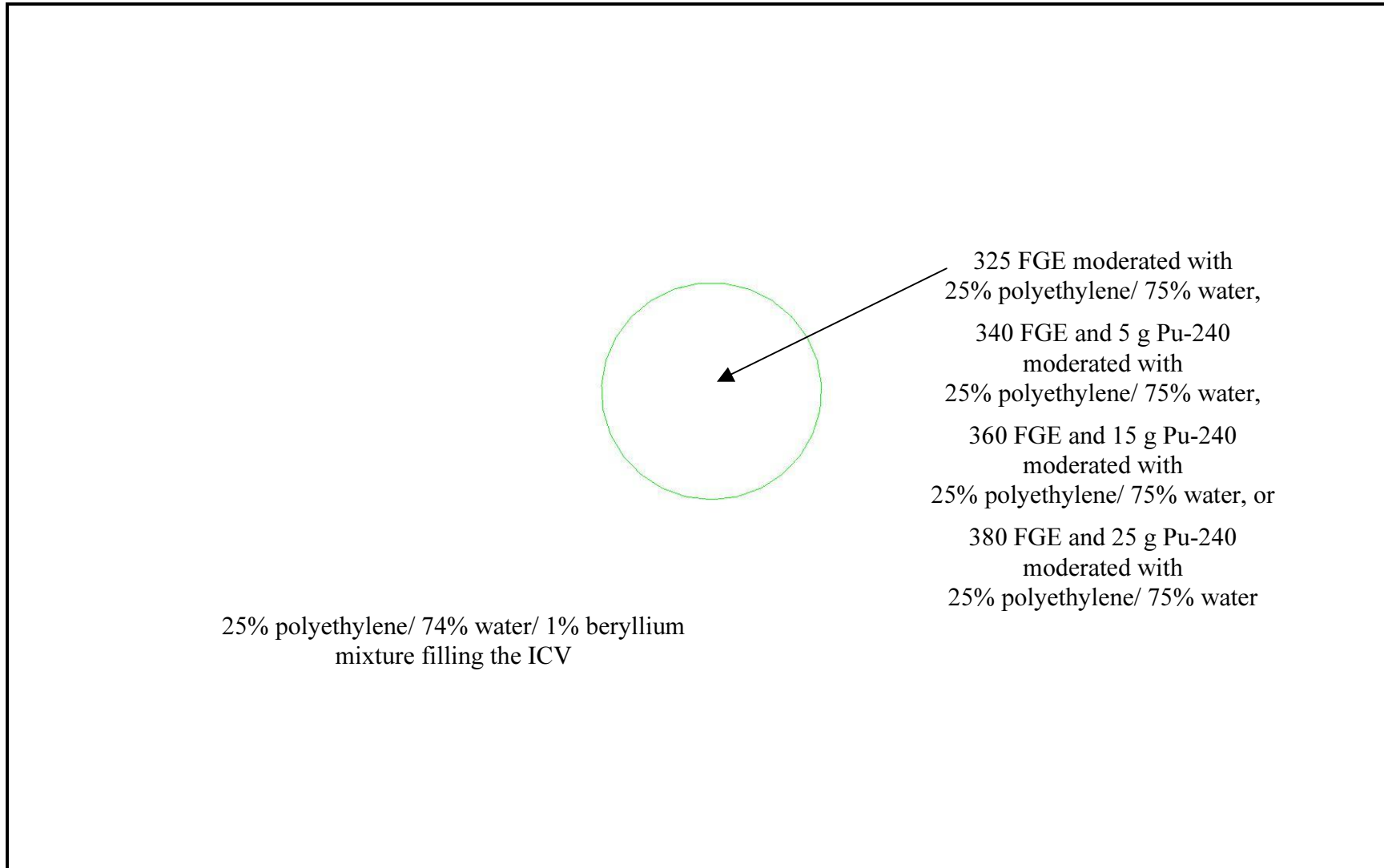


Figure 6.3-1 – Case A Contents Model

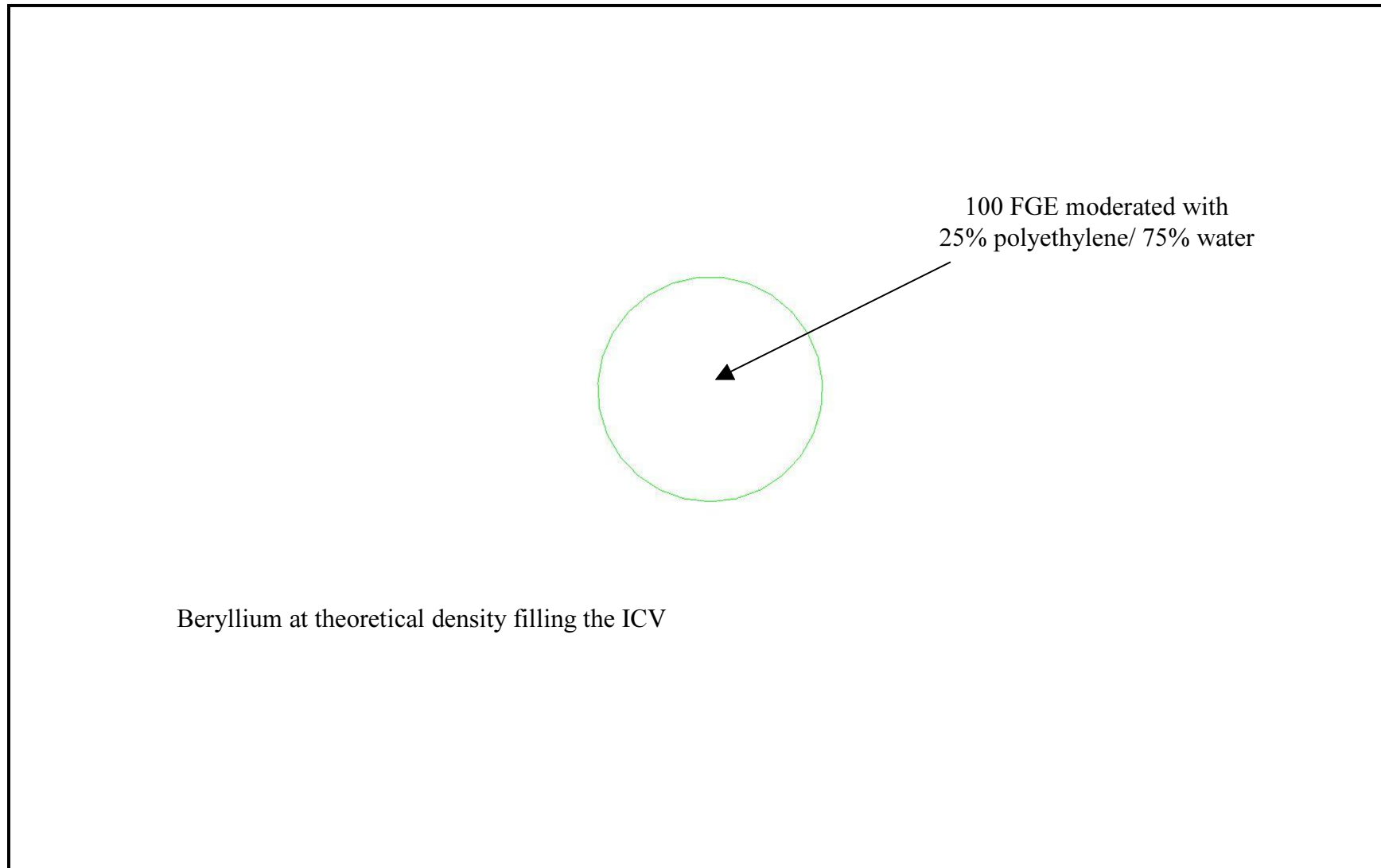


Figure 6.3-2 – Case B Contents Model

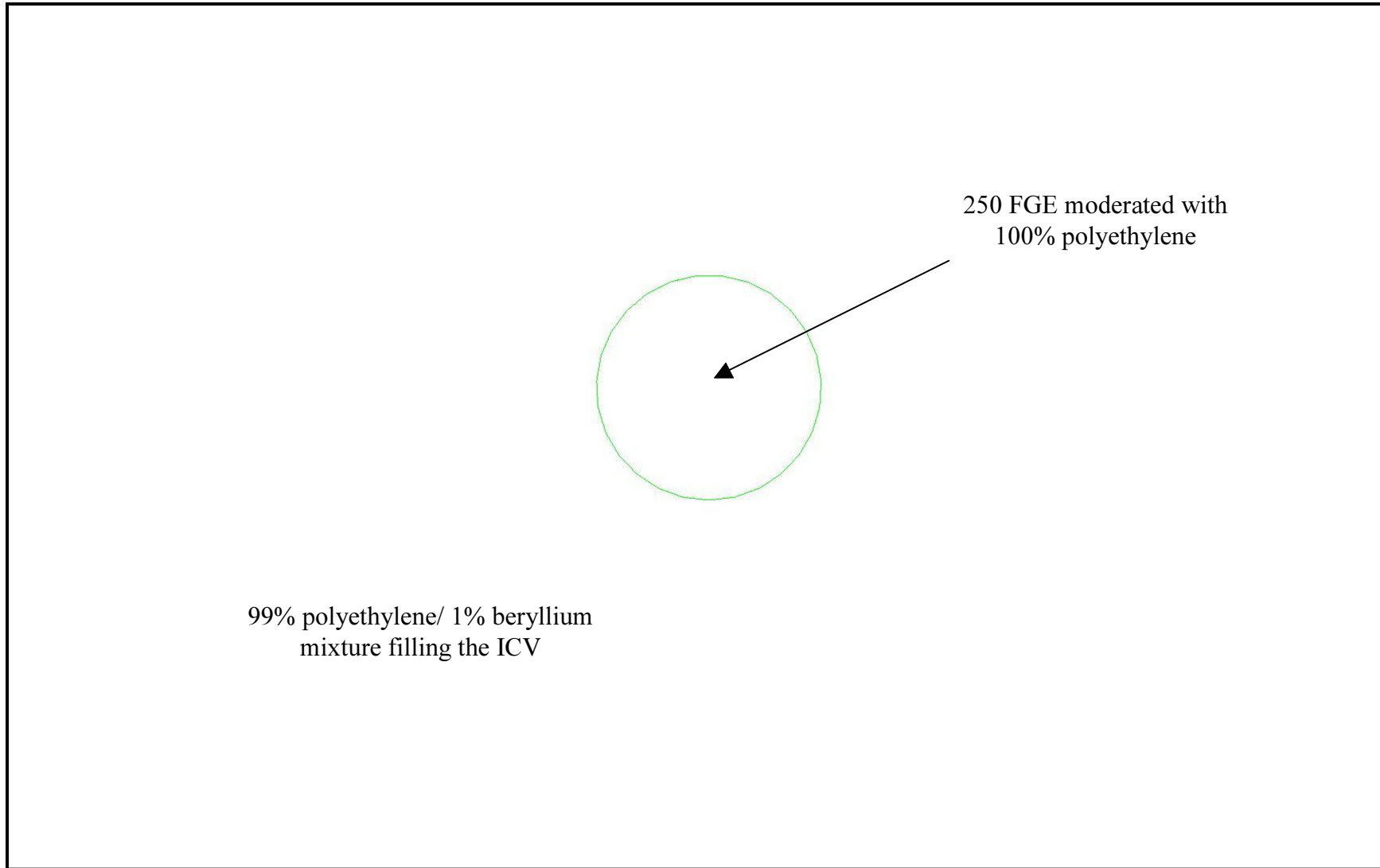


Figure 6.3-3 – Case C Contents Model

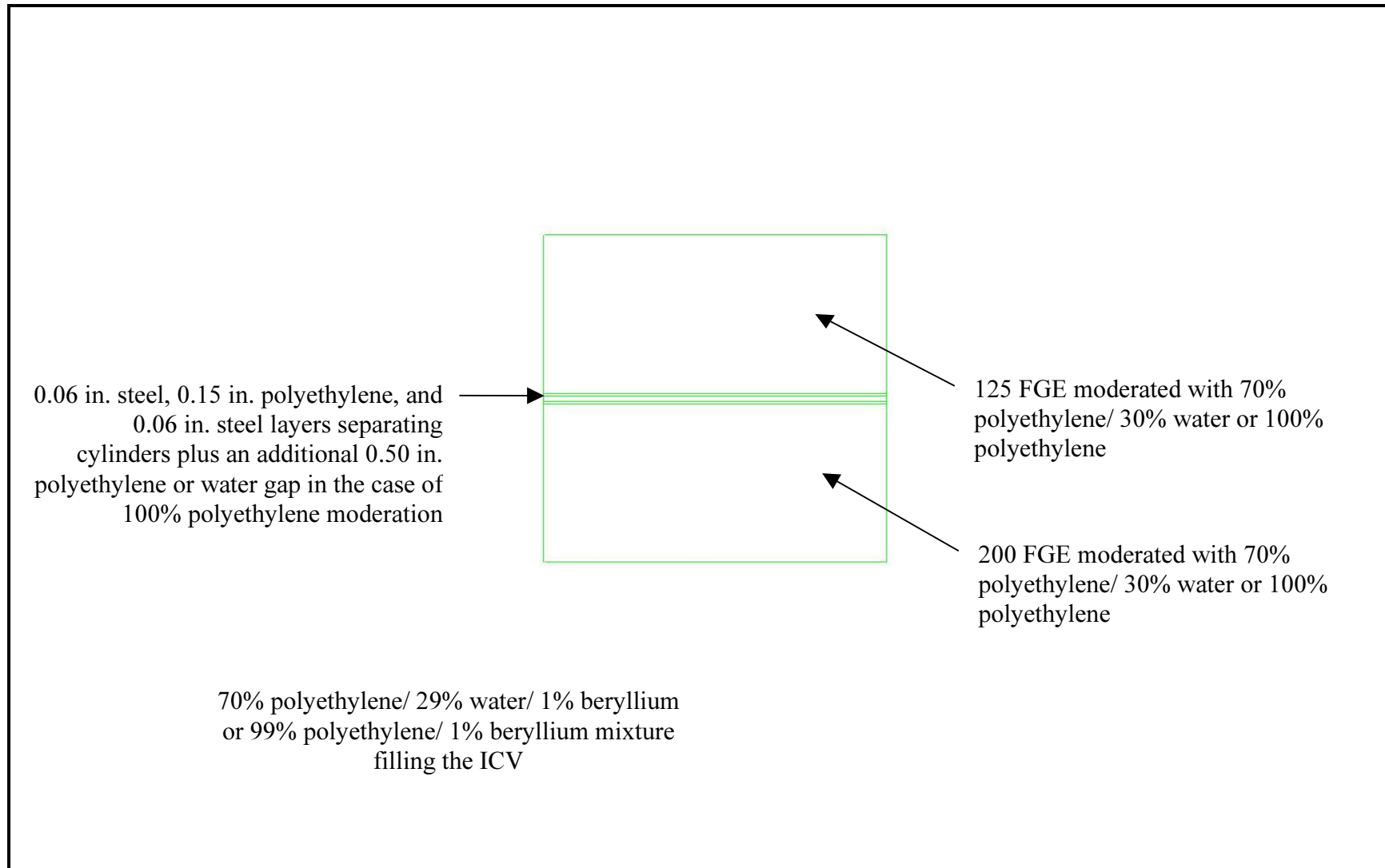


Figure 6.3-4 – Case D Contents Model

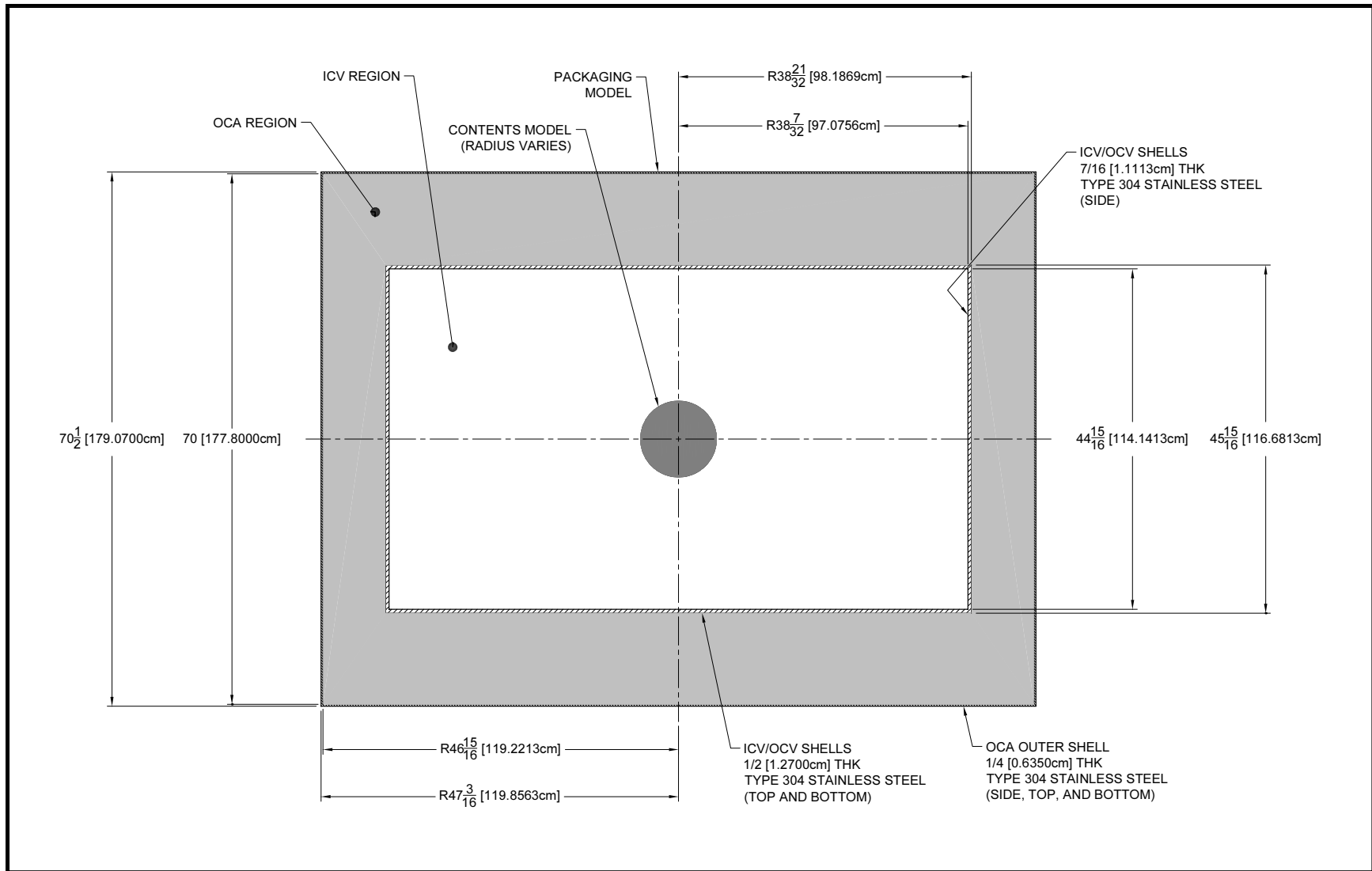


Figure 6.3-5 – NCT, Single-Unit Model; R-Z Slice

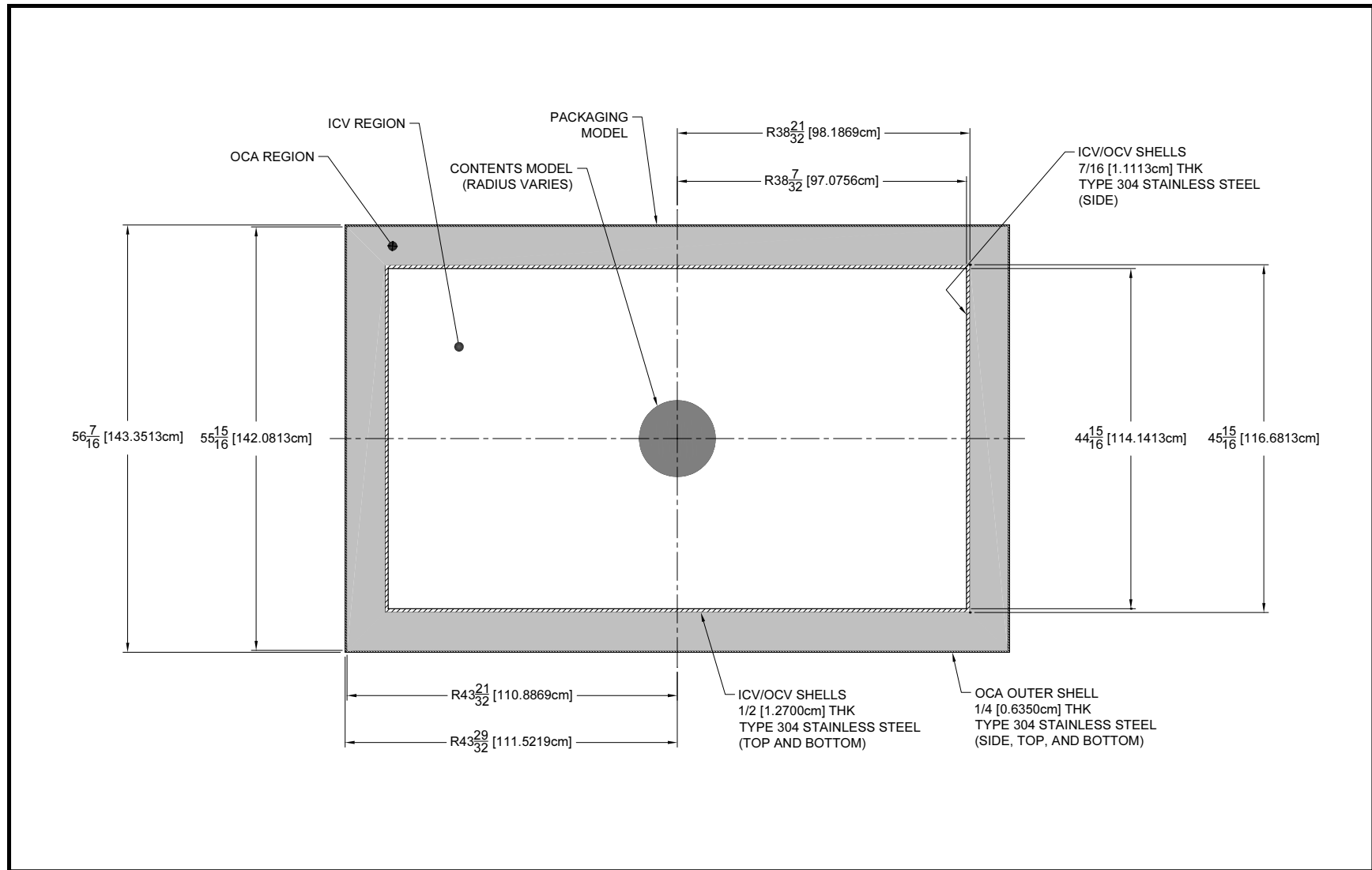


Figure 6.3-6 – HAC, Single-Unit Model; R-Z Slice

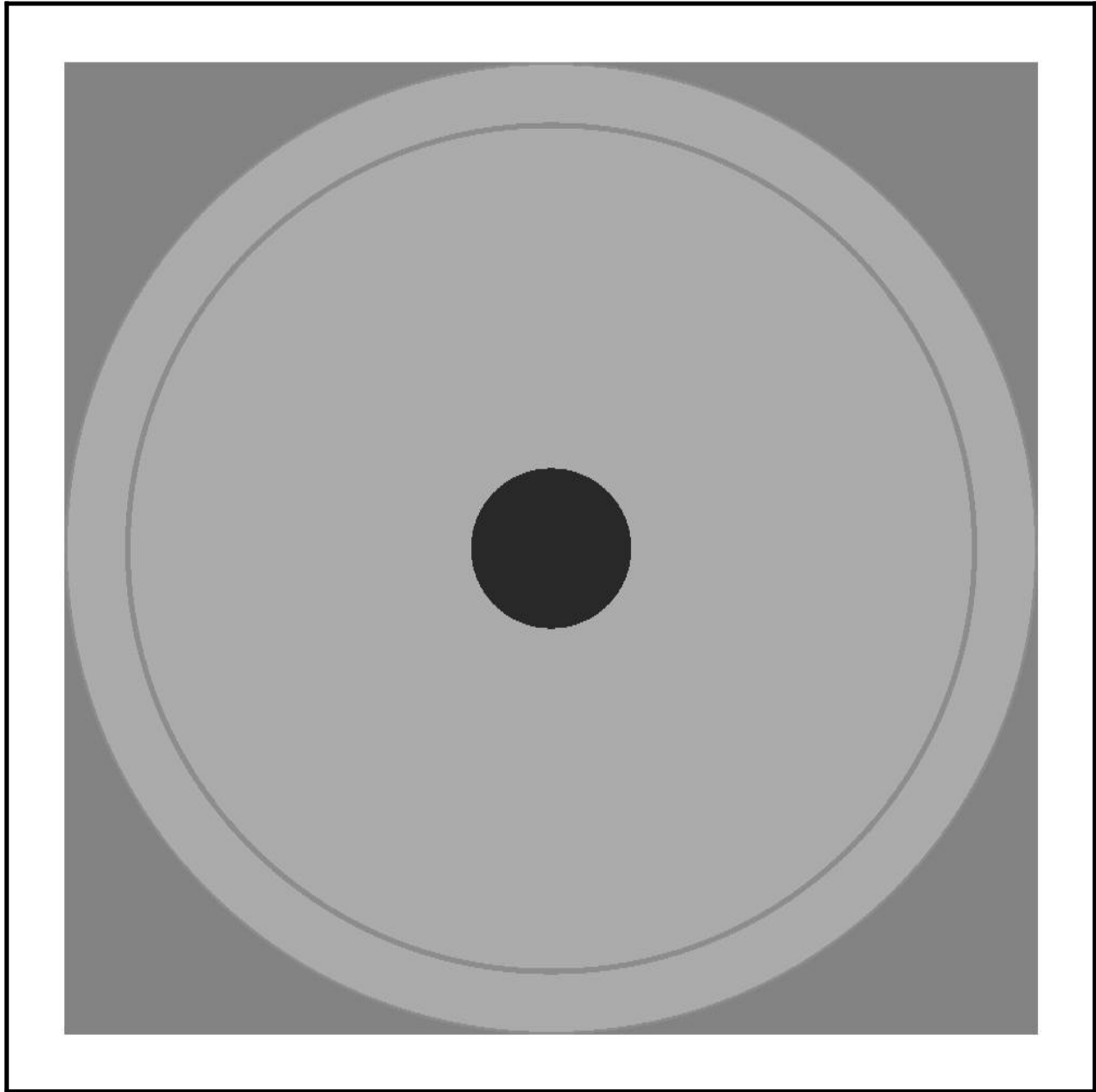


Figure 6.3-7 – Array Model Variation 0 (Reflective Boundary Conditions Imposed)

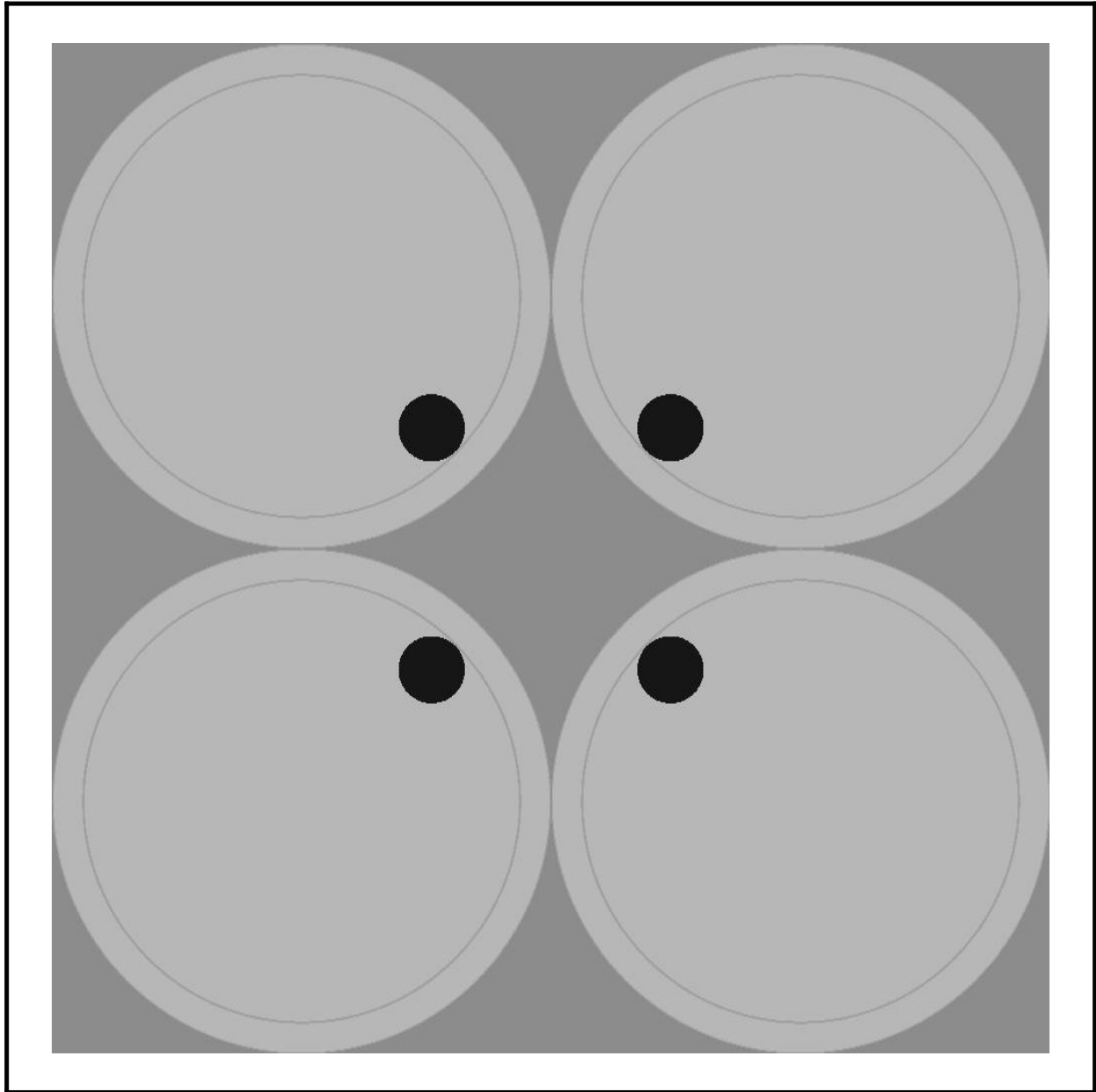


Figure 6.3-8 – Array Model Variation 1; X-Y Slice Through Top Axial Layer

6.4 Criticality Calculations

A description of the criticality calculations performed for the HalfPACT package is presented in this section. The calculational methodology is discussed in [Section 6.4.1, *Calculational or Experimental Method*](#). The optimization of the payload model is discussed in [Section 6.4.2, *Fuel Loading or Other Contents Loading Optimization*](#). The results of all calculations are presented in [Section 6.4.3, *Criticality Results*](#).

The intent of the analysis is to demonstrate that the HalfPACT package is safely subcritical under normal conditions of transport (NCT) and hypothetical accident conditions (HAC).

6.4.1 Calculational or Experimental Method

Calculations for the HalfPACT package are performed with the three-dimensional Monte Carlo transport theory code, KENO-V.a¹. The SCALE-PC v4.4a², CSAS25 utility³ is used as a driver for the KENO code. In this role, CSAS25 determines nuclide number densities, performs resonance processing, and automatically prepares the necessary input for the KENO code based on a simplified input description. The 238 energy-group (238GROUPNDF5), cross-section library based on ENDF/B-V cross-section data⁴ is used as the nuclear data library for the KENO-V.a code.

The KENO code has been used extensively in the criticality safety industry. KENO-V.a is an extension of earlier versions of the KENO code and includes many versatile geometry capabilities and screen plots to facilitate geometry verification. The KENO-V.a code and the associated 238GROUPNDF5 cross-section data set are validated for proper operation on the PC platform by performing criticality analyses of a number of relevant benchmark criticality experiments. A description of these benchmark calculations, along with justification for the computed bias in the code and library for the relevant region of applicability, is provided in [Section 6.5, *Critical Benchmark Experiments*](#).

6.4.2 Fuel Loading or Other Contents Loading Optimization

The allowable fuel loading for a single HalfPACT package is based on the FGE package fissile loading limit established in the [CH-TRAMPAC](#)⁵. The analysis demonstrates that the HalfPACT package is safely subcritical under NCT and HAC. Calculations are based on the following conservative assumptions:

¹ L. M. Petrie and N. F. Landers, *KENO-V.a: An Improved Monte Carlo Criticality Program with Supergrouping*, ORNL/NUREG/CSD-2/V2/R6, Volume 2, Section F11, March 2000.

² Oak Ridge National Laboratory (ORNL), *SCALE 4.4a: Modular Code System for Performing Standardized Computer Analyses for Licensing Evaluation for Workstations and Personal Computers*, ORNL/NUREG/CSD-2/R6, March 2000.

³ N. F. Landers and L. M. Petrie, *CSAS: Control Module For Enhanced Criticality Safety Analysis Sequences*, ORNL/NUREG/CSD-2/V1/R6, Volume 1, Section C4, March 2000.

⁴ W. C. Jordan and S. M. Bowman, *Scale Cross-Section Libraries*, ORNL/NUREG/CSD-2/V3/R6, Volume 3, Section M4, March 2000.

⁵ U.S. Department of Energy (DOE), *Contact-Handled Transuranic Waste Authorized Methods for Payload Control (CH-TRAMPAC)*, U.S. Department of Energy, Carlsbad Field Office, Carlsbad, New Mexico.

1. Pu-239 is present at the fissile gram equivalent (FGE) limit. FGE limits with 0 g, 5 g, 15 g, and 25 g Pu-240 are calculated for Case A. FGE limits ignoring Pu-240 are calculated for Cases B, C and D.
2. All Pu is assumed to be optimally moderated and reflected with the optimal degree of moderation determined in each case for the applicable moderator. Studies indicate that the presence of voids in the optimal spherical contents model significantly reduces k_{eff} . The presence of less than or equal to 1% by weight beryllium in the moderator was also shown to have a small effect on k_{eff} , and at larger quantities, k_{eff} is reduced.
3. The reflector material is tight fitting around the fissile geometry and assumed to fill the inner containment vessel (ICV) at up to 100% of theoretical density. Especially in Case B with a beryllium reflector, results in [Section 6.4.3, Criticality Results](#) show that the presence of voids in the reflector reduces k_{eff} .

The two additional conservative assumptions below are applicable to Cases A, B and C but not to Case D. As discussed in [Section 6.3.1.4, Case D Contents Model](#), Case D is applicable to a very specific scenario and thus details of the specific configuration are credited.

4. The fissile material is represented in a spherical geometry. Calculations performed for other geometries, such as cylinders and cubes, indicate a reduction in k_{eff} for these other geometries
5. All structural material comprising the payload drums and material within the payload drums, other than Pu-239 and hydrogenous material (represented as a polyethylene/water/beryllium mixture), are conservatively neglected.

The same conservative assumptions that are used to analyze the single-unit HalfPACT package are used for the infinite array calculations. However, the presence of reflector in the ICV and outer containment assembly (OCA) region and water around the package tends to isolate the replicated fissile regions from each other. In order to identify the limiting case, the volume fraction of the materials in these regions are varied in order to maximize reactivity of the configuration. Additional conservative assumptions used to model the HalfPACT package are delineated in [Section 6.2, Package Contents](#).

6.4.3 Criticality Results

The results of the calculations for the HalfPACT package criticality evaluation are divided into two sections. Results for a single HalfPACT package are presented in [Section 6.4.3.1, Criticality Results for a Single HalfPACT Package](#), and results for arrays of HalfPACT packages are presented in [Section 6.4.3.2, Criticality Results for Infinite Arrays of HalfPACT Packages](#). Reported multiplication factors represent the computed k_{eff} values plus twice the standard deviation in the result calculated for each case, as follows:

$$k_s = k_{\text{eff}} + 2\sigma$$

This quantity is then compared with the upper subcriticality limit (USL) in order to demonstrate an adequate margin of subcriticality. Generally, the Monte Carlo calculations reported here are performed with sufficient histories to bring the computed relative standard deviation in the result to

approximately 0.1%. Typical KENO parameters required to obtain this level of uncertainty are 1000 generations of 1000 histories per generation, with the initial 50 generations skipped.

6.4.3.1 Criticality Results for a Single HalfPACT Package

With the model described in [Section 6.3.3, *Single-Unit Models*](#), subcriticality of the HalfPACT package under both NCT and HAC is demonstrated for each case.

6.4.3.1.1 Case A Single Unit Results

The results of studies that identify optimal model parameters for NCT calculations are summarized in [Table 6.4-1](#) and [Table 6.4-2](#). Although tabulated values of both k_s and the reported Monte-Carlo standard deviation, σ , are provided, recall that k_s includes the 2σ uncertainty in the result. Calculations were performed for the single-unit HalfPACT package model to demonstrate the reactivity effect of adding less than or equal to 1% by weight quantities of beryllium to the package under NCT and HAC. First, the reactivity of a 325 FGE sphere of ^{239}Pu , polyethylene and water with a polyethylene/water mixture filling the ICV and OCA (25% by volume polyethylene and 75% by volume water in both the moderator and reflector) was calculated. Optimal moderation of the contents model is determined by parametrically varying the H/Pu ratio in the fissile sphere. Then, two different compositions for the fissile moderator were considered, namely one in which the moderator consisted only of ^{239}Pu , polyethylene and water and the other in which the moderator contained less than or equal to 1% by weight quantities of beryllium resulting in a conservative mixture of ^{239}Pu and 25% polyethylene, 74% water and 1% by volume beryllium. In both cases, the ICV and OCA regions were filled with a 25% polyethylene, 74% water and 1% by volume beryllium. The results of these calculations are shown in [Table 6.4-1](#). The difference in reactivity for the cases with beryllium in the moderator and those without is statistically insignificant. However, the maximum reactivity occurs when beryllium is not included in the moderator but is included in the reflector. Thus, a polyethylene/water moderator and polyethylene/water/beryllium reflector were modeled in the remainder of the calculations.

[Table 6.4-2](#) shows that the reactivity of the NCT single-unit model decreases as the volume fraction of the reflector material is decreased. As expected for a single unit, the full density reflector case is limiting, with a k_s value of 0.9339.

Thus, optimal reactivity parameters for the single-unit, NCT model with a 25% polyethylene and 75% water moderator are H/Pu(900) at maximum reflection conditions with a 25% polyethylene, 74% water, and 1% beryllium reflector composition.

For HAC conditions, variation of k_s with H/Pu ratio at maximum reflection conditions is shown in [Table 6.4-3](#). The maximum k_s value (0.9331) for the single-unit, HAC occurs at H/Pu(1000). Note that the maximum reactivity of the NCT single unit model (0.9339) is statistically the same as the maximum reactivity for the HAC single unit model. This is expected because of the similarity of the models and the fact that maximum reflection increases the reactivity of a single unit. Although the OCA region is thinner under HAC vs. NCT, the single-unit package model contains a 30 cm external water reflector to ensure that the package is infinitely reflected under both HAC and NCT.

6.4.3.1.2 Case B Single Unit Results

Section 6.4.3.2.1, *Case A Infinite Array Results*, found that the maximum reactivity of a single-unit HalfPACT package under NCT or HAC conditions is statistically equivalent to that of an infinite array of HAC packages under maximum reflection conditions. Thus the analysis given in Section 6.4.3.2.2, *Case B Infinite Array Results* is bounding for the Case B single unit.

6.4.3.1.3 Case C Single Unit Results

Section 6.4.3.2.1, *Case A Infinite Array Results*, found that the maximum reactivity of a single-unit HalfPACT package under NCT or HAC conditions is statistically equivalent to that of an infinite array of HAC packages under maximum reflection conditions. Thus the analysis given in Section 6.4.3.2.3, *Case C Infinite Array Results* is bounding for the Case C single unit.

6.4.3.1.4 Case D Single Unit Results

Section 6.4.3.2.1, *Case A Infinite Array Results*, found that the maximum reactivity of a single-unit HalfPACT package under NCT or HAC conditions is statistically equivalent to that of an infinite array of HAC packages under maximum reflection conditions. Thus the analysis given in Section 6.4.3.2.4, *Case D Infinite Array Results* is bounding for the Case D single unit.

6.4.3.1.5 Conclusions from Single Unit Calculations

Based on optimum moderation of the fissile contents and the maximum reflection conditions modeled by filling the ICV and OCA regions with full density materials appropriate for each case and surrounding the package by an additional 30 cm of water, all single unit results are less than the USL. Thus, a single HalfPACT package will remain subcritical under both NCT and HAC conditions.

6.4.3.2 Criticality Results for Infinite Arrays of HalfPACT Packages

The infinite array model studies the interaction between the fissile contents in adjacent HalfPACT packages. The models described in Section 6.3, *Model Specification* provide the basis for the KENO-V.a calculations. The only difference in the NCT and HAC models is that the thickness of the OCA area is reduced to 5 inches (12.7000 cm) in the HAC model. Thus, the interaction between HAC packages will be greater compared to NCT packages as the spacing between fissile regions is smaller. Also, the results shown below indicate that the reactivity effects of array interaction are less than those of close, full reflection of the package contents. Thus, the infinite array calculations based on the HAC model performed in the following subsections demonstrate that an infinite array of HalfPACT packages is safely subcritical under both NCT and HAC conditions.

In addition, the infinite array calculations assume the presence of interspersed water between the damaged packages. The volume fraction of water in the array interstitial space, abbreviated Int in the tables, is varied to determine the most reactive condition.

6.4.3.2.1 Case A Infinite Array Results

As in the single unit calculations for Case A, additional moderation of the spheres of fissile contents is assumed by in-leakage of water into the ICV. The maximum polyethylene density in the cavity is 25% and 1% by volume beryllium is present. The fissile material is assumed to mix homogeneously

with a 25% polyethylene/75% water moderator (by volume). The ICV and OCA areas are filled with a 25% polyethylene/74% water/1% beryllium composition (by volume) reflector. The moderator does not contain 1% by volume beryllium based on the slight reduction in k_s obtained from the single-unit model when beryllium was added to the moderator as discussed in [Section 6.4.3.1.1, Case A Single Unit Results](#). The optimum H/Pu ratio for the HAC infinite array model is determined to be 1000 from the results in [Table 6.4-4](#).

Results for an infinite number of HalfPACT packages arranged in a close-packed, square-pitched array with contents models centered in each package (model variation 0) and various reflector volume fractions are shown in [Table 6.4-5](#). These results indicate that the reactivity effect of tight reflection of the fissile contents by the full density 25% polyethylene/74% water/1% beryllium mixture is greater than that of array interaction. With the reflector removed and the ICV, OCA and exterior regions of the package voided, the array interaction effect is maximized. However, in this case the computed reactivity is less than that at full moderator density in which the packages are effectively isolated from one another.

These results also indicate that the HAC infinite array maximum reactivity (0.9331) achieved with maximum reflection is statistically equivalent to the HAC single-unit maximum reactivity (0.9331) and the NCT single-unit maximum reactivity (0.9339). Thus, the HAC infinite array model with maximum reflection is equivalent to the single-unit model and is used in the remainder of the calculations.

The reactivity results for the fissile contents displacement Variation 1 described in [Section 6.3.4, Array Models](#), are shown in [Table 6.4-6](#) as a function of H/Pu for the case with only the ICV filled with the polyethylene/water/beryllium reflector mixture and the case with the entire interior and exterior of the package voided. The case with maximum array interaction resulted in a lower k_s compared to the case with the ICV region filled with the polyethylene/water/beryllium mixture. Both model Variation 1 cases, however, were less reactive than the Variation 0 model with the spheres centered in the package surrounded by the full density reflector mixture.

The addition of Pu-240 to the fissile sphere was also studied and FGE limits calculated based on the Pu-240 gram content in the package. As shown in [Table 6.4-7](#), a package containing 5 g Pu-240 is subcritical at a FGE limit of 340, a package containing 15 g Pu-240 is subcritical at a FGE limit of 360 and a package containing 25 g Pu-240 is subcritical at a FGE limit of 380. The fissile sphere was modeled centered in the package with the polyethylene/water/beryllium mixture filling the ICV and OCA regions and water in the interstitial region between packages as these parameters were found to result in the most reactive configuration for the cases without Pu-240. These limits are based on the grams of Pu-240 present, not wt% Pu-240 in order to allow the limits to apply to packages containing both U and Pu fissile isotopes. Calculations were performed based on the 340 FGE limit with 5 g Pu-240 with varying mixtures of U-235 and Pu-239 to verify applicability of this limit to mixed fissile systems. The conversion factor of 0.643 g U-235 per FGE given in the [CH-TRAMPAC](#)⁶ was used. The results shown in [Table 6.4-8](#) verify that mixed fissile systems will remain subcritical under this limit. In fact, the most reactive scenario occurs with 100% Pu-239. The case with 100% U-235 and 5 g Pu-240 is obviously unrealistic but shown for comparison purposes.

⁶ U.S. Department of Energy (DOE), *Contact-Handled Transuranic Waste Authorized Methods for Payload Control (CH-TRAMPAC)*, U.S. Department of Energy, Carlsbad Field Office, Carlsbad, New Mexico.

All infinite array results are less than the USL. Thus, an infinite array of HalfPACT packages containing 325 FGE per package (with 0 g Pu-240), 340 FGE per package (with ≥ 5 g Pu-240), 360 FGE per package (with ≥ 15 g Pu-240), and 380 FGE per package (with ≥ 25 g Pu-240) under the limitations imposed for Case A is subcritical.

6.4.3.2.2 Case B Infinite Array Results

The results for the Case B beryllium reflected cases are consistent with the results for Case A in that the maximum reactivity occurs at maximum reflection conditions. The maximum reactivity (0.9184) occurs at an H/Pu ratio of 800 for the 100 FGE beryllium reflected, polyethylene/water moderated scenario as shown in Table 6.4-9. The addition of beryllium to the fissile sphere was also studied as beryllium was found to increase reactivity when added to a polyethylene/water moderator in a water reflected system per SAIC-1322-001⁷. Volume fractions in the fissile sphere from 1 to 60% beryllium were modeled and the results shown in Table 6.4-10 indicate that k_s is reduced as more beryllium is added to this beryllium reflected system. The results in Table 6.4-11 indicate that the reactivity is reduced as the volume fraction of the reflectors in the ICV, OCA and interstitial regions are reduced. As expected from the Case A results, array Variation 1 with the fissile spheres moved off-center in the ICV to minimize distance between spheres in adjacent packages is significantly less reactive than the Variation 0 base model. These results are shown in Table 6.4-12. Overall, these calculations indicate that an infinite array of HalfPACT packages is subcritical with 100 FGE and an unlimited mass of special reflectors.

6.4.3.2.3 Case C Infinite Array Results

The Case C results support the 250 FGE package limit for mechanically compacted waste that does not meet the Case D specifications. As shown in Table 6.4-13, the reactivity is increased when 1% beryllium is added to the polyethylene reflector in the ICV and the maximum reactivity (0.9345) occurs at an H/Pu ratio of 900. The results in Table 6.4-14 indicate that the reactivity is lower as the volume fraction of the reflector materials in the ICV, OCA and interstitial regions are reduced. Again, moving the fissile spheres off-center in the ICV reduces reactivity based on the results tabulated in Table 6.4-15. Thus, again the maximum reactivity occurs at maximum reflection conditions with the fissile spheres centered in the packages and remains below the USL. Thus, an infinite array of HalfPACT packages containing machine compacted waste is subcritical at 250 FGE per package.

6.4.3.2.4 Case D Infinite Array Results

The results of the Case D calculations show that at a maximum packing fraction of 70%, machine compacted pucks are subcritical when each overpack drum is limited to 200 FGE and the package is limited to 325 FGE or if the packing fraction is not limited, when a minimum gap of 0.50 inches exists between the puck drums. The results shown in Table 6.4-16 indicate that the highest reactivity for the modeled configuration at 70% packing fraction (0.9325) occurs at an H/Pu ratio of 800 and the highest reactivity at 100% packing fraction (0.9349) also occurs at

⁷ Neeley, G. W., D. L. Newell, S. L. Larson, and R. J. Green, *Reactivity Effects of Moderator and Reflector Materials on a Finite Plutonium System*, SAIC-1322-001, Revision 1, Science Applications International Corporation, Oak Ridge, Tennessee, May 2004.

an H/Pu ratio of 800. At 100% packing fraction, the required separation distance between the puck drums, in addition to the ½ thickness of the the drum steel and the ½ thickness of the slip sheet/ reinforcing plate thicknesses modeled, is 0.50 inches. The reactivity resulting from filling the gap with polyethylene versus water is statistically equivalent. As in the other cases, the results in [Table 6.4-17](#) show that reducing the volume fraction of reflector material in the ICV, OCA and interstitial regions reduces reactivity as does placing the fissile material off-center in the package (i.e., infinite array variation 1) as shown in [Table 6.4-18](#). The cases in these tables were only calculated at the 70% packing fraction, but the results are obviously also applicable to the 100% packing fraction case. Thus, an infinite array of HalfPACT packages containing machine compacted waste under the specific restrictions applied to Case D is subcritical at 325 FGE per package.

6.4.3.2.5 Conclusions from Infinite Array Calculations

The calculations reported in this section are performed with conservative representations of arrays of damaged HalfPACT packages. The HAC model used gives a smaller center-to-center spacing between packages compared to the NCT model. In addition, the results indicate that the reactivity effects of array interaction are less than those of close, full reflection of the package contents. Hence, maximum reactivity results for arrays of HalfPACT packages under NCT are essentially the same as those under HAC at optimal moderation conditions. Therefore, infinite arrays of HalfPACT packages are safely subcritical under both NCT and HAC, and the requirements of 10 CFR §71.59⁸ are satisfied. Furthermore, a CSI of zero (0.0) is justified.

6.4.3.3 Special Reflectors in CH-TRU Waste

As described previously, the only “special reflectors” credibly applicable to CH-TRU waste criticality analysis are: beryllium (Be), beryllium oxide (BeO), carbon (C), deuterium (D₂O), magnesium oxide (MgO), and depleted uranium ($\geq 0.3\%$ ²³⁵U) when present in quantities greater than 1 weight percent. Each special reflector with regard to its possible presence in CH-TRU waste is discussed below:

Beryllium and Beryllium Oxide – Be, and/or BeO, may be present in CH-TRU waste in quantities greater than 1% by weight. The limits for payload containers other than pipe overpacks are found in [Table 6.1-1](#) and [Table 6.1-2](#) under Case B. As described in [Section 6.2.1](#), beryllium is the limiting special reflector for CH-TRU waste. For pipe overpack configurations, beryllium may be present in neutron sources and other source materials where the beryllium is completely bound to the fissile material in the source. Therefore, for pipe overpack configurations, Case E limits in [Table 6.1-1](#) and [Table 6.1-2](#) apply.

Carbon – Carbon is present as a constituent in CH-TRU waste but not in forms that can credibly reconfigure as a reflector. For example: (1) Carbon may be present as graphite molds or crucibles. In these forms the carbon will be chemically and irreversibly bound to the plutonium or other fissile material and cannot be separated. (2) Carbon may be present in filter media as spent or activated carbon. The plutonium or other fissile material would then be attached to the carbon filter media and would not be easily separated. (3) Granular activated carbon (GAC)

⁸ Title 10, Code of Federal Regulations, Part 71 (10 CFR 71), *Packaging and Transportation of Radioactive Material*, 01-01-07 Edition.

pads may also be present in an enclosed bag for the purpose of absorbing volatile organic compounds. Once the GAC pad is placed inside the payload container, there is no credible method for the carbon to fully-surround the fissile material and reconfigure as a reflector.

(4) Carbon may also be present in alloys, which are by definition chemically and/or mechanically bound. In summary, there is no identified mechanism that could cause the carbon in CH-TRU waste to be separated from the fissile material and/or to be reconfigured as a reflector.

Deuterium – The presence of liquid waste in the payload containers, except for residual amounts in well-drained containers, is prohibited. As specified by the CH-TRAMPAC, the total volume of residual liquid in a payload container shall be less than 1 percent (volume) of the payload container. This limitation on the authorized contents is such that D₂O will not be present in greater than 1% by weight.

Magnesium Oxide – Magnesium oxide crucibles used in high temperature-controlled applications, such as reduction processes, may be present in solid inorganic waste forms such as glass, metal, and pyrochemical salts. If present, MgO will be bound to the fissile material and would not be easily separated. MgO used for neutralization in solidified material cannot be separated out as it is chemically reacted in the waste generation process. There is no identified mechanism that could cause the magnesium oxide in CH-TRU waste to be reconfigured as a reflector.

Depleted Uranium ($\geq 0.3\% \text{ }^{235}\text{U}$) – Depleted uranium may be present in CH-TRU waste, but it will be chemically and/or mechanically bound to the plutonium or physically inseparable because the densities of U and Pu are similar. Separation by mechanical means or by leaching is extremely difficult and is considered highly unlikely in CH-TRU waste. Depleted uranium in CH-TRU waste will, therefore, not be separated from the fissile material and/or reconfigured as a reflector.

6.4.3.4 Machine Compacted CH-TRU Waste

Three criticality cases were analyzed for machine compacted CH-TRU waste:

Case C assumes all the machine compacted waste reconfigures into a single sphere during the hypothetical accident conditions and is applicable to machine compacted waste in a 55-gallon drum, 85-gallon drum, 100-gallon drum, or SWB. As shown in Table 6.1-1 and Table 6.1-2, the limits for Case C are 200 FGE per drum, 250 FGE per SWB, and 250 FGE per package.

Case D assumes either a maximum 70% packing fraction or a minimum vertical spacing of at least 0.50 inches is maintained between two cylinders during the hypothetical accident conditions (in addition to credit for the steel and slipsheets as described in Section 6.3.1.4).

Case D is applicable to machine compacted waste in the form of compacted pucks in a 55-gallon drum, 85-gallon drum, or 100-gallon drum. As shown in Table 6.1-1 and Table 6.1-2, the limits for Case D are 200 FGE per payload container and 325 FGE per package.

Case H assumes all the machine compacted waste reconfigures into a single sphere during the hypothetical accident conditions and is applicable to machine compacted waste in a shielded container. As shown in Table 6.1-1 and Table 6.1-2, the limits for Case H are 200 FGE per shielded container and 245 FGE per package.

6.4.3.5 Applicable Criticality Limits for CH-TRU Waste

In conclusion, the only special reflector in CH-TRU waste requiring special controls is Be/BeO. The criticality analyses for CH-TRU waste with greater than 1% by weight Be/BeO in any form is bounded by Case B (excluding shielded containers). Non-machine compacted CH-TRU waste payloads are covered by Cases A, E, and G. Machine compacted CH-TRU waste payloads are covered by Cases C, D, and H. The applicable FGE limits are specified by case in [Table 6.1-1](#) and [Table 6.1-2](#). Considering machine compaction and special reflectors in CH-TRU waste, as discussed in [Sections 6.4.3.3](#) and [6.4.3.4](#), the applicable FGE limits are summarized below.

FGE Limits Considering Machine Compaction and Special Reflectors

Contents	Payload Container	Fissile Limit per Payload Container (Pu-239 FGE)	Fissile Limit per Package (Pu-239 FGE)	Applicable Analysis Case
Not machine compacted with $\leq 1\%$ by weight Be/BeO ^①	Drum	200	325	A
	Pipe Overpack	200	1,400	E
	SWB	325	325	A
	Shielded Container	200	325	G
Not machine compacted with $> 1\%$ by weight Be/BeO ^①	Drum	100	100	B
	Pipe Overpack	200	1,400	E ^②
	SWB	100	100	B
	Shielded Container	Unauthorized	Unauthorized	N/A
Machine compacted with $\leq 1\%$ by weight Be/BeO ^①	Drum	200	250	C
	Pipe Overpack	Unauthorized	Unauthorized	N/A
	SWB	250	250	C
	Shielded Container	200	245	H
Machine compacted with controls ^③ and $\leq 1\%$ by weight Be/BeO ^①	Drum	200	325	D
	Pipe Overpack	Unauthorized	Unauthorized	N/A
	SWB	Unauthorized	Unauthorized	N/A
	Shielded Container	Unauthorized	Unauthorized	N/A
Machine compacted with $> 1\%$ by weight Be/BeO ^①	Drum	Unauthorized	Unauthorized	N/A
	Pipe Overpack	Unauthorized	Unauthorized	N/A
	SWB	Unauthorized	Unauthorized	N/A
	Shielded Container	Unauthorized	Unauthorized	N/A

Notes:

- ① Special reflectors other than Be/BeO in greater than 1% by weight quantities are exempted by the evaluation given in [Section 6.4.3.3](#).
- ② Case E is applicable in lieu of Case F because Be/BeO is always mechanically or chemically bound to fissile material in pipe overpack payloads (see [Section 6.4.3.3](#)).
- ③ The contents shall be machine compacted waste in the form of “puck” drums with the payload controls specified in [Sections 6.2.4](#) and [6.3.1.4](#).

Table 6.4-1 – Single-Unit, NCT, Case A, 325 FGE; k_s vs. H/Pu Ratio with Different Moderator and Reflector Compositions

Case	H/Pu	Composition	k_{eff}	σ	k_s
NPWPW5	500	Moderator and Reflector in ICV and OCA = 25% poly/75% water	0.8981	0.0011	0.9003
NPWPW6	600		0.9141	0.0010	0.9161
NPWPW7	700		0.9242	0.0010	0.9262
NPWPW8	800		0.9280	0.0010	0.9300
NPWPW9	900		0.9299	0.0010	0.9319
NPWPW10	1,000		0.9288	0.0009	0.9306
NPWPW11	1,100		0.9247	0.0010	0.9267
NPWPW12	1,200		0.9216	0.0010	0.9236
NPWPW13	1,300		0.9155	0.0009	0.9173
NPWPWB5	500		Moderator = 25% poly/75% water Reflector in ICV and OCA = 25% poly/74% water/1% beryllium	0.9000	0.0009
NPWPWB6	600	0.9149		0.0011	0.9171
NPWPWB7	700	0.9259		0.0010	0.9279
NPWPWB8	800	0.9297		0.0009	0.9315
NPWPWB9	900	0.9319		0.0010	0.9339
NPWPWB10	1,000	0.9308		0.0009	0.9326
NPWPWB11	1,100	0.9281		0.0009	0.9299
NPWPWB12	1,200	0.9211		0.0009	0.9229
NPWPWB13	1,300	0.9169		0.0009	0.9187
N2PWB5	500	Moderator and Reflector in ICV and OCA = 25% poly/74% water/1% beryllium	0.9015	0.0011	0.9037
N2PWB6	600		0.9155	0.0010	0.9175
N2PWB7	700		0.9265	0.0010	0.9285
N2PWB8	800		0.9302	0.0010	0.9322
N2PWB9	900		0.9318	0.0010	0.9338
N2PWB10	1,000		0.9302	0.0010	0.9322
N2PWB11	1,100		0.9277	0.0008	0.9293
N2PWB12	1,200		0.9224	0.0009	0.9242
N2PWB13	1,300		0.9173	0.0010	0.9193

Table 6.4-2 – Single Unit, NCT, Case A, 325 FGE; Variation of Reflector Volume Fraction (VF) at Near-Optimal H/Pu Ratio

Case	H/Pu	Reflector	VF	k_{eff}	σ	k_s
NPWPWB9	900		1.00	0.9319	0.0010	0.9339
NWCVOL95		ICV = OCA	0.95	0.9283	0.0010	0.9303
NWCVOL90		= 25% poly/ 74% water/ 1% Be at VF	0.90	0.9256	0.0009	0.9274
NWCVOL75		given	0.75	0.9157	0.0010	0.9177
NWCVOL50			0.50	0.8888	0.0009	0.8906
NWCVOL25		Int = water at VF given	0.25	0.8434	0.0010	0.8454
NWCVOL10			0.10	0.7963	0.0011	0.7985
NWCVOL00			0	0.7583	0.0010	0.7603

Table 6.4-3 – Single-Unit, HAC, Case A, 325 FGE; k_s vs. H/Pu at Maximum Reflection Conditions

Case	H/Pu	Reflector	k_{eff}	σ	k_s
HPWPWB5	500	ICV = OCA = 25% poly/ 74% water/ 1% Be at VF=1.0 Int = water at VF=1.0	0.8996	0.0010	0.9016
HPWPWB6	600		0.9149	0.0011	0.9171
HPWPWB7	700		0.9234	0.0009	0.9252
HPWPWB8	800		0.9296	0.0010	0.9316
HPWPWB9	900		0.9295	0.0009	0.9313
HPWPWB10	1,000		0.9311	0.0010	0.9331
HPWPWB11	1,100		0.9273	0.0009	0.9291
HPWPWB12	1,200		0.9219	0.0009	0.9237
HPWPWB13	1,300		0.9170	0.0009	0.9188

Table 6.4-4 – Infinite Array Variation 0, HAC, Case A, 325 FGE;
 k_s vs. H/Pu at Extremes of Reflection Conditions

Case	H/Pu	Reflector	k_{eff}	σ	k_s	
HINFAR5	500	ICV = OCA = 25% poly/ 74% water/ 1% Be at VF=1.0 Int = water at VF=1.0	0.8997	0.0012	0.9021	
HINFAR6	600		0.9163	0.0010	0.9183	
HINFAR7	700		0.9275	0.0009	0.9293	
HINFAR8	800		0.9291	0.0010	0.9311	
HINFAR9	900		0.9307	0.0009	0.9325	
HINFAR10	1,000		0.9311	0.0010	0.9331	
HINFAR11	1,100		0.9266	0.0010	0.9286	
HINFAR12	1,200		0.9224	0.0008	0.9240	
HINFAR13	1,300		0.9161	0.0008	0.9177	
HVINAR8	800		ICV = Void OCA = Void Int = Void	0.8677	0.0010	0.8697
HVINAR9	900			0.8759	0.0009	0.8777
HVINAR10	1,000			0.8832	0.0010	0.8852
HVINAR11	1,100			0.8859	0.0008	0.8875
HVINAR12	1,200	0.8878		0.0009	0.8896	
HVINAR13	1,300	0.8860		0.0008	0.8876	
HVINAR14	1,400	0.8840		0.0009	0.8858	
HVINAR15	1,500	0.8814		0.0008	0.8830	

Table 6.4-5 – Infinite Array Variation 0, HAC, Case A, 325 FGE;
Variation of Reflector Volume Fraction at Near-Optimal H/Pu Ratios

Case	H/Pu	Reflector	VF	k_{eff}	σ	k_s
HINFAR10	1000	ICV = OCA = 25% poly/ 74% water/ 1% Be at VF given Int = water at VF given	1.00	0.9311	0.0010	0.9331
HWC10VOL95			0.95	0.9266	0.0009	0.9284
HWC10VOL90			0.90	0.9244	0.0011	0.9266
HWC10VOL75			0.75	0.9159	0.0010	0.9179
HWC10VOL50			0.50	0.8915	0.0010	0.8935
HWC10VOL25			0.25	0.8483	0.0010	0.8503
HWC10VOL10			0.10	0.8047	0.0009	0.8065
HWC10VOL1			0.01	0.7888	0.0009	0.7906
HWC10VOL01			0.001	0.8439	0.0009	0.8457
HVINAR10			0	0.8832	0.0010	0.8852
HINFAR12	1,200	ICV = OCA = 25% poly/ 74% water/ 1% Be at VF given Int = water at VF given	1.00	0.9224	0.0008	0.9240
HWC12VOL90			0.95	0.9190	0.0009	0.9208
HWC12VOL95			0.90	0.9201	0.0009	0.9219
HWC12VOL75			0.75	0.9098	0.0009	0.9116
HWC12VOL50			0.50	0.8888	0.0010	0.8908
HWC12VOL25			0.25	0.8543	0.0010	0.8563
HWC12VOL10			0.10	0.8129	0.0009	0.8147
HWC12VOL1			0.01	0.7972	0.0010	0.7992
HWC12VOL01			0.001	0.8014	0.0010	0.8034
HVINAR12			0	0.8878	0.0009	0.8896

**Table 6.4-6 – Infinite Array Variation 1, HAC, Case A, 325 FGE;
Variation of H/Pu Ratio at Extremes of Reflection Conditions**

					σ	
HINFAROFF9		900	ICV = 25% poly/74% water/1% Be at VF=1.0 OCA = Int = Void	0.9226	0.0009	0.9244
HINFAROFF10		1,000		0.9239	0.0010	0.9259
HINFAROFF11		1,100		0.9209	0.0010	0.9229
HINFAROFF12		1,200		0.9188	0.0010	0.9208
HVINAROFF9		900		0.8948	0.0010	0.8968
HVINAROFF10		1,000		0.9006	0.0009	0.9024
HVINAROFF11		1,100		0.9027	0.0010	0.9047
HVINAROFF12		1,200		0.9022	0.0009	0.9040
HVINAROFF13		1,300		0.8997	0.0009	0.9015

Table 6.4-7 – Infinite Array Variation 0, HAC, Case A; Variation of H/Pu Ratio for Various Gram Quantities of Pu-240 at Maximum Reflection Conditions

	Pu-240 (g)	Pu-239 (g)					
5PU340H6			600		0.9144	0.0011	0.9166
5PU340H7			700		0.9237	0.0022	0.9281
5PU340H8			800		0.9313	0.0009	0.9331
5PU340H9			900		0.9316	0.0010	0.9336
5PU340H10			1,000		0.9304	0.0009	0.9322
5PU340H11			1,100		0.9278	0.0009	0.9296
5PU340H12			1,200		0.9248	0.0011	0.9270
5PU340H13			1,300		0.9196	0.0010	0.9216
15PU360H6			600		0.9136	0.0009	0.9154
15PU360H7			700		0.9233	0.0008	0.9249
15PU360H8			800		0.9307	0.0009	0.9325
15PU360H9			900		0.9337	0.0011	0.9359
15PU360H10			1,000		0.9302	0.0009	0.9320
15PU360H11			1,100		0.9308	0.0008	0.9324
15PU360H12			1,200		0.9254	0.0010	0.9274
15PU360H13			1,300		0.9197	0.0008	0.9213
25PU380H6			600		0.9121	0.0009	0.9139
25PU380H7			700		0.9246	0.0010	0.9266
25PU380H8			800		0.9299	0.0009	0.9317
25PU380H9			900		0.9316	0.0010	0.9336
25PU380H10			1,000		0.9339	0.0009	0.9357
25PU380H11			1,100		0.9298	0.0010	0.9318
25PU380H12			1,200		0.9268	0.0009	0.9286
25PU380H13			1,300		0.9206	0.0008	0.9222

Table 6.4-8 – Infinite Array Variation 0, HAC, Case A, 5 g Pu-240, 340 FGE; k_s vs. H/Pu for Various Combinations of U-235 and Pu-239 under Maximum Reflection Conditions

Case	Fissile Material	H/X	k_{eff}	σ	k_s
U100H3	FGE = 100% U-235 ^① = 528.7 g U-235	300	0.9000	0.0011	0.9022
U100H4		400	0.9198	0.0009	0.9216
U100H5		500	0.9261	0.0009	0.9279
U100H6		600	0.9214	0.0009	0.9232
U100H7		700	0.9131	0.0010	0.9151
U75H4	FGE = 75% U-235/ 25% Pu-239 = 396.6 g U-235/ 85.0 g Pu-239	400	0.9141	0.0010	0.9161
U75H5		500	0.9245	0.0009	0.9263
U75H6		600	0.9272	0.0010	0.9292
U75H7		700	0.9224	0.0010	0.9244
U75H8		800	0.9162	0.0008	0.9178
U50H5	FGE = 50% U-235/ 50% Pu-239 = 264.4 g U-235/ 170.0 g Pu-239	500	0.9188	0.0009	0.9206
U50H6		600	0.9272	0.0009	0.9290
U50H7		700	0.9275	0.0010	0.9295
U50H8		800	0.9240	0.0008	0.9256
U50H9		900	0.9194	0.0010	0.9214
U25H5	FGE = 25% U-235/ 75% Pu-239 = 132.2 g U-235/ 255 g Pu-239	500	0.9152	0.0010	0.9172
U25H6		600	0.9253	0.0011	0.9275
U25H7		700	0.9310	0.0010	0.9330
U25H8		800	0.9295	0.0010	0.9315
U25H9		900	0.9289	0.0010	0.9309
5PU340H7	FGE = 100% Pu-239 = 340 g Pu-239	700	0.9237	0.0022	0.9281
5PU340H8		800	0.9313	0.0009	0.9331
5PU340H9		900	0.9316	0.0010	0.9336
5PU340H10		1,000	0.9304	0.0009	0.9322
5PU340H11		1,100	0.9278	0.0009	0.9296

Note:

① 1 g U-235 = 0.643 FGE

Table 6.4-9 – Infinite Array Variation 0, HAC, Case B, 100 FGE;
 k_s vs. H/Pu at Maximum Reflection Conditions

Case	H/Pu	Reflector	k_{eff}	σ	k_s
HINFAR5B	500	ICV = Be at	0.8892	0.0009	0.8910
HINFAR6B	600	VF=1.0	0.9041	0.0009	0.9059
HINFAR7B	700	OCA =	0.9127	0.0008	0.9143
HINFAR8B	800	25% poly/ 74% water/	0.9168	0.0008	0.9184
HINFAR9B	900	1% Be at	0.9127	0.0009	0.9145
HINFAR10B	1,000	VF =1.0	0.9095	0.0008	0.9111
HINFAR11B	1,100	Int = water	0.9042	0.0008	0.9058
HINFAR12B	1,200	at VF=1.0	0.8988	0.0008	0.9004

Table 6.4-10 – Infinite Array Variation 0, HAC, Case B, 100 FGE; k_s vs. H/Pu for Various Moderator Volume Fractions of Beryllium under Maximum Reflection Conditions

Case	VF Beryllium in Moderator	H/Pu	k_{eff}	σ	k_s
B01H6	1	600	0.9027	0.0008	0.9043
B01H7		700	0.9102	0.0009	0.9120
B01H8		800	0.9144	0.0010	0.9164
B01H9		900	0.9129	0.0009	0.9147
B01H10		1,000	0.9101	0.0008	0.9117
B10H6	10	600	0.9027	0.0009	0.9045
B10H7		700	0.9102	0.0009	0.9120
B10H8		800	0.9125	0.0008	0.9141
B10H9		900	0.9104	0.0009	0.9122
B10H10		1,000	0.9075	0.0009	0.9093
B20H6	20	600	0.9001	0.0010	0.9021
B20H7		700	0.9081	0.0009	0.9099
B20H8		800	0.9093	0.0009	0.9111
B20H9		900	0.9094	0.0009	0.9112
B20H10		1,000	0.9042	0.0008	0.9058
B40H6	40	600	0.8972	0.0010	0.8992
B40H7		700	0.9012	0.0009	0.9030
B40H8		800	0.9022	0.0009	0.9040
B40H9		900	0.9010	0.0009	0.9028
B40H10		1,000	0.8960	0.0008	0.8976
B60H6	60	600	0.8822	0.0009	0.8840
B60H7		700	0.8859	0.0008	0.8875
B60H8		800	0.8846	0.0009	0.8864
B60H9		900	0.8815	0.0008	0.8831
B60H10		1,000	0.8771	0.0008	0.8787

Table 6.4-11 – Infinite Array Variation 0, HAC, Case B, 100 FGE;
Variation of Reflector Volume Fraction at Near-Optimal H/Pu Ratio

Case	H/Pu	Reflector	VF	k_{eff}	σ	k_s
HINFAR8B	800	ICV = Be at	1.00	0.9168	0.0008	0.9184
HINFAR8B95		VF given	0.95	0.8973	0.0009	0.8991
HINFAR8B90		OCA =	0.90	0.8838	0.0009	0.8856
HINFAR8B75		25% poly/	0.75	0.8320	0.0008	0.8336
HINFAR8B50		74% water/	0.50	0.7188	0.0009	0.7206
HINFAR8B25		1% Be at	0.25	0.5671	0.0008	0.5687
HINFAR8B10		VF given	0.10	0.4678	0.0009	0.4696
HINFAR8B00		Int = water at VF given	0	0.5013	0.0008	0.5029

Table 6.4-12 – Infinite Array Variation 1, HAC, Case B, 100 FGE;
Variation of H/Pu Ratio at Reflector Volume Fraction to Maximize
Interaction while Maintaining Beryllium Reflection

					σ	
HINFAR8BOFF		800		0.7680	0.0010	0.7700
HINFAR9BOFF		900		0.7752	0.0009	0.7770
HINFAR10BOFF		1,000		0.7795	0.0009	0.7813
HINFAR11BOFF		1,100		0.7798	0.0009	0.7816
HINFAR12BOFF		1,200		0.7800	0.0008	0.7816
HINFAR13BOFF		1,300		0.7782	0.0007	0.7796

Table 6.4-13 – Infinite Array Variation 0, HAC, Case C, 250 FGE;
 k_s vs. H/Pu at Maximum Reflection Conditions

Case	H/Pu	Reflector	k_{eff}	σ	k_s
C0B250H6	600	ICV =	0.9152	0.0010	0.9172
C0B250H7	700	100% poly	0.9248	0.0010	0.9268
C0B250H8	800	OCA =	0.9287	0.0010	0.9307
C0B250H9	900	25% poly/ 74% water/ 1% Be	0.9320	0.0010	0.9340
C0B250H10	1,000		0.9305	0.0009	0.9323
C0B250H11	1,100	Int = water	0.9274	0.0009	0.9292
C0B250H12	1,200	All at	0.9223	0.0010	0.9243
C0B250H13	1,300	VF=1.0	0.9148	0.0008	0.9164
C1B250H5	500	ICV =	0.8969	0.0010	0.8989
C1B250H6	600	99% poly/ 1% Be	0.9148	0.0009	0.9166
C1B250H7	700		0.9250	0.0009	0.9268
C1B250H8	800	OCA =	0.9309	0.0011	0.9331
C1B250H9	900	25% poly/ 74% water/ 1% Be	0.9325	0.0010	0.9345
C1B250H10	1,000		0.9296	0.0010	0.9316
C1B250H11	1,100	Int = water	0.9271	0.0009	0.9289
C1B250H12	1,200	All at	0.9237	0.0008	0.9253
C1B250H13	1,300	VF=1.0	0.9188	0.0009	0.9206

Table 6.4-14 – Infinite Array Variation 0, HAC, Case C, 250 FGE;
Variation of Reflector Volume Fraction at Near-Optimal H/Pu Ratio

Case	H/Pu	Reflector	VF	k_{eff}	σ	k_s
C1B250H9	900	ICV = 99%	1.00	0.9325	0.0010	0.9345
C1B250H9V95		poly/1% Be at VF given	0.95	0.9295	0.0009	0.9313
C1B250H9V90		OCA = 25%	0.90	0.9269	0.0010	0.9289
C1B250H9V75		poly/ 74%	0.75	0.9149	0.0010	0.9169
C1B250H9V50		water/ 1%	0.50	0.8880	0.0009	0.8898
C1B250H9V25		Be at VF given	0.25	0.8460	0.0010	0.8480
C1B250H9V10		Int = water at VF given	0.10	0.7974	0.0010	0.7994
C1B250H9V00			0	0.8560	0.0009	0.8578

Table 6.4-15 – Infinite Array Variation 1, HAC, Case C, 250 FGE;
Variation of H/Pu Ratio at Reflector Volume Fraction to Maximize
Interaction while Maintaining Reflection

					σ	
C1BOFF7		700		0.9134	0.0010	0.9154
C1BOFF8		800		0.9202	0.0009	0.9220
C1BOFF9		900		0.9218	0.0011	0.9240
C1BOFF10		1,000		0.9224	0.0009	0.9242
C1BOFF11		1,100		0.9185	0.0009	0.9203

Table 6.4-16 – Infinite Array Variation 0, HAC, Case D, 325 FGE;
 k_s vs. H/Pu at Maximum Reflection Conditions

Case	H/Pu	Reflector	k_{eff}	σ	k_s
70% Polyethylene/ 30% Water Moderator and No Separation Between Pucks					
CASED70H5	500	ICV =	0.9123	0.0010	0.9143
CASED70H6	600	70% poly/	0.9245	0.0010	0.9265
CASED70H7	700	29% water/	0.9298	0.0010	0.9318
CASED70H8	800	1% Be	0.9307	0.0009	0.9325
CASED70H9	900	OCA =	0.9292	0.0010	0.9312
CASED70H10	1,000	25% poly/	0.9257	0.0010	0.9277
CASED70H11	1,100	74% water/	0.9183	0.0008	0.9199
CASED70H12	1,200	1% Be Int = water All VF=1.0	0.9144	0.0009	0.9162
100% Polyethylene Moderator and 0.50 in. Separation Between Pucks Filled with Water					
CASED100H5	500	ICV =	0.9154	0.0010	0.9174
CASED100H6	600	99% poly/	0.9258	0.0009	0.9276
CASED100H7	700	1% Be	0.9319	0.0009	0.9337
CASED100H8	800	OCA =	0.9320	0.0008	0.9336
CASED100H9	900	25% poly/	0.9310	0.0009	0.9328
CASED100H10	1,000	74% water/	0.9263	0.0009	0.9281
CASED100H11	1,100	1% Be Int = water	0.9233	0.0010	0.9253
CASED100H12	1,200	All VF=1.0	0.9147	0.0009	0.9165
100% Polyethylene Moderator and 0.50 in. Separation Between Pucks Filled with Polyethylene					
CASED100H5P	500	ICV =	0.9159	0.0010	0.9179
CASED100H6P	600	99% poly/	0.9261	0.0009	0.9279
CASED100H7P	700	1% Be	0.9319	0.0010	0.9339
CASED100H8P	800	OCA =	0.9329	0.0010	0.9349
CASED100H9P	900	25% poly/	0.9308	0.0009	0.9326
CASED100H10P	1,000	74% water/	0.9260	0.0009	0.9278
CASED100H11P	1,100	1% Be Int = water	0.9210	0.0009	0.9228
CASED100H12P	1,200	All VF=1.0	0.9136	0.0009	0.9154

Table 6.4-17 – Infinite Array Variation 0, HAC, Case D, 325 FGE;
Variation of Reflector Volume Fraction at Near-Optimal H/Pu Ratio

Case	H/Pu	Reflector	VF	k_{eff}	σ	k_s
CASED70H8	800	ICV = 70%	1.00	0.9307	0.0009	0.9325
CASED70H8V95		poly/29%	0.95	0.9292	0.0009	0.9310
CASED70H8V90		water/1% Be at VF given	0.90	0.9252	0.0009	0.9270
CASED70H8V75		OCA = 25%	0.75	0.9143	0.0009	0.9161
CASED70H8V50		poly/74%	0.50	0.8893	0.0009	0.8911
CASED70H8V25		water/1% Be at VF given	0.25	0.8382	0.0011	0.8404
CASED70H8V10		Int = water at VF given	0.10	0.7828	0.0010	0.7848
CASED70H8V00				0	0.8501	0.0010

Table 6.4-18 – Infinite Array Variation 1, HAC, Case D, 325 FGE;
Variation of H/Pu Ratio at Reflector Volume Fraction to Maximize
Interaction while Maintaining Reflection

					σ	
D1BOFF70H6		600	ICV = 70%	0.9037	0.0010	0.9057
D1BOFF70H7		700	poly/29%	0.9125	0.0011	0.9147
D1BOFF70H8		800	water/1% Be at VF=1.0	0.9144	0.0008	0.9160
D1BOFF70H9		900	OCA = Int = Void	0.9153	0.0009	0.9171

This page intentionally left blank.

6.5 Critical Benchmark Experiments

The KENO-V.a Monte Carlo criticality code¹ has been used extensively in criticality evaluations. The 238 energy-group, ENDF-B/V cross-section library² employed here has been selected based on its relatively fine neutron energy group structure. This section justifies the validity of this computation tool and data library combination for application to the HalfPACT package criticality analysis.

The ORNL USLSTATS code, described in Appendix C, *User's Manual for USLSTATS V1.0*, of NUREG/CR-6361³, is used to establish an upper subcriticality limit, USL, for the analysis. Computed multiplication factors, k_{eff} , for the HalfPACT package are deemed to be adequately subcritical if the computed value of k_{eff} plus two standard deviations is below the USL as follows:

$$k_s = k_{\text{eff}} + 2\sigma < \text{USL}$$

The USL includes the combined effects of code bias, uncertainty in the benchmark experiments, uncertainty in the computational evaluation of the benchmark experiments, and an administrative margin of subcriticality. The USL is determined using the confidence band with administrative margin technique (USLSTATS Method 1).

The result of the statistical analysis of the benchmark experiments is a USL of 0.9382. Due to the significant positive bias exhibited by the code and library for the benchmark experiments, the USL is constant with respect to the various parameters selected for the benchmark analysis.

6.5.1 Benchmark Experiments and Applicability

A total of 196 benchmark experiments of water-reflected solutions of plutonium nitrate are evaluated using the KENO-V.a Monte Carlo criticality code with the SCALE-PC v4.4a⁴, 238 energy-group, ENDF-B/V cross-section library. The benchmark cases are evaluated with respect to three independent parameters: 1) the H/Pu ratio, 2) the average fission energy group (AEG), and 3) the ratio of Pu-240 to total Pu.

Detailed descriptions of the benchmark experiments are obtained from the OECD Nuclear Energy Agency's *International Handbook of Evaluated Criticality Safety Benchmark Experiments*⁵. The critical experiments selected for this analysis are presented in [Table 6.5-1](#). Experiments with beryllium and Pu as the fissile component are not available. The only experiments with beryllium in the thermal energy range identified from the OECD Handbook

¹ L. M. Petrie and N. F. Landers, *KENO-V.a: An Improved Monte Carlo Criticality Program with Supergrouping*, ORNL/NUREG/CSD-2/V2/R6, Volume 2, Section F11, March 2000.

² W. C. Jordan and S. M. Bowman, *Scale Cross-Section Libraries*, ORNL/NUREG/CSD-2/V3/R6, Volume 3, Section M4, March 2000.

³ J. J. Lichtenwalter, S. M. Bowman, M. D. DeHart, C. M. Hopper, *Criticality Benchmark Guide for Light-Water-Reactor Fuel in Transportation and Storage Packages*, NUREG/CR-6361, ORNL/TM-13211, March 1997.

⁴ Oak Ridge National Laboratory (ORNL), *SCALE 4.4a: Modular Code System for Performing Standardized Computer Analyses for Licensing Evaluation for Workstations and Personal Computers*, ORNL/NUREG/CSD-2/R6, March 2000.

⁵ OECD Nuclear Energy Agency, *International Handbook of Evaluated Criticality Safety Benchmark Experiments*, NEA/NSC/DOC(95)03, September 2002.

contained U-233 as the fissile isotope. Thus, 31 benchmarks with U-233 and beryllium in the thermal energy range and 15 benchmarks with U-233 and no beryllium also in the thermal energy range were evaluated. With respect to validation of polyethylene, CH₂, in the models, some of the U-233 benchmarks contained polyethylene and some of the plutonium experiments contained Plexiglas, which also contains carbon. All criticality models of the HalfPACT package fall within the range of applicability of the benchmark experiments for the H/Pu ratio and AEG trending parameters as follows:

Range of Applicability for Trending Parameters

$$45 \leq \text{H/Pu Ratio} \leq 2,730$$

$$173 \leq \text{AEG} \leq 220$$

$$4.95 \times 10^{-3} \leq \text{Pu-240/Pu Ratio} \leq 2.32 \times 10^{-1}$$

The intent of using the Pu-240/Pu ratio is to demonstrate the validity of an extension of the range of applicability of this parameter to the HalfPACT package criticality models. The Case A models include a Pu-240/Pu Ratio of up to 6.6×10^{-2} , which is within the range of applicability.

Only thermal benchmark experiments are analyzed. Criticality analysis of the HalfPACT package and package arrays demonstrate that multiplication factors are insignificant when the package contents are unmoderated.

6.5.2 Details of Benchmark Calculations

A total of 196 experimental benchmarks with Pu in the thermal energy range were evaluated with the KENO-V.a code with the SCALE-PC v4.4a, 238 group, ENDF-B/V cross-section library. Detailed descriptions of these experiments are found in the OECD Handbook. A summary of the experiment titles is provided in [Table 6.5-1](#). The benchmark results were evaluated using the USLSTATS program as discussed in the next section.

6.5.3 Results of Benchmark Calculations

[Table 6.5-2](#) summarizes the trending parameter values, computed k_{eff} values, and uncertainties for each case. The uncertainty value, σ_c , assigned to each case is a combination of the experimental uncertainty for each experiment, σ_{exp} , and the Monte Carlo uncertainty associated with the particular computational evaluation of the case, σ_{comp} , or:

$$\sigma_c = (\sigma_{\text{exp}}^2 + \sigma_{\text{comp}}^2)^{1/2}$$

These values were input into the USLSTATS program in addition to the following parameters:

- P, proportion of population falling above lower tolerance level = 0.995
- $1-\gamma$, confidence on fit = 0.95
- α , confidence on proportion P = 0.95
- x_{min} , minimum value of AEG for which USL correlation are computed = N/A, minimum of supplied data used by code

- x_{\max} , maximum value of AEG for which USL correlation are computed = N/A, maximum of supplied data used by code
- σ_{eff} , estimate in average standard deviation of all input values of $k_{\text{eff}} = -1.0$, use supplied values
- Δk_m , administrative margin used to ensure subcriticality = 0.05.

This data is followed by triplets of trending parameter value, computed k_{eff} , and uncertainty for each case. The USL Method 1 result was chosen which performs a confidence band analysis on the data for the trending parameter.

Three trending parameters are identified for determination of the bias. First, the AEG is used in order to characterize any code bias with respect to neutron spectral effects. The USL is calculated vs. AEG separately for the Pu experiments, U-233 experiments with beryllium and U-233 experiments without beryllium in addition to the combined results of the Pu and U-233 with beryllium experiments. Because the U-233 fissile isotope introduces a component that is not relative to the calculations performed for the HalfPACT and may have a distinct bias of its own, comparison of the USL for the U-233 experiments with beryllium to the USL for those without beryllium allows the effect of the beryllium reflector to be separated from the effect of the U-233 isotope. Next, the H/Pu ratio of each experimental case containing Pu is used in order to characterize the material and geometric properties of each sphere. Finally, since all the Pu experiments include Pu-240 to some extent and the HalfPACT models contain varying amount of Pu-240, a trending analysis of the results of the Pu experiments with respect to Pu-240/Pu ratio is performed. The U-233 results are not considered in the trending with respect to H/Pu as the optimum H/Pu range will be significantly different for a U-233 system vs. a Pu system. For obvious reasons, the U-233 results are also not considered in the trending with respect to the Pu-240/Pu ratio.

The USLs calculated using USLSTATS Method 1 for the benchmark combinations discussed above are tabulated in [Table 6.5-3](#). The USL calculated based on the combined results of the U-233 with beryllium and Pu experiments of 0.9382 is chosen as the USL for this analysis. This USL value is ~ 0.001 below that of the Pu experiments alone. The ^{233}U benchmarks without Be result in a lower USL (0.0032) than calculated from the U-233 benchmark results with beryllium. This difference is greater than the experimental uncertainty of each benchmark case (~ 0.001). Both of the U-233 USL values are lower than the Pu experiment USL values indicating that the U-233 isotope in the experiments has a more significant effect on the USL than the beryllium. Thus, the USL based on the combined results of the U-233 with beryllium and Pu experiments chosen adequately accounts for any bias attributable to beryllium. In addition, the USLs calculated for the Pu experiments using either H/X or the Pu-240/Pu ratio as the trending parameter do not differ significantly from the Pu USL vs. AEG and are bounded by the chosen USL value of 0.9382. USLSTATS calculated constant USL values with respect to H/Pu and Pu-240/Pu ratio indicating no appreciable trend with respect to these parameters.

Table 6.5-1 – Benchmark Experiment Description with Experimental Uncertainties

Series	Title
PU-SOL-THERM-001	Water-reflected 11.5 inch diameter spheres of plutonium nitrate solutions
PU-SOL-THERM-002	Water-reflected 12 inch diameter spheres of plutonium nitrate solutions
PU-SOL-THERM-003	Water-reflected 13 inch diameter spheres of plutonium nitrate solutions
PU-SOL-THERM-004	Water-reflected 14 inch diameter spheres of plutonium nitrate solutions 0.54% to 3.43% Pu-240
PU-SOL-THERM-005	Water-reflected 14 inch diameter spheres of plutonium nitrate solutions 4.05% and 4.40% Pu-240
PU-SOL-THERM-006	Water-reflected 15 inch diameter spheres of plutonium nitrate solutions
PU-SOL-THERM-007	Water-reflected 11.5 inch diameter spheres partly filled with plutonium nitrate solutions
PU-SOL-THERM-009	Unreflected 48 inch-diameter sphere of plutonium nitrate solution
PU-SOL-THERM-010	Water-reflected 9-, 10-, 11-, and 12 inch-diameter cylinders of plutonium nitrate solutions
PU-SOL-THERM-011	Bare 16- and 18 inch-diameter spheres of plutonium nitrate solutions
PU-SOL-THERM-014	Interacting cylinders of 300-mm diameter with plutonium nitrate solution (115.1gPu/l) in air
PU-SOL-THERM-015	Interacting cylinders of 300-mm diameter with plutonium nitrate solution (152.5gPu/l) in air
PU-SOL-THERM-016	Interacting cylinders of 300-mm and 256-mm diameters with plutonium nitrate solution (152.5 and 115.1gPu/l) and nitric acid (2n) in air
PU-SOL-THERM-017	Interacting cylinders of 256-mm and 300-mm diameters with plutonium nitrate solution (115.1gPu/l) in air
PU-SOL-THERM-020	Water-reflected and water-cadmium reflected 14-inch diameter spheres of plutonium nitrate solutions
PU-SOL-THERM-021	Water-reflected and bare 15.2-inch-diameter spheres of plutonium nitrate solutions
PU-SOL-THERM-024	Slabs of plutonium nitrate solutions reflected by 1-inch-thick Plexiglas
U233-SOL-THERM-001	Unreflected spheres of ²³³ U nitrate solutions
U233-SOL-THERM-003	Paraffin-reflected 5-, 5.4-, 6-, 6.6-, 7.5- 8-, 8.5-, 9- and 12-inch-diameter cylinders of ²³³ U uranyl fluoride solutions
U233-SOL-THERM-015	Uranyl-fluoride (²³³ U) solutions in spherical stainless steel vessels with reflectors of Be, CH ₂ , and Be-CH ₂ composites

Table 6.5-2 – Benchmark Case Parameters and Computed Results

Case Name	k_{eff}	σ_{comp}	AEG	H/X[Ⓞ]	Pu-240/ Pu Ratio	Experiment Uncertainty σ_{exp}
PUST001_CASE_1	1.0080	0.0010	212.494	352.9	0.04650	0.0050
PUST001_CASE_2	1.0100	0.0010	209.961	258.1	0.04650	0.0050
PUST001_CASE_3	1.0133	0.0010	207.777	204.1	0.04650	0.0050
PUST001_CASE_4	1.0073	0.0010	206.439	181	0.04650	0.0050
PUST001_CASE_5	1.0111	0.0011	205.757	171.2	0.04650	0.0050
PUST001_CASE_6	1.0089	0.0010	195.766	86.7	0.04650	0.0050
PUST002_CASE_1	1.0074	0.0010	214.693	508	0.03110	0.0047
PUST002_CASE_2	1.0088	0.0011	214.457	489.2	0.03110	0.0047
PUST002_CASE_3	1.0074	0.0010	213.798	437.3	0.03110	0.0047
PUST002_CASE_4	1.0103	0.0010	213.343	407.5	0.03110	0.0047
PUST002_CASE_5	1.0125	0.0011	212.898	380.6	0.03110	0.0047
PUST002_CASE_6	1.0099	0.0010	211.974	333.5	0.03110	0.0047
PUST002_CASE_7	1.0101	0.0010	211.146	299.3	0.03110	0.0047
PUST003_CASE_1	1.0089	0.0010	216.630	774.1	0.01750	0.0047
PUST003_CASE_2	1.0076	0.0011	216.438	742.7	0.01750	0.0047
PUST003_CASE_3	1.0103	0.0010	216.055	677.2	0.03110	0.0047
PUST003_CASE_4	1.0094	0.0010	215.948	660.5	0.03110	0.0047
PUST003_CASE_5	1.0097	0.0010	215.535	607.2	0.03110	0.0047
PUST003_CASE_6	1.0099	0.0011	214.960	545.3	0.03110	0.0047
PUST003_CASE_7	1.0121	0.0009	216.482	714.8	0.03110	0.0047
PUST003_CASE_8	1.0091	0.0011	216.321	692.1	0.03110	0.0047
PUST004_CASE_1	1.0080	0.0010	217.470	981.7	0.00538	0.0047
PUST004_CASE_2	1.0032	0.0009	217.408	898.6	0.04180	0.0047
PUST004_CASE_3	1.0059	0.0008	217.241	864	0.04500	0.0047
PUST004_CASE_4	1.0033	0.0009	217.034	842	0.03260	0.0047
PUST004_CASE_5	1.0043	0.0010	217.257	780.2	0.03630	0.0047
PUST004_CASE_6	1.0074	0.0009	217.195	668	0.00495	0.0047
PUST004_CASE_7	1.0104	0.0010	217.030	573.3	0.00495	0.0047
PUST004_CASE_8	1.0040	0.0009	216.917	865	0.00504	0.0047
PUST004_CASE_9	1.0041	0.0009	216.580	872.2	0.01530	0.0047

Case Name	k_{eff}	σ_{comp}	AEG	H/X ^①	Pu-240/ Pu Ratio	Experiment Uncertainty σ_{exp}
PUST004_CASE_10	1.0078	0.0009	215.881	971.6	0.02510	0.0047
PUST004_CASE_11	1.0041	0.0010	215.106	929.6	0.02330	0.0047
PUST004_CASE_12	1.0094	0.0009	217.031	884.1	0.03160	0.0047
PUST004_CASE_13	1.0042	0.0009	217.074	925.5	0.03350	0.0047
PUST005_CASE_1	1.0072	0.0010	217.069	866.4	0.04030	0.0047
PUST005_CASE_2	1.0084	0.0009	216.909	832.7	0.04030	0.0047
PUST005_CASE_3	1.0092	0.0009	216.749	800.7	0.04030	0.0047
PUST005_CASE_4	1.0091	0.0010	216.360	734.4	0.04030	0.0047
PUST005_CASE_5	1.0102	0.0010	215.906	666.1	0.04030	0.0047
PUST005_CASE_6	1.0112	0.0010	215.451	607.9	0.04030	0.0047
PUST005_CASE_7	1.0099	0.0010	215.004	557.2	0.04030	0.0047
PUST005_CASE_8	1.0024	0.0010	216.903	830.6	0.04030	0.0047
PUST005_CASE_9	1.0078	0.0010	216.687	788.9	0.04030	0.0047
PUST006_CASE_1	1.0059	0.0008	217.615	1028.2	0.03110	0.0035
PUST006_CASE_2	1.0079	0.0009	217.459	986.2	0.03110	0.0035
PUST006_CASE_3	1.0072	0.0010	217.147	910.9	0.03110	0.0035
PUST007_CASE_2	1.0090	0.0011	198.911	102.6	0.04570	0.0047
PUST007_CASE_3	1.0024	0.0010	199.553	110.11	0.04570	0.0047
PUST007_CASE_5	1.0099	0.0010	209.885	253.3	0.04570	0.0047
PUST007_CASE_6	1.0054	0.0011	209.689	247.3	0.04570	0.0047
PUST007_CASE_7	1.0072	0.0010	209.816	250.5	0.04570	0.0047
PUST007_CASE_8	1.0007	0.0012	209.577	246.5	0.04570	0.0047
PUST007_CASE_9	0.9996	0.0011	209.628	246.5	0.04570	0.0047
PUST007_CASE_10	1.0009	0.0011	210.426	275.5	0.04570	0.0047
PUST009_CASE_1	1.0202	0.0007	219.730	2579.3	0.02510	0.0033
PUST009_CASE_2	1.0242	0.0005	219.819	2706.5	0.02510	0.0033
PUST009_CASE_3	1.0232	0.0006	219.830	2729.8	0.02510	0.0033
PUST010_CASE_1.11	1.0158	0.0011	219.830	471.3	0.02840	0.0048
PUST010_CASE_1.12	1.0125	0.0009	214.122	527.7	0.02890	0.0048
PUST010_CASE_1.9	1.0183	0.0012	214.895	259.3	0.02840	0.0048
PUST010_CASE_2.11	1.0124	0.0011	210.075	542.3	0.02840	0.0048

Case Name	k_{eff}	σ_{comp}	AEG	H/X ^①	Pu-240/ Pu Ratio	Experiment Uncertainty σ_{exp}
PUST010_CASE_2.12	1.0136	0.0010	214.882	600.5	0.02890	0.0048
PUST010_CASE_2.9	1.0140	0.0011	215.514	346.8	0.02840	0.0048
PUST010_CASE_3.11	1.0128	0.0011	212.361	542.3	0.02840	0.0048
PUST010_CASE_3.12	1.0208	0.0009	215.036	707	0.02890	0.0048
PUST010_CASE_3.9	1.0120	0.0010	216.250	470.4	0.02840	0.0048
PUST010_CASE_4.11	1.0055	0.0011	214.300	588.7	0.02840	0.0048
PUST010_CASE_4.12	1.0142	0.0009	215.366	825.1	0.02890	0.0048
PUST010_CASE_5.11	1.0068	0.0010	216.852	646.5	0.02840	0.0048
PUST010_CASE_6.11	1.0176	0.0012	215.739	402.3	0.02890	0.0048
PUST010_CASE_7.11	1.0065	0.0010	213.340	519.8	0.02890	0.0048
PUST011_CASE_1.16	1.0135	0.0010	214.790	733	0.04150	0.0052
PUST011_CASE_1.18	1.0001	0.0009	215.818	1157.3	0.04180	0.0052
PUST011_CASE_2.16	1.0196	0.0010	217.686	705.5	0.04150	0.0052
PUST011_CASE_2.18	1.0065	0.0011	215.633	1103.2	0.04180	0.0052
PUST011_CASE_3.16	1.0213	0.0010	217.509	662.8	0.04150	0.0052
PUST011_CASE_3.18	1.0027	0.0010	215.281	1109.8	0.04180	0.0052
PUST011_CASE_4.16	1.0139	0.0011	217.525	653.4	0.04150	0.0052
PUST011_CASE_4.18	0.9991	0.0011	215.196	1053.7	0.04180	0.0052
PUST011_CASE_5.16	1.0113	0.0010	217.313	550.7	0.04150	0.0052
PUST011_CASE_5.18	1.0099	0.0010	214.156	995.4	0.04180	0.0052
PUST011_CASE_6.18	1.0068	0.0010	217.071	870.4	0.04180	0.0052
PUST011_CASE_7.18	1.0050	0.0010	216.471	1056.4	0.04180	0.0052
PUST014_CASE_1	1.0068	0.0012	205.455	210.2	0.04230	0.0032
PUST014_CASE_3	1.0065	0.0010	205.477	210.2	0.04230	0.0032
PUST014_CASE_4	1.0079	0.0011	205.504	210.2	0.04230	0.0032
PUST014_CASE_5	1.0065	0.0011	205.510	210.2	0.04230	0.0032
PUST014_CASE_6	1.0073	0.0013	205.516	210.2	0.04230	0.0032
PUST014_CASE_7	1.0082	0.0012	205.434	210.2	0.04230	0.0043
PUST014_CASE_8	1.0051	0.0012	205.462	210.2	0.04230	0.0032
PUST014_CASE_9	1.0068	0.0012	205.477	210.2	0.04230	0.0032
PUST014_CASE_10	1.0060	0.0011	205.499	210.2	0.04230	0.0032

Case Name	k_{eff}	σ_{comp}	AEG	H/X ^①	Pu-240/ Pu Ratio	Experiment Uncertainty σ_{exp}
PUST014_CASE_11	1.0046	0.0010	205.526	210.2	0.04230	0.0032
PUST014_CASE_12	1.0076	0.0010	205.522	210.2	0.04230	0.0032
PUST014_CASE_13	1.0080	0.0011	205.420	210.2	0.04230	0.0043
PUST014_CASE_14	1.0062	0.0011	205.458	210.2	0.04230	0.0043
PUST014_CASE_15	1.0067	0.0011	205.507	210.2	0.04230	0.0043
PUST014_CASE_16	1.0057	0.0011	205.512	210.2	0.04230	0.0043
PUST014_CASE_17	1.0033	0.0011	205.506	210.2	0.04230	0.0043
PUST014_CASE_18	1.0070	0.0011	205.430	210.2	0.04230	0.0043
PUST014_CASE_19	1.0045	0.0011	205.469	210.2	0.04230	0.0043
PUST014_CASE_20	1.0061	0.0011	205.487	210.2	0.04230	0.0043
PUST014_CASE_21	1.0066	0.0012	205.514	210.2	0.04230	0.0043
PUST014_CASE_22	1.0060	0.0012	205.527	210.2	0.04230	0.0043
PUST014_CASE_23	1.0048	0.0012	205.530	210.2	0.04230	0.0043
PUST014_CASE_24	1.0080	0.0012	205.393	210.2	0.04230	0.0043
PUST014_CASE_25	1.0042	0.0011	205.445	210.2	0.04230	0.0043
PUST014_CASE_26	1.0066	0.0011	205.490	210.2	0.04230	0.0043
PUST014_CASE_27	1.0044	0.0011	205.504	210.2	0.04230	0.0043
PUST014_CASE_28	1.0052	0.0011	205.534	210.2	0.04230	0.0043
PUST014_CASE_29	1.0050	0.0011	205.525	210.2	0.04230	0.0043
PUST014_CASE_30	1.0060	0.0010	205.416	210.2	0.04230	0.0043
PUST014_CASE_31	1.0046	0.0011	205.444	210.2	0.04230	0.0043
PUST014_CASE_33	1.0021	0.0011	205.446	210.2	0.04230	0.0043
PUST014_CASE_34	1.0045	0.0011	205.480	210.2	0.04230	0.0043
PUST015_CASE_1	1.0065	0.0010	201.243	155.3	0.04230	0.0038
PUST015_CASE_2	1.0069	0.0011	201.272	155.3	0.04230	0.0038
PUST015_CASE_3	1.0060	0.0011	201.289	155.3	0.04230	0.0038
PUST015_CASE_4	1.0056	0.0012	201.324	155.3	0.04230	0.0038
PUST015_CASE_5	1.0072	0.0011	201.311	155.3	0.04230	0.0038
PUST015_CASE_6	1.0078	0.0012	201.327	155.3	0.04230	0.0038
PUST015_CASE_7	1.0078	0.0011	201.209	155.3	0.04230	0.0047
PUST015_CASE_8	1.0056	0.0011	201.255	155.3	0.04230	0.0047

Case Name	k_{eff}	σ_{comp}	AEG	H/X ^①	Pu-240/ Pu Ratio	Experiment Uncertainty σ_{exp}
PUST015_CASE_9	1.0062	0.0012	201.292	155.3	0.04230	0.0047
PUST015_CASE_10	1.0060	0.0011	201.333	155.3	0.04230	0.0047
PUST015_CASE_11	1.0012	0.0010	201.196	155.3	0.04230	0.0047
PUST015_CASE_12	1.0053	0.0011	201.280	155.3	0.04230	0.0047
PUST015_CASE_13	1.0084	0.0010	201.307	155.3	0.04230	0.0047
PUST015_CASE_14	1.0065	0.0012	201.335	155.3	0.04230	0.0047
PUST015_CASE_15	1.0082	0.0013	201.196	155.3	0.04230	0.0047
PUST015_CASE_16	1.0064	0.0010	201.222	155.3	0.04230	0.0047
PUST015_CASE_17	1.0067	0.0010	201.299	155.3	0.04230	0.0047
PUST016_CASE_1	1.0077	0.0011	201.225	155.3	0.04230	0.0043
PUST016_CASE_2	1.0048	0.0011	201.265	155.3	0.04230	0.0043
PUST016_CASE_3	1.0072	0.0011	201.295	155.3	0.04230	0.0043
PUST016_CASE_4	1.0075	0.0011	201.318	155.3	0.04230	0.0043
PUST016_CASE_5	1.0054	0.0012	205.463	210.2	0.04230	0.0038
PUST016_CASE_6	1.0047	0.0011	205.476	210.2	0.04230	0.0038
PUST016_CASE_7	1.0093	0.0013	205.511	210.2	0.04230	0.0038
PUST016_CASE_8	1.0072	0.0011	205.508	210.2	0.04230	0.0038
PUST016_CASE_9	1.0070	0.0012	205.607	210.2	0.04230	0.0033
PUST016_CASE_10	1.0065	0.0012	205.556	210.2	0.04230	0.0033
PUST016_CASE_11	1.0063	0.0011	205.516	210.2	0.04230	0.0033
PUST017_CASE_1	1.0076	0.0011	205.535	210.2	0.04230	0.0038
PUST017_CASE_2	1.0050	0.0011	205.488	210.2	0.04230	0.0038
PUST017_CASE_3	1.0041	0.0011	205.492	210.2	0.04230	0.0038
PUST017_CASE_4	1.0054	0.0012	205.482	210.2	0.04230	0.0038
PUST017_CASE_5	1.0066	0.0012	205.488	210.2	0.04230	0.0038
PUST017_CASE_6	1.0056	0.0011	205.479	210.2	0.04230	0.0038
PUST017_CASE_7	1.0069	0.0011	205.485	210.2	0.04230	0.0038
PUST017_CASE_8	1.0051	0.0011	205.497	210.2	0.04230	0.0038
PUST017_CASE_9	1.0071	0.0012	205.525	210.2	0.04230	0.0038
PUST017_CASE_10	1.0060	0.0011	205.500	210.2	0.04230	0.0038
PUST017_CASE_11	1.0050	0.0011	205.531	210.2	0.04230	0.0038

Case Name	k_{eff}	σ_{comp}	AEG	H/X^⓪	Pu-240/ Pu Ratio	Experiment Uncertainty σ_{exp}
PUST017_CASE_12	1.0057	0.0011	205.509	210.2	0.04230	0.0038
PUST017_CASE_13	1.0047	0.0011	205.490	210.2	0.04230	0.0038
PUST017_CASE_14	1.0049	0.0013	205.487	210.2	0.04230	0.0038
PUST017_CASE_15	1.0072	0.0012	205.533	210.2	0.04230	0.0038
PUST017_CASE_16	1.0075	0.0010	205.522	210.2	0.04230	0.0038
PUST017_CASE_17	1.0068	0.0012	205.519	210.2	0.04230	0.0038
PUST017_CASE_18	1.0056	0.0010	205.487	210.2	0.04230	0.0038
PUST020_CASE_1	1.0075	0.0010	215.482	596.5	0.04570	0.0059
PUST020_CASE_2	1.0117	0.0010	215.622	615.6	0.04570	0.0059
PUST020_CASE_3	1.0049	0.0009	216.499	743.8	0.04570	0.0059
PUST020_CASE_5	1.0074	0.0010	213.992	462.9	0.04570	0.0059
PUST020_CASE_6	1.0078	0.0009	213.637	450.5	0.04570	0.0059
PUST020_CASE_7	1.0022	0.0009	216.277	722.9	0.04570	0.0059
PUST020_CASE_8	1.0066	0.0011	210.650	341.1	0.04570	0.0059
PUST020_CASE_9	1.0004	0.0010	214.048	543.2	0.04570	0.0059
PUST021_CASE_7	1.0109	0.0011	215.405	662	0.04570	0.0032
PUST021_CASE_8	1.0044	0.0010	197.712	125	0.04570	0.0065
PUST021_CASE_9	1.0117	0.0010	215.136	634	0.04570	0.0032
PUST021_CASE_10	1.0123	0.0008	218.033	1107	0.04570	0.0025
PUST024_CASE_1	1.0018	0.0010	191.676	87.5	0.18400	0.0062
PUST024_CASE_2	0.9999	0.0009	191.828	87.5	0.18400	0.0062
PUST024_CASE_3	1.0002	0.0011	191.933	87.5	0.18400	0.0062
PUST024_CASE_4	1.0020	0.0010	192.026	87.5	0.18400	0.0062
PUST024_CASE_5	0.9986	0.0011	192.017	87.5	0.18400	0.0062
PUST024_CASE_6	0.9988	0.0009	173.477	44.9	0.18400	0.0077
PUST024_CASE_7	1.0072	0.0010	201.097	143.9	0.18400	0.0053
PUST024_CASE_8	1.0073	0.0010	201.200	143.9	0.18400	0.0053
PUST024_CASE_9	1.0068	0.0010	201.253	143.9	0.18400	0.0053
PUST024_CASE_10	1.0090	0.0010	201.353	143.9	0.18400	0.0053
PUST024_CASE_11	1.0065	0.0011	201.418	143.9	0.18400	0.0053
PUST024_CASE_12	1.0069	0.0010	201.452	143.9	0.18400	0.0053

Case Name	k_{eff}	σ_{comp}	AEG	H/X ^①	Pu-240/ Pu Ratio	Experiment Uncertainty σ_{exp}
PUST024_CASE_13	1.0066	0.0010	201.493	143.9	0.18400	0.0053
PUST024_CASE_14	1.0019	0.0011	197.708	115.8	0.23200	0.0053
PUST024_CASE_15	1.0033	0.0012	197.781	115.8	0.23200	0.0053
PUST024_CASE_16	1.0017	0.0009	197.845	115.8	0.23200	0.0053
PUST024_CASE_17	1.0026	0.0010	197.990	115.8	0.23200	0.0053
PUST024_CASE_18	1.0085	0.0010	212.039	367.3	0.18400	0.0051
PUST024_CASE_19	1.0079	0.0009	212.057	367.3	0.18400	0.0051
PUST024_CASE_20	1.0100	0.0010	212.074	367.3	0.18400	0.0051
PUST024_CASE_21	1.0075	0.0010	212.106	367.3	0.18400	0.0051
PUST024_CASE_22	1.0054	0.0010	212.142	367.3	0.18400	0.0051
PUST024_CASE_23	1.0068	0.0011	212.166	367.3	0.18400	0.0051
233ST001CASE_1	0.9975	0.0008	218.415	1531.5	N/A	0.0031
233ST001CASE_2	0.9959	0.0008	218.224	1471.7	N/A	0.0033
233ST001CASE_3	0.9955	0.0007	218.055	1420.1	N/A	0.0033
233ST001CASE_4	0.9970	0.0007	217.875	1369.7	N/A	0.0033
233ST001CASE_5	0.9956	0.0008	217.697	1325.4	N/A	0.0033
233ST003CASE_40	1.0029	0.0011	192.780	74.1	N/A	0.0087
233ST003CASE_41	1.0164	0.0011	191.195	74.1	N/A	0.0151
233ST003CASE_42	1.0002	0.0013	191.824	74.1	N/A	0.0087
233ST003CASE_45	1.0040	0.0013	180.246	45.9	N/A	0.0126
233ST003CASE_55	1.0102	0.0011	176.271	39.4	N/A	0.0122
233ST003CASE_57	1.0196	0.0012	204.026	154	N/A	0.0087
233ST003CASE_58	1.0119	0.0012	209.393	250	N/A	0.0087
233ST003CASE_61	1.0056	0.0011	211.723	329	N/A	0.0087
233ST003CASE_62	1.0079	0.0012	213.031	396	N/A	0.0087
233ST003CASE_65	1.0039	0.0010	216.519	775	N/A	0.0087
233ST015_CASE_1	0.9928	0.0012	175.241	51.58	N/A	0.0075
233ST015_CASE_2	0.9869	0.0013	173.581	51.58	N/A	0.0070
233ST015_CASE_3	0.9863	0.0012	181.133	51.58	N/A	0.0068
233ST015_CASE_4	0.9863	0.0012	181.133	51.58	N/A	0.0041
233ST015_CASE_5	0.9844	0.0012	172.140	51.58	N/A	0.0055

Case Name	k_{eff}	σ_{comp}	AEG	H/X [ⓐ]	Pu-240/ Pu Ratio	Experiment Uncertainty σ_{exp}
233ST015_CASE_6	0.9750	0.0012	171.626	51.58	N/A	0.0099
233ST015_CASE_7	0.9807	0.0012	179.879	51.58	N/A	0.0070
233ST015_CASE_8	0.9719	0.0012	171.311	51.58	N/A	0.0067
233ST015_CASE_9	0.9664	0.0013	171.019	51.58	N/A	0.0050
233ST015_CASE_10	0.9841	0.0012	174.951	51.58	N/A	0.0051
233ST015_CASE_11	0.9937	0.0012	181.620	64.23	N/A	0.0075
233ST015_CASE_12	0.9942	0.0012	180.243	64.23	N/A	0.0069
233ST015_CASE_13	0.9924	0.0011	179.562	64.23	N/A	0.0069
233ST015_CASE_14	0.9930	0.0011	187.157	64.23	N/A	0.0036
233ST015_CASE_15	0.9881	0.0012	178.911	64.23	N/A	0.0060
233ST015_CASE_16	0.9877	0.0013	178.599	64.23	N/A	0.0043
233ST015_CASE_17	0.9924	0.0012	186.084	64.23	N/A	0.0029
233ST015_CASE_18	0.9727	0.0014	178.045	64.23	N/A	0.0056
233ST015_CASE_19	0.9728	0.0012	177.964	64.23	N/A	0.0052
233ST015_CASE_20	0.9969	0.0011	193.458	102.54	N/A	0.0079
233ST015_CASE_21	0.9992	0.0012	192.290	102.54	N/A	0.0070
233ST015_CASE_22	0.9966	0.0011	191.669	102.54	N/A	0.0062
233ST015_CASE_23	0.9949	0.0011	191.140	102.54	N/A	0.0055
233ST015_CASE_24	0.9901	0.0013	190.850	102.54	N/A	0.0051
233ST015_CASE_25	0.9917	0.0012	196.919	102.54	N/A	0.0023
233ST015_CASE_26	0.9964	0.0011	204.143	199.4	N/A	0.0066
233ST015_CASE_27	0.9982	0.0011	203.709	199.4	N/A	0.0063
233ST015_CASE_28	0.9948	0.0010	203.459	199.4	N/A	0.0058
233ST015_CASE_29	0.9928	0.0012	203.220	199.4	N/A	0.0051
233ST015_CASE_30	0.9940	0.0011	203.118	199.4	N/A	0.0048
233ST015_CASE_31	0.9946	0.0012	203.041	199.4	N/A	0.0055

ⓐ X refers to Pu or U-233 as applicable for the benchmark cases

All cases were run with 1000 neutrons per generation for 1000 generations with the initial 50 generations skipped.

Table 6.5-3 – Calculation of USL

Benchmark Set	Number of Cases	USL vs. AEG	USL vs. H/X	USL vs. Pu-240/Pu
U-233 without Be	15	0.9270	N/A	N/A
U-233 with Be	31	0.9302 (204.14) ^①	N/A	N/A
Pu	196	0.9395	0.9393	0.9395
Pu + U-233 with Be	227	0.9382 ^②	N/A	N/A

① Calculated at maximum AEG of the set 204.14. USL increases with AEG such that this is conservative for the AEG of the calculations (~217)

② Range of applicability is $195.928 < \text{AEG} < 219.83$

This page intentionally left blank.

7.0 OPERATING PROCEDURES

7.1 Procedures for Loading the Package

This section delineates the procedures for loading a payload into the HalfPACT packaging, and leakage rate testing both the outer containment vessel (OCV) and the inner containment vessel (ICV). Hereafter, reference to specific HalfPACT packaging components may be found in [Appendix 1.3.1, *Packaging General Arrangement Drawings*](#).

The loading operation shall be performed in a dry environment. In the event of precipitation during outdoor loading operations, precautions, such as covering the OCV and ICV cavities shall be implemented to prevent water or precipitation from entering the cavities. If precipitation enters the cavities, the free-standing water shall be removed prior to loading the payload.

Based on the current configuration of the HalfPACT packaging when preparing for loading, begin at the section applicable to the following criteria:

- If the HalfPACT package will be loaded while on the transport trailer or railcar, proceed directly to [Section 7.1.2, *Outer Containment Assembly \(OCA\) Lid Removal*](#).
- If the outer containment assembly (OCA) lid has already been removed, proceed directly to [Section 7.1.3, *Inner Containment Vessel \(ICV\) Lid Removal*](#).
- If both the outer containment assembly and inner containment vessel (ICV) lids have already been removed, proceed directly to [Section 7.1.4, *Loading the Payload into the HalfPACT Package*](#).

7.1.1 Removal of the HalfPACT Package from the Transport Trailer/Railcar

1. Uncover the forklift pockets located at the base of the OCA body.
2. Disengage each of the four (4) tie-down devices on the transport trailer or railcar from the corresponding tie-down lugs on the package.

CAUTION: Failure to disengage the tie-down devices may cause damage to the packaging and/or transport trailer/railcar.

3. Using a forklift of appropriate size, position the forklift's forks inside the forklift pockets.
4. Lift the package from the transport trailer or railcar and move the package to the loading station.
5. Place the package in the loading station and remove the forklift.

7.1.2 Outer Containment Assembly (OCA) Lid Removal

1. If necessary, clean the surfaces around the joint between the OCA lid and body as required.
2. Remove the OCV seal test port access plug, OCV seal test port thermal plug, and OCV seal test port plug.

3. Remove the OCV vent port access plug, OCV vent port thermal plug, and OCV vent port cover.
4. Remove the OCV vent port plug to vent the OCV cavity to ambient atmospheric pressure.
5. Remove the six 1/2 inch lock bolts (socket head cap screws) from the exterior of the OCA thermal shield.
6. Install a vacuum pump to the OCV vent port and evacuate the OCV cavity sufficiently to allow the OCV locking ring to freely rotate. Rotate the OCV locking ring approximately 10° counterclockwise until the exterior alignment mark indicates the unlocked position. Disconnect the vacuum system and equalize pressure to the OCV cavity.
7. Rig an overhead crane, or equivalent, with an appropriate lift fixture capable of handling the OCA lid. Engage the lift fixture and remove the OCA lid from the OCA body. Store the OCA lid in a manner such that potential damage to the OCA lid's sealing region is minimized.

7.1.3 Inner Containment Vessel (ICV) Lid Removal

1. Remove the ICV vent port cover, the ICV outer vent port plug, and ICV inner vent port plug to vent the ICV cavity to ambient atmospheric pressure.
2. Remove the ICV seal test port plug.
3. Remove the three 1/2 inch lock bolts (socket head cap screws) from the exterior of the ICV locking ring.
4. Install a vacuum pump to the ICV vent port and evacuate the ICV cavity sufficiently to allow the ICV locking ring to freely rotate. Rotate the ICV locking ring approximately 10° counterclockwise until the exterior alignment mark indicates the unlocked position. Disconnect the vacuum system and equalize pressure to the ICV cavity.
5. Rig an overhead crane, or equivalent, with an appropriate lift fixture capable of handling the ICV lid. Engage the lift fixture and remove the ICV lid from the ICV body. Store the ICV lid in a manner such that potential damage to the ICV lid's sealing region and ICV upper aluminum honeycomb spacer assembly is minimized.

7.1.4 Loading the Payload into the HalfPACT Package

The following loading sequence requires that a payload configuration has been properly prepared per the requirements of the *Contact-Handled Transuranic Waste Authorized Methods for Payload Control (CH-TRAMPAC)*¹.

1. Verify the presence of an ICV upper aluminum honeycomb spacer assembly in the ICV lid, and an ICV lower aluminum honeycomb spacer assembly in the ICV body.
2. Utilizing the 3-inch diameter hole in the ICV lower aluminum honeycomb spacer assembly, inspect the ICV lower head for the presence of water. Remove all free-standing water prior to loading the payload assembly into the ICV cavity.

¹ U.S. Department of Energy (DOE), *Contact-Handled Transuranic Waste Authorized Methods for Payload Control (CH-TRAMPAC)*, U.S. Department of Energy, Carlsbad Field Office, Carlsbad, New Mexico.

3. If the payload assembly is a 55-gallon drum configuration, short 85-gallon drum configuration, 100-gallon drum configuration, or a standard waste box (SWB), install a payload spacer into the bottom of the ICV cavity. If the payload assembly is a shielded container configuration, install an axial dunnage into the bottom of the ICV cavity.
4. Connect an appropriate lifting device to the payload assembly.
5. Balance the payload assembly to ensure the payload does not damage either the ICV or the OCV sealing regions during the loading operation.
6. Lower the payload assembly into the ICV cavity; disconnect and remove the lifting device. If the payload assembly is a shielded container configuration, install an axial dunnage onto the top of the payload assembly.

7.1.5 Inner Containment Vessel (ICV) Lid Installation

1. Visually inspect each of the following ICV components for wear or damage that could impair their function and, if necessary, replace or repair per the requirements of the drawings in [Appendix 1.3.1, Packaging General Arrangement Drawings](#).
 - a. ICV debris shield
 - b. ICV wiper O-ring seal and wiper O-ring holder
 - c. ICV seal test port plug and accompanying O-ring seal
 - d. ICV inner vent port plug and accompanying O-ring seal
 - e. ICV vent port cover and accompanying seal (O-ring or gasket)
 - f. Lock bolts
2. Visually inspect both ICV main O-ring seals. If necessary, remove the O-ring seal(s) and clean the seal(s) and sealing surface(s) on the ICV lid and body to remove contamination. If, during the visual examination, it is determined that damage to the O-ring seal(s) and/or sealing surface(s) is sufficient to impair ICV containment integrity, replace the damaged seal(s) and/or repair the damaged sealing surface(s) per [Section 8.2.3.3.1, Seal Area Routine Inspection and Repair](#).
3. Visually inspect the O-ring seal on the ICV outer vent port plug. If necessary, remove the O-ring seal and clean the seal and sealing surfaces on the ICV outer vent port plug and in the ICV vent port to remove contamination. If, during the visual examination, it is determined that damage to the O-ring seal and/or sealing surface(s) is sufficient to impair ICV containment integrity, replace the damaged seal and/or repair the damaged sealing surface(s) per [Section 8.2.3.3.1, Seal Area Routine Inspection and Repair](#).
4. As an option, sparingly apply vacuum grease to the O-ring seals and install into the appropriate O-ring seal grooves in the ICV body, ICV seal test port and vent port plugs.
5. Rig an overhead crane, or equivalent, with an appropriate lift fixture capable of handling the ICV lid. Engage the lift fixture and install the ICV lid onto the ICV body. Remove the lift fixture.

6. Install a vacuum pump to the ICV vent port and evacuate the ICV cavity sufficiently to allow the ICV locking ring to freely rotate. Rotate the ICV locking ring approximately 10° clockwise until the exterior alignment mark indicates the locked position. After rotating the ICV locking ring, disconnect the vacuum system and equalize pressure to the ICV cavity.
7. Install the three 1/2 inch lock bolts (socket head cap screws) through the cutouts in the ICV locking ring to secure the ICV locking ring in the locked position. Tighten the lock bolts to 28 - 32 lb-ft torque, lubricated.
8. Leakage rate testing of the ICV main O-ring seal shall be performed based on the following criteria:
 - a. If the ICV upper main O-ring seal (containment) is replaced, or the corresponding sealing surface(s) was repaired, then perform the maintenance/periodic leakage rate test per [Section 8.2.2.2, Helium Leakage Rate Testing the ICV Main O-ring Seal](#).
 - b. If there are no changes to the ICV upper main O-ring seal (containment) and no repairs made to the corresponding sealing surfaces, then perform preshipment leakage rate testing per [Section 7.4, Preshipment Leakage Rate Test](#), or per [Section 8.2.2.2, Helium Leakage Rate Testing the ICV Main O-ring Seal](#).
9. Install the ICV seal test port plug; tighten to 55 - 65 lb-in torque.
10. Install the ICV outer vent port plug; tighten to 55 - 65 lb-in torque.
11. Leakage rate testing of the ICV outer vent port plug O-ring seal shall be performed based on the following criteria:
 - a. If the ICV outer vent port plug O-ring seal is replaced, or the corresponding ICV vent port sealing surface was repaired, then perform the maintenance/periodic leakage rate test per [Section 8.2.2.3, Helium Leakage Rate Testing the ICV Outer Vent Port Plug O-ring Seal](#).
 - b. If the ICV outer vent port plug and accompanying O-ring seal are the same as previously removed, and no repairs made to the corresponding sealing surfaces, then perform preshipment leakage rate testing per [Section 7.4, Preshipment Leakage Rate Test](#), or per [Section 8.2.2.3, Helium Leakage Rate Testing the ICV Outer Vent Port Plug O-ring Seal](#).
12. Install the ICV vent port cover; tighten to 55 - 65 lb-in torque.

7.1.6 Outer Containment Assembly (OCA) Lid Installation

1. Visually inspect each of the following OCA components for wear or damage that could impair their function and, if necessary, replace or repair per the requirements of the drawings in [Appendix 1.3.1, Packaging General Arrangement Drawings](#).
 - a. OCV seal test port plug and accompanying O-ring seal
 - b. OCV vent port cover and accompanying O-ring seal
 - c. Lock bolts
2. Visually inspect both OCV main O-ring seals. If necessary, remove the O-ring seal(s) and clean the seal(s) and sealing surface(s) on the OCA lid and body to remove contamination.

If, during the visual examination, it is determined that damage to the O-ring seal(s) and/or sealing surface(s) is sufficient to impair OCV containment integrity, replace the damaged seal(s) and/or repair the damaged sealing surface(s) per [Section 8.2.3.3.1, Seal Area Routine Inspection and Repair](#).

3. Visually inspect the O-ring seal on the OCV vent port plug. If necessary, remove the O-ring seal and clean the seal and sealing surfaces on the OCV vent port plug and in the OCV vent port to remove contamination. If, during the visual examination, it is determined that damage to the O-ring seal and/or sealing surface(s) is sufficient to impair OCV containment integrity, replace the damaged seal and/or repair the damaged sealing surface(s) per [Section 8.2.3.3.1, Seal Area Routine Inspection and Repair](#).
4. As an option, sparingly apply vacuum grease to the O-ring seals and install into the appropriate O-ring seal grooves in the OCV body, OCV seal test port plug and OCV vent port plug.
5. Rig an overhead crane, or equivalent, with an appropriate lift fixture capable of handling the OCA lid. Engage the lift fixture and install the OCA lid onto the OCA body. Remove the lift fixture.
6. Install a vacuum pump to the OCV vent port and evacuate the OCV cavity sufficiently to allow the OCV locking ring to freely rotate. Rotate the OCV locking ring approximately 10° clockwise until the alignment mark indicates the locked position. After rotating the OCV locking ring, disconnect the vacuum system and equalize pressure to the OCV cavity.
7. Install the six 1/2 inch lock bolts (socket head cap screws) through the cutouts in the OCA outer thermal shield to secure the OCV locking ring in the locked position. Tighten the lock bolts to 28 - 32 lb-ft torque, lubricated.
8. Leakage rate testing of the OCV main O-ring seal shall be performed based on the following criteria:
 - a. If the OCV upper main O-ring seal (containment) is replaced, or the corresponding sealing surface(s) was repaired, then perform the maintenance/periodic leakage rate test per [Section 8.1.3.6, Helium Leakage Rate Testing the OCV Main O-ring Seal Integrity](#).
 - b. If there are no changes to the OCV upper main O-ring seal (containment) and no repairs made to the corresponding sealing surfaces, then perform preshipment leakage rate testing per [Section 7.4, Preshipment Leakage Rate Test](#), or per [Section 8.1.3.6, Helium Leakage Rate Testing the OCV Main O-ring Seal Integrity](#).
9. Install the OCV seal test port plug; tighten to 55 - 65 lb-in torque. Install the OCV seal test port thermal plug and the OCV seal test port access plug; tighten to 28 - 32 lb-ft torque.
10. Install the OCV vent port plug; tighten to 55 - 65 lb-in torque.
11. Leakage rate testing of the OCV vent port plug O-ring seal shall be performed based on the following criteria:
 - a. If the OCV vent port plug O-ring seal is replaced, or the corresponding OCV vent port sealing surface was repaired, then perform the maintenance/periodic leakage rate test per [Section 8.1.3.7, Helium Leakage Rate Testing the OCV Vent Port Plug O-ring Seal Integrity](#).

- b. If the OCV vent port plug and accompanying O-ring seal are the same as previously removed, and no repairs made to the corresponding sealing surfaces, then perform preshipment leakage rate testing per [Section 7.4, *Preshipment Leakage Rate Test*](#), or per [Section 8.1.3.7, *Helium Leakage Rate Testing the OCV Vent Port Plug O-ring Seal Integrity*](#).

12. Install the OCV vent port cover; tighten to 55 – 65 lb-in torque.

13. Install the OCV vent port thermal plug and the OCV vent port access plug; tighten to 28 - 32 lb-ft torque.

7.1.7 Final Package Preparations for Transport (Loaded)

1. Install the two tamper-indicating devices (security seals). One security seal is located at the OCA vent port access plug; the second is located at an OCA lock bolt.
2. If the HalfPACT package is not already loaded onto the transport trailer or railcar, perform the following steps:
 - a. Using a forklift of appropriate size, position the forklift's forks inside the forklift pockets.
 - b. Lift the loaded HalfPACT package, aligning the packaging over the tie-down points on the transport trailer or railcar.
 - c. Secure the loaded HalfPACT package to the transport trailer or railcar using the appropriate tie-down devices.
 - d. Load as many as three HalfPACT packages per transport trailer or up to seven HalfPACT packages per railcar.
 - e. Install forklift pocket covers over the four forklift pockets located at the base of the OCA body.
3. Monitor external radiation for each loaded HalfPACT package per the guidelines of 49 CFR §173.441².
4. Determine that surface contamination levels for each loaded HalfPACT package are per the guidelines of 49 CFR §173.443.
5. Determine the shielding Transport Index (TI) for each loaded HalfPACT package per the guidelines of 49 CFR §173.403.
6. Complete all necessary shipping papers in accordance with Subpart C of 49 CFR 172³.
7. HalfPACT package marking shall be in accordance with 10 CFR §71.85(c)⁴ and Subpart D of 49 CFR 172. Package labeling shall be in accordance with Subpart E of 49 CFR 172. Package placarding shall be in accordance with Subpart F of 49 CFR 172.

² Title 49, Code of Federal Regulations, Part 173 (49 CFR 173), *Shippers—General Requirements for Shipments and Packagings*, 10-01-06 Edition.

³ Title 49, Code of Federal Regulations, Part 172 (49 CFR 172), *Hazardous Materials Tables and Hazardous Communications Regulations*, 10-01-06 Edition.

⁴ Title 10, Code of Federal Regulations, Part 71 (10 CFR 71), *Packaging and Transportation of Radioactive Material*, 01-01-07 Edition.

7.2 Procedures for Unloading the Package

This section delineates the procedures for unloading a payload from the HalfPACT packaging. Hereafter, reference to specific HalfPACT packaging components may be found in [Appendix 1.3.1, *Packaging General Arrangement Drawings*](#).

The unloading operation shall be performed in a dry environment. In the event of precipitation during outdoor unloading operations, precautions, such as covering the outer containment vessel (OCV) and inner containment vessel (ICV) cavities shall be implemented to prevent water or precipitation from entering the cavities. If precipitation enters the cavities, the free-standing water shall be removed prior to installing the lids.

- If the HalfPACT package will be unloaded while on the transport trailer or railcar, proceed directly to [Section 7.2.2, *Outer Containment Assembly \(OCA\) Lid Removal*](#).

7.2.1 Removal of the HalfPACT Package from the Transport Trailer/Railcar

1. Uncover the forklift pockets located at the base of the OCA body.
2. Disengage each of the four (4) tie-down devices on the transport trailer or railcar from the corresponding tie-down lugs on the package.

CAUTION: Failure to disengage the tie-down devices may cause damage to the packaging and/or transport trailer/railcar.

3. Using a forklift of appropriate size, position the forklift's forks inside the forklift pockets.
4. Lift the package from the transport trailer or railcar and move the package to the loading station.
5. Place the package in the loading station and remove the forklift.

7.2.2 Outer Containment Assembly (OCA) Lid Removal

1. If necessary, clean the surfaces around the joint between the OCA lid and body as required.
2. Remove the OCV seal test port access plug, OCV seal test port thermal plug, and OCV seal test port plug.
3. Remove the OCV vent port access plug, OCV vent port thermal plug, and OCV vent port cover.
4. Remove the OCV vent port plug to vent the OCV cavity to ambient atmospheric pressure.
5. Remove the six 1/2 inch lock bolts (socket head cap screws) from the exterior of the OCA thermal shield.
6. Install a vacuum pump to the OCV vent port and evacuate the OCV cavity sufficiently to allow the OCV locking ring to freely rotate. Rotate the OCV locking ring approximately 10° counterclockwise until the exterior alignment mark indicates the unlocked position. Disconnect the vacuum system and equalize pressure to the OCV cavity.

7. Rig an overhead crane, or equivalent, with an appropriate lift fixture capable of handling the OCA lid. Engage the lift fixture and remove the OCA lid from the OCA body. Store the OCA lid in a manner such that potential damage to the OCA lid's sealing region is minimized.

7.2.3 Inner Containment Vessel (ICV) Lid Removal

1. Remove the ICV vent port cover, the ICV outer vent port plug, and ICV inner vent port plug to vent the ICV cavity to ambient atmospheric pressure.
2. Remove the ICV seal test port plug.
3. Remove the three 1/2 inch lock bolts (socket head cap screws) from the exterior of the ICV locking ring.
4. Install a vacuum pump to the ICV vent port and evacuate the ICV cavity sufficiently to allow the ICV locking ring to freely rotate. Rotate the ICV locking ring approximately 10° counterclockwise until the alignment mark indicates the unlocked position. Disconnect the vacuum system and equalize pressure to the ICV cavity.
5. Rig an overhead crane, or equivalent, with an appropriate lift fixture capable of handling the ICV lid. Engage the lift fixture and remove the ICV lid from the ICV body. Store the ICV lid in a manner such that potential damage to the ICV lid's sealing region and ICV upper aluminum honeycomb spacer assembly is minimized.

7.2.4 Unloading the Payload from the HalfPACT Package

1. Connect an appropriate lifting device to the payload assembly. If the payload assembly is a shielded container configuration, remove the axial dunnage from the top of the payload assembly first.
2. Balance the payload assembly sufficiently to ensure the payload does not damage either the ICV or the OCV sealing regions during the unloading operation.
3. Remove the payload assembly from the ICV cavity; disconnect and remove the lifting device.

7.2.5 Inner Containment Vessel (ICV) Lid Installation

1. Visually inspect each of the following ICV components for wear or damage that could impair their function and, if necessary, replace or repair per the requirements of the drawings in [Appendix 1.3.1, *Packaging General Arrangement Drawings*](#).
 - a. ICV debris shield
 - b. ICV wiper O-ring seal and wiper O-ring holder
 - c. ICV main O-ring seals and sealing surfaces
 - d. ICV seal test port plug and accompanying O-ring seal
 - e. ICV inner and outer vent port plugs and accompanying O-ring seals
 - f. ICV vent port cover and accompanying seal (O-ring or gasket)

- g. Lock bolts
2. As an option, sparingly apply vacuum grease to the O-ring seals and install into the appropriate O-ring seal grooves in the ICV body, ICV seal test port and vent port plugs.
 3. Rig an overhead crane, or equivalent, with an appropriate lift fixture capable of handling the ICV lid. Engage the lift fixture and install the ICV lid onto the ICV body. Remove the lift fixture.
 4. Install a vacuum pump to the ICV vent port and evacuate the ICV cavity sufficiently to allow the ICV locking ring to freely rotate. Rotate the ICV locking ring approximately 10° clockwise until the alignment mark indicates the locked position. After rotating the ICV locking ring, disconnect the vacuum system and equalize pressure to the ICV cavity.
 5. Install the three 1/2 inch lock bolts (socket head cap screws) through the cutouts in the ICV locking ring to secure the ICV locking ring in the locked position. Tighten the lock bolts to 28 - 32 lb-ft torque, lubricated.
 6. Install the ICV seal test port plug; tighten to 55 - 65 lb-in torque.
 7. Install the ICV inner and outer vent port plugs, followed by the ICV vent port cover; tighten each to 55 - 65 lb-in torque.

7.2.6 Outer Containment Assembly (OCA) Lid Installation

1. Visually inspect each of the following OCA components for wear or damage that could impair their function and, if necessary, replace or repair per the requirements of the drawings in [Appendix 1.3.1, *Packaging General Arrangement Drawings*](#).
 - a. OCV main O-ring seals and sealing surfaces
 - b. OCV seal test port plug and accompanying O-ring seal
 - c. OCV vent port plug and accompanying O-ring seal
 - d. OCV vent port cover and accompanying O-ring seal
 - e. Lock bolts
2. As an option, sparingly apply vacuum grease to the O-ring seals and install into the appropriate O-ring seal grooves in the OCV body, OCV seal test port and vent port plugs.
3. Rig an overhead crane, or equivalent, with an appropriate lift fixture capable of handling the OCA lid. Engage the lift fixture and install the OCA lid onto the OCA body. Remove the lift fixture.
4. Install a vacuum pump to the OCV vent port and evacuate the OCV cavity sufficiently to allow the OCV locking ring to freely rotate. Rotate the OCV locking ring approximately 10° clockwise until the alignment mark indicates the locked position. After rotating the OCV locking ring, disconnect the vacuum system and equalize pressure to the OCV cavity.
5. Install the six 1/2 inch lock bolts (socket head cap screws) through the cutouts in the OCA outer thermal shield to secure the OCV locking ring in the locked position. Tighten the lock bolts to 28 - 32 lb-ft torque, lubricated.

6. Install the OCV seal test port plug; tighten to 55 - 65 lb-in torque. Install the OCV seal test port thermal plug and the OCV seal test port access plug; tighten to 28 - 32 lb-ft torque.
7. Install the OCV vent port plug and OCV vent port cover; tighten each to 55 - 65 lb-in torque. Install the OCV vent port thermal plug and the OCV vent port access plug; tighten to 28 - 32 lb-ft torque.

7.2.7 Final Package Preparations for Transport (Unloaded)

1. If the HalfPACT package is not already loaded onto the transport trailer or railcar, perform the following steps:
 - a. Using a forklift of appropriate size, position the forklift's forks inside the forklift pockets.
 - b. Lift the HalfPACT package, aligning the packaging over the tie-down points on the transport trailer or railcar.
 - c. Secure the HalfPACT package to the transport trailer or railcar using the appropriate tie-down devices.
 - d. Load as many as three HalfPACT packages per transport trailer or up to seven HalfPACT packages per railcar.
 - e. Install forklift pocket covers over the four forklift pockets located at the base of the OCA body.
2. Transport the HalfPACT package in accordance with [Section 7.3, *Preparation of an Empty Package for Transport*](#).

7.3 Preparation of an Empty Package for Transport

Previously used and empty HalfPACT packagings shall be prepared and transported per the requirements of 49 CFR §173.428¹.

¹ Title 49, Code of Federal Regulations, Part 173 (49 CFR 173), *Shippers—General Requirements for Shipments and Packagings*, 10-01-06 Edition.

This page intentionally left blank.

7.4 Preshipment Leakage Rate Test

After the HalfPACT package is assembled and prior to shipment, leakage rate testing shall be performed to confirm proper assembly of the package following the guidelines of Section 7.6, *Preshipment Leakage Rate Test*, and Appendix A.5.2, *Gas Pressure Rise*, of ANSI N14.5¹.

7.4.1 Gas Pressure Rise Leakage Rate Test Acceptance Criteria

In order to demonstrate containment integrity in preparation for shipment, no leakage shall be detected when tested to a sensitivity of 1×10^{-3} reference cubic centimeters per second (scc/s) air, or less, per Section 7.6, *Preshipment Leakage Rate Test*, of ANSI N14.5.

7.4.2 Determining the Test Volume and Test Time

1. Assemble a leakage rate test apparatus that consists of, at a minimum, the components illustrated in Figure 7.4-1, using a calibrated volume with a range of 100 - 500 cubic centimeters, and a calibrated pressure transducer with a minimum sensitivity of 100 millitorr. Connect the test apparatus to the test volume (i.e., the OCV or ICV seal test port, or OCV or ICV vent port, as appropriate).
2. Set the indicated sensitivity on the digital readout of the calibrated pressure transducer, ΔP , to, at a minimum, the resolution (i.e., sensitivity) of the calibrated pressure transducer (e.g., $\Delta P = 1, 10, \text{ or } 100$ millitorr for a pressure transducer with a 1 millitorr sensitivity).
3. Open all valves (i.e., the vent valve, calibration valve, and vacuum pump isolation valve), and record ambient atmospheric pressure, P_{atm} .
4. Isolate the calibrated volume by closing the vent and calibration valves.
5. Evacuate the test volume to a pressure less than the indicated sensitivity on the digital readout of the calibrated pressure transducer or 0.76 torr, whichever is less.
6. Isolate the vacuum pump from the test volume by closing the vacuum pump isolation valve. Allow the test volume pressure to stabilize and record the test volume pressure, P_{test} (e.g., $P_{\text{test}} < 1$ millitorr for an indicated sensitivity of 1 millitorr).
7. Open the calibration valve and, after allowing the system to stabilize, record the total volume pressure, P_{total} .
8. Knowing the calibrated volume, V_c , calculate and record the test volume, V_t , using the following equation:

$$V_t = V_c \left(\frac{P_{\text{atm}} - P_{\text{total}}}{P_{\text{total}} - P_{\text{test}}} \right)$$

9. Knowing the indicated sensitivity on the digital readout of the calibrated pressure transducer, ΔP , calculate and record the test time, t , using the following equation:

$$t = \Delta P(1.32)V_t$$

¹ ANSI N14.5-1997, *American National Standard for Radioactive Materials - Leakage Tests on Packages for Shipment*, American National Standards Institute, Inc. (ANSI).

7.4.3 Performing the Gas Pressure Rise Leakage Rate Test

1. Isolate the calibrated volume by closing the calibration valve.
2. Open the vacuum pump isolation valve and evacuate the test volume to a pressure less than the test volume pressure, P_{test} , determined in step 6 of [Section 7.4.2, *Determining the Test Volume and Test Time*](#).
3. Isolate the vacuum pump from the test volume by closing the vacuum pump isolation valve. Allow the test volume pressure to stabilize and record the beginning test pressure, P_1 . After a period of time equal to “t” seconds, determined in step 9 of [Section 7.4.2, *Determining the Test Volume and Test Time*](#), record the ending test pressure, P_2 . To be acceptable, there shall be no difference between the final and initial pressures such that the requirements of [Section 7.4.1, *Gas Pressure Rise Leakage Rate Test Acceptance Criteria*](#), are met.
4. If, after repeated attempts, the O-ring seal fails to pass the leakage rate test, replace the damaged seal and/or repair the damaged sealing surfaces per [Section 8.2.3.3.1, *Seal Area Routine Inspection and Repair*](#). Perform verification leakage rate test per the applicable procedure delineated in [Section 8.2.2, *Maintenance/Periodic Leakage Rate Tests*](#).

7.4.4 Optional Preshipment Leakage Rate Test

As an option to [Section 7.4.3, *Performing the Gas Pressure Rise Leakage Rate Test*](#), [Section 8.2.2, *Maintenance/Periodic Leakage Rate Tests*](#), may be performed.

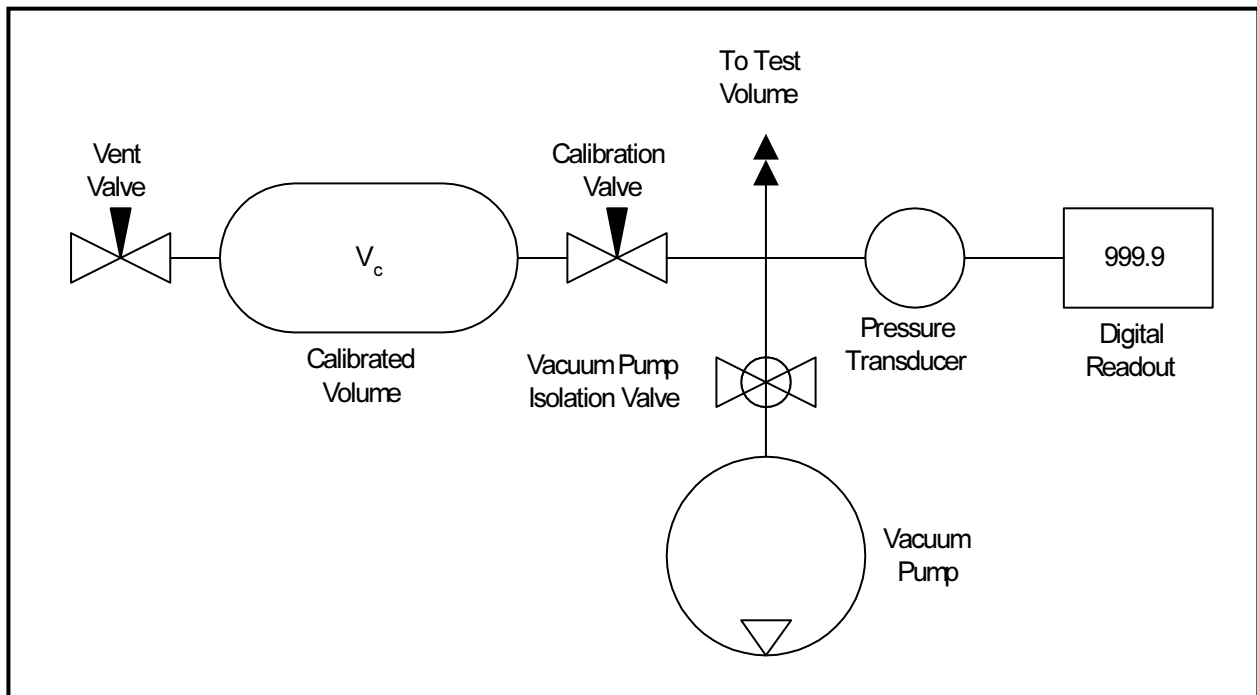


Figure 7.4-1 – Pressure Rise Leakage Rate Test Schematic

8.0 ACCEPTANCE TESTS AND MAINTENANCE PROGRAM

8.1 Acceptance Tests

Per the requirements of 10 CFR §71.85¹, this section discusses the inspections and tests to be performed prior to first use of the HalfPACT packaging.

8.1.1 Visual Inspection

All HalfPACT packaging materials of construction and welds shall be examined in accordance with requirements delineated on the drawings in [Appendix 1.3.1, *Packaging General Arrangement Drawings*](#), per the requirements of 10 CFR §71.85(a). Furthermore, the inspections and tests of [Section 8.2.3.3, *Seal Areas and Grooves*](#), shall be performed prior to pressure and leakage rate testing.

8.1.2 Structural and Pressure Tests

8.1.2.1 Lifting Device Load Testing

The bounding design load of the OCA lid lifting devices is 7,500 pounds total, or 2,500 pounds per lifting point. Load test each set of OCA lid lifting devices to 150% of their bounding design load, 11,250 pounds total, or 3,750 pounds per lifting point. Perform load testing of the OCA lid lifting devices prior to polyurethane foam installation.

The bounding design load of the ICV lifting sockets is 5,000 pounds total, or 1,667 pounds per lifting socket. Load test each set of ICV lifting sockets to 150% of their bounding design load, 7,500 pounds total, or 2,500 pounds per lifting socket.

Following load testing, all accessible base material and welds and adjacent base metal (minimum 1/2 inch on each side of the weld) directly related to load testing shall be visually inspected for plastic deformation or cracking, and liquid penetrant inspected per ASME Boiler and Pressure Vessel Code, Section V², Article 6, and ASME Boiler and Pressure Vessel Code, Section III³, Division 1, Subsection NB, Article NB-5000. Indications of cracking or distortion shall be recorded on a nonconformance report and dispositioned prior to final acceptance in accordance with the cognizant quality assurance program.

8.1.2.2 Containment Vessel Pressure Testing

Per the requirements of 10 CFR §71.85(b), the outer containment vessel (OCV) and inner containment vessel (ICV) shall be pressure tested to 150% of the maximum normal operating

¹ Title 10, Code of Federal Regulations, Part 71 (10 CFR 71), *Packaging and Transportation of Radioactive Material*, 01-01-07 Edition.

² American Society of Mechanical Engineers (ASME) Boiler and Pressure Vessel Code, Section V, *Nondestructive Examination*, 1995 Edition, 1997 Addenda.

³ American Society of Mechanical Engineers (ASME) Boiler and Pressure Vessel Code, Section III, *Rules for Construction of Nuclear Power Plant Components*, 1995 Edition, 1997 Addenda.

pressure (MNOP) to verify structural integrity. The MNOP of the OCV and ICV is equal to the 50 psig design pressure. Thus, each containment vessel shall be pressure tested to $50 \times 1.5 = 75$ psig.

Following containment vessel pressure testing, all accessible welds and adjacent base metal (minimum 1/2 inch on each side of the weld) directly related to the pressure testing of the containment vessels shall be visually inspected for plastic deformation or cracking, and liquid penetrant inspected per ASME Boiler and Pressure Vessel Code, Section V, Article 6, and ASME Boiler and Pressure Vessel Code, Section III, Division 1, Subsection NB, Article NB-5000, as delineated on the drawings in [Appendix 1.3.1, Packaging General Arrangement Drawings](#). Indications of cracking or distortion shall be recorded on a nonconformance report and dispositioned prior to final acceptance in accordance with the cognizant quality assurance program.

Leakage rate testing per [Section 8.1.3, Fabrication Leakage Rate Tests](#), shall be performed after completion of pressure testing to verify package configuration and performance to design criteria.

8.1.3 Fabrication Leakage Rate Tests

This section provides the generalized procedure for fabrication leakage rate testing of the containment vessel boundaries and penetrations following the completion of fabrication. Fabrication leakage rate testing shall follow the guidelines of Section 7.3, *Fabrication Leakage Rate Test*, of ANSI N14.5⁴.

Prior to leakage rate testing, internal components such as the payload and spacer pallets, ICV aluminum honeycomb spacer assemblies, etc., shall be removed. For ease of leakage rate testing, each containment vessel should be thoroughly cleaned.

Fabrication leakage rate testing shall be performed on the inner containment vessel (ICV) and outer containment vessel (OCV). Six separate tests comprise the series with three on each containment vessel. Each test shall meet the acceptance criteria delineated in [Section 8.1.3.1, Fabrication Leakage Rate Test Acceptance Criteria](#).

8.1.3.1 Fabrication Leakage Rate Test Acceptance Criteria

1. To be acceptable, each leakage rate test shall demonstrate a “leaktight” leakage rate of 1×10^{-7} reference cubic centimeters per second (scc/s), air, or less, per Section 6.3, *Application of Referenced Air Leakage Rate (L_R)*, of ANSI N14.5.
2. In order to demonstrate a leaktight leakage rate, the sensitivity of the leakage rate test procedure shall be 5×10^{-8} scc/s, air, or less, per Section 8.4, *Sensitivity*, of ANSI N14.5.

8.1.3.2 Helium Leakage Rate Testing the ICV Structure Integrity

1. The fabrication leakage rate test of the ICV structure shall be performed following the guidelines of Section A.5.4, *Evacuated Envelope – Gas Detector*, of ANSI N14.5.
2. The ICV shall be assembled with both main O-ring seals installed into the ICV lower seal flange. Assembly is as shown in [Appendix 1.3.1, Packaging General Arrangement Drawings](#).

⁴ ANSI N14.5-1997, *American National Standard for Radioactive Materials – Leakage Tests on Packages for Shipment*, American National Standards Institute, Inc. (ANSI).

3. Install the assembled ICV into a functional OCV body.
4. Remove the ICV vent port cover, ICV outer vent port plug, and ICV inner vent port plug.
5. Connect a vacuum pump to the ICV vent port and evacuate the ICV cavity to 90% vacuum or better (i.e., $\leq 10\%$ ambient atmospheric pressure).
6. Provide a helium atmosphere inside the ICV cavity by backfilling with helium gas to a pressure slightly greater than atmospheric pressure (+1 psi, -0 psi).
7. Install the ICV outer vent port plug, followed by the ICV vent port cover; tighten each to 55 - 65 lb-in torque.
8. Ensure the OCV vent port access plug, OCV vent port thermal plug, OCV vent port cover, and OCV vent port plug have been removed from the OCV body.
9. With both main O-ring seals installed into the OCV lower seal flange, install the OCV lid. Assembly is as shown in [Appendix 1.3.1, *Packaging General Arrangement Drawings*](#).
10. Install a helium mass spectrometer leak detector to the OCV vent port. Evacuate through the OCV vent port until the vacuum is sufficient to operate the helium mass spectrometer leak detector.
11. Perform the helium leakage rate test to the requirements of [Section 8.1.3.1, *Fabrication Leakage Rate Test Acceptance Criteria*](#). If, after repeated attempts, the ICV structure fails to pass the leakage rate test, isolate the leak path and, prior to repairing the leak path and repeating the leakage rate test, record on a nonconformance report and disposition prior to final acceptance in accordance with the cognizant quality assurance program.

8.1.3.3 Helium Leakage Rate Testing the ICV Main O-ring Seal

1. The fabrication leakage rate test of the ICV main O-ring seal shall be performed following the guidelines of Section A.5.4, *Evacuated Envelope – Gas Detector*, of ANSI N14.5.
2. The ICV shall be assembled with both main O-ring seals installed into the ICV lower seal flange. Assembly is as shown in [Appendix 1.3.1, *Packaging General Arrangement Drawings*](#).
3. Remove the ICV vent port cover, outer vent port plug, and inner vent port plug.
4. Connect a vacuum pump to the ICV vent port and evacuate the ICV cavity to 90% vacuum or better (i.e., $\leq 10\%$ ambient atmospheric pressure).
5. Remove the ICV seal test port plug and install a helium mass spectrometer leak detector to the ICV seal test port. Evacuate through the ICV seal test port until the vacuum is sufficient to operate the helium mass spectrometer leak detector.
6. Provide a helium atmosphere inside the ICV cavity by backfilling with helium gas to a pressure slightly greater than atmospheric pressure (+1 psi, -0 psi).
7. Perform the helium leakage rate test to the requirements of [Section 8.1.3.1, *Fabrication Leakage Rate Test Acceptance Criteria*](#). If, after repeated attempts, the ICV main O-ring seal fails to pass the leakage rate test, isolate the leak path and, prior to repairing the leak path and repeating the leakage rate test, record on a nonconformance report and disposition prior to final acceptance in accordance with the cognizant quality assurance program.

8.1.3.4 Helium Leakage Rate Testing the ICV Outer Vent Port Plug O-ring Seal

1. The fabrication leakage rate test of the ICV outer vent port plug O-ring seal shall be performed following the guidelines of Section A.5.4, *Evacuated Envelope – Gas Detector*, of ANSI N14.5.
2. The ICV shall be assembled with both main O-ring seals installed into the ICV lower seal flange. Assembly is as shown in [Appendix 1.3.1, Packaging General Arrangement Drawings](#).
3. Remove the ICV vent port cover, ICV outer vent port plug, and the ICV inner vent port plug.
4. Connect a vacuum pump to the ICV vent port and evacuate the ICV cavity to 90% vacuum or better (i.e., $\leq 10\%$ ambient atmospheric pressure).
5. Provide a helium atmosphere inside the ICV cavity by backfilling with helium gas to a pressure slightly greater than atmospheric pressure (+1 psi, -0 psi).
6. Install the ICV outer vent port plug; tighten to 55 - 65 lb-in torque.
7. Install a helium mass spectrometer leak detector to the ICV vent port. Evacuate through the ICV vent port until the vacuum is sufficient to operate the helium mass spectrometer leak detector.
8. Perform the helium leakage rate test to the requirements of [Section 8.1.3.1, Fabrication Leakage Rate Test Acceptance Criteria](#). If, after repeated attempts, the ICV outer vent port plug O-ring seal fails to pass the leakage rate test, isolate the leak path and, prior to repairing the leak path and repeating the leakage rate test, record on a nonconformance report and disposition prior to final acceptance in accordance with the cognizant quality assurance program.

8.1.3.5 Helium Leakage Rate Testing the OCV Structure Integrity

1. The fabrication leakage rate test of the OCV structure shall be performed following the guidelines of Section A.5.3, *Gas Filled Envelope – Gas Detector*, of ANSI N14.5.
2. Remove the OCV vent port access plug, OCV vent port thermal plug, OCV vent port cover, and OCV vent port plug.
3. Install the OCV lid with both main O-ring seals installed into the OCV lower seal flange. As an option, an assembled ICV may be placed within the OCV cavity for volume reduction. Assembly is as shown in [Appendix 1.3.1, Packaging General Arrangement Drawings](#).
4. Install a helium mass spectrometer leak detector to the OCV vent port. Evacuate through the OCV vent port until the vacuum is sufficient to operate the helium mass spectrometer leak detector.
5. Surround the assembled OCV with an envelope filled with helium.
6. Perform the helium leakage rate test to the requirements of [Section 8.1.3.1, Fabrication Leakage Rate Test Acceptance Criteria](#). If, after repeated attempts, the OCV structure fails to pass the leakage rate test, isolate the leak path and, prior to repairing the leak path and repeating the leakage rate test, record on a nonconformance report and disposition prior to final acceptance in accordance with the cognizant quality assurance program.

8.1.3.6 Helium Leakage Rate Testing the OCV Main O-ring Seal Integrity

1. The fabrication leakage rate test of the OCV main O-ring seal shall be performed following the guidelines of Section A.5.4, *Evacuated Envelope – Gas Detector*, of ANSI N14.5.
2. The OCA shall be assembled with both main O-ring seals installed into the OCV lower seal flange. Assembly is as shown in [Appendix 1.3.1, *Packaging General Arrangement Drawings*](#).
3. Remove the OCV vent port access plug, OCV vent port thermal plug, OCV vent port cover, and OCV vent port plug.
4. Connect a vacuum pump to the OCV vent port and evacuate the OCV cavity to 90% vacuum or better (i.e., $\leq 10\%$ ambient atmospheric pressure).
5. Remove the OCV seal test port access plug, OCV seal test port thermal plug, and OCV seal test port plug and install a helium mass spectrometer leak detector to the OCV seal test port. Evacuate through the OCV seal test port until the vacuum is sufficient to operate the helium mass spectrometer leak detector.
6. Provide a helium atmosphere inside the OCV cavity by backfilling with helium gas to a pressure slightly greater than atmospheric pressure (+1 psi, -0 psi).
7. Perform the helium leakage rate test to the requirements of [Section 8.1.3.1, *Fabrication Leakage Rate Test Acceptance Criteria*](#). If, after repeated attempts, the OCV main O-ring seal fails to pass the leakage rate test, isolate the leak path and, prior to repairing the leak path and repeating the leakage rate test, record on a nonconformance report and disposition prior to final acceptance in accordance with the cognizant quality assurance program.

8.1.3.7 Helium Leakage Rate Testing the OCV Vent Port Plug O-ring Seal Integrity

1. The fabrication leakage rate test of the OCV vent port plug O-ring seal shall be performed following the guidelines of Section A.5.4, *Evacuated Envelope – Gas Detector*, of ANSI N14.5.
2. The OCV shall be assembled with both main O-ring seals installed into the OCV lower seal flange. Assembly is as shown in [Appendix 1.3.1, *Packaging General Arrangement Drawings*](#).
3. Remove the OCV vent port access plug, OCV vent port thermal plug, OCV vent port cover, and OCV vent port plug.
4. Connect a vacuum pump to the OCV vent port and evacuate the OCV cavity to 90% vacuum or better (i.e., $\leq 10\%$ ambient atmospheric pressure).
5. Provide a helium atmosphere inside the OCV cavity by backfilling with helium gas to a pressure slightly greater than atmospheric pressure (+1 psi, -0 psi).
6. Install the OCV vent port plug; tighten to 55 - 65 lb-in torque.
7. Install a helium mass spectrometer leak detector to the OCV vent port. Evacuate through the OCV vent port until the vacuum is sufficient to operate the helium mass spectrometer leak detector.

8. Perform the helium leakage rate test to the requirements of [Section 8.1.3.1, *Fabrication Leakage Rate Test Acceptance Criteria*](#). If, after repeated attempts, the OCV vent port plug O-ring seal fails to pass the leakage rate test, isolate the leak path and, prior to repairing the leak path and repeating the leakage rate test, record on a nonconformance report and disposition prior to final acceptance in accordance with the cognizant quality assurance program.

8.1.4 Component Tests

8.1.4.1 Polyurethane Foam

This section establishes the requirements and acceptance criteria for installation, inspection, and testing of rigid, closed-cell, polyurethane foam utilized within the HalfPACT packaging.

8.1.4.1.1 Introduction and General Requirements

The polyurethane foam used within the HalfPACT packaging is comprised of a specific “formulation” of foam constituents that, when properly apportioned, mixed, and reacted, produce a polyurethane foam material with physical characteristics consistent with the requirements given in this section. In practice, the chemical constituents are batched into multiple parts (e.g., parts A and B) for later mixing in accordance with a formulation. Therefore, a foam “batch” is considered to be a specific grouping and apportionment of chemical constituents into separate and controlled vats or bins for each foam formulation part. Portions from each batch part are combined in accordance with the foam formulation requirements to produce the liquid foam material for pouring into a component. Thus, a foam “pour” is defined as apportioning and mixing the batch parts into a desired quantity for subsequent installation (pouring).

The following sections describe the general requirements for chemical composition, constituent storage, foamed component preparation, foam material installation, and foam pour and test data records.

8.1.4.1.1.1 Polyurethane Foam Chemical Composition

The foam supplier shall certify that the chemical composition of the polyurethane foam is as delineated below, with the chemical component weight percents falling within the specified ranges. In addition, the foam supplier shall certify that the finished (cured) polyurethane foam does not contain halogen-type flame retardants or trichloromonofluoromethane (Freon 11).

Carbon.....	50% – 70%	Phosphorus.....	0% – 2%
Oxygen.....	14% – 34%	Silicon	< 1%
Nitrogen	4% – 12%	Chlorine	< 1%
Hydrogen.....	4% – 10%	Other	< 1%

8.1.4.1.1.2 Polyurethane Foam Constituent Storage

The foam supplier shall certify that the polyurethane foam constituents have been properly stored prior to use, and that the polyurethane foam constituents have been used within their shelf life.

8.1.4.1.1.3 Foamed Component Preparation

Prior to polyurethane foam installation, the foam supplier shall visually verify to the extent possible (i.e., looking through the foam fill ports) that the ceramic fiber insulation is still attached to the component shell interior surfaces. In addition, due to the internal pressures generated during the foam pouring/curing process, the foam supplier shall visually verify that adequate bracing/shoring of the component shells is provided to maintain the dimensional configuration throughout the foam pouring/curing process.

8.1.4.1.1.4 Polyurethane Foam Installation

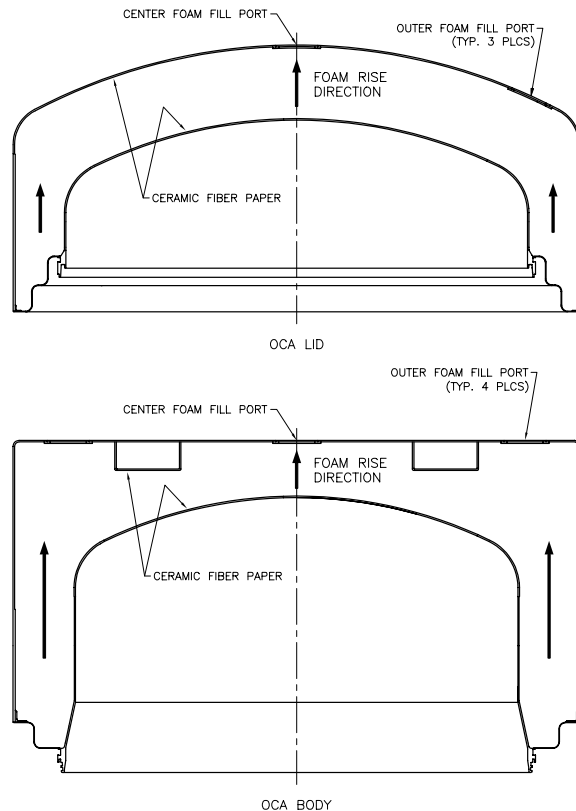
As illustrated in the accompanying illustration, the direction of foam rise shall be vertically aligned with the shell component axis.

The surrounding walls of the component shell where the liquid foam material is to be installed shall be between 55 °F and 95 °F prior to foam installation. Measure and record the component shell temperature to an accuracy of ± 2 °F prior to foam installation.

In the case of multiple pours into a single foamed component, the cured level of each pour shall be measured and recorded to an accuracy of ± 1 inch.

Measure and record the weight of liquid foam material installed during each pour to an accuracy of ± 10 pounds.

All test samples shall be poured into disposable containers at the same time as the actual pour it represents, clearly marking the test sample container with the pour date and a unique pour identification number. All test samples shall be cut from a larger block to obtain freshly cut faces. Prior to physical testing, each test sample shall be cleaned of superfluous foam dust.



8.1.4.1.1.5 Polyurethane Foam Pour and Test Data Records

A production pour and testing record shall be compiled by the foam supplier during the foam pouring operation and subsequent physical testing. Upon completion of production and testing, the foam supplier shall issue certification referencing the production record data and test data pertaining to each foamed component. At a minimum, relevant pour and test data shall include:

- formulation, batch, and pour numbers, with foam material traceability, and pour date,
- foamed component description, part number, and serial number,
- instrumentation description, serial number, and calibration due date,

- pour and test data (e.g., date, temperature, dimensional, and/or weight measurements, compressive modulus, thermal conductivity, compressive stress, etc., as applicable), and
- technician and Quality Assurance/Quality Control (QA/QC) sign-off.

8.1.4.1.2 Physical Characteristics

The following subsections define the required physical characteristics of the polyurethane foam material used for the HalfPACT packaging design.

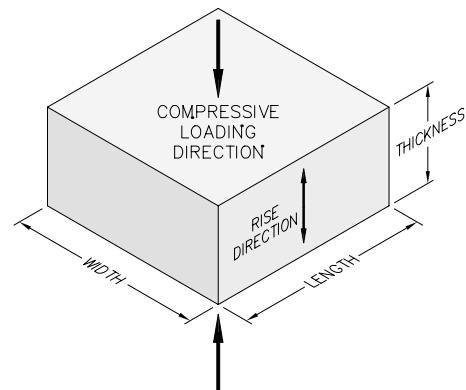
Testing for the various polyurethane foam physical characteristics is based on a “formulation”, “batch”, or “pour”, as appropriate, as defined in [Section 8.1.4.1.1, *Introduction and General Requirements*](#). The physical characteristics determined for a specific foam formulation are relatively insensitive to small variations in chemical constituents and/or environmental conditions, and therefore include physical testing for compressive modulus, Poisson’s ratio, thermal expansion coefficient, thermal conductivity, and specific heat. Similarly, the physical characteristics determined for a batch are only slightly sensitive to small changes in formulation and/or environmental conditions during batch mixing, and therefore include physical testing for flame retardancy, intumescence, and leachable chlorides. Finally, the physical characteristics determined for a pour are also only slightly sensitive to small changes in formulation and slightly more sensitive to variations in environmental conditions during pour mixing, and therefore include physical testing for density and compressive stress.

8.1.4.1.2.1 Physical Characteristics Determined for a Foam Formulation

Foam material physical characteristics for the following parameters shall be determined once for a particular foam formulation. If multiple components are to be foamed utilizing a specific foam formulation, then additional physical testing, as defined below, need not be performed.

8.1.4.1.2.1.1 Parallel-to-Rise Compressive Modulus

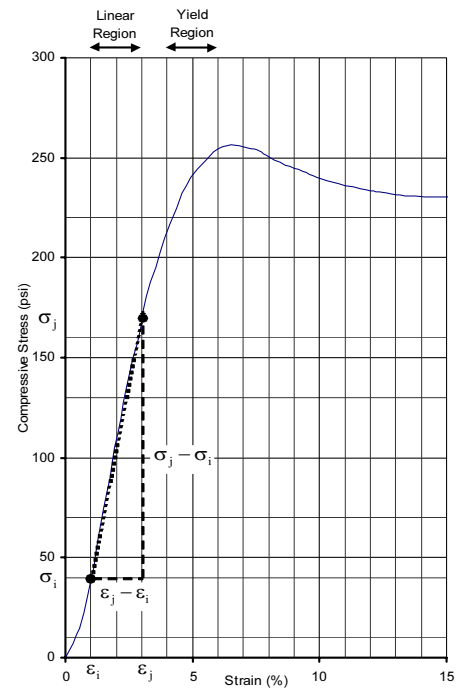
1. Three (3) test samples shall be taken from the sample pour. Each test sample shall be a rectangular prism with nominal dimensions of 1.0 inch thick (T) × 2.0 inches wide (W) × 2.0 inches long (L). The thickness dimension shall be in the parallel-to-rise direction.
2. Place the test samples in a room (ambient) temperature environment (i.e., 65 °F to 85 °F) for sufficient time to thermally stabilize the test samples. Measure and record the room temperature to an accuracy of ± 2 °F.
3. Measure and record the thickness, width, and length of each test sample to an accuracy of ± 0.001 inches.
4. Compute and record the surface area of each test sample by multiplying the width by the length (i.e., $W \times L$).
5. Place a test sample in a Universal Testing Machine. Lower the machine’s crosshead until it touches the test sample. Set the machine’s parameters for the thickness of the test sample.



6. Apply a compressive load to each test sample at a rate of 0.10 ± 0.05 inches/minute until the compressive stress somewhat exceeds the elastic range of the foam material (i.e., the elastic range is typically 0% – 6% strain). Plot the compressive stress versus strain for each test sample.
7. Determine and record the parallel-to-rise compressive modulus, E , of each test sample by computing the slope in the linear region of the elastic range of the stress-strain curve, where ϵ_i and ϵ_j , and σ_i and σ_j are the strain and compressive stress at two selected points i and j , respectively, in the linear region of the stress-strain curve (see example curve to right) as follows:

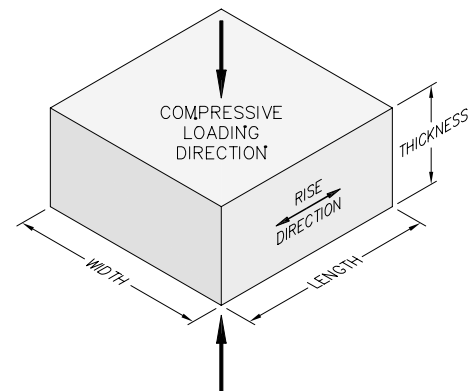
$$E = \frac{\sigma_j - \sigma_i}{\epsilon_j - \epsilon_i}, \text{ psi}$$

8. Determine and record the average parallel-to-rise compressive modulus of the three test samples. The numerically averaged, parallel-to-rise compressive modulus of the three test samples shall be 6,810 psi $\pm 20\%$ (i.e., within the range of 5,448 to 8,172 psi).



8.1.4.1.2.1.2 Perpendicular-to-Rise Compressive Modulus

1. Three (3) test samples shall be taken from the sample pour. Each test sample shall be a rectangular prism with nominal dimensions of 1.0 inch thick (T) \times 2.0 inches wide (W) \times 2.0 inches long (L). The thickness dimension shall be in the perpendicular-to-rise direction.
2. Place the test samples in a room (ambient) temperature environment (i.e., 65 °F to 85 °F) for sufficient time to thermally stabilize the test samples. Measure and record the room temperature to an accuracy of ± 2 °F.
3. Measure and record the thickness, width, and length of each test sample to an accuracy of ± 0.001 inches.
4. Compute and record the surface area of each test sample by multiplying the width by the length (i.e., $W \times L$).
5. Place a test sample in a Universal Testing Machine. Lower the machine's crosshead until it touches the test sample. Set the machine's parameters for the thickness of the test sample.
6. Apply a compressive load to each test sample at a rate of 0.10 ± 0.05 inches/minute until the compressive stress somewhat exceeds the elastic range of the foam material (i.e., the elastic range is typically 0% – 6% strain). Plot the compressive stress versus strain for each test sample.



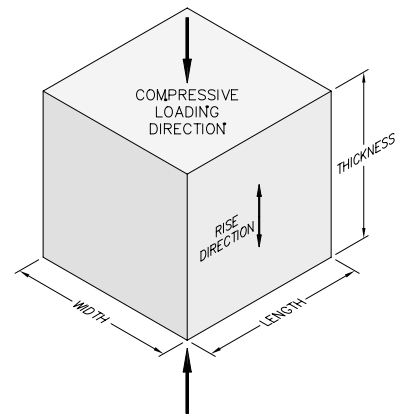
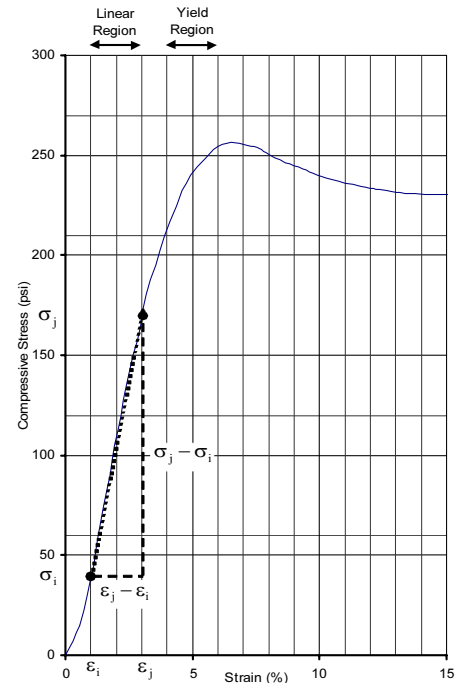
7. Determine and record the perpendicular-to-rise compressive modulus, E , of each test sample by computing the slope in the linear region of the elastic range of the stress-strain curve, where ϵ_i and ϵ_j , and σ_i and σ_j are the strain and compressive stress at two selected points i and j , respectively, in the linear region of the stress-strain curve (see example curve to right) as follows:

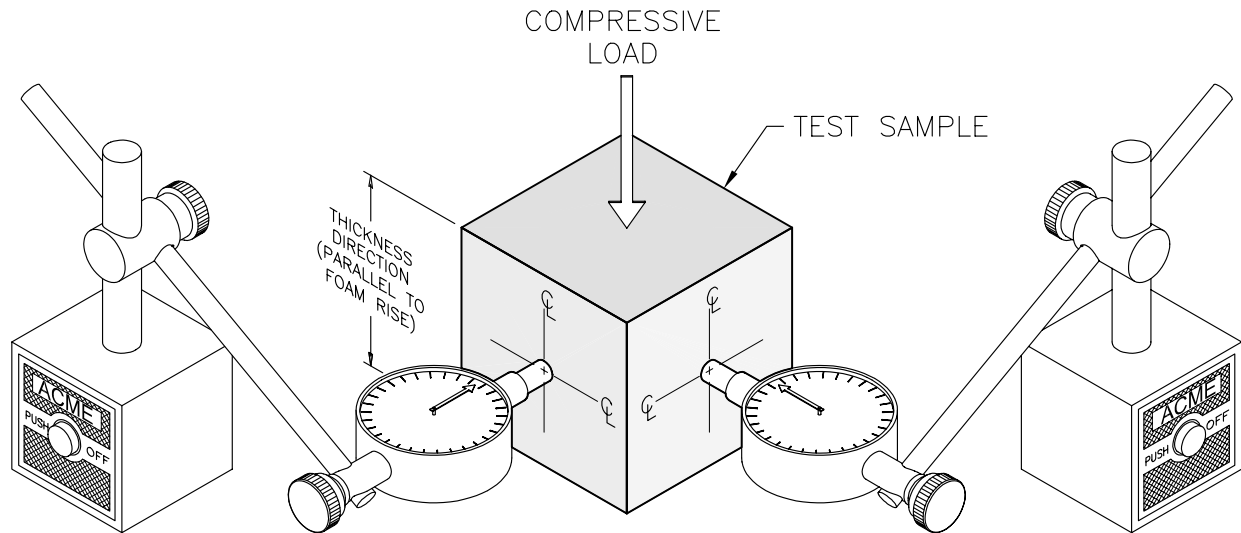
$$E = \frac{\sigma_j - \sigma_i}{\epsilon_j - \epsilon_i}, \text{ psi}$$

8. Determine and record the average perpendicular-to-rise compressive modulus of the three test samples. The numerically averaged, perpendicular-to-rise compressive modulus of the three test samples shall be 4,773 psi $\pm 20\%$ (i.e., within the range of 3,818 to 5,728 psi).

8.1.4.1.2.1.3 Poisson's Ratio

- Three (3) test samples shall be taken from the sample pour. Each test sample shall be a rectangular prism with nominal dimensions of 2.0 inches thick (T) \times 2.0 inches wide (W) \times 2.0 inches long (L). The thickness dimension shall be in the parallel-to-rise direction.
- Place the test samples in a room (ambient) temperature environment (i.e., 65 °F to 85 °F) for sufficient time to thermally stabilize the test samples. Measure and record the room temperature to an accuracy of ± 2 °F.
- Measure and record the thickness, width, and length of each test sample to an accuracy of ± 0.001 inches.
- Place a test sample in a Universal Testing Machine. Lower the machine's crosshead until it touches the test sample. Set the machine's parameters for the thickness of the test sample.
- As illustrated below, place two orthogonally oriented dial indicators at the mid-plane of one width face and one length face of the test sample to record the lateral deflections. The dial indicators shall be capable of measuring to an accuracy of ± 0.001 inches.
- Apply a compressive load to each test sample so that the strain remains within the elastic range of the material, as determined in [Section 8.1.4.1.2.1.1, *Parallel-to-Rise Compressive Modulus*](#). Record the axial crosshead displacement (δ_T) and both dial indicator displacements (δ_W and δ_L) at one strain point within the elastic range for each test sample.





7. Determine and record Poisson's ratio of each test sample as follows:

$$\mu = \frac{\delta_W/W + \delta_L/L}{\delta_T/T}$$

8. Determine and record the average Poisson's ratio of the three test samples. The numerically averaged Poisson's ratio of the three test samples shall be $0.33 \pm 20\%$ (i.e., within the range of 0.26 to 0.40).

8.1.4.1.2.1.4 Thermal Expansion Coefficient

- Three (3) test samples shall be taken from the sample pour. Each test sample shall be a rectangular prism with a nominal cross-section of 1.0 inch square and a nominal length of 6.0 inches.
- Place the test samples in a room (ambient) temperature environment (i.e., 65 °F to 85 °F) for sufficient time to thermally stabilize the test samples. Measure and record the room temperature (T_{RT}) to an accuracy of ± 2 °F.
- Measure and record the room temperature length (L_{RT}) of each test sample to an accuracy of ± 0.001 inches.
- Place the test samples in a -40 °F to -60 °F cold environment for a minimum of three hours. Measure and record the cold environment temperature (T_C) to an accuracy of ± 2 °F.
- Measure and record the cold environment length (L_C) of each test sample to an accuracy of ± 0.001 inches.
- Determine and record the cold environment thermal expansion coefficient for each test sample as follows:

$$\alpha_C = \frac{(L_C - L_{RT})}{(L_{RT})(T_C - T_{RT})}, \text{ in/in/}^\circ\text{F}$$

7. Place the test samples in a 180 °F to 200 °F hot environment for a minimum of three hours. Measure and record the hot environment temperature (T_H) to an accuracy of ± 2 °F.
8. Measure and record the hot environment length (L_H) of each test sample to an accuracy of ± 0.001 inches.
9. Determine and record the hot environment thermal expansion coefficient for each test sample as follows:

$$\alpha_H = \frac{(L_H - L_{RT})}{(L_{RT})(T_H - T_{RT})}, \text{ in/in/}^\circ\text{F}$$

10. Determine and record the average thermal expansion coefficient of each test sample as follows:

$$\alpha = \frac{\alpha_C + \alpha_H}{2}, \text{ in/in/}^\circ\text{F}$$

11. Determine and record the average thermal expansion coefficient of the three test samples. The numerically averaged thermal expansion coefficient of the three test samples shall be 3.5×10^{-5} in/in/°F $\pm 20\%$ (i.e., within the range of 2.8×10^{-5} to 4.2×10^{-5} in/in/°F).

8.1.4.1.2.1.5 Thermal Conductivity

1. The thermal conductivity test shall be performed using a heat flux meter (HFM) apparatus. The HFM establishes steady state unidirectional heat flux through a test specimen between two parallel plates at constant but different temperatures. By measurement of the plate temperatures and plate separation, Fourier's law of heat conduction is used by the HFM to automatically calculate thermal conductivity. Description of a typical HFM is provided in ASTM C518⁵. The HFM shall be calibrated against a traceable reference specimen per the HFM manufacturer's operating instructions.
2. Three (3) test samples shall be taken from the sample pour. Each test sample shall be of sufficient size to enable testing per the HFM manufacturer's operating instructions.
3. Measure and record the necessary test sample parameters as input data to the HFM per the HFM manufacturer's operating instructions.
4. Perform thermal conductivity testing and record the measured thermal conductivity for each test sample following the HFM manufacturer's operating instructions.
5. Determine and record the average thermal conductivity of the three test samples. The numerically averaged thermal conductivity of the three test samples shall be 0.230 Btu-in/hr-ft²-°F $\pm 20\%$ (i.e., within the range of 0.184 to 0.276 Btu-in/hr-ft²-°F).

8.1.4.1.2.1.6 Specific Heat

1. The specific heat test shall be performed using a differential scanning calorimeter (DSC) apparatus. The DSC establishes a constant heating rate and measures the differential heat

⁵ ASTM C518, *Standard Test Method for Steady-State Heat Flux Measurements and Thermal Transmission Properties by Means of the Heat Flux Meter Apparatus*, American Society of Testing and Materials (ASTM).

flow into both a test specimen and a reference specimen. Description of a typical DSC is provided in ASTM E1269⁶. The DSC shall be calibrated against a traceable reference specimen per the DSC manufacturer's operating instructions.

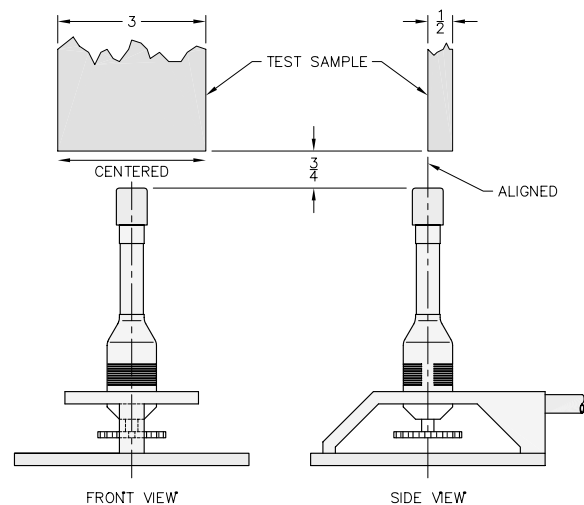
2. Three (3) test samples shall be taken from the sample pour. Each test sample shall be of sufficient size to enable testing per the DSC manufacturer's operating instructions.
3. Measure and record the necessary test sample parameters as input data to the DSC per the DSC manufacturer's operating instructions.
4. Perform specific heat testing and record the measured specific heat for each test sample following the DSC manufacturer's operating instructions.
5. Determine and record the average specific heat of the three test specimens. The numerically averaged specific heat at 77 °F of the three test samples shall be 0.30 Btu/lb-°F \pm 20% (i.e., within the range of 0.24 to 0.36 Btu/lb-°F).

8.1.4.1.2.2 Physical Characteristics Determined for a Foam Batch

Foam material physical characteristics for the following parameters shall be determined once for a particular foam batch based on the [batch definition from Section 8.1.4.1.1, Introduction and General Requirements](#). If a single or multiple components are to be poured utilizing multiple pours from a single foam batch, then additional physical testing, as defined below, need not be performed for each foam pour.

8.1.4.1.2.2.1 Flame Retardancy

1. Three (3) test samples shall be taken from a pour from each foam batch. Each test sample shall be a rectangular prism with nominal dimensions of 0.5 inches thick, 3.0 inches wide, and a minimum length of 6.0 inches. In addition, individual sample lengths must not be less than the total burn length observed for the sample when tested.
2. Place the test samples in a room (ambient) temperature environment (i.e., 65 °F to 85 °F) for sufficient time to thermally stabilize the test samples. Measure and record the room temperature to an accuracy of \pm 2 °F.
3. Measure and record the length of each test sample to an accuracy of \pm 0.1 inches.
4. Install a $\text{\O}3/8$ inches (10 mm), or larger, Bunsen or Tirrill burner inside an enclosure of sufficient size to perform flame retardancy testing. Adjust the burner flame height to $1\frac{1}{2} \pm 1/8$ inches. Verify that the burner flame temperature is 1,550 °F, minimum.

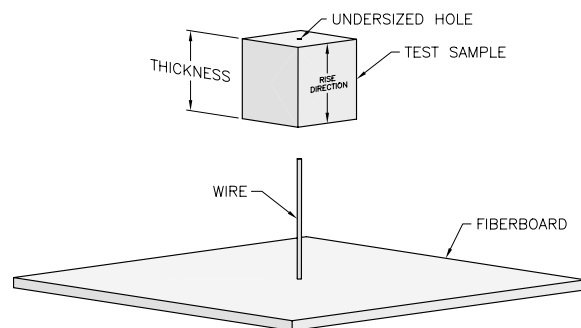


⁶ ASTM E1269, *Standard Test Method for Determining Specific Heat Capacity by Differential Scanning Calorimetry*, American Society of Testing and Materials (ASTM).

5. Support the test sample with the long axis oriented vertically within the enclosure such that the test sample's bottom edge will be $3/4 \pm 1/16$ inches above the top edge of the burner.
6. Move the burner flame under the test sample for an elapsed time of 60 ± 2 seconds. As illustrated, align the burner flame with the front edge of the test sample thickness and the center of the test sample width.
7. Immediately after removal of the test sample from the burner flame, measure and record the following data:
 - a. Measure and record, to the nearest second, the elapsed time until flames from the test sample extinguish.
 - b. Measure and record, to the nearest second, the elapsed time from the occurrence of drips, if any, until drips from the test sample extinguish.
 - c. Measure and record, to the nearest 0.1 inches, the burn length following cessation of all visible burning and smoking.
8. Flame retardancy testing acceptance is based on the following criteria:
 - a. The numerically averaged flame extinguishment time of the three test samples shall not exceed fifteen (15) seconds.
 - b. The numerically averaged flame extinguishment time of drips from the three test samples shall not exceed three (3) seconds.
 - c. The numerically averaged burn length of the three test samples shall not exceed six (6) inches.

8.1.4.1.2.2.2 Intumescence

1. Three (3) test samples shall be taken from a pour from each foam batch. Each test sample shall be a cube with nominal dimensions of 2.0 inches.
2. Place the test samples in a room (ambient) temperature environment (i.e., 65 °F to 85 °F) for sufficient time to thermally stabilize the test samples. Measure and record the room temperature to an accuracy of ± 2 °F.
3. Preheat a furnace to $1,475 \text{ °F} \pm 18 \text{ °F}$.
4. Identify two opposite faces on each test sample as the thickness direction. The thickness dimension shall be in the parallel-to-rise direction. Measure and record the initial thickness (t_i) of each test sample to an accuracy of ± 0.01 inches.
5. Mount a test sample onto a fire resistant fiberboard, with one face of the thickness direction contacting to the board. As illustrated above, the test samples may be



mounted by installing onto a 12 to 16 gauge wire (Ø0.105 to Ø0.063 inches, respectively) of sufficient length, oriented perpendicular to the fiberboard face. The test samples may be pre-drilled with an undersized hole to allow installation onto the wire.

6. Locate the test sample/fiberboard assembly over the opening of the pre-heated furnace for a 90 ± 3 second duration. After removal of the test sample/fiberboard assembly from the furnace, gently extinguish any remaining flames and allow the test sample to cool.
7. Measure and record the final thickness (t_f) of the test sample to an accuracy of ± 0.1 inches.
8. For each sample tested, determine and record the intumescence, I , as a percentage of the original sample length as follows:

$$I = \left(\frac{t_f - t_i}{t_i} \right) \times 100$$

9. Determine and record the average intumescence of the three test samples. The numerically averaged intumescence of the three test samples shall be a minimum of 50%.

8.1.4.1.2.2.3 Leachable Chlorides

1. The leachable chlorides test shall be performed using an ion chromatograph (IC) apparatus. The IC measures inorganic anions of interest (i.e., chlorides) in water. Description of a typical IC is provided in EPA Method 300.0⁷. The IC shall be calibrated against a traceable reference specimen per the IC manufacturer's operating instructions.
2. One (1) test sample shall be taken from the sample pour. The test sample shall be a cube with dimensions of 2.00 ± 0.03 inches.
3. Place the test sample in a room (ambient) temperature environment (i.e., 65 °F to 85 °F) for sufficient time to thermally stabilize the test sample. Measure and record the room temperature to an accuracy of ± 2 °F.
4. Measure and record the thickness, width, and length of each test sample to an accuracy of ± 0.001 inches.
5. Obtain a minimum of 550 ml of distilled or de-ionized water for testing. The test water shall be from a single source to ensure consistent anionic properties for testing control.
6. Obtain a 400 ml, or larger, contaminant free container that is capable of being sealed. Fill the container with 262 ± 3 ml of test water. Fully immerse the test sample inside the container for a duration of 72 ± 3 hours. If necessary, use an inert standoff to ensure the test sample is completely immersed for the full test duration. Seal the container prior to the 72 hour duration.
7. Obtain a second, identical container to use as a "control". Fill the control container with 262 ± 3 ml of the same test water. Seal the control container for a 72 ± 3 hour duration.

⁷ EPA Method 300.0, *Determination of Inorganic Anions in Water by Ion Chromatography*, U.S. Environmental Protection Agency.

8. At the end of the test period, measure and record the leachable chlorides in the test water per the IC manufacturer's operating instructions. The leachable chlorides in the test water shall not exceed one part per million (1 ppm).
9. Should leachable chlorides in the test water exceed 1 ppm, measure and record the leachable chlorides in the test water from the "control" container. The difference in leachable chlorides from the test water and "control" water sample shall not exceed 1 ppm.

8.1.4.1.2.3 Physical Characteristics Determined for a Foam Pour

Foam material physical characteristics for the following parameters shall be determined for each foam pour based on the [pour definition from Section 8.1.4.1.1, *Introduction and General Requirements*](#).

8.1.4.1.2.3.1 Density

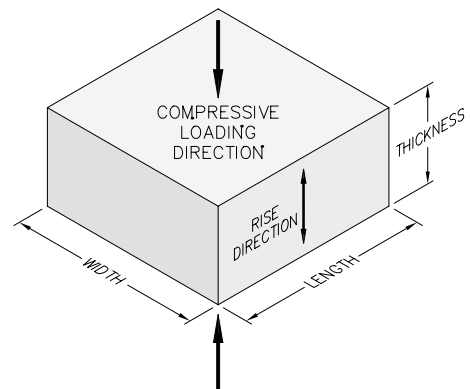
1. Three (3) test samples shall be taken from the foam pour. Each test sample shall be a rectangular prism with nominal dimensions of 1.0 inch thick (T) × 2.0 inches wide (W) × 2.0 inches long (L).
2. Place the test samples in a room (ambient) temperature environment (i.e., 65 °F to 85 °F) for sufficient time to thermally stabilize the test samples. Measure and record the room temperature to an accuracy of ±2 °F.
3. Measure and record the weight of each test sample to an accuracy of ±0.01 grams.
4. Measure and record the thickness, width, and length of each test sample to an accuracy of ±0.001 inches.
5. Determine and record the room temperature density of each test sample utilizing the following formula:

$$\rho_{\text{foam}} = \frac{\text{Weight, g}}{453.6 \text{ g/lb}} \times \frac{1,728 \text{ in}^3/\text{ft}^3}{T \times W \times L \text{ in}^3}, \text{ pcf}$$

6. Determine and record the average density of the three test samples. The numerically averaged density of the three test samples shall be 8¼ pcf ±15% (i.e., within the range of 7 to 9½ pcf).

8.1.4.1.2.3.2 Parallel-to-Rise Compressive Stress

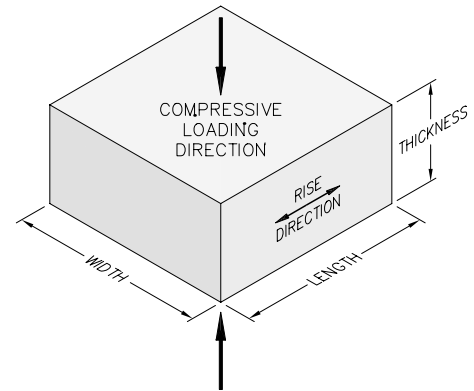
1. Three (3) test samples shall be taken from the foam pour. Each test sample shall be a rectangular prism with nominal dimensions of 1.0 inch thick (T) × 2.0 inches wide (W) × 2.0 inches long (L). The thickness dimension shall be the parallel-to-rise direction.
2. Place the test samples in a room (ambient) temperature environment (i.e., 65 °F to 85 °F) for sufficient time to thermally stabilize the test samples. Measure and record the room temperature to an accuracy of ±2 °F.



3. Measure and record the thickness, width, and length of each test sample to an accuracy of ± 0.001 inches.
4. Compute and record the surface area of each test sample by multiplying the width by the length (i.e., $W \times L$).
5. Place a test sample in a Universal Testing Machine. Lower the machine's crosshead until it touches the test sample. Set the machine's parameters for the thickness of the test sample.
6. Apply a compressive load to each test sample at a rate of 0.10 ± 0.05 inches/minute until a strain of 70%, or greater, is achieved. For each test sample, plot the compressive stress versus strain and record the compressive stress at strains of 10%, 40%, and 70%.
7. Determine and record the average parallel-to-rise compressive stress of the three test samples from each pour. As delineated in [Table 8.1-1](#), the average parallel-to-rise compressive stress for each pour shall be the nominal compressive stress $\pm 20\%$ at strains of 10%, 40%, and 70%.
8. Determine and record the average parallel-to-rise compressive stress of all test samples from each foamed component. As delineated in [Table 8.1-1](#), the average parallel-to-rise compressive stress for a foamed component shall be the nominal compressive stress $\pm 15\%$ at strains of 10%, 40%, and 70%.

8.1.4.1.2.3.3 Perpendicular-to-Rise Compressive Stress

1. Three (3) test samples shall be taken from the foam pour. Each test sample shall be a rectangular prism with nominal dimensions of 1.0 inch thick (T) \times 2.0 inches wide (W) \times 2.0 inches long (L). The thickness dimension shall be the perpendicular-to-rise direction.
2. Place the test samples in a room (ambient) temperature environment (i.e., 65 °F to 85 °F) for sufficient time to thermally stabilize the test samples. Measure and record the room temperature to an accuracy of ± 2 °F.
3. Measure and record the thickness, width, and length of each test sample to an accuracy of ± 0.001 inches.
4. Compute and record the surface area of each test sample by multiplying the width by the length (i.e., $W \times L$).
5. Place a test sample in a Universal Testing Machine. Lower the machine's crosshead until it touches the test sample. Set the machine's parameters for the thickness of the test sample.
6. Apply a compressive load to each test sample at a rate of 0.10 ± 0.05 inches/minute until a strain of 70%, or greater, is achieved. For each test sample, plot the compressive stress versus strain and record the compressive stress at strains of 10%, 40%, and 70%.
7. Determine and record the average perpendicular-to-rise compressive stress of the three test samples from each pour. As delineated in [Table 8.1-1](#), the average perpendicular-to-rise compressive stress for each pour shall be the nominal compressive stress $\pm 20\%$ at strains of 10%, 40%, and 70%.



8. Determine and record the average perpendicular-to-rise compressive stress of all test samples from each foamed component. As delineated in [Table 8.1-1](#), the average perpendicular-to-rise compressive stress for a foamed component shall be the nominal compressive stress $\pm 15\%$ at strains of 10%, 40%, and 70%.

8.1.5 Tests for Shielding Integrity

The HalfPACT packaging does not contain any biological shielding.

8.1.6 Thermal Acceptance Test

Material properties utilized in [Chapter 3.0, Thermal Evaluation](#), are consistently conservative for the normal conditions of transport (NCT) and hypothetical accident condition (HAC) thermal analyses performed. In addition, HAC fire certification testing of the HalfPACT package (see [Appendix 2.10.3, Certification Tests](#)) served to verify material performance in the HAC thermal environment. As such, with the exception of the tests required for polyurethane foam, as shown in [Section 8.1.4, Component Tests](#), specific acceptance tests for material thermal properties are not performed.

Table 8.1-1 – Acceptable Compressive Stress Ranges for Foam (psi)

Sample Range	Parallel-to-Rise at Strain, $\epsilon_{//}$			Perpendicular-to-Rise at Strain, ϵ_{\perp}		
	$\epsilon=10\%$	$\epsilon=40\%$	$\epsilon=70\%$	$\epsilon=10\%$	$\epsilon=40\%$	$\epsilon=70\%$
Nominal –20%	188	216	544	156	188	536
Nominal –15%	200	230	578	166	200	570
Nominal	235	270	680	195	235	670
Nominal +15%	270	311	782	224	270	771
Nominal +20%	282	324	816	234	282	804

8.2 Maintenance Program

This section describes the maintenance program used to ensure continued performance of the HalfPACT package.

8.2.1 Structural and Pressure Tests

8.2.1.1 Containment Vessel Pressure Testing

Perform structural pressure testing on both the inner containment vessel (ICV) and the outer containment vessel (OCV) per the requirements of [Section 8.1.2.2, *Containment Vessel Pressure Testing*](#), once every five years. Upon completing the structural pressure test, perform leakage rate testing per the requirements of [Section 8.1.3, *Fabrication Leakage Rate Tests*](#).

8.2.1.2 ICV Interior Surfaces Inspection

Annual inspection shall be performed of the accessible interior surfaces of the ICV for evidence of chemically induced stress corrosion. After removal of the ICV spacer assemblies, perform a visual inspection for indications of ICV interior surface corrosion. Should evidence of corrosion exist, a liquid penetrant inspection of the ICV interior surfaces, including accessible shell, head, flange, and weld surfaces, shall be performed per ASME Boiler and Pressure Vessel Code, Section V¹, Article 6, and ASME Boiler and Pressure Vessel Code, Section III², Division 1, Subsection NB, Article NB-5000, as delineated on the drawings in [Appendix 1.3.1, *Packaging General Arrangement Drawings*](#). Indications of cracking or distortion shall be recorded on a nonconformance report and dispositioned prior to corrective actions.

Once the packaging is put into service, at a maximum interval of five (5) years, an examination shall be performed on the accessible interior surfaces of the ICV for evidence of chemically induced stress corrosion. This examination shall consist of a liquid penetrant inspection of the entire ICV interior surfaces, including the accessible shell, head, flange, and weld surfaces, and shall be performed per ASME Boiler and Pressure Vessel Code, Section V, Article 6, and ASME Boiler and Pressure Vessel Code, Section III, Division 1, Subsection NB, Article NB-5000, as delineated on the drawings in [Appendix 1.3.1, *Packaging General Arrangement Drawings*](#). Indications of cracking or distortion shall be recorded on a nonconformance report and dispositioned prior to corrective actions.

8.2.2 Maintenance/Periodic Leakage Rate Tests

This section provides the generalized procedure for maintenance and periodic leakage rate testing of the containment vessel penetrations during routine maintenance, or at the time of seal replacement or seal area repair. Maintenance/periodic leakage rate testing shall follow the

¹ American Society of Mechanical Engineers (ASME) Boiler and Pressure Vessel Code, Section V, *Nondestructive Examination*, 1995 Edition, 1997 Addenda, United Engineering Center, 345 East 47th Street, New York, NY.

² American Society of Mechanical Engineers (ASME) Boiler and Pressure Vessel Code, Section III, *Rules for Construction of Nuclear Power Plant Components*, 1995 Edition, 1997 Addenda, United Engineering Center, 345 East 47th Street, New York, NY.

guidelines of Section 7.4, *Maintenance Leakage Rate Test*, and Section 7.5, *Periodic Leakage Rate Test*, of ANSI N14.5³.

Maintenance/periodic leakage rate testing shall be performed on the main O-ring seal and vent port plug seal for the inner containment vessel (ICV) in accordance with [Section 8.2.2.2, *Helium Leakage Rate Testing the ICV Main O-ring Seal*](#), and [Section 8.2.2.3, *Helium Leakage Rate Testing the ICV Outer Vent Port Plug O-ring Seal*](#). Leakage rate testing of the outer containment vessel (OCV) main O-ring seal and OCV vent port plug shall be performed in accordance with [Section 8.1.3.6, *Helium Leakage Rate Testing the OCV Main O-ring Seal Integrity*](#), and [Section 8.1.3.7, *Helium Leakage Rate Testing the OCV Vent Port Plug O-ring Seal Integrity*](#). Each leakage rate test shall meet the acceptance criteria delineated in [Section 8.2.2.1, *Maintenance/Periodic Leakage Rate Test Acceptance Criteria*](#).

8.2.2.1 Maintenance/Periodic Leakage Rate Test Acceptance Criteria

Maintenance/periodic leakage rate test acceptance criteria are identical to the criteria delineated in [Section 8.1.3.1, *Fabrication Leakage Rate Test Acceptance Criteria*](#).

8.2.2.2 Helium Leakage Rate Testing the ICV Main O-ring Seal

1. The maintenance/periodic leakage rate test of the ICV main O-ring seal shall be performed following the guidelines of A.5.4, *Evacuated Envelope – Gas Detector*, of ANSI N14.5.
2. The ICV shall be assembled with both main O-ring seals installed into the ICV lower seal flange and the wiper O-ring installed into the holder. Assembly is as shown in [Appendix 1.3.1, *Packaging General Arrangement Drawings*](#).
3. Verify that the ICV vent port cover and ICV outer vent port plug have been removed. Verify that the ICV inner vent port plug is installed and tighten to 55 - 65 lb-in torque.
4. Connect a vacuum pump to the ICV vent port and evacuate the ICV vent port cavity to 90% vacuum or better (i.e., $\leq 10\%$ ambient atmospheric pressure). If the ICV vent port cavity cannot be evacuated to the required vacuum, remove the ICV lid and inspect the ICV wiper O-ring seal, the ICV upper main O-ring seal, and sealing surfaces for damage. Replace any damaged O-ring seals and repair any damaged sealing surfaces prior to re-performing the ICV main O-ring seal test.
5. Remove the ICV seal test port plug and install a helium mass spectrometer leak detector to the ICV seal test port. Evacuate the ICV seal test port cavity until the vacuum is sufficient to operate the helium mass spectrometer leak detector.
6. Provide a helium atmosphere inside the ICV vent port cavity by backfilling with helium gas to a pressure slightly greater than atmospheric pressure (+1 psi, -0 psi).
7. Perform the helium leakage rate test to the requirements of [Section 8.2.2.1, *Maintenance/Periodic Leakage Rate Test Acceptance Criteria*](#). If, after repeated attempts, the ICV main O-ring seal fails to pass the leakage rate test, isolate the leak path and, prior to repairing the leak path and repeating

³ ANSI N14.5-1997, *American National Standard for Radioactive Materials – Leakage Tests on Packages for Shipment*, American National Standards Institute, Inc. (ANSI).

the leakage rate test, record on a nonconformance report and disposition prior to final acceptance in accordance with the cognizant quality assurance program.

8.2.2.3 Helium Leakage Rate Testing the ICV Outer Vent Port Plug O-ring Seal

1. The maintenance/periodic leakage rate test of the ICV outer vent port plug O-ring seal shall be performed following the guidelines of A.5.4, *Evacuated Envelope – Gas Detector*, of ANSI N14.5.
2. The ICV shall be assembled with both main O-ring seals installed into the ICV lower seal flange and the wiper O-ring installed into the holder. Assembly is as shown in [Appendix 1.3.1, Packaging General Arrangement Drawings](#).
3. Verify that the ICV vent port cover and ICV outer vent port plug have been removed. Verify that the ICV inner vent port plug is installed and tighten to 55 - 65 lb-in torque.
4. Connect a vacuum pump to the ICV vent port and evacuate the ICV vent port cavity to 90% vacuum or better (i.e., $\leq 10\%$ ambient atmospheric pressure). If the ICV vent port cavity cannot be evacuated to the required vacuum, remove the ICV lid and inspect the ICV wiper O-ring seal, the ICV upper main O-ring seal, and sealing surfaces for damage. Replace any damaged O-ring seals and repair any damaged sealing surfaces prior to re-performing the ICV main O-ring seal test.
5. Provide a helium atmosphere inside the ICV vent port cavity by backfilling with helium gas to a pressure slightly greater than atmospheric pressure (+1 psi, -0 psi).
6. Install the ICV outer vent port plug and tighten to 55 - 65 lb-in torque.
7. Install a helium mass spectrometer leak detector to the ICV vent port. Evacuate the ICV vent port cavity until the vacuum is sufficient to operate the helium mass spectrometer leak detector.
8. Perform the helium leakage rate test to the requirements of [Section 8.2.2.1, Maintenance/Periodic Leakage Rate Test Acceptance Criteria](#). If, after repeated attempts, the ICV outer vent port plug O-ring seal fails to pass the leakage rate test, isolate the leak path and, prior to repairing the leak path and repeating the leakage rate test, record on a nonconformance report and disposition prior to final acceptance in accordance with the cognizant quality assurance program.

8.2.3 Subsystems Maintenance

8.2.3.1 Fasteners

All threaded components shall be inspected annually for deformed or stripped threads. Damaged components shall be repaired or replaced prior to further use. The threaded components to be visually inspected include the lock bolts, the OCV and ICV seal test port and vent port plugs, the OCV and ICV vent port covers, and OCV access plugs.

8.2.3.2 Locking Rings

Before each use, inspect the OCV and ICV locking ring assemblies for restrained motion. Any motion-impairing components shall be corrected prior to further use.

8.2.3.3 Seal Areas and Grooves

8.2.3.3.1 Seal Area Routine Inspection and Repair

Before each use and at the time of seal replacement, the OCV and ICV sealing surfaces shall be visually inspected for damage that could impair the sealing capabilities of the HalfPACT packaging. Damage shall be corrected prior to further use (e.g., using emery cloth restore sealing surfaces) to the surface finish specified in [Section 8.2.3.3.2.4, *Surface Finish of Sealing Areas*](#).

Upon completion of containment seal area repairs, verify depth of O-ring groove does not exceed the value in [Table 8.2-1](#) when repairs are in the O-ring groove; perform leakage rate test per the applicable section of [Section 8.2.2, *Maintenance/Periodic Leakage Rate Tests*](#).

8.2.3.3.2 Annual Seal Area Dimensional Inspection

In order to demonstrate compliance of the OCV and ICV main O-ring seal regions, annual inspection of sealing area dimensions and surface finishes shall be performed as defined in [Section 8.2.3.3.2.1, *Groove Widths*](#), through [Section 8.2.3.3.2.5, *O-ring Groove Depth*](#).

Allowable measurements for these dimensions are based on a minimum O-ring compression of 12.5%, which will ensure “leaktight” seals are maintained (see calculation in [Table 8.2-1](#)).

Table 8.2-1 – Calculation of Minimum O-ring Compression

Calculation	Value
G = Maximum allowed upper seal flange groove width, in ^①	0.560
T = Minimum allowed lower seal flange tab width, in ^②	0.494
R = Maximum allowed radial gap due to axial play, in ^③	0.010
D = Maximum allowed O-ring groove depth, in ^④	0.253
M = Maximum gap that O-ring must fill, in ^⑤	0.329
W = Minimum O-ring cross section diameter, in ^⑥	0.376
C = Minimum O-ring compression, % ^⑦	12.5%
Notes: Refer to Appendix 1.3.1, <i>Packaging General Arrangement Drawings</i> , Sheet 6 of 12 and Sheet 1 of 12, Note 42, for key dimension: ① Measured 0.250 inches from bottom of groove, $G = 0.543 + 0.25(\tan 3.95^\circ)$ ② Measured 0.250 inches from top of tab, $T = 0.477 + 0.25(\tan 3.85^\circ)$ ③ Derived from axial play measurements, $R = 0.153(\tan 3.90^\circ)$ ④ Measured at center of groove ⑤ $M = (G - T) + R + D$ ⑥ Minimum production O-ring cross section diameter including the effects of maximum stretch = 0.376 in ⑦ $C = [1 - (M / W)] \times 100$	

All measurement results shall be recorded and retained as part of the overall inspection record for the HalfPACT package. Measurements not in compliance with the following dimensional requirements require repairs. Upon completion of repairs, perform a maintenance/periodic leakage rate test per the applicable section of [Section 8.2.2, Maintenance/Periodic Leakage Rate Tests](#).

8.2.3.3.2.1 Groove Widths

The method of measuring the OCV and ICV upper (lid) seal flange groove width is illustrated in [Figure 8.2-1](#). Remove the ICV debris shield to measure the ICV upper seal flange groove width. As an option, the lid may be inverted to facilitate the measurement process. The measuring equipment includes a $\text{Ø}0.560 \pm 0.001$ inch pin gauge of any convenient length, and a $\text{Ø}0.250 \pm 0.001$ inch ball. With reference to [Figure 8.2-1](#), the pin gauge is aligned parallel with the inner lip of the upper seal flange. Acceptability is based on the following conditions:

- Having *contact* at location ①-① and a *gap* at location ②-② is a NO-GO condition indicating that the upper seal flange groove width is acceptable.
- Having *contact* or a *gap* at location ①-① and *contact* at location ②-② is a GO condition indicating that the upper seal flange groove width is unacceptable.

The method of measuring the OCV and ICV lower (body) seal flange groove width is illustrated in [Figure 8.2-2](#). The measuring equipment includes a $\text{Ø}0.273 \pm 0.001$ inch pin gauge of any convenient length, and a $\text{Ø}0.250 \pm 0.001$ inch ball. With reference to [Figure 8.2-2](#), the pin gauge is aligned parallel with the outer lip of the lower seal flange. Acceptability is based on the following conditions:

- Having *contact* at location ①-① and a *gap* at location ②-② is a NO-GO condition indicating that the lower seal flange groove width is acceptable.
- Having *contact* or a *gap* at location ①-① and *contact* at location ②-② is a GO condition indicating that the lower seal flange groove width is unacceptable.

Groove width measurements shall be taken and recorded at six equally spaced locations around the circumference of the seal flanges.

8.2.3.3.2.2 Tab Widths

The method of measuring the OCV and ICV upper (lid) seal flange tab width is illustrated in [Figure 8.2-3](#). As an option, the lid may be inverted to facilitate the measurement process. The measuring device is a tab width gauge of any convenient size, with a 0.234 ± 0.001 inch inside width \times 0.428 ± 0.001 inch inside height \times 0.375 ± 0.005 inch thickness. With reference to [Figure 8.2-3](#), the tab width gauge is aligned parallel with the lowermost lip of the upper seal flange. Acceptability is based on the following conditions:

- Having *contact* at location ①-① and a *gap* at location ②-② is a NO-GO condition indicating that the upper seal flange tab width is acceptable.
- Having *contact* or a *gap* at location ①-① and *contact* at location ②-② is a GO condition indicating that the upper seal flange tab width is unacceptable.

The method of measuring the OCV and ICV lower (body) seal flange tab width is illustrated in [Figure 8.2-4](#). The measuring device is a 0.494 ± 0.001 inch inside width \times 0.250 ± 0.001 inch inside height \times 0.375 ± 0.005 inch thick tab width gauge of any convenient size. With reference to [Figure 8.2-4](#), the tab width gauge is aligned parallel with the uppermost lip of the lower seal flange. Acceptability is based on the following conditions:

- Having *contact* at location ①-① and a *gap* at location ②-② is a NO-GO condition indicating that the lower seal flange tab width is acceptable.
- Having *contact* or a *gap* at location ①-① and *contact* at location ②-② is a GO condition indicating that the lower seal flange tab width is unacceptable.

Tab width measurements shall be taken and recorded at six equally spaced locations around the circumference of the seal flanges.

8.2.3.3.2.3 Axial Play

Measurement of axial play shall be performed to ensure that O-ring compression is sufficient to maintain package configuration and performance to design criteria. Axial play is the maximum axial distance that a lid can move relative to a body. Because the seal flange sealing surfaces are tapered, any axial movement where the lid moves *away* from the body results in a separation of the sealing surfaces and a slight reduction in O-ring compression. The procedure for measuring OCV and ICV axial play is as follows:

1. Remove the vent port access plug (OCV only), vent port thermal plug (OCV only), vent port cover, and vent port plug(s). Remove the ICV debris seal (ICV only).
2. Assemble the lid onto the body.
3. Locate a minimum of six equally spaced locations around the exterior circumference of the lid and body. At each location, place vertically aligned temporary reference marks on the lid and body.
4. Install a vacuum pump to the vent port and evacuate the containment vessel sufficiently to fully compress the upper seal flange to the lower seal flange.
5. At each location, scribe a horizontal mark that intersects both the lid and the body vertical marks.
6. Install a source of pressure to the vent port and pressurize the containment vessel sufficiently to fully separate the upper seal flange from the lower seal flange.
7. At each location, scribe a second horizontal mark that intersects either the lid or the body vertical mark (select either the lid or body mark as a base point).
8. Measure and record the difference between the initial and final horizontal marks at each location. The maximum acceptable axial play at any location is 0.153 inch.
9. Other measuring devices, such as dial indicators, digital calipers, etc., may be used in lieu of the reference marking method, provided that the axial play is measured at a minimum of six equally spaced locations.

8.2.3.3.2.4 Surface Finish of Sealing Areas

The surface finish in the main O-ring sealing regions shall be a 125 micro-inch finish, or better, to maintain package configuration and performance to design criteria. Perform surface finish inspections for the bottom of the grooves on the lower seal flange and the mating sealing surfaces on the upper seal flange. If the surface condition is determined to exceed 125 micro-inch, repair the surface per the requirements of [Section 8.2.3.3.1, *Seal Area Routine Inspection and Repair*](#).

8.2.3.3.2.5 O-ring Groove Depth

Verify the OCV and ICV O-ring groove depth to be less than 0.253 inches at six equally spaced locations around the circumference of the seal flanges.

8.2.4 Valves, Rupture Discs, and Gaskets on the Containment Vessel

8.2.4.1 Valves

The HalfPACT packaging does not contain any valves.

8.2.4.2 Rupture Discs

The HalfPACT packaging does not contain any rupture discs.

8.2.4.3 Gaskets

Containment boundary O-ring seals shall be replaced within the 12-month period prior to shipment or when damaged (whichever is sooner), per the size and material requirements delineated on the drawings in [Appendix 1.3.1, *Packaging General Arrangement Drawings*](#). Following containment O-ring seal replacement and prior to a loaded shipment, the new seals shall be leakage rate tested to the requirements of [Section 8.2.2, *Maintenance/Periodic Leakage Rate Tests*](#).

The Inner Containment Vessel debris shield and wiper O-ring seal shall be replaced within the 12-month period prior to shipment or when damaged (whichever is sooner), per the size and material requirements delineated on the drawings in [Appendix 1.3.1, *Packaging General Arrangement Drawings*](#).

8.2.5 Shielding

The HalfPACT packaging does not contain any biological shielding.

8.2.6 Thermal

No thermal tests are necessary to ensure continued performance of the HalfPACT packaging.

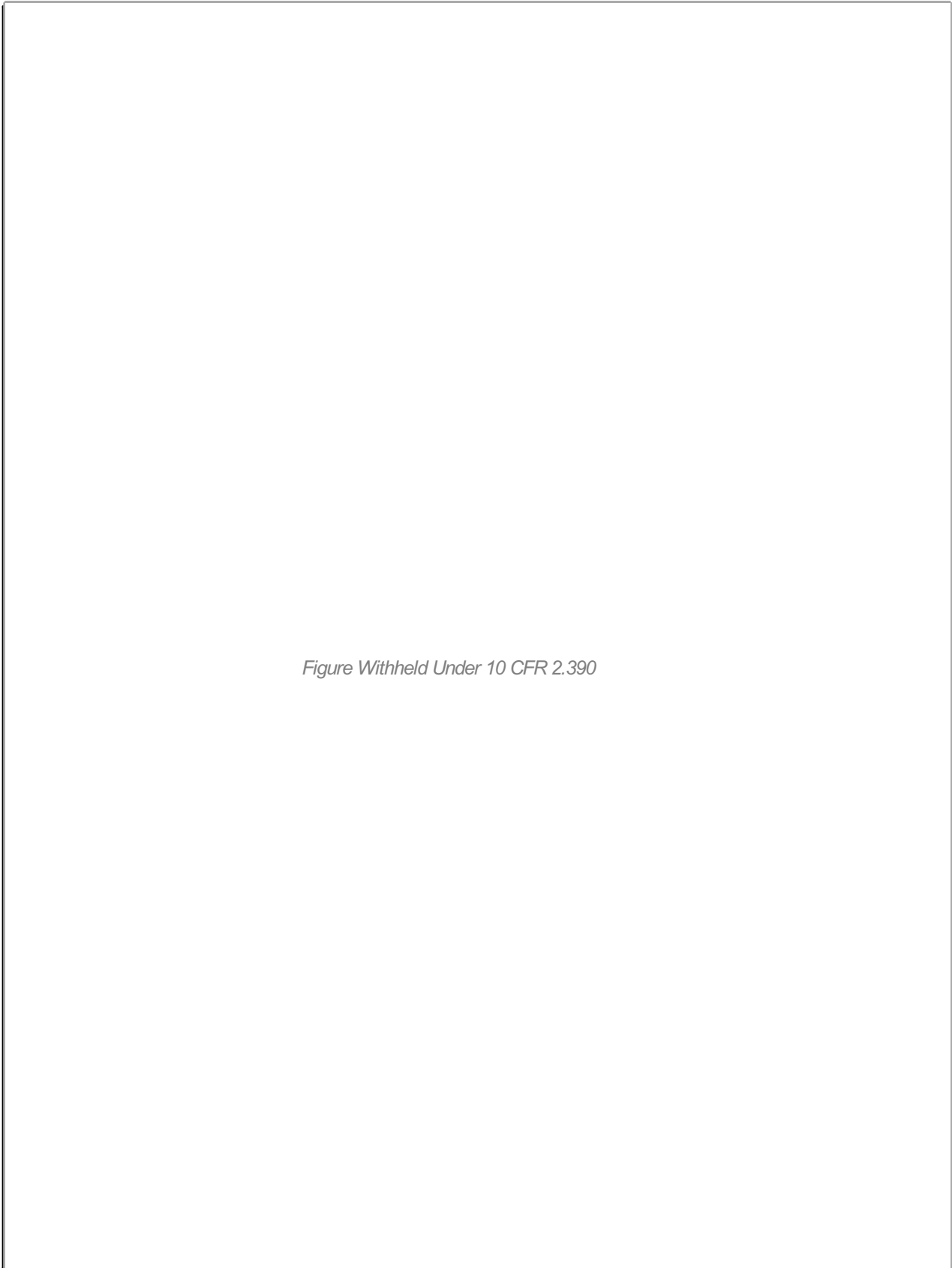


Figure Withheld Under 10 CFR 2.390

Figure 8.2-1 – Method of Measuring Upper Seal Flange Groove Widths

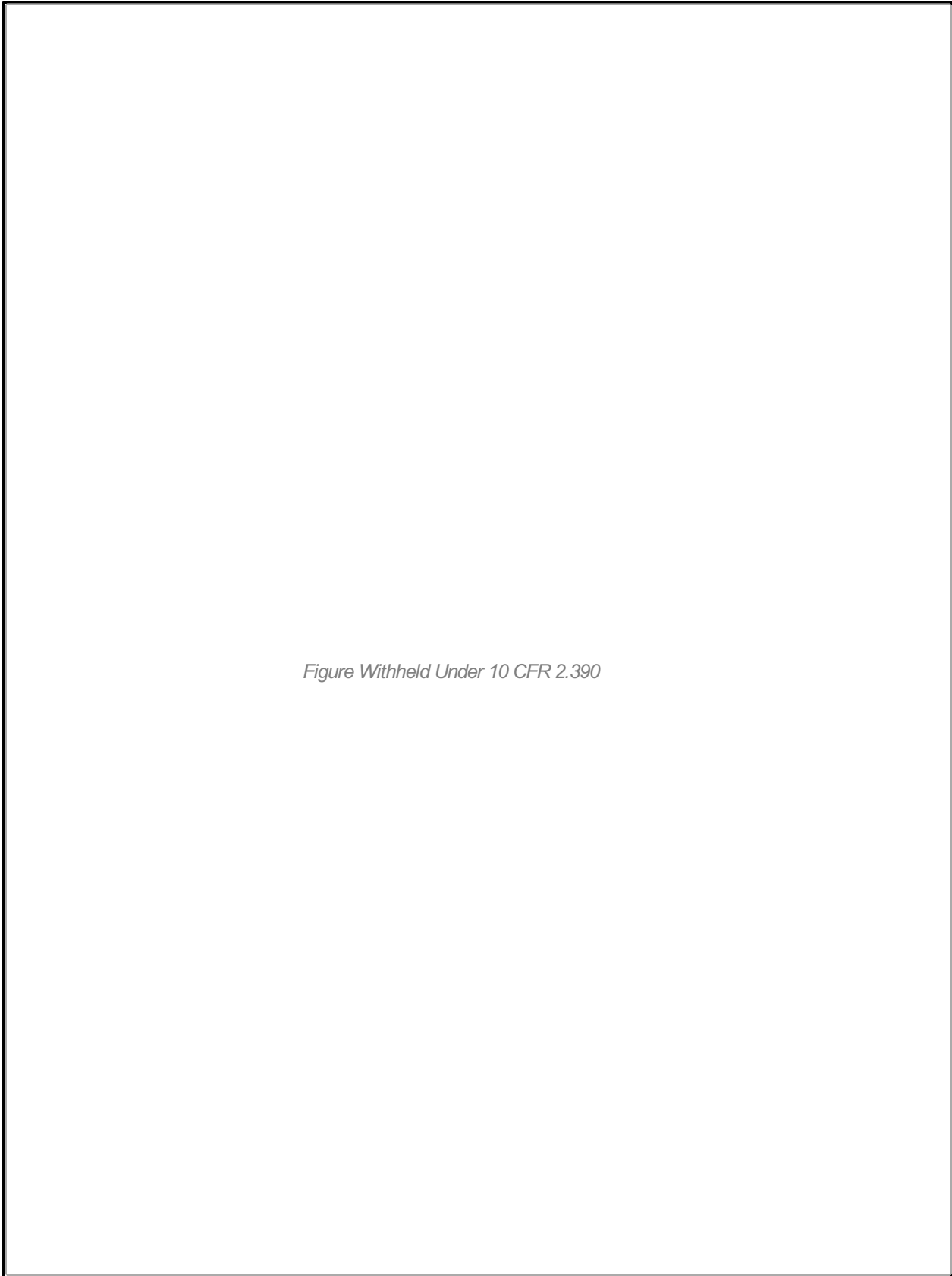


Figure Withheld Under 10 CFR 2.390

Figure 8.2-2 – Method of Measuring Lower Seal Flange Groove Widths



Figure Withheld Under 10 CFR 2.390

Figure 8.2-3 – Method of Measuring Upper Seal Flange Tab Widths

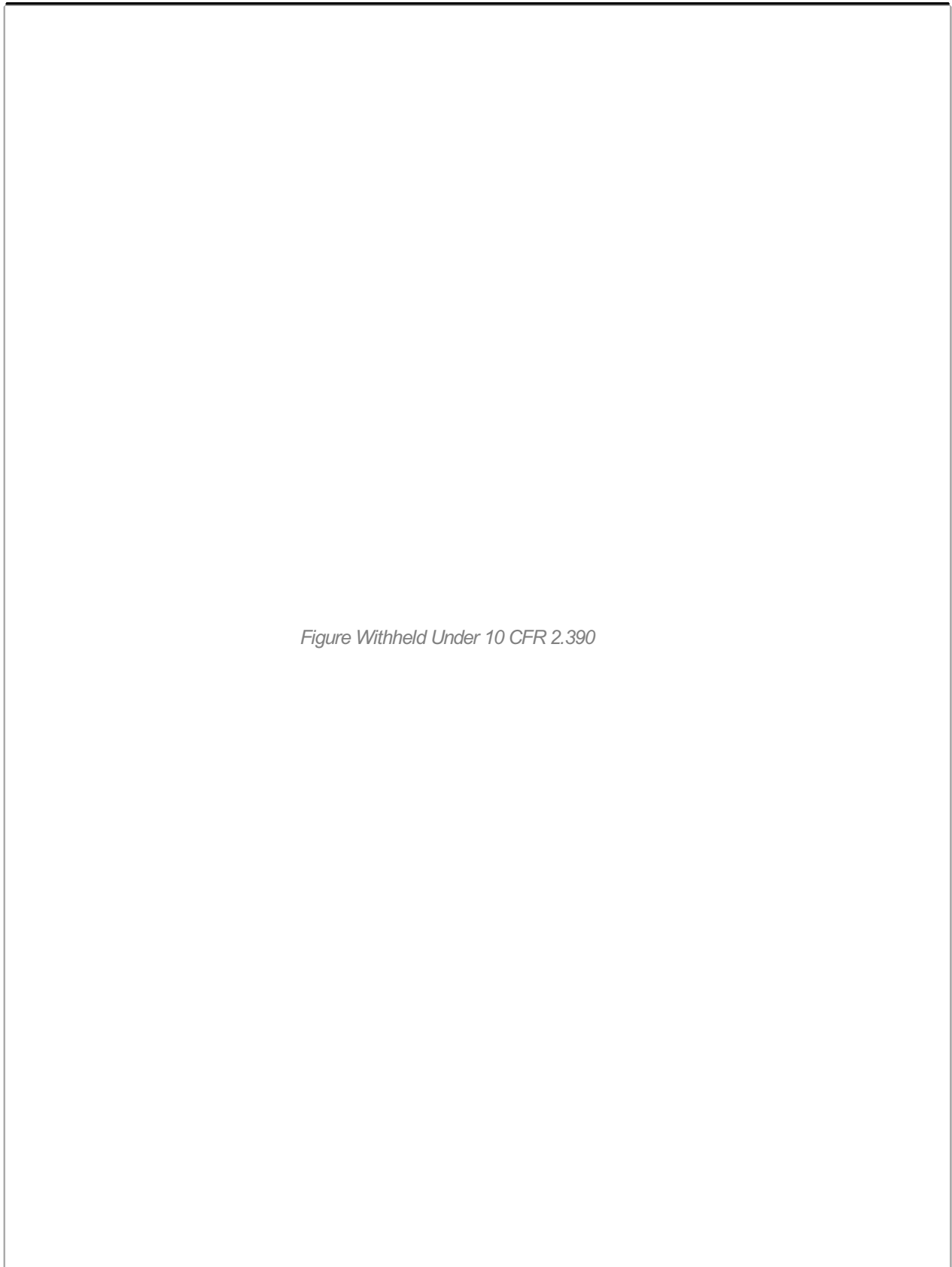


Figure Withheld Under 10 CFR 2.390

Figure 8.2-4 – Method of Measuring Lower Seal Flange Tab Widths

This page intentionally left blank.

9.0 QUALITY ASSURANCE

This section describes the quality assurance (QA) requirements and methods of compliance applicable to the HalfPACT package.

9.1 Introduction

The HalfPACT package is designed and shall be built for the U.S. Department of Energy (DOE), and must be approved by the U.S. Nuclear Regulatory Commission (NRC) for the shipment of radioactive material in accordance with the applicable provisions of the U.S. Department of Transportation, described in Subpart I of 49 CFR Part 173¹. Procurement, design, fabrication, assembly, testing, maintenance, repair, modification, and use of the HalfPACT package are all done under QA programs that meet all applicable NRC and DOE QA requirements. QA requirements for payloads to be transported in the HalfPACT package are discussed in the *Contact-Handled Transuranic Waste Authorized Methods for Payload Control (CH-TRAMPAC)*².

¹ Title 49, Code of Federal Regulations, Part 173 (49 CFR 173), *Shippers—General Requirements for Shipments and Packagings*, 10-01-06 Edition.

² U.S. Department of Energy (DOE), *Contact-Handled Transuranic Waste Authorized Methods for Payload Control (CH-TRAMPAC)*, U.S. Department of Energy, Carlsbad Field Office, Carlsbad, New Mexico.

This page intentionally left blank.

9.2 Quality Assurance Requirements

9.2.1 U.S. Nuclear Regulatory Commission

The QA requirements for packaging established by the NRC are described in Subpart H of 10 CFR 71¹. Subpart H is an 18 criteria QA program based on ANSI/ASME NQA-1². Guidance for QA programs for packaging is provided in Regulatory Guide 7.10³.

9.2.2 U.S. Department of Energy

The QA requirements of DOE for the use of NRC certified packaging are described in Chapter 4 of DOE Order 460.1⁴. According to Chapter 4.(4)(b), the DOE and its contractors may use NRC certified Type B packaging only under the conditions specified in the certificate of compliance.

9.2.3 Transportation to or from WIPP

Public Law 102-579, enacted by the 102nd Congress, reads as follows:

SEC. 16. TRANSPORTATION.

- (a) SHIPPING CONTAINERS. - No transuranic waste may be transported by or for the Secretary [of Energy] to or from WIPP, except in packages -
- (1) the design of which has been certified by the Nuclear Regulatory Commission; and
 - (2) that have been determined by the Nuclear Regulatory Commission to satisfy its quality assurance requirements.

The determination under paragraph (2) shall not be subject to rulemaking or judicial review.

¹ Title 10, Code of Federal Regulations, Part 71 (10 CFR 71), *Packaging and Transportation of Radioactive Material*, 01-01-07 Edition.

² ANSI/ASME NQA-1, *Quality Assurance Requirements of Nuclear Power Plants*, American National Standards Institute.

³ U.S. Nuclear Regulatory Commission, Regulatory Guide 7.10, *Establishing Quality Assurance Programs for Packaging Used in the Transport of Radioactive Material*, Revision 1, June 1986.

⁴ U.S. Department of Energy Order 460.1, *Packaging and Transportation Safety*, September 1995.

This page intentionally left blank.

9.3 Quality Assurance Program

9.3.1 NRC Regulatory Guide 7.10

Guidance for QA programs applicable to design, fabrication, assembly, and testing of packaging used in transport of radioactive material is covered in Annex 1 of the NRC's Regulatory Guide 7.10¹; procurement, use, maintenance and repair are covered in Annex 2.

9.3.2 Design

The HalfPACT package was designed under a QA program approved by the NRC for packaging design. Requests for modification or changes to the design will be submitted to the NRC for approval prior to modification of the HalfPACT packaging. Any future design changes shall be made under an appropriate NRC approved QA program.

9.3.3 Fabrication, Assembly, and Testing

Fabrication, assembly, and testing of each HalfPACT packaging are performed under a QA program approved by the NRC for these activities.

9.3.4 Procurement

Procurement of each HalfPACT packaging is performed under a QA program that meets the applicable QA requirements of the NRC.

9.3.5 Use

The HalfPACT package will be used primarily by the DOE for shipments of authorized contents to the WIPP site. However, it may also be used between DOE sites other than WIPP (inter-site), and for DOE on-site shipments within site boundaries (intra-site). The DOE is registered with the NRC as a user of the HalfPACT package under the general license provisions of 49 CFR §173.471². The HalfPACT package may also be used for non-DOE shipments as authorized by the NRC.

9.3.5.1 DOE Shipments: To/From WIPP

Use of the HalfPACT packaging for shipments to or from the WIPP site shall be made under a QA program that meets the QA requirements of the NRC. The appropriate DOE Field Office(s) shall inspect and approve the QA programs of the DOE contractors that make shipments to or from WIPP in the HalfPACT package. DOE or the DOE managing and operating contractor for the WIPP shall perform surveillances of the HalfPACT package users' QA programs to ensure that the package is used in accordance with the requirements of the certificate of compliance.

¹ U.S. Nuclear Regulatory Commission, Regulatory Guide 7.10, *Establishing Quality Assurance Programs for Packaging Used in the Transport of Radioactive Material*, Revision 1, June 1986.

² Title 49, Code of Federal Regulations, Part 173 (49 CFR 173), *Shippers—General Requirements for Shipments and Packagings*, 10-01-06 Edition.

9.3.5.2 Other DOE Shipments: Non-WIPP

The appropriate DOE Field Office(s) shall inspect and approve the shippers' and receivers' QA programs for equivalency to the NRC's QA program requirements in Subpart H of 10 CFR 71. For example, a contractor working under an 18 criteria QA program per ANSI/ASME NQA-1³ could be deemed acceptable if the program is applicable to packaging. DOE or the DOE managing and operating contractor for the WIPP shall perform surveillances of the HalfPACT package users' QA programs to ensure that the package is used in accordance with the requirements of the Certificate of Compliance.

9.3.5.3 Non-DOE Users of HalfPACT

Non-DOE users of the HalfPACT package shall have QA programs approved by the NRC.

9.3.6 Maintenance and Repair

Minor maintenance such as changing seals or fasteners may be performed under the user's QA program. Major maintenance such as cutting or welding a containment boundary shall be performed under an appropriate QA program that has been approved by the NRC.

³ ANSI/ASME NQA-1, *Quality Assurance Requirements of Nuclear Power Plants*, American National Standards Institute.